Feedback Circuit Analysis

S. S. HAKIM, PH.D., B.SC., A.M.I.E.E.
Professor of Electrical Engineering
at the McMaster University, Hamilton
Ontario, Canada

LONDON ILIFFE BOOKS LTD

Preface

This book is devoted to a detailed study of feedback theory as applied to linear electronic circuits. It has been written with two particular objectives in mind. The first is to develop a generalised feedback theory which does not rely on the separation of a feedback circuit into an amplifier and feedback network component, and yet it is capable of accounting for all the effects associated with feedback. The need for such a theory is more necessary than ever before owing to the more complex manner in which a transistor behaves compared with a thermionic valve. The second objective is to provide a broad view of the important problem of stability and its relation to the closed-loop transient response, open-loop frequency response and driving-point impedances of the feedback circuit. In all this, we shall find that Bode's classic work on feedback plays a major role.

The book is written at a level suitable for a final year electronics undergraduate or a postgraduate student. It is hoped that the book will also prove useful to the practising electronics engineer who is seeking a sound understanding of the feedback problem and its various circuit implications.

The first chapter introduces the idea of feedback in fairly general terms, and Chapter 2 introduces brief discussions of the concept of a controlled source, the Laplace transformation, frequency response analysis, matrices, two-port networks, the indefinite admittance matrix and its applications to valve and transistor circuits. Much of this chapter is essential to a serious study of feedback. It is, however, assumed that the reader is familiar with the mesh and nodal methods of circuit analysis.

In Chapter 3 the classical feedback theory, is developed, assuming a distinct separation between the amplifier and feedback network. Then after discussing the limitations of this theory, the need for a more generalised feedback theory is established. In the development of this generalised theory the approach adopted is based on the Mason-Truxal flow graph exposition of Bode's mathematical theory of feedback.

The stability problem in feedback amplifiers is first studied in Chapter 4 in terms of the complex frequency (i.e. the p-) plane and the associated

Routh's criterion and Evans's root locus diagram. In the Appendix at the end of the book it is shown that a great deal of useful information about the relative locations of the closed-loop poles in the left half of the p-plane can be obtained by applying certain transformations.

Next in Chapter 5 the stability problem is studied in terms of the open-loop frequency response. Nyquist's criterion is developed from first principles, and some of the more widely used integral relationships between the gain and phase characteristics of minimum phase transfer functions are derived. By now sufficient background material has been covered to develop Bode's ideal loop gain characteristic, the realisation of which assures specified mid-band open-loop gain and stability margins. An important link with Chapter 4 is established by showing how the principal oscillatory mode of the closed-loop transient response can be determined from the open-loop frequency response.

Chapter 6 is concerned with the problem of designing suitable compensating networks required to shape the open-loop frequency response. In Chapter 7, it is shown that much useful information about stability can be also obtained by examining the driving-point impedance at an appropriate pair of terminals in the feedback circuit.

In Chapter 8 the transient and frequency responses of various wideband amplifier configurations employing negative feedback are examined. Chapter 9 gives a fairly detailed treatment of the operational amplifier and its use in transfer function simulation.

The last chapter of the book is devoted to a study of sinusoidal feedback oscillators. By using chain matrices to describe the overall behaviours of the internal amplifier and feedback network components connected in cascade, a generalised method of analysis is established and the various LC- and RC-oscillators are considered as special cases. This chapter ends with an account of the various frequency stabilisation techniques.

At the end of each chapter I have included a list of references which I have found invaluable in the course of writing this book. I was first introduced to the work of H. W. Bode on feedback by Professor J. T. Allanson of the Electrical Engineering Department of Birmingham University; to him I am deeply indebted.

Finally I should like to thank the Senate of London University and the Institution of Electrical Engineers for granting me permission to reproduce a number of problems taken from their previous examination papers. I am solely responsible for the answers to problems given at the end of the book.

Coventry, 1965 S.S.H.

CHAPTER 1

Introduction

Feedback is said to exist in a circuit when the output signal is wholly or partially fed back to be combined with the input signal. If the feedback signal opposes the input signal the feedback is said to be *negative*, whereas if the feedback signal aids the input then *positive feedback* results.

In electronic circuits feedback can exist in a variety of ways:

1. Feedback may appear in a circuit unintentionally as a result of parasitic capacitances or leakage resistances. For example, in the common cathode stage of Fig. 1.1 using a triode valve the anode-grid interelectrode capacitance C_{ag} privides a return path for the output signal at high frequencies, thereby giving rise to the well known *Miller effect* and its various consequences. Another example is that of a common emitter stage using a junction transistor. Here we find that, at low as well as high frequencies, the transistor transmits a signal in the reverse direction (i.e. from output to input) in addition to the forward direction (i.e. from input to output) with the result that the electrical conditions across the input terminals of the stage affect those across the output terminals and vice-versa. This form of feedback is usually referred to as *internal feedback*.
2. Feedback can also arise as a secondary result of circuit design, as in the valve amplifier of Fig. 1.2 employing self-bias by means of the cathode resistor R_k. Normally this resistor is shunted with a suitably large capacitor, C_k, to ensure that, in the useful frequency band of the amplifier, the cathode bias resistor is effectively short-circuited for a.c. signals. At low frequencies, however, the by-pass capacitor no longer presents an effective short-circuit across the cathode bias resistor R_k because the impedance of a capacitor is inversely proportional to frequency. The result is that, at very low frequencies, the resistor R_k applies a certain amount of

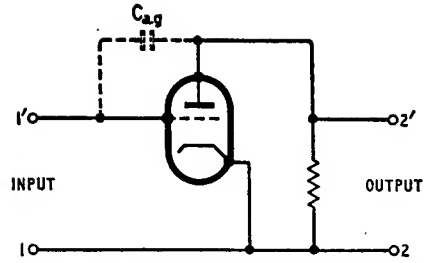

Fig. 1.1. Illustrating feedback due to anode to grid interelectrode capacitance C_{ag}

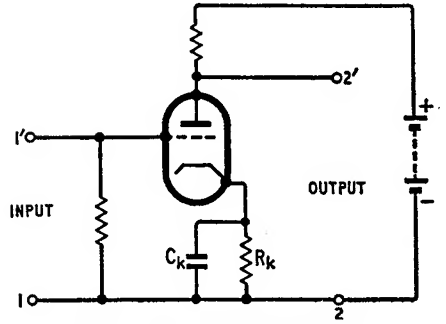

Fig. 1.2. Self-bias circuit

Fig. 1.3. Block diagram of non-feedback amplifier

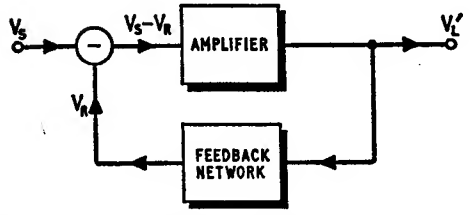

Fig. 1.4. Block diagram of negative feedback amplifier

negative feedback to the stage, thereby causing a reduction in the magnitude of its voltage gain.

3. Feedback is purposefully applied to a circuit with the object of realising certain useful circuit properties. It is with this form of feedback that we shall be largely concerned.

1.1 Advantages and cost of feedback

One of the effects of negative feedback when it is applied to an amplifier circuit is that it results in a reduction of the sensitivity of the overall gain of the circuit to variations in valve or transistor parameters due to changes in ambient temperature, d.c. supply voltage or aging. To appreciate this important effect, let us first consider Fig. 1.3 which shows the block diagram representation of a non-feedback amplifier having a forward gain K defined as the ratio of the load voltage V_L to the source voltage V_S, that is

$$K = \frac{V_L}{V_S} \tag{1.1}$$

Here we see that a fractional change in the gain K causes an equal fractional change in the load voltage V_L. Thus if the source voltage is maintained constant and the gain K changes by 10%, say, we find that the load voltage changes by 10% too.

Let us consider next a negative feedback amplifier represented by the block diagram of Fig. 1.4.† The load voltage V_L' is fed back to the input through the feedback network producing the feedback voltage V_R which is 180° out of phase with the source voltage V_S. The result is that the input signal of the internal amplifier becomes equal to $V_S - V_R$, and the *closed-loop gain* K' (i.e. gain with feedback) assumes the following value

$$K' = \frac{V_L'}{V_S} = \frac{K}{1 + \beta K} \tag{1.2}$$

where β equals the ratio V_R/V_L' and is determined by the feedback network. If the product term βK, which is known as the *open-loop gain*, is chosen very large compared to unity, the gain K' with feedback approximates very closely to $1/\beta$. Then it becomes practically independent of variations in the parameters of the transistors or valves which constitute the internal amplifier and depends only on

† The reason for adopting the convention shown in the block diagram of Fig. 1.4 is that it enables us to unify the treatment of feedback circuits with other feedback control systems.

the constancy of the β-network. This is a very attractive feature of negative feedback.

The application of negative feedback also tends to reduce the harmonic distortion and noise generated inside the internal amplifier. In addition the input and output impedances of the amplifier can be increased or decreased by suitable interconnections of the internal amplifier and feedback network components.

The above advantages of negative feedback are achieved at the cost of, firstly, a reduced value for the closed-loop gain K'; this follows from Equation 1.2 where we see that K' is less than K if the denominator $1 + \beta K$ is greater than unity, as is the case in negative feedback. Secondly in certain cases the amplifier can become unstable as a result of the applied feedback and therefore break into oscillation as soon as the d.c. power supply is switched on. Then it becomes necessary to add suitable corrective circuit elements to the internal amplifier and/or the feedback network so as to ensure that the amplifier remains stable under all possible operating conditions.

1.2 Analysis of feedback circuits

In the analysis and design of feedback circuits it is found that the following two problems are of particular importance:

Evaluation of the various effects of feedback on the circuit performance of the amplifier

This can be carried out by applying the *classical feedback theory* which leads to Equation 1.2. It is based on the assumption that there exists a clear cut separation between the internal amplifier and the feedback network as illustrated in the idealised block diagram representation of Fig. 1.4. In a practical circuit, however, we invariably find that the feedback network loads the internal amplifier in such a way that an absolute and clear cut separation between the two is non-existent. Therefore, a much more elegant approach is the development of a *generalised feedback theory* which does not rely on the decomposition of the feedback amplifier into its two basic network components. H. W. Bode[1] has developed such a theory which not only explains all the effects of feedback but can be applied to any feedback circuit irrespective of its complexity.

Investigation of the stability problem

This can be usefully studied by considering the closed-loop transient response, or the open-loop frequency response or the input and output impedances of the feedback amplifier; each particular method brings out a different aspect of the important

problem of stability. An allied problem is that of designing the corrective networks which, when added to the internal amplifier and/or the feedback network, would assure the desired stability of the amplifier.

The major part of the book is devoted to a detailed study of these two aspects of feedback. However, before undertaking this task, we shall find it beneficial to consider first the various established methods of analysing linear electric circuits. This we shall do in the next chapter.

REFERENCES

1. BODE, H. W., *Network Analysis and Feedback Amplifier Design*, Van Nostrand, New York (1945).
2. BLACK, H. S., 'Stabilised Feedback Amplifiers' *Bell System Tech. J.*, **13**, 1, (1934).

CHAPTER 2

Linear Circuit Analysis

Electric circuits can be broadly classified as *linear* and *non-linear*. A circuit is said to be linear when its output signal is directly proportional to the input signal, otherwise the circuit is non-linear. Linear circuits have the important property of *superposition*, that is, if a number of electrical sources exist in a linear circuit then the total voltage (or current) in any part of the circuit is equal to the sum of the voltages (or currents) that would result if the various sources were to act individually. This is known as the *superposition theorem*. In the category of linear circuits we can include a valve or transistor provided it is operated under small signal conditions, that is, the deviations from the quiescent operating point are sufficiently small to assure a negligible departure from linear behaviour. Another example is the tunnel diode which can present an essentially linear negative resistance over part of its characteristic curve.

Alternatively electric circuits can be classified into *passive* and *active* networks. A two-terminal network component is said to be passive when the signal power input into it is always positive regardless of the conditions imposed by its environment. The resistor, capacitor and inductor are examples of passive network elements, and a circuit composed of such elements is usually referred to as a *passive network*. If, on the other hand, the signal power input into a two-terminal network component is negative (i.e. it delivers power to its environment) then it is said to be an active element. The negative resistance exhibited by a tunnel diode is an example of a two-terminal active network element. A transistor or a valve operated in its linear region is also an example of an active network element because the output signal power which it delivers to its load can exceed the input signal power supplied from the external source. Circuits containing negative resistance elements, valves or transistors are usually referred to as *active networks*. A characteristic of an active network is that it can, under certain circumstances, become unstable and therefore break into oscillation. This is in direct

contrast to a passive network which is inherently stable. We shall have more to say about the passivity and activity of electric networks later on in the chapter.

2.1 Circuit elements and sources

The voltage-current relationships for a resistor R, an inductor L and a capacitor C are as follows, respectively

$$v(t) = Ri(t) \tag{2.1}$$

$$v(t) = L\frac{di(t)}{dt} \tag{2.2}$$

$$v(t) = \frac{1}{C}\int_0^t i(t)\,dt + v(0) \tag{2.3}$$

where the voltage $v(t)$ and current $i(t)$ are both functions of time t and are as shown defined in Fig. 2.1. Also $v(0)$ is the voltage across the capacitor at the reference time $t = 0$.

In Equations 2.1 to 2.3 the current $i(t)$ is the independent variable.

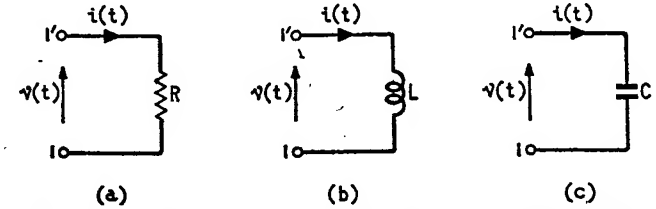

Fig. 2.1. Voltage–current relationships in passive circuit elements: (a) resistor, (b) inductor, (c) capacitor

If the voltage $v(t)$ is regarded as the independent variable, we obtain the following inverse relations for the resistor, the inductor and the capacitor, respectively

$$i(t) = Gv(t) \tag{2.4}$$

$$i(t) = \frac{1}{L}\int_0^t v(t)\,dt + i(0) \tag{2.5}$$

$$i(t) = C\frac{dv(t)}{dt} \tag{2.6}$$

where $G = 1/R$ is the conductance, and $i(0)$ is the current flowing through the inductor at $t = 0$.

In addition to the resistance, inductance and capacitance there exists a fourth network parameter, namely, the mutual inductance M which arises when two inductors are magnetically coupled, as in the transformer of Fig. 2.2. In this diagram, L_1 is the self-inductance of the primary winding when $i_2(t) = 0$ and L_2 is the self-inductance

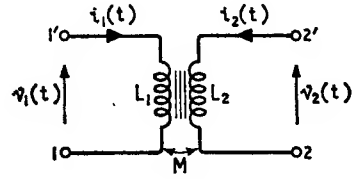

Fig. 2.2. Transformer

of the secondary winding when $i_1(t) = 0$. The voltage-current relationships for the transformer of Fig. 2.2 are

$$\left.\begin{aligned} v_1(t) &= L_1 \frac{di_1(t)}{dt} + M \frac{di_2(t)}{dt} \\ v_2(t) &= M \frac{di_1(t)}{dt} + L_2 \frac{di_2(t)}{dt} \end{aligned}\right\} \tag{2.7}$$

The mutual inductance M is related to the self-inductances L_1 and L_2 by

$$M = k\sqrt{(L_1 L_2)} \tag{2.8}$$

where k is termed the *coefficient of coupling* and is always less than unity.

If the primary and secondary windings of the transformer are joined together in the manner shown in Fig. 2.3 (a), then it can be replaced by the T-equivalent circuit of Fig. 2.3 (b) or the π-equivalent circuit of Fig. 2.3 (c). Here we are assuming that both windings of the transformer are dissipationless.

When the coefficient of coupling is unity, and the primary and secondary inductances are infinite but so proportioned that their

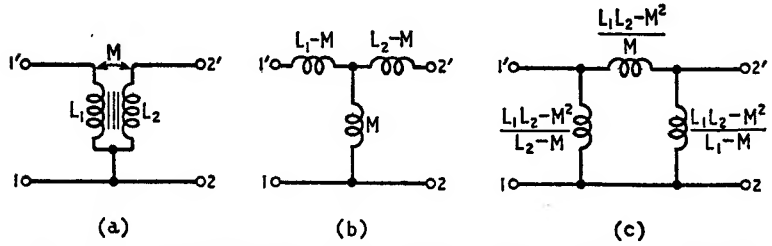

Fig. 2.3. (a) Transformer, (b) T-equivalent circuit, (c) π-equivalent circuit

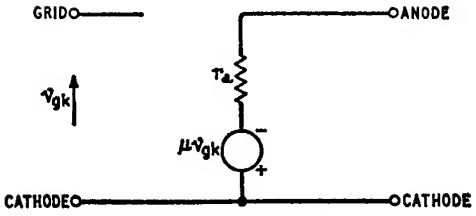

Fig. 2.4. Equivalent circuit for a triode valve

ratio is finite, the transformer is said to be *ideal*. In an ideal transformer $v_2(t) = nv_1(t)$ and $i_2(t) = i_1(t)/n$ where n is the turns ratio.

2.1.1 CONTROLLED SOURCES

In the analysis of circuits containing active devices such as valves and transistors it is found convenient to replace the particular device by a suitable equivalent circuit consisting of ordinary passive

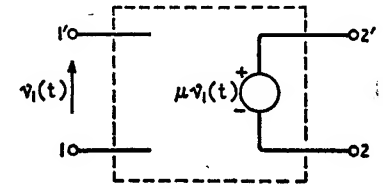

Fig. 2.5. Voltage-controlled voltage source

circuit elements and a *controlled source* whose value is proportional to a *control signal* applied at another point in the circuit. For example, in the equivalent circuit representation of Fig. 2.4 for a triode valve the voltage source μv_{gk} is controlled by means of the grid-cathode voltage v_{gk}

In general, each of the control signal and the controlled source can be either a voltage or a current one. Hence, it follows that there are four basic types of controlled sources; they are

1. A *voltage-controlled voltage source*. This is shown in Fig. 2.5 where the input voltage $v_1(t)$ is the control signal, and the *control parameter* μ is dimensionless.
2. A *current-controlled voltage source*. This is shown in Fig. 2.6 where the input current $i_1(t)$ is the control signal, and the control parameter r_m has the dimensions of a resistance.
3. A *current-controlled current source*. This is shown in Fig. 2.7 where the control parameter α is dimensionless.
4. A *voltage-controlled current source*. This is shown in Fig. 2.8 where the control parameter g_m has the dimensions of a conductance.

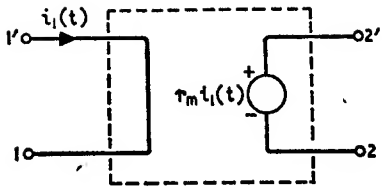

Fig. 2.6. Current-controlled voltage source

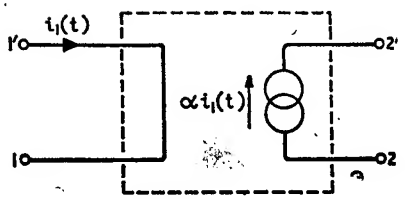

Fig. 2.7. Current-controlled current source

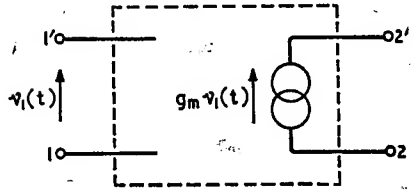

Fig. 2.8. Voltage-controlled current source

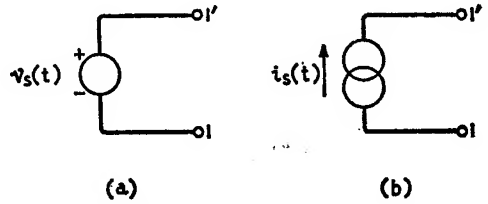

Fig. 2.9. Independent sources: (a) voltage source, (b) current source

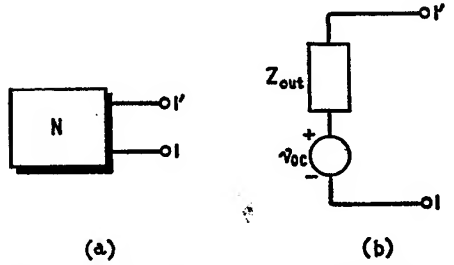

Fig. 2.10. (a) Network N containing controlled sources, (b) Thévenin equivalent circuit

Any of the controlled sources of Figs. 2.5 to 2.8 is seen to be a *two-port network* in that it has two ports, one port being constituted by terminals 1,1′ and the other port constituted by terminals 2,2′. In this respect they differ from the independent voltage and current sources of Fig. 2.9, both of which are seen to be *one-port network* elements having one pair of terminals only.

Special consideration must be given to the presence of controlled sources when applying *Thévenin's* and *Norton's theorems* to active networks. Thus the Thévenin equivalent circuit of Fig. 2.10 (b) for an active network containing controlled sources consists of a source of voltage v_{oc} equal to the open-circuit voltage which appears across the output terminals 1,1′ of the network N, connected in series with an impedance Z_{out} equal to the impedance measured

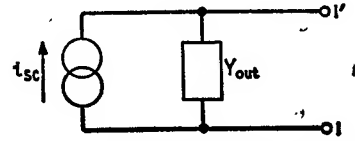

Fig. 2.11. Norton equivalent circuit

looking into the output terminals when all independent voltage sources inside the network N are short-circuited and all independent current sources are open-circuited. It is, however, important to note that the controlled sources must not be removed when calculating the impedance Z_{out}. This is because a controlled source is, by nature, dependent on the control signal such that any change in the control signal produces a corresponding change in the magnitude of the controlled source; hence controlled sources do contribute to the value of Z_{out} as well as v_{oc}.

Similarly, the Norton equivalent circuit of Fig. 2.11 for the active network N of Fig. 2.10 (a) consists of a source of current i_{sc} equal to the short-circuit current which flows through the output terminals 1,1′ of the network N, connected in parallel with an admittance $Y_{out} = 1/Z_{out}$, where Z_{out} is as calculated above.

2.2 Transient response

The transient response of a linear circuit can be studied by using the classical method of solving ordinary integro-differential equations or by applying operational methods based on the widely used *Laplace transform*. In the classical method the solution of the particular transient problem is carried out directly in the *time domain*. On the other hand, the Laplace transformation converts the problem from the time domain to the *complex frequency domain* where the transform of the solution can be obtained by simple

algebraic means. Next, by applying the *inverse Laplace transformation*, the desired solution as a function of time can be determined.

Another important and useful feature of the Laplace transform method of solving differential equations is that initial conditions are taken into account at an early stage in the solution. This avoids the need for evaluating arbitrary constants, as required in the classical method. Also, as we shall see later, the Laplace transformation enables the unification of the transient and frequency responses of a network. For these reasons we shall only consider the Laplace transform method of solving transient response problems.

2.2.1 LAPLACE TRANSFORM THEORY

Consider a function $\phi(t)$ of time t that is zero for $t < 0$. Its Laplace transform $\Phi(p)$ is defined to be

$$\Phi(p) = \int_0^\infty \phi(t)\, e^{-pt}\, dt \qquad (2.9)$$

where $p = \sigma + j\omega$, with both σ and ω being real. The variable p has the dimensions of frequency and is therefore termed the *complex frequency variable.*† Equation 2.9 transforms the function $\phi(t)$ in the time domain into another function $\Phi(p)$ in the complex frequency domain. $\phi(t)$ and $\Phi(p)$ are said to constitute a *transform pair*. The exponential factor e^{-pt} assures the convergence of the integral in Equation 2.9 when applied to functions of time commonly met in the study of electrical systems.

The Laplace transform is characterised in having a number of important properties which follow from the basic definition of Equation 2.9. Some of these properties are discussed below.

Linearity

This property provides a basis for the transformation of a sum of two functions of time into the sum of their respective Laplace transforms. Consider two functions $\phi_1(t)$ and $\phi_2(t)$ and suppose that k_1 and k_2 are any constants. Then

$$\int_0^\infty k_1\phi_1(t)\, e^{-pt}\, dt = k_1\int_0^\infty \phi_1(t)\, e^{-pt}\, dt = k_1\Phi_1(p) \qquad (2.10)$$

Similarly,

$$\int_0^\infty k_2\phi_2(t)\, e^{-pt}\, dt = k_2\Phi_2(p) \qquad (2.11)$$

† The notation s is also widely used for denoting the complex frequency variable.

where $\Phi_1(p)$ and $\Phi_2(p)$ are the Laplace transforms of $\phi_1(t)$ and $\phi_2(t)$, respectively. Therefore

$$\int_0^\infty [k_1\phi_1(t) + k_2\phi_2(t)]\, e^{-pt}\, dt = k_1\Phi_1(p) + k_2\Phi_2(p) \qquad (2.12)$$

Transforms of derivatives

From Equation 2.9 we see that the Laplace transform of

$$\frac{d}{dt}\phi(t)$$

which is the derivative of $\phi(t)$ with respect to time, is given by

$$\int_0^\infty \left[\frac{d}{dt}\phi(t)\right] e^{-pt}\, dt$$

Integrating by parts, we obtain

$$\begin{aligned}\int_0^\infty \left[\frac{d}{dt}\phi(t)\right] e^{-pt}\, dt &= \Big[\phi(t)\, e^{-pt}\Big]_0^\infty - \int_0^\infty \phi(t)\frac{d}{dt}e^{-pt}\, dt \\ &= -\phi(0^+) + \int_0^\infty p\phi(t)\, e^{-pt}\, dt \\ &= p\Phi(p) - \phi(0^+) \qquad (2.13)\end{aligned}$$

where $\phi(0^+)$ signifies the initial condition and equals the limit of $\phi(t)$ as t approaches zero from positive time values. We thus see that differentiation with respect to t transforms into multiplication of $\Phi(p)$ with the complex variable p and subtraction of the initial value $\phi(0^+)$.

Next for the second derivative, we can show that the Laplace transform is given by

$$\int_0^\infty \left[\frac{d^2}{dt^2}\phi(t)\right] e^{-pt}\, dt = p^2\Phi(p) - p\phi(0^+) - \phi'(0^+) \qquad (2.14)$$

where $\phi'(0^+)$ denotes the initial value of $d\phi(t)/dt$. In a similar fashion, the Laplace transforms of higher derivatives can be obtained.

Transforms of integrals

The Laplace transform of the integral of $\phi(t)$ with respect to time follows from Equation 2.9 to be

$$\int_0^\infty [\int \phi(t)\,dt]\,e^{-pt}\,dt$$

Integrating by parts we find that

$$\int_0^\infty [\int \phi(t)\,dt]\,e^{-pt}\,dt = \left[-\frac{1}{p}e^{-pt}\int \phi(t)\,dt\right]_0^\infty + \int_0^\infty \frac{1}{p}e^{-pt}\phi(t)\,dt$$

$$= \frac{\Phi(p)}{p} + \frac{1}{p}\phi^{-1}(0^+) \qquad (2.15)$$

where $\phi^{-1}(0^+)$ is the initial value of $\int\phi(t)\,dt$. Similarly we can evaluate the Laplace transforms of higher integrals.

Shifting theorem

Consider a function $\phi(t-\tau)$ which is zero for $t < \tau$. The Laplace transform of such a function follows from Equation 2.9 to be

$$\int_\tau^\infty \phi(t-\tau)\,e^{-pt}\,dt$$

In this integral, we shall make the substitution $x = t - \tau$. Hence $dx = dt$. Since $x = 0$ when $t = \tau$, we find that

$$\int_\tau^\infty \phi(t-\tau)\,e^{-pt}\,dt = \int_0^\infty \phi(x)\,e^{-p(\tau+x)}\,dx$$

$$= e^{-p\tau}\int_0^\infty \phi(x)\,e^{-px}\,dx$$

$$= e^{-p\tau}\,\Phi(p) \qquad (2.16)$$

Therefore, a shift to the right of τ seconds in the time domain corresponds to multiplying by the factor $e^{-p\tau}$ in the complex frequency domain.

2.2.2 UNIT-STEP, UNIT-IMPULSE AND UNIT-RAMP FUNCTIONS

In studying the transient response of electric circuits, it is found that a number of excitations are of fundamental importance. Consider first the function of Fig. 2.12 where it is seen to be equal to zero for $t < 0$ and unity for $t > 0$. This function is known as the *unit-step function* or *Heaviside's unit function* after Oliver Heaviside. We shall denote it by $u_{-1}(t)$; thus

$$\left.\begin{aligned} u_{-1}(t) &= 0 \text{ for } t < 0 \\ u_{-1}(t) &= 1 \text{ for } t > 0 \end{aligned}\right\} \qquad (2.17)$$

From Equation 2.9 we find that the Laplace transform of the unit-step function is

$$\int_0^\infty u_{-1}(t)\,e^{-pt}\,dt = \int_0^\infty e^{-pt}\,dt$$

$$= \left[-\frac{1}{p}e^{-pt}\right]_0^\infty$$

$$= \frac{1}{p} \qquad (2.18)$$

If the step function has an amplitude equal to k, then its Laplace transform is equal to k/p.

From Fig. 2.12 we see that the initial value of the step function is zero. Therefore, from Equation 2.13 we deduce that the Laplace

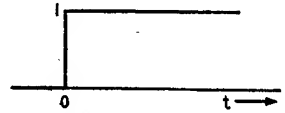

Fig. 2.12. Unit-step function

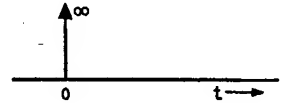

Fig. 2.13. Impulse function

transform of the first derivative of the unit-step function is equal to unity which is the simplest possible transform. The waveform obtained by differentiating the unit-step function with respect to time is shown illustrated in Fig. 2.13. This function is known as the *unit-impulse function* or *delta function*. It is seen to be zero everywhere except at $t = 0$ where it is infinite. We shall use $u_0(t)$ to denote the unit-impulse function, thus

$$\left.\begin{aligned} u_0(t) &= 0 \quad \text{for } t \neq 0 \\ u_0(t) &= \infty \text{ for } t = 0 \\ \int_{0^-}^{0^+} u_0(t)\,dt &= 1 \end{aligned}\right\} \qquad (2.19)$$

The unit-impulse function may be synthesised by considering a rectangle pulse of duration δ and amplitude $1/\delta$ as shown shaded in

Fig. 2.14. The rectangle is seen to have unit area. If now δ is allowed to approach zero then, in the limit, the rectangular pulse of Fig. 2.14 becomes a unit impulse.

The function $ku_0(t)$, where k is a constant, is referred to as an impulse function of strength k. Its Laplace transform is equal to k since that of the unit-impulse function $u_0(t)$ is equal to unity.

Consider next integrating the unit-step function $u_{-1}(t)$ with respect to time. The resulting function is shown in Fig. 2.15 where

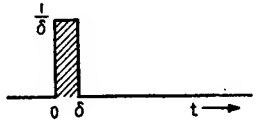

Fig. 2.14. Rectangular pulse of duration δ and amplitude $1/\delta$

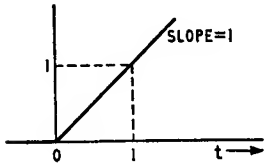

Fig. 2.15. Unit-ramp function

it is seen to increase with time at a constant slope of unity. This function is usually referred to as the *unit-ramp function* which we shall denote by $u_{-2}(t)$. Therefore

$$\left.\begin{aligned} u_{-2}(t) &= 0 \text{ for } t \leqslant 0 \\ u_{-2}(t) &= t \text{ for } t > 0 \end{aligned}\right\} \qquad (2.20)$$

Now the Laplace transform of the unit-step function is equal to $1/p$ and since the initial conditions are zero, then from Equation 2.15 it follows that the Laplace transform of the unit-ramp function is equal to $1/p^2$. If, however, the ramp function has a slope equal to k, then its Laplace transform will be equal to k/p^2.

By further differentiations and integrations of the unit-step function it is possible to generate additional forms of excitation but, in the present book, we shall find that the step, impulse and ramp functions are quite adequate.

2.2.3 LAPLACE TRANSFORM PAIRS TABLE

By applying the basic definition of the Laplace transform as given in Equation 2.9, to a variety of functions of time such as e^{-at}, $\cos \omega t$, $\sin \omega t$ etc. we can develop the Table 2.1 shown below. This table is usually referred to as the *Laplace transform pairs table.* We shall find it to be particularly useful later in the solution of transient response problems.

Table 2.1 SHORT TABLE OF LAPLACE TRANSFORM PAIRS†

No.	*Time Function $\phi(t)$*	*Laplace Transform $\Phi(p)$*
1	$u_0(t)$ or unit-impulse	1
2	$u_{-1}(t)$ or unit-step	$\frac{1}{p}$
3	$u_{-2}(t)$ or unit-ramp	$\frac{1}{p^2}$
4	t^n	$\frac{n!}{p^{n+1}}$
5	e^{-at}	$\frac{1}{p+a}$
6	te^{-at}	$\frac{1}{(p+a)^2}$
7	$\sin \omega t$	$\frac{\omega}{p^2+\omega^2}$
8	$\cos \omega t$	$\frac{p}{p^2+\omega^2}$
9	$e^{-at} \sin \omega t$	$\frac{\omega}{(p+a)^2+\omega^2}$
10	$e^{-at} \cos \omega t$	$\frac{p+a}{(p+a)^2+\omega^2}$
11	$t \sin \omega t$	$\frac{2\omega p}{(p^2+\omega^2)^2}$
12	$t \cos \omega t$	$\frac{p^2-\omega^2}{(p^2+\omega^2)^2}$
13	$\sinh at$	$\frac{a}{p^2-a^2}$
14	$\cosh at$	$\frac{p}{p^2-a^2}$
15	$\frac{1}{2\omega}(\sin \omega t - \omega t \cos \omega t)$	$\frac{\omega^2}{(p^2+\omega^2)^2}$

† A more comprehensive table of Laplace transform pairs is given by (1) Churchill, R. V., *Operational Mathematics*, (2nd Ed.), McGraw-Hill (1958).
(2) Carslaw, H. S. and Jaeger, J. C., *Operational Methods in Applied Mathematics*, (2nd. Ed.), Oxford University Press (1948)

2.2.4 NETWORK FUNCTIONS

For linear electric networks the *output* or *response* function is related to the *input* or *excitation* function by a linear ordinary differential equation. Thus, if the excitation is $\phi_i(t)$, which signifies a voltage or current, and $\phi_0(t)$ is the resulting response function, the relation is of the following form

$$a_n \frac{d^n}{dt^n}\phi_0(t) + a_{n-1}\frac{d^{n-1}}{dt^{n-1}}\phi_0(t) + \ldots + a_1\frac{d}{dt}\phi_0(t) + a_0\phi_0(t)$$

$$= b_m\frac{d^m}{dt^m}\phi_i(t) + b_{m-1}\frac{d^{m-1}}{dt^{m-1}}\phi_i(t) + \ldots b_1\frac{d}{dt}\phi_i(t) + b_0\phi_i(t) \tag{2.21}$$

where $a_0, a_1 \ldots a_{n-1}, a_n$ and $b_0, b_1 \ldots b_{m-1}, b_m$ are all real coefficients. Assuming the initial conditions to be zero and taking the Laplace transform of both sides of Equation 2.21, we obtain

$$(a_n p^n + a_{n-1}p^{n-1} + \ldots a_1 p + a_0)\Phi_0(p)$$

$$= (b_m p^m + b_{m-1}p^{m-1} + \ldots b_1 p + b_0)\Phi_i(p)$$

Therefore

$$\Phi_0(p) = \frac{b_m p^m + b_{m-1}p^{m-1} + \ldots b_1 p + b_0}{a_n p^n + a_{n-1}p^{n-1} + \ldots a_1 p + a_0}\Phi_i(p) \tag{2.22}$$

$\Phi_i(p)$ is the Laplace transform of the excitation $\phi_i(t)$ and is therefore termed the *excitation transform.* $\Phi_0(p)$ is the Laplace transform of the response function $\phi_0(t)$ and is termed the *response transform.* The ratio of the response transform to the excitation transform is referred to as the *system function* $G(p)$ of the network, Thus

(Response Transform) = (System Function) (Excitation Transform) (2.23)

Alternatively,

$$\text{(System Function)} = \frac{\text{(Response Transform)}}{\text{(Excitation Transform)}} \tag{2.24}$$

Hence, Equation 2.24 gives

$$G(p) = \frac{\Phi_0(p)}{\Phi_i(p)}$$

$$= \frac{b_m p^m + b_{m-1}p^{m-1} + \ldots b_1 p + b_0}{a_n p^n + a_{n-1}p^{n-1} + \ldots a_1 p + a_0} \tag{2.25}$$

Thus the system function of a linear network is a rational function of p, that is, the ratio of two polynomials each with constant coefficients.

If in Equation 2.25 the numerator and denominator polynomials are both factorised, the numerator into m factors and the denominator into n factors, we obtain the following alternative but equivalent form for the system function

$$G(p) = H\frac{(p - z_1)(p - z_2)\ldots(p - z_m)}{(p - p_1)(p - p_2)\ldots(p - p_n)} = H\frac{\prod_{k=1}^{m}(p - z_k)}{\prod_{k=1}^{n}(p - p_k)} \tag{2.26}$$

where H is equal to b_m/a_n and is termed the *scale factor.* The numbers z_1 to z_m are the values of p for which $G(p)$ is zero and so therefore they are termed the *zeros* of the system function. The numbers p_1 to p_n are the values of p for which $G(p)$ becomes infinite,

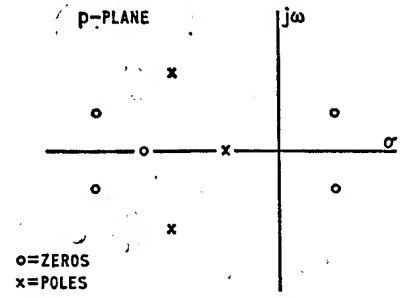

Fig. 2.16. Pole-zero pattern

and so they are termed the *poles* of the system function. In Equation 2.26 we shall refer to each factor $(p - z_k)$ in the numerator as a *zero factor* and to each factor $(p - p_k)$ in the denominator as a *pole factor.* The system function $G(p)$ is completely determined by specifying its poles and zeros and its scale factor. It is to be noted that both poles and zeros have the dimensions of frequency.

With the coefficients a_0 to a_n and b_0 to b_m all real, we find that the poles and zeros of a system function can be either real or else occur in complex conjugate pairs. It is customary practice to plot the poles and zeros of the system function in the complex p-plane. We shall use circles ○ to represent the locations of zeros and crosses × to represent the locations of the poles. The resulting plot is referred to as the *pole-zero pattern.* An example of such a plot is shown in Fig. 2.16.

There are two kinds of system functions of interest; they are the *driving-point function* and the *transfer function.* The driving-point function expresses a relationship between the voltage and current

transforms at the same pair of terminals. On the other hand, a transfer function expresses a relationship between the voltage or current transform at one pair of terminals and the voltage or current transform at another pair of terminals of the same network. Consider the two-terminal network N of Fig. 2.17 (a) assumed to consist

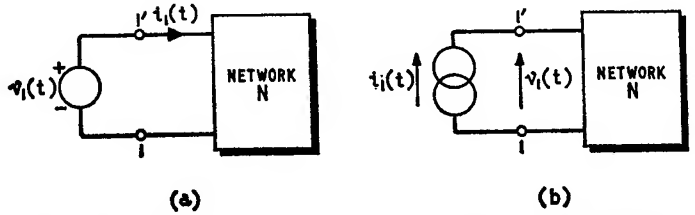

Fig. 2.17. One-port network: (a) with driving voltage source, and (b) with driving current source

of passive elements and controlled sources only. The voltage source $v_1(t)$ is assumed to be the excitation and the current $i_1(t)$ is the resulting response function. Then

$$Y(p) = \frac{I_1(p)}{V_1(p)} \tag{2.27}$$

where $I_1(p)$ and $V_1(p)$ are the Laplace transforms of $i_1(t)$ and $v_1(t)$, respectively. The function $Y(p)$ has the dimensions of an admittance and is therefore termed the *driving-point admittance.*

In Fig. 2.17 (b) the current source $i_1(t)$ is assumed to be the excitation and the voltage $v_1(t)$ developed across the terminal pair 1,1′ is the response function. Then

$$Z(p) = \frac{V_1(p)}{I_1(p)} \tag{2.28}$$

The function $Z(p)$ has the dimensions of an impedance and is termed the *driving-point impedance.* It is equal to the reciprocal of the driving-point admittance.

Consider next the two-port network N of Fig. 2.18 (a) consisting of passive elements and controlled sources only. The voltage source $v_1(t)$ connected across the port 1,1′ is the excitation. If the voltage $v_2(t)$ developed across the load, that is, terminal pair 2,2′ is the response function, then

$$K_V(p) = \frac{V_2(p)}{V_1(p)} \tag{2.29}$$

The function $K_V(p)$ is termed the *voltage gain* of the two-port

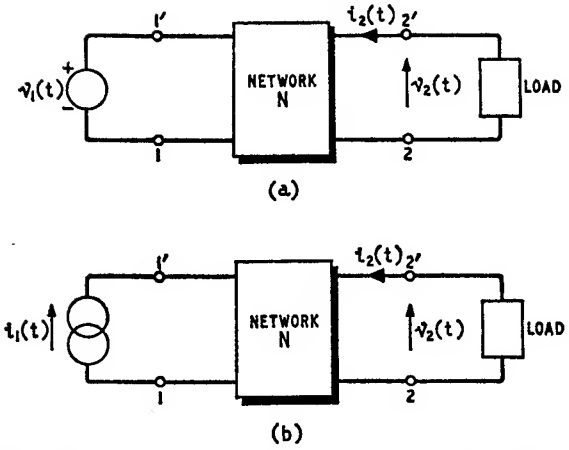

Fig. 2.18. Two-port network: (a) with driving voltage source, and (b) with driving current source

network. If, however, the output current $i_2(t)$ flowing through the load is the response function of interest, then

$$Y_{21}(p) = \frac{I_2(p)}{V_1(p)} \tag{2.30}$$

where $Y_{21}(p)$ is termed the *transfer admittance.*

In Fig. 2.18 (b) the current source $i_1(t)$ connected across the terminal pair 1,1′ is regarded as the excitation. If the output current $i_2(t)$ is the response function of interest, then

$$K_I(p) = \frac{I_2(p)}{I_1(p)} \tag{2.31}$$

where $K_I(p)$ is termed the *current gain.*

If, however, the output voltage $v_2(t)$ is the desired response function, then

$$Z_{21}(p) = \frac{V_2(p)}{I_1(p)} \tag{2.32}$$

where $Z_{21}(p)$ is the *transfer impedance.*

It is important to note that, unlike the driving-point functions $Z(p)$ and $Y(p)$, the transfer functions $Z_{21}(p)$ and $Y_{21}(p)$ are not the reciprocals of each other.

The above definitions relating to the various system functions have been summarised in Table 2.2.

Table 2.2 SYSTEM FUNCTIONS

	System Function G(p)	*Excitation Transform $\Phi_i(p)$*	*Response Transform $\Phi_0(p)$*
Driving-point Functions	$Y(p)$ $Z(p)$	$V_1(p)$ $I_1(p)$	$I_1(p)$ $V_1(p)$
Transfer Functions	$K_V(p)$ $Y_{21}(p)$ $K_I(p)$ $Z_{21}(p)$	$V_1(p)$ $V_1(p)$ $I_1(p)$ $I_1(p)$	$V_2(p)$ $I_2(p)$ $I_2(p)$ $V_2(p)$

2.2.5 INVERSE TRANSFORMATION BY THE METHOD OF PARTIAL FRACTIONS

Having determined the response transform of a given circuit to a specified excitation, the problem then becomes one of evaluating the required response as a function of time. A simple method of carrying out this evaluation is to use the Laplace transform pairs table given earlier. If the particular transform is found to be listed in this table, then the corresponding response function can be deduced directly. If, however, it is found that the transform has not been listed, then the next step is to express it, as the sum of partial fractions. The functions of time that correspond to the various partial fractions are noted from the table and their sum gives the required response function. This follows from the linearity property which is a characteristic of the Laplace transform.

2.2.6 STEP-FUNCTION RESPONSE OF NETWORK HAVING ONE POLE

Consider the simple *RC*-network of Fig. 2.19 where $v_1(t)$ is the excitation and $v_2(t)$ is the response function. These are related by the first order differential equation

$$\frac{1}{\omega_0}\frac{d}{dt}v_2(t) + v_2(t) = v_1(t) \tag{2.33}$$

where $\omega_0 = 1/RC$. Suppose that the initial conditions are zero. Then taking the Laplace transform of both sides of Equation 2.33

$$\left(\frac{p}{\omega_0} + 1\right)V_2(p) = V_1(p)$$

Therefore,

$$K_V(p) = \frac{V_2(p)}{V_1(p)} = \frac{\omega_0}{p + \omega_0} \tag{2.34}$$

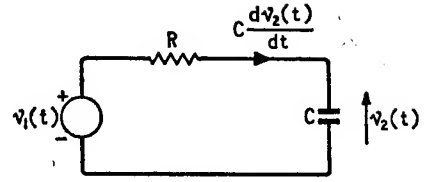

Fig. 2.19. Simple RC-network

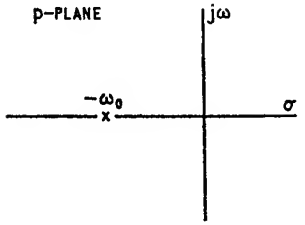

Fig. 2.20. Pole-zero pattern of Equation 2.34

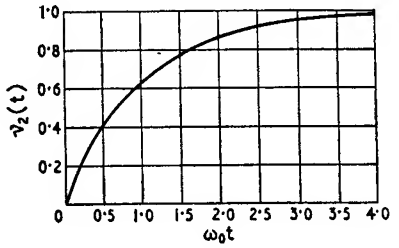

Fig. 2.21. Unit-step function response of a circuit having one pole

This corresponds to a real pole at $p = -\omega_0$ as shown in Fig. 2.20. If $v_1(t)$ is a unit-step function, $V_1(p) = 1/p$ and Equation 2.34 gives

$$V_2(p) = \frac{\omega_0}{p(p + \omega_0)} \tag{2.35}$$

Expanding into partial fractions, we have

$$V_2(p) = \frac{1}{p} - \frac{1}{p + \omega_0} \tag{2.36}$$

From pairs 2 and 5 of Table 2.1 we find that the response function $v_2(t)$ is

$$v_2(t) = 1 - e^{-\omega_0 t} \tag{2.37}$$

This is shown plotted aginst the *normalised time* $\omega_0 t$ in Fig. 2.21. At $t = 1/\omega_0$ we see that the output voltage reaches 63·3% of its final value which occurs at $t = \infty$.

2.2.7 STEP-FUNCTION RESPONSE OF NETWORK HAVING TWO POLES

Consider next the series LCR-network of Fig. 2.22. The response function $v_2(t)$ is related to the excitation $v_1(t)$ by the second order differential equation

$$\frac{1}{\omega_0^2}\frac{d^2}{dt^2}v_2(t) + \frac{2\zeta}{\omega_0}\frac{d}{dt}v_2(t) + v_2(t) = v_1(t) \qquad (2.38)$$

where $\omega_0^2 = 1/LC$ and $2\zeta = R\sqrt{(C/L.)}$. Assuming the initial conditions to be zero and taking the Laplace transform of both sides of Equation 2.38, we obtain

$$K_V(p) = \frac{V_2(p)}{V_1(p)} = \frac{\omega_0^2}{p^2 + 2\,\zeta\omega_0 p + \omega_0^2} \qquad (2.39)$$

By setting the denominator polynomial of the rational function on the right hand side equal to zero, and solving for the two roots

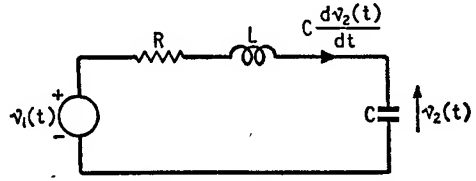

Fig. 2.22. Series LCR-network

of the resulting quadratic equation, we find that the transfer function of Equation 2.39 has the following two poles

$$p_1, p_2 = -\zeta\omega_0 \pm j\omega_0\sqrt{(1-\zeta^2)} \qquad (2.40)$$

The following three cases arise depending upon the value of the parameter ζ:

(1) $\zeta > 1$ In this case Equation 2.40 becomes

$$p_1, p_2 = -\zeta\omega_0 \pm \omega_0\sqrt{(\zeta^2 - 1)} \qquad (2.41)$$

The two poles of the transfer function are seen to be both real and negative. The corresponding transient response is said to be *overdamped.*

(2) $\zeta = 1$ Equation 2.40 reduces to

$$p_1, p_2 = -\omega_0 \qquad (2.42)$$

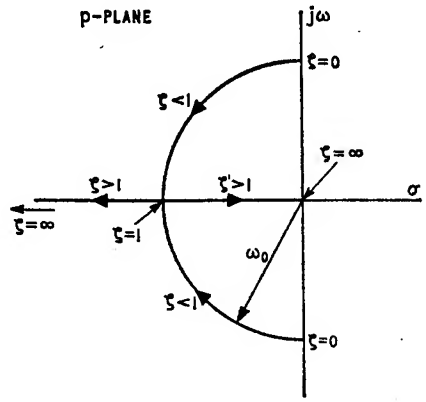

Fig. 2.23. Migration of the two poles of Equation 2.39 for varying ζ

Then the transfer function has a *double pole* at $p = -\omega_0$. The corresponding transient response is said to be *critically damped.*

(3) $\zeta < 1$ In this case we see from Equation 2.40 that the two poles of the transfer function become complex conjugate. The resulting transient response is oscillatory and is said to be *underdamped.*

Suppose that ω_0 is held constant and ζ is varied from zero to infinity. In the network of Fig. 2.22, this can be achieved by keeping L and C constant and varying R. Then the two poles of the transfer function will move in the p-plane along the paths indicated in Fig. 2.23. In the range $1 > \zeta > 0$ the two poles move along a circular path of radius ω_0. They meet at $p = -\omega_0$ when $\zeta = 1$. When $\zeta > 1$ the two poles separate along the negative σ-axis, with one pole moving towards the origin and the second one moving towards infinity.

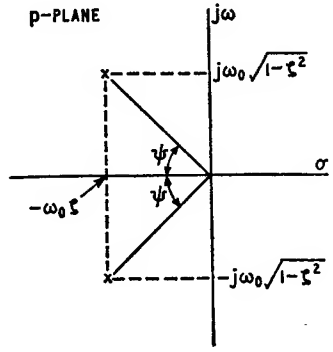

Fig. 2.24. Pair of complex conjugate poles with $\zeta < 1$

Consider the case when $1 > \zeta > 0$ and the two poles are complex conjugate as shown in Fig. 2.24. The angle ψ, between the σ-axis of the p-plane and the radial line to either of the two complex poles, is related to the parameter ζ as follows

$$\cos \psi = \zeta \tag{2.43}$$

If the circuit is initially at rest and the driving signal $v_1(t)$ is a unit-step function, then $V_1(p) = 1/p$ and Equation 2.39 gives the corresponding response transform to be

$$V_2(p) = \frac{\omega_0^2}{p(p^2 + 2\zeta\omega_0 p + \omega_0^2)} \tag{2.44}$$

Expanding into partial fractions, we obtain

$$V_2(p) = \frac{1}{p} - \frac{p + 2\zeta\omega_0}{p^2 + 2\zeta\omega_0 p + \omega_0^2} \tag{2.45}$$

This can be re-written as follows

$$V_2(p) = \frac{1}{p} - \frac{p + \zeta\omega_0}{(p + \zeta\omega_0)^2 + \omega_0^2(1 - \zeta^2)} - \frac{\zeta}{\sqrt{(1 - \zeta^2)}} \cdot \frac{\omega_0\sqrt{(1 - \zeta^2)}}{(p + \zeta\omega_0)^2 + \omega_0^2(1 - \zeta^2)} \tag{2.46}$$

Therefore, from pairs 2, 9 and 10 of Table 2.1 we deduce that the response function $v_2(t)$ is given by

$$v_2(t) = 1 - \frac{e^{-\zeta\omega_0 t}}{\sqrt{(1 - \zeta^2)}} [\sqrt{(1 - \zeta^2)} \cdot \cos \omega_n t + \zeta \sin \omega_n t] \tag{2.47}$$

where

$$\omega_n = \omega_0\sqrt{(1 - \zeta^2)} \tag{2.48}$$

ω_n is the natural (i.e. damped) angular frequency of oscillation.

Using the relationship between ψ and ζ (see Equation 2.43) we can re-write the expression for $v_2(t)$ as follows

$$v_2(t) = 1 - \frac{e^{-\zeta\omega_0 t}}{\sqrt{(1 - \zeta^2)}} \cdot (\sin \psi \cos \omega_n t + \cos \psi \sin \omega_n t)$$

$$v_2(t) = 1 - \frac{e^{-\zeta\omega_0 t}}{\sqrt{(1 - \zeta^2)}} \cdot \sin (\omega_n t + \psi) \tag{2.49}$$

Here we see that the response is oscillatory having a frequency equal to ω_n. The dimensionless parameter ζ controls the damping of the oscillations and is, therefore, referred to as the *damping ratio.*

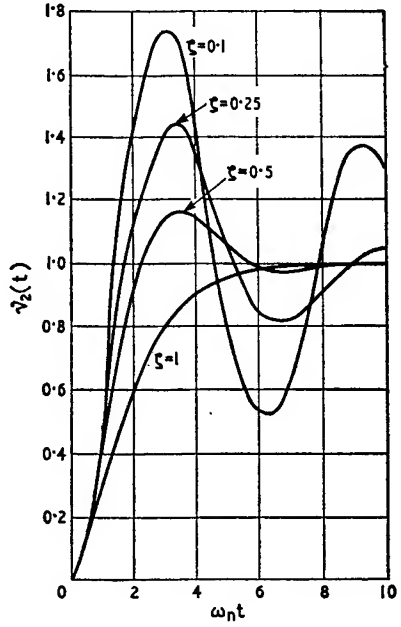

Fig. 2.25 Unit-step function response of a circuit having two poles

As ζ decreases in value the response becomes more oscillatory. When $\zeta = 0$ we see from Equations 2.48 and 2.49 that $\omega_n = \omega_0$ and $v_2(t) = 1 - \sin(\omega_0 t + \psi)$ which corresponds to sustained oscillations. Therefore, ω_0 is the *angular frequency of undamped oscillation.*

In Fig. 2.25 the response function $v_2(t)$ is shown plotted against the normalised time $\omega_n t$ for various values of damping ratio ζ.

For the case of an oscillatory response let V_{max} denote the first maximum value of $v_2(t)$, Then $V_{max} - 1$ is a quantitative measure of the extent to which V_{max} exceeds unity, that is, the ultimate value of $v_2(t)$. Thus

$$\gamma = V_{max} - 1 \tag{2.50}$$

where γ is termed the *fractional overshoot.* It is informative to relate the fractional overshoot to the damping ratio. For this

purpose we shall first differentiate Equation 2.49 with respect to time and so obtain

$$\frac{\mathrm{d}}{\mathrm{d}t}v_2(t) = \frac{\zeta\omega_0\,\mathrm{e}^{-\zeta\omega_0 t}}{\sqrt{(1-\zeta^2)}}\cdot\sin(\omega_n t+\psi) - \frac{\omega_n\,\mathrm{e}^{-\zeta\omega_0 t}}{\sqrt{(1-\zeta^2)}}\cdot\cos(\omega_n t+\psi) \tag{2.51}$$

Setting $\mathrm{d}v_2(t)/\mathrm{d}t$ equal to zero, using Equations 2.43 and 2.48 and then simplifying we find that the instances of time at which $v_2(t)$ reaches its maxima and minima are defined by

$$\tan(\omega_n t+\psi) = \frac{\omega_n}{\zeta\omega_0} = \tan\psi$$

from which it follows that

$$t = \frac{k\pi}{\omega_n}$$

$$= \frac{k\pi}{\omega_0\sqrt{(1-\zeta^2)}} \tag{2.52}$$

where $k = 0, 1, 2, \ldots$ and where use has been made of Equation 2.48. The first maximum value $V_{\max}$ of the response function $v_2(t)$ occurs when $k = 1$. Therefore, if $t_{\max}$ denotes the instance of time at which $v_2(t)$ equals $V_{\max}$, we deduce from Equation 2.52 that

$$t_{\max} = \frac{\pi}{\omega_0\sqrt{(1-\zeta^2)}} \tag{2.53}$$

Next, if in Equation 2.49 we put $t = t_{\max}$ and then use Equation 2.48 and 2.53, we find that

$$V_{\max} = 1 + \mathrm{e}^{-\pi\cot\psi} \tag{2.54}$$

which, together with Equations 2.43 and 2.50, leads to

$$\gamma = \mathrm{e}^{-\pi\zeta/\sqrt{(1-\zeta^2)}} \tag{2.55}$$

This relationship shows that the fractional overshoot γ is uniquely determined by the damping ratio ζ. Fig. 2.26 shows γ plotted against ζ; we see that the overshoot increases as the damping ratio is reduced.

It is of interest to note that the transfer functions of Equations 2.34 and 2.39 could have been obtained directly from Figs. 2.19 and 2.22 respectively, without having to write down the respective differential equations. Now from Equations 2.1 to 2.3 we find that, in the complex frequency domain, a resistor presents an impedance equal to R, an inductor presents an impedance equal to pL and a capacitor presents an impedance equal to $1/pC$, provided the initial conditions are zero. Hence, using these results and then applying the conventional mesh or nodal method of analysis, it is possible to directly determine the system function of any network.

2.3 Steady-state frequency response

If a sinusoidal excitation is suddenly applied to an electric network, the resulting response function will in general consist of two components: a *transient* and a *steady-state* component; the latter component is itself sinusoidal having the same frequency as the excitation.

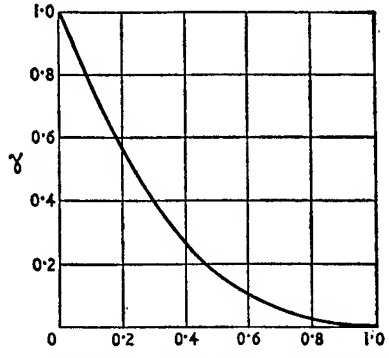

Fig. 2.26. Effect of damping ratio ζ on overshoot γ

In the case of a stable network the transient component dies away with time, and so after a sufficiently long time only the sinusoidal steady-state component remains of importance. A great deal of useful information about the behaviour of a network can be obtained by studying its sinusoidal steady-state response.

Consider a sinusoidal function of time defined by

$$\phi(t) = |\Phi(\mathrm{j}\omega)|\cdot\cos(\omega t+\theta) \tag{2.56}$$

where $|\Phi(\mathrm{j}\omega)|$ is the *amplitude*, ω is the *angular frequency* and θ is the *phase angle* of $\phi(t)$. Equation 2.56 can be also written as follows

$$\phi(t) = \mathscr{R}[|\Phi(\mathrm{j}\omega)|\cdot\mathrm{e}^{\mathrm{j}(\omega t+\theta)}]$$

$$= \mathscr{R}[\Phi(\mathrm{j}\omega)\cdot\mathrm{e}^{\mathrm{j}\omega t}] \tag{2.57}$$

where

$$\Phi(\mathrm{j}\omega) = |\Phi(\mathrm{j}\omega)|\cdot\mathrm{e}^{\mathrm{j}\theta} \tag{2.58}$$

and where $\mathscr{R}$ denotes the real part of the expression that follows it.

The complex quantity $\Phi(j\omega)$ is usually referred to as a *vector* or a *phasor*; it contains all the information needed to determine the amplitude and phase angle of the sinusoidal time function $\phi(t)$. To obtain $\phi(t)$ we multiply $\Phi(j\omega)$ by $e^{j\omega t}$ and take the real part of the product. Thus the sinusoidal function $\phi(t)$ is completely defined in terms of $\Phi(j\omega)$ and the multiplying factor $e^{j\omega t}$.

The vector $\Phi(j\omega)$ can be determined in the following manner. Let us consider the general case of a network described by the differential equation 2.21, and assume that

$$\left.\begin{aligned}\phi_i(t) &= \Phi_i(j\omega)\, e^{j\omega t}\\ \phi_0(t) &= \Phi_0(j\omega)\, e^{j\omega t}\end{aligned}\right\} \tag{2.59}$$

Then from Equations 2.21 and 2.59 we find that

$$[a_n(j\omega)^n + a_{n-1}(j\omega)^{n-1} + \ldots a_1(j\omega) + a_0]\Phi_0(j\omega) = [b_m(j\omega)^m + b_{m-1}(j\omega)^{m-1} + \ldots b_1(j\omega) + b_0]\Phi_i(j\omega) \tag{2.60}$$

Therefore, for sinusoidal excitation we can define a *steady-state system function* $G(j\omega)$ as follows

$$G(j\omega) = \frac{\Phi_0(j\omega)}{\Phi_i(j\omega)}$$

$$= \frac{b_m(j\omega)^m + b_{m-1}(j\omega)^{m-1} + \ldots + b_1(j\omega) + b_0}{a_n(j\omega)^n + a_{n-1}(j\omega)^{n-1} + \ldots + a_1(j\omega) + a_0} \tag{2.61}$$

$$= H\frac{(j\omega - z_1)(j\omega - z_2)\ldots(j\omega - z_m)}{(j\omega - p_1)(j\omega - p_2)\ldots(j\omega - p_n)} \tag{2.62}$$

On examining Equations 2.25, 2.26 and 2.61, 2.62 we see that $G(j\omega)$ can be derived directly from $G(p)$ by simply replacing p with $j\omega$. Conversely, $G(p)$ can be derived from $G(j\omega)$ by replacing $j\omega$ with p. This demonstrates the fundamental relationship between the transient and sinusoidal steady-state response of a linear network. For a one-port network we can define a *steady-state impedance* $Z(j\omega)$ to be

$$Z(j\omega) = \frac{V_1(j\omega)}{I_1(j\omega)} \tag{2.63}$$

which is the value of the driving-point impedance $Z(p)$ of Equation 2.28 at $p = j\omega$. In a similar fashion we can define steady-state values for all the other network functions.

Returning to Equation 2.62, suppose that the scale factor H is positive. Further let the m complex zero factors and the n complex pole factors of $G(j\omega)$ be expressed as follows, respectively,

$$j\omega - z_q = M_q\, e^{j\alpha_q} \quad \text{where} \quad q = 1, 2, \ldots, m$$

$$j\omega - p_r = N_r\, e^{j\beta_r} \quad \text{where} \quad r = 1, 2, \ldots, n$$

The transfer function $G(j\omega)$ can then be expressed as

$$G(j\omega) = |G(j\omega)|\, e^{jB(\omega)} \tag{2.64}$$

where

$$|G(j\omega)| = H\frac{M_1 M_2 \ldots M_m}{N_1 N_2 \ldots N_n} \tag{2.65}$$

$$B(\omega) = (\alpha_1 + \alpha_2 + \ldots + \alpha_m) - (\beta_1 + \beta_2 + \ldots + \beta_n) \tag{2.66}$$

From here on we shall refer to $|G(j\omega)|$ as the *magnitude function* and to $B(\omega)$ as the *phase angle function*. From Equation 2.65 we see that the magnitude function is equal to the scale factor multiplied by the product of all the zero factor magnitudes and divided by the product of all pole factor magnitudes, and from Equation 2.66 we see that at any frequency the phase angle function is equal to the sum of the angles of all the zero factors minus the sum of the angles of all the pole factors. Therefore, given the scale factor and the poles and zeros of the system function $G(p)$, it is possible to determine the magnitude and phase angle of $G(j\omega)$ from Equations 2.65 and 2.66, respectively.

It is also possible to determine the magnitude and phase angle functions from the pole-zero pattern of $G(p)$ by a graphical procedure which further illustrates the relationship between the transient and steady-state response of a network. Consider first the case of Fig. 2.27 showing a pair of complex conjugate poles. For values of p restricted to the $j\omega$-axis of the p-plane we see that, at the operating frequency ω_1, the magnitude of the pole factor $(j\omega_1 - p_1)$ is proportional to the length of a vector directed from p_1 to $j\omega_1$, and its phase angle is equal to the angle θ_1, shown defined in Fig. 2.27. In a similar manner we can evaluate the magnitude and phase angle of the factor $(j\omega_1 - p_2)$ and all other pole and zero factors that make up the given system function. Then at the point $p = j\omega_1$, the magnitude function is proportional to the product of all the vector lengths to all the zeros divided by the product of the vector lengths to all the poles. The phase angle function is equal to the sum of the angles between the σ-axis of the p-plane and the vectors to all the

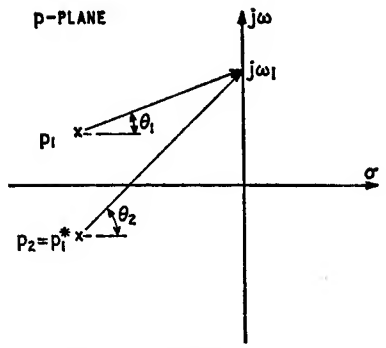

Fig. 2.27. Graphical calculation of steady state response

zeros minus the sum of all the angles between the σ-axis and the vectors to all the poles. If these evaluations are repeated for a number of points on the jω-axis, then it is possible to plot the magnitude and phase angle of $G(j\omega)$ as functions of frequency.

Suppose next we take the natural logarithm of both sides of Equation 2.64; then we have

$$\log_e G(j\omega) = A(\omega) + jB(\omega) \tag{2.67}$$

where

$$A(\omega) = \log_e |G(\omega)| \tag{2.68}$$

The function $A(\omega)$, which is the natural logarithm of the magnitude function $|G(j\omega)|$, is termed the *logarithmic gain* of the network; its unit is the *neper*. Alternatively we can express the gain in *decibels* abbreviated as dB; thus

$$A'(\omega) = 20 \log_{10} |G(j\omega)| \tag{2.69}$$

The two gain functions $A(\omega)$ and $A'(\omega)$ are related by

$$A'(\omega) = \frac{20}{\log_e 10} A(\omega) = 8{\cdot}69A(\omega) \tag{2.70}$$

In other words, one neper is equal to 8·69 decibels.

In Equation 2.67 the gain and phase angle functions are the real and imaginary parts, respectively, of the logarithm of the steady-state system function. Further, from Equations 2.65 and 2.68

$$A(\omega) = \log_e H + (\log_e M_1 + \log_e M_2 + \ldots\ldots \log_e M_m) - (\log_e N_1 + \log_e N_2 + \ldots\ldots \log_e N_n) \tag{2.71}$$

Here we see that multiplication and division of the various zero factor and pole factor magnitudes have been transformed into addition and subtraction, and each zero factor and pole factor appears separately. For these reasons the logarithm of $|G(j\omega)|$ is often preferred to $|G(j\omega)|$ itself as the function of interest.

Up to now we have assumed that the scale factor H is positive. If, however, H is negative then in Equations 2.65 and 2.71 it should be replaced by $|H|$, and a phase angle equal to π radians must be added to Equation 2.66.

2.3.1 STEADY-STATE RESPONSE OF NETWORK HAVING ONE REAL POLE

Consider the case of a system function $G(p)$ having one real pole at $p = -\omega_0$; thus

$$G(p) = \frac{\omega_0}{p + \omega_0} = \frac{1}{1 + p/\omega_0} \tag{2.72}$$

This, for example, represents the transfer function of the *RC*-circuit of Fig. 2.19 (see Equation 2.34). Replacing p with jω in Equation 2.72, we obtain

$$G(j\omega) = \frac{1}{1 + j\omega/\omega_0} \tag{2.73}$$

Therefore,

$$|G(j\omega)| = \frac{1}{\sqrt{[1 + (\omega/\omega_0)^2]}} \tag{2.74}$$

$$B(\omega) = -\tan^{-1}(\omega/\omega_0) \tag{2.75}$$

Expressing the gain function in decibels

$$A'(\omega) = -10 \log_{10}[1 + (\omega/\omega_0)^2] \tag{2.76}$$

Let us examine the behaviour of this equation at very low and very high frequencies. At low frequencies we have

$$\frac{\omega}{\omega_0} \ll 1 \text{ and } A'(\omega) \simeq -10 \log_{10} 1 = 0 \tag{2.77}$$

Therefore, the low frequency behaviour of Equation 2.76 can be approximated by the horizontal zero dB line as in Fig. 2.28a.

Next, at high frequencies we have

$$\frac{\omega}{\omega_0} \gg 1 \text{ and } A'(\omega) \simeq -10 \log_{10}\left(\frac{\omega}{\omega_0}\right)^2 = -20 \log_{10}\left(\frac{\omega}{\omega_0}\right) \tag{2.78}$$

Suppose that $x = \log_{10}(\omega/\omega_0)$ is considered as the variable instead of ω. Then we see that Equation 2.78 is a straight line of the form $A'(\omega) = -20x$ having a slope equal to -20, that is, $A'(\omega)$ decreases by 20 dB when x increases by one unit. Since $x = \log_{10}(\omega/\omega_0)$, it follows that the *normalised frequency variable* (ω/ω_0), must increase by a factor of 10 (i.e. one decade) if x is to increase by one unit. Therefore, the high frequency behaviour of Equation 2.76 can be approximated by a straight line having a slope equal to -20 dB per decade. The slope of the *high frequency asymptote* can be also stated in a different but equivalent form as follows. Every time ω is doubled the number of decibels is decreased by a constant amount equal to

$$20\log_{10}\left(\frac{2\omega}{\omega_0}\right) - 20\log_{10}\left(\frac{\omega}{\omega_0}\right) = 20\log_{10}2 = 6$$

Thus, when the characteristic of Equation 2.76 is plotted against $\log_{10}\omega$ we find that the high frequency asymptote is a straight line

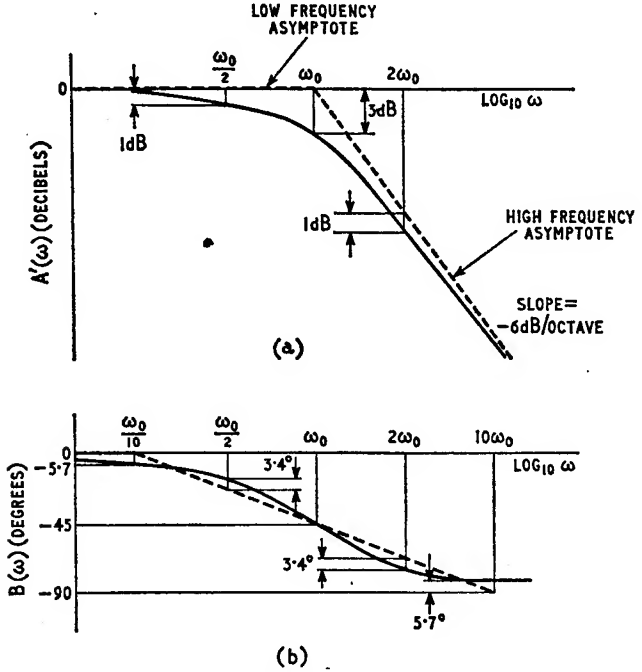

Fig. 2.28. Gain and phase angle characteristics of pole factor $1\Big/\left(1+\frac{j\omega}{\omega_0}\right)$. *(Note: actual characteristics are shown in solid lines and approximating characteristics are shown in dashed lines)*

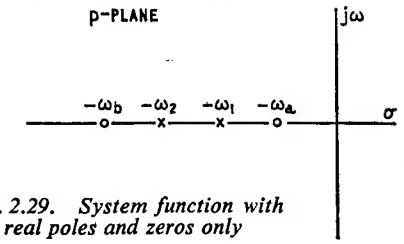

Fig. 2.29. System function with real poles and zeros only

with a slope of -6 dB per octave (doubling) of ω as shown in Fig. 2.28 (a).

From Equation 2.78 we see that the high frequency asymptote reaches zero dB at $(\omega/\omega_0) = 1$, that is, $\omega = \omega_0$. Therefore, the low and high frequency asymptotes defined by Equations 2.77 and 2.78 intersect at $\omega = \omega_0$. For this reason ω_0 is termed the *break* or *corner frequency*. Together, the two asymptotes provide a broken line approximation to the actual characteristic of Equation 2.76, which is also shown plotted in Fig. 2.28 (a). The broken line approximation is termed the *semi-infinite constant slope* characteristic. From Equation 2.76 we see that at $\omega = \omega_0$, $A'(\omega) = -10\log_{10}2 = -3$ dB. Hence, the maximum error occurs at $\omega = \omega_0$ and equals 3 dB. Further at both $\omega = \omega_0/2$ and $\omega = 2\omega_0$, that is, one octave away from the point $\omega = \omega_0$, the error is equal to 1 dB. The actual characteristic can be thus sketched with reasonable accuracy from the asymptotic approximations taking account of the errors involved.

Consider next the phase angle characteristic of Equation 2.75. For small values of ω the phase angle $B(\omega)$ is nearly zero, and for large values of ω it is nearly $-90°$. At the corner frequency ω_0 the phase angle is $-45°$. The phase angle is shown plotted against $\log_{10}\omega$ in Fig. 2.28 (b) where it is seen to be symmetrical about the point $\omega = \omega_0$.

The actual phase angle characteristic can be approximated reasonably well by the three straight line segments shown in Fig. 2.28 (b). The maximum error of 5·7° occurs at $\omega = \omega_0/10$ and $\omega = 10\omega_0$.

2.3.2 STEADY-STATE RESPONSE OF NETWORK HAVING REAL POLES AND ZEROS

The results that we have obtained for the logarithmic gain and phase angle characteristic of a single real pole factor can be extended to a multiplicity of real pole and real zero factors in the following manner. As an illustration consider a system function having poles at $-\omega_1$ and $-\omega_2$, and zeros at $-\omega_a$ and $-\omega_b$ all located on the negative σ-axis, as shown in Fig. 2.29. The corresponding system function $G(p)$ is

$$G(p) = H \cdot \frac{(p + \omega_a)(p + \omega_b)}{(p + \omega_1)(p + \omega_2)} \tag{2.79}$$

For sinusoidal excitation we replace p with $j\omega$ and so obtain

$$G(j\omega) = H \cdot \frac{(j\omega + \omega_a)(j\omega + \omega_b)}{(j\omega + \omega_1)(j\omega + \omega_2)} \tag{2.80}$$

This can be re-written in the following form

$$G(j\omega) = H' \frac{(1 + j\omega/\omega_a)(1 + j\omega/\omega_b)}{(1 + j\omega/\omega_1)(1 + j\omega/\omega_2)} \tag{2.81}$$

where

$$H' = \frac{H\omega_a\omega_b}{\omega_1\omega_2} \tag{2.82}$$

From Equation 2.81 we deduce that with the scale factor H' positive

$$\begin{aligned} A'(\omega) &= 20 \log_{10} |G(j\omega)| \\ &= 20 \log_{10} H' + 10 \log_{10}\left[1 + \left(\frac{\omega}{\omega_a}\right)^2\right] + 10 \log_{10}\left[1 + \left(\frac{\omega}{\omega_b}\right)^2\right] \\ &\quad - 10 \log_{10}\left[1 + \left(\frac{\omega}{\omega_1}\right)^2\right] - 10 \log_{10}\left[1 + \left(\frac{\omega}{\omega_2}\right)^2\right] \end{aligned} \tag{2.83}$$

Each term on the right hand side, except the constant term, has the same form as Equation 2.76. The two zero factors contribute positive terms with corner frequencies at ω_a and ω_b, and high frequency asymptotes of slopes 6 dB per octave. The two pole factors contribute negative terms with corner frequencies at ω_1 and ω_2 and high frequency asymptotes of slopes -6 dB per octave. Thus, assuming that $\omega_b > \omega_2 > \omega_1 > \omega_a$ we find that the individual contributions are as shown in Fig. 2.30 (a). The broken line approximation to the actual overall characteristic is obtained by summing the contributions of the constant term and the various pole and zero factors; the result of this summation is shown in Fig. 2.30 (b) where it is assumed that $H' > H$.

2.3.3 STEADY-STATE RESPONSE OF NETWORK HAVING A PAIR OF COMPLEX CONJUGATE POLES

Let us next consider the case of a system function having a pair of complex conjugate poles. Thus

$$G(p) = \frac{\omega_0^2}{p^2 + 2\zeta\omega_0 p + \omega_0^2} = \frac{1}{1 + 2\zeta(p/\omega_0) + (p/\omega_0)^2} \tag{2.84}$$

This, for example, corresponds to the transfer function of the *RLC*-circuit of Fig. 2.22 (see Equation 2.39). When $\zeta < 1$, the two poles of $G(p)$ become complex conjugate

Replacing p with $j\omega$, we have

$$G(j\omega) = \frac{1}{1 - (\omega/\omega_0)^2 + j2\zeta(\omega/\omega_0)} \tag{2.85}$$

Therefore

$$\begin{aligned} A'(\omega) &= 20 \log_{10} |G(j\omega)| \\ &= -10 \log_{10}[(1 - (\omega/\omega_0)^2)^2 + 4\zeta^2(\omega/\omega_0)^2] \end{aligned} \tag{2.86}$$

$$B(\omega) = -\tan^{-1}\left[\frac{2\zeta(\omega/\omega_0)}{1 - (\omega/\omega_0)^2}\right] \tag{2.87}$$

Consider first equation 2.86. At very low frequencies, we have

$$\frac{\omega}{\omega_0} \ll 1 \text{ and } A'(\omega) \simeq -10 \log_{10} 1 = 0 \tag{2.88}$$

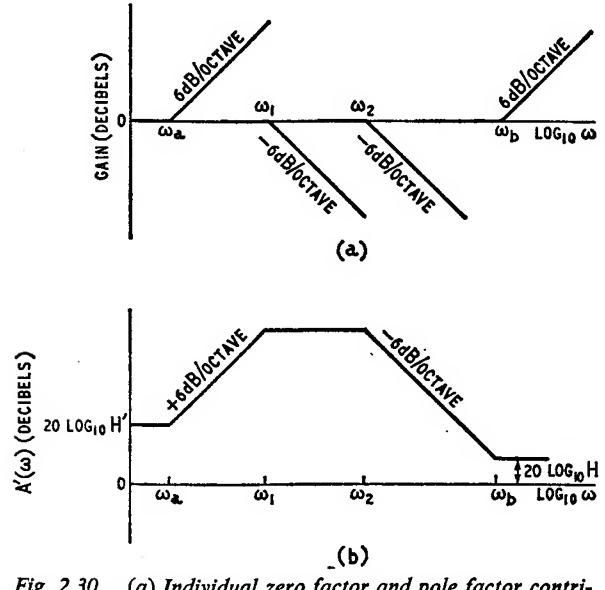

Fig. 2.30. (a) Individual zero factor and pole factor contributions, (b) Overall gain characteristic

Hence, the low frequency asymptote is the horizontal zero dB line.

At very high frequencies, we have

$$\frac{\omega}{\omega_0} \gg 1 \text{ and } A'(\omega) \simeq -10 \log_{10}\left(\frac{\omega}{\omega_0}\right)^4 = -40 \log_{10}\left(\frac{\omega}{\omega_0}\right) \tag{2.89}$$

Therefore, the high frequency asymptote is a straight line with a slope of — 40 dB per decade, that is, — 12 dB per octave. The low and high frequency asymptotes intersect at $\omega = \omega_0$, as is shown by the dashed lines in Fig. 2.31. In this diagram, the actual characteristics, as calculated from Equation 2.86, are also shown plotted for different values of the damping ratio ζ. The corresponding phase angle characteristics as calculated from Equation 2.87, are shown plotted in Fig. 2.32.

The characteristics of Figs. 2.31 and 2.32 can be also used for calculating the logarithmic gain and phase angle characteristics of a pair of complex conjugate zeros with the following modification: the results for the zeros are the negatives of those obtained for the poles.

2.4 Matrix algebra

Matrix algebra provides a convenient and compact form of expressing and analysing the response of linear networks. A matrix can

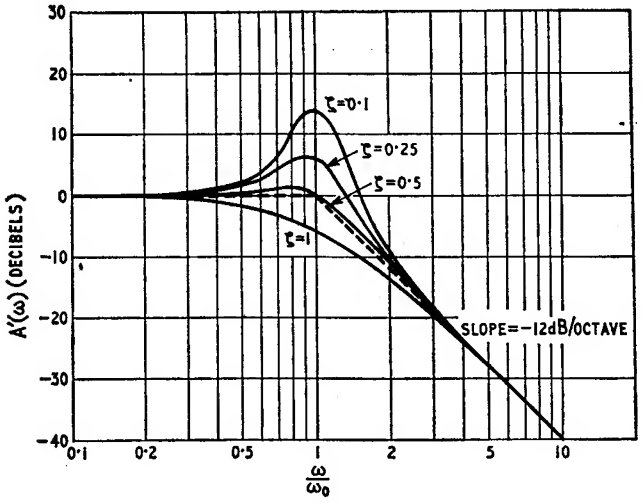

Fig. 2.31. Gain-frequency characteristic of second order pole factor

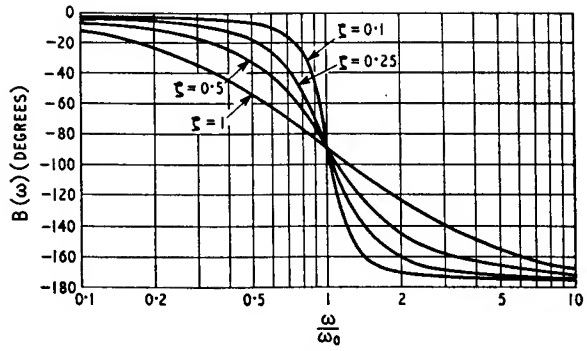

Fig. 2.32. Phase angle-frequency characteristic of second order pole factor

be regarded as a rectangular array of numbers. Matrices obey most of the laws of linear algebra provided that suitable definitions are introduced for the operations of addition, multiplication etc.; yet there are certain laws which are not obeyed by matrices, for example matrix multiplication is not commutative.

Consider the following set of three simultaneous linear equations:

$$\left.\begin{aligned} y_1 &= a_{11}x_1 + a_{12}x_2 + a_{13}x_3 \\ y_2 &= a_{21}x_1 + a_{22}x_2 + a_{23}x_3 \\ y_3 &= a_{31}x_1 + a_{32}x_2 + a_{33}x_3 \end{aligned}\right\} \tag{2.90}$$

where the a's are known coefficients, and the x's are the unknown quantities. We can re-write Equation 2.90 in matrix form as

$$\begin{bmatrix} y_1 \\ y_2 \\ y_3 \end{bmatrix} = \begin{bmatrix} a_{11} & a_{12} & a_{13} \\ a_{21} & a_{22} & a_{23} \\ a_{31} & a_{32} & a_{33} \end{bmatrix} \begin{bmatrix} x_1 \\ x_2 \\ x_3 \end{bmatrix} \tag{2.91}$$

which, in turn, can be abbreviated to

$$[y] = [a][x] \tag{2.92}$$

The matrices $[y]$, $[a]$ and $[x]$ are given by

$$[y] = \begin{bmatrix} y_1 \\ y_2 \\ y_3 \end{bmatrix} \tag{2.93}$$

$$[a] = \begin{bmatrix} a_{11} & a_{12} & a_{13} \\ a_{21} & a_{22} & a_{23} \\ a_{31} & a_{32} & a_{33} \end{bmatrix} \tag{2.94}$$

$$[x] = \begin{bmatrix} x_1 \\ x_2 \\ x_3 \end{bmatrix} \tag{2.95}$$

The matrix $[a]$ has three rows and three columns, and is therefore referred to as a 3×3 matrix or a *square matrix* of order 3. Each of the matrices $[x]$ and $[y]$ has three rows and only one column and is known as a *column matrix* of order 3. From Equation 2.94 we see that the matrix $[a]$ is an array of the coefficients a_{jk} arranged in rows and columns in exactly the same order as they appear in Equation 2.90. Thus a matrix is similar to a determinant in that it contains elements in rows and columns, but they differ in two fundamental respects: a matrix need not have equal numbers of rows and columns, and secondly, a matrix does not possess a numerical value.

2.4.1 ADDITION

The addition of two matrices is possible only when they have an equal number of rows and an equal number of columns. It is achieved by adding their corresponding elements. As an illustration suppose that $[b]$ and $[d]$ are 3×2 matrices given by

$$[b] = \begin{bmatrix} b_{11} & b_{12} \\ b_{21} & b_{22} \\ b_{31} & b_{32} \end{bmatrix} \tag{2.96}$$

$$[d] = \begin{bmatrix} d_{11} & d_{12} \\ d_{21} & d_{22} \\ d_{31} & d_{32} \end{bmatrix} \tag{2.97}$$

Then

$$[b] + [d] = \begin{bmatrix} b_{11} + d_{11} & b_{12} + d_{12} \\ b_{21} + d_{21} & b_{22} + d_{22} \\ b_{31} + d_{31} & b_{32} + d_{32} \end{bmatrix} \tag{2.98}$$

2.4.2 MULTIPLICATION

Let $[a]$ be a matrix of order $m \times n$ and $[b]$ be a matrix of order $n \times p$. The product of $[a]$ $[b]$ is defined to be a matrix $[c]$ of order $m \times p$; the element c_{ij} of this product term is given by

$$c_{ij} = \sum_{k=1}^{n} a_{ik} b_{kj} \tag{2.99}$$

which states that the element c_{ij} of the matrix $[c] = [a]\,[b]$ is obtained by multiplying the corresponding elements of the ith row of matrix $[a]$ and the jth column of the matrix $[b]$, and adding the products obtained. The product $[a]$ $[b]$ exists only when the number of columns in the matrix $[a]$ is equal to the number of rows in the matrix $[b]$.

As an example let us evaluate $[a]$ $[b]$ given that $[a]$ is the 3×3 matrix of Equation 2.94 and $[b]$ is the 3×2 matrix of Equation 2.96. Then the product $[a]\,[b]$ is a 3×2 matrix given by

$$\begin{bmatrix} a_{11} & a_{12} & a_{13} \\ a_{21} & a_{22} & a_{23} \\ a_{31} & a_{32} & a_{33} \end{bmatrix} \begin{bmatrix} b_{11} & b_{12} \\ b_{21} & b_{22} \\ b_{31} & b_{32} \end{bmatrix}$$

$$= \begin{bmatrix} (a_{11}b_{11} + a_{12}b_{21} + a_{13}b_{31}) & (a_{11}b_{12} + a_{12}b_{22} + a_{13}b_{32}) \\ (a_{21}b_{11} + a_{22}b_{21} + a_{23}b_{31}) & (a_{21}b_{12} + a_{22}b_{22} + a_{23}b_{32}) \\ (a_{31}b_{11} + a_{32}b_{21} + a_{33}b_{31}) & (a_{31}b_{12} + a_{32}b_{22} + a_{33}b_{32}) \end{bmatrix}$$

In this example we see that it is not possible to define the product $[b]$ $[a]$.

Matrix multiplication is not *commutative*, that is, the matrix product $[a]$ $[b]$ is not, in general, equal to $[b]$ $[a]$; even though both products may be defined. But matrix multiplication is *distributive* so that

$$[b]([c] + [d]) = [b]\,[c] + [b]\,[d] \tag{2.101}$$

and it is also *associative*, that is

$$[b]([c]\,[d]) = ([b]\,[c])\,[d] \tag{2.102}$$

Multiplication of a matrix by a constant k is obtained by multiplying each of its elements with k. Thus multiplying the matrix $[a]$ of Equation 2.94 with k, we obtain

$$k[a] = \begin{bmatrix} ka_{11} & ka_{12} & ka_{13} \\ ka_{21} & ka_{22} & ka_{23} \\ ka_{31} & ka_{32} & ka_{33} \end{bmatrix} \tag{2.103}$$

2.4.3 INVERSION

Suppose that in Equation 2.90 the y's and the a's are known quantities. Then solving these equations for x_1, x_2 and x_3 by *Cramer's rule* we obtain

$$\left.\begin{aligned} x_1 &= \frac{\Delta_{11}}{\Delta} y_1 + \frac{\Delta_{21}}{\Delta} y_2 + \frac{\Delta_{31}}{\Delta} y_3 \\ x_2 &= \frac{\Delta_{12}}{\Delta} y_1 + \frac{\Delta_{22}}{\Delta} y_2 + \frac{\Delta_{32}}{\Delta} y_3 \\ x_3 &= \frac{\Delta_{13}}{\Delta} y_1 + \frac{\Delta_{23}}{\Delta} y_2 + \frac{\Delta_{33}}{\Delta} y_3 \end{aligned}\right\} \tag{2.104}$$

where Δ is the determinant

$$\Delta = \begin{vmatrix} a_{11} & a_{12} & a_{13} \\ a_{21} & a_{22} & a_{23} \\ a_{31} & a_{32} & a_{33} \end{vmatrix} \tag{2.105}$$

and where Δ_{jk} is the *cofactor* of the element a_{jk} and is obtained from Δ by deleting both row j and column k and multiplying the result by $(-1)^{j+k}$. In matrix form Equation 2.104 becomes

$$[x] = [a'][y] \tag{2.106}$$

where the matrices $[x]$ and $[y]$ are as defined in Equations 2.95 and 2.93, respectively, and the matrix $[a']$ is given by

$$[a'] = \frac{1}{\Delta} \begin{bmatrix} \Delta_{11} & \Delta_{21} & \Delta_{31} \\ \Delta_{12} & \Delta_{22} & \Delta_{32} \\ \Delta_{13} & \Delta_{23} & \Delta_{33} \end{bmatrix} \tag{2.107}$$

If the matrix $[a']$ exists, it is referred to as the *inverse* of the matrix $[a]$ of Equation 2.94 and is written as follows

$$[a'] = [a]^{-1} \tag{2.108}$$

The inverse of a matrix exists only if the matrix is a square one and its determinant Δ is non-zero.

The product of a square matrix and its inverse is another square matrix whose diagonal terms are all unity and the remaining ones are zero. Such a matrix is called the *unit matrix*. Thus in the case of Equation 2.94 we have

$$[a]\,[a]^{-1} = \begin{bmatrix} 1 & 0 & 0 \\ 0 & 1 & 0 \\ 0 & 0 & 1 \end{bmatrix} \tag{2.109}$$

Also for a square matrix $[a]\,[a]^{-1} = [a]^{-1}\,[a]$.

2.5 Two-port networks

Two-port networks† form a very important class of electric net-

Fig. 2.33. Two-port network

works. We saw examples of such networks in Figs. 2.5 to 2.8 which illustrated the various controlled source types. Fig. 2.33 shows a generalised representation for a two-port network together with the terminal currents and voltages. We shall refer to terminals 1, 1′ as the *input port* and to terminals 2, 2′ as the *output port*.

The external behaviour of the two-port network of Fig. 2.33 is completely determined if the input current I_1, input voltage V_1, output current I_2 and output voltage V_2 are known. The interrelationships between I_1, V_1, I_2, and V_2 can be expressed in six different ways depending upon which two of these four quantities are regarded as independent variables and which two are regarded as dependent variables. These six possibilities lead to six sets of parameters, namely the *z-*, *y-*, *h-*, *g-*, *chain matrix* and *inverse chain matrix* parameters. These we shall consider in turn.

z-parameters

Suppose that I_1 and I_2 are chosen as the independent variables (i.e. excitations), and V_1 and V_2 are the dependent variables (i.e. response functions). Then we obtain the following set of relationships

† Two-port networks are also referred to as *two-terminal pair* networks, *four-terminal* networks, *four-pole* networks and *quadripole* networks.

$$\left.\begin{aligned} V_1 &= z_{11}I_1 + z_{12}I_2 \\ V_2 &= z_{21}I_1 + z_{22}I_2 \end{aligned}\right\} \qquad (2.110)$$

where z_{11}, z_{12}, z_{21} and z_{22} are known as the *z-parameters* of the two-port network. It is to be noted that the various currents and voltages and the z-parameters are all functions of p or $j\omega$ depending

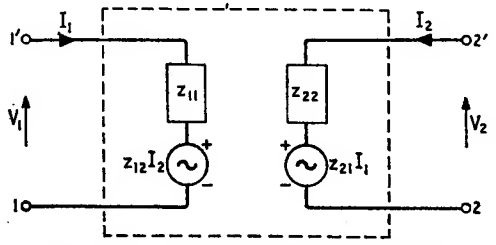

Fig. 2.34. z-parameters equivalent circuit

on whether we are considering network behaviour in the p-plane or along the $j\omega$-axis. The functional dependences have been omitted only for simplicity. This remark applies to all the other parameters to be considered later.

Returning to Equations 2.110, we can deduce the following definitions for the z-parameters

$$\left.\begin{aligned} z_{11} &= \left(\frac{V_1}{I_1}\right)_{I_2=0} \\ z_{12} &= \left(\frac{V_1}{I_2}\right)_{I_1=0} \\ z_{21} &= \left(\frac{V_2}{I_1}\right)_{I_2=0} \\ z_{22} &= \left(\frac{V_2}{I_2}\right)_{I_1=0} \end{aligned}\right\} \qquad (2.111)$$

The condition $I_1 = 0$ corresponds to open-circuiting the input port, and $I_2 = 0$ corresponds to open-circuiting the output port.

From Equations 2.111 we see that all the z-parameters have the dimensions of an impedance. Further z_{11} is the *input driving-point impedance* or simply *input impedance* and z_{21} is the *forward transfer impedance* (i.e. from input to output) of the network with its output port open-circuited. On the other hand, z_{22} is the *output driving-point impedance* or simply *output impedance* and z_{12} is the *reverse transfer impedance* (i.e. from output to input) of the network with its input port open-circuited.

Equations 2.110 lead to the *z-parameters equivalent circuit* of Fig. 2.34 for the two-port network. It involves two current-controlled voltage sources.

In matrix form Equations 2.110 can be expressed as

$$\begin{bmatrix} V_1 \\ V_2 \end{bmatrix} = \begin{bmatrix} z_{11} & z_{12} \\ z_{21} & z_{22} \end{bmatrix} \begin{bmatrix} I_1 \\ I_2 \end{bmatrix} \qquad (2.112)$$

where $\begin{bmatrix} V_1 \\ V_2 \end{bmatrix}$ and $\begin{bmatrix} I_1 \\ I_2 \end{bmatrix}$ are column matrices, and the square matrix $\begin{bmatrix} z_{11} & z_{12} \\ z_{21} & z_{22} \end{bmatrix}$ is known as the *z-matrix* of the two-port network.

y-parameters

Let us next choose the voltages V_1, V_2 to be independent variables and the currents I_1, I_2 to be the dependent variables. Then we obtain

$$\left.\begin{aligned} I_1 &= y_{11}V_1 + y_{12}V_2 \\ I_2 &= y_{21}V_1 + y_{22}V_2 \end{aligned}\right\} \qquad (2.113)$$

where y_{11}, y_{12}, y_{21} and y_{22} are known as the *y-parameters* of the two-port network. From Equations 2.113 we deduce the following definitions for the y-parameters.

$$\left.\begin{aligned} y_{11} &= \left(\frac{I_1}{V_1}\right)_{V_2=0} \\ y_{12} &= \left(\frac{I_1}{V_2}\right)_{V_1=0} \\ y_{21} &= \left(\frac{I_2}{V_1}\right)_{V_2=0} \\ y_{22} &= \left(\frac{I_2}{V_2}\right)_{V_1=0} \end{aligned}\right\} \qquad (2.114)$$

The condition $V_1 = 0$ is equivalent to short-circuiting the input port, and $V_2 = 0$ is equivalent to short-circuiting the output port.

From Equations 2.114 we see that all the y-parameters have the dimensions of an admittance. Further, the parameter y_{11} is the *input driving-point admittance* or simply *input admittance* and y_{21} is the *forward transfer admittance* of the two-port network when its output is short-circuited. y_{22} is the *output driving-point admittance*

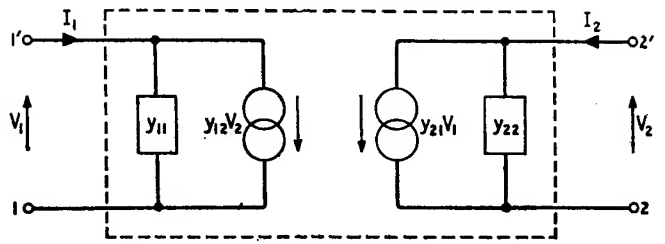

Fig. 2.35. y-parameters equivalent circuit

or simply *output admittance* and y_{12} is the *reverse transfer admittance* of the two-port network with its input port short-circuited.

Equations 2.113 lead to the *y-parameters equivalent circuit* of Fig. 2.35 involving two voltage-controlled current sources.

In matrix form we can re-write Equation 2.113 as follows

$$\begin{bmatrix} I_1 \\ I_2 \end{bmatrix} = \begin{bmatrix} y_{11} & y_{12} \\ y_{21} & y_{22} \end{bmatrix} \begin{bmatrix} V_1 \\ V_2 \end{bmatrix} \tag{2.115}$$

where the square matrix $\begin{bmatrix} y_{11} & y_{12} \\ y_{21} & y_{22} \end{bmatrix}$ is known as the *y-matrix* of the two-port network.

h-parameters

If I_1 and V_2 are the independent variables, and V_1 and I_2 are the dependent variables, we have

$$\left.\begin{aligned} V_1 &= h_{11}I_1 + h_{12}V_2 \\ I_2 &= h_{21}I_1 + h_{22}V_2 \end{aligned}\right\} \tag{2.116}$$

where h_{11}, h_{12}, h_{21} and h_{22} constitute of *h-parameters* of the two-port network. From Equations 2.116 we deduce the following definitions

$$\left.\begin{aligned} h_{11} &= \left(\frac{V_1}{I_1}\right)_{V_2=0} \\ h_{12} &= \left(\frac{V_1}{V_2}\right)_{I_1=0} \\ h_{21} &= \left(\frac{I_2}{I_1}\right)_{V_2=0} \\ h_{22} &= \left(\frac{I_2}{V_2}\right)_{I_1=0} \end{aligned}\right\} \tag{2.117}$$

Therefore, h_{11} is the input impedance and h_{21} is the *forward current gain* of the two-port network when its output is short-circuited. h_{22} is the output admittance and h_{12} is the *reverse voltage gain* of the two-port network with its input port open-circuited. h_{11} has the dimensions of an impedance, h_{22} has the dimensions of an admittance, and h_{12} and h_{21} are both dimensionless.

From Equation 2.116 we deduce the *h-parameters equivalent circuit* of Fig. 2.36 involving a current-controlled current source and

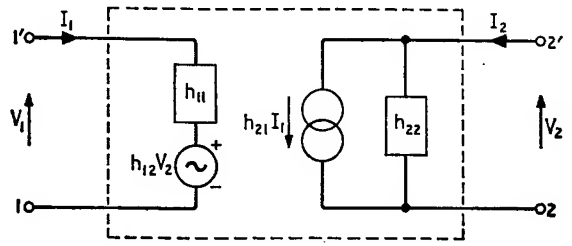

Fig. 2.36. h-parameters equivalent circuit

a voltage-controlled voltage source. This circuit further illustrates the hybrid nature of the *h*-parameters.

Re-writing Equations 2.116 in matrix form, we obtain

$$\begin{bmatrix} V_1 \\ I_2 \end{bmatrix} = \begin{bmatrix} h_{11} & h_{12} \\ h_{21} & h_{22} \end{bmatrix} \begin{bmatrix} I_1 \\ V_2 \end{bmatrix} \tag{2.118}$$

where the square matrix $\begin{bmatrix} h_{11} & h_{12} \\ h_{21} & h_{22} \end{bmatrix}$ is called the *h-matrix* of the two-port network.

g-parameters

Next, choosing V_1 and I_2 to be the independent variables and I_1 and V_2 to be the dependent variables, we find that they are related by

$$\left.\begin{aligned} I_1 &= g_{11}V_1 + g_{12}I_2 \\ V_2 &= g_{21}V_1 + g_{22}I_2 \end{aligned}\right\} \tag{2.119}$$

where g_{11}, g_{12}, g_{21} and g_{22} are the *g-parameters* and are defined by

$$g_{11} = \left(\frac{I_1}{V_1}\right)_{I_2=0}$$

$$g_{12} = \left(\frac{I_1}{I_2}\right)_{V_1=0}$$
$$g_{21} = \left(\frac{V_2}{V_1}\right)_{I_1=0} \qquad (2.120)$$
$$g_{22} = \left(\frac{V_2}{I_2}\right)_{V_1=0}$$

Hence, g_{11} is the input admittance and g_{21} is the *forward voltage gain* of the two-port network when its output port is open-circuited. g_{22} is the output impedance and g_{12} is the *reverse current gain* when

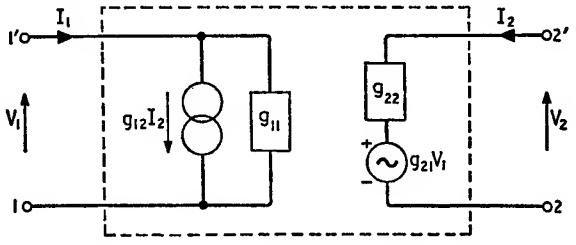

Fig. 2.37. g-parameters equivalent circuit

the input port is short-circuited. g_{11} has the dimensions of an admittance, g_{22} has the dimensions of an impedance and g_{12} and g_{21} are both dimensionless. From Equation 2.119 we deduce the *g-parameters equivalent circuit* of Fig. 2.37 involving a current-controlled current source and a voltage-controlled voltage source and so further stressing the hybrid nature of the *g*-parameters too.

In matrix form we can re-write Equation 2.119 as follows

$$\begin{bmatrix} I_1 \\ V_2 \end{bmatrix} = \begin{bmatrix} g_{11} & g_{12} \\ g_{21} & g_{22} \end{bmatrix} \begin{bmatrix} V_1 \\ I_2 \end{bmatrix} \qquad (2.121)$$

where the square matrix $\begin{bmatrix} g_{11} & g_{12} \\ g_{21} & g_{22} \end{bmatrix}$ is known as the *g-matrix* of the two-port network.

Chain matrix parameters

Let us next choose V_2 and I_2 to be the independent variables, and V_1 and I_1 to be the dependent variables. Then we have

$$\left.\begin{aligned} V_1 &= a_{11}V_2 - a_{12}I_2 \\ I_1 &= a_{21}V_2 - a_{22}I_2 \end{aligned}\right\} \qquad (2.122)$$

where a_{11}, a_{12}, a_{21} and a_{22} are called the *chain matrix parameters* because, as we shall see later, they are particularly useful for analysing a chain of two-port networks connected in cascade. They are defined as follows

$$\left.\begin{aligned} a_{11} &= \left(\frac{V_1}{V_2}\right)_{I_2=0} \\ a_{12} &= \left(\frac{V_1}{-I_2}\right)_{V_2=0} \\ a_{21} &= \left(\frac{I_1}{V_2}\right)_{I_2=0} \\ a_{22} &= \left(\frac{I_1}{-I_2}\right)_{V_2=0} \end{aligned}\right\} \qquad (2.123)$$

Therefore, a_{11} is the reciprocal of the open-circuit voltage gain for signal transmission in the forward direction whereas the parameter a_{22} is the reciprocal of the short-circuit current gain for the same direction of signal transmission. Further, the parameters a_{12} and a_{21} are reciprocals of the short-circuit transfer admittance and the open-circuit transfer impedance respectively, again for the forward direction of signal transmission.

Equations 2.122 can be re-written in matrix form as follows

$$\begin{bmatrix} V_1 \\ I_1 \end{bmatrix} = \begin{bmatrix} a_{11} & a_{12} \\ a_{21} & a_{22} \end{bmatrix} \begin{bmatrix} V_2 \\ -I_2 \end{bmatrix} \qquad (2.124)$$

where the matrix $\begin{bmatrix} a_{11} & a_{12} \\ a_{21} & a_{22} \end{bmatrix}$ is known as the *a-matrix* or the *chain matrix* of the two-port network.

Historically the chain matrix parameters† were the first set to be used in the study of transmission lines. In such networks if the input current I_1 flows into the line, then the output current naturally flows out. The latter is opposite to the convention adopted in Fig. 2.33. This accounts for the introduction of the minus sign in Equations 2.122 and 2.124.

Inverse-chain matrix parameters

For this set of parameters V_1 and I_1 are regarded to be the independent variables, and V_2 and I_2 to be the dependent variables; thus

† The notations A, B, C, D are also widely used for denoting the elements of the chain matrix. Thus $A \equiv a_{11}$, $B \equiv a_{12}$, $C \equiv a_{21}$, and $D \equiv a_{22}$.

$$\left.\begin{aligned} V_2 &= b_{11}V_1 - b_{12}I_1 \\ I_2 &= b_{21}V_1 - b_{22}I_1 \end{aligned}\right\} \qquad (2.125)$$

where b_{11}, b_{12}, b_{21} and b_{22} are termed the *inverse chain matrix parameters*. They are useful in analysing a cascade of two-port networks viewed from the output end, that is, in the reverse direction to the case of the chain matrix parameters. They can be evaluated from the following definitions

$$\left.\begin{aligned} b_{11} &= \left(\frac{V_2}{V_1}\right)_{I_1=0} \\ b_{12} &= \left(\frac{V_2}{-I_1}\right)_{V_1=0} \\ b_{21} &= \left(\frac{I_2}{V_1}\right)_{I_1=0} \\ b_{22} &= \left(\frac{I_2}{-I_1}\right)_{V_1=0} \end{aligned}\right\} \qquad (2.126)$$

These relationships show that b_{11} and b_{22} are the reciprocals of the open-circuit voltage gain and the short-circuit current gain of the two-port network, both measured in the reverse direction of signal

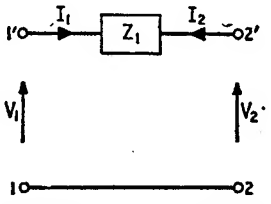

Fig. 2.38. Series impedance

transmission. Also b_{12} and b_{21} are the reciprocals of the short-circuit transfer admittance and the open-circuit transfer impedance, for the same direction of transmission.

In matrix form we can express Equations 2.125 as

$$\begin{bmatrix} V_2 \\ I_2 \end{bmatrix} = \begin{bmatrix} b_{11} & b_{12} \\ b_{21} & b_{22} \end{bmatrix} \begin{bmatrix} V_1 \\ -I_1 \end{bmatrix} \qquad (2.127)$$

where $\begin{bmatrix} b_{11} & b_{12} \\ b_{21} & b_{22} \end{bmatrix}$ is the *b-matrix* or the *inverse chain matrix* of the two-port network.

It is to be noted that, owing to the nature of the chain matrix parameters, it is not possible to formulate an equivalent circuit representation for the two-port network based on Equations 2.122 or 2.125.

2.5.1 EXAMPLES

Consider first the network of Fig. 2.38. From Equations 2.111 we see that this network does not possess a finite z-matrix while Equations 2.114 give its y-matrix to be

Fig. 2.39. Shunt impedance

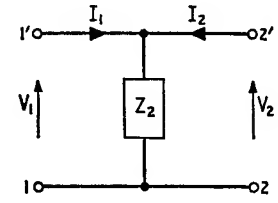

$$\begin{bmatrix} y_{11} & y_{12} \\ y_{21} & y_{22} \end{bmatrix} = \begin{bmatrix} Y_1 & -Y_1 \\ -Y_1 & Y_1 \end{bmatrix} \qquad (2.128)$$

where $Y_1 = 1/Z_1$. Equations 2.117 give the following h-matrix

$$\begin{bmatrix} h_{11} & h_{12} \\ h_{21} & h_{22} \end{bmatrix} = \begin{bmatrix} Z_1 & 1 \\ -1 & 0 \end{bmatrix} \qquad (2.129)$$

From Equations 2.120 we find that the g-matrix is

$$\begin{bmatrix} g_{11} & g_{12} \\ g_{21} & g_{22} \end{bmatrix} = \begin{bmatrix} 0 & -1 \\ 1 & Z_1 \end{bmatrix} \qquad (2.130)$$

Equations 2.123 give the chain matrix to be

$$\begin{bmatrix} a_{11} & a_{12} \\ a_{21} & a_{22} \end{bmatrix} = \begin{bmatrix} 1 & Z_1 \\ 0 & 1 \end{bmatrix} \qquad (2.131)$$

Consider next the network of Fig. 2.39. Equations 2.111 give its z-matrix to be

$$\begin{bmatrix} z_{11} & z_{12} \\ z_{21} & z_{22} \end{bmatrix} = \begin{bmatrix} Z_2 & Z_2 \\ Z_2 & Z_2 \end{bmatrix} \qquad (2.132)$$

From Equations 2.114 we see that the network of Fig. 2.39 does not possess a finite y-matrix, and from Equations 2.117 we deduce the following h-matrix

$$\begin{bmatrix} h_{11} & h_{12} \\ h_{21} & h_{22} \end{bmatrix} = \begin{bmatrix} 0 & 1 \\ -1 & Y_2 \end{bmatrix} \tag{2.133}$$

where $Y_2 = 1/Z_2$. Equations 2.120 give the g-matrix to be

$$\begin{bmatrix} g_{11} & g_{12} \\ g_{21} & g_{22} \end{bmatrix} = \begin{bmatrix} Y_2 & -1 \\ 1 & 0 \end{bmatrix} \tag{2.134}$$

The corresponding chain matrix is deduced from Equations 2.123 to be

$$\begin{bmatrix} a_{11} & a_{12} \\ a_{21} & a_{22} \end{bmatrix} = \begin{bmatrix} 1 & 0 \\ Y_2 & 1 \end{bmatrix} \tag{2.135}$$

As a third example consider the ideal transformer of Fig. 2.40. From Equations 2.111, 2.114, 2.117 and 2.120 we see that none of

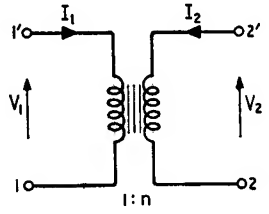

Fig. 2.40. Ideal transformer

the z-, y-, h-, and g-matrices is finite, while from Equations 2.123 we find that the chain matrix is

$$\begin{bmatrix} a_{11} & a_{12} \\ a_{21} & a_{22} \end{bmatrix} = \begin{bmatrix} n^{-1} & 0 \\ 0 & n \end{bmatrix} \tag{2.136}$$

where n is the transformer turns ratio defined in Fig. 2.40.

2.5.2 INTER-RELATIONSHIPS BETWEEN MATRIX PARAMETERS

Very often it is required to convert one set of matrix parameters to another, and for this purpose it is found desirable to develop the inter-relationships between the various matrix parameters of the two-port network. We first see from Equations 2.112 and 2.115 that the z- and y-matrices are the inverse of each other, that is

$$\begin{bmatrix} z_{11} & z_{12} \\ z_{21} & z_{22} \end{bmatrix} = \begin{bmatrix} y_{11} & y_{12} \\ y_{21} & y_{22} \end{bmatrix}^{-1} \tag{2.137}$$

and

$$\begin{bmatrix} y_{11} & y_{12} \\ y_{21} & y_{22} \end{bmatrix} = \begin{bmatrix} z_{11} & z_{12} \\ z_{21} & z_{22} \end{bmatrix}^{-1} \tag{2.138}$$

On evaluating the inverse matrix we find that Equation 2.137 has the following form

$$\begin{bmatrix} z_{11} & z_{12} \\ z_{21} & z_{22} \end{bmatrix} = \frac{1}{\Delta y} \begin{bmatrix} y_{22} & -y_{12} \\ -y_{21} & y_{11} \end{bmatrix} \tag{2.139}$$

where Δy is the determinant of the y-matrix and is given by

$$\Delta y = \begin{vmatrix} y_{11} & y_{12} \\ y_{21} & y_{22} \end{vmatrix} = y_{11}\, y_{22} - y_{12}\, y_{21} \tag{2.140}$$

In a similar way we can evaluate the inverse matrix of Equation 2.138, and so evaluate the y-parameters in terms of the z-parameters.

Next, from Equations 2.118 and 2.121 we find that the h- and g-matrices are the inverse of each other, that is

$$\begin{bmatrix} h_{11} & h_{12} \\ h_{21} & h_{22} \end{bmatrix} = \begin{bmatrix} g_{11} & g_{12} \\ g_{21} & g_{22} \end{bmatrix}^{-1} \tag{2.141}$$

and

$$\begin{bmatrix} g_{11} & g_{12} \\ g_{21} & g_{22} \end{bmatrix} = \begin{bmatrix} h_{11} & h_{12} \\ h_{21} & h_{22} \end{bmatrix}^{-1} \tag{2.142}$$

Then, the h- and g-parameters can be related to each other in the same way as we related the z- and y-parameters.

Similarly, from Equations 2.124 and 2.127 it follows that the a- and b-matrices are related by

$$\begin{bmatrix} a_{11} & a_{12} \\ a_{21} & a_{22} \end{bmatrix} = \begin{bmatrix} b_{11} & -b_{12} \\ -b_{21} & b_{22} \end{bmatrix}^{-1} \tag{2.143}$$

and

$$\begin{bmatrix} b_{11} & b_{12} \\ b_{21} & b_{22} \end{bmatrix} = \begin{bmatrix} a_{11} & -a_{12} \\ -a_{21} & a_{22} \end{bmatrix}^{-1} \tag{2.144}$$

Additional relationships between the various matrix parameters can be obtained by using the various sets of voltage-current relationships of the two-port network. Suppose we wish to evaluate the chain matrix parameters in terms of the h-parameters. Solving the second line of Equations 2.116 for I_1 gives

$$I_1 = -\frac{h_{22}V_2}{h_{21}} + \frac{I_2}{h_{21}} \tag{2.145}$$

Eliminating I_1 between this relationship and the first line of Equations 2.116, we obtain

$$V_1 = -\frac{\Delta h}{h_{21}}V_2 + \frac{h_{11}}{h_{21}}I_2 \tag{2.146}$$

where Δh is the determinant of the h-matrix, that is

$$\Delta h = \begin{vmatrix} h_{11} & h_{12} \\ h_{21} & h_{22} \end{vmatrix} = h_{11}h_{22} - h_{12}h_{21} \tag{2.147}$$

Comparing Equations 2.146 with the first line of Equations 2.122, and comparing Equations 2.145 with the second line of Equations 2.122, we find that

$$\begin{bmatrix} a_{11} & a_{12} \\ a_{21} & a_{22} \end{bmatrix} = \frac{-1}{h_{21}} \begin{bmatrix} \Delta h & h_{11} \\ h_{22} & 1 \end{bmatrix} \tag{2.148}$$

In a similar fashion we can go on developing further relationships between the various matrix parameters and so obtain the *matrix conversion table* given below (Table 2.3). Δy and Δh are defined by Equations 2.140 and 2.147, respectively, and

$$\Delta z = \text{determinant of } z\text{-matrix.}$$
$$= \begin{vmatrix} z_{11} & z_{12} \\ z_{21} & z_{22} \end{vmatrix} = z_{11}z_{22} - z_{12}z_{21} \tag{2.149}$$

$$\Delta g = \text{determinant of } g\text{-matrix}$$
$$= \begin{vmatrix} g_{11} & g_{12} \\ g_{21} & g_{22} \end{vmatrix} = g_{11}g_{22} - g_{12}g_{21} \tag{2.150}$$

$$\Delta a = \text{determinant of } a\text{-matrix}$$
$$= \begin{vmatrix} a_{11} & a_{12} \\ a_{21} & a_{22} \end{vmatrix} = a_{11}a_{22} - a_{12}a_{21} \tag{2.151}$$

$$\Delta b = \text{determinant of } b\text{-matrix}$$
$$= \begin{vmatrix} b_{11} & b_{12} \\ b_{21} & b_{22} \end{vmatrix} = b_{11}b_{22} - b_{12}b_{21} \tag{2.152}$$

2.5.3 COUPLING OF TWO-PORT NETWORKS

Thus far we have presented the various ways of expressing the external behaviour of two-port networks with impartiality. The usefulness of each set of matrix parameters becomes evident when

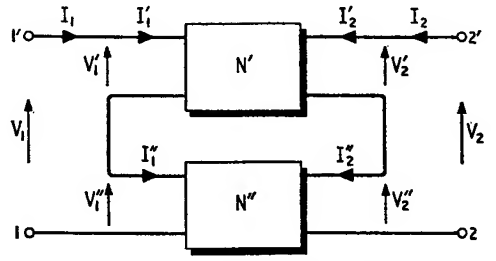

Fig. 2.41. Series-series coupling

we consider the various ways of coupling two-port networks. Consider two such networks N′ and N″. They can be connected together in any of the five different ways shown in Figs. 2.41 to 2.45. We shall see that the z-parameters are useful for dealing with the *series-series* coupling of Fig. 2.41, the y-parameters are useful for the *shunt-shunt coupling* of Fig. 2.42, the h-parameters are useful for the *series-shunt coupling* of Fig. 2.43, the g-parameters are useful for the *shunt-series coupling* of Fig. 2.44 and the a- and b-parameters are useful for the *cascade coupling* of Fig. 2.45.

Series-series coupling

Consider first Fig. 2.41 where the two-port networks N′ and N″ are connected together in series at their input and output ports. In terms of the z-parameters, we have for network N′

$$\begin{bmatrix} V_1' \\ V_2' \end{bmatrix} = \begin{bmatrix} z_{11}' & z_{12}' \\ z_{21}' & z_{22}' \end{bmatrix} \begin{bmatrix} I_1' \\ I_2' \end{bmatrix} \tag{2.153}$$

For network N″ we have

$$\begin{bmatrix} V_1'' \\ V_2'' \end{bmatrix} = \begin{bmatrix} z_{11}'' & z_{12}'' \\ z_{21}'' & z_{22}'' \end{bmatrix} \begin{bmatrix} I_1'' \\ I_2'' \end{bmatrix} \tag{2.154}$$

Table 2.3 MATRIX CONVERSION TABLE

To \ From	$z's$		$y's$		$h's$		$g's$		$a's$		$b's$	
$z's$	z_{11}	z_{12}	$\frac{y_{22}}{\Delta y}$	$\frac{-y_{12}}{\Delta y}$	$\frac{\Delta h}{h_{22}}$	$\frac{h_{12}}{h_{22}}$	$\frac{1}{g_{11}}$	$\frac{-g_{12}}{g_{11}}$	$\frac{a_{11}}{a_{21}}$	$\frac{\Delta a}{a_{21}}$	$\frac{b_{22}}{b_{21}}$	$\frac{1}{b_{21}}$
	z_{21}	z_{22}	$\frac{-y_{21}}{\Delta y}$	$\frac{y_{11}}{\Delta y}$	$\frac{-h_{21}}{h_{22}}$	$\frac{1}{h_{22}}$	$\frac{g_{21}}{g_{11}}$	$\frac{\Delta g}{g_{11}}$	$\frac{1}{a_{21}}$	$\frac{a_{22}}{a_{21}}$	$\frac{\Delta b}{b_{21}}$	$\frac{b_{11}}{b_{21}}$
$y's$	$\frac{z_{22}}{\Delta z}$	$\frac{-z_{12}}{\Delta z}$	y_{11}	y_{12}	$\frac{1}{h_{11}}$	$\frac{-h_{12}}{h_{11}}$	$\frac{\Delta g}{g_{22}}$	$\frac{g_{12}}{g_{22}}$	$\frac{a_{22}}{a_{12}}$	$\frac{-\Delta a}{a_{12}}$	$\frac{b_{11}}{b_{12}}$	$\frac{-1}{b_{12}}$
	$\frac{-z_{21}}{\Delta z}$	$\frac{z_{11}}{\Delta z}$	y_{21}	y_{22}	$\frac{h_{21}}{h_{11}}$	$\frac{\Delta h}{h_{11}}$	$\frac{-g_{21}}{g_{22}}$	$\frac{1}{g_{22}}$	$\frac{-1}{a_{12}}$	$\frac{a_{11}}{a_{12}}$	$\frac{-\Delta b}{b_{12}}$	$\frac{b_{22}}{b_{12}}$
$h's$	$\frac{\Delta z}{z_{22}}$	$\frac{z_{12}}{z_{22}}$	$\frac{1}{y_{11}}$	$\frac{-y_{12}}{y_{11}}$	h_{11}	h_{12}	$\frac{g_{22}}{\Delta g}$	$\frac{-g_{12}}{\Delta g}$	$\frac{a_{12}}{a_{22}}$	$\frac{\Delta a}{a_{22}}$	$\frac{b_{12}}{b_{11}}$	$\frac{1}{b_{11}}$
	$\frac{-z_{21}}{z_{22}}$	$\frac{1}{z_{22}}$	$\frac{y_{21}}{y_{11}}$	$\frac{\Delta y}{y_{11}}$	h_{21}	h_{22}	$\frac{-g_{21}}{\Delta g}$	$\frac{g_{11}}{\Delta g}$	$\frac{-1}{a_{22}}$	$\frac{a_{21}}{a_{22}}$	$\frac{-\Delta b}{b_{11}}$	$\frac{b_{21}}{b_{11}}$

F.C.A.—5

To \ From	$z's$		$y's$		$h's$		$g's$		$a's$		$b's$	
$g's$	$\frac{1}{z_{11}}$	$\frac{-z_{12}}{z_{11}}$	$\frac{\Delta y}{y_{22}}$	$\frac{y_{12}}{y_{22}}$	$\frac{h_{22}}{\Delta h}$	$\frac{-h_{12}}{\Delta h}$	g_{11}	g_{12}	$\frac{a_{21}}{a_{11}}$	$\frac{-\Delta a}{a_{11}}$	$\frac{b_{21}}{b_{22}}$	$\frac{-1}{b_{22}}$
	$\frac{z_{21}}{z_{11}}$	$\frac{\Delta z}{z_{11}}$	$\frac{-y_{21}}{y_{22}}$	$\frac{1}{y_{22}}$	$\frac{-h_{21}}{\Delta h}$	$\frac{h_{11}}{\Delta h}$	g_{21}	g_{22}	$\frac{1}{a_{11}}$	$\frac{a_{12}}{a_{11}}$	$\frac{\Delta b}{b_{22}}$	$\frac{b_{12}}{b_{22}}$
$a's$	$\frac{z_{11}}{z_{21}}$	$\frac{\Delta z}{z_{21}}$	$\frac{-y_{22}}{y_{21}}$	$\frac{-1}{y_{21}}$	$\frac{-\Delta h}{h_{21}}$	$\frac{-h_{11}}{h_{21}}$	$\frac{1}{g_{21}}$	$\frac{g_{22}}{g_{21}}$	a_{11}	a_{12}	$\frac{b_{22}}{\Delta b}$	$\frac{b_{12}}{\Delta b}$
	$\frac{1}{z_{21}}$	$\frac{z_{22}}{z_{21}}$	$\frac{-\Delta y}{y_{21}}$	$\frac{-y_{11}}{y_{21}}$	$\frac{-h_{22}}{h_{21}}$	$\frac{-1}{h_{21}}$	$\frac{g_{11}}{g_{21}}$	$\frac{\Delta g}{g_{21}}$	a_{21}	a_{22}	$\frac{b_{21}}{\Delta b}$	$\frac{b_{11}}{\Delta b}$
$b's$	$\frac{z_{22}}{z_{12}}$	$\frac{\Delta z}{z_{12}}$	$\frac{-y_{11}}{y_{12}}$	$\frac{-1}{y_{12}}$	$\frac{1}{h_{12}}$	$\frac{h_{11}}{h_{12}}$	$\frac{-\Delta g}{g_{12}}$	$\frac{-g_{22}}{g_{12}}$	$\frac{a_{22}}{\Delta a}$	$\frac{a_{12}}{\Delta a}$	b_{11}	b_{12}
	$\frac{1}{z_{12}}$	$\frac{z_{11}}{z_{12}}$	$\frac{-\Delta y}{y_{12}}$	$\frac{-y_{22}}{y_{12}}$	$\frac{h_{22}}{h_{12}}$	$\frac{\Delta h}{h_{12}}$	$\frac{-g_{11}}{g_{12}}$	$\frac{-1}{g_{12}}$	$\frac{a_{21}}{\Delta a}$	$\frac{a_{11}}{\Delta a}$	b_{21}	b_{22}

However, in Fig. 2.41 we see that

$$\begin{bmatrix} I_1 \\ I_2 \end{bmatrix} = \begin{bmatrix} I_1' \\ I_2' \end{bmatrix} = \begin{bmatrix} I_1'' \\ I_2'' \end{bmatrix} \tag{2.155}$$

and

$$\begin{bmatrix} V_1 \\ V_2 \end{bmatrix} = \begin{bmatrix} V_1' + V_1'' \\ V_2' + V_2'' \end{bmatrix} = \begin{bmatrix} V_1' \\ V_2' \end{bmatrix} + \begin{bmatrix} V_1'' \\ V_2'' \end{bmatrix} \tag{2.156}$$

Therefore, using Equations 2.153 to 2.156 we find that

$$\begin{bmatrix} V_1 \\ V_2 \end{bmatrix} = \begin{bmatrix} z_{11}' & z_{12}' \\ z_{21}' & z_{22}' \end{bmatrix} \begin{bmatrix} I_1 \\ I_2 \end{bmatrix} + \begin{bmatrix} z_{11}'' & z_{12}'' \\ z_{21}'' & z_{22}'' \end{bmatrix} \begin{bmatrix} I_1 \\ I_2 \end{bmatrix}$$

$$= \begin{bmatrix} z_{11}' + z_{11}'' & z_{12}' + z_{12}'' \\ z_{21}' + z_{21}'' & z_{22}' + z_{22}'' \end{bmatrix} \begin{bmatrix} I_1 \\ I_2 \end{bmatrix} \tag{2.157}$$

We thus see that the series-series coupled arrangement of Fig. 2.41 is equivalent to a single two-port network whose z-matrix is equal to the sum of the z-matrices of the individual two-port networks.

Shunt-shunt coupling

Consider next Fig. 2.42 where the two-port networks are connected together in parallel at their input and output ports. If we describe each network in terms of its respective y-parameters, we obtain

$$\begin{bmatrix} I_1' \\ I_2' \end{bmatrix} = \begin{bmatrix} y_{11}' & y_{12}' \\ y_{21}' & y_{22}' \end{bmatrix} \begin{bmatrix} V_1' \\ V_2' \end{bmatrix} \tag{2.158}$$

$$\begin{bmatrix} I_1'' \\ I_2'' \end{bmatrix} = \begin{bmatrix} y_{11}'' & y_{12}'' \\ y_{21}'' & y_{22}'' \end{bmatrix} \begin{bmatrix} V_1'' \\ V_2'' \end{bmatrix} \tag{2.159}$$

In Fig. 2.42 we see that

$$\begin{bmatrix} I_1 \\ I_2 \end{bmatrix} = \begin{bmatrix} I_1' \\ I_2' \end{bmatrix} + \begin{bmatrix} I_1'' \\ I_2'' \end{bmatrix} \tag{2.160}$$

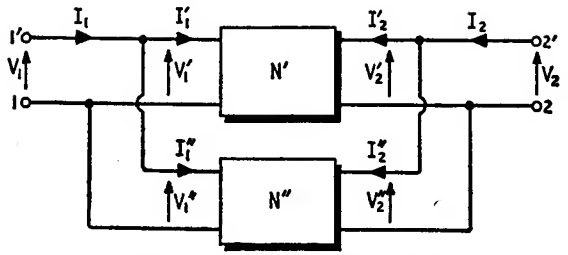

Fig. 2.42. Shunt-shunt coupling

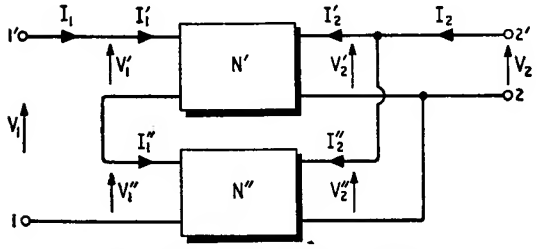

Fig. 2.43. Series-shunt coupling

and that the two networks have equal input voltages and equal output voltages. Therefore, adding Equations 2.158 and 2.159 and using Equation 2.160 we get

$$\begin{bmatrix} I_1 \\ I_2 \end{bmatrix} = \begin{bmatrix} y_{11}' + y_{11}'' & y_{12}' + y_{12}'' \\ y_{21}' + y_{21}'' & y_{22}' + y_{22}'' \end{bmatrix} \begin{bmatrix} V_1 \\ V_2 \end{bmatrix} \tag{2.161}$$

Thus, the shunt-shunt coupled arrangement of Fig. 2.42 can be replaced by a two-port network whose y-matrix is equal to the sum of the y-matrices of the individual networks.

Series-shunt coupling

Fig. 2.43 shows the two-port networks N′ and N″ having their input ports connected in series and their output ports connected in parallel. The overall voltage V_1 at the input port 1,1′ is equal to the sum of the input voltages V_1' and V_1'' of the individual networks. Further, the overall output current I_2 is the sum of the output currents I_2' and I_2'' of the individual networks. Therefore, if each network is described in terms of its h-parameters, we find that the overall behaviour can be expressed by

$$\begin{bmatrix} V_1 \\ I_2 \end{bmatrix} = \begin{bmatrix} h_{11}' + h_{11}'' & h_{12}' + h_{12}'' \\ h_{21}' + h_{21}'' & h_{22}' + h_{22}'' \end{bmatrix} \begin{bmatrix} I_1 \\ V_2 \end{bmatrix} \tag{2.162}$$

In other words, the series-shunt coupled arrangement of Fig. 2.43 is equivalent to a single two-port network having an h-matrix equal to the sum of the h-matrices of the component two-port networks.

Shunt-series coupling

Consider next Fig. 2.44 where the two-port networks have their input ports connected in parallel and their output ports connected in series. Here we see that the overall input current I_1 is equal to the sum of the input currents I_1' and I_1'' of the component networks, and the overall output voltage V_2 is equal to the sum of their output voltages V_2' and V_2''. Hence if we describe each component network by its g-parameters, we find that for the complete arrangement

$$\begin{bmatrix} I_1 \\ V_2 \end{bmatrix} = \begin{bmatrix} g_{11}' + g_{11}'' & g_{12}' + g_{12}'' \\ g_{21}' + g_{21}'' & g_{22}' + g_{22}'' \end{bmatrix} \begin{bmatrix} V_1 \\ I_2 \end{bmatrix} \tag{2.163}$$

which states that the shunt-series coupled arrangement of Fig. 2.44 is equivalent to a two-port network with a g-matrix equal to the sum of the g-matrices of the individual two-port networks.

It is important to note that the various statements which we have made regarding the above four ways of interconnecting two-port networks are valid if, and only if, the matrices describing the individual networks are not modified as a result of the particular method of interconnection.†

Cascade coupling

In Fig. 2.45 the two-port networks N′ and N″ are connected together in cascade. Viewing this cascade from left to right, we can make use of the a-matrix. For network N′ we have

$$\begin{bmatrix} V_1 \\ I_1 \end{bmatrix} = \begin{bmatrix} a_{11}' & a_{12}' \\ a_{21}' & a_{22}' \end{bmatrix} \begin{bmatrix} V_2' \\ -I_2' \end{bmatrix} \tag{2.164}$$

and for network N″ we have

$$\begin{bmatrix} V_1'' \\ I_1'' \end{bmatrix} = \begin{bmatrix} a_{11}'' & a_{12}'' \\ a_{21}'' & a_{22}'' \end{bmatrix} \begin{bmatrix} V_2 \\ -I_2 \end{bmatrix} \tag{2.165}$$

† For a more complete discussion of this problem, see E. A. Guillemin[1].

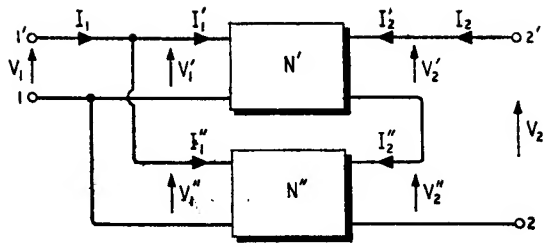

Fig. 2.44. Shunt-series coupling

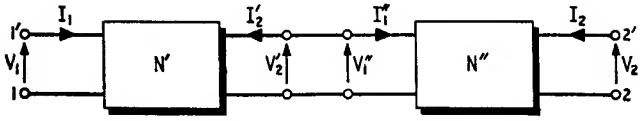

Fig. 2.45. Cascade coupling

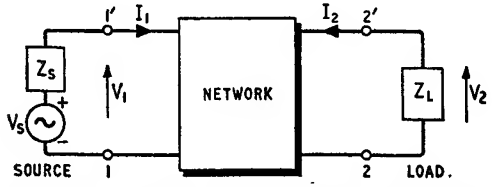

Fig. 2.46. Double-terminated two-port network

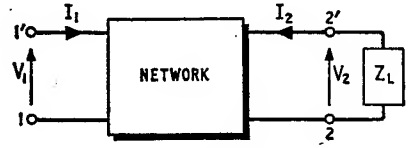

Fig. 2.47. Two-port network terminated at its output port

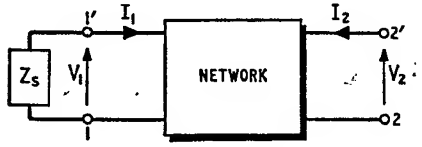

Fig. 2.48. Two-port network terminated at its input port

However, in Fig. 2.45 we see that

$$\begin{bmatrix} V_2' \\ -I_2' \end{bmatrix} = \begin{bmatrix} V_1'' \\ I_1'' \end{bmatrix} \tag{2.166}$$

Then, if the common voltage and current at the junction are eliminated from Equations 2.164 and 2.165 by using Equation 2.166 we find that

$$\begin{bmatrix} V_1 \\ I_1 \end{bmatrix} = \begin{bmatrix} a_{11}' & a_{12}' \\ a_{21}' & a_{22}' \end{bmatrix} \begin{bmatrix} a_{11}'' & a_{12}'' \\ a_{21}'' & a_{22}'' \end{bmatrix} \begin{bmatrix} V_2 \\ -I_2 \end{bmatrix} \tag{2.167}$$

Therefore, the overall a-matrix of the cascade coupling of Fig. 2.45 when viewed from the left, is equal to the product of the a-matrices of the individual networks.

If, however, the cascade coupling of Fig. 2.45 is viewed from the right, then we can show that

$$\begin{bmatrix} V_2 \\ I_2 \end{bmatrix} = \begin{bmatrix} b_{11}'' & b_{12}'' \\ b_{21}'' & b_{22}'' \end{bmatrix} \begin{bmatrix} b_{11}' & b_{12}' \\ b_{21}' & b_{22}' \end{bmatrix} \begin{bmatrix} V_1 \\ -I_1 \end{bmatrix} \tag{2.168}$$

where the b-parameters with one prime refer to network N′ and those with two primes refer to network N″.

2.5.4 EXTERNAL CIRCUIT PROPERTIES OF THE TERMINATED TWO-PORT NETWORK

The two-port network is normally used to couple a source to a load. Fig. 2.46 illustrates the general case of a voltage source V_S of internal impedance Z_S coupled to a load of impedance Z_L by means of a two-port network. When studying this double-terminated two-port network it is found that its *input impedance* Z_{in}, *output impedance* Z_{out}, *voltage gain* K_V and *current gain* K_I are of particular interest. Z_{in} is defined as the impedance measured looking into the input port 1,1′ when the output port 2,2′ is terminated with the load Z_L as in Fig. 2.47; then

$$Z_{in} = \frac{V_1}{I_1} \tag{2.169}$$

The output impedance Z_{out} is equal to the impedance measured looking into the output port when the input port is terminated with the source impedance Z_S as in Fig. 2.48; thus

$$Z_{out} = \frac{V_2}{I_2} \tag{2.170}$$

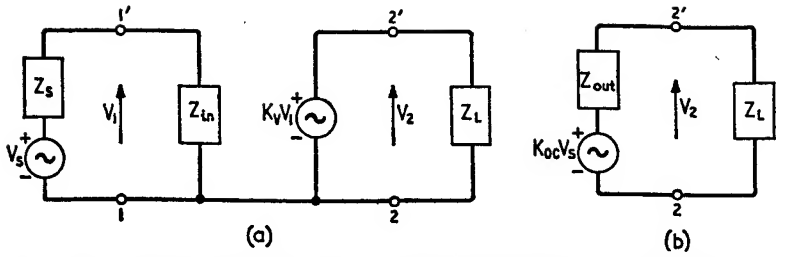

Fig. 2.49. (a) Equivalent circuit for double-terminated two-port network, (b) Another equivalent circuit for double terminated two-port network

The voltage and current gains are both transfer functions. They were defined earlier in Equations 2.29 and 2.31 which are re-written here for convenience

$$K_V = \frac{V_2}{V_1} \tag{2.171}$$

$$K_I = \frac{I_2}{I_1} \tag{2.172}$$

where the various currents and voltages are as shown in Fig. 2.47 Now

$$V_2 = -Z_L I_2 \tag{2.173}$$

Therefore, from Equations 2.169 and 2.171 to 2.173 we find that the input impedance, voltage and current gains are related by

$$K_V = -\frac{Z_L K_I}{Z_{in}} \tag{2.174}$$

In terms of the input impedance and voltage gain we can develop the equivalent circuit representation of Fig. 2.49(a) for the double-terminated two-port network. Here we see that

$$K = \frac{V_2}{V_S} = \frac{Z_{in} K_V}{Z_{in} + Z_S} \tag{2.175}$$

where K is termed the *external voltage gain.* It depends on the two-port network parameters and the terminating source and load impedances, whereas the voltage and current gains are both independent of the source impedance.

When $Z_S = Z_{in}$, we see from Equation 2.175 that $K = K_V/2$. We therefore have a second definition for the input impedance Z_{in} of a two-port network in that it is equal to the particular value of source impedance which causes the external voltage gain of the network to become half its voltage gain.

Let K_{oc} denote the value of K that results when the output port is open-circuited, that is, $Z_L = \infty$. Then we can deduce the equivalent circuit of Fig. 2.49 (b) to represent the double-terminated two-port network in terms of Z_{out} and K_{oc}, thus

$$K = \frac{Z_L K_{oc}}{Z_L + Z_{out}} \tag{2.176}$$

When $Z_L = Z_{out}$, we find from Equation 2.176 that $K = K_{oc}/2$. Since K_{oc} is independent of the load impedance, we deduce that the output impedance Z_{out} of a two-port network can be also defined as the special value of load impedance which causes the external voltage gain K to assume half its open-circuit value K_{oc}.
From Equations 2.175 and 2.176 we deduce that

$$\frac{Z_{in} K_V}{Z_{in} + Z_S} = \frac{Z_L K_{oc}}{Z_L + Z_{out}} \tag{2.177}$$

Let us next evaluate Z_{in}, Z_{out}, K_V and K_I in terms of the various matrix parameters. As an example, consider the case of z-parameters. Eliminating V_2 between Equations 2.173 and the second line of Equations 2.110 we obtain

$$K_I = \frac{I_2}{I_1} = \frac{-z_{21}}{z_{22} + Z_L} \tag{2.178}$$

Next, eliminating I_2 between Equations 2.178 and the first line of Equations 2.110 gives

$$\begin{aligned} Z_{in} &= z_{11} - \frac{z_{12} z_{21}}{z_{22} + Z_L} \\ &= \frac{\Delta z + z_{11} Z_L}{z_{22} + Z_L} \end{aligned} \tag{2.179}$$

where Δz is as defined in Equation 2.149. From Equations 2.174, 2.178 and 2.179 we find that the voltage gain is

$$K_V = \frac{z_{21} Z_L}{\Delta z + z_{11} Z_L} \tag{2.180}$$

For evaluating the output impedance, consider Fig. 2.48 where

$$V_1 = -I_1 Z_S$$

Therefore, eliminating V_1 between this relation and the first line of Equations 2.110, and then solving for I_1, we obtain

$$I_1 = -\frac{z_{12} I_2}{z_{11} + Z_S} \tag{2.181}$$

Next, on eliminating I_1 between Equation 2.181 and the second line of Equations 2.110, we find that

$$\begin{aligned} Z_{out} &= z_{22} - \frac{z_{21} z_{12}}{z_{11} + Z_S} \\ &= \frac{\Delta z + z_{22} Z_S}{z_{11} + Z_S} \end{aligned} \tag{2.182}$$

In a similar way we can go on to evaluate Z_{in}, Z_{out}, K_V and K_I in terms of the remaining matrix parameters, and so obtain the results of Table 2.4 where the determinants Δz, Δy, Δh, Δg and Δb are as defined in Equations 2.149, 2.140, 2.147, 2.150 and 2.152, respectively.

2.5.5 RECIPROCITY AND PASSIVITY

In passive two-port networks composed of such bilateral elements as resistors, capacitors and inductors, we find that the following relationships are always satisfied:

$$\left.\begin{aligned} z_{12} &= z_{21} \\ y_{12} &= y_{21} \\ h_{12} &= -h_{21} \\ g_{12} &= -g_{21} \\ a_{11}a_{22} - a_{12}a_{21} &= 1 \end{aligned}\right\} \tag{2.183}$$

These relationships are all consequences of the 'reciprocity theorem' which states that a passive two-port network, containing bilateral elements only, transmits electric signals equally in the forward and reverse directions provided that the external impedances presented to the input and output ports of the network remain unchanged.

On the other hand, in an active two-port network containing controlled sources we find that none of the relationships of Equations 2.183 are satisfied because a controlled source is, by nature, a unilateral and therefore non-reciprocal element. It must be, however, emphasised that a two-port network is not necessarily non-reciprocal if it is active. As an example, consider the symmetrical T-network of Fig. 2.50 having equal series resistance elements of 1 Ω and a shunt branch made up of a negative resistance element of −R Ω. Such a network can have a 'maximum power

Table 2.4 EXTERNAL CIRCUIT PROPERTIES OF TERMINATED TWO-PORT NETWORK

	z's	y's	h's	g's	a's	b's
Z_{in}	$\dfrac{\Delta z + z_{11}Z_L}{z_{22} + Z_L}$	$\dfrac{1 + y_{22}Z_L}{y_{11} + \Delta yZ_L}$	$\dfrac{h_{11} + \Delta hZ_L}{1 + h_{22}Z_L}$	$\dfrac{g_{22} + Z_L}{\Delta g + g_{11}Z_L}$	$\dfrac{a_{12} + a_{11}Z_L}{a_{22} + a_{21}Z_L}$	$\dfrac{b_{12} + b_{22}Z_L}{b_{11} + b_{21}Z_L}$
Z_{out}	$\dfrac{\Delta z + z_{22}Z_S}{z_{11} + Z_S}$	$\dfrac{1 + y_{11}Z_S}{y_{22} + \Delta yZ_S}$	$\dfrac{h_{11} + Z_S}{\Delta h + h_{22}Z_S}$	$\dfrac{g_{22} + \Delta gZ_S}{1 + g_{11}Z_S}$	$\dfrac{a_{12} + a_{22}Z_S}{a_{11} + a_{21}Z_S}$	$\dfrac{b_{12} + b_{11}Z_S}{b_{22} + b_{21}Z_S}$
K_V	$\dfrac{z_{21}Z_L}{\Delta z + z_{11}Z_L}$	$\dfrac{-y_{21}Z_L}{1 + y_{22}Z_L}$	$\dfrac{-h_{21}Z_L}{h_{11} + \Delta hZ_L}$	$\dfrac{g_{21}Z_L}{g_{22} + Z_L}$	$\dfrac{Z_L}{a_{12} + a_{11}Z_L}$	$\dfrac{\Delta bZ_L}{b_{12} + b_{22}Z_L}$
K_I	$\dfrac{-z_{21}}{z_{22} + Z_L}$	$\dfrac{y_{21}}{y_{11} + \Delta yZ_L}$	$\dfrac{h_{21}}{1 + h_{22}Z_L}$	$\dfrac{-g_{21}}{\Delta g + g_{11}Z_L}$	$\dfrac{-1}{a_{22} + a_{21}Z_L}$	$\dfrac{-\Delta b}{b_{11} + b_{21}Z_L}$

gain'† greater than unity, and therefore behave as an active two-port network, provided that its z-parameters satisfy the following condition[2],

$$4r_{11}r_{22} - (r_{12} + r_{21})^2 - (x_{12} - x_{21})^2 < 0 \qquad (2.184)$$

where the r's and x's are the resistive and reactive components of the respective z-parameters; thus

$$z_{11} = r_{11} + jx_{11}$$
$$z_{12} = r_{12} + jx_{12}$$
$$z_{21} = r_{21} + jx_{21}$$
$$z_{22} = r_{22} + jx_{22}$$

Now for the symmetrical T-network of Fig. 2.50 we have,

$$z_{11} = z_{22} = 1 - R$$
$$z_{12} = z_{21} = \quad -R$$

Fig. 2.50. A possible active but reciprocal two-port network

† The power gain K_P of a two-port network is defined as the ratio of output power, delivered to the load, over the input power supplied to the network from the external source. Let $Z_L = R_L + jX_L$ be the load impedance, and $Z_{in} = R_{in} + jX_{in}$ be the input impedance of the network when its output port is terminated with the load impedance Z_L. Then we find that the input power $= R_{in}|I_1|^2$ and the output power $= R_L|I_1|^2$, which give the power gain of the network to be

$$K_P = \frac{R_L}{R_{in}}|K_I|^2$$

where $|K_I| = |I_2/I_1|$ is the magnitude of the current gain of the network. Now R_{in} and $|K_I|$ are both functions of R_L and X_L. Therefore, to evaluate the maximum power gain, we set

$$\frac{\partial K_P}{\partial R_L} = 0$$

and

$$\frac{\partial K_P}{\partial X_L} = 0$$

These two conditions uniquely determine, in terms of the network parameters, the optimum load impedance which results in the maximum power gain. Then after some manipulations we find that, in terms of the z-parameters, the maximum power gain of the network is greater than unity provided that the necessary condition of Equation 2.184 is satisfied.

Hence, from Equation 2.184 it follows that provided the absolute value R of the negative resistance element exceeds $\frac{1}{2}\,\Omega$, the T-network of Fig. 2.50 behaves as an active two-port network, and yet it is reciprocal for all R because it has $z_{12} = z_{21}$.

Furthermore, not all passive networks are necessarily reciprocal. Thus in a 'gyrator', which was first introduced by B. D. H. Tellegen[3], we have

$$y_{11} = y_{22} = 0$$

$$y_{12} = -y_{21} = g$$

where g is termed the 'gyration conductance'. The gyrator is therefore a two-port network for which $I_2 = -gV_1$ and $V_2 = I_1/g$ where the currents I_1, I_2 and the voltages V_1, V_2 are as defined in Fig. 2.46. If an impedance Z_L is connected across the output port of a gyrator, we find that the impedance measured, looking into its input port, is equal to $1/g^2Z_L$. Thus the gyrator behaves somewhat like an ideal transformer except that it interchanges the roles of voltage and current at the output port in the sense that the output current I_2 becomes directly proportional to the input voltage V_1, and the output voltage V_2 becomes directly proportional to the input current I_1. However, since $|I_1V_1| = |I_2V_2|$ it follows that the instantaneous power input is equal to the instantaneous power output for all loads. Therefore, we conclude that the gyrator is basically a lossless passive element as it does not store or dissipate energy, and yet it is non-reciprocal because the condition $y_{12} = y_{21}$ is not satisfied.

2.6 Basic valve and transistor configurations

2.6.1 EQUIVALENT CIRCUITS

Valves and transistors are inherently non-linear circuit elements, as can be seen from examining their static characteristic curves. But if the level of the applied signal is sufficiently low, then the external behaviour of the valve or transistor can be simulated, with reasonable accuracy, by means of a *linear equivalent circuit* which consists of a suitable combination of passive elements and controlled sources.

Consider first the triode valve of Fig. 2.51 (a). Under small signal conditions its external behaviour can be represented by the Thévenin equivalent circuit of Fig. 2.51 (b) which involves a voltage-controlled voltage source or by the Norton equivalent circuit of Fig. 2.15 (c) which involves a voltage-controlled current source[4]. In both cases the grid-cathode voltage V_{gk} is the control signal. In the case of Fig. 2.51 (b) the element r_a is termed the *anode slope resistance* and μ is termed the *amplification factor*. Thus

$$V_{ak} = r_aI_a - \mu V_{gk} \tag{2.185}$$

where I_a is the anode current and V_{ak} is the anode-cathode voltage.

The control parameter g_m of Fig. 2.51 (c) is termed the *mutual conductance* and is related to r_a and μ by

$$\mu = r_ag_m \tag{2.186}$$

From Fig. 2.51 (c) we deduce that

$$I_a = \frac{1}{r_a}V_{ak} + g_mV_{gk} \tag{2.187}$$

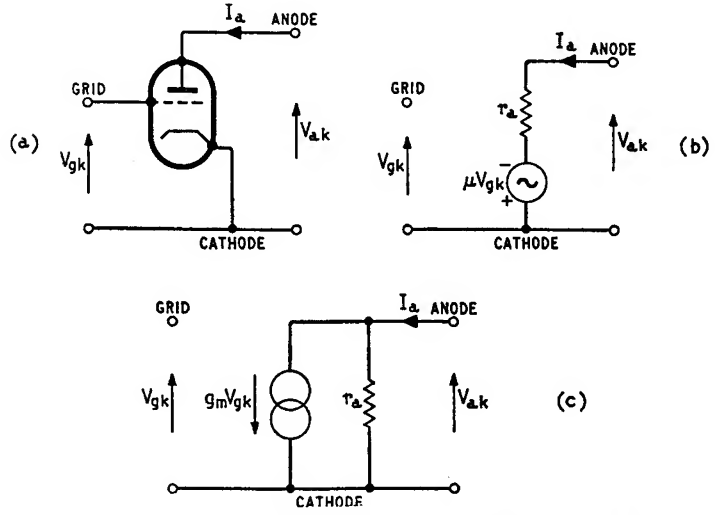

Fig. 2.51. (a) Triode valve, (b) Equivalent circuit with controlled voltage source, (c) Equivalent circuit with controlled current source

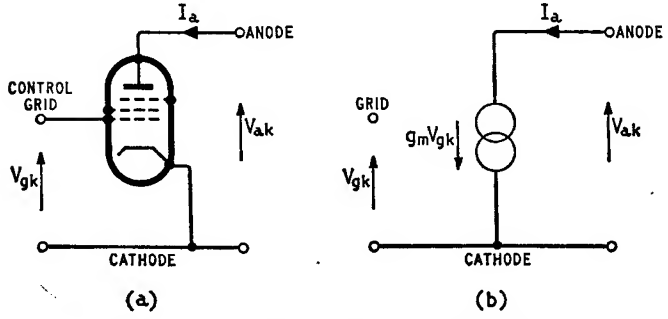

Fig. 2.52. (a) Pentode valve, (b) Equivalent circuit

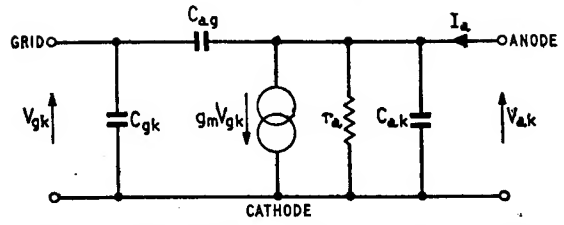

Fig. 2.53. High frequency equivalent circuit for triode valve

In a pentode valve the anode slope resistance r_a is very large; it is of the order of 1 MΩ. Consequently, we are normally justified in ignoring the shunting effect of r_a in the equivalent circuit of Fig. 2.51 (c), which then reduces to the simpler form shown in Fig. 2.52 (b).

If the operating frequency is high, the effect of inter-electrode capacitances can become important. This can be taken into account by adding the anode-grid capacitance C_{ag}, the grid-cathode capacitance C_{gk} and anode-cathode capacitance C_{ak} as in Fig. 2.53. In a pentode valve C_{ag} is much smaller than in a triode valve.

The case of the transistor is more involved than the valve in that very many different equivalent circuits have been developed for describing the external behaviour of a transistor, with each one having certain advantages and disadvantages. In the present book we shall only consider a few of the more widely used ones.

Consider the pnp transistor of Fig. 2.54 (a). Its external behaviour can be represented by the *common emitter h-parameters equivalent circuit* of Fig. 2.54 (b). It is so called because the emitter is arranged common to the input and output ports, as in Fig. 2.54 (a). From Fig. 2.54 (b) it follows that

$$\left.\begin{aligned} V_{be} &= h_{11e} I_b + h_{12e} V_{ce} \\ I_c &= h_{21e} I_b + h_{22e} V_{ce} \end{aligned}\right\} \qquad (2.188)$$

where I_b is the base current, I_c is the collector current, V_{be} is the

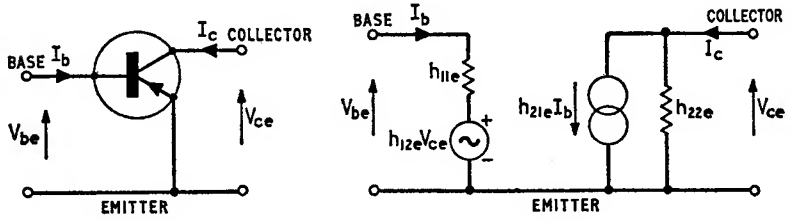

Fig. 2.54. (a) pnp transistor, (b) Common emitter h-parameters equivalent circuit

base-emitter voltage and V_{ce} is the collector-emitter voltage. The parameter h_{11e} is the *short-circuit input impedance* and is defined as

$$h_{11e} = \left(\frac{V_{be}}{I_b}\right)_{V_{ce}=0} \qquad (2.189)$$

The parameter h_{21e} is termed the *forward current amplification factor* and is defined as

$$h_{21e} = \left(\frac{I_c}{I_b}\right)_{V_{ce}=0} \qquad (2.190)$$

Next, h_{12e} is termed the *reverse voltage amplification factor* and is defined as

$$h_{12e} = \left(\frac{V_{be}}{V_{ce}}\right)_{I_b=0} \qquad (2.191)$$

Finally, h_{22e} is the *open-circuit output admittance* and is defined as

$$h_{22e} = \left(\frac{I_c}{V_{ce}}\right)_{I_b=0} \qquad (2.192)$$

The subscript e in each of the parameters h_{11e}, h_{12e}, h_{21e} and h_{22e} signifies the fact that they apply to a transistor operated with its

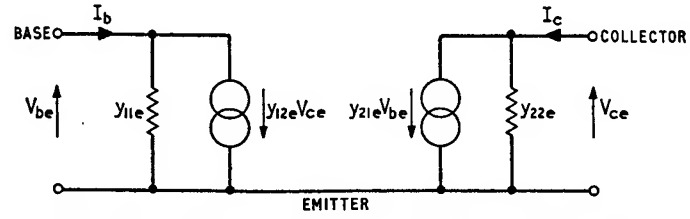

Fig. 2.55. Common emitter y-parameters equivalent circuit

emitter terminal common to the input and output ports. They are known as the *common emitter h-parameters*†.

Another useful equivalent circuit for the transistor is the *common emitter y-parameters equivalent circuit* of Fig. 2.55. From the matrix conversion Table 2.3 we deduce that the *common emitter y-parameters*‡ y_{11e}, y_{12e}, y_{21e}, and y_{22e} are related to the common emitter

† The common emitter h-parameters are also denoted by h_{ie}, h_{re}, h_{fe} and h_{oe}. Thus $h_{ie} \equiv h_{11e}$, $h_{re} \equiv h_{12e}$, $h_{fe} \equiv h_{21e}$, and $h_{oe} \equiv h_{22e}$.

‡ The common emitter y-parameters are also denoted by y_{ie}, y_{re}, y_{fe} and y_{oe}. Thus $y_{ie} \equiv y_{11e}$, $y_{re} \equiv y_{12e}$, $y_{fe} \equiv y_{21e}$ and $y_{oe} \equiv y_{22e}$.

h-parameters as follows

$$\left.\begin{aligned} y_{11e} &= \frac{1}{h_{11e}} \\ y_{12e} &= \frac{-h_{12e}}{h_{11e}} \\ y_{21e} &= \frac{h_{21e}}{h_{11e}} \\ y_{22e} &= \frac{\Delta h_e}{h_{11e}} \end{aligned}\right\} \qquad (2.193)$$

where

$$\Delta h_e = h_{11e}h_{22e} - h_{12e}h_{21e} \qquad (2.194)$$

At this stage it is instructive to compare the relative merits of the common emitter h- and y-parameters. The great advantage of the h-parameters is the relative ease with which they can be all measured directly and accurately. Thus the measurement of h_{11e} and h_{21e} requires short-circuiting the collector to emitter for a.c. signals, while the measurement of h_{12e} and h_{22e} requires open-circuiting the base terminal for a.c. signals. A transistor operated with its emitter terminal common has a relatively low input impedance and high output impedance. Therefore, it is possible to simulate open-circuit and short-circuit conditions across its input and output ports, respectively, quite accurately and so the h-parameters are easy to measure. On the other hand, the measurement of y-parameters requires the simulation of short-circuit conditions across both the input and output ports. Thus we find that the parameters y_{11e} and y_{21e} can be measured quite easily but a direct and accurate measurement of y_{12e} and y_{22e} may be more difficult. However, the y-parameters equivalent circuit has the advantage in that it is quite suitable for a direct application of the nodal analysis as it involves controlled current sources only, whereas the h-parameters equivalent circuit has the analytical disadvantage of involving controlled voltage and current sources.

The common emitter h- and y-parameters have real values only when the operating frequency is sufficiently low. At high frequencies both sets of parameters become frequency dependent and assume complex values. Therefore, the analysis of transistor circuits at high frequencies in terms of the y- or h- parameters can become quite involved. In such cases the *hybrid-π equivalent circuit* of Fig. 2.56 (a) is found to be more convenient. The great advantage of this equivalent circuit is that all of its elements are independent of frequency. If the terminating load resistance is small then the effect of the elements $r_{b'c}$ and r_{ce} of Fig. 2.56 (a) can be neglected, and so

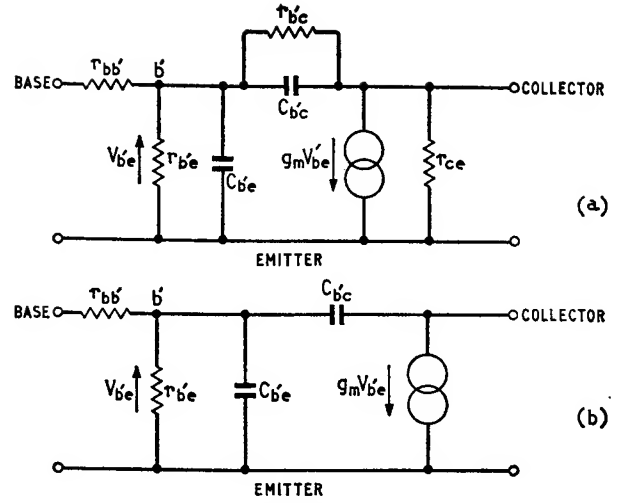

Fig. 2.56. (a) High frequency hybrid-π equivalent circuit, (b) Simplified hybrid-π equivalent circuit

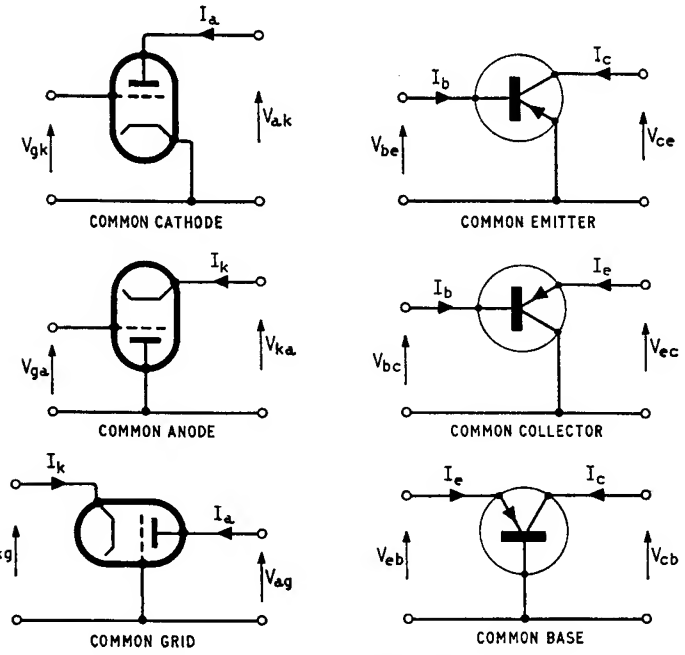

Fig. 2.57. Valve and transistor configurations

we obtain the *simplified hybrid-π equivalent circuit* of Fig. 2.56 (b) which we shall find quite adequate for later work.

The resistance $r_{bb'}$ of Figs. 2.56 is known as the *base resistance*, and $C_{b'c}$ is known as the *collector depletion layer capacitance*. The remaining elements $r_{b'e}$, g_m and $C_{b'e}$ of Fig. 2.56 (b) are defined as follows[5]

$$\left.\begin{aligned} r_{b'e} &= h_{11e} - r_{bb'} \\ g_m &= \frac{h_{21e}}{h_{11e} - r_{bb'}} \\ C_{b'e} &= \frac{1}{2\pi f_\beta r_{b'e}} \end{aligned}\right\} \qquad (2.195)$$

where f_β is termed the *common emitter beta cut off frequency*. In Equations 2.195 it is to be noted that h_{11e} and h_{21e} both refer to low frequency values.

2.6.2 THE BASIC CONFIGURATIONS

The triode valve and transistor have the common feature in that they are both basically *three-terminal networks*. Each one has three useful modes of operation depending upon which of the three terminals is arranged common to the input and output ports. The valve can thus be operated in the *common cathode*, *common anode* (that is, *cathode follower*) and *common grid* configurations, while the transistor can be operated in the *common emitter*, *common collector*, (i.e. emitter follower) and *common base* configurations as shown in Fig. 2.57. This diagram also illustrates the correspondence between the various basic valve and transistor configurations.

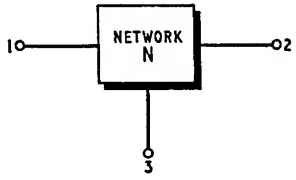

Fig. 2.58. Three-terminal network

For a unified treatment of various valve and transistor configurations we shall use the indefinite admittance matrix, to be considered next, as the basic tool of analysis.

2.6.3 THE INDEFINITE ADMITTANCE MATRIX

Consider the generalised three-terminal network N of Fig. 2.58 which is assumed to represent a valve or transistor. Let y_{11}, y_{12}, y_{21} and y_{22} signify the y-parameters of this network when its terminal

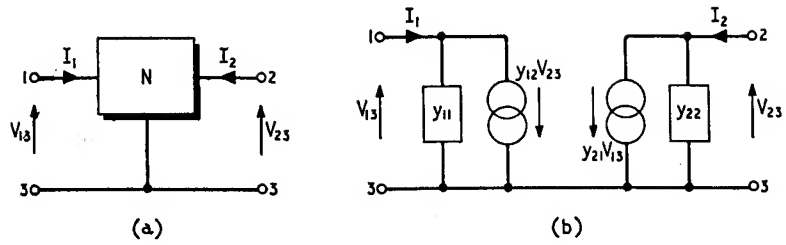

Fig. 2.59. (a) Network N with terminal 3 common, (b) Equivalent circuit

3 is common to the input and output ports as in Fig. 2.59 (a). Then, we can represent this configuration with the y-parameters equivalent circuit of Fig. 2.59 (b). Consider next Fig. 2.60 (a) where the currents I_1, I_2 and I_3 are applied to the network, and the resulting terminal voltages V_1, V_2 and V_3 are shown defined with respect to an arbitrary earth terminal. If in Fig. 2.60 (a) we replace the network N with the equivalent circuit of Fig. 2.59 (b), we obtain the circuit of Fig. 2.60 (b). Analysing this circuit by the nodal method gives

$$\left.\begin{aligned} I_1 - y_{12}V_{23} &= y_{11}V_1 - y_{11}V_3 \\ I_2 - y_{21}V_{13} &= y_{22}V_2 - y_{22}V_3 \\ I_3 + y_{12}V_{23} + y_{21}V_{13} &= -y_{11}V_1 - y_{22}V_2 + (y_{11} + y_{22})V_3 \end{aligned}\right\} \qquad (2.196)$$

The voltage differences V_{23} and V_{13} are given by

$$\left.\begin{aligned} V_{23} &= V_2 - V_3 \\ V_{13} &= V_1 - V_3 \end{aligned}\right\} \qquad (2.197)$$

Therefore, eliminating V_{23} and V_{13} between Equations 2.196 and 2.197 and collecting terms, we get

$$\left.\begin{aligned} I_1 &= y_{11}V_1 + y_{12}V_2 - (y_{11} + y_{12})V_3 \\ I_2 &= y_{21}V_1 + y_{22}V_2 - (y_{21} + y_{22})V_3 \\ I_3 &= -(y_{11} + y_{21})V_1 - (y_{12} + y_{22})V_2 + (y_{11} + y_{12} + y_{21} + y_{22})V_3 \end{aligned}\right\} \qquad (2.198)$$

Re-writing these equations in matrix form, we have

$$\begin{bmatrix} I_1 \\ I_2 \\ I_3 \end{bmatrix} = [y] \begin{bmatrix} V_1 \\ V_2 \\ V_3 \end{bmatrix} \qquad (2.199)$$

where the square matrix $[y]$ of order 3 is defined as

$$[y] = \begin{bmatrix} y_{11} & y_{12} & -(y_{11}+y_{12}) \\ y_{21} & y_{22} & -(y_{21}+y_{22}) \\ -(y_{11}+y_{21}) & -(y_{12}+y_{22}) & (y_{11}+y_{12}+y_{21}+y_{22}) \end{bmatrix} \tag{2.200}$$

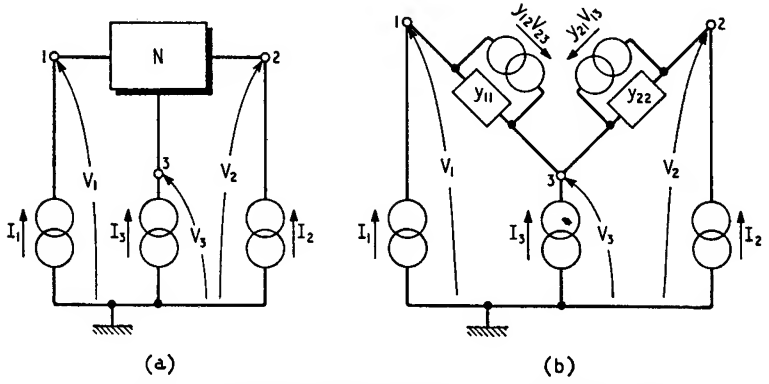

Fig. 2.60. (a) Three-terminal network, (b) Equivalent circuit

The matrix $[y]$ is known as the *indefinite admittance matrix* because in Fig. 2.60 the reference terminal has been left undefined. An important property of this matrix is that the sum of the admittances in any one of its three rows or three columns is zero as can be easily established from Equations 2.200. Further, if we delete the third row and third column of the matrix of Equation 2.200, the submatrix which remains is the matrix of the y-parameters y_{11}, y_{12}, y_{21} and y_{22} of the two-port network obtained by arranging terminal 3

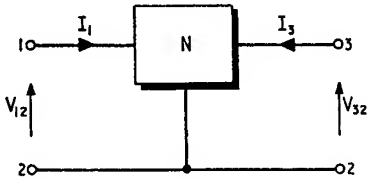

Fig. 2.61. Network N with terminal 2 common

of the network common to the input and output ports as in Fig. 2.59 (a). Next, if the second row and second column of the matrix $[y]$ are deleted, the remaining submatrix is the matrix of the y-parameters y_{11}, y_{13}, y_{31}, and y_{33} of the two-port network having terminal 2

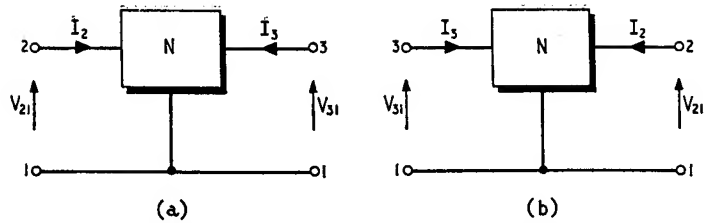

Fig. 2.62. Network N with terminal 1 common: (a) Terminal 2 as input and terminal 3 as output, (b) Terminal 3 as input and terminal 2 as output

common to the input and output ports as in Fig. 2.61, that is,

$$\begin{bmatrix} y_{11} & y_{13} \\ y_{31} & y_{33} \end{bmatrix} = \begin{bmatrix} y_{11} & -(y_{11}+y_{12}) \\ -(y_{11}+y_{21}) & (y_{11}+y_{12}+y_{21}+y_{22}) \end{bmatrix} \tag{2.201}$$

Similarly, if the first row and first column of the matrix $[y]$ are deleted, the remaining submatrix is the matrix of the y-parameters y_{22}, y_{23}, y_{32} and y_{33} of the two-port network that results when terminal 1 is arranged common as in Fig. 2.62 (a).

Thus

$$\begin{bmatrix} y_{22} & y_{23} \\ y_{32} & y_{33} \end{bmatrix} = \begin{bmatrix} y_{22} & -(y_{21}+y_{22}) \\ -(y_{12}+y_{22}) & (y_{11}+y_{12}+y_{21}+y_{22}) \end{bmatrix} \tag{2.202}$$

Suppose next that terminal 1 is left common but terminal 3 is arranged as the input terminal and terminal 2 is arranged as the output terminal, as shown in Fig. 2.62 (b). The y-matrix of this configuration is deduced directly from Equation 2.202 to be

$$\begin{bmatrix} y_{33} & y_{32} \\ y_{23} & y_{22} \end{bmatrix} = \begin{bmatrix} (y_{11}+y_{12}+y_{21}+y_{22}) & -(y_{12}+y_{22}) \\ -(y_{21}+y_{22}) & y_{22} \end{bmatrix} \tag{2.203}$$

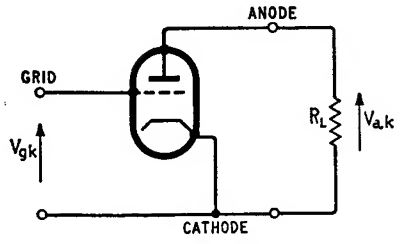

Fig. 2.63. Common cathode stage

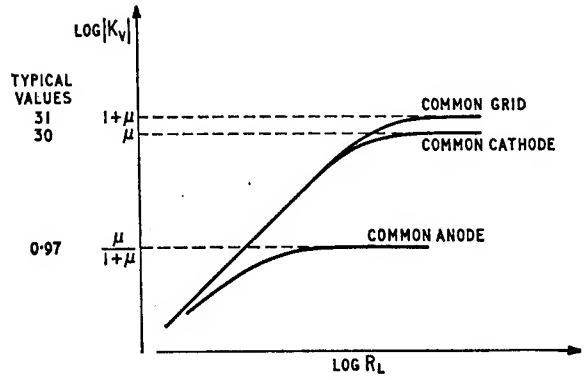

Fig. 2.64. Variation of voltage gain with load resistance for the three valve configurations

We thus see that if the y-parameters of the configuration of Fig. 2.59 (a) are known, then the y-parameters of the configurations of Figs. 2.61 and 2.62 can be determined by the applications of Equations 2.201 and 2.203. We shall use these results in evaluating the circuit behaviour of the various valve and transistor configurations. In this way we shall have unified the valve and transistor as special cases of the generalised three-terminal network.

2.6.4 EXTERNAL CIRCUIT RESPONSE OF BASIC VALVE CONFIGURATIONS

Common cathode stage

Consider a common cathode stage connected to a load resistance R_L as in Fig. 2.63, and suppose that y_{11k}, y_{12k}, y_{21k} and y_{22k} denote the y-parameters of the stage. Then from the equivalent circuit of Fig. 2.51 (c) we find that at low frequencies

$$\begin{bmatrix} y_{11k} & y_{12k} \\ y_{21k} & y_{22k} \end{bmatrix} = \begin{bmatrix} 0 & 0 \\ g_m & g_a \end{bmatrix} \tag{2.204}$$

where

$$g_a = 1/r_a \tag{2.205}$$

From Table 2.4 we deduce that the voltage gain of the stage of Fig. 2.63 is given by

$$K_V = \frac{V_{ak}}{V_{gk}} = \frac{-y_{21k}R_L}{1 + y_{22k}R_L}$$

$$= \frac{-g_m R_L}{1 + g_a R_L}$$

$$K_V = \frac{-\mu R_L}{r_a + R_L} \tag{2.206}$$

where the minus sign indicates that the common cathode stage provides 180° phase shift between its input and output voltage signals at low frequencies. Further, K_V is zero at $R_L = 0$ and reaches the maximum value of $-\mu$ at $R_L = \infty$, and so it varies with R_L in the manner shown in Fig. 2.64.

The common cathode stage has an infinite input impedance and an output impedance equal to r_a at low frequencies.

Common anode stage (Cathode follower)

Fig. 2.65 shows a common anode stage connected to a load resistance R_L. Suppose that terminals 1, 2 and 3 of the three-terminal network N of Fig. 2.59 (a) correspond to the grid, anode and cathode

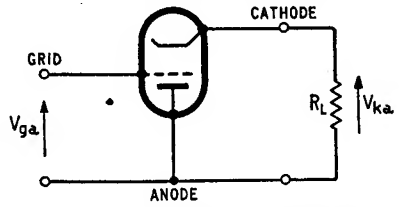

Fig. 2.65. Common anode stage

of the triode valve, respectively. Then, if y_{11a}, y_{12a}, y_{21a}, and y_{22a} denote the *common anode y-parameters* we deduce from Equations 2.201 that they are related to the common cathode y-parameters as follows

$$\begin{bmatrix} y_{11a} & y_{12a} \\ y_{21a} & y_{22a} \end{bmatrix} = \begin{bmatrix} y_{11k} & -(y_{11k} + y_{12k}) \\ -(y_{11k} + y_{21k}) & (y_{11k} + y_{12k} + y_{21k} + y_{22k}) \end{bmatrix}$$

$$= \begin{bmatrix} 0 & 0 \\ -g_m & g_m + g_a \end{bmatrix} \tag{2.207}$$

Then the low frequency value of the voltage gain of the common anode stage follows from Table 2.4 to be

$$K_V = \frac{V_{ka}}{V_{ga}} = \frac{-y_{21a}R_L}{1 + y_{22a}R_L}$$

$$= \frac{g_m R_L}{1 + (g_m + g_a)R_L}$$

$$= \frac{\mu R_L}{r_a + (1 + \mu)R_L} \tag{2.208}$$

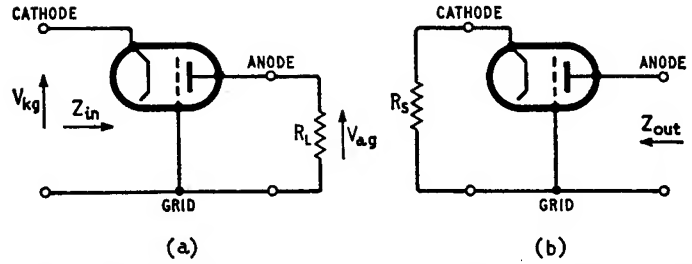

Fig. 2.66. Common grid stage: (a) Stage terminated at output, (b) Stage terminated at input

Here we see that at $R_L = \infty$ the voltage gain K_V reaches its maximum value of $\mu/(1 + \mu)$. Since normally $\mu \gg 1$ it follows that the voltage gain of a common anode stage can approximate closely to unity at relatively high load resistances. Fig. 2.64 also includes variation of the common anode voltage gain with load resistance.

The input impedance of the common anode stage of Fig. 2.65 is infinite at low frequencies. Its output impedance is equal to $1/(g_m + g_a)$, that is, $r_a/(1 + \mu)$ which is much smaller than the output impedance r_a of the common cathode stage.

Common grid stage

Consider next a triode valve operated with its grid common as in Fig. 2.66. Assuming that the common cathode stage corresponds to the network configuration of Fig. 2.59 (a), we find that the common grid stage corresponds to the network configuration of Fig. 2.62 (b). Therefore, if y_{11g}, y_{12g}, y_{21g} and y_{22g} denote the *common grid y-parameters*, then it follows from Equations 2.203 that they are related to the common cathode y-parameters as follows

$$\begin{bmatrix} y_{11g} & y_{12g} \\ y_{21g} & y_{22g} \end{bmatrix} = \begin{bmatrix} (y_{11k} + y_{12k} + y_{21k} + y_{22k}) & -(y_{12k} + y_{22k}) \\ -(y_{21k} + y_{22k}) & y_{22k} \end{bmatrix}$$

$$= \begin{bmatrix} g_m + g_a & -g_a \\ -(g_m + g_a) & g_a \end{bmatrix} \qquad (2.209)$$

Hence the common grid stage has finite values for all of its y-parameters. This is in direct contrast to the common cathode and common anode stages, both of which have zero values for their short-circuit input admittance and reverse transfer admittance parameters at low frequencies. From Table 2.4 the low frequency value of the voltage gain of the common grid stage of Fig. 2.66 (a) is

$$K_V = \frac{V_{ag}}{V_{kg}} = \frac{-y_{21g}R_L}{1 + y_{22g}R_L}$$

$$= \frac{(g_m + g_a)R_L}{1 + g_aR_L}$$

$$= \frac{(1 + \mu)R_L}{r_a + R_L} \qquad (2.210)$$

Hence, K_V reaches its maximum value of $(1 + \mu)$ at $R_L = \infty$, and it decreases with decreasing R_L as illustrated in Fig. 2.64. Since $\mu \gg 1$ it follows that, for a given load resistance, the magnitudes of the common cathode and common grid voltage gains are very nearly equal.

From Table 2.4 we also deduce that the common grid stage has the following input impedance at low frequencies

$$Z_{in} = \frac{1 + y_{22g}R_L}{y_{11g} + R_L\Delta y_g}$$

$$= \frac{1 + g_aR_L}{g_m + g_a}$$

$$= \frac{r_a + R_L}{1 + \mu} \qquad (2.211)$$

Notice that $\Delta y_g = y_{11g}y_{22g} - y_{12g}y_{21g} = 0$ as can be easily verified from Equation 2.209.

For evaluating the output impedance of the common grid stage, consider Fig. 2.66 (b) where the input port has been terminated with a resistance equal to R_S. Then, from Table 2.4 we find that

$$Z_{out} = \frac{1 + y_{11g}R_S}{y_{22g} + \Delta y_gR_S}$$

$$= \frac{1 + (g_m + g_a)R_S}{g_a}$$

$$= r_a + (1 + \mu)R_S \qquad (2.212)$$

We therefore see from Equations 2.211 and 2.212 that, unlike the common cathode and common anode stages, the input and output impedances of a common grid stage depend on the terminating load and source resistances, respectively. This is due to the finite value of the short-circuit reverse transfer admittance parameter of the common grid stage. Further, the common grid stage has a relatively low input impedance and a relatively high output impedance as $\mu \gg 1$.

2.6.5 EXTERNAL CIRCUIT RESPONSE OF BASIC TRANSISTOR CONFIGURATIONS

Common emitter stage

Fig. 2.67 shows a transistor operated with its emitter terminal common to the input and output ports. In terms of the common emitter y-parameters y_{11e}, y_{12e}, y_{21e}, and y_{22e} we find from Table 2.4 that the stage of Fig. 2.67 (a) has the following current gain

$$K_I = \frac{I_c}{I_b} = \frac{y_{21e}}{y_{11e} + R_L \Delta y_e} \tag{2.213}$$

K_I increases with decreasing load resistance, as shown in Fig. 2.68. It has the maximum value of y_{21e}/y_{11e} which occurs at $R_L = 0$.

From Table 2.4 we also find that the voltage gain of the common emitter stage of Fig. 2.67 (a) is

$$K_V = \frac{V_{ce}}{V_{be}} = \frac{-y_{21e}R_L}{1 + y_{22e}R_L} \tag{2.214}$$

K_V increases with increasing load resistance, as shown in Fig. 2.69. It reaches the maximum value of $-y_{21e}/y_{22e}$ at $R_L = \infty$.

The input impedance of the common emitter stage of Fig. 2.67 (a) is deduced from Table 2.4 to be

$$Z_{in} = \frac{1 + y_{22e}R_L}{y_{11e} + \Delta y_e R_L} \tag{2.215}$$

Therefore, $Z_{in} = 1/y_{11e}$ at $R_L = 0$, and $Z_{in} = y_{22e}/\Delta y_e$ at $R_L = \infty$. From the following typical values

$$\begin{aligned} y_{11e} &= 1 \text{ m}\mho \\ y_{12e} &= -0{\cdot}4\ \mu\mho \\ y_{21e} &= 50 \text{ m}\mho \\ y_{12e} &= 25\ \mu\mho \end{aligned} \tag{2.216}$$

we see that the parameter y_{12e} has a negative value. Hence, $\Delta y_e = y_{11e}y_{22e} - y_{12e}y_{21e}$ is invariably greater than the product term $y_{11e}y_{22e}$, and accordingly we see from Equation 2.215 that the input impedance of a common emitter stage decreases with increasing load resistance as in Fig. 2.70.

Consider next Fig. 2.67 (b) where a resistance R_S has been connected across the input port of the common emitter stage. From Table 2.4 we see that the output impedance of this stage is

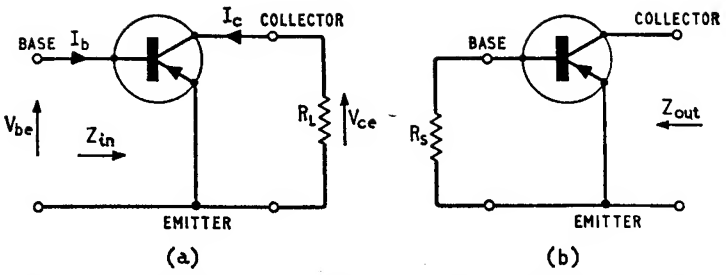

Fig. 2.67. Common emitter stage: (a) Stage terminated at output, (b) Stage terminated at input

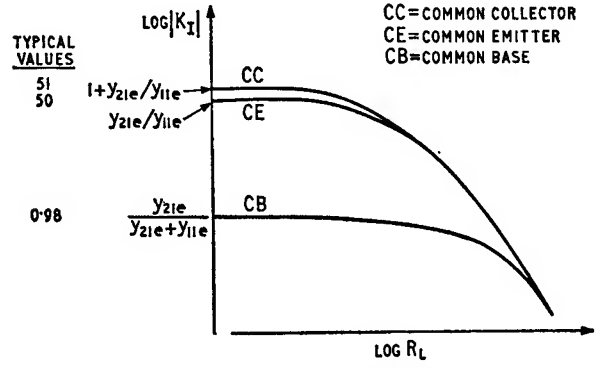

Fig. 2.68. Variation of current gain with load resistance for the three transistor configurations

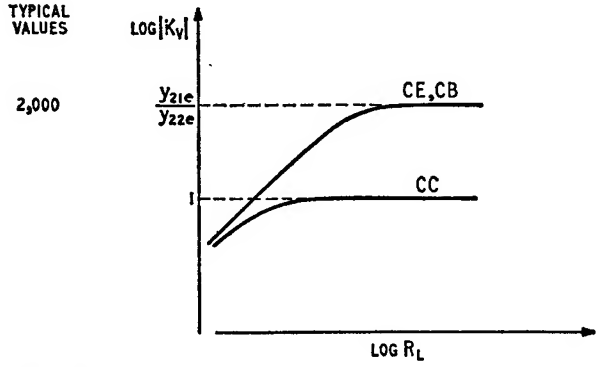

Fig. 2.69. Variation of voltage gain with load resistance for the three transistor configurations

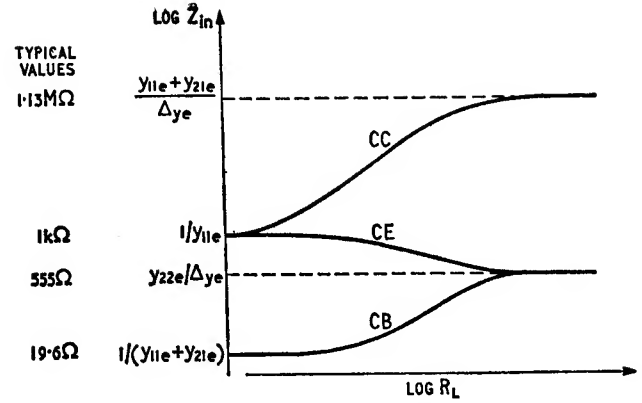

Fig. 2.70. Variation of input impedance with load resistance for the three transistor configurations

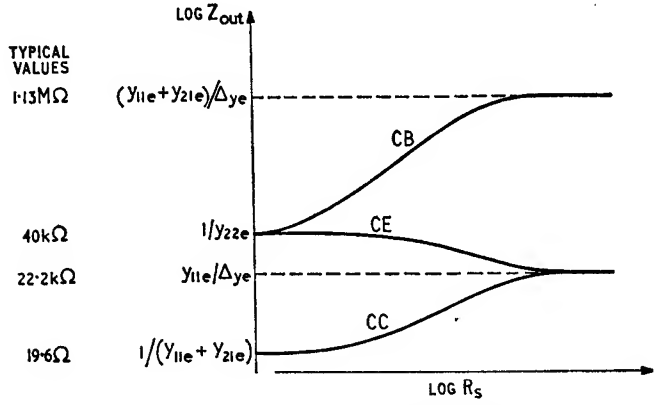

Fig. 2.71. Variations of output impedance with source resistance for the three transistor configurations

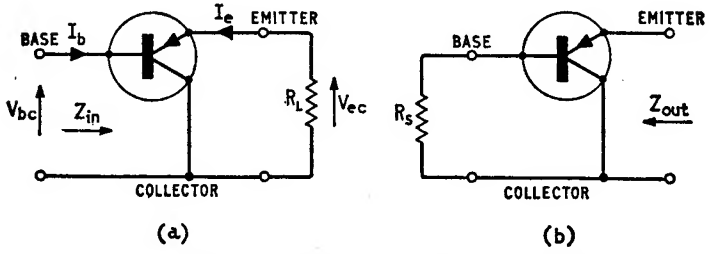

Fig. 2.72. Common collector stage: (a) Terminated at output, (b) Terminated at input

$$Z_{out} = \frac{1 + y_{11e}R_S}{y_{22e} + \Delta y_e R_S} \tag{2.217}$$

At $R_S = 0$, $Z_{out} = 1/y_{22e}$ and at $R_S = \infty$, $Z_{out} = y_{11e}/\Delta y_e$. Since $\Delta y_e > y_{11e}y_{22e}$ as explained above, it follows that the output impedance of a common emitter stage decreases with increasing load resistance, as in Fig. 2.71.

Equations 2.213 to 2.217 express the external circuit response of the common emitter stage in terms of its y-parameters. It is also useful to express the circuit response in terms of the common emitter h-parameters. Using Equations 2.193 and 2.213 to 2.217 we obtain the results given in Table 2.5.

Common collector stage (Emitter follower)

Consider Fig. 2.72 where the transistor is operated with its collector terminal common to the input and output ports. If we assume that the common emitter stage of Fig. 2.67 (a) corresponds to the network configuration of Fig. 2.59 (a), we see that the terminals 1, 2 and 3 of Fig. 2.59 (a) correspond to the base, collector and emitter terminals of the transistor, and so the common collector stage corresponds to the network configuration of Fig. 2.61. Hence, if y_{11c}, y_{12c}, y_{21c} and y_{22c} denote the *common collector y-parameters*, we deduce from Equations 2.201 that they are related to the common emitter y-parameters as follows

$$\begin{bmatrix} y_{11c} & y_{12c} \\ y_{21c} & y_{22c} \end{bmatrix} = \begin{bmatrix} y_{11e} & -(y_{11e} + y_{12e}) \\ -(y_{11e} + y_{21e}) & (y_{11e} + y_{12e} + y_{21e} + y_{22e}) \end{bmatrix}$$

Then, from Table 2.4 we see that the current gain of the common collector stage of Fig. 2.72 (a) is

$$K_I = \frac{I_e}{I_b} = \frac{y_{21c}}{y_{11c} + R_L\Delta y_c} = \frac{-(y_{11e} + y_{21e})}{y_{11e} + R_L\Delta y_e} \tag{2.219}$$

where it is to be noted that

$$\begin{aligned} \Delta y_c &= y_{11c}y_{22c} - y_{12c}y_{21c} \\ &= y_{11e}(y_{11e} + y_{12e} + y_{21e} + y_{22e}) - (y_{11e} + y_{12e})(y_{11e} + y_{21e}) \\ &= y_{11e}y_{22e} - y_{12e}y_{21e} \\ &= \Delta y_e \end{aligned} \tag{2.220}$$

Table 2.5 EXTERNAL CIRCUIT RESPONSE OF TRANSISTOR CONFIGURATIONS IN TERMS OF COMMON EMITTER h-PARAMETERS

	Common emitter	*Common collector*	*Common base*
K_I	$\frac{h_{21e}}{1+h_{22e}R_L}$	$\frac{-(1+h_{21e})}{1+h_{22e}R_L}$	$\frac{-h_{21e}}{1+h_{21e}+h_{22e}R_L}$
K_V	$\frac{-h_{21e}R_L}{h_{11e}+\Delta h_e R_L}$	$\frac{(1+h_{21e})R_L}{h_{11e}+(1+h_{21e})R_L}$	$\frac{h_{21e}R_L}{h_{11e}+\Delta h_e R_L}$
Z_{in}	$\frac{h_{11e}+\Delta h_e R_L}{1+h_{22e}R_L}$	$\frac{h_{11e}+(1+h_{21e})R_L}{1+h_{22e}R_L}$	$\frac{h_{11e}+\Delta h_e R_L}{1+h_{21e}+h_{22e}R_L}$
Z_{out}	$\frac{h_{11e}+R_S}{\Delta h_e+h_{22e}R_S}$	$\frac{h_{11e}+R_S}{1+h_{21e}+h_{22e}R_S}$	$\frac{h_{11e}+(1+h_{21e})R_S}{\Delta h_e+h_{22e}R_S}$

Normally $y_{21e} \gg y_{11e}$ (see the typical values of Equations 2.216). Therefore, for a given load resistance we see from Equations 2.213 and 2.219 that the common emitter and common collector stages have nearly the same magnitudes for their current gains, as illustrated in Fig. 2.68. Next, the voltage gain of the common collector stage of Fig. 2.72 (a) is deduced from Table 2.4 to be

$$K_V = \frac{V_{ec}}{V_{bc}} = \frac{-y_{21c}R_L}{1+y_{22c}R_L} = \frac{(y_{11e}+y_{21e})R_L}{1+(y_{11e}+y_{12e}+y_{21e}+y_{22e})R_L} \tag{2.221}$$

Normally, we find that

$$y_{11e}+y_{21e} \gg y_{12e}+y_{22e} \tag{2.222}$$

as can be seen from the typical values of Equation 2.216. Hence Equation 2.221 reduces to

$$K_V \simeq \frac{(y_{11e}+y_{21e})R_L}{1+(y_{11e}+y_{21e})R_L} \tag{2.223}$$

and so the voltage gain of the common collector stage varies with the load resistance in the manner shown in Fig. 2.69. When $R_L \gg 1/(y_{11e}+y_{21e})$ we find that $K_V \simeq 1$.

The input impedance of the common collector stage of Fig. 2.72 (a) follows from Table 2.4 to be

$$Z_{in} = \frac{1+y_{22c}R_L}{y_{11c}+\Delta y_c R_L} = \frac{1+(y_{11e}+y_{12e}+y_{21e}+y_{22e})R_L}{y_{11e}+\Delta y_e R_L}$$

$$Z_{in} \simeq \frac{1+(y_{11e}+y_{21e})R_L}{y_{11e}+\Delta y_e R_L} \tag{2.224}$$

where we have made use of Equations 2.220 and 2.222. At $R_L = 0$, $Z_{in} = 1/y_{11e}$ and at $R_L = \infty$, $Z_{in} = (y_{11e}+y_{21e})/\Delta y_e$. Thus the common emitter and common collector stages have the same short-circuit input impedances. Further, the input impedance of the common collector stage increases with the load resistance as in Fig. 2.70.

Consider next Fig. 2.72 (b) where the common collector stage has been terminated at its input port with the source resistance R_S. From Table 2.4 we deduce that the output impedance is

$$Z_{out} = \frac{1+y_{11c}R_S}{y_{22c}+\Delta y_c R_S} = \frac{1+y_{11e}R_S}{y_{11e}+y_{12e}+y_{21e}+y_{22e}+\Delta y_e R_S} \simeq \frac{1+y_{11e}R_S}{y_{11e}+y_{21e}+\Delta y_e R_S} \tag{2.225}$$

At $R_S = 0$, $Z_{out} = 1/(y_{11e}+y_{21e})$, and at $R_S = \infty$, $Z_{out} = y_{11e}/\Delta y_e$ Therefore, the common emitter and common collector stages have the same open-circuit output impedances. Further, the output impedance of the common collector stage increases with increasing source resistance as in Fig. 2.71.

Using Equations 2.193, 2.219 and 2.223 to 2.225 we can express the current and voltage gains, input and output impedances of the common collector stage in terms of the common emitter h-parameters and so obtain the results of Table 2.5.

Common base stage

In Fig. 2.73 the transistor is operated with its base terminal common to the input and output ports. If the common emitter stage

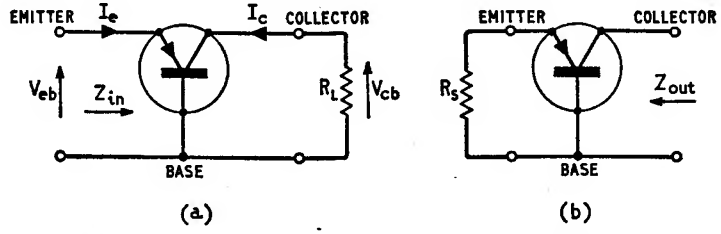

Fig. 2.73. Common base stage: (a) Terminated at output, (b) Terminated at input

corresponds to the network configuration of Fig. 2.59 (a), we see that the common base stage corresponds to the network configuration of Fig. 2.62 (b). Hence, if y_{11b}, y_{12b}, y_{21b} and y_{22b} denote the *common base y-parameters*, we find from Equations 2.203 that they are related to the common emitter y-parameters by

$$\begin{bmatrix} y_{11b} & y_{12b} \\ y_{21b} & y_{22b} \end{bmatrix} = \begin{bmatrix} y_{11e} + y_{12e} + y_{21e} + y_{22e} & -(y_{12e} + y_{22e}) \\ -(y_{21e} + y_{22e}) & y_{22e} \end{bmatrix} \tag{2.226}$$

Then, from Table 2.4 we deduce that the current gain of the common base stage of Fig. 2.73 (a) is

$$K_I = \frac{I_c}{I_e} = \frac{y_{21b}}{y_{11b} + R_L \Delta y_b} = \frac{-(y_{21e} + y_{22e})}{y_{11e} + y_{12e} + y_{21e} + y_{22e} + R_L \Delta y_e} \tag{2.227}$$

where it is noted that

$$\begin{aligned} \Delta y_b &= y_{11b}y_{22b} - y_{12b}y_{21b} \\ &= (y_{11e} + y_{12e} + y_{21e} + y_{22e})y_{22e} - (y_{12e} + y_{22e})(y_{21e} + y_{22e}) \\ &= y_{11e}y_{22e} - y_{12e}y_{21e} \\ &= \Delta y_e \end{aligned} \tag{2.228}$$

Normally $y_{21e} \gg y_{22e}$, therefore, using this inequality and that of Equation 2.222, we can simplify Equation 2.227 as follows

$$K_I \simeq \frac{-y_{21e}}{y_{11e} + y_{21e} + R_L \Delta y_e} \tag{2.229}$$

At $R_L = 0$, K_I reaches the maximum value of $-y_{21e}/(y_{11e} + y_{21e})$. This is very close to unity in magnitude because normally $y_{21e} \gg y_{11e}$, and so the current gain of the common base stage of Fig. 2.73 (a) varies with R_L as shown in Fig. 2.68.

Next, from Table 2.4 we deduce that the common base stage of Fig. 2.73 (a) has the following voltage gain

$$K_V = \frac{V_{cb}}{V_{eb}} = \frac{-y_{21b}R_L}{1 + y_{22b}R_L} = \frac{(y_{21e} + y_{22e})R_L}{1 + y_{22e}R_L}$$

$$K_V \simeq \frac{y_{21e}R_L}{1 + y_{22e}R_L} \tag{2.230}$$

where we have noted the inequality $y_{21e} \gg y_{22e}$. Therefore, for a given load resistance we see from Equations 2.214 and 2.230 that the common emitter and common base stages have practically the same magnitudes for their voltage gains, as is shown in Fig. 2.69.

From Table 2.4 we also see that the input impedance of the common base stage of Fig. 2.73 (a) is

$$\begin{aligned} Z_{in} &= \frac{1 + y_{22b}R_L}{y_{11b} + \Delta y_b R_L} \\ &= \frac{1 + y_{22e}R_L}{y_{11e} + y_{12e} + y_{21e} + y_{22e} + \Delta y_e R_L} \\ &\simeq \frac{1 + y_{22e}R_L}{y_{11e} + y_{21e} + \Delta y_e R_L} \end{aligned} \tag{2.231}$$

where we have made use of the inequality of Equation 2.222. At $R_L = 0$, $Z_{in} = 1/(y_{11e} + y_{21e})$ and at $R_L = \infty$, $Z_{in} = y_{22e}/\Delta y_e$. Hence, the common emitter and common base stages have the same open-circuit input impedances, and the input impedance of the common base stage increases with the load resistance as in Fig. 2.70.

Consider next the common base stage of Fig. 2.73 (b) having its input port terminated with R_S. From Table 2.4 we find that the output impedance of this stage is

$$\begin{aligned} Z_{out} &= \frac{1 + y_{11b}R_S}{y_{22b} + \Delta y_b R_S} \\ &= \frac{1 + (y_{11e} + y_{12e} + y_{21e} + y_{22e})R_S}{y_{22e} + \Delta y_e R_S} \\ &\simeq \frac{1 + (y_{11e} + y_{21e})R_S}{y_{22e} + \Delta y_e R_S} \end{aligned} \tag{2.232}$$

At $R_S = 0$, $Z_{out} = 1/y_{22e}$ and at $R_S = \infty$, $Z_{out} = (y_{11e} + y_{21e})/\Delta y_e$. Hence, the common emitter and common base stages have the same short-circuit output impedances, and the output impedance of the common base stage increases with the source resistance as in Fig. 2.71.

Next, using Equations 2.193 and 2.229 to 2.232 we can also express the current and voltage gains, input and output impedances of the common base stage in terms of the common emitter h-parameters and so obtain the results given in Table 2.5.

In the diagrams of Figs. 2.68 to 2.71 we have included typical

values for the various circuit parameters of the three transistor configurations. These are based on the parameter values given by Equation 2.216.

A special case which occurs quite often in practice is that of a transistor stage connected to a load resistance R_L small compared to $1/h_{22e}$. This is equivalent to saying that

$$h_{22e}R_L \ll 1 \tag{2.233}$$

Since $\Delta h_e = h_{11e}h_{22e} - h_{12e}h_{21e}$ and both h_{12e} and h_{21e} are positive, it follows that provided R_L satisfies the above inequality then it will certainly satisfy the following one too

$$\Delta h_e R_L \ll h_{11e} \tag{2.234}$$

In such a situation we find that the expressions for the current gain, voltage gain and input impedance for the three transistor configurations simplify as in Table 2.6. It is also of interest to note that the h-parameter equivalent circuit for the common emitter reduces to the form shown in Fig. 2.74.

2.6.6 HIGH FREQUENCY RESPONSE

Common cathode stage

Consider the common cathode stage of Fig. 2.63 and suppose that the operating frequency is high enough for the influence of the interelectrode capacitances to become noticeable. From the high frequency equivalent circuit of Fig. 2.53 we deduce that

$$\begin{bmatrix} y_{11k} & y_{12k} \\ y_{21k} & y_{22k} \end{bmatrix} = \begin{bmatrix} j\omega(C_{gk} + C_{ag}) & -j\omega C_{ag} \\ g_m - j\omega C_{ag} & g_a + j\omega(C_{ag} + C_{ak}) \end{bmatrix} \tag{2.235}$$

We therefore see that at high frequencies all the common cathode y-parameters assume finite values. From Table 2.4 we deduce that the corresponding voltage gain of the stage is

$$\begin{aligned} K_V(j\omega) &= \frac{-y_{21k}R_L}{1 + y_{22k}R_L} \\ &= \frac{-(g_m - j\omega C_{ag})R_L}{1 + g_a R_L + j\omega(C_{ag} + C_{ak})R_L} \\ &= \frac{-\mu R_L}{r_a + R_L} \cdot \frac{1 - j\omega/\omega_1}{1 + j\omega/\omega_2} \end{aligned} \tag{2.236}$$

Table 2.6 APPROXIMATE RELATIONS FOR THE EXTERNAL CIRCUIT RESPONSE OF TRANSISTOR CONFIGURATIONS

	Common emitter	*Common collector*	*Common base*
K_I	h_{21e}	$-(1 + h_{21e})$	$\frac{-h_{21e}}{1 + h_{21e}}$
K_V	$\frac{-h_{21e}R_L}{h_{11e}}$	$\frac{(1 + h_{21e})R_L}{h_{11e} + (1 + h_{21e})R_L}$	$\frac{h_{21e}R_L}{h_{11e}}$
Z_{in}	h_{11e}	$h_{11e} + (1 + h_{21e})R_L$	$\frac{h_{11e}}{1 + h_{21e}}$

where

$$\omega_1 = \frac{g_m}{C_{ag}} \tag{2.237}$$

$$\omega_2 = \frac{r_a + R_L}{r_a R_L(C_{ag} + C_{ak})} \tag{2.238}$$

Normally ω_1 is much greater than ω_2.

From Table 2.4 we also see that the input admittance Y_{in} of the common cathode stage is

$$\begin{aligned} Y_{in} &= \frac{1}{Z_{in}} \\ &= y_{11k} - \frac{y_{12k}y_{21k}R_L}{1 + y_{22k}R_L} \\ &= y_{11k} + y_{12k}K_V(j\omega) \\ &= j\omega C_{gk} + j\omega C_{ag}[1 - K_V(j\omega)] \end{aligned} \tag{2.239}$$

where $K_V(j\omega)$ is as given by Equation 2.236. If the operating frequency is low compared to both ω_1 and ω_2, we find that the voltage gain remains practically real and equal to $-\mu R_L/(r_a + R_L)$. Then

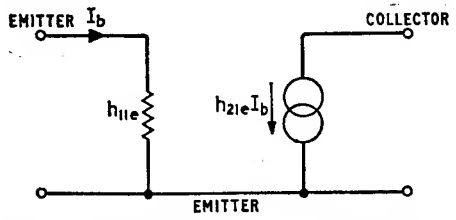

Fig. 2.74. Simplified h-parameters equivalent circuit

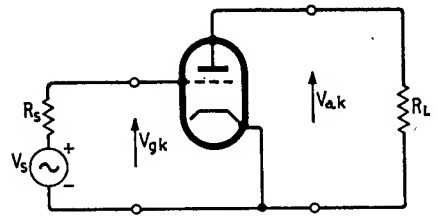

Fig. 2.75. Double-terminated common cathode stage

Equation 2.239 gives the input capacitance C_{in} of the common cathode stage to be

$$C_{in} = \frac{Y_{in}}{j\omega}$$

$$= C_{gk} + C_{ag}\left(1 + \frac{\mu R_L}{r_a + R_L}\right) \qquad (2.240)$$

We therefore see that, owing to the voltage gain of the stage, the input capacitance C_{in} can be much greater than the value we may expect from the interelectrode capacitances on their own. This effect is known as the *Miller effect.*

Consider next Fig. 2.75 where the common cathode stage is driven from a voltage source V_S of internal resistance R_S. Then, from Equation 2.175 we deduce that the external voltage gain of the stage is

$$K(j\omega) = \frac{K_V(j\omega)}{1 + R_S Y_{in}(j\omega)}$$

$$\simeq \frac{-\mu R_L}{r_a + R_L} \cdot \frac{1}{1 + j\omega/\omega_{0k}} \qquad (2.241)$$

where

$$\omega_{0k} = \frac{1}{C_{in} R_S} \qquad (2.242)$$

From Equation 2.241 we find that $20 \log_{10}|K(j\omega)|$ and $\angle K(j\omega)$ vary with frequency as shown in Fig. 2.76. The corner frequency ω_{0k} is referred to as the *common cathode cut off frequency.* At $\omega = \omega_{0k}$ the gain drops by 3 dB below its low frequency value and the phase angle is equal to 135°.

Common emitter stage

Fig. 2.77 (a) shows a common emitter stage connected to a load resistance R_L. Provided that R_L is small (of the order of 1 kΩ) we can represent the transistor with the simplified hybrid-π

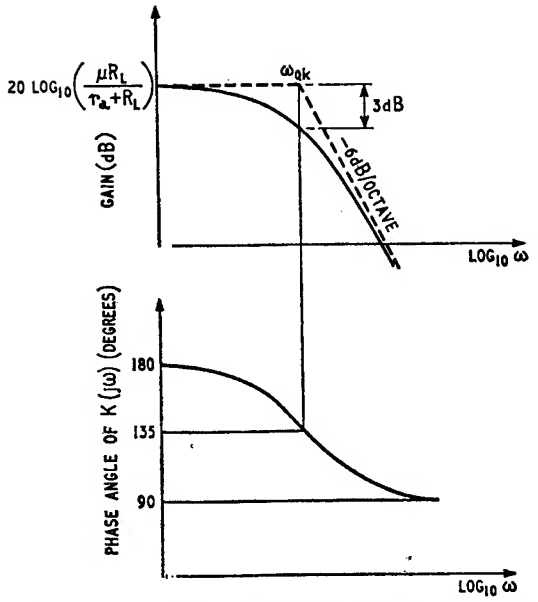

Fig. 2.76. Gain and phase response of common cathode stage

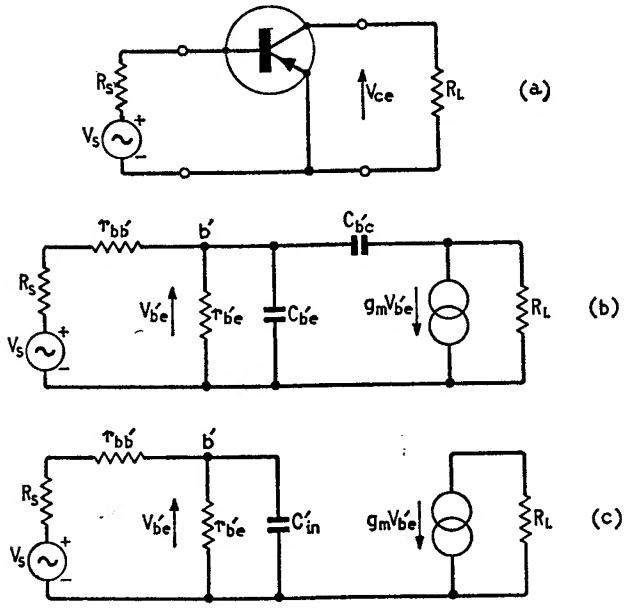

Fig. 2.77. (a) Double terminated common emitter stage, (b) Equivalent circuit, (c) Simplified equivalent circuit

equivalent circuit as in Fig. 2.77 (b). Owing to the Miller effect of the capacitance $C_{b'c}$, we find that the input capacitance C_{in}' measured between the emitter terminal and the internal node labelled b' is given by

$$C_{in}' = C_{b'e} + C_{b'c}(1 + g_m R_L) \tag{2.243}$$

where $g_m R_L$ is magnitude of the internal voltage gain from node b' to the collector terminal. Normally $C_{b'e}$ is very large compared to $C_{b'c}$; therefore, Equation 2.243 approximates to

$$C_{in}' \simeq C_{b'e} + C_{b'c} g_m R_L \tag{2.244}$$

We can thus reduce the equivalent circuit of Fig. 2.77 (b) to the simpler form shown in Fig. 2.77 (c), and so deduce that the external voltage gain of the common emitter stage is†

$$K(j\omega) \simeq \frac{-g_m r_{b'e} R_L}{r_{bb'} + r_{b'e} + R_S} \cdot \frac{1}{1 + j\omega/\omega_{0e}} \tag{2.245}$$

where ω_{0e} is termed the *common emitter cut off frequency* and is given by

$$\omega_{0e} = \frac{1}{C_{in}'}\left(\frac{1}{r_{b'e}} + \frac{1}{r_{bb'} + R_S}\right) \tag{2.246}$$

Hence, the frequency response of a common emitter stage is essentially similar in form to that of the common cathode stage.

PROBLEMS

1. The circuit of Fig. 2.78 involves a current-controlled voltage source $r_m i_1$, where $r_m = 9{\cdot}8$ kΩ. Determine the internal voltage (in terms of v_S) and the series impedance of the Thévenin equivalent circuit with respect to the terminals 1, 1′.
2. The circuit of Fig. 2.79 involves a voltage-controlled current source $g_m v_1$, where $g_m = 50$ mA/V. Determine the internal current (in terms of i_S) and the shunt impedance of the Norton equivalent circuit with respect to the terminals 1, 1′.
3. A step function of amplitude E is applied to the terminals 1,1′ of the network shown in Fig. 2.80. Determine (a) the voltage $v(t)$ developed across the capacitor C, and (b) the initial rate of change of the input current $i(t)$.
   Assume that the capacitor is initially uncharged.

† To be more precise, we should place a capacitance equal to $C_{b'c}$ across the load resistance R_L in Fig. 2.77 (c). However, provided that at frequencies of interest $1 \gg \omega C_{b'c} R_L$, then we are justified in using the simplified equivalent circuit of Fig. 2.77 (c).

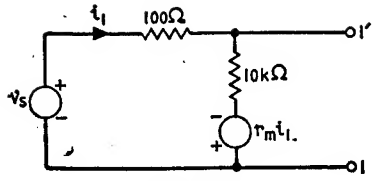

Fig. 2.78

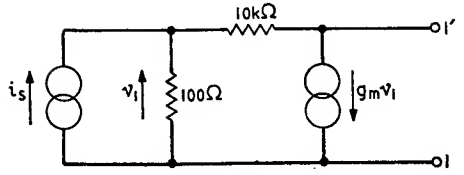

Fig. 2.79

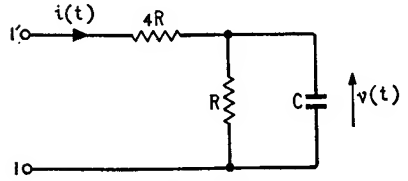

Fig. 2.80

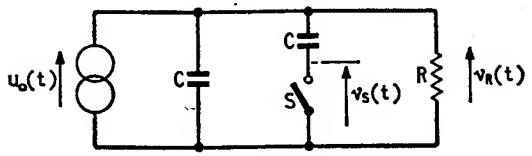

Fig. 2.81

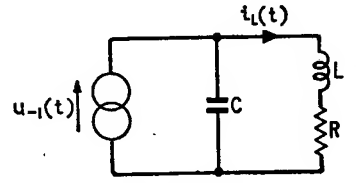

Fig. 2.82

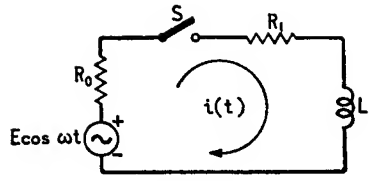

Fig. 2.83

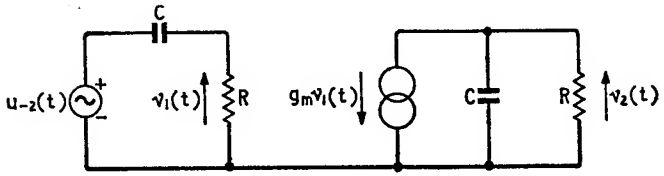

Fig. 2.84

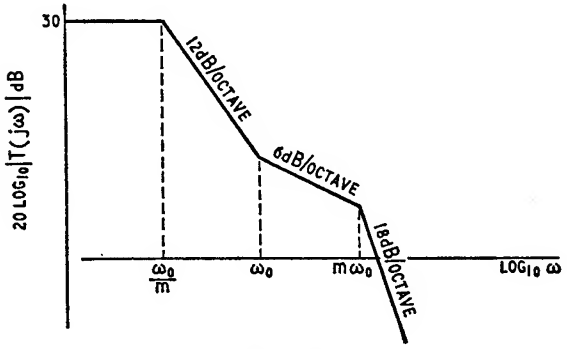

Fig. 2.85

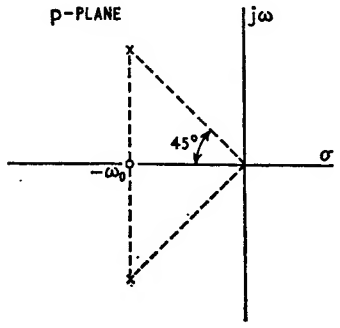

Fig. 2.86

4. In the network of Fig. 2.81 the switch S is opened at time $t = 0^+$, that is, just after the unit-impulse current $u_0(t)$ is over. Determine the voltages $v_R(t)$ and $v_S(t)$ developed across the resistor R and the switch S, respectively, for $t \geqslant 0^+$.
5. A unit-step current is applied to the parallel LRC network of Fig. 2.82. Assuming that the initial conditions are zero and that $R^2 < 4L/C$, determine the current $i_L(t)$ through the inductor L.
6. The switch S in the circuit of Fig. 2.83 is closed at $t = 0$. Evaluate the resulting current $i(t)$ for $t \geqslant 0^+$.
7. A unit-ramp voltage $u_{-2}(t)$ is applied to the network of Fig. 2.84, containing the controlled source $g_m v_1(t)$. Determine the voltages $v_1(t)$ and $v_2(t)$, assuming that both capacitors are initially uncharged.
8. Sketch the gain-frequency and phase-frequency characteristic for the transfer function

$$G(p) = \frac{50(1 + 0{\cdot}2p)}{(1 + p)(1 + 0{\cdot}5p)(1 + 0{\cdot}1p)}$$

9. The characteristic of Fig. 2.85 shows the approximation to the open-loop gain function $T(j\omega)$ of a feedback amplifier. Determine $T(j\omega)$ and sketch the associated phase-frequency characteristic, given that the parameter $m = 10$.
10. The diagram of Fig. 2.86 shows the pole-zero pattern for the transfer function of an amplifier stage. Determine the angular frequency at which the gain of the stage drops by 3dB below its low frequency. What is the associated phase angle at this cut off frequency?
11. Show that the *twin-T network* of Fig. 2.87 has a zero output voltage for an input angular frequency of $1/CR$. (Hint: The twin-T network can be regarded as two sub-networks connected in parallel at their input as well as output ports).
12. Show that the *bridged-T network* of Fig. 2.88 has a null angular frequency at $\omega_0 = \sqrt{[2/LC]}$ provided that $2rRC = L$.
13. A transistor has the following values for its common emitter h-parameters

$$h_{11e} = 1400\ \Omega$$
$$h_{12e} = 5 \times 10^{-4}$$
$$h_{21e} = 49$$
$$h_{22e} = 25\ \mu\mho$$

It is operated as a common base stage with a voltage source of internal resistance 100 Ω and a load resistance 10 kΩ. Evaluate its input and output impedances, voltage and current gains.

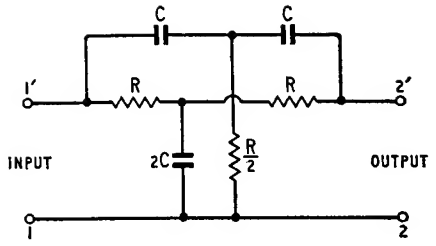

Fig. 2.87

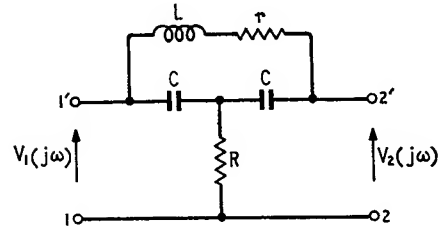

Fig. 2.88

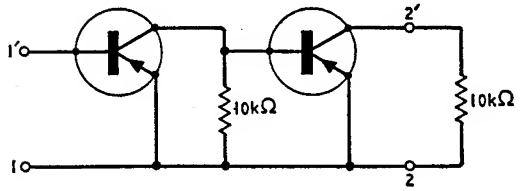

Fig. 2.89

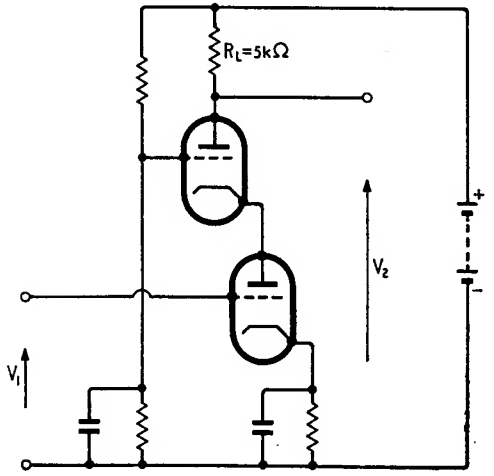

Fig. 2.90

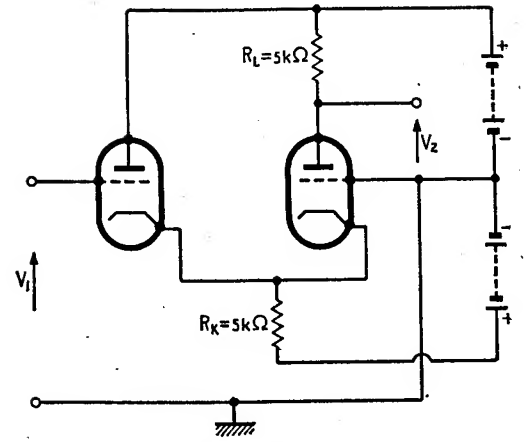

Fig. 2.91

14. The two-stage transistor amplifier of Fig. 2.89 uses a cascade of two identical common emitter stages, each one having the common emitter *h*-parameters of Problem 13. Determine the input impedance and voltage gain of the complete amplifier. (Hint: Convert the *h*-parameters into *a*-matrix parameters, then evaluate the overall *a*-matrix of the cascade).
15. Fig. 2.90 shows the circuit diagram of a *cascode* amplifier. Evaluate its overall voltage gain, given that the two triode valves are identical having the parameters $r_a = 10\ \text{k}\Omega$ and $g_m = 4\text{mA/V}$. It is assumed that the capacitors are sufficiently large to have negligible effects at the operating frequency. (Hint: The cascode can be regarded as a common cathode and common grid stage connected in tandem).
16. Determine the overall voltage gain of the *cathode coupled pair* shown in Fig. 2.91. The two valves are identical having the parameters given in Problem 15.
(Hint: The cathode coupled pair can be regarded as a cascade of common anode and common grid stages).
17. Show that the input capacitance of a common anode stage, with a load resistance R_L is equal to

$$C_{ga} + C_{gk}(1 - K_V)$$

where

$$K_V = \frac{\mu R_L}{r_a + (1 + \mu)R_L}$$

Comment on the practical significance of the result.

18. The power gain of a two-port network is defined as the ratio of power output to power input. In terms of the z-parameters show that a purely resistive two-port network has a maximum power gain $K_{p\,\max}$ given by

$$K_{p\,\max} = \left(\frac{z_{21}}{\sqrt{(z_{11}z_{22})} + \sqrt{(\Delta z)}}\right)^2$$

and that this value occurs when the terminating load resistance is equal to

$$\sqrt{(\Delta_z z_{22}/z_{11})}$$

Determine the maximum power gain of a certain two-port network having the following z-parameters.

$$z_{11} = 625\ \Omega$$
$$z_{12} = 601\ \Omega$$
$$z_{21} = 0{\cdot}98\ \text{M}\Omega$$
$$z_{22} = 1\ \text{M}\Omega$$

and hence state whether or not the network is active.

REFERENCES

1. GUILLEMIN, E. A., *Communication Networks*, Vol. 2, Wiley, New York (1935).
2. DE PIAN, L., *Linear Active Network Theory*, Prentice-Hall, Englewood Cliffs (1962).
3. TELLEGEN, B. D. H., 'The Gyrator, A New Electric Network Element', *Philips Research Rep.*, 3, 81 (1948).
4. ANGELO, E. J., *Electronic Circuits*, McGraw-Hill, New York (1958).
5. HAKIM, S. S., *Junction Transistor Circuit Analysis*, Iliffe Books (1962).
6. MASON, S. J., and ZIMMERMANN, H. J., *Electronic Circuits, Signals and Systems*, Wiley, New York (1960).
7 REZA, F. M., and SEELY, S., *Modern Network Analysis*, McGraw-Hill, New York (1959).
8. SESHU, S., and BALABANIAN, N., *Linear Network Analysis*, Wiley, New York (1959).

CHAPTER 3

Theory of Feedback

The performance of a feedback circuit, like any other electrical circuit, can be determined by applying the conventional mesh and nodal methods of circuit analysis, the basic principles of which are not in any way affected by the presence of feedback in the particular circuit. Alternatively, we can apply the matrix methods developed in Section 2.5.3.

In this chapter, however, we shall develop yet another method of circuit analysis which has certain attractive features when the feedback is objectively applied to a circuit: we shall see that the method not only spotlights the presence of feedback but also provides a quantitative measure for the various effects of feedback on the behaviour of the circuit.

3.1 Classical feedback theory

Basically a feedback circuit consists of an active *internal amplifier* and a passive 'feedback network' component interconnected in the manner illustrated in the idealised 'block diagram' of Fig. 3.1. The internal amplifier provides signal amplification in the forward direction (i.e. from input to output). The feedback network, on the other hand, provides a means of monitoring the actual state of the output signal, it does this by feeding back to the input of the circuit a controlled fraction of the output signal.

If the internal amplifier has a forward gain K, then by definition

$$K = \frac{V_L}{V_D} \tag{3.1}$$

where V_L is the output (or load) signal and V_D is the 'error signal' representing the difference between the source signal V_S and the feedback signal V_R. Further, if β is the *reverse transfer function* of the feedback network, the signal V_R returned to the input is given by

$$V_R = \beta V_L \tag{3.2}$$

In Fig. 3.1 the small circle containing the minus sign signifies that differencing action takes place at the input end of the feedback circuit. Therefore at this junction we have

$$\begin{aligned} V_D &= V_S - V_R \\ &= V_S - \beta V_L \end{aligned} \tag{3.3}$$

Eliminating V_D between Equations 3.1 and 3.3 we find that the

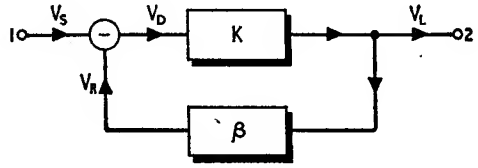

Fig. 3.1. Block diagram of basic negative feedback circuit

closed-loop gain K' (i.e. the gain with feedback) of the circuit of Fig. 3.1 is equal to

$$\begin{aligned} K' &= \frac{V_L}{V_S} \\ &= \frac{K}{1 + \beta K} \end{aligned} \tag{3.4}$$

The product term βK, which we shall denote by T, is termed the *open-loop gain* of the feedback circuit; it is equal to the overall gain of the internal amplifier and the feedback network if connected in cascade.

Alternatively, we can define the open-loop gain as the ratio of the feedback signal V_R to the error signal V_D. This definition follows simply from the fact that the feedback signal is equal to βV_L and the error signal is equal to (V_L/K); their ratio is

$$\frac{V_R}{V_D} = \frac{\beta V_L}{V_L/K} = \beta K = T$$

The term $1 + \beta K$ is a measure of the amount of applied feedback and is referred to as the *feedback factor* F; it is related to the open-loop gain by

$$\begin{aligned} F &= 1 + \beta K \\ &= 1 + T \end{aligned} \tag{3.5}$$

If the phase of the feedback signal V_R is such that it opposes the

source signal V_S, the applied feedback is said to be *negative* or *degenerative*. If, on the other hand, the phase of the feedback signal is such that it aids the source signal, the applied feedback is *positive* or *regenerative*. Therefore, in a negative feedback circuit the feedback factor has a value greater than unity with the result that the closed-loop gain K' is less than the gain K without feedback. In a positive feedback circuit the feedback factor $F < 1$, and accordingly K' can be greater than K.

3.1.1 SENSITIVITY

In a negative feedback amplifier, if the magnitude of the open loop gain is large compared to unity, we find that $1 + \beta K$ closely approaches the value βK and accordingly Equation 3.4 reduces to

$$K' \simeq \frac{1}{\beta} \tag{3.6}$$

which states that the closed-loop gain is essentially determined by the passive feedback network and becomes practically independent of variations in the parameters of the valves or transistors that constitute the internal amplifier. This important result can be also explained in physical terms as follows. As the open-loop gain is increased in magnitude, the error signal becomes progressively smaller, and the feedback signal approximates more closely to the source signal. In this situation we find that, with the error signal negligibly small, $V_S \simeq \beta V_L$ which is equivalent to saying that the closed-loop gain of the feedback amplifier is effectively equal to $1/\beta$.

In fact, even when the magnitude of the open-loop gain is not large, we find that the effect of variations in the internal amplifier parameters is reduced as a result of the applied negative feedback. To demonstrate this, let us differentiate both sides of Equation 3.4 with respect to the gain K of the internal amplifier obtaining

$$\frac{dK'}{dK} = \frac{1}{(1 + \beta K)^2} \tag{3.7}$$

In assessing the effect of changes in the gain K of the internal amplifier it is convenient to consider the *sensitivity* S_K of the closed-loop gain K' of the feedback amplifier. S_K is defined as the ratio of a fractional change in K' to the fractional change in K, which produced the initial change in K'. Provided that all changes concerned are small, we get

$$S_K = \frac{dK'/K'}{dK/K} \tag{3.8}$$

Then, noting that $\beta K = T$ we obtain the following important result from Equations 3.4 to 3.8

$$S_K = \frac{1}{1+T} \tag{3.9}$$

This states that the effectiveness of the applied negative feedback in minimising the influence of a change in the gain K depends solely on the magnitude of the open-loop gain T which is under the designer's control. As an example, let us suppose that owing to temperature

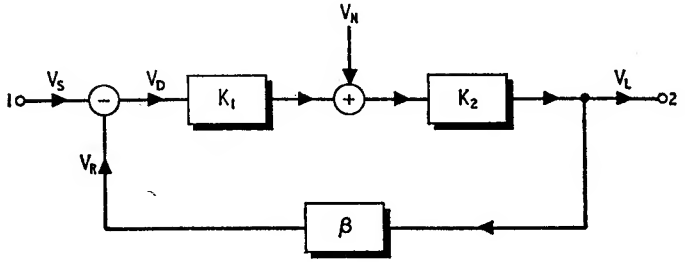

Fig. 3.2. Feedback circuit with extraneous signal

variations, aging of components or manufacturing tolerances, the gain K of the internal amplifier changes by 10%, and that the corresponding change in the closed-loop gain K' is required not to exceed 1%. From Equation 3.9 we find that $1 + T = 10$, that is, $T = 9$. The reduction in the effect of parameter variations has, of course, been achieved at the cost of reduced gain.

3.1.2 HARMONIC DISTORTION AND NOISE

Another important property of negative feedback is that it reduces the effects of harmonic distortion and noise generated inside the internal amplifier. To appreciate this effect, let us consider Fig. 3.2 where the internal amplifier is assumed to consist of two stages having forward gains K_1 and K_2. The extraneous signal source V_N represents harmonic distortion or noise introduced at an arbitrary point in the interior of the amplifier component. From Fig. 3.2 we see that

$$\begin{aligned} V_L &= K_2(K_1 V_D + V_N) \\ &= KV_D + K_2 V_N \end{aligned} \tag{3.10}$$

where $K_1 K_2 = K$ is the overall forward gain of the internal amplifier. Using Equation 3.10 together with Equations 3.2 and 3.3 which still apply to the circuit of Fig. 3.2, we find that the load voltage V_L is

$$V_L = \frac{KV_S}{1+\beta K} + \frac{K_2 V_N}{1+\beta K} \tag{3.11}$$

The first term on the right hand side of this equation represents the contribution of the source signal V_S to the output, whereas the second term represents the contribution of the noise signal V_N. The ratio of these two contributions gives the output *signal to noise ratio* with feedback; from Equation 3.11 we see that it is equal to KV_S/K_2V_N. In the absence of feedback the signal V_R is zero making $V_S = V_D$ in which case we find from Equation 3.10 that the output signal to noise ratio without feedback is also equal to KV_S/K_2V_N. Hence, the output signal to noise ratio is unaffected by the application of feedback if the source signal V_S is maintained constant, with and without feedback. If, however, negative feedback is applied and at the same time the source signal V_S is increased such that the load signal V_L remains at the same level it had before the application of feedback, then from Equations 3.10 and 3.11 we see that the net effect at the output terminal will be to reduce the contribution of the extraneous signal V_N by the factor $1/(1 + \beta K)$. In other words, provided that the output power is maintained the same with and without feedback, the application of negative feedback results in a reduction in the harmonic distortion and noise component at the output. This improvement in circuit performance is, however, possible only if the extraneous signal V_N is generated within the internal amplifier. Thus if the extraneous signal originates at the input of the internal amplifier, we have a case equivalent to $K_1 = 1$ and $K_2 = K$ in Fig. 3.2. Then the signal and noise components add directly and are amplified by the same amount, in which case the application of negative feedback would prove to be of no help at all.

3.2 Basic feedback circuit types

The internal amplifier and feedback network components of a feedback circuit are both essentially two-port structures which can be interconnected in any of the four basic ways illustrated in Figs. 3.3 to 3.6. In the circuit of Fig. 3.3 the two components are connected in series at their input as well as output ports; it is therefore referred to as the *series-series* feedback circuit. In Fig. 3.4 the internal amplifier and feedback network are connected in parallel at both their input and output ports; this feedback circuit is thus referred to as the *shunt-shunt* type. Similarly, the feedback circuit of Fig. 3.5 is of the *series-shunt* type, and that of Fig. 3.6 is of the *shunt-series* type.

In both the series-series and the shunt-series feedback circuits the feedback signal is proportional to the load current; in such cases the applied feedback is sometimes referred to as *current feedback*. On the other hand, in the shunt-shunt and series-shunt feedback circuits

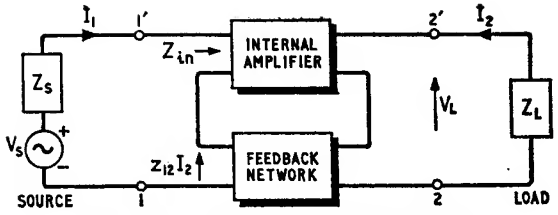

Fig. 3.3. Series-series feedback circuit

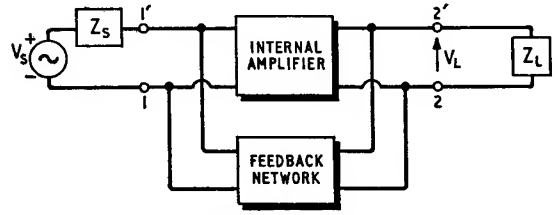

Fig. 3.4. Shunt-shunt feedback circuit

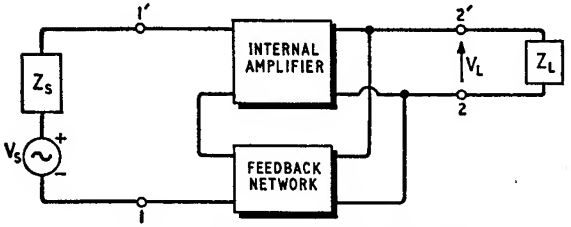

Fig. 3.5. Series-shunt feedback circuit

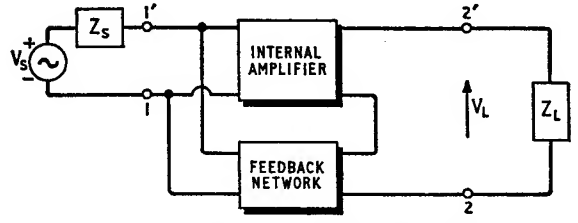

Fig. 3.6. Shunt-series feedback circuit

the feedback signal is proportional to the load voltage; accordingly the applied feedback is referred to as *voltage feedback.*

The closed-loop gain of each of the basic feedback circuits of Figs. 3.3 to 3.6 can be determined from Equation 3.4 provided the following assumptions are satisfied:

1. The internal amplifier transmits signals in the forward direction only.
2. The feedback network transmits signals in the reverse direction only.
3. The feedback network presents negligible loading to the internal amplifier at both the input and output ports.

Then in the case of the series-series feedback circuit of Fig. 3.3 we find that

$$(Z_S + Z_{in})I_1 = V_S - z_{12}I_2 \tag{3.12}$$

where z_{12} is the reverse open-circuit transfer impedance of the feedback network, and Z_{in} is the input impedance of the internal amplifier. Comparing the terms of this equation with those of Equation 3.3 we deduce that the error signal V_D is equal to $(Z_S + Z_{in})I_1$, and the feedback signal V_R is equal to $z_{12}I_2$. Therefore, the ratio of the feedback signal to error signal gives the open-loop gain of the series–series feedback circuit of Fig. 3.3 to be

$$T = \frac{z_{12}I_2}{(Z_S + Z_{in})I_1}$$

$$= \frac{z_{12}K_I}{Z_S + Z_{in}} \tag{3.13 (a)}$$

where $K_I = I_2/I_1$ is the current gain of the internal amplifier.

In a similar manner we can show that for the shunt—shunt feedback circuit of Fig. 3.4, the open-loop gain is given by

$$T = \frac{y_{12}K_V}{Y_S + Y_{in}} \tag{3.13 (b)}$$

where y_{12} is the reverse short-circuit transfer admittance of the feedback network, K_V is the voltage gain of the internal amplifier and Y_{in} is its input admittance. $Y_S = 1/Z_S$ is the source admittance.

For the series-shunt feedback circuit of Fig. 3.5, we have

$$T = \frac{h_{12}Z_{21}}{Z_S + Z_{in}} \tag{3.14 (a)}$$

where h_{12} is the reverse open-circuit voltage transfer function of the feedback network, and Z_{21} is the forward transfer impedance of the internal amplifier.

Lastly, for the shunt-series feedback circuit of Fig. 3.6 we find that

$$T = \frac{g_{12}Y_{21}}{Y_S + Y_{in}} \qquad (3.14\,(b))$$

where g_{12} is the reverse short-circuit current transfer function of the feedback network, and Y_{21} is the forward transfer admittance of the internal amplifier. It must be, however, emphasised that Y_{21} is not the same as the reciprocal of Z_{21}.

It is of particular interest to note that if at the input (or output) port the internal amplifier and feedback network are connected together in parallel, the feedback signal is reduced to zero by putting the terminating source (or load) impedance equal to zero. If, on the other hand, the two components are connected together in series at their input (or output) port, then the feedback signal is reduced to zero by putting the source (or load) impedance equal to infinity.

3.3 Limitations of the classical feedback theory and the need for a more generalised feedback theory

The classical feedback theory presented in Section 3.1 is based on the fundamental assumption that there exists a clear-cut separation between the K-network (i.e. the internal amplifier component) and the β-network (i.e. the feedback network component), each one having a prescribed circuit performance independent of the other. In many circuits, however, it is found that the circuit elements constituting the β-network also form part of the K-network. Further, in a *multiple-loop feedback circuit*, where signals can be returned to some point inside the internal amplifier by more than one path, it may be quite difficult to separate the circuit into β- and K-networks.

Accordingly we find that the true meaning of the gain K without feedback is somewhat vague in the sense that when evaluating K in practice it is not quite clear whether we should just simply remove the feedback network, or whether we should make some allowances for the loading effects of the feedback network at the input and output ports of the amplifier, and if so, what these allowances ought to be.

Another limitation of the classical feedback theory is that it does not account for the direct transmission from the source to the load, which can in practice occur through the feedback network. In certain instances this direct transmission can be quite appreciable.

The above shortcomings can, in the case of the four basic feedback circuits of Figs. 3.3 to 3.6, be overcome by using the matrix methods of Section 2.5.3. There it was shown that the overall behaviour of each of these coupled network arrangements can be determined by describing the individual network components with a set of matrix parameters appropriate to the particular type of coupling. Thus the series-series feedback circuit of Fig. 3.3 can be replaced by a single

two-port network having a z-matrix equal to the sum of the z-matrices of the internal amplifier and feedback network. The shunt-shunt feedback circuit of Fig. 3.4 is equivalent to a single two-port network whose y-matrix is equal to the sum of the y-matrices of the two network components. The series-shunt feedback circuit of Fig. 3.5 is equivalent to a single two-port network having an h-matrix equal to the sum of the h-matrices of the internal amplifier and the feedback network. The shunt-series feedback

Fig. 3.7. Graphical representation of Equation 3.15

circuit of Fig. 3.6 is equivalent to a single two-port network whose g-matrix is equal to the sum of the g-matrices of the two network components. Having, in each case, determined the matrix parameters of the equivalent two-port network, then the input and output impedances, voltage and current gains of the particular feedback circuit type can be evaluated from Table 2.4.

Alternatively, we can determine the performance of the feedback circuit by using Bode's *generalised feedback theory* which applies to any circuit irrespective of its complexity, and has none of the limitations of the classical theory. This generalised feedback theory can be developed in terms of the *circuit determinant* as originally carried out by H. W. Bode[1] or in terms of *signal flow graphs* as first proposed by S. J. Mason[2] and later extended by J. G. Truxal.[3] The use of signal flow graphs has the advantage of providing an invaluable aid in interpreting and understanding the various results. For this reason we shall adopt the Mason-Truxal approach in developing the generalised feedback theory.

3.4 Signal flow graphs

Consider two variables x_0 and x_1, which can signify voltage or current signals, related as follows

$$x_1 = t_{01}x_0 \qquad (3.15)$$

where t_{01} is a coefficient defining the dependence of x_1 on x_0. This simple relationship can be portrayed graphically as in Fig. 3.7 where the *nodes* x_0 and x_1 represent the respective variables, and the *branch* directed from the node x_0 to node x_1 expresses the dependence of variable x_1 on x_0.

As a second example let us suppose that

$$x_3 = t_{03}x_0 + t_{13}x_1 + t_{23}x_2 \qquad (3.16)$$

This equation can be represented graphically as in Fig. 3.8.

For our next example we shall consider the graphical representation of the following set of equations

$$\left.\begin{aligned} x_1 &= t_{01}x_0 + t_{21}x_2 \\ x_2 &= t_{12}x_1 + t_{32}x_3 \end{aligned}\right\} \qquad (3.17)$$

Fig. 3.9 (a) shows the graph of the first line of these equations, and Fig. 3.9 (b) shows that of the second line. By superimposing these diagrams, as in Fig. 3.9 (c), we obtain the complete graph of Equation 3.17.

The diagrams of Figs. 3.7 to 3.9 are known as *signal flow graphs;* they clearly illustrate the flow of signals between the various nodes. A variable represented by a node is known as a *node signal.* The coefficient t_{ij} defining the dependence of node signal x_j on node signal x_i is referred to as a *branch transmittance.*

From the defining Equations 3.15 to 3.17 and the corresponding signal flow graphs we deduce that such graphs have the following properties:

1. The nodes represent the variables of the system defined by the given set of equations.
2. Signal flows along a branch only in the direction defined by the arrow and is multiplied by the transmittance of that branch.
3. A node signal is equal to the sum of all node signals entering the corresponding node.
4. A node signal is applied to all branches leaving the particular node independently of transmittances of the outgoing branches.

3.5 Basic feedback flow graph

In developing the generalised feedback theory let us first consider Fig. 3.10 where the two-port network N is assumed to represent a feedback circuit driven from a voltage source V_S of internal impedance Z_S, and having a load of impedance Z_L connected across its output port. Within the network N we necessarily find one or more controlled sources, the type of which depends on the equivalent circuit representation adopted for the valves or transistors that make up the internal amplifier component of the feedback circuit. If, in the general case, θ_a denotes the control signal and ϕ_b denotes the controlled source, then we have that $\phi_b = k\theta_a$ where k is the control parameter. The dimensions of the variables θ_a, ϕ_b and the parameter k depend on the type of the controlled source, as shown in Table 3.1. As an example consider Fig. 3.11 where we have selected a voltage-controlled voltage source inside the network N. In this case we see that $\theta_a = V_a$, $k = \mu$ and $\phi_b = \mu V_a$.

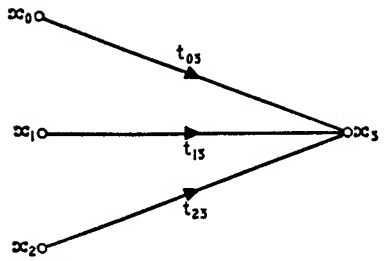

Fig. 3.8. Graphical representation of Equation 3.16

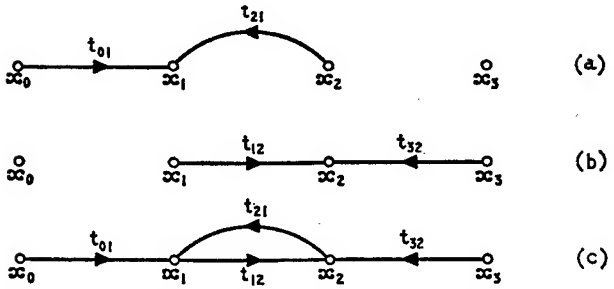

Fig. 3.9. (a) Graph of first line of Equation 3.17, (b) Graph of second line of Equation 3.17, (c) Graph of complete set of Equation 3.17

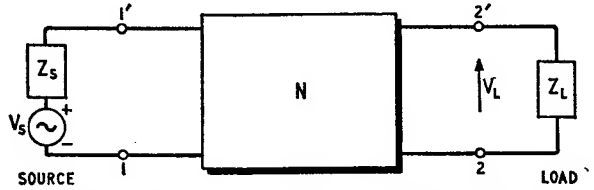

Fig. 3.10. Two-port network N assumed to represent a feedback circuit

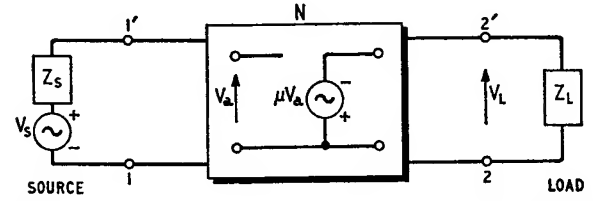

Fig. 3.11. Feedback circuit with a voltage-controlled voltage source selected for special consideration

Table 3.1 POSSIBLE DIMENSIONS OF θ_a, ϕ_b AND k

	Control signal θ_a	*Controlled source* ϕ_b	*Controlled parameter* k
Voltage-controlled voltage source	Voltage	Voltage	Dimensionless
Voltage-controlled current source	Voltage	Current	Admittance
Current-controlled current source	Current	Current	Dimensionless
Current-controlled voltage source	Current	Voltage	Impedance

Assuming that the circuit is linear, it follows from the superposition theorem that we can add the separate effects of the independent voltage source V_S and controlled source ϕ_b upon both the load signal V_L and control signal θ_a; thus

$$\left.\begin{aligned} V_L &= t_{sl}V_S + t_{bl}\phi_b \\ \theta_a &= t_{sa}V_S + t_{ba}\phi_b \end{aligned}\right\} \tag{3.18}$$

where

$$\phi_b = k\theta_a \tag{3.19}$$

From Equations 3.18 we obtain the following definitions for the coefficients t_{sl}, t_{bl}, t_{sa} and t_{ba}

$$\left.\begin{aligned} t_{sl} &= \left(\frac{V_L}{V_S}\right)_{\phi_b=0} \\ t_{bl} &= \left(\frac{V_L}{\phi_b}\right)_{V_S=0} \\ t_{sa} &= \left(\frac{\theta_a}{V_S}\right)_{\phi_b=0} \\ t_{ba} &= \left(\frac{\theta_a}{\phi_b}\right)_{V_S=0} \end{aligned}\right\} \tag{3.20}$$

Therefore, by setting $V_S = 1$ and $\phi_b = 0$ we find that $V_L = t_{sl}$ and $\theta_a = t_{sa}$. Further, when $V_S = 0$ and $\phi_b = 1$ we find that $V_L = t_{bl}$ and $\theta_a = t_{ba}$.

With the aid of the rules given in Section 3.4 we can construct the signal flow graph of Fig. 3.12 for Equations 3.18 and 3.19. In this diagram we see that the transmittance t_{sl} accounts for all paths from the independent source to the load that by-pass the controlled source; it is therefore termed the *direct transmittance*. We also see that the transmittance t_{ba} enables feeding a certain portion of the controlled source ϕ_b back to its control signal θ_a; it is therefore

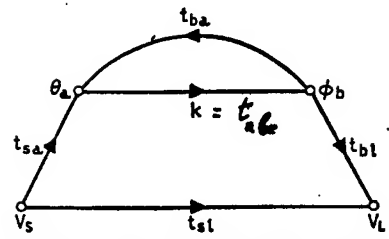

Fig. 3.12. Basic feedback flow graph

responsible for the feedback acting around the controlled source. If t_{ba} is zero, then there is no feedback acting around the controlled source.

The signal flow graph of Fig. 3.12 is the basis of the generalised feedback theory to be developed in the following sections. Accordingly, it is referred to as the *basic feedback flow graph.*

3.6 The concepts of return ratio, return difference and null return difference

3.6.1 RETURN RATIO AND RETURN DIFFERENCE

Let us suppose that the feedback loop, constituted by the two branches with transmittances k and t_{ba}, is opened as in Fig. 3.13. Also, let the source signal V_S be reduced to zero and a unit signal be transmitted from point a'. Then, from Fig. 3.13 we see that the signal returned to the point a is equal to kt_{ba}. The negative of this product term is referred to as the *return ratio* T, for the control parameter k, that is

$$T = -kt_{ba} \tag{3.21}$$

This relation suggests the following definition for the return ratio T. If we reduce the source signal V_S to zero, replace the controlled source $k\theta_a$ by an independent source k, and determine the value of the variable θ_a in the resulting system, then the return ratio T for the control parameter k is equal to $-\theta_a$.

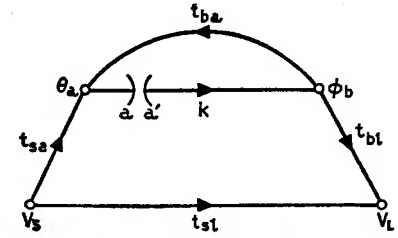

Fig. 3.13. Feedback loop broken for calculation of return difference

Going back to the signal flow graph of Fig. 3.13, the difference between the transmitted unit signal and the returned signal, under the condition $V_S = 0$, is referred to as the *return difference F*. It is related to the return ratio as follows

$$\begin{aligned} F &= 1 + T \\ &= 1 - kt_{ba} \end{aligned} \tag{3.22}$$

Therefore, the return difference with reference to the control parameter k is a quantitative measure of the amount of feedback acting around k. When there is no feedback acting around k, we have $t_{ba} = 0$ and $F = 1$.

The return ratio is thus analogous to the open-loop gain and the return difference is analogous to the feedback factor of Section 3.1. In a *single-loop feedback amplifier*, which involves a cascade of amplifier stages each providing signal transmission in the forward direction only, the return ratios with reference to the control parameters of the individual stages are exactly the same and equal to the open-loop gain of the feedback amplifier.†

It must be emphasised that the return difference F is measurable experimentally. This measurement is quite straightforward in the case of valve feedback amplifiers, because a triode or a pentode valve operated in its common cathode mode has a very high input impedance. On the other hand, in a transistor feedback amplifier the measurement of return difference is more complicated principally because of the internal feedback which exists within a transitor irrespective of the mode in which it is operated.‡ This internal feedback manifests itself in the interaction between the input and output ports of the stage.

3.6.2 NULL RETURN DIFFERENCE

Another useful concept is the *null return difference* F_N which is defined as the return difference that results when the source signal V_S is adjusted so as to reduce the load signal V_L to zero. Thus, with a unit signal transmitted from point a' of Fig. 3.13 we find that $\phi_b = k$ and

† According to H. W. Bode[1] the return ratio is the negative of the loop gain. On the other hand many modern writers (for example J. G. Truxal[3] and I. M. Horowitz[8]) on feedback control systems have chosen to define the loop gain as the negative of the actual transmittance round the feedback loop, and have consequently made it identical to the return ratio in the sense of Bode. In the present book we have followed the convention adopted by Truxal, Horowitz and others, and thereby unified the treatment of feedback circuits with other feedback control systems.

‡ For the measurement of return difference in transistor feedback amplifiers, refer to F. H. Blecher[4] and S. S. Hakim.[5,11]

$$\left.\begin{aligned} V_L &= t_{sl}V_S + kt_{bl} \\ \theta_a &= t_{sa}V_S + kt_{ba} \end{aligned}\right\} \tag{3.23}$$

Putting $V_L = 0$ and solving for the corresponding value of returned signal θ_a, we obtain

$$\theta_a = kt_{ba} - \frac{kt_{bl}t_{sa}}{t_{sl}} \tag{3.24}$$

The null return difference is equal to the unit transmitted signal minus the returned signal of Equation 3.24; thus

$$F_N = 1 - kt_{ba} + \frac{kt_{bl}t_{sa}}{t_{sl}} \tag{3.25}$$

3.7 Closed-loop circuit response

3.7.1 CLOSED-LOOP GAIN

When the feedback loop is closed as in Fig. 3.12, the ratio V_L/V_S is equal to the *closed-loop gain K'*. From Equations 3.18 and 3.19

$$\begin{aligned} K' &= \frac{V_L}{V_S} \\ &= t_{sl} + \frac{kt_{bl}t_{sa}}{1 - kt_{ba}} \end{aligned} \tag{3.26}$$

Comparing this expression with the basic feedback Equation 3.4 we see that the product term $kt_{bl}t_{sa}$ is analogous to the *gain without feedback K*, and $-kt_{ba}$ is analogous to the open-loop gain βK. However, the direct transmittance t_{sl} has no counterpart in the classical feedback theory based on Equation 3.4. As we shall see later, many practical feedback circuits do in fact exhibit a finite value for t_{sl}.

Multiplying Equation 3.25 by the expression $t_{sl}/(1 - kt_{ba})$ and then using Equations 3.22 and 3.26 we see that the closed-loop gain, the direct transmittance and the two return differences are related simply by the expression

$$K' = t_{sl}\frac{F_N}{F} \tag{3.27}$$

A special case occurs when the direct transmittance t_{sl} is zero, then the basic feedback flow graph of Fig. 3.12 reduces to the form shown in Fig. 3.14, and Equation 3.26 simplifies to

$$K' = \frac{kt_{bl}t_{sa}}{1 - kt_{ba}} \tag{3.28}$$

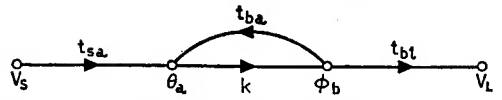

Fig. 3.14. Feedback flow graph for the special case of zero direct transmittance

which has a form similar to that of Equation 3.4 derived from the classical feedback theory.

3.7.2 SENSITIVITY AGAIN

Suppose that the control parameter k changes by a small amount dk. The corresponding change in the closed-loop gain is found from Equation 3.26 to be

$$dK' = \frac{\partial K'}{\partial k}\,dk \tag{3.29}$$

$$= \frac{t_{bl}t_{sa}}{(1 - kt_{ba})^2}\,dk$$

Hence, the sensitivity S_k of the closed-loop gain K' with respect to the control parameter k is given by

$$S_k = \frac{dK'/K'}{dk/k}$$

$$= \frac{kt_{bl}t_{sa}}{K'(1 - kt_{ba})^2} \tag{3.30}$$

Using Equations 3.22, 3.26 and 3.30, we get

$$S_k = \frac{1}{F}\left(1 - \frac{t_{sl}}{K'}\right) \tag{3.31}$$

Another useful expression relating the sensitivity S_k to the two return differences F and F_N is obtained by eliminating t_{sl}/K' between Equations 3.27 and 3.31; thus

$$S_k = \frac{1}{F} - \frac{1}{F_N} \tag{3.32}$$

Normally the closed-loop gain K' is very large compared to the direct transmittance t_{sl}; this is equivalent to saying that the null return difference F_N is much larger than the return difference F. We therefore deduce the important result that the sensitivity S_k of the closed-loop gain with respect to the control parameter k is very

nearly equal to the reciprocal of the return difference with reference to k.

Remembering that the product term $kt_{sa}t_{bl}$ and the return difference in the generalised feedback theory, correspond to the forward gain K and the feedback factor in the classical feedback theory, respectively, we see that the sensitivity S_k calculated from the generalised theory is practically the same as the sensitivity S_K of the closed-loop gain with respect to the forward gain K of the internal amplifier, as calculated from the classical theory, provided that the direct transmittance t_{sl} is negligible.

3.7.3 DRIVING-POINT IMPEDANCE

We have discussed the effect of feedback on the gain of an amplifier. Another effect of feedback that is of fundamental engineering importance is its influence on the input and output impedances which

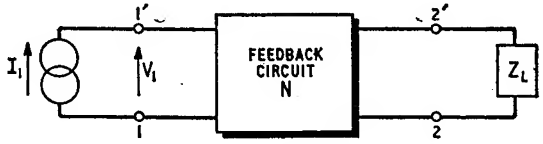

Fig. 3.15. Evaluation of input impedance Z_{in}'

the amplifier presents to its source and load, respectively. To evaluate this effect, consider first Fig. 3.15 where it is required to determine the input impedance Z_{in}'. For this evaluation a current source I_1 is connected across the input port 1,1′, then if V_1 is the resulting voltage developed across this port, we find that $Z_{in}' = V_1/I_1$.

Let us assume that a generalised controlled source $\phi_b = k\theta_a$ has been selected inside the network N. Then adding the separate effects of the sources I_1 and ϕ_b, we obtain

$$\left.\begin{aligned} V_1 &= Z^0{}_{in}I_1 + t_{b1}\phi_b \\ \theta_a &= t_{1a}I_1 + t_{1oc}\phi_b \end{aligned}\right\} \tag{3.33}$$

from which we deduce the following definitions for the various transmittances

$$\left.\begin{aligned} Z^0{}_{in} &= \left(\frac{V_1}{I_1}\right)_{\phi_b=0} \\ t_{b1} &= \left(\frac{V_1}{\phi_b}\right)_{I_1=0} \end{aligned}\right\} \tag{3.34}$$

$$\left.\begin{aligned} t_{1a} &= \left(\frac{\theta_a}{I_1}\right)_{\phi_b=0} \\ t_{1oc} &= \left(\frac{\theta_a}{\phi_b}\right)_{I_1=0} \end{aligned}\right\} \qquad (3.34)$$

Therefore, when $I_1 = 1$ and $\phi_b = 0$ we find that $V_1 = Z^0_{in}$ and $\theta_a = t_{1a}$; when $I_1 = 0$ and $\phi_b = 1$ we get $V_1 = t_{b1}$ and $\theta_a = t_{1oc}$. The coefficient Z^0_{in} is the value assumed by the impedance Z_{in}' when signal flow through the controlled source is reduced to zero. The coefficient t_{1oc} is the value of the transmittance t_{ba} which occurs when the input port 1,1′ is open-circuited.

The relationship $\phi_b = k\theta_a$ and Equation 3.33 lead to the signal flow diagram of Fig. 3.16 which is seen to be of the same form as that of Fig. 3.12. The signals I_1 and V_1 of Fig. 3.16 correspond to V_S and V_L of Fig. 3.12, respectively. Therefore, the ratio V_1/I_1 of Fig. 3.16 corresponds to the ratio V_L/V_S of Fig. 3.12, and so we can make use of Equation 3.27 for deducing an expression for the input impedance Z_{in}'.

Let F_{1oc} denote the return difference, with reference to the control parameter k, which results when the port 1,1′ of Fig. 3.15 is open-circuited. Since open-circuiting this port is equivalent to putting I_1 equal to zero, and since the node signal I_1 of Fig. 3.16 corresponds to the node signal V_S of Fig. 3.12, it follows that the *open-circuit return difference* F_{1oc} corresponds to the return difference F which is evaluated under the condition $V_S = 0$. Thus

$$F_{1oc} = 1 - kt_{1oc} \qquad (3.35)$$

Next, let F_{1sc} be the value of the return difference, with reference to k, which results when the port 1,1′ is short-circuited, that is, when $V_1 = 0$. Since the node signal V_1 of Fig. 3.16 corresponds to the node signal V_L of Fig. 3.12, it follows that the *short-circuit return difference* F_{1sc} corresponds to the null return difference F_N which is evaluated under the condition $V_L = 0$. The transmittances

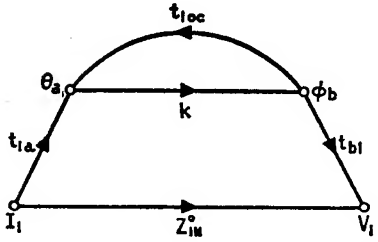

Fig. 3.16. Feedback flow graph for evaluattng Z_{in}'

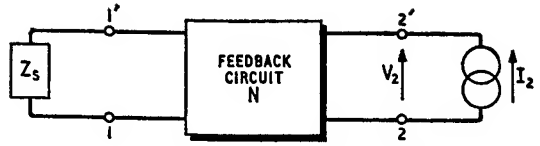

Fig. 3.17. Evaluation of output impedance Z_{out}'

Z^0_{in}, t_{1a}, t_{b1}, and t_{1oc} of Fig. 3.16, correspond to the transmittances t_{sl}, t_{sa}, t_{bl} and t_{ba} of Fig. 3.12 respectively. Hence, from Equation 3.25 we deduce that F_{1sc} is given by

$$F_{1sc} = 1 - kt_{1oc} + \frac{kt_{b1}t_{1a}}{Z^0_{in}} \qquad (3.36)$$

Having established the above correspondences between the signal flow diagrams of Figs. 3.12 and 3.16, we can now make use of Equation 3.27 and so deduce the following expression for the input impedance

$$Z_{in}' = Z^0_{in}\frac{F_{1sc}}{F_{1oc}} \qquad (3.37)$$

Similarly, we can show that the output impedance Z_{out}' measured at the port 2,2′ (see Fig. 3.17) is given by

$$Z_{out}' = Z^0_{out}\frac{F_{2sc}}{F_{2oc}} \qquad (3.38)$$

where Z^0_{out} is the value of Z_{out}' that results when the controlled source ϕ_b is reduced to zero. F_{2oc} and F_{2sc} are the return differences which result when the output port 2,2′ is open-circuited and short-circuited, respectively; both return differences being measured with reference to the control parameter k.

The important results of Equations 3.37 and 3.38 apply to all forms of feedback. Let us use them to study the following special cases:

(a) The series-series feedback circuit of Fig. 3.3. In such a circuit F_{1oc} and F_{2oc} are both equal to unity because the feedback signal is reduced to zero if either the input port or output port is open-circuited. Then Equations 3.37 and 3.38 simplify to

$$Z_{in}' = Z^0_{in}F_{1sc} \qquad (3.39\ (a))$$

$$Z_{out}' = Z^0_{out}F_{2sc} \qquad (3.39\ (b))$$

(*b*) The shunt-shunt feedback circuit of Fig. 3.4. In this case F_{1sc} and F_{2sc} are both equal to unity as the feedback signal is reduced to

zero by short-circuiting the input port or output port. Then Equations 3.37 and 3.38 reduce to

$$Z_{in}' = \frac{Z^0_{in}}{F_{ioc}} \qquad (3.40\,(a))$$

$$Z_{out}' = \frac{Z^0_{out}}{F_{oc}} \qquad (3.40\,(b))$$

We can therefore summarise the effects of feedback on the input and output impedances of an amplifier as follows:

1. The input impedance of a negative feedback amplifier is increased if the internal amplifier and feedback network are connected in series at the input port, while it is reduced if at this port they are connected in parallel.
2. The output impedance of a negative feedback amplifier is increased if the internal amplifier and feedback network are connected in series at the output port, and is reduced if at this port they are connected in parallel.
3. The effect of feedback on impedance at the input port is independent of the manner in which the internal amplifier and feedback network are coupled together at the output port, and vice versa.

As an illustration of this last point, we find that the input impedance of the shunt-series feedback circuit of Fig. 3.6 is given by Equation 3.40 (a), and its output impedance is given by Equation 3.39 (b). The input impedance of the series-shunt feedback circuit of Fig. 3.5 is given by Equation 3.39 (a) and its output impedance is given by Equation 3.40 (b).

3.8 Examples

We shall next illustrate the feedback theory developed above by considering the analysis and design of a number of different feedback circuits involving valves and transistors. In these various examples we shall find that the great virtue of the generalised feedback theory is that it enables the analysis of a given feedback circuit to be broken down to one of analysing a number of much simpler circuits. Also throughout the analysis a physical touch with the problem is maintained.

3.8.1 INTERNAL FEEDBACK IN TWO-PORT NETWORKS

In Section 2.5 we developed the z-, y-, h- and g-matrix representations for defining the external behaviour of a two-port network. In each

of these four cases the parameter with subscripts 21, that is the parameter z_{21}, y_{21}, h_{21}, or g_{21} accounts for the forward transmission of the input signal. On the other hand, the parameter with subscripts 12, that is, the parameter z_{12}, y_{12}, h_{12} or g_{12} accounts for signal transmission in the reverse direction, thereby giving rise to a certain amount of internal feedback within the two-port network. As an example, let us evaluate this internal feedback in terms of the h-parameters.

The diagram of Fig. 3.18 shows the h-parameter equivalent circuit for a double-terminated two-port network. The presence of internal

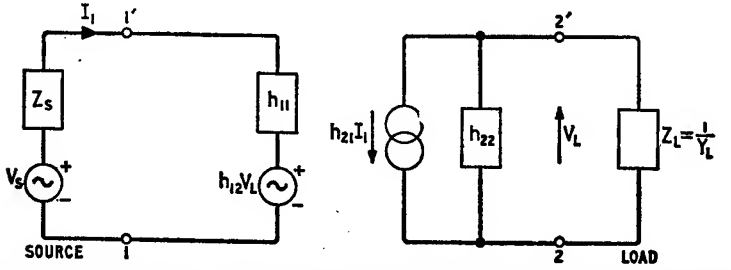

Fig. 3.18. h-parameters equivalent circuit for double-terminated two-port network

feedback is clearly seen to be due to the voltage-controlled voltage source $h_{12}V_L$, which provides a return path for the output signal back to the input port.

To evaluate the return difference F_h with reference to the control parameter h_{21} and so obtain a quantitative measure of the internal feedback existing within the two-port network, we put $V_S = 0$ and $h_{21}I_1 = 1$; then the resulting value of the returned signal I_1 is found to be $h_{12}/(h_{11} + Z_S)\,(h_{22} + Y_L)$. Hence

$$F_h = 1 - \frac{h_{12}h_{21}}{(h_{11} + Z_S)\,(h_{22} + Y_L)} \qquad (3.41)\,(a)$$

In this case we deduce that if either the source impedance Z_S is large or if the load impedance $Z_L = 1/Y_L$ is small, then F_h approaches unity and the effect of internal feedback is diminished.

It is to be emphasised that the amount of internal feedback existing with a two-port network is not unique in that it depends, amongst other factors, on the particular matrix representation adopted for describing its external circuit performance. Thus for specified source and load impedances, the return difference with reference to h_{21} can have quite a different value from the return difference F_y with reference to y_{21}, which is given by

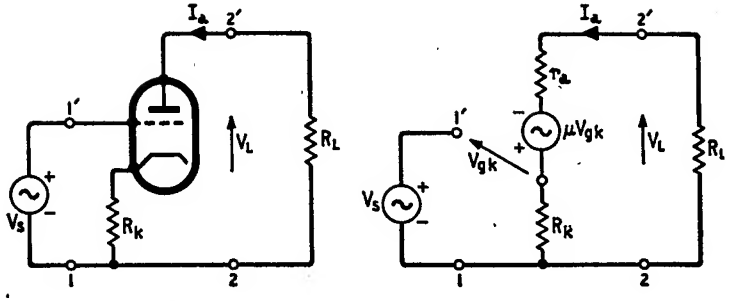

(a) (b)

Fig. 3.19. (a) Common cathode stage with local series feedback, (b) Equivalent circuit

$$F_y = 1 - \frac{y_{12}y_{21}}{(y_{11} + Y_S)(y_{22} + Y_L)} \qquad (3.41\text{ (b)})$$

where $Y_S = 1/Z_S$ is the source admittance.

As a numerical example, consider a transistor having the following common emitter *h*-parameters

$$h_{11e} = 1\text{ k}\Omega$$
$$h_{12e} = 0{\cdot}25 \times 10^{-3}$$
$$h_{21e} = 50$$
$$h_{22e} = 25\ \mu\text{℧}$$

and operated as a common emitter stage with $Z_S = 4$ kΩ, and $Z_L = 20$ kΩ (i.e. $Y_L = 50\ \mu$℧). From Equation 3.41 (a) we find that the return difference F_h with reference to h_{21e} has the corresponding value of 0·9. Therefore, it is to be anticipated that there would exist a certain degree of interaction between the input and output ports. The fact that the calculated value for F_h is less than unity indicates that the internal feedback existing in a common emitter stage is positive when it is represented by its *h*-parameter equivalent circuit.

If, on the other hand, we were to use the *y*-parameters to represent the common emitter stage and calculate the return difference F_y with reference to y_{21e}, we shall find from Equation 3.41 (b) that $F_y = 1{\cdot}16$. This result assumes that the terminating admittances for the stage are, as before, $Y_S = 0{\cdot}25$ m℧ and $Y_L = 50\ \mu$℧, and that the transistor has the following common emitter *y*-parameters:

$$y_{11e} = 1\text{ m}\text{℧}$$
$$y_{12e} = -0{\cdot}25\ \mu\text{℧}$$

$$y_{21e} = 50\text{ m}\text{℧}$$
$$y_{22e} = 12{\cdot}5\ \mu\text{℧}$$

which are equivalent to the previous set of common emitter *h*-parameter values, as obtained from the matrix conversion Table 2.3. We therefore deduce that because F_y is greater than unity, the internal feedback existing in a common emitter stage is negative when it is represented by its *y*-parameters.

This example clearly illustrates the non-uniqueness of the return difference in active two-port networks in the sense that its value depends on the matrix representation adopted to describe the device.†

3.8.2 LOCAL FEEDBACK

When external feedback is applied to a single-stage amplifier (e.g. common cathode or common emitter stage) it is usually referred to as *local feedback*. We shall illustrate this form of feedback by considering three different examples.

Common cathode stage with local series feedback

In Fig. 3.19 (a) local feedback is applied to a common cathode stage by means of the resistor R_k connected in series with the cathode terminal and arranged to be common to the input and output ports. Replacing the valve with its equivalent circuit, we obtain the diagram of Fig. 3.19 (b) where we see that the control signal θ_a = the grid-cathode voltage V_{gk}, the control parameter k = the amplification factor μ, and the controlled source $\phi_b = \mu V_{gk}$.

To evaluate the transmittances t_{sa} and t_{sl} we put $V_S = 1$ and $\mu = 0$ (i.e. $\phi_b = 0$), in which case the anode current I_a is reduced to zero and V_{gk} becomes equal to V_S. Hence

$$\left.\begin{aligned} t_{sa} &= 1 \\ t_{sl} &= 0 \end{aligned}\right\} \qquad (3.42)$$

Next, to evaluate the transmittances t_{ba} and t_{bl} we put $V_S = 0$ and $\mu V_{gk} = 1$, as in Fig. 3.20. Then noting that the resulting values of V_{gk} and V_L are equal to t_{ba} and t_{bl}, respectively, we find directly that

$$t_{ba} = \frac{-R_k}{r_a + R_L + R_k} \qquad (3.43\text{ (a)})$$

† For a further discussion of the non-uniqueness of return difference in active two-port networks, see J. H. Mulligan.[6]

$$t_{bl} = \frac{-R_L}{r_a + R_L + R_k} \qquad (3.43\ (b))$$

Further, since $k = \mu$ it follows from Equations 3.22 and 3.43 (a) that the return difference F with reference to μ is given by

$$F = 1 + \frac{\mu R_k}{r_a + R_L + R_k} \qquad (3.44)$$

Also Equations 3.26, 3.42 and 3.43 give the closed-loop gain V_L/V_S

$$K' = \frac{-\mu R_L}{r_a + R_L + R_k(1 + \mu)} \qquad (3.45)$$

Common emitter stage with local series feedback

Consider next the transistor feedback circuit of Fig. 3.21 (a) where local series feedback has been applied to the common emitter stage by means of the resistor R_e connected in series with the emitter terminal. Replacing the transistor with its common emitter h-parameter equivalent circuit, we obtain the diagram of Fig. 3.21 (b). Here it is to be noted that the effect of the feedback parameter h_{12e} has been assumed negligible. This assumption is quite justified provided that the amount of feedback applied externally to the stage by the resistor R_e is large compared to the internal feedback due to h_{12e}, as is normally the case.

In Fig. 3.21 (b) we see that the control signal θ_a = the input base current I_b, the control parameter k = the forward current amplification factor h_{21e}, and the controlled source $\phi_b = h_{21e}I_b$. To evaluate the return difference with reference to h_{21e} we require to know the transmittance t_{ba}. This can be found from Fig. 3.22 where we have put $V_S = 0$ and $h_{21e}I_b = 1$. Normally the feedback resistance R_e is small compared to the total resistance $(R_L + 1/h_{22e})$, that is

$$(R_L + 1/h_{22e}) \gg R_e \qquad (3.46)$$

Then from Fig. 3.22 we find directly that the transmittance t_{ba}, which equals the returned signal I_b is given by

$$t_{ba} \simeq \frac{1}{1 + h_{22e}R_L} \cdot \frac{-R_e}{R_e + R_S + h_{11e}} \qquad (3.47)$$

Remembering that $k = h_{21e}$ and using Equations 3.22 and 3.47, the return difference F with reference to h_{21e} is

$$F \simeq 1 + \frac{h_{21e}R_e}{(1 + h_{22e}R_L)(R_e + R_S + h_{11e})} \qquad (3.48)$$

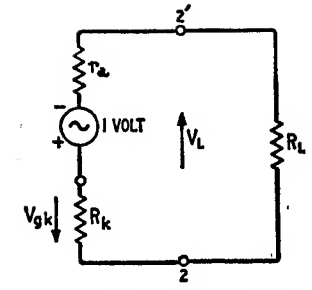

Fig. 3.20. Circuit for evaluating the transmittances t_{ba} and t_{bl} of common cathode stage with local series feedback

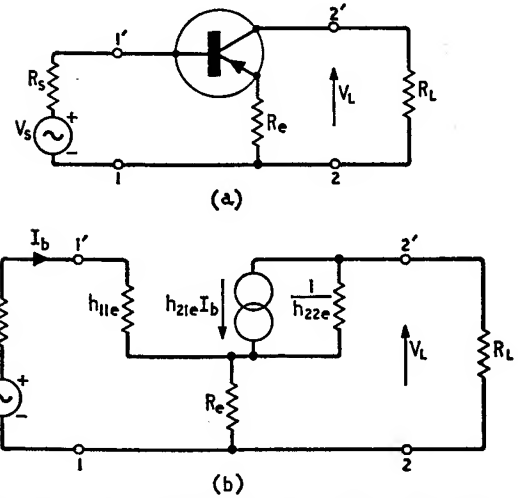

Fig. 3.21. (a) Common emitter stage with local series feedback, (b) Equivalent circuit

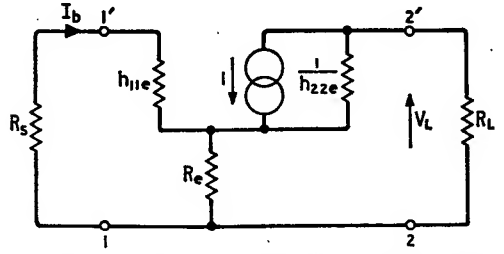

Fig. 3.22. Evaluation of transmittances t_{ba} and t_{bl} for common emitter stage with local series feedback

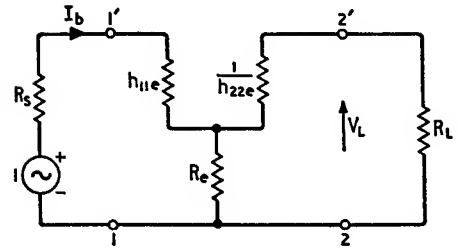

Fig. 3.23. Evaluation of transmittances t_{sa} and t_{sl} for common emitter stage with local series feedback

From Fig. 3.22 we also deduce that the transmittance t_{bl} which, by definition, equals V_L is

$$t_{bl} \simeq \frac{-R_L}{1 + h_{22e}R_L} \tag{3.49}$$

The transmittances t_{sa} and t_{sl} can be found from Fig. 3.23 where we have put $V_S = 1$ and $h_{21e} = 0$. Then noting that $I_b = t_{sa}$ and $V_L = t_{sl}$ and making use of the inequality of Equation 3.46, we get

$$t_{sa} \simeq \frac{1}{R_e + R_S + h_{11e}} \tag{3.50}$$

$$t_{sl} \simeq \frac{R_e}{R_e + R_S + h_{11e}} \cdot \frac{h_{22e}R_L}{1 + h_{22e}R_L} \tag{3.51}$$

In most practical cases the direct transmittance t_{sl} is small enough to justify using Equation 3.28 for evaluating the closed-loop gain $K' = V_L/V_S$. Hence, the relationship $k = h_{21e}$ together with Equations 3.47, 3.49 and 3.50 give the closed-loop gain of the stage of Fig. 3.21 (a) to be

$$K' \simeq \frac{-h_{21e}R_L}{(1 + h_{22e}R_L)(R_e + R_S + h_{11e}) + h_{21e}R_e} \tag{3.52}$$

For evaluating the input impedance Z_{in}' of the stage of Fig. 3.21 (a) we can apply Equation 3.39 (a) which involves Z^0_{in} and F_{isc}. Putting $R_S = 0$ in Equation 3.48 gives

$$F_{isc} \simeq 1 + \frac{h_{21e}R_e}{(1 + h_{22e}R_L)(R_e + h_{11e})} \tag{3.53}$$

The impedance Z^0_{in}, which is the value of Z_{in}' when $h_{21e} = 0$, can be found from Fig. 3.23. Using the inequality of Equation 3.46, we get

$$Z^0_{in} \simeq h_{11e} + R_e \tag{3.54}$$

Therefore, Equations 3.39 (a), 3.53 and 3.54 lead to

$$Z_{in}' \simeq h_{11e} + R_e + \frac{h_{21e}R_e}{1 + h_{22e}R_L} \tag{3.55}$$

The output impedance Z_{out}' of the stage of Fig. 3.21 (a) can be determined from Equation 3.39 (b) which requires a knowledge of F_{2sc} and Z^0_{out}. Putting $R_L = 0$ in Equation 3.48 gives F_{2sc} to be

$$F_{2sc} \simeq 1 + \frac{h_{21e}R_e}{R_e + R_S + h_{11e}} \tag{3.56}$$

The impedance Z^0_{out}, which is the value of Z_{out}' when $h_{21e} = 0$, can be also found from Fig. 3.23; thus

$$Z^0_{out} \simeq \frac{1}{h_{22e}} \tag{3.57}$$

where we have made use of the inequality $1/h_{22e} \gg R_e$. Hence, Equations 3.39 (b), 3.56 and 3.57 give the output impedance Z_{out}' to be

$$Z_{out}' \simeq \frac{1}{h_{22e}}\left(1 + \frac{h_{21e}R_e}{R_e + R_S + h_{11e}}\right) \tag{3.58}$$

If the load resistance R_L is small compared to $1/h_{22e}$, we obtain the approximate relations of Table 3.2 for the return difference, closed-loop gain and input impedance for the stage of Fig. 3.21(a).

As a numerical example, let it be required to determine the feedback resistor R_e so as to realise a value of 4 for the return difference F with reference to h_{21e} when $R_S = 4\,\text{k}\Omega$, $R_L = 2\,\text{k}\Omega$ and the transistor has the following common emitter h-parameters

Table 3.2 APPROXIMATE RELATIONS FOR TRANSISTOR STAGE WITH LOCAL FEEDBACK

	Local series feedback	*Local shunt feedback*
F	$1 + \frac{h_{21e}R_e}{R_e + R_S + h_{11e}}$	$1 + \frac{h_{21e}R_LR_S}{(R_L + R_c)(R_S + h_{11e})}$
K'	$\frac{-h_{21e}R_L}{R_e(1 + h_{21e}) + R_S + h_{11e}}$	$\frac{-h_{21e}R_LR_c}{(R_L + R_c)(R_S + h_{11e}) + h_{21e}R_LR_S}$
Z_{in}'	$h_{11e} + R_e(1 + h_{21e})$	$h_{11e}\frac{R_L + R_c}{R_c + R_L(1 + h_{21e})}$

$$h_{11e} = 1\ \text{k}\Omega$$
$$h_{21e} = 50$$
$$h_{22e} = 25\ \mu\text{℧}$$

Substituting these values into Equation 3.48 gives

$$4 = 1 + \frac{50R_e}{(1 + 25 \times 10^{-6} \times 2 \times 10^3)(R_e + 4 + 1)}$$

where R_e is in kΩ. Simplifying and solving for R_e we find that

$$R_e = 0{\cdot}336\ \text{k}\Omega = 336\ \Omega$$

which satisfies the assumed inequality of Equation 3.46.

Using the above value let us next determine the resulting values of closed-loop gain, input and output impedances for the stage of Fig. 3.21 (a). First, Equation 3.52 gives the closed-loop gain to be

$$K' = \frac{-50 \times 2}{(1 + 25 \times 10^{-6} \times 2 \times 10^3)(0{\cdot}336 + 4 + 1) + 50 \times 0{\cdot}336}$$
$$= -4{\cdot}46$$

Next, Equation 3.55 gives the input impedance to be

$$Z_{in}' = 1 + 0{\cdot}336 + \frac{50 \times 0{\cdot}336}{1 + 25 \times 10^{-6} \times 2 \times 10^3}$$
$$= 17{\cdot}3\ \text{k}\Omega$$

Equation 3.58 gives the output impedance to be

$$Z_{out}' = \frac{1}{25 \times 10^{-6}}\left(1 + \frac{50 \times 0{\cdot}336}{0{\cdot}336 + 4 + 1}\right)$$
$$= 166\ \text{k}\Omega$$

Common emitter stage with local shunt feedback

The diagram of Fig. 3.24 (a) shows local shunt feedback applied to a common emitter stage by means of a resistor R_c, connected between the base and collector terminals. Replacing the transistor with its common emitter h-parameter equivalent circuit, we obtain the circuit of Fig. 3.24 (b). Here again we have ignored the effect of the parameter h_{12e} on the assumption that the external feedback applied to the stage by means of the resistor R_c is large compared to the internal feedback due to h_{12e}.

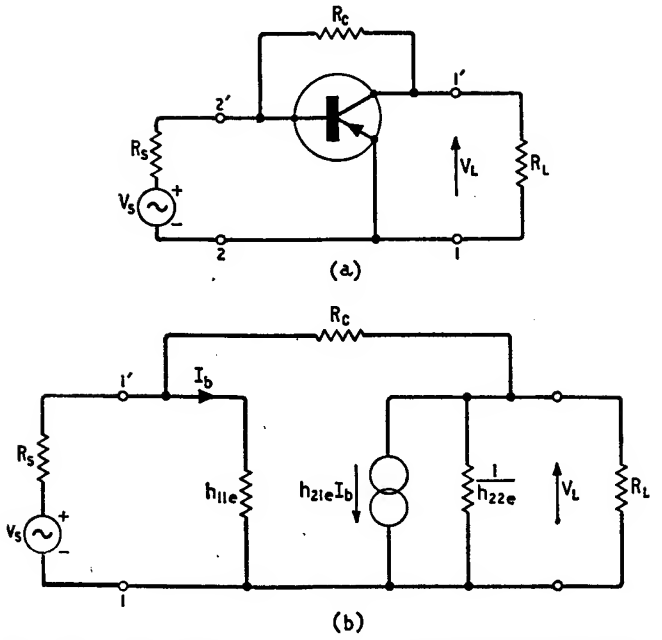

Fig. 3.24. (a) Common emitter stage with local shunt feedback, (b) Equivalent circuit

In Fig. 3.24 (b) we have $\theta_a = I_b$, $k = h_{21e}$ and $\phi_b = h_{21e}I_b$. To evaluate the transmittances t_{ba} and t_{bl} we put $V_S = 0$ and $h_{21e}I_b = 1$, as in Fig. 3.25. Normally the feedback resistance R_c is large compared to the parallel combination of resistances h_{11e} and R_S, that is

$$R_c \gg \frac{R_S h_{11e}}{R_S + h_{11e}} \tag{3.59}$$

Then noting that, in Fig. 3.25, $I_b = t_{ba}$ and $V_L = t_{bl}$ we get

$$t_{ba} \simeq \frac{-G_c}{G_c + G_L + h_{22e}} \cdot \frac{R_S}{R_S + h_{11e}} \tag{3.60}$$

$$t_{bl} \simeq \frac{-1}{G_c + G_L + h_{22e}} \tag{3.61}$$

where $G_c = 1/R_c$ and $G_L = 1/R_L$.

Since $k = h_{21e}$, it follows from Equation 3.22 and 3.60 that the return difference with reference to h_{21e} is

$$F \simeq 1 + \frac{h_{21e}G_cR_S}{(G_c + G_L + h_{22e})(R_S + h_{11e})} \tag{3.62}$$

Next, putting $V_S = 1$ and $h_{21e} = 0$ we obtain the circuit of Fig. 3.26 where $I_b = t_{sa}$ and $V_L = t_{sl}$. Therefore, using the inequality of Equation 3.59 we have

$$t_{sa} \simeq \frac{1}{R_S + h_{11e}} \tag{3.63}$$

$$t_{sl} \simeq \frac{h_{11e}}{R_S + h_{11e}} \cdot \frac{G_c}{G_c + G_L + h_{22e}} \tag{3.64}$$

The direct transmittance t_{sl} is normally so small that, to a good degree of approximation, we can neglect its effect. Then, Equations 3.28, 3.60, 3.61 and 3.63 give the closed-loop gain V_L/V_S for the

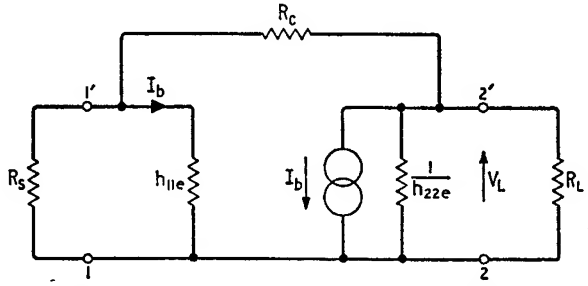

Fig. 3.25. Evaluation of transmittances t_{ba} and t_{bl} for common emitter stage with local shunt feedback

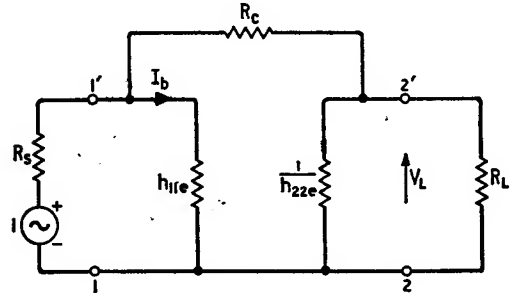

Fig. 3.26. Evaluation of transmittances t_{sa} and t_{sl} for common emitter stage with local shunt feedback

feedback stage of Fig. 3.24 (a) to be

$$K' \simeq \frac{-h_{21e}}{(G_c + G_L + h_{22e})(R_S + h_{11e}) + h_{21e}G_cR_S} \tag{3.65}$$

The input impedance Z_{in}' of the stage of Fig. 3.24 (a) can be determined from Equation 3.40 (a) which requires a knowledge of F_{1oc} and Z^0_{in}. If we put $R_S = \infty$ in Equation 3.62, we get

$$F_{1oc} \simeq 1 + \frac{h_{21e}G_c}{G_c + G_L + h_{22e}} \tag{3.66}$$

The impedance Z^0_{in}, which equals Z_{in}' when $h_{21e} = 0$ can be found from Fig. 3.26; assuming that $R_c \gg h_{11e}$ we have

$$Z^0_{in} \simeq h_{11e} \tag{3.67}$$

Therefore Equations 3.40 (a), 3.66 and 3.67 lead to

$$Z_{in}' \simeq \frac{h_{11e}(G_L + h_{22e} + G_c)}{G_L + h_{22e} + G_c(1 + h_{21e})} \tag{3.68}$$

To evaluate the output impedance Z_{out}' of the stage of Fig. 3.24 (a), we can apply Equation 3.40 (b) involving F_{2oc} and Z^0_{out}. Putting $R_L = \infty$ (i.e. $G_L = 0$) in Equation 3.62 gives

$$F_{2oc} \simeq 1 + \frac{h_{21e}G_cR_S}{(G_c + h_{22e})(R_S + h_{11e})} \tag{3.69}$$

The impedance Z^0_{out}, which is the value of Z_{out}' when $h_{21e} = 0$, can be also found from Fig. 3.26; thus, assuming the inequality of Equation 3.59, we get

$$Z^0_{out} \simeq \frac{1}{G_c + h_{22e}} \tag{3.70}$$

Combining Equations 3.40 (b), 3.69 and 3.70 gives the output impedance Z_{out}' to be

$$Z_{out}' = \frac{R_S + h_{11e}}{(G_c + h_{22e})(R_S + h_{11e}) + h_{21e}G_cR_S} \tag{3.71}$$

If the load resistance R_L is small compared to $1/h_{22e}$, that is, $G_L \gg h_{22e}$, we obtain the approximate relations of Table 3.2 for the return difference, closed-loop gain, input impedance of the stage of Fig. 3.24 (a).

To illustrate the above results with a numerical example, let us suppose that it is required to evaluate the feedback resistor R_c which

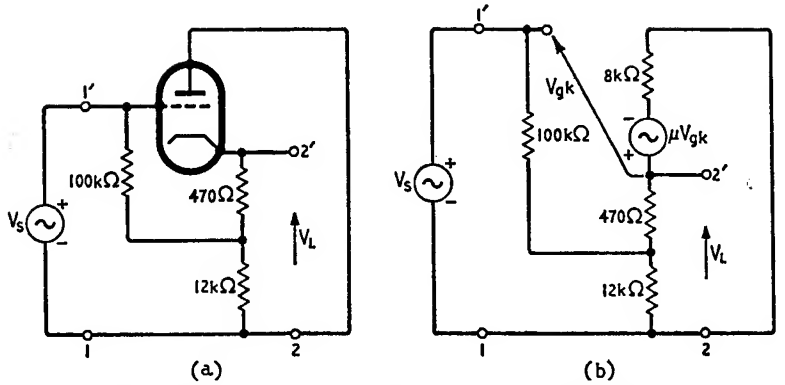

Fig. 3.27. (a) Common anode stage, (b) Equivalent circuit

results in a return difference, with reference to h_{21e}, equal to 4 when $R_S = 4$ kΩ, $R_L = 2$k Ω (i.e. $G_L = 0{\cdot}5$ mʊ) and the common emitter h-parameters have the values

$$h_{11e} = 1 \text{ k}\Omega$$
$$h_{21e} = 50$$
$$h_{22e} = 25\ \mu\text{ʊ}$$

Substitution in Equation 3.62 gives

$$4 = 1 + \frac{50 \times 4G_c}{(G_c + 0{\cdot}5 + 0{\cdot}025)(4 + 1)}$$

where G_c is in mʊ, that is, R_c is in kΩ. Simplifying and solving for G_c, we obtain

$$G_c = 0{\cdot}0426 \text{ mʊ}$$

that is,

$$R_c = 23{\cdot}5 \text{ k}\Omega$$

which satisfies the inequality of Equation 3.59.

Using the above value for G_c we find from Equation 3.65 that the closed-loop gain is

$$K' = \frac{-50}{(0{\cdot}0426 + 0{\cdot}5 + 0{\cdot}025)(4 + 1) + 50 \times 0{\cdot}0426 \times 4}$$
$$= -4{\cdot}4$$

Equation 3.68 gives the input impedance Z_{in}' to be

$$Z_{in}' = \frac{1(0{\cdot}5 + 0{\cdot}025 + 0{\cdot}0426)}{0{\cdot}5 + 0{\cdot}025 + 0{\cdot}0426(1 + 50)}$$
$$= 0{\cdot}21 \text{ k}\Omega$$

From Equation 3·71 we find that the output impedance has the value

$$Z_{out}' = \frac{4 + 1}{(0{\cdot}0426 + 0{\cdot}025)(4 + 1) + 50 \times 0{\cdot}0426 \times 4}$$
$$= 0{\cdot}565 \text{ k}\Omega$$

Comparing the results of this example with those obtained for the local series feedback stage involving a common emitter stage, we see that for the same terminating resistances R_S and R_L and for the same transistor the closed-loop gains of the two stages of Figs. 3.21 (a) and 3.24 (a) are practically the same when both stages have equal return differences with reference to h_{21e}. The major differences between the two stages are in the values of their input and output impedances; the input and output impedances of the series feedback stage of

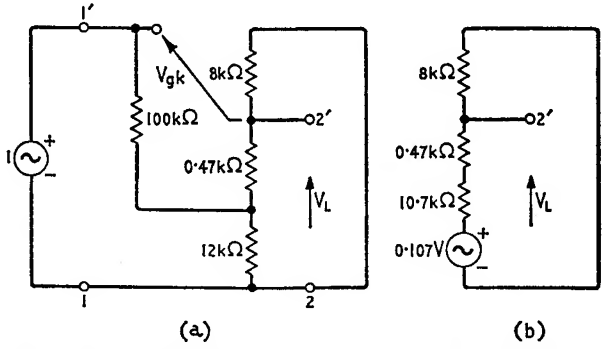

Fig. 3.28. Evaluation of transmittances t_{s1} and t_{sa} of common anode stage

Fig. 3.21 (a) are both increased as a result of the applied negative feedback, whereas the input and output impedances of the shunt feedback stage of Fig. 3.24 (a) are both reduced due to the applied negative feedback.

3.8.3 COMMON ANODE STAGE (CATHODE FOLLOWER)

For our next example we shall evaluate the voltage gain, input and output impedances of the common anode stage shown in Fig. 3.27 (a). The triode valve has an anode slope resistance $r_a = 8$ kΩ and an amplification factor $\mu = 30$.

In Fig. 3.27 (b) the triode valve is represented by its equivalent circuit involving the voltage-controlled voltage source μV_{gk}. Thus $\theta_a = V_{gk}$, $k = \mu$ and $\phi_b = \mu V_{gk}$. For evaluating the transmittances t_{sa} and t_{sl} we put $V_S = 1$ and $\mu = 0$, as in Fig. 3.28 (a). Applying Thévenin's theorem to the 12 kΩ and 100 kΩ resistances and the unit voltage source, we obtain the simpler circuit of

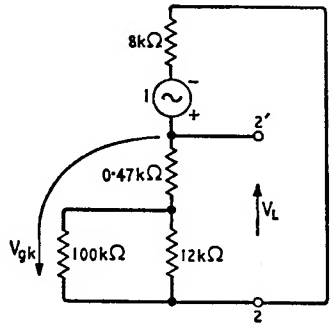

Fig. 3.29. Evaluation of transmittances t_{bl} and t_{ba} for common anode stage

Fig. 3.28 (b). Noting that $V_L = t_{sl}$ and $V_{gk} = t_{sa}$ we find from Fig. 3.28 (b) that

$$t_{sl} = \frac{8 \times 0{\cdot}107}{8 + 0{\cdot}47 + 10{\cdot}7} = 0{\cdot}045$$

and from Fig. 3.28 (a) we get

$$t_{sa} = 1 - V_L = 1 - 0{\cdot}045 = 0{\cdot}955$$

Next, to evaluate the transmittances t_{bl} and t_{ba}, we put $V_S = 0$ and $\mu V_{gk} = 1$, as in Fig. 3.29. Since in this diagram $V_L = t_{bl}$ and $V_{gk} = t_{ba}$, we get

$$t_{bl} = \frac{10{\cdot}7 + 0{\cdot}47}{10{\cdot}7 + 0{\cdot}47 + 8} = 0{\cdot}583$$

$$t_{ba} = -0{\cdot}583$$

Using the above values, together with $k = \mu = 30$, in Equations 3.22 and 3.26 we find that the return difference F with reference to μ and the voltage gain $K' = V_L/V_S$ for the stage of Fig. 3.27 (a) are equal to, respectively,

$$F = 1 + 30 \times 0{\cdot}583 = 18{\cdot}5$$

$$K' = 0{\cdot}045 + \frac{30 \times 0{\cdot}583 \times 0{\cdot}955}{18{\cdot}5}$$

$$= 0{\cdot}948$$

Here we see that 4·6% of the closed-loop gain K′ is due to the direct transmittance t_{sl}.

The common anode stage of Fig. 3.27 (a) is of the series-shunt type of a feedback circuit; its return difference with reference to μ is reduced to unity when its output is short circuited (i.e. $V_L = 0$). Therefore, its output impedance Z_{out}' can be determined from Equation 3.40 (b) which involves F_{2oc} and Z^0_{out}. The return difference F_{2oc} results when the output port of the stage is left open-circuited; this is in fact the case in Figs. 3.27 (a) and 3.29. Hence $F_{2oc} = F = 18{\cdot}5$. Next when $\mu = 0$ as in Fig. 3.28 (b), we find that the resulting output impedance Z^0_{out} is

$$Z^0_{out} = \frac{8(0{\cdot}47 + 10{\cdot}7)}{8 + 0{\cdot}47 + 10{\cdot}7} = 4{\cdot}66 \text{ kΩ}$$

Then Equation 3.40 (b) gives the output impedance Z_{out}' of the stage to be

$$Z_{out}' = \frac{4{\cdot}66}{18{\cdot}5} = 0{\cdot}25 \text{ kΩ}$$

Although in Fig. 3.27 (a) the feedback signal is applied in series at the input, it is not reduced to zero when the input port of the complete stage is open-circuited; this is owing to the presence of the

Fig. 3.30. Evaluation of F_{1oc}

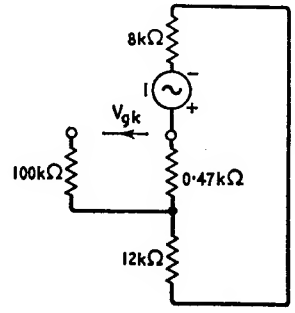

0·47 kΩ resistance. Therefore, in evaluating the input impedance Z_{in}' of the common anode stage of Fig. 3.27 (a) by means of the method developed in Section 3.7.3, it is necessary to use the general expression of Equation 3.37, which involves F_{1oc}, F_{1sc} and Z^0_{in}. The return difference F_{1oc} can be determined from Fig. 3.30. Here we see that, with $\mu V_{gk} = 1$ the returned signal

$$V_{gk} = \frac{-0{\cdot}47}{0{\cdot}47 + 12 + 8} = -0{\cdot}023$$

Thus the return difference F_{10c} with reference to μ is equal to

$$F_{10c} = 1 + 30 \times 0{\cdot}023 = 1{\cdot}69$$

The return difference F_{1sc} results when the input port of the stage is short-circuited, as in Fig. 3.29. Hence, we have $F_{1sc} = F = 18{\cdot}5$. Next, when $\mu = 0$ we find that the resulting value Z^0_{in} of the input impedance is given by (see Fig. 3.28 (a))

$$Z^0_{in} = 100 + \frac{12 \times (8 + 0{\cdot}47)}{12 + 8 + 0{\cdot}47}$$
$$= 105\ \text{k}\Omega$$

Then Equation 3.37 gives the input impedance Z_{in}' of the common anode stage of Fig. 3.27 (a) to be

$$Z_{in}' = 105\,\frac{18{\cdot}5}{1{\cdot}69}$$
$$= 1{,}150\ \text{k}\Omega = 1{\cdot}15\ \text{M}\Omega$$

3.8.4 TWO-STAGE FEEDBACK AMPLIFIERS

The benefits that result from the application of negative feedback in reducing the sensitivity of the gain to parameter variations, in

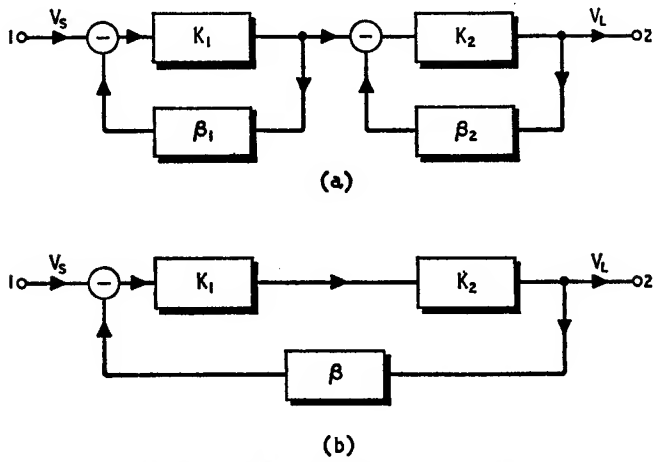

Fig. 3.31. (a) Two-stage amplifier with individual local feedbacks, (b) Two-stage amplifier with overall feedback

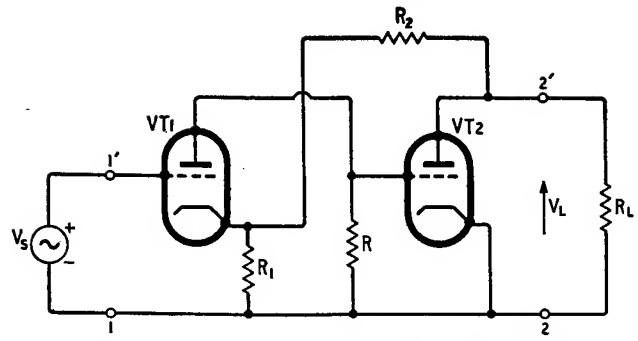

Fig. 3.32. Two-stage valve feedback amplifier of the series-shunt type

reducing harmonic distortion, etc. become greater as the available forward gain of the internal amplifier is increased. Thus overall negative feedback applied to an amplifier consisting of a cascade of two or more stages can improve the amplifier performance to a greater extent than is possible if feedback is applied to each of the stages individually. To illustrate this remark, let us consider Fig. 3.31 (a) showing the block diagram of an amplifier consisting of two stages of gains K_1 and K_2, with negative feedback applied to each stage. The overall gain K_a' is given by

$$K_a' = \frac{K_1}{1 + \beta_1 K_1} \cdot \frac{K_2}{1 + \beta_2 K_2} \tag{3.72}$$

Consider next the block diagram of Fig. 3.31 (b) where overall negative feedback is applied to the cascade of the stages K_1 and K_2. The resulting closed-loop gain K_b' is

$$K_b' = \frac{K_1 K_2}{1 + \beta K_1 K_2} \tag{3.73}$$

If the overall gains K_a' and K_b' of the two circuit arrangements of Fig. 3.31 are required to be equal, we must have

$$(1 + \beta_1 K_1)(1 + \beta_2 K_2) = 1 + \beta K_1 K_2 \tag{3.74}$$

This equation states that, with $K_a' = K_b'$ the amount of feedback acting on each of the individual stages in Fig. 3.31 (a) is necessarily less than in Fig. 3.31 (b). Therefore, with the proviso $K_a' = K_b'$, a greater improvement in amplifier performance is possible with the circuit of Fig. 3.31 (b) than is with the circuit of Fig. 3.31 (a).

Let us next examine the practical ways in which negative feedback can be applied to a cascade of two valve or transistor stages. In a

cascade of two common cathode stages each stage produces a phase shift of 180° between its input and output voltage signals when operating at low frequencies; the result is that the input and output voltage signals of the complete cascade are in phase. Hence, overall negative feedback can be applied to a cascade of two common cathode stages if the feedback network is connected between the anode of the second stage and the cathode of the first stage, as in Fig. 3.32, or if the feedback network is connected between the cathode of the second stage and the grid of the first valve stage. Similarly, overall negative feedback can be applied to a cascade of two common emitter stages by connecting the feedback network between the emitter of the second stage and the base of the first stage, as in Fig. 3.33, or between the collector of the second stage and the emitter of the first stage.

The feedback circuit of Fig. 3.32 is recognised to be of the series-shunt type, whereas the feedback circuit of Fig. 3.33 is of the shunt-series type. These feedback amplifiers have one common feature in

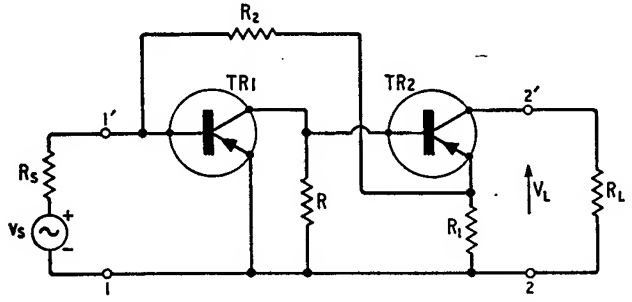

Fig. 3.33. Two-stage transistor feedback amplifier of the shunt-series type

that they are both essentially multiple-loop feedback circuits. Thus, for example, in the case of Fig. 3.32 local feedback is applied to the first valve-stage by the resistor R_1, and overall negative feedback embracing the two stages is provided by the resistor R_2.

Two-stage valve feedback amplifier of the series-shunt type

Let us suppose that it is required to determine the return difference F_2 of the feedback circuit of Fig. 3.32 with reference to the amplification factor μ_2 of the second common cathode stage $VT2$ given that

$$R = R_L = 10\ \text{k}\Omega$$
$$R_1 = 1\ \text{k}\Omega$$
$$R_2 = 15\ \text{k}\Omega$$

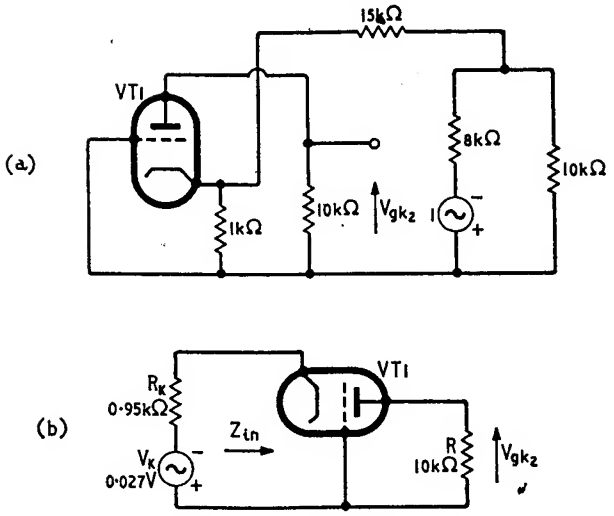

Fig. 3.34. Calculation of return difference with reference to μ_2

and that the two triode valves are identical having the parameters

$$r_{a1} = r_{a2} = 8\ \text{k}\Omega$$
$$\mu_1 = \mu_2 = 30$$

For the purpose of the above calculation the source voltage V_S is reduced to zero and the common cathode stage $VT2$ is replaced with its equivalent circuit. Then we obtain the circuit of Fig. 3.34 (a) where $\mu_2 V_{gk2} = 1$. On applying Thévenin's theorem to the circuit connected between the common terminal and the cathode of $VT1$, we obtain the simpler circuit of Fig. 3.34 (b). Here we see that the triode valve $VT1$ is operated in its common grid mode; its input impedance Z_{in1} and voltage gain K_{V1} are given by (see Equations 2.211 and 2.210)

$$Z_{in1} = \frac{r_{a1} + R}{1 + \mu_1}$$
$$= \frac{8 + 10}{1 + 30} = 0{\cdot}58\ \text{k}\Omega$$
$$K_{V1} = \frac{(1 + \mu_1)R}{r_{a1} + R}$$
$$= \frac{(1 + 30)10}{8 + 10} = 17{\cdot}2$$

Therefore, the voltage developed across the interstage resistor $R = 10\ \text{k}\Omega$, which is the same as the voltage V_{gk_2} returned to the grid of the stage $VT2$, is equal to

$$V_{gk_2} = -K_{V_1}\frac{Z_{in_1}V_k}{Z_{in_1} + R_k}$$

$$= -17{\cdot}2\frac{0{\cdot}58 \times 0{\cdot}027}{0{\cdot}58 + 0{\cdot}95} = -0{\cdot}176$$

In other words the transmittance $t_{ba} = -0{\cdot}176$, and since the control parameter $k = \mu_2 = 30$, it follows from Equation 3.22 that the return difference F_2 with reference to μ_2 is

$$F_2 = 1 + 30 \times 0{\cdot}176 = 6{\cdot}3$$

Owing to the additional local feedback applied to the first stage $VT1$ by the resistor R_1, the return difference F_1 with reference to the amplification factor μ_1 of the first stage is necessarily greater than F_2 calculated above. The value of F_1 can be calculated quite conveniently from the following relationship†

$$\frac{F_1}{F_2} = \frac{(F_1)_{k_2=0}}{(F_2)_{k_1=0}} \tag{3.75}$$

where $(F_1)_{k_2=0}$ is the value of the return difference F_1, with reference to k_1, that results when the control parameter k_2 of the second stage is zero. Similarly $(F_2)_{k_1=0}$ is the value of the return difference F_2 with reference to k_2, which occurs when the control parameter k_1 of the first stage is zero. In the case of Fig. 3.32 we have $k_1 = \mu_1$ and $k_2 = \mu_2$.

When the amplification factor μ_2 of the second stage is reduced to zero, the feedback amplifier of Fig. 3.32 reduces simply to a common cathode stage with local series feedback provided by a cathode resistor R_k equal to 0·95 kΩ and with a load resistance $R = 10\ \text{k}\Omega$. Hence from Equation 3.44 we deduce that $(F_1)_{\mu_2=0}$ has the value

$$(F_1)_{\mu_2=0} = 1 + \frac{\mu_1 R_k}{r_{a_1} + R + R_k}$$

$$= 1 + \frac{30 \times 0{\cdot}95}{8 + 10 + 0{\cdot}95} = 2{\cdot}51$$

Next, the return difference $(F_2)_{\mu_1=0}$ can be evaluated fr om Fig 3.35 (a) where we have put $\mu_2 V_{gk_2} = 1$. This circuit can be

† The relationship of Equation 3.75 is proved by Truxal, J. G. on p. 141 of *Automatic Feedback Control System Synthesis*, McGraw-Hill (1955).

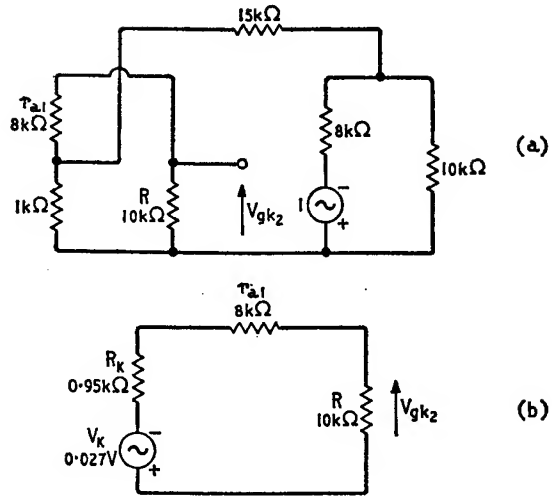

Fig. 3.35. Calculation of return difference with reference to μ_2 and with $\mu_1 = 0$

simplified to the form shown in Fig. 3.35 (b) where we find directly that the voltage V_{gk_2} returned to the grid of the second stage is equal to

$$V_{gk_2} = -\frac{RV_k}{R + r_{a_1} + R_k}$$

$$= -\frac{10 \times 0{\cdot}027}{10 + 8 + 0{\cdot}95} = -0{\cdot}0142$$

Hence, the return difference $(F_2)_{\mu_1=0}$ has the value

$$(F_2)_{\mu_1=0} = 1 + 30 \times 0{\cdot}0142 = 1{\cdot}43$$

Therefore, from Equation 3.75 we find that the return difference F_1 of the two-stage feedback circuit of Fig. 3.35, with reference to μ_1 is given by

$$F_1 = F_2 \cdot \frac{(F_1)_{\mu_2=0}}{(F_2)_{\mu_1=0}}$$

$$= 6{\cdot}3\frac{2{\cdot}51}{1{\cdot}43} = 11{\cdot}1$$

The fact that, in the feedback amplifier of Fig. 3.32, F_1 is greater than F_2 implies that the overall gain of the amplifier is less sensitive to variations in the parameter μ_1 of the first stage than it is to variations in the parameter μ_2 of the second stage.

Two-stage transistor feedback amplifier of the shunt-series type

In the two-stage transistor feedback amplifier of Fig. 3.33 the resistor R represents the shunting effect of interstage biasing resistors, while R_1 and R_2 are responsible for the applied negative feedback. This amplifier can have a very low input impedance and a very high output impedance provided that a large amount of overall feedback is applied to it. Therefore it is most suited for the amplification of current signals. In the analysis to follow we shall assume that the amplifier is driven from an ideal current source, as in Fig. 3.36, and that the collector current I_L of the stage $TR2$ provides the desired output signal.

As a numerical example let it be assumed that

$$R = 13{\cdot}3\ \text{k}\Omega$$
$$R_1 = 0{\cdot}1\ \text{k}\Omega$$
$$R_2 = 15\ \text{k}\Omega$$
$$R_L = 1\ \text{k}\Omega$$

and that the transistors are identical having the following common emitter h-parameters

$$h_{11e}' = h_{11e}'' = 1\ \text{k}\Omega$$
$$h_{21e}' = h_{21e}'' = 50$$
$$h_{22e}' = h_{22e}'' = 25\mu\text{℧}$$

where the parameters with one prime refer to transistor $TR1$ and those with two primes refer to transistor $TR2$.

For calculating the return difference F_1 with reference to the forward current amplification factor h_{21e}' of the first stage, we replace $TR1$ with its common emitter h-parameter equivalent circuit,

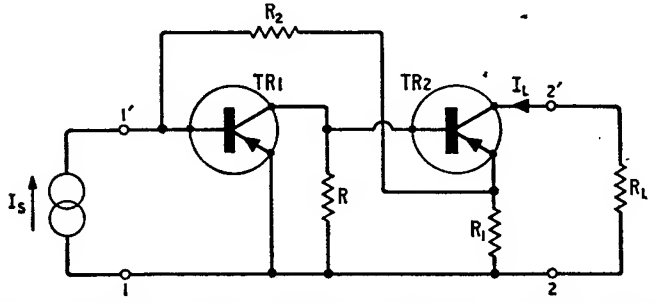

Fig. 3.36. Two-stage transistor feedback amplifier for current amplification

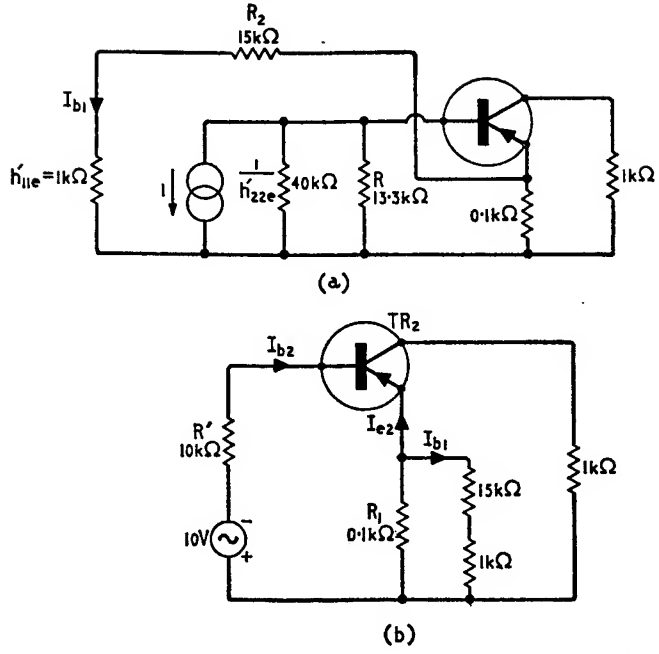

Fig. 3.37. Calculation of return difference with reference to h_{21e}'

set $h_{21e}'I_{b1} = 1$ and $I_S = 0$, as is shown in Fig. 3.37 (a). The unit current source and the shunting resistors $R = 13{\cdot}3$ kΩ and $1/h_{22e}' = 40$ kΩ can be represented by an equivalent voltage source in series with a 10 kΩ resistance (equal to R and $1/h_{22e}'$ in parallel), as in Fig. 3.37 (b). Since the load resistance $R_L = 1$ kΩ is quite small compared to $1/h_{22e}''$, the stage $TR2$ behaves essentially as a common collector stage having the following input impedance Z_{in2} and current gain K_{I2} (see the approximate relations of Table 2.6)

$$Z_{in2} \simeq h_{11e}'' + (1 + h_{21e}'')R_e$$
$$K_{I2} \simeq -(1 + h_{21e}'')$$

where R_e is the total resistance connected in series with the emitter terminal of stage $TR2$; it is effectively equal to $R_1 = 0{\cdot}1$ kΩ owing to the negligible shunting effect of the series combination of $R_2 = 15$ kΩ and $h_{11e}' = 1$ kΩ.

Therefore

$$Z_{in2} \simeq 1 + (1 + 50) \times 0{\cdot}1 = 6{\cdot}1\ \text{k}\Omega$$

$$K_{I_2} \simeq -51$$

The base current I_{b_2} of the stage $TR2$ is

$$I_{b_2} \simeq \frac{-10}{10 + 6{\cdot}1} = -0{\cdot}62$$

and its emitter current I_{e_2} is

$$I_{e_2} = K_{I_2} I_{b_2}$$
$$\simeq (-51) \times (-0{\cdot}62) = 31{\cdot}6$$

Hence, the transmittance t_{ba}, which equals the current I_{b_1} returned to the base of stage $TR1$, has the value

$$t_{ba} = \frac{-R_1 I_{e_2}}{R_1 + R_2 + h_{11e}'}$$
$$\simeq \frac{-0{\cdot}1 \times 31{\cdot}6}{0{\cdot}1 + 15 + 1} = -0{\cdot}196$$

With the control parameter $k = h_{21e}'$ it follows from Equation 3.22 that the return difference F_1 with reference to h_{21e}' is given by

$$F_1 = 1 + 50 \times 0{\cdot}196 = 10{\cdot}8$$

The return difference F_2 with reference to h_{21e}'' is necessarily greater than F_1 owing to the additional local feedback applied to the second stage $TR2$ by means of the resistor R_1. To determine F_2 we

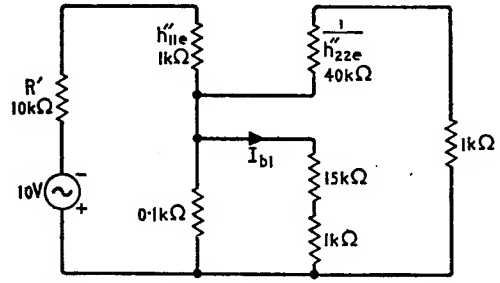

Fig. 3.38. Calculation of return difference with reference to h_{21e}' and with $h_{21e}'' = 0$

can use the relationship of Equation 3.75, where $k_1 = h_{21e}'$ and $k_2 = h_{21e}''$. The return difference $(F_1)_{h_{21e}''=0}$ can be evaluated from Fig. 3.38 to which form the circuit of Fig. 3.37 (b) reduces when $h_{21e}'' = 0$. The corresponding value of the current I_{b_1} returned to the base of transistor $TR1$ is found to be effectively

$$I_{b_1} \simeq \frac{-10}{10 + 1 + 0{\cdot}1} \times \frac{0{\cdot}1}{15 + 1 + 0{\cdot}1} = -0{\cdot}0056$$

Hence,

$$(F_1)_{h_{21e}''=0} = 1 + 50 \times 0{\cdot}0056 = 1{\cdot}28$$

To determine $(F_2)_{h_{21e}'=0}$ we set $h_{21e}' = 0$ in which case the two-stage transistor amplifier of Fig. 3.36 reduces simply to a common emitter stage with local series feedback provided by an emitter resistor R_e effectively equal to 0·1 kΩ, and with a source resistance $R' = 10$ kΩ. Then from the approximate relations of Table 3.2 we find that

$$(F_2)_{h_{21e}'=0} = 1 + \frac{h_{21e}'' R_e}{R_e + R' + h_{11e}''}$$
$$= 1 + \frac{50 \times 0{\cdot}1}{0{\cdot}1 + 10 + 1} = 1{\cdot}45$$

The return difference F_2 with reference to h_{21e}'' is deduced from Equation 3.75 to be

$$F_2 = F_1 \frac{(F_2)_{h_{21e}'=0}}{(F_1)_{h_{21}''=0}}$$
$$= 10{\cdot}8 \frac{1{\cdot}45}{1{\cdot}28} = 12{\cdot}2$$

We therefore find that, in the feedback amplifier of Fig. 3.36, because F_2 is greater than F_1 the overall current gain I_L/I_S is less sensitive to variations in the parameter h_{21e}'' of stage $TR2$ than it is to variations in the parameter h_{21e}' of stage $TR1$.

3.8.5 THREE-STAGE FEEDBACK AMPLIFIERS

There are many different ways of applying overall negative feedback to a cascade of three valve or transistor stages. We shall consider only three representative examples, widely used in practice.

Shunt-shunt feedback type

The circuit of Fig. 3.39 shows this type of feedback applied to a cascade of three common emitter stages; the internal amplifier and feedback network are seen to be connected in parallel at their input as well as output ports. The feedback amplifier of Fig. 3.39 can have very low input and output impedances provided that a large feedback is applied.

In Fig. 3.39 the internal amplifier, as one whole unit, exhibits practically no interaction between its input and output ports.

Also the forward gain is very high; accordingly, even if the required open-loop gain is large, the elements of the feedback network normally turn out to have such values that negligible loading is presented at the input and output ports. Then, provided that we are interested only in the effects of the externally applied feedback, the classical feedback theory developed in the early part of the chapter may prove quite adequate.

The open-loop gain T of the feedback amplifier of Fig. 3.39 is given by Equations 3.13 (b), which is reproduced here for convenience

$$T = \frac{y_{12}K_V}{Y_{\text{in}} + Y_S} \tag{3.76}$$

where y_{12} is the reverse short-circuit transfer admittance of the feedback network.

The internal amplifier component can be represented by the equivalent circuit shown in Fig. 3.40, where Y_{in} and Y_{out} are the input and output admittances, respectively; Y_m is the mutual admittance responsible for signal amplification in the forward direction. Neglecting the internal feedback associated with each of the three stages, we have

$$Y_{\text{in}} \simeq \frac{1}{h_{11e}'} \tag{3.77}$$

$$Y_{\text{out}} \simeq h_{22e}''' \tag{3.78}$$

$$Y_m \simeq \frac{h_{21e}'h_{21e}''h_{21e}'''}{h_{11e}'(1 + h_{22e}'h_{11e}'' + h_{11e}''/R')\,(1 + h_{22e}''h_{11e}''' + h_{11e}'''/R'')} \tag{3.79}$$

The elements R' and R'' account for the interstage biasing resistors (see Fig. 3.39). The common emitter h-parameters with one prime

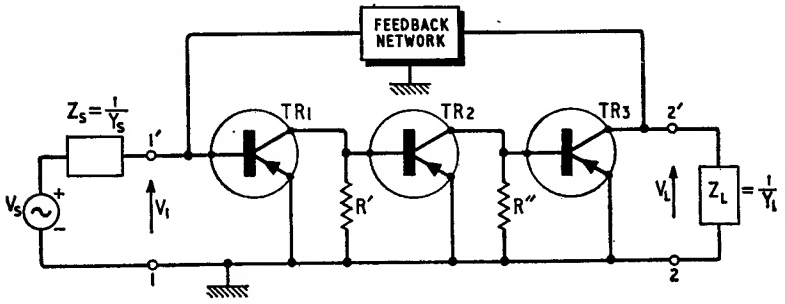

Fig. 3.39. Three-stage transistor amplifier with shunt-shunt feedback

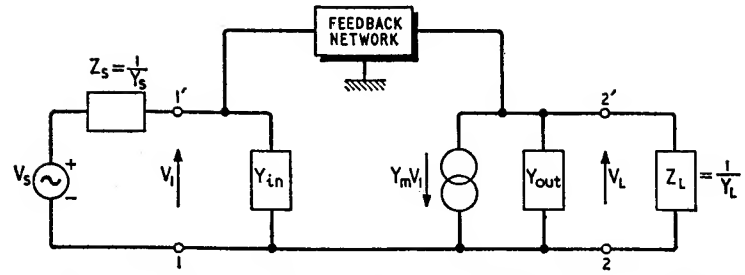

Fig. 3.40. Equivalent circuit for the three-stage feedback amplifier of Fig. 3.39

refer to transistor $TR1$, those with two primes refer to transistor $TR2$, and those with three primes refer to transistor $TR3$.

The feedback network will present a negligible loading effect at the input as well as the output ports provided its y-parameters y_{11} and y_{22} satisfy the following inequalities

$$\left.\begin{aligned} Y_{\text{in}} + Y_S &\gg y_{11} \\ Y_{\text{out}} + Y_L &\gg y_{22} \end{aligned}\right\} \tag{3.80}$$

Then we find that the voltage gain K_V of the loaded internal amplifier without feedback is given by

$$K_V \simeq \frac{-Y_m}{Y_{\text{out}} + Y_L} \tag{3.81}$$

Therefore, Equation 3.76 and 3.81 give the open-loop gain T of the feedback amplifier of Fig. 3.39 to be

$$T \simeq \frac{-y_{12}Y_m}{(Y_{\text{in}} + Y_S)(Y_{\text{out}} + Y_L)} \tag{3.82}$$

In this equation we can regard the factor $-Y_m/(Y_{\text{out}} + Y_L)$ as the effective forward voltage gain of the loaded internal amplifier, and the factor $-y_{12}/(Y_{\text{in}} + Y_S)$ as the effective reverse voltage gain of the loaded feedback network.

If we assume that the magnitude of the open-loop gain is large compared to unity, then as explained in Section 3.1.1, the closed-loop gain $K' = V_L/V_S$ becomes effectively equal to $1/\beta$, which for the shunt-shunt feedback amplifier of Fig. 3.39 has the value of

$$K' \simeq \frac{Y_S}{y_{12}} \tag{3.83}$$

As a numerical example let us assume that

$$R' = R'' = 10\ \text{k}\Omega$$
$$Z_S = 4\ \text{k}\Omega\ (\text{i.e. } Y_S = 0{\cdot}25\ \text{m}\mho)$$
$$Z_L = 2\ \text{k}\Omega\ (\text{i.e. } Y_L = 0{\cdot}5\ \text{m}\mho)$$

and that all three transistors constituting the internal amplifier are identical and have the following common emitter h-parameters

$$h_{11e}' = h_{11e}'' = h_{11e}''' = 1\ \text{k}\Omega$$
$$h_{21e}' = h_{21e}'' = h_{21e}''' = 50$$
$$h_{22e}' = h_{22e}'' = h_{22e}''' = 25\mu\mho$$

The feedback network is to be in the form of a T section as in Fig. 3.41, and the problem is to evaluate its elements so as to realise an open-loop gain T of 30.

The y-parameters y_{11}, y_{12}, y_{21} and y_{22} of the feedback network can

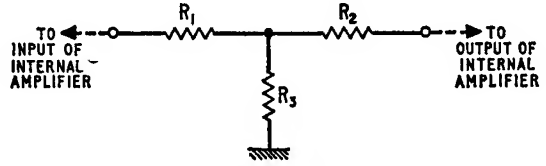

Fig. 3.41. Feedback network in the form of a T section

be determined from the definitions of Equations 2.114; then we find that they are given as follows

$$\left.\begin{aligned} y_{11} &= \frac{R_2 + R_3}{R_1R_2 + R_1R_3 + R_2R_3} \\ y_{12} = y_{21} &= \frac{-R_3}{R_1R_2 + R_1R_3 + R_2R_3} \\ y_{22} &= \frac{R_1 + R_3}{R_1R_2 + R_1R_3 + R_2R_3} \end{aligned}\right\} \qquad (3.84)$$

The second line of these equations can be solved for R_3 giving

$$R_3 = \frac{R_1R_2}{(-1/y_{12}) - (R_1 + R_2)} \qquad (3.85)$$

Now since y_{11} and y_{22} are necessarily smaller than $1/R_1$ and $1/R_2$ respectively, it follows that the inequalities of Equation 3.80 are certainly satisfied provided we choose R_1 and R_2 such that

$$\left.\begin{aligned} R_1 &\gg \frac{1}{Y_{\text{in}} + Y_S} \\ R_2 &\gg \frac{1}{Y_{\text{out}} + Y_L} \end{aligned}\right\} \qquad (3.86)$$

In addition R_1 and R_2 must satisfy the following condition if R_3 is to be assured of a positive value (see Equation 3.85)

$$(-1/y_{12}) > R_1 + R_2 \qquad (3.87)$$

It must be remembered that in a passive network y_{12} is negative.

From Equation 3.79 we find that the mutual admittance of the internal amplifier has the following value

$$Y_m \simeq \frac{50^3}{1(1 + 1 \times 0{\cdot}025 + 1/10)^2} = 98{\cdot}7 \times 10^3\ \text{m}\mho$$

Then with $T = 30$ it follows from Equation 3.82, that the required value of y_{12} is

$$y_{12} \simeq \frac{-T}{Y_m}(Y_{\text{in}} + Y_S)\,(Y_{\text{out}} + Y_L) \qquad (3.88)$$

$$= \frac{-30}{98{\cdot}7 \times 10^3}(1 + 0{\cdot}25)\,(0{\cdot}025 + 0{\cdot}5)$$

$$= -0{\cdot}2 \times 10^{-3}\ \text{m}\mho$$

Further

$$\frac{1}{Y_{\text{in}} + Y_S} \simeq \frac{1}{1 + 0{\cdot}25} = 0{\cdot}8\ \text{k}\Omega$$

$$\frac{1}{Y_{\text{out}} + Y_L} \simeq \frac{1}{0{\cdot}025 + 0{\cdot}5} = 1{\cdot}9\ \text{k}\Omega$$

Therefore choosing $R_1 = 33\ \text{k}\Omega$ and $R_2 = 75\ \text{k}\Omega$ will satisfy the conditions of both Equations 3.86 and 3.87. Then Equation 3.85 gives the value of the remaining element R_3 to be

$$R_3 = \frac{33 \times 75}{(10^3/0{\cdot}2) - (33 + 75)} = 0{\cdot}505\ \text{k}\Omega$$

An approximate value for the closed-loop gain K' can be found from Equation 3.83; it is

$$K' \simeq \frac{0{\cdot}25}{-0{\cdot}2 \times 10^{-3}} = -1{,}250$$

Series-series feedback type

For our next example we shall consider the series-series feedback amplifier of Fig. 3.42 involving a cascade of three common cathode stages. The interstage resistors are denoted by R' and R'', and R_g is the grid resistor of the first stage. The element R_1 is responsible for the applied negative feedback.

The internal amplifier as one whole unit, can be represented by the equivalent circuit shown in Fig. 3.43 where

$$K_{oc} = \text{open-circuit voltage gain}$$

$$= \frac{\mu_1\mu_2\mu_3 R' R''}{(R' + r_{a1})(R'' + r_{a2})} \tag{3.89}$$

The parameters r_{a1}, μ_1, refer to the valve $VT1$; r_{a2}, μ_2, refer to valve $VT2$, and r_{a3}, μ_3 refer to valve $VT3$.

Normally the feedback resistor R_1 is quite small compared with both the grid resistor R_g of the first stage and the anode slope resistance r_{a3} of the last stage. Hence the feedback network will

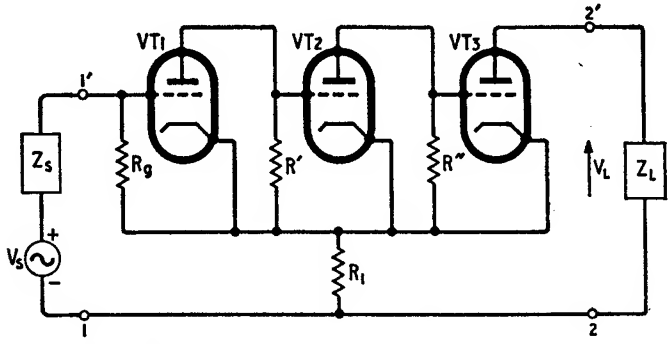

Fig. 3.42. Three-stage valve amplifier with series-series feedback

present a negligible loading effect, and so we find that the forward voltage gain K_V of the loaded internal amplifier is effectively given by

$$K_V \simeq \frac{-K_{oc} Z_L}{Z_L + r_{a3}} \tag{3.90}$$

We also find that normally the grid resistor R_g is very large compared to the source impedance. Therefore, if in Equation 3.13 (a) we neglect Z_S and remember that $K_V Z_{in} = -K_I Z_L$, we find that the open-loop gain T of the valve feedback amplifier of Fig. 3.42 has the value

$$T = \frac{-z_{12} K_V}{Z_L} \tag{3.91}$$

where z_{12} is the reverse open-circuit transfer impedance of the feedback network. Therefore, Equations 3.90 and 3.91 give

$$T \simeq \frac{z_{12} K_{oc}}{Z_L + r_{a3}} \tag{3.92}$$

The z-parameters z_{11}, z_{12}, z_{21} and z_{22} of the feedback network of Fig. 3.43 are all equal having the common value R_1; thus

$$z_{12} = R_1 \tag{3.93}$$

If the open-loop gain T has a large magnitude compared with

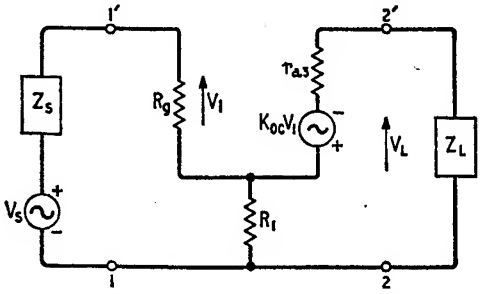

Fig. 3.43. Equivalent circuit of the feedback amplifier of Fig. 3.42

unity, the closed-loop gain K' assumes the following approximate value

$$K' \simeq -\frac{Z_L}{z_{12}}$$

$$= -\frac{Z_L}{R_1} \tag{3.94}$$

To illustrate the above results with a numerical example let it be required to realise an open-loop gain of 30 given that

$$R' = R'' = 6{\cdot}8\ \text{k}\Omega$$

$$Z_L = 10\ \text{k}\Omega$$

and that the three valves are identical having the following parameters

$$r_{a1} = r_{a2} = r_{a3} = 8\ \text{k}\Omega$$

$$\mu_1 = \mu_2 = \mu_3 = 30$$

From Equation 3.89 we find that

$$K_{oc} = \frac{(30)^3 \times 6{\cdot}8^2}{(6{\cdot}8 + 8)^2} = 5{,}700$$

Then Equation 3.92 gives the required value of z_{12} to be

$$z_{12} \simeq \frac{T}{K_{oc}}(Z_L + r_{a3}) \qquad (3.95)$$

$$= \frac{30}{5700}(10 + 8) = 0{\cdot}095\ \text{k}\Omega = 95\ \Omega$$

Hence the required feedback resistor R_1 follows from Equation 3.93 to be 95 Ω, which is quite small compared both with $r_{a3} = 8$ kΩ and with the normal value of 100 kΩ to 1 MΩ for the grid resistor R_g of the first stage. This then justifies ignoring the loading effects of the feedback network.

With $T = 30$ we shall be quite justified in using Equation 3.94 for obtaining an approximate value for the closed-loop gain, thus

$$K' \simeq -\frac{10}{0{\cdot}095} = -105$$

Bridge feedback

The simple shunt and series feedback circuits shown in Figs. 3.39 and 3.42, which are quite suitable for most applications, suffer from two major disadvantages. First, the applied negative feedback causes the input and output impedances presented to the source and load, respectively, to assume either very low values or very high values. Therefore, if the feedback amplifier is required to match the internal impedance of the source at its input port, and the load impedance at its output port so as to minimise reflection effects, it will become necessary to pad the input and output ports of the amplifier with appropriate impedances in the manner illustrated in Fig. 3.44. With these arrangements, however, the impedance matching is achieved at the cost of reduced gain and reduced useful power output.

The second major disadvantage of the shunt and series feedback circuits is that in both cases the open-loop gain T depends on the source and load impedances with the result that any variation in either terminating impedance will produce a corresponding change in the open-loop gain. In certain cases this effect can be appreciable enough to cause instability.

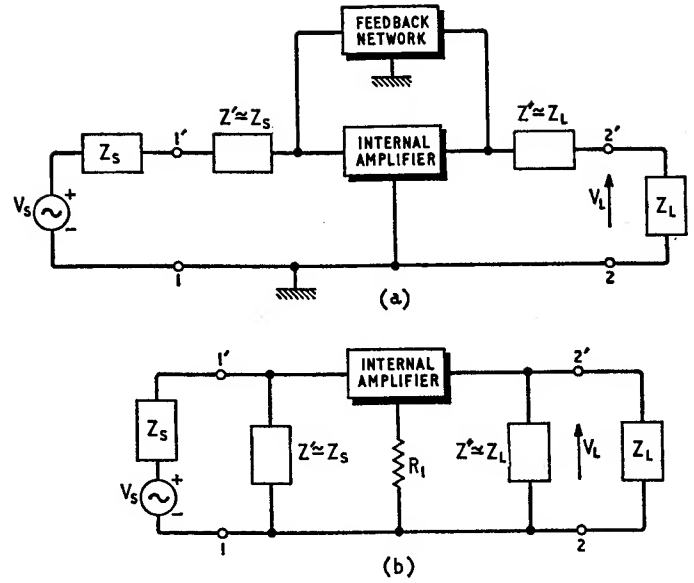

Fig. 3.44. (a) Shunt-shunt feedback amplifier with series padding elements for impedance matching, (b) Series-series feedback amplifier with shunt padding elements for impedance matching

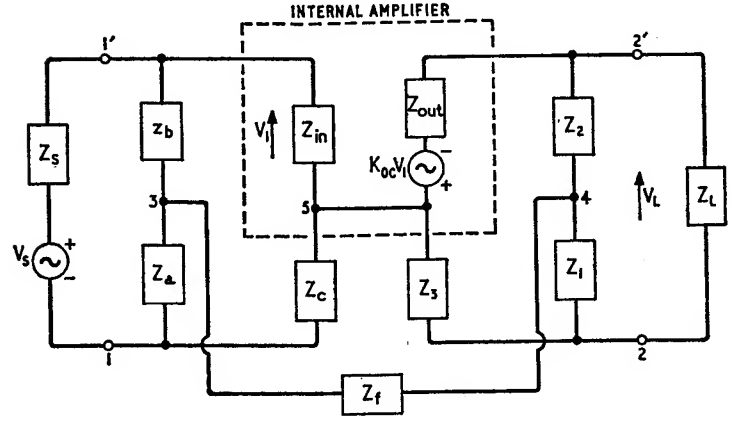

Fig. 3.45. Bridge feedback

These difficulties, experienced with shunt and series feedback circuits, are overcome by the use of *bridge feedback* shown illustrated in Fig. 3.45. At the output port the elements Z_1 and Z_2 forming a potential divider across the load apply shunt feedback, whereas the element Z_3 applies series feedback. Similarly, at the input port the elements Z_a, Z_b and Z_c are responsible for applying the feedback signal to the input port of the internal amplifier in parallel and series, respectively.

In Fig. 3.45 the parameter K_{oc} denotes the open-circuit voltage gain of the internal amplifier, and Z_{in} and Z_{out} represent its input and output impedances, respectively. The elements Z_a, Z_b, Z_c and Z_{in}

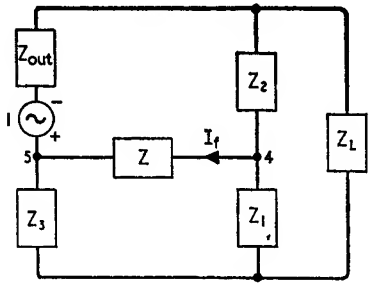

Fig. 3.46. Calculation of return difference with reference to K_{oc}

are seen to form the four arms of a Wheatstone bridge at the input end of the circuit, while the elements Z_1, Z_2, Z_3 and Z_{out} form the four arms of another Wheatstone bridge at the output end. Both these bridges will be balanced provided the following conditions are satisfied

$$\frac{Z_a}{Z_c} = \frac{Z_b}{Z_{in}} \qquad (3.96\text{ (a)})$$

$$\frac{Z_1}{Z_3} = \frac{Z_2}{Z_{out}} \qquad (3.96\text{ (b)})$$

Then with the first balance condition satisfied, we find that the input impedance Z_{in}' measured looking into the port 1,1′ becomes independent of the feedback impedance Z_f, that is Z_{in}' remains unchanged for zero or infinite feedback impedance. Hence

$$Z_{in}' = \frac{(Z_a + Z_b)(Z_c + Z_{in})}{Z_a + Z_b + Z_c + Z_{in}} \qquad (3.97)$$

Eliminating Z_{in} between Equations 3.96 (a) and 3.97 gives

$$Z_{in}' = \frac{Z_c(Z_a + Z_b)}{Z_a + Z_c} \qquad (3.98)$$

Similarly the output impedance Z_{out}' measured looking into the port 2,2′ becomes independent of any variations in the feedback impedance Z_f if the second balance condition of Equation 3.96 (b) is satisfied. Then we find that

$$Z_{out}' = \frac{(Z_1 + Z_2)(Z_3 + Z_{out})}{Z_1 + Z_2 + Z_3 + Z_{out}} \qquad (3.99)$$

Eliminating Z_{out} between Equations 3.96 (b) and 3.99 gives

$$Z_{out}' = \frac{Z_3(Z_1 + Z_2)}{Z_1 + Z_3} \qquad (3.100)$$

Next, let us evaluate the return difference of the feedback amplifier of Fig. 3.45 with reference to K_{oc} assuming that both bridges are balanced. For this purpose, consider first Fig. 3.46 where the controlled source $K_{oc}V_1$ has been set equal to unity. The impedance Z is equal to the feedback impedance Z_f plus the impedance $Z_{3,5}$ measured between the point 3 and the common terminal 5 of the internal amplifier. Provided that Equation 3.96 (a) is satisfied, the impedance $Z_{3,5}$ becomes independent of the source impedance Z_S, and so we obtain

$$Z = Z_f + \frac{(Z_a + Z_c)(Z_b + Z_{in})}{Z_a + Z_b + Z_c + Z_{in}} \qquad (3.101)$$

Eliminating Z_c between Equations 3.96 (a) and 3.101, and then simplifying, we get

$$Z = Z_f + n_a(Z_b + Z_{in}) \qquad (3.102)$$

where n_a = the input potential divider ratio

$$= \frac{Z_a}{Z_a + Z_b} \qquad (3.103)$$

The current I_f flowing through the impedance Z (see Fig. 3.46) remains unchanged for zero or infinite load impedance provided Equation 3.96 (b) is satisfied. Thus we find

$$I_f = \frac{-(Z_1 + Z_3)/(Z + Z_1 + Z_3)}{Z_2 + Z_{out} + Z(Z_1 + Z_3)/(Z + Z_1 + Z_3)} \qquad (3.104)$$

Eliminating Z_3 between Equations 3.96 (b) and 3.104, and then simplifying, we have

$$I_f = \frac{-n_1}{Z + n_1(Z_2 + Z_{out})} \qquad (3.105)$$

where n_1 = the output potential divider ratio

$$= \frac{Z_1}{Z_1 + Z_2} \tag{3.106}$$

The current I_f flowing through the feedback impedance Z_f in turn, produces a voltage V_1 across the impedance Z_{in}. This voltage will, because of Equation 3.96 (a), be independent of the source impedance Z_S and is given by

$$V_1 = \frac{Z_{in}(Z_a + Z_c)I_f}{Z_a + Z_b + Z_c + Z_{in}} \tag{3.107}$$

Eliminating Z_c between Equations 3.96 (a) and 3.107, and then using Equations 3.103, 3.105 and 3.102 we get

$$\begin{aligned} V_1 &= \frac{Z_a Z_{in} I_f}{Z_a + Z_b} \\ &= \frac{-n_a n_1 Z_{in}}{Z + n_1(Z_2 + Z_{out})} \\ &= \frac{-n_a n_1 Z_{in}}{Z_f + n_a(Z_b + Z_{in}) + n_1(Z_2 + Z_{out})} \end{aligned} \tag{3.108}$$

Noting that the control parameter k corresponds to K_{oc}, and that the returned signal V_1 is equal to the transmittance t_{ba}, we find from Equations 3.22 and 3.108 that the return difference F with reference to K_{oc} is equal to

$$F = 1 + \frac{n_1 n_a K_{oc} Z_{in}}{Z_f + n_a(Z_b + Z_{in}) + n_1(Z_2 + Z_{out})} \tag{3.109}$$

In the case of an internal amplifier consisting of a cascade of three common cathode stages the open-circuit voltage gain K_{oc} is given by Equation 3.89. If, however, the internal amplifier involves three common emitter stages, then K_{oc} has the following value

$$K_{oc} = Y_m Z_{out} \tag{3.110}$$

where $Z_{out} = 1/Y_{out}$ and Y_m are as given by Equations 3.78 and 3.79, respectively. We thus see that in both cases K_{oc} has a positive value, making the return difference F greater than unity.

From Equations 3.98, 3.100 and 3.109 we can summarise the important properties of the feedback amplifier of Fig. 3.45 having balanced input and output bridge circuits, as follows:

1. Its input and output impedances are independent of the feedback impedance Z_f.
2. The return difference F, which increases with decreasing Z_f, is independent of both the source and load impedances.

By choosing the source impedance $Z_S = Z_{in}'$ and the load impedance $Z_L = Z_{out}'$, where Z_{in}' and Z_{out}' are as given by Equations 3.98 and 3.100, we ensure that the feedback amplifier is perfectly matched to both its source and load.

Unbalanced Bridge Feedback

Owing to the unavoidable variations that occur in the parameters of the transistors or valves which constitute the internal amplifier component, we find that the actual input and output impedances of the internal amplifier depart from the desired values which are necessary to satisfy the balance conditions of Equation 3.96. Furthermore, quite often the bridge feedback is deliberately made unbalanced in an effort to save useful power. In such situations we find that a certain degree of impedance mismatch occurs at the input and output ports of the feedback amplifier. In fact it can be shown that if the output impedance of the internal amplifier component has a value different from the Z_{out} required to satisfy the balance condition of Equation 3.96 (b), then

$$\rho_2 = \frac{\rho_2^0}{F_1} \tag{3.111}$$

In this equation we have

F_1 = return difference with reference to K_{oc} after the change in the output impedance of the internal amplifier is made,

ρ_2 = reflection coefficient at the output port 2,2′ resulting from the change in the output impedance of the internal amplifier

$$= \frac{Z_{out_1} - Z_L}{Z_{out_1} + Z_L} \tag{3.112}$$

ρ_2^0 = reflection coefficient, at the output port 2,2′, that results if the internal amplifier were made passive by inactivating the controlled source $K_{oc}V_1$

$$= \frac{Z^0_{out_1} - Z_L}{Z^0_{out_1} + Z_L} \tag{3.113}$$

Z_{out_1}, which is different from the Z_{out}' of Equation 3.100, is the impedance measured looking into the output port 2,2′ after the

balance of the output bridge in the feedback amplifier has been disturbed by the change in the output impedance of the internal amplifier component. The impedance Z^0_{out1} is the value of Z_{out1} which results when the controlled source $K_{oc}V_1$ is set equal to zero. It is to be noted that in Equation 3.111 it is assumed that, as before, the load impedance Z_L has been chosen equal to the Z_{out}' of Equation 3.100.

The reflection coefficient $\rho_2{}^0$ is always less than unity in absolute value. Therefore, from Equation 3.111 it follows that provided the applied feedback is large, then the absolute value of the output

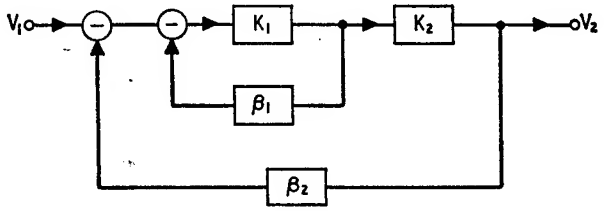

Fig. 3.47

reflection coefficient ρ_2 will be small compared to unity. In other words, the departures produced in the output impedance which the feedback amplifier presents to the load will be small even though the actual output impedance of the internal amplifier may depart considerably from the value required to satisfy the balance condition of Equation 3.96 (b). However, the other important property of the balanced output bridge, that the return difference with reference to K_{oc} is independent of the load impedance, is no longer applicable once the balance of the output bridge has been disturbed.

Assuming that we are only interested in the magnitudes of the quantities in Equation 3.111, we find that on taking the natural logarithm of the magnitudes of both sides of this equation, and then multiplying throughout by -1, we get

$$-\log_e|\rho_2| = -\log_e|\rho_2{}^0| + \log_e F_1 \qquad (3.114)$$

The term $-\log_e|\rho|$ is referred to as the 'return loss' in nepers. To obtain the return loss in decibels, we simply multiply the value in nepers by 8·69.

Now because $|\rho_2{}^0| \leqslant 1$, we deduce from Equation 3.114 that in an unbalanced bridge feedback having a load impedance Z_L equal to the Z_{out}' of Equation 3.100, the return loss (in nepers) measured at the output port 2,2′ of the feedback amplifier is necessarily greater than the amount of feedback (in nepers) acting in the circuit. Therefore, in practice we should ensure that the return difference with reference to K_{oc} equals at least the required output

return loss. Similar remarks apply to the bridge feedback at the input end of the amplifier.

PROBLEMS

1. Fig. 3.47 illustrates the block diagram of a multiple-loop feedback amplifier. If $\beta_1 K_1 = -1$, show that (a) the closed-loop gain becomes independent of variations in K_2, and (b) harmonic distortion produced by nonlinearities associated with the K_2-stage is completely eliminated from the output signal. What practical difficulties can be experienced in the design of such an amplifier?
2. State the advantages gained from the application of negative feedback to an amplifier. Derive an expression for the factor by which the amplification without feedback must be multiplied to give the amplification in the presence of feedback. Show that, with certain assumptions, the harmonic distortion present in the output is reduced in the same ratio.

   Discuss the effect of negative feedback on noise introduced into (a) the input, (b) the output stage, of an amplifier.

   A certain amplifier has 1/5000th part of its output fed back in antiphase to the input, the gain of the amplifier itself (without feedback) being 55,000.

   Calculate the percentage reduction in the amplification if the overall amplification without feedback falls to 40,000.

   (London University, B.Sc. Eng., Part III, Telecommunication, 1959).
3. A negative feedback amplifier, involving three identical stages, has a closed-loop gain of 50. It is found that a change of 5 per cent in the gain of each of the three stages causes the closed-loop gain to change by 0·5 per cent. Calculate the gain of each individual stage. Assume that the direct transmittance from source to load is zero.
4. The circuit of Fig. 3.48 shows local shunt feedback applied to a common cathode stage. Show that

   K' = closed-loop gain of the stage

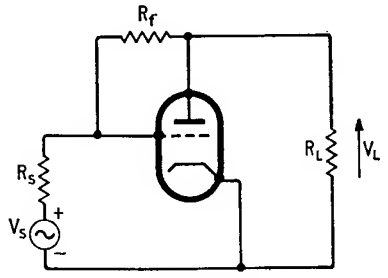

Fig. 3.48

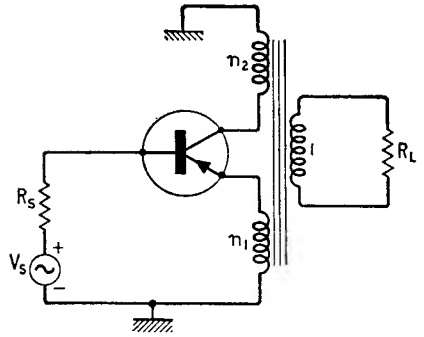

Fig. 3.49

$$K' = \frac{1 - g_m R_f}{1 + (R_S + R_f)(g_a + G_L) + g_m R_S}$$

F = return difference with reference to g_m

$$= 1 + \frac{g_m R_S}{1 + (R_S + R_f)(g_a + G_L)}$$

where g_a = anode slope conductance, g_m = mutual conductance of the triode, and $G_L = 1/R_L$ is the load conductance.

5. Assuming that the transformer of the *split-load stage* of Fig. 3.49 is ideal, and that the parameters h_{12e} and h_{22e} have negligible effects, show that the return difference F with reference to h_{21e} is

$$F = 1 + \frac{n_1 h_{21e} R_L (n_1 + n_2)}{n_1^2 R_L + h_{11e} + R_S}$$

6. In the transistor stage of Fig. 3.50 the series and shunt types of local feedback are combined together. Neglecting the effects of h_{12e} and h_{22e}, determine the return difference with reference to h_{21e}. Show that when $R_e R_f = h_{11e} R_L$, the input impedance of the stage becomes independent of h_{21e}.

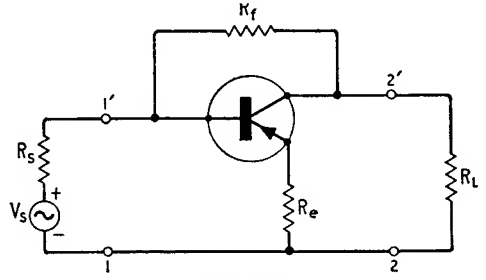

Fig. 3.50

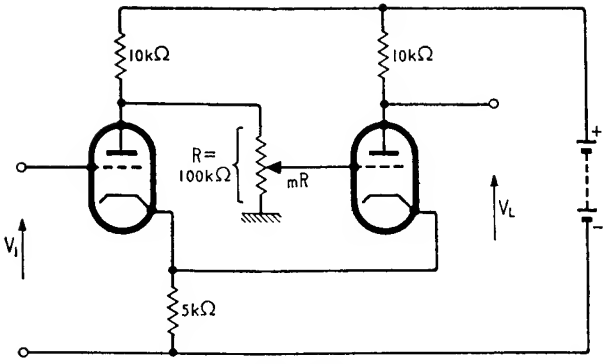

Fig. 3.51

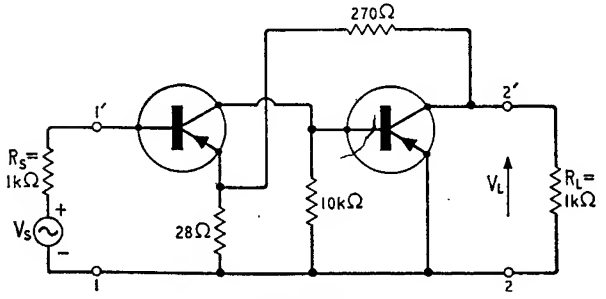

Fig. 3.52

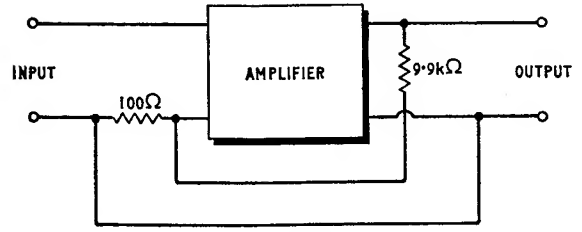

Fig. 3.53

7. Fig. 3.51 shows the *Schmitt trigger circuit*. Assuming that the circuit is operated in its linear region, calculate the critical value of the potential divider ratio m that will cause the closed-loop gain to become infinite. The two valves are identical, each having $r_a = 10$ kΩ and $\mu = 20$.
8. Calculate the closed-loop gain and input impedance of the transistor feedback amplifier of Fig. 3.52. The two transistors are identical, for each one of which $h_{11e} = 1{\cdot}06$ kΩ and $h_{21e} = 38$. Neglect effects of the h_{12e} and h_{22e} parameters of both stages.
9. The voltage gain of a two-stage direct-coupled amplifier is 1,000 when the output terminals are open-circuited. The input impedance is infinite and the final stage of the amplifier is equivalent to a generator having an internal resistance of 8 kΩ. Feedback is provided by the network shown in Fig. 3.53.
   What is the voltage gain of the amplifier when the feedback is operative? What is the output impedance of the amplifier including the feedback circuit shown in Fig. 3.53?
   (London University, B.Sc., Eng., Part III Electronics, 1959)
10. A common emitter stage has a load resistance $R_L = 10$ kΩ and is driven from a voltage source of internal resistance $R_S = 1$ kΩ. The transistor has the following common emitter h-parameters.

$$h_{11e} = 1 \text{ k}\Omega$$
$$h_{12e} = 10^{-4}$$
$$h_{21e} = 50$$
$$h_{22e} = 25\ \mu\mho$$

   Determine the return difference of the stage with reference to
   (a) the h_{21e} parameter
   (b) the y_{21e} parameter
   (c) the z_{21e} parameter
   (d) the g_{21e} parameter

   Comment on the results.
11. In a single-loop feedback amplifier show that

$$F = F_{1oc}\frac{Z_S + Z_{in}'}{Z_S + Z_{in}^0}$$
$$= F_{1sc}\frac{Y_S + Y_{in}'}{Y_S + Y_{in}^0}$$

   where F is the return difference with reference to a specified control parameter when the input port is terminated with the source impedance $Z_S = 1/Y_S$, F_{1oc} and F_{1sc} are the values of F when the input port port is open-circuited and short-circuited, respectively,
   $Z_{in}' = 1/Y_{in}'$ is the input impedance of the feedback amplifier,
   $Z_{in}^0 = 1/Y_{in}^0$ is the value of the input impedance which results when the control parameter is set equal to zero.
   What are the corresponding relations for the output port?
   To what forms do these various relations reduce when they are applied to the basic series—series and shunt–shunt feedback circuits?
12. Using the impedance formula of Equation 3.38, derive the relation of Equation 3.111 which applies to an unbalanced bridge feedback circuit.

REFERENCES

1. BODE, H. W., *Network Analysis and Feedback Amplifier Design*, Van Nostrand, New York (1945).
2. MASON, S. J. 'Feedback Theory—some properties of signal flow graphs', *Proc. I.R.E.*, **41**, 1144 (1953).
3. TRUXAL, J. G., *Automatic Feedback Control Systems Synthesis*, McGraw-Hill (1955).
4. BLECHER, F. H., 'Design Principles for Single-Loop Transistor Feedback Amplifiers', *I.R.E. Trans.*, **CT-4**, 145 (1957).
5. HAKIM, S. S., *Junction Transistor Circuit Analysis*, Iliffe Books (1962).
6. MULLIGAN, J. H., 'Signal Transmission in Non-Reciprocal Systems', *International Symposium on Active Networks and Feedback Systems, Polytechnic Institute of Brooklyn*, New York, 125 (1960).
7. BURMAN, D. F., FEY, L. J., and INGRAM, D. G. W., 'Transistor Feedback Amplifiers in Carrier Telephony Systems', *Proc. I.E.E.*, Supplement No. 16, **106B**, 587 (1959).
8. HOROWITZ, I. M., *Synthesis of Feedback Systems*, Academic Press, New York (1963).
9. HOSKINS, R. F., 'Signal Flow Graph Analysis and Feedback Theory', *Proc. I.E.E.*, **108C**, 12 (1961).
10. SHEA, R. F., *Principles of Transistor Circuits*, Wiley, New York (1953).
11. HAKIM, S. S., 'Aspects of Return Difference Evaluation in Transistor Feedback Amplifiers', *Proc. I.E.E.*, **112**, 1700 (1965).

CHAPTER 4

Analysis in the p-plane

Feedback circuits can be classified as stable or unstable depending on the nature of their closed-loop response. The circuit is stable if its output signal decays with time ultimately becoming zero when the applied input signal is an impulse. Thus, the stability problem of a feedback circuit can be studied in terms of its closed-loop transient response; this we shall do in the present chapter. Alternatively, as we shall see in Chapters 5 and 7, it is possible to investigate the stability performance of a feedback circuit in terms of its open-loop frequency response or its driving-point impedances.

4.1 Impulse response

Consider a linear circuit having the following transfer function $G(p)$

$$G(p) = \frac{b_m p^m + b_{m-1} p^{m-1} + \ldots + b_1 p + b_0}{a_n p^n + a_{n-1} p^{n-1} + \ldots + a_1 p + a_0} \tag{4.1}$$

where p is the complex frequency variable, $a_0, a_1 \ldots a_{n-1}, a_n$ and $b_0, b_1 \ldots b_{m-1}, b_m$ are all real coefficients. Suppose that this circuit is subjected to a unit impulse. Then, the excitation transform will be equal to unity, and from Equation 2.23 we see that the corresponding response transform $\Phi_0(p)$ is

$$\Phi_0(p) = G(p) \cdot 1 \tag{4.2}$$

Therefore, the transfer function of a circuit that is initially at rest and that is subjected to a unit impulse is equal to the Laplace transform of the resulting response function $\phi_0(t)$ which represents a voltage or current.

Expressing $G(p)$ in terms of its poles and zeros, we see from Equations 4.1 and 4.2 that

$$\begin{aligned}\Phi_0(p) &= \frac{b_m p^m + b_{m-1} p^{m-1} + \ldots + b_1 p + b_0}{a_n p^n + a_{n-1} p^{n-1} + \ldots + a_1 p + a_0} \\ &= H \frac{(p - z_1)(p - z_2) \ldots (p - z_m)}{(p - p_1)(p - p_2) \ldots (p - p_n)}\end{aligned} \tag{4.3}$$

where H is the scale factor; $z_1, z_2 \ldots z_m$ are the zeros of $G(p)$ and $p_1, p_2 \ldots p_n$ are its poles.

Owing to the nature of any linear feedback circuit, the transfer function is restricted to have $n > m$. Then, assuming that all the poles are simple ones, we can expand Equation 4.3 into partial fractions as follows

$$\begin{aligned}\Phi_0(p) &= \frac{A_1}{p - p_1} + \frac{A_2}{p - p_2} + \ldots \frac{A_n}{p - p_n} \\ &= \sum_{i=1}^{i=n} \frac{A_i}{p - p_i}\end{aligned} \tag{4.4}$$

where the coefficient A_i is given by

$$A_i = [(p - p_i)\, \Phi_0(p)]_{p=p_i} \tag{4.5}$$

From pair No. 5 of the Laplace Transform pairs Table 2.1 we see that the term $1/(p - p_i)$ will contribute the component $e^{p_i t}$ to the response function $\phi_0(t)$. Therefore,

$$\begin{aligned}\phi_0(t) &= A_1 e^{p_1 t} + A_2 e^{p_2 t} + \ldots + A_n e^{p_n t} \\ &= \sum_{i=1}^{i=n} A_i e^{p_i t}\end{aligned} \tag{4.6}$$

With the coefficients $a_0, a_1 \ldots a_{n-1}, a_n$ all real, we find that the poles of $G(p)$ can be either real numbers or occur in pairs of complex conjugate numbers. Hence, there are two cases to consider:

1. *Real poles*

In this case the pole at p_i is real and contributes $A_i e^{p_i t}$ to the impulse response. If p_i is negative, that is, the pole is located on the σ-axis and in the left half of the p-plane as in Fig. 4.1 (a), then as t increases the value of $e^{p_i t}$ decreases exponentially and reduces to zero at infinite time as illustrated in Fig. 4.1 (b). If, however, p_i is positive, that is, the real pole lies in the right half of the p-plane as in Fig. 4.2 (a), then the value of $e^{p_i t}$ increases exponentially with increasing time and becomes infinite at $t = \infty$ as shown in Fig. 4.2 (b).

2. *Complex conjugate poles*

In this case p_i and A_i are both complex and so we can write $p_i = \sigma_i + j\omega_i$ and $A_i = a_i + jb_i$ where σ_i, ω_i, a_i and b_i are all real numbers. Then the pole at p_i contributes

$$A_i e^{p_i t} = (a_i + jb_i) e^{\sigma_i t} e^{j\omega_i t}$$
$$= e^{\sigma_i t}(a_i + jb_i)(\cos \omega_i t + j \sin \omega_i t) \qquad (4.7)$$

to the impulse response of the circuit. Since the poles occur in complex conjugate pairs, it follows that there must be a second pole at $p_i^* = \sigma_i - j\omega_i$ where p_i^* denotes the complex conjugate of p_i. Therefore, the contribution of this second pole to the impulse response is equal to $A_i^* e^{p_i^* t}$ where A_i^* is the complex conjugate of A_i, that is, $A_i^* = a_i - jb_i$. Thus

$$A_i^* e^{p_i^* t} = (a_i - jb_i) e^{\sigma_i t} e^{-j\omega_i t}$$
$$= e^{\sigma_i t}(a_i - jb_i)(\cos \omega_i t - j \sin \omega_i t) \qquad (4.8)$$

Adding Equations 4.7 and 4.8 gives the total contribution of a pair of complex conjugate poles at p_i and p_i^* to the impulse response to be

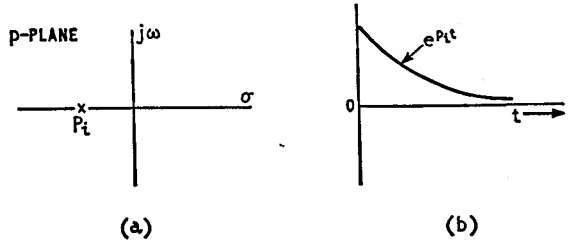

Fig. 4.1. (*a*) *Real pole located in left half of p-plane* ($p_1 < 0$), (*b*) *Impulse response*

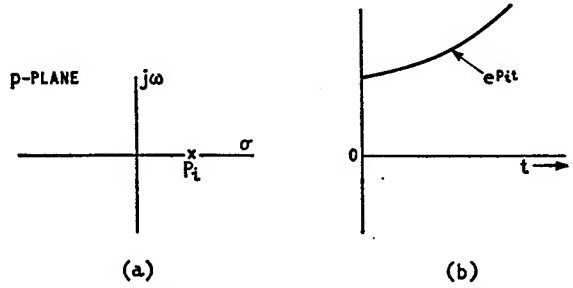

Fig. 4.2. (*a*) *Real pole located in right half of p-plane* ($p_1 > 0$), (*b*) *Impulse response*

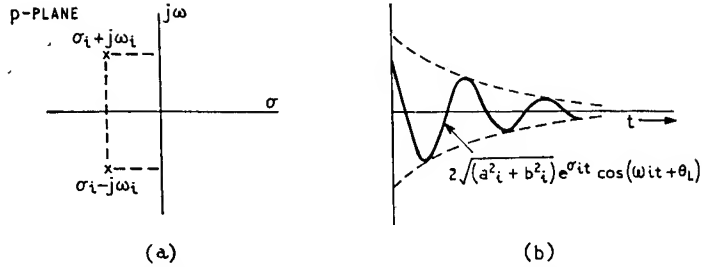

Fig. 4.3. (*a*) *Pair of complex conjugate poles in left half of p-plane* ($\sigma_1 < 0$), (*b*) *Impulse response*

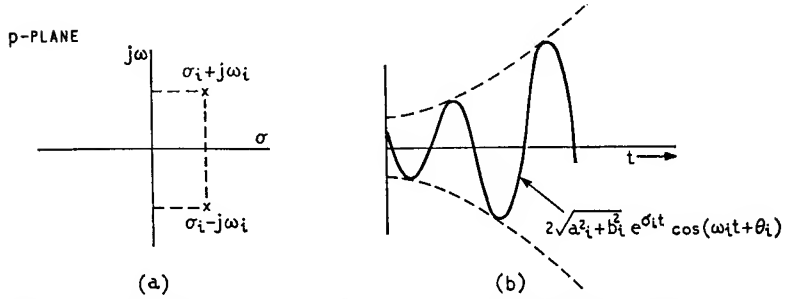

Fig. 4.4. (*a*) *Pair of complex conjugate poles in right half of p-plane* ($\sigma_i > 0$), (*b*) *Impulse response*

$$2 e^{\sigma_i t}(a_i \cos \omega_i t - b_i \sin \omega_i t) = 2\sqrt{(a_i^2 + b_i^2)} \cdot e^{\sigma_i t} \cos(\omega_i t + \theta_i) \qquad (4.9)$$

where

$$\theta_i = \tan^{-1}\left(\frac{b_i}{a_i}\right)$$

If the poles at p_i and p_i^* lie in the left half of the *p*-plane as in Fig. 4.3 (a), then σ_i is negative and the corresponding impulse response contribution is of a damped cosine form as illustrated in Fig. 4.3 (b).

But if the two complex conjugate poles lie in the right half of the *p*-plane as in Fig. 4.4 (a), then σ_i is positive and the corresponding impulse response contribution will be of an exponentially increasing cosine form as shown in Fig. 4.4 (b).

Finally, if the two complex conjugate poles lie on the jω-axis of the *p*-plane as in Fig. 4.5 (a), then σ_i is zero and Equation 4.9 reduces to $2\sqrt{(a_i^2 + b_i^2)} \cos(\omega_i t + \theta_i)$. This corresponds to a sustained oscillatory function as shown in Fig. 4.5 (b).

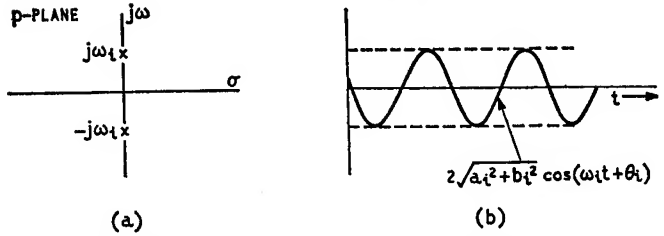

Fig. 4.5. (a) Pair of complex conjugate poles on imaginary axis ($\sigma_1 = 0$), (b) Impulse response

From the above discussion we can draw the following important conclusions regarding the transfer function $G(p)$ of any linear circuit:

1. The location of the poles of $G(p)$ in the p-plane uniquely defines the nature of the transient response. Real poles and the real parts of complex conjugate poles contribute exponential terms; hence, they control the damping of the response. The imaginary part of a pair of complex conjugate poles controls the frequency of their oscillatory response contribution.
2. The exponential terms contributed to the impulse response by poles located in the right half of the p-plane increase with increasing time despite the fact that the driving impulse function is zero for $t > 0$. Therefore, a transfer function having any pole in the right half of the p-plane corresponds to an *unstable circuit.*
3. For a stable response it is necessary that all the poles of the transfer function are located in the left half of the p-plane.
4. The $j\omega$-axis of the p-plane is the dividing line between the domains of stability and instability.

4.2 Stability considerations of feedback circuits

Consider a single-loop feedback circuit represented by the signal flow graph of Fig. 4.6 where all the transmittances have been assumed to be functions of the complex frequency variable p so as to keep the discussion quite general. The closed-loop gain function $K'(p)$ of the feedback circuit is thus given by (see Section 3.7.1.)

$$K'(p) = \frac{V_L(p)}{V_S(p)} = t_{sl}(p) + \frac{K(p)}{1 + T(p)} \tag{4.10}$$

where

$$K(p) = t_{sa}(p)k(p)t_{bl}(p) \tag{4.11 (a)}$$

$$T(p) = -k(p)t_{ba}(p) \tag{4.11 (b)}$$

In a single-loop feedback circuit we normally find that both the direct transmittance $t_{sl}(p)$ and the gain function $K(p)$ of Equation 4.11 (a) represent stable transfer functions in that they have all their poles located in the left half of the p-plane. We therefore see from Equation 4.10 that the closed-loop gain function $K'(p)$ can have poles in the right half of the p-plane if the return difference $F(p) = 1 + T(p)$ happens to have zeros in the right half of the p-plane. Conversely, if $F(p)$ has zeros in the right half of the p-plane, then $K'(p)$ must have poles there except in the extremely unlikely case that the $K(p)$ of Equation 4.11 (a) should have zeros

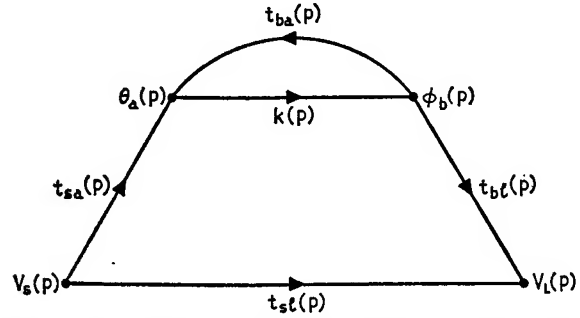

Fig. 4.6. The signal flow graph for a single-loop feedback circuit

at the correct positions to cancel all the zeros of $F(p)$. We therefore conclude that the closed-loop gain function $K'(p)$ represents a stable transfer function if and only if the return difference $F(p)$ has no zeros at all in the right half of the p-plane. In other words, the stability performance of a single-loop feedback circuit is completely determined by the location of the zeros of $F(p) = 1 + T(p)$ in the p-plane.

Let us assume that the open-loop gain function $T(p)$ is expressed as follows:

$$T(p) = H\frac{N(p)}{D(p)} \tag{4.12}$$

where H is the scale factor, and $D(p)$ and $N(p)$ are two polynomials in p. Then the zeros of $F(p)$ are the same as the roots of the *characteristic equation*

$$D(p) + H \cdot N(p) = 0 \tag{4.13}$$

By evaluating the roots of this equation it is possible to establish whether or not the closed-loop gain function $K'(p)$ has any poles in the right half of the p-plane. The numerical evaluation of the roots of the characteristic equation is quite straightforward; but it becomes more time consuming as the order of the highest power of p increases. A simpler method of establishing that $K'(p)$ corresponds to a stable circuit is to apply to the characteristic equation a criterion developed by E. J. Routh[1] in 1877.

4.3 Routh's criterion†

Suppose that for a given feedback circuit the characteristic equation is of the following form

$$\alpha_0 p^n + \alpha_1 p^{n-1} + \alpha_2 p^{n-2} + \ldots + \alpha_n = 0 \qquad (4.14)$$

where it is assumed that all the coefficients are real and α_0 is positive. By inspecting the coefficients α_0 to α_n and applying *Routh's criterion* it is possible to detect the presence of roots with positive real roots, that is, roots located in the right half of the p-plane. As an illustration; consider the case of $n = 5$; then Equation 4.14 becomes

$$\alpha_0 p^5 + \alpha_1 p^4 + \alpha_2 p^3 + \alpha_3 p^2 + \alpha_4 p + \alpha_5 = 0 \qquad (4.15)$$

The various coefficients of this equation are arranged first into two rows as follows

Row 1	α_0	α_2	α_4
Row 2	α_1	α_3	α_5

(4.16)

The next step is to construct the following array of terms

α_0	α_2	α_4
α_1	α_3	α_5
B_1	B_3	
C_1	C_3	
D_1		
E_1		

(4.17)

where the coefficients B_1, B_3, C_1, C_3, D_1 and E_1 are related to the coefficients α_0 to α_5 as follows

† Routh's criterion is also referred to as the 'Routh-Hurwitz Criterion'. A. Hurwitz, who was unaware of Routh's work, developed essentially the same result in 1895, but in a somewhat different form.

$$B_1 = \frac{\alpha_0 \times \alpha_2 \;\; \alpha_1 \times \alpha_3}{\alpha_1} = \frac{\alpha_1\alpha_2 - \alpha_0\alpha_3}{\alpha_1} \qquad (4.18)$$

$$B_3 = \frac{\alpha_0 \times \alpha_4 \;\; \alpha_1 \times \alpha_5}{\alpha_1} = \frac{\alpha_1\alpha_4 - \alpha_0\alpha_5}{\alpha_1} \qquad (4.19)$$

$$C_1 = \frac{\alpha_1 \times \alpha_3 \;\; B_1 \times B_3}{B_1} = \frac{B_1\alpha_3 - \alpha_1 B_3}{B_1} \qquad (4.20)$$

$$C_3 = \frac{\alpha_1 \times \alpha_5 \;\; B_1 \times 0}{B_1} = \frac{B_1\alpha_5 - \alpha_1 \times 0}{B_1} = \alpha_5 \qquad (4.21)$$

$$D_1 = \frac{B_1 \times B_3 \;\; C_1 \times C_3}{C_1} = \frac{C_1B_3 - B_1C_2}{C_1} \qquad (4.22)$$

$$E_1 = \frac{C_1 \times C_3 \;\; D_1 \times 0}{D_1} = \frac{D_1C_3 - C_1 \times 0}{D_1} = C_3 \qquad (4.23)$$

The final step is to examine the signs of the elements in the first column of the table of Equation 4.17. If all these elements are positive, then the given characteristic equation has all its roots located in the left half of the p-plane. If, however, there are elements with negative signs in the first column of Equation 4.17, then the number of sign changes will be equal to the number of roots located in the right half of the p-plane.

A special case that is found to occur in the study of feedback circuits is that of a row having zero for all of its elements. Normally this means the presence of conjugate roots on the $j\omega$-axis of the p-plane. In such a case we speak of the feedback circuit being on the *threshold of instability.*

Further, in certain cases it is not necessary to form the table of Equation 4.17 because a preliminary inspection of the given characteristic equation may reveal a missing term or the coefficients having different signs, in which case it is immediately deduced that the given equation must have roots in the right half of the p-plane.

4.4 Three-stage feedback amplifier

To illustrate the application of Routh's criterion, consider a single-loop feedback amplifier involving three common cathode or common emitter stages and having a purely resistive feedback network. The corresponding open-loop gain function is given by

$$T(p) = \frac{T(0)}{\left(1+\frac{p}{\omega_1}\right)\left(1+\frac{p}{\omega_2}\right)\left(1+\frac{p}{\omega_3}\right)}$$

$$= \frac{\omega_1\omega_2\omega_3 T(0)}{(p+\omega_1)(p+\omega_2)(p+\omega_3)}$$

$$= \frac{\omega_1\omega_2\omega_3 T(0)}{p^3+(\omega_1+\omega_2+\omega_3)p^2+(\omega_1\omega_2+\omega_1\omega_3+\omega_2\omega_3)p+\omega_1\omega_2\omega_3} \tag{4.24}$$

where $T(0)$ is the low frequency value of the open-loop gain and ω_1, ω_2, ω_3 are the individual stage cut off frequencies. From Equations 4.12 and 4.24 we see that

$$\left.\begin{aligned} H\cdot N(p) &= \omega_1\omega_2\omega_3 T(0) \\ D(p) &= p^3+(\omega_1+\omega_2+\omega_3)p^2 \\ &\quad +(\omega_1\omega_2+\omega_1\omega_3+\omega_2\omega_3)p+\omega_1\omega_2\omega_3 \end{aligned}\right\} \tag{4.25}$$

Then, Equations 4.13 and 4.25 give the corresponding characteristic equation to be

$$p^3+\alpha_1 p^2+\alpha_2 p+\alpha_3 = 0 \tag{4.26}$$

where

$$\left.\begin{aligned} \alpha_1 &= \omega_1+\omega_2+\omega_3 \\ \alpha_2 &= \omega_1\omega_2+\omega_1\omega_3+\omega_2\omega_3 \\ \alpha_3 &= (1+T(0))\omega_1\omega_2\omega_3 \end{aligned}\right\} \tag{4.27}$$

From the coefficients of Equation 4.26 we can develop the following table

$$\begin{array}{cc} 1 & \alpha_2 \\ \alpha_1 & \alpha_3 \\ (\alpha_1\alpha_2-\alpha_3)/\alpha_1 & 0 \\ \alpha_3 & 0 \end{array} \tag{4.28}$$

The elements of the first column of this table will be all positive and so the feedback amplifier will be stable provided that

$$\alpha_1\alpha_2-\alpha_3 > 0 \tag{4.29}$$

Using Equations 4.27 and 4.29 we deduce that the necessary condition for stability is

$$T(0) < (\omega_1+\omega_2+\omega_3)\left(\frac{1}{\omega_1}+\frac{1}{\omega_2}+\frac{1}{\omega_3}\right)-1 \tag{4.30}$$

Hence, a three-stage feedback amplifier, having the open loop gain function of Equation 4.24, will remain stable as long as its low frequency open-loop gain $T(0)$ satisfies the inequality of Equation 4.30.

From the table of Equation 4.28 we also see that if $\alpha_1\alpha_2 = \alpha_3$ then the third row will have zero for both of its elements and the amplifier will be on the threshold of instability. Using T_{0m} to denote the corresponding value of the open-loop gain, we get

$$T_{0m} = (\omega_1+\omega_2+\omega_3)\left(\frac{1}{\omega_1}+\frac{1}{\omega_2}+\frac{1}{\omega_3}\right)-1 \tag{4.31}$$

This is the low frequency value of open-loop gain which is just sufficient to cause the feedback amplifier to become oscillatory. T_{0m} is therefore termed the *threshold open-loop gain.*

In order to ensure that the feedback amplifier remains stable under all possible operating conditions, it is found necessary to have $T(0)$ sufficiently less than T_{0m}; thus

$$T(0) = \frac{T_{0m}}{T_m} \tag{4.32}$$

where $T_m > 1$. Expressing the various loop gains in decibels we obtain

$$20\log_{10} T(0) = 20\log_{10} T_{0m} - 20\log_{10} T_m \tag{4.33}$$

where $20\log_{10} T_m$ is termed the *gain margin* expressed in decibels. It can be defined as the number of decibels by which the low frequency open-loop gain can be increased to make the amplifier just unstable. It is intended to guard against the effect of parameter variations caused by changes in the d.c. supply voltage and/or ambient temperature.

Suppose that the individual stage cut off frequencies of the internal amplifier are such that $\omega_3 > \omega_2 > \omega_1$. Then, Equation 4.24 corresponds to the pole-zero pattern of Fig. 4.7. If ω_2 and ω_3 are

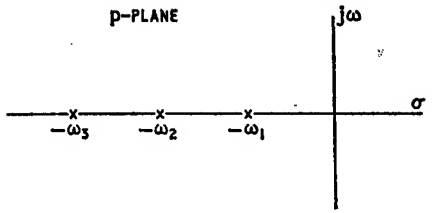

Fig. 4.7. Pole-zero pattern of open-loop gain function of three-stage feedback circuit

maintained constant, we deduce from Equation 4.31 that it is possible to increase the threshold open-loop gain T_{0m} by allowing the pole at $p = -\omega_1$ to come closer to the origin. This is referred to as *narrowbanding* because it results in a reduced cut off frequency for the stage concerned, and it can be achieved by shunting the input port of the particular transistor or valve stage with a suitable capacitor as shown in Fig. 4.8. Here it is assumed that ω_1 refers to the first stage.

Alternatively, T_{0m} can be increased by shifting the pole at

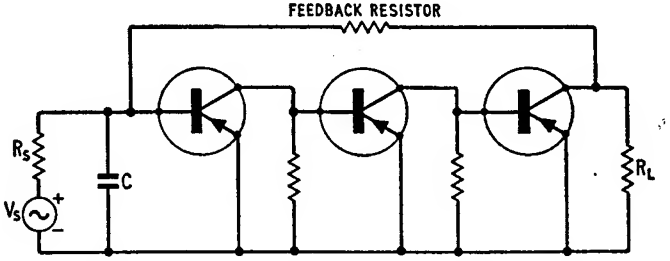

Fig. 4.8. Feedback amplifier with its first stage narrowbanded by means of capacitor C

$p = -\omega_3$ further away from the origin. This is known as *broadbanding* as it results in an increased cut off frequency for the particular stage, and it can be achieved by applying local feedback to the particular stage.†

4.5 Root locus diagrams

The *root locus method* of studying the behaviour of closed-loop feedback circuits was first introduced by W. R. Evans[2] in 1948. It provides a graphical technique for determining the roots of the

† Effect of local feedback on frequency response is discussed in Chapter 8.

characteristic equation of a single-loop feedback circuit from a knowledge of the poles and zeros of its open-loop gain function.

In Section 4.2 it was shown that the stability of a single-loop feedback circuit is determined by the location of the roots of its characteristic equation in the p-plane. The *root loci* are plots of the

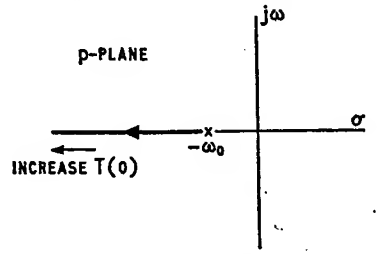

Fig. 4.9. Root locus diagram of single-stage feedback circuit

roots of the characteristic equation as a function of a suitable circuit parameter such as the low frequency open-loop gain.

As an illustration consider a single-stage feedback circuit having the following open-loop gain function

$$T(p) = \frac{T(0)}{1 + \frac{p}{\omega_0}} = \frac{\omega_0 T(0)}{p + \omega_0} \tag{4.34}$$

where $T(0)$ is the low frequency value of $T(p)$, and ω_0 is the stage cut off frequency. From Equations 4.12 and 4.34 we see that

$$\left.\begin{aligned} H \cdot N(p) &= \omega_0 T(0) \\ D(p) &= p + \omega_0 \end{aligned}\right\} \tag{4.37}$$

Then, Equation 4.13 gives the corresponding characteristic equation to be

$$p + \omega_0(1 + T(0)) = 0 \tag{4.38}$$

which has a single root at $-\omega_0(1 + T(0))$. As $T(0)$ is increased, this root moves along the σ-axis of the p-plane further away from the origin as depicted in Fig. 4.9. Therefore, a single-stage amplifier with negative feedback is inherently stable.

As a second example consider a two-stage feedback circuit whose open-loop gain function is

$$T(p) = \frac{T(0)}{\left(1 + \frac{p}{\omega_1}\right)\left(1 + \frac{p}{\omega_2}\right)}$$

$$= \frac{\omega_1\omega_2 T(0)}{(p + \omega_1)(p + \omega_2)} \tag{4.37}$$

where ω_1 and ω_2 are the individual stage cut off frequencies. Comparing Equations 4.12 and 4.37 we have

$$\left.\begin{aligned} H \cdot N(p) &= \omega_1\omega_2 T(0) \\ D(p) &= (p + \omega_1)(p + \omega_2) \\ &= p^2 + (\omega_1 + \omega_2)p + \omega_1\omega_2 \end{aligned}\right\} \tag{4.38}$$

Hence, Equations 4.13 and 4.38 give the characteristic equation of the two-stage feedback circuit to be

$$p^2 + (\omega_1 + \omega_2)p + \omega_1\omega_2(1 + T(0)) = 0 \tag{4.39}$$

This is a quadratic equation in p and has the following two roots

$$p_1, p_2 = \tfrac{1}{2}\left[-(\omega_1 + \omega_2) \pm \sqrt{[(\omega_1 + \omega_2)^2 - 4\omega_1\omega_2(1 + T(0))]}\right] \tag{4.40}$$

Here we see that when $T(0) = 0$, the two roots are equal to $-\omega_1$ and $-\omega_2$ which are the poles of $T(p)$ as given by Equation 4.37. Next, the two roots become equal to $-\frac{1}{2}(\omega_1 + \omega_2)$ when $T(0)$ satisfies the condition

$$(\omega_1 + \omega_2)^2 - 4\omega_1\omega_2(1 + T(0)) = 0$$

that is, when

$$T(0) = \frac{(\omega_2 - \omega_1)^2}{4\omega_1\omega_2} \tag{4.41}$$

When $T(0)$ assumes a value greater than that of Equation 4.41 the two roots of the characteristic equation become complex conjugate and located on a line parallel to, and a distance of $-\frac{1}{2}(\omega_1 + \omega_2)$ from the jω-axis of the p-plane. We thus find that as $T(0)$ is increased from zero, the two roots of Equation 4.39 trace out the loci shown in Fig. 4.10. From this root locus diagram we deduce that with both ω_1 and ω_2 positive:

(a) The circuit remains stable for all positive values of $T(0)$
(b) The transient response is overdamped when

$$\frac{(\omega_2 - \omega_1)^2}{4\omega_1\omega_2} > T(0) > 0 \tag{4.42}$$

It is critically damped when $T(0)$ has the value defined by Equation 4.41, and it becomes underdamped when

$$T(0) > \frac{(\omega_2 - \omega_1)^2}{4\omega_1\omega_2} \tag{4.43}$$

In the case of open-loop gain functions having more poles and zeros than those considered above, the construction of the root loci is facilitated by applying a number of rules to be developed.

4.5.1 CONSTRUCTION OF THE ROOT LOCI

From Equations 4.12 and 4.13 we see that the characteristic equation of a single-loop feedback circuit can be also expressed as follows

$$T(p) = -1 \tag{4.44}$$

This equation is satisfied if the magnitude and phase angle of the open-loop gain function meet the following conditions, respectively,

$$|T(p)| = 1 \tag{4.45}$$

$$\angle T(p) = (1 + 2k)\pi \tag{4.46}$$

where k is any integer, including zero. In general, the open-loop gain function can be expressed in terms of its poles and zeros by

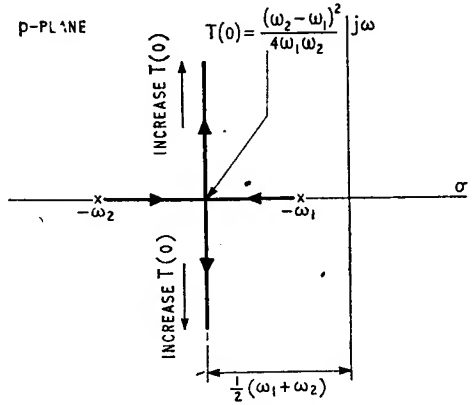

Fig. 4.10. Root locus diagram of two-stage feedback circuit

$$T(p) = H\frac{(p-z_1)(p-z_2)\ldots(p-z_m)}{(p-p_1)(p-p_2)\ldots(p-p_n)}$$

$$= H\frac{\prod_{i=1}^{m}(p-z_i)}{\prod_{j=1}^{n}(p-p_j)} \qquad (4.47)$$

where $n > m$ and H is the scale factor. From Equation 4.47 it follows that H is related to the low frequency value $T(0)$ of the open-loop gain as follows

$$T(0) = H\cdot\frac{z_1 z_2 \ldots z_m}{p_1 p_2 \ldots p_n}(-1)^{n-m} \qquad (4.48)$$

With negative feedback assumed to exist in the circuit, $T(0)$ will have a positive value.

Using Equation 4.47 we find that the two conditions of Equations 4.45 and 4.46 are equivalent to, respectively

$$H\cdot\frac{\prod_{i=1}^{m}|p-z_i|}{\prod_{j=1}^{n}|p-p_j|} = 1 \qquad (4.49)$$

$$\sum_{i=1}^{m}\angle\underline{p-z_i} - \sum_{j=1}^{n}\angle\underline{p-p_j} = (1+2k)\pi \qquad (4.50)$$

Equation 4.50 is seen to be independent of the scale factor H; it therefore applies over all points of the root loci.

We shall next develop the various rules, and later on in the chapter we shall illustrate them by considering three examples.

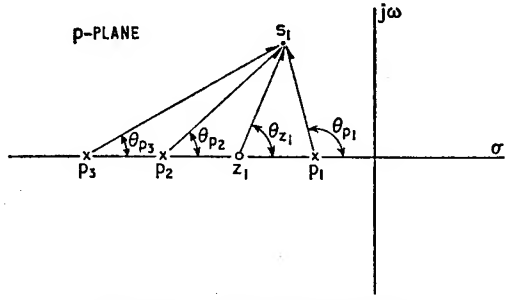

Fig. 4.11. Illustrating rule No. 5

4.5.2 RULES FOR CONSTRUCTION OF THE ROOT LOCI

Rule 1: *The root loci start at the poles of the open-loop gain function (with $H = 0$)*

Referring to Equation 4.47 we see that at each of the poles p_1, p_2, . . . p_n of the open-loop gain function, the value of the denominator is equal to zero. Therefore, to satisfy Equation 4.45, it is necessary for the scale factor H to be zero too. In other words, as H approaches zero, p approaches the poles of $T(p)$.

Rule 2: *The root loci terminate on the zeros of the open-loop gain function (with $H = \infty$)*

Again with reference to Equation 4.47 we see that at each of the zeros z_1, z_2 . . . z_m of the open-loop gain function, the value of the numerator is equal to zero. Hence, the scale factor H must equal infinity if the condition of Equation 4.45 is to be satisfied. In other words, as H approaches infinity, p approaches the zeros of $T(p)$.

Rule 3: *The root loci are symmetrical with respect to the σ-axis of the p-plane*

This rule follows simply from the fact that complex poles and zeros always occur in conjugate pairs.

Rule 4: *The number of root loci is equal to the number of poles of the open-loop gain function*

This follows from Equation 4.13 when it is remembered that the order of the denominator polynomial $D(p)$ of the open-loop gain function is greater than that of the numerator polynomial $N(p)$, that is, $n > m$ in Equation 4.47.

Rule 5: *A root locus is the locus of those points in the p-plane for which the phase angle of the open-loop gain function is equal to $(1 + 2k)\pi$ where k is any integer*

This is re-stating the condition of Equation 4.46 and enables us to determine whether a given point in the p-plane lies on the root locus or not. As an illustration consider Fig. 4.11 where it is assumed that the open-loop gain function $T(p)$ has one zero at z_1 and three poles at p_1, p_2 and p_3. Let us next draw vectors directed from the poles and zeros of $T(p)$ to an arbitrary point s_1 in the p-plane. For s_1 to lie on a root locus it is necessary that the sum $(\theta_{z_1} - \theta_{p_1} - \theta_{p_2} - \theta_{p_3})$ is an odd multiple of 180°; the angles θ_{z_1}, θ_{p_1}, θ_{p_2} and θ_{p_3} are as defined in Fig. 4.11.

Rule 6: *For very large values of p, the root loci become asymptotic to straight lines making angles of* $-(1 + 2k)\pi/(n - m)$ *with the σ-axis of the p-plane, where n and m are the number of poles and zeros of the open-loop gain function respectively, and* $k = 0, 1, 2, \ldots$ *up to* $k = n - m$

When $p \to \infty$, we find from Equation 4.47 that

$$T(p) \to Hp^{m-n} \tag{4.51}$$

Then, the condition of Equation 4.46 gives

$$\angle p^{m-n} = (1 + 2k)\pi$$

or

$$\angle p = -\frac{(1 + 2k)\pi}{n - m} \tag{4.52}$$

Thus, if $n - m = 3$, that is, $T(p)$ has a triple zero at infinity, then the asymptotes make angles of $-60°$, $-180°$ and $-300° \equiv +60°$ with the σ-axis as indicated in Fig. 4.12.

Rule 7: *The asymptotes meet at a point located along the σ-axis and determined by the relationship* (Σ *poles* $-$ Σ *zeros*)/(*number of poles — number of zeros*)

From Equation 4.47 we see that

$$T(p) = H\frac{p^m + d_{m-1}p^{m-1} + \ldots + d_0}{p^n + c_{n-1}p^{n-1} + \ldots c_0} \tag{4.53}$$

where

$$d_{m-1} = -(z_1 + z_2 + \ldots z_m) = -\sum_{i=1}^{m} z_i \tag{4.54}$$

$$c_{n-1} = -(p_1 + p_2 + \ldots p_n) = -\sum_{j=1}^{n} p_j \tag{4.55}$$

If in Equation 4.53 the numerator polynomial is divided into the denominator polynomial, we get

$$T(p) = \frac{H}{p^{n-m} + (c_{n-1} - d_{m-1})p^{n-m-1} + \ldots} \tag{4.56}$$

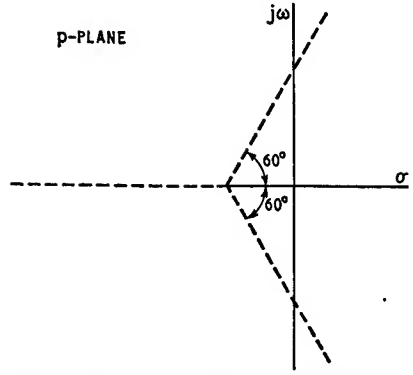

Fig. 4.12. Asymptotes of the root loci for the case of $n - m = 3$

Then, from Equations 4.44 and 4.56 it follows that the root loci are described by

$$p^{n-m} + (c_{n-1} - d_{m-1})p^{n-m-1} + \ldots = -H \tag{4.57}$$

For very large values of p the first two terms on the left hand side predominate and Equation 4.57 becomes practically indistinguishable from the following

$$\left(p + \frac{c_{n-1} - d_{m-1}}{n - m}\right)^{n-m} = -H \tag{4.58}$$

This equation defines a family of $(n - m)$ straight lines, that is, asymptotes whose intersection point corresponds to $H = 0$. Then, if $p = \sigma_0$ denotes the point at which the asymptotes meet, we find from Equation 4.58 that

$$\sigma_0 = -\frac{c_{n-1} - d_{m-1}}{n - m} \tag{4.59}$$

Therefore, Equations 4.54, 4.55 and 4.59 give

$$\sigma_0 = \frac{\sum_{j=1}^{n} p_j - \sum_{i=1}^{m} z_i}{n - m} = \frac{\sum \text{poles} - \sum \text{zeros}}{(\text{number of poles}) - (\text{number of zeros})} \tag{4.60}$$

Rule 8: *On the σ-axis the root loci lie on alternate sections connecting the real poles and zeros of the open-loop gain function, starting from the real pole or zero farthest to the right*

For any point $p = \sigma_1$ on the σ-axis of the p-plane, the sum of the angles of the vectors directed from any pair of complex conjugate poles and zeros is always zero. Therefore, when it is required to satisfy the condition of Equation 4.46 for values of p on the σ-axis, we can justifiably ignore the effect of complex conjugate poles and

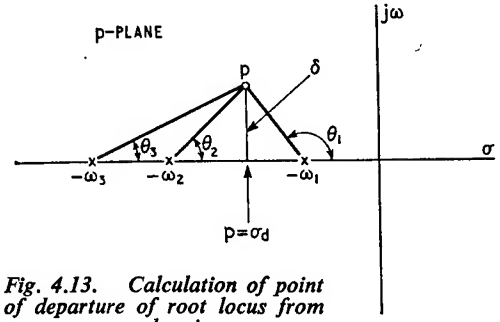

Fig. 4.13. Calculation of point of departure of root locus from real axis

zeros of $T(p)$, if any. Further, the angle contributed by a real pole or zero to the left of point σ_1 is zero, while the angle contributed by a real pole or zero to the right of σ_1, is equal to $-\pi$ or $+\pi$, respectively. Hence, along the σ-axis the root loci lie to the left of an odd number of open-loop poles and zeros.

Rule 9: *Any two real poles connected by a section of the root locus move towards each other, as the scale factor is increased, till they become coincident whereafter they separate from the σ-axis initially at right angles, to form a pair of complex conjugate roots*

To illustrate the procedure for evaluating the point of departure from the σ-axis, consider an open-loop gain function having three real poles at $-\omega_1$, $-\omega_2$ and $-\omega_3$ as in Fig. 4.13. The point of departure is at $p = \sigma_d$. At a neighbouring point $p = \sigma_d + j\delta$ we see from Fig. 4.13 that if δ is small then

$$\left.\begin{aligned}(\pi - \theta_1) \simeq \tan(\pi - \theta_1) &= \frac{-\delta}{\sigma_d + \omega_1}\\ \theta_2 \simeq \tan\theta_2 &= \frac{\delta}{\sigma_d + \omega_2}\\ \theta_3 \simeq \tan\theta_3 &= \frac{\delta}{\sigma_d + \omega_3}\end{aligned}\right\} \qquad (4.61)$$

The point $p = \sigma_d + j\delta$ will lie on the root locus if

$$-\theta_1 - \theta_2 - \theta_3 = -\pi \qquad (4.62)$$

Therefore, using Equations 4.61 and 4.62 we see that σ_d is given by the solution of the following equation

$$\frac{1}{\sigma_d + \omega_1} + \frac{1}{\omega_2 + \sigma_d} + \frac{1}{\omega_3 + \sigma_d} = 0 \qquad (4.63)$$

Rule 10: *The points at which the root loci cross the jω-axis of the p-plane can be determined from the application of Routh's criterion to the characteristic equation*

As an illustration consider the characteristic Equation 4.26 which applies to an open-loop gain function having real poles at $-\omega_1$, $-\omega_2$, and $-\omega_3$. From the table of Equation 4.28 we deduce that this characteristic equation will have a pair of complex conjugate poles on the jω-axis when $\alpha_1\alpha_2 = \alpha_3$, in which case Equation 4.26 becomes $(p + \alpha_1)(p^2 + \alpha_2) = 0$. Therefore, the root loci cross the jω-axis at

$$p = \pm j\sqrt{\alpha_2} = \pm j\sqrt{(\omega_1\omega_2 + \omega_1\omega_3 + \omega_2\omega_3)} \qquad (4.64)$$

where we have made use of the second line of Equation 4.27.

Rule 11: *The angle of departure of the root locus from a complex pole and the angle of arrival at a complex zero can be determined from Equation* 4.50

Suppose that it is required to determine the angle of departure θ_{p3} at the complex pole p_3 shown in Fig. 4.14. At a point on the root locus and very close to the pole p_3, we have from Equation 4.50 that

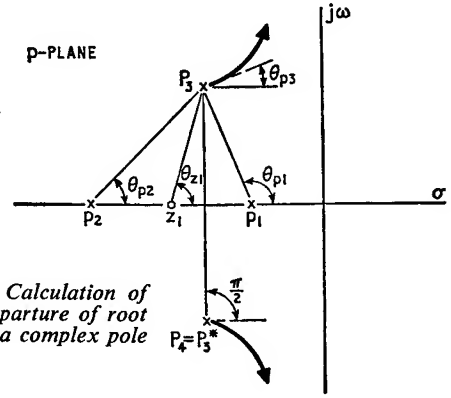

Fig. 4.14. Calculation of angle of departure of root locus from a complex pole

$$\theta_{z1} - \left(\theta_{p1} + \theta_{p2} + \theta_{p3} + \frac{\pi}{2}\right) = (1 + 2k)\pi \qquad (4.65)$$

Having measured the angles θ_{z1}, θ_{p1} and θ_{p2}, we can solve Equation 4.65 for the angle θ_{p3}. In a similar way we can determine the angle at which the root locus arrives at a complex zero.

Rule 12: *Having constructed the root loci, the value of the scale factor H at any point on the root loci can be determined from Equation* 4.49

As an example, consider Fig. 4.15 where it is required to evaluate H at the point s_1 on the root locus. Suppose that A, B and C are the

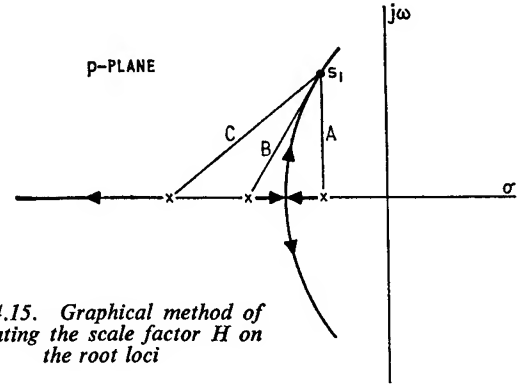

Fig. 4.15. Graphical method of evaluating the scale factor H on the root loci

lengths of the vecots directed from the poles of $T(p)$ to the point s_1. Then, from Equation 4.49 it follows that $H = A.B.C.$ at $p = s_1$.

4.6 Examples

We shall next illustrate the application of the above twelve rules to facilitate construction of the root loci by considering three examples.

Example 1

Consider a single-loop three-stage feedback amplifier with a purely resistive feedback network and having the following open-loop gain function:

$$T(p) = \frac{T(0)}{(1 + 10p)(1 + p)(1 + 0{\cdot}5p)}$$

which has three poles at $-0{\cdot}1$, -1 and -2 all located on the σ-axis of the p-plane. All the zeros of $T(p)$ are at infinity. Therefore, there

are three loci starting at $p = -0{\cdot}1$, $p = -1$ and $p = -2$ and terminating at infinity. The asymptotes make angles of $-60°$, $-180°$ and $-300°$ ($\equiv +60°$) with the σ-axis, and from Equation 4.60 we see that they intersect at

$$p = \sigma_0 = \frac{(-0{\cdot}1 - 1 - 2)}{3} = -1{\cdot}03$$

The point of departure from the σ-axis is determined from Equation 4.63; thus

$$\frac{1}{\sigma_d + 0{\cdot}1} + \frac{1}{1 + \sigma_d} + \frac{1}{2 + \sigma_d} = 0$$

Simplifying, we obtain

$$3\sigma_d^2 + 6{\cdot}2\sigma_d + 2{\cdot}3 = 0$$

Solving for σ_d, we find that $\sigma_d = -0{\cdot}483$ or $\sigma_d = -1{\cdot}58$. The former solution is the acceptable one, because the point of departure must be between the poles at $p = -0{\cdot}1$ and $p = -1$.

From Equation 4.64 we find that the points at which the root loci cross the $j\omega$-axis are given by

$$p = \pm j\sqrt{2{\cdot}3} = \pm j1{\cdot}52$$

At this intersection point, we see from Equation 4.31 that $T(0) = 34{\cdot}7$.

Using the above results and rule No. 5 we can go on to construct the root loci of Fig. 4.16.

Example 2

In the second example, we shall assume that the open-loop gain function has one real zero and three real poles; thus

$$T(p) = T(0)\frac{1 + 2p}{(1 + 10p)(1 + p)(1 + 0{\cdot}5p)}$$

The root loci start at the poles $p = -0{\cdot}1$, -1 and -2, and finish at the zero $p = -0{\cdot}5$ and the two zeros at infinity. Since there are three finite poles and one finite zero, that is $n = 3$ and $m = 1$, it follows that there are two asymptotes at angles of $-90°$ and $-270°$ ($\equiv +90°$). They intersect the σ-axis at

$$p = \sigma_0 = \frac{(-0{\cdot}1 - 1 - 2 + 0{\cdot}5)}{(3 - 1)} = -1{\cdot}3$$

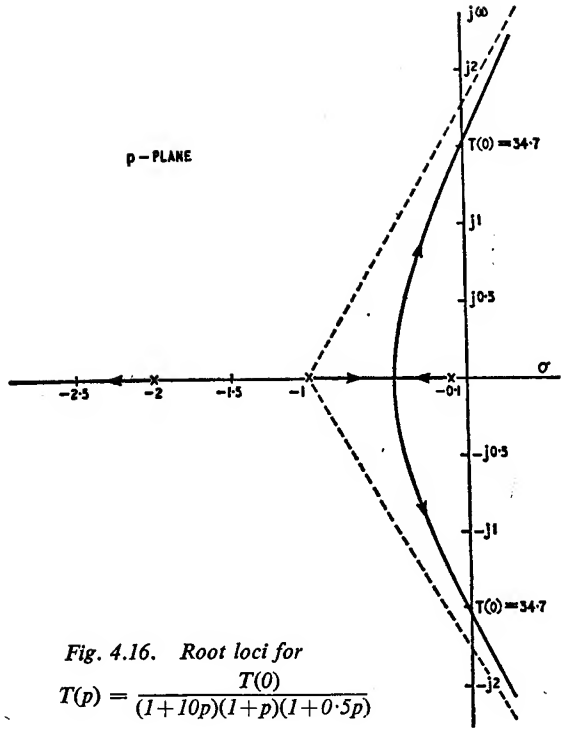

Fig. 4.16. Root loci for $T(p) = \dfrac{T(0)}{(1+10p)(1+p)(1+0{\cdot}5p)}$

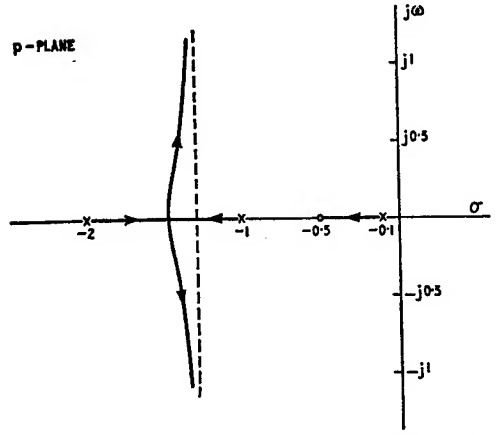

Fig. 4.17. Root loci for $T(p) = \dfrac{T(0)(1+2p)}{(1+10p)(1+p)(1+0{\cdot}5p)}$

Extending Equation 4.63 to the case of three real poles and one zero, then the point of departure $p = \sigma_d$ can be determined from

$$\frac{1}{\sigma_d + 0{\cdot}5} - \frac{1}{\sigma_d + 0{\cdot}1} - \frac{1}{\sigma_d + 1} - \frac{1}{2 + \sigma_d} = 0$$

Simplifying, we get

$$2\sigma_d^3 + 4{\cdot}6\sigma_d^2 + 4\sigma_d + 2{\cdot}3 = 0$$

Solving this cubic by Newton's method† we find that $\sigma_d = -1{\cdot}47$.

In Fig. 4.17 the root loci do not intersect the $j\omega$ axis of the p-plane; therefore, it represents a stable feedback circuit and clearly demonstrates the stabilising influence of the zero at $p = -0{\cdot}5$.

Example 3

For the final example consider the open-loop gain function

$$T(p) = T(0)\frac{1 + 0{\cdot}1p + 0{\cdot}1p^2}{(1+p)(1+p+p^2)}$$

which has a pair of complex conjugate zeros at $p = -0{\cdot}5 \pm j3{\cdot}12$, a real pole at $p = -1$ and a pair of complex conjugate poles at $p = -0{\cdot}5 \pm j0{\cdot}866$. As p tends to infinity, $T(p)$ behaves as $0{\cdot}1\ T(0)/p$. Therefore, there are three root loci, two of which start at the complex conjugate poles and terminate on the complex conjugate zeros; the remaining one starts at the real pole and terminates at infinity.

To determine the values of $T(0)$ at which the root loci intersect the $j\omega$-axis, we apply Routh's criterion to the characteristic equation

$$(1+p)(1+p+p^2) + T(0)(1 + 0{\cdot}1p + 0{\cdot}1p^2) = 0$$

that is

$$p^3 + p^2(2 + 0{\cdot}1\ T(0)) + p(2 + 0{\cdot}1\ T(0)) + (1 + T(0)) = 0$$

Thus we obtain the following array of elements

1	$2 + 0{\cdot}1T(0)$
$2 + 0{\cdot}1T(0)$	$1 + T(0)$
$2 + 0{\cdot}1T(0) - \dfrac{1 + T(0)}{2 + 0{\cdot}1T(0)}$	0
$1 + T(0)$	0

† Turnbull, H. W., *Theory of Equations*, Oliver and Boyd, Edinburgh (1946).

The characteristic equation has imaginary roots when

$$2 + 0{\cdot}1T(0) - \frac{1 + T(0)}{2 + 0{\cdot}1T(0)} = 0$$

which simplifies to

$$3 - 0{\cdot}6T(0) + 0{\cdot}01T^2(0) = 0$$

Solution of this quadratic equation gives $T(0) = 5{\cdot}5$ or $T(0) = 54{\cdot}5$. We therefore deduce that the feedback circuit is stable provided

$$T(0) < 5{\cdot}5 \text{ or else } T(0) > 54{\cdot}5$$

The two root loci starting from the complex conjugate poles cross into the right half of the p-plane when $T(0)$ exceeds 5·5. Then as $T(0)$ is increased further, these two root loci cross back again into the

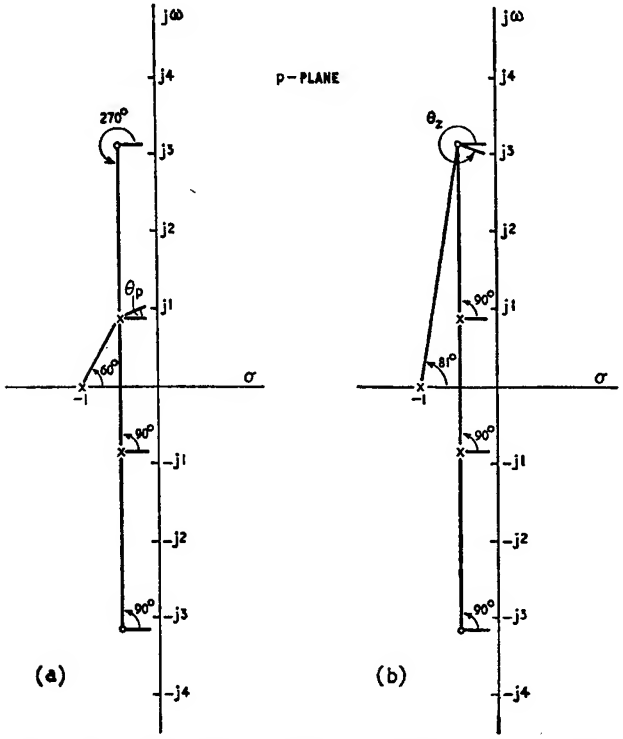

Fig. 4.18. Evaluation of angles of departure from complex poles and angles of arrival at complex zeros

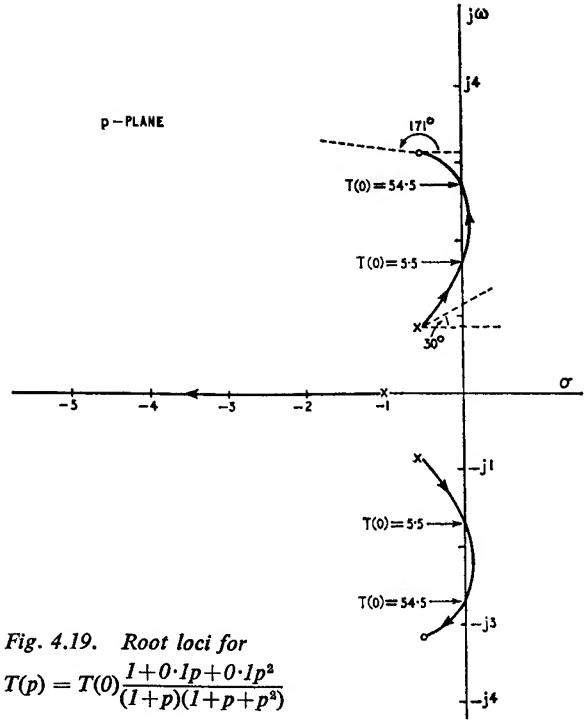

Fig. 4.19. Root loci for $T(p) = T(0)\frac{1+0{\cdot}1p+0{\cdot}1p^2}{(1+p)(1+p+p^2)}$

left half of the p-plane when $T(0)$ exceeds 54·5. This form of stability is referred to as *conditional stability* because it is conditioned by the value of $T(0)$.

For evaluating the angle θ_p of departure from the pole at $p = -0{\cdot}5 + j0{\cdot}866$ we can make use of rule No. 11. Thus if vectors are drawn from this pole to all the other poles and zeros, and the angles at these poles and zeros are measured, we find that (see Fig. 4.18 (a))

$$270° + 90° - (90° + 60° + \theta_p) = 180°$$

Therefore

$$\theta_p = 30°$$

Similarly, to determine the angle θ_z of arrival of the locus at the zero $p = -0{\cdot}5 + j3{\cdot}12$, we draw vectors from this zero to the other zero and all the poles as in Fig. 4.18 (b), and measure the various angles; then we get

$$90° + \theta_z - (90° + 90° + 81°) = 180°$$

Hence, $\theta_z = 351°$; this is equivalent to $\theta_z = -9°$. Then with the aid of rule No. 5 the complete root locus can be sketched as in Fig. 4.19, which is seen to be symmetrical with respect to the σ-axis.

4.7 Significance of closed-loop poles in the p-plane

The root locus method of design directly relates the *closed-loop poles*, that is, poles of the closed-loop gain function, to the open-loop poles and zeros, that is, poles and zeros of the open-loop gain

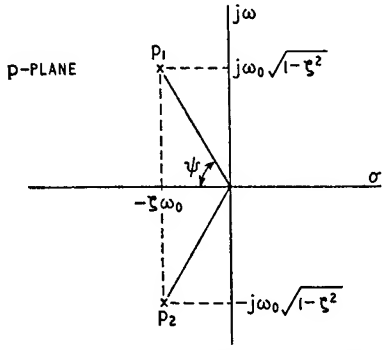

Fig. 4.20. Pair of complex conjugate poles

function. It provides a convenient method for adjusting the open-loop poles and zeros and the multiplying factor $T(0)$ or H in such a way as to produce satisfactory positions for the closed-loop poles in the p-plane.

The transient response of the circuit is very largely controlled by the location of the closed-loop poles. Therefore, it is important to be able to relate the location of the closed-loop poles to the form of the associated transient response.

Consider a pair of complex conjugate poles located at

$$p_1, p_2 = -\zeta\omega_0 \pm j\omega_0\sqrt{(1-\zeta^2)} \qquad (4.66)$$

as shown in Fig. 4.20. The step function response of a circuit having such a pair of poles was studied in Section 2.2.7 where it was shown that the response function $v_2(t)$ to a unit-step is given by

$$v_2(t) = 1 - \frac{e^{-\zeta\omega_0 t}}{\sqrt{(1-\zeta^2)}} \sin(\omega_0 \cdot t\sqrt{(1-\zeta^2)} + \psi) \qquad (4.67)$$

where $\zeta = \cos\psi$. From Equation 4.67 we see that the factor $\zeta\omega_0$ which is equal to the real part of either complex pole, controls the time required for the transient response to decay. Therefore all

closed-loop poles located on a vertical line parallel to the $j\omega$-axis contribute to the transient response terms which decay with time at the same rate; the closer the vertical line is to the imaginary axis the slower is the rate of decay.

From Equation 4.67 we also see that the frequency of oscillation is controlled by the factor $\omega_0\sqrt{(1-\zeta^2)}$, which is equal to the imaginary part of either complex pole in Fig. 4.20. Hence, all closed-loop poles located on a horizontal line parallel to the σ-axis contribute to the overall transient response, terms which have the same frequency of oscillation; the closer the horizontal line is to the σ-axis the smaller is the frequency of oscillation.

Another significant factor in connection with the location of closed-loop poles is the damping ratio ζ which controls the amount of overshoot γ of the oscillatory response (see Equation 2.55). The closer ζ is to unity, that is, the closer the angle ψ of Fig. 4.20 is to zero, the smaller is the overshoot. For a constant amount of overshoot, we must have the closed-loop poles located along a pair of radial lines through the origin and symmetrically placed with respect to the σ-axis of the p-plane. Motion of a pair of complex conjugate poles along such a pair of radial lines does not change the form of the associated transient response component, but only alters the time scale.

In the study of linear feedback circuits it is usually found that there exists a pair of complex conjugate closed-loop poles lying in close

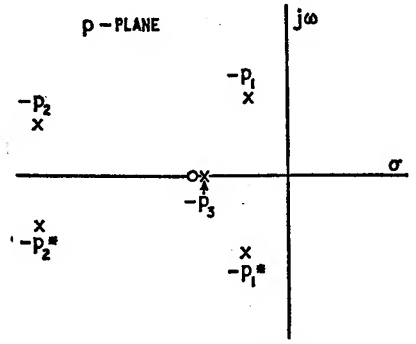

Fig. 4.21. Illustrating the dominant closed-loop poles

proximity to the $j\omega$-axis of the p-plane (as $-p_1$ and $-p_1^*$ in the example of Fig. 4.21). Such a pair of poles gives rise to the *principal oscillatory mode* of the transient response; it is so-called because it has the longest decay time. The other closed-loop poles are either located so far out to the left in the p-plane (as $-p_2$ and $-p_2^*$ in Fig. 4.21) or else lie so close to a closed-loop zero (as $-p_3$ in Fig. 4.21) that they contribute negligibly to the transient response.

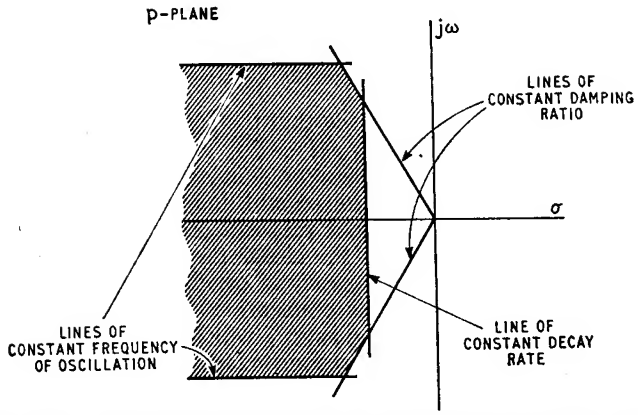

Fig. 4.22. Restrictions on location of closed-loop poles in the p-plane

Accordingly we find that the transient response of the circuit is dominated by the two closed loop poles $-p_1$ and $-p_1^*$ and any zeros that lie in the significant part of the p-plane.

We thus see that if the damping rate, frequency of oscillation and amount of overshoot of the closed-loop transient response are not to exceed specified values, then when constructing the root loci it is necessary to restrict the dominant closed-loop poles and the other roots of the characteristic equation to lie within the shaded region of Fig. 4.22. In the appendix at the end of the book it is shown that much useful information about the relative positions of the various closed-loop poles in the left half of the p-plane can be obtained from the characteristic equation by applying certain transformations.

4.8 Effect of parameter variations

It is often required to know how sensitive the roots of a characteristic equation are to changes in the low frequency value $T(0)$ of the open-loop gain, and to changes in the open-loop pole and zero positions. Such an evaluation would be most useful in assessing, for example, the effect of valve or transistor parameter variations on the closed-loop pole positions of a feedback circuit.

Let us assume that the open-loop gain function $T(p)$ is defined as in Equation 4.47, then

$$T(p) = H\frac{N(p)}{D(p)} \tag{4.68}$$

where

$$N(p) = (p - z_1)(p - z_2)\ldots(p - z_m)$$

$$N(p) = \prod_{i=1}^{m}(p - z_i) \tag{4.69}$$

$$D(p) = (p - p_1)(p - p_2)\ldots(p - p_n) = \prod_{j=1}^{n}(p - p_j) \tag{4.70}$$

The scale factor H is directly proportional to the low frequency open-loop gain $T(0)$, as in Equation 4.48. Since the number of characteristic roots is equal to the number of open-loop poles, it follows that the characteristic polynomial

$$Q(p) = D(p) + H\cdot N(p) \tag{4.71}$$

can be expressed in factorised form as follows

$$D(p) + H\cdot N(p) = (p - s_1)(p - s_2)\ldots(p - s_n) = \prod_{\lambda=1}^{n}(p - s_\lambda) \tag{4.72}$$

where $s_1, s_2 \ldots s_n$ denote the characteristic roots. Taking the natural logarithm of both sides of Equation 4.72, we have

$$\log_e[D(p) + H\cdot N(p)] = \log_e(p - s_1) + \log_e(p - s_2) + \ldots + \log_e(p - s_n) = \sum_{\lambda=1}^{n}\log_e(p - s_\lambda) \tag{4.73}$$

Suppose the open-loop poles and zeros are maintained fixed, and the scale factor H is changed by a small amount δH. The corresponding change δs_λ in the characteristic root at $p = s_\lambda$ is given by

$$\delta s_\lambda = \frac{\partial s_\lambda}{\partial H}\cdot\delta H \tag{4.74}$$

Differentiating both sides of Equation 4.73 with respect to H gives

$$\frac{N(p)}{D(p) + H\cdot N(p)} = \sum_{\lambda=1}^{n}\frac{-1}{p - s_\lambda}\cdot\frac{\partial s_\lambda}{\partial H} \tag{4.75}$$

Noting the definition of Equation 4.71 for $Q(p)$, we deduce that

$$\frac{\partial s_\lambda}{\partial H} = \operatorname*{Limit}_{p\to s_\lambda} -\frac{(p - s_\lambda).N(p)}{Q(p)}$$

$$\frac{\partial s_\lambda}{\partial H} = \underset{p \to s_\lambda}{\text{Limit}} \frac{-\frac{d}{dp}[(p - s_\lambda).N(p)]}{\frac{d}{dp}Q(p)}$$

$$= \underset{p \to s_\lambda}{\text{Limit}} - \frac{N(p) + (p - s_\lambda)\cdot N'(p)}{Q'(p)}$$

$$= -\frac{N(s_\lambda)}{Q'(s_\lambda)} \qquad (4.76)$$

where

$$Q'(s_\lambda) = \left[\frac{d}{dp}Q(p)\right]_{p=s_\lambda}$$

But $p = s_\lambda$ is an assumed root of the characteristic equation, therefore

$$D(s_\lambda) + H\cdot N(s_\lambda) = 0$$

and Equations 4.74 and 4.76 give

$$\delta s_\lambda = \frac{D(s_\lambda)}{Q'(s_\lambda)}\cdot\frac{\delta H}{H} \qquad (4.77)$$

When the positions of the open-loop poles and zeros are unaltered as assumed above, we see from Equation 4.48 that a fractional change $\delta H/H$ in the scale factor is equal to the fractional change $\delta T(0)/T(0)$ in the low frequency value of the open-loop gain. Hence the sensitivity of the characteristic root at $p = s_\lambda$ to a variation in $T(0)$ is given by

$$\frac{\delta s_\lambda}{\delta T(0)/T(0)} = \frac{D(s_\lambda)}{Q'(s_\lambda)} \qquad (4.78)$$

In the special case of an open-loop gain function having no finite zeros, the numerator polynomial $N(p)$ reduces to a constant, and its derivative with respect to p is zero. Then $Q'(p) = D'(p)$, and Equation 4.78 becomes

$$\frac{\delta s_\lambda}{\delta T(0)/T(0)} = \frac{D(s_\lambda)}{D'(s_\lambda)} \qquad (4.79)$$

where

$$D'(s_\lambda) = \left[\frac{d}{dp}D(p)\right]_{p=s_\lambda}$$

Numerical example

A single-loop feedback amplifier involving two identical stages has the open-loop gain function

$$T(p) = \frac{T(0)}{(1 + p)^2}$$

where p is normalised with respect to the stage cut off frequency. The normal value of $T(0)$ is equal to 9, and it is required to evaluate the effect of a 10% increase in the value of $T(0)$ on the closed-loop poles.

For $T(0) = 9$ the characteristic equation is

$$(1 + p)^2 + 9 = 0$$

that is,

$$p^2 + 2p + 10 = 0$$

This is a quadratic equation in p; hence the normal positions of the two closed-loop poles are

$$s_\lambda = -1 \pm j3 \qquad \lambda = 1, 2$$

Now

$$D(p) = (1 + p)^2$$

$$D'(p) = 2(1 + p)$$

Hence Equation 4.79 gives the sensitivity of the root at $p = -1 + j3$ to be

$$\frac{\delta s_\lambda}{0{\cdot}1} = \frac{(1 - 1 + j3)^2}{2(1 - 1 + j3)} = j1{\cdot}5$$

$$\delta s_\lambda = j0{\cdot}15$$

Thus the characteristic root at $p = -1 + j3$ moves to the new position of $p = -1 + j3{\cdot}15$ as a result of 10% increase in the value of $T(0)$. Similarly the root at $p = -1 - j3$ moves to the new position of $p = -1 - j3{\cdot}15$.

4.8.1 SENSITIVITY OF CHARACTERISTIC ROOTS TO VARIATIONS IN OPEN-LOOP POLES AND ZEROS

Let us next evaluate the effect of a small shift in an open-loop pole position. Suppose $T(p)$ has a pole of order b at $p = p_a$, then

$$T(p) = H\frac{N(p)}{D(p)} = H\frac{N(p)}{q(p)\cdot(p - p_a)^b} \qquad (4.80)$$

where the polynomial $q(p)$ is non-zero at $p = p_a$. The characteristic polynomial $Q(p)$ is

$$q(p)\cdot(p-p_a)^b + H\cdot N(p) = \prod_{\lambda=1}^{n}(p-s_\lambda) \tag{4.81}$$

Taking natural logarithms, we get

$$\log_e [q(p)\cdot(p-p_a)^b + H\cdot N(p)] = \sum_{\lambda=1}^{n} \log_e (p-s_\lambda) \tag{4.82}$$

If the scale factor H is maintained constant but the open-loop pole at $p = p_a$ shifts by a small amount δp_a, then the corresponding shift δs_λ in the position of the characteristic root at $p = s_\lambda$ is equal to

$$\delta s_\lambda = \frac{\partial s_\lambda}{\partial p_a}\delta p_a \tag{4.83}$$

Differentiating Equation 4.82 with respect to p_a gives

$$\frac{-q(p)\cdot b(p-p_a)^{b-1}}{q(p)\cdot(p-p_a)^b + H\cdot N(p)} = \sum_{\lambda=1}^{n}\frac{-1}{p-s_\lambda}\frac{\partial s_\lambda}{\partial p_a} \tag{4.84}$$

Remembering that

$$q(p)\,(p-p_a)^b = D(p)$$

and

$$q(p)\,(p-p_a)^b + H\cdot N(p) = Q(p)$$

we find from Equation 4.84 that

$$\begin{aligned}\frac{\partial s_\lambda}{\partial p_a} &= b \operatorname*{Limit}_{p\to s_\lambda} \frac{p-s_\lambda}{p-p_a}\cdot\frac{D(p)}{Q(p)} \\ &= b \operatorname*{Limit}_{p\to s_\lambda} \frac{\frac{\mathrm{d}}{\mathrm{d}p}[(p-s_\lambda)\cdot D(p)]}{\frac{\mathrm{d}}{\mathrm{d}p}[(p-p_a)\cdot Q(p)]} \\ &= b \operatorname*{Limit}_{p\to s_\lambda} \frac{D(p)+(p-s_\lambda)D'(p)}{Q(p)+(p-p_a)Q'(p)} \\ &= \frac{bD(s_\lambda)}{(s_\lambda-p_a)Q'(s_\lambda)}\end{aligned} \tag{4.85}$$

where we have made use of the fact that $Q(p) = 0$ at the root $p = s_\lambda$. Hence Equation 4.83 gives

$$\delta s_\lambda = b\frac{\delta p_a}{s_\lambda - p_a}\cdot\frac{D(s_\lambda)}{Q'(s_\lambda)} \tag{4.86}$$

In a similar manner we can show that a small shift δz_x in the position of an open-loop zero of order y at $p = z_x$ is to displace a characteristic root at $p = s_\lambda$ by an amount equal to

$$\delta s_\lambda = -\,y\cdot\frac{\delta z_x}{s_\lambda - z_x}\cdot\frac{D(s_\lambda)}{Q'(s_\lambda)} \tag{4.87}$$

The combined effect of variations occuring in the low frequency open-loop gain as well as the open-loop poles and zeros upon the position of a given characteristic root can be determined by summing the individual effects, provided that the changes involved are relatively small.

PROBLEMS

1. By applying Routh's criterion determine whether the feedback circuits having the following characteristic equations are stable or not

   (a) $p^3 + 11p^2 + 11p + 10 = 0$

   (b) $8p^3 + 7p^2 + 4p + 16 = 0$

   (c) $4p^4 + 3p^3 + 7p^2 + 3p + 4 = 0$

   (d) $4p^4 + 5p^3 + 9p^2 + 5p + 4 = 0$

2. A negative feedback circuit has the following loop gain function

$$T(p) = T(0)\frac{1+\frac{p}{4}+\frac{p^2}{20}}{1+2p+\frac{p^2}{2}+\frac{p^3}{2}}$$

   Determine by means of Routh's criterion the range of values of $T(0)$ for which the amplifier is unstable.

3. Sketch the root locus diagram for a negative feedback amplifier having the open-loop gain function

$$T(p) = \frac{T(0)}{(1+5p)(1+p)\left(1+\frac{p}{5}\right)}$$

On the diagram indicate such important data as the asymptotes, points of departure from the σ-axis, points of intersection with the $j\omega$-axis, and the threshold value of $T(0)$.

What is the value of $T(0)$ that gives critical damping?

4. A negative feedback amplifier, with a purely resistive feedback network, has the open-loop gain function

$$T(p) = \frac{T(0)}{(1 + 10p)(1 + p + p^2)}$$

Sketch the root locus diagram indicating such important data as angle of departure from the complex conjugate open-loop poles, points of intersection with the $j\omega$ axis, and the threshold value of $T(0)$.

If $T(0)$ has the value of 10, determine the percentage overshoot of the closed-loop transient response to a step function.

5. The open-loop gain function of a three-stage amplifier having a purely resistive feedback network is

$$T(p) = \frac{T(0)}{1 + 10p + 30p^2 + 20p^3}$$

The normal value of $T(0)$ is 12. Determine the corresponding positions of the closed-loop poles.

What is the effect of 20% increase in the value of $T(0)$ on the closed-loop pole positions? Comment on the result.

6. A three-stage feedback amplifier with a purely resistive feedback network is required to realise a low-frequency open-loop gain $T(0) = 49{\cdot}5$ and a gain margin of 6 dB. Two of the stages have cut off frequencies at 10^6 rad/sec. Determine the necessary cut off frequency of the third stage.

7. A single-loop negative feedback amplifier has three identical stages and employs a purely resistive feedback network. Determine the low-frequency value T(0) of the open-loop gain required to realise a pair of complex conjugate closed-loop poles with a damping ratio of $\zeta = 0{\cdot}097$ and a normalised frequency of oscillation $\omega_n = 1{\cdot}48$ rad./sec. What is the position of the remaining closed-loop pole? Hence obtain an approximate value for the fractional overshoot exhibited by the closed-loop transient response to an input step function.

REFERENCES

1. ROUTH, E. J., *Dynamics of a System of Rigid Bodies*, Macmillan, London, (1884).
2. EVANS, W. R., *Control Systems Dynamics*, McGraw-Hill, New York, (1954).
3. MULLIGAN, J. H., 'The Effect of Pole and Zero Locations on the Transient Response of Linear Dynamic Systems', *Proc. I.R.E.*, 37, 516 (1949).

4. CHESTNUT, H., and MAYER, R. W., *Servomechanisms and Regulating System Design*, Vol. 1, Wiley, New York (1959), Second Edition.
5. HOROWITZ, I. M., *Synthesis of Feedback Systems*, Academic Press, New York (1963).
6. HUANG, R. Y. 'The Sensitivity of The Poles of Linear Closed-Loop Systems', *Trans. A.I.E.E., Part II*, 77, 182 (1958).
7. TRUXAL, J. G., *Automatic Feedback Control System Synthesis*, McGraw-Hill, New York (1955).

CHAPTER 5

Frequency Response

In the previous chapter, the stability of a feedback circuit was studied in terms of the location of the closed-loop poles in the p-plane and the associated transient response. It is also possible to study the stability problem by considering the open-loop response of the feedback circuit in the real frequency domain. This method of analysis not only indicates the absolute stability and degree of stability of the feedback circuit, but also provides adequate information about how the stability performance of the feedback circuit may be improved.

A branch of mathematics that is essential to a detailed study of the open-loop frequency response is the theory of functions of a complex variable, which we shall briefly discuss in the next section.

5.1 Functions of a complex variable

A function $f(p)$ of the complex frequency variable $p = \sigma + j\omega$ will itself be complex; that is

$$f(p) = f(\sigma + j\omega) = x(\sigma, \omega) + jy(\sigma, \omega) \tag{5.1}$$

where the real part $x(\sigma, \omega)$ and the imaginary part $y(\sigma, \omega)$ are both real functions of the real variables σ and ω.

The derivative of the function $f(p)$ with respect to p at the point $p = s_1$ is defined by

$$f'(s_1) = \underset{p \to s_1}{\text{Limit}} \frac{f(p) - f(s)}{p - s_1} \tag{5.2}$$

where $f(s_1)$ is the value of $f(p)$ at the point $p = s_1$. Necessary and sufficient conditions for the derivative of $f(p)$ to be independent of the direction along which the variable p approaches the point s_1 are that the real and imaginary parts of $f(p)$ satisfy the *Cauchy-Riemann equations* which state that

$$\left.\begin{aligned} \frac{\partial x}{\partial \omega} &= -\frac{\partial y}{\partial \sigma} \\ \frac{\partial y}{\partial \omega} &= \frac{\partial x}{\partial \sigma} \end{aligned}\right\} \tag{5.3}$$

The function $f(p)$ is said to be finite if both its real and imaginary parts are finite. It is single valued if, for any given value of p there exists one and only one value for $f(p)$. When the function $f(p)$ is finite, single valued and possesses a derivative, then it is said to be *analytic*. Those points in the p-plane at which $f(p)$ is not analytic are referred to as *singularities*. An important kind of singularity is the *pole* defined as follows. If at any point $p = p_1$ we find that the function $(p - p_1)^n f(p)$ approaches a finite value as p approaches p_1, then $f(p)$ is said to have a pole of order n at the point $p = p_1$. When $n = 1$, the pole is referred to as a *simple* one.

If $f(p)$ has a pole of order n at $p = p_1$ then we can expand it as a *Laurent series* in the neighbourhood of $p = p_1$ to give

$$f(p) = a_0 + a_1(p - p_1) + a_2(p - p_1)^2 + \ldots + \frac{b_1}{p - p_1} + \frac{b_2}{(p - p_1)^2} + \ldots \frac{b_n}{(p - p_1)^n} \tag{5.4}$$

The coefficient b_1 is termed the *residue* of the function $f(p)$ at the pole $p = p_1$; it is given by

$$b_1 = \frac{1}{(n-1)!} \underset{p \to p_1}{\text{Limit}} \frac{d^{n-1}}{dp^{n-1}}[(p - p_1)^n f(p)] \tag{5.5}$$

In the special case of a simple pole, we have

$$b_1 = \underset{p \to p_1}{\text{Limit}} (p - p_1) f(p) \tag{5.6}$$

5.1.1 CAUCHY'S THEOREM

Consider next the integral of $f(p)$ with respect to p between the limits s_1 and s_2, that is,

$$\int_{s_1}^{s_2} f(p)\, dp$$

Fig. 5.1 shows two possible paths a and b along which the variable p can move from the point s_1 to s_2. If $f(p)$ is analytic at all points within and on the closed contour C of Fig. 5.1, then

$$\int_a^{s_2} f(p)\, dp = \int_b^{s_2} f(p)\, dp \tag{5.7}$$

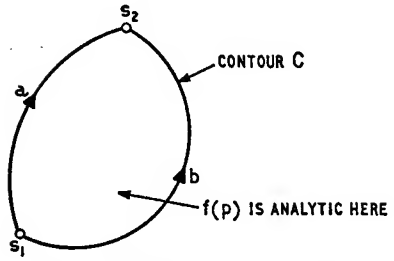

Fig. 5.1. Illustrating Cauchy's theorem

i.e. the integrals along the different paths a and b are equal. However

$$\int_b^{s_1} f(p)\,dp = -\int_b^{s_2} f(p)\,dp \tag{5.8}$$

and the contour C consists of the paths a and b; therefore the integral round C is

$$\int_C f(p)\,dp = \int_a^{s_1} f(p)\,dp + \int_b^{s_1} f(p)\,dp \tag{5.9}$$

Hence, from Equations 5.7 to 5.9 it follows that

$$\int_C f(p)\,dp = 0 \tag{5.10}$$

We have thus shown that if the function $f(p)$ is analytic inside and on the closed contour C in the p-plane, then the integral of $f(p)$ round the contour C is zero. This is known as *Cauchy's theorem.*

Consider next a closed contour C enclosing a second such contour γ, and suppose that $f(p)$ is analytic at all points between and on these two contours. In Fig. 5.2 the contours C and γ are connected together by the cuts a_1b_1 and a_2b_2 which eventually run into coinci-

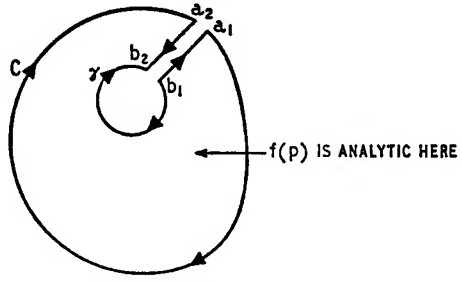

Fig. 5.2. Illustrating extension to Cauchy's theorem

dence. Then, applying Cauchy's theorem to the composite contour $\mathscr{C}$ consisting of the sum of paths C, a_1b_1, γ and a_2b_2, we get

$$\int_{\mathscr{C}} f(p)\,dp = 0 \tag{5.11}$$

But

$$\int_{\mathscr{C}} = \int_C + \int_{a_2b_2} - \int_\gamma + \int_{b_1a_1} \tag{5.12}$$

and in the limit we have

$$\int_{a_2b_2} = -\int_{b_1a_1} \tag{5.13}$$

Hence, Equations 5.11 to 5.13 give

$$\int_C f(p)\,dp = \int_\gamma f(p)\,dp \tag{5.14}$$

where both integrals are taken round the contours in the clockwise direction. Similarly if C encloses a number of closed contours $\gamma_1, \gamma_2, \ldots \gamma_q$ then we have

$$\begin{aligned}\int_C f(p)\,dp &= \int_{\gamma_1} f(p)\,dp + \int_{\gamma_2} f(p)\,dp + \ldots \int_{\gamma_q} f(p)\,dp \\ &= \sum_{i=1}^{q} \int_{\gamma_i} f(p)\,dp \end{aligned} \tag{5.15}$$

This result is referred to as the *extension to Cauchy's theorem.*

5.1.2 CAUCHY'S RESIDUE THEOREM

Suppose that $f(p)$ is analytic inside and on a closed contour C except for the points $p_1, p_2, \ldots p_q$ where it has poles of orders $n_1, n_2, \ldots n_q$ respectively. Let these poles be surrounded by circles $\gamma_1, \gamma_2, \ldots \gamma_q$ of radii $r_1, r_2, \ldots r_q$ respectively and centred at the poles as shown in Fig. 5.3. The radii are to be such that the circles do not intersect. Then, $f(p)$ will be analytic at all points between the contours C and $\gamma_1, \gamma_2, \ldots \gamma_q$, and so the integral of $f(p)$ round C can be determined by using Equation 5.15.

In the neighbourhood of the point $p = p_1$ we can express $f(p)$ as a Laurent series as follows

$$f(p) = g(p) + \sum_{m=1}^{n_1} \frac{b_m}{(p - p_1)^m} \tag{5.16}$$

where $g(p) = a_0 + a_1(p - p_1) + a_2(p - p_1)^2 + \ldots$ From this we see that $g(p)$ is analytic inside and on the circle γ_1; hence, the integral of $g(p)$ round the circle γ_1 is zero. Thus

$$\int_{\gamma_1} f(p)\,dp = \sum_{m=1}^{n_1} \int_{\gamma_1} \frac{b_m}{(p - p_1)^m}\,dp \tag{5.17}$$

On the circle γ_1 we have $p - p_1 = r_1 e^{j\theta}$ and $dp = jr_1 e^{j\theta}\,d\theta$. Also, as p moves along γ_1 once, the angle θ decreases from 2π to zero. Therefore

$$\int_{\gamma_1} \frac{b_m}{(p - p_1)^m}\,dp = \int_{2\pi}^{0} \frac{b_m}{(r_1 e^{j\theta})^m} jr_1 e^{j\theta}\,d\theta$$

$$= jb_m r_1^{1-m} \int_{2\pi}^{0} e^{(1-m)j\theta}\,d\theta \tag{5.18}$$

When $m = 1$, Equation 5.18 becomes

$$\int_{\gamma_1} \frac{b_1}{p - p_1}\,dp = jb_1 \int_{2\pi}^{0} d\theta$$

$$= -j2\pi b_1 \tag{5.19}$$

For any other value of m greater than unity, we find from Equation 5.18 that the integral vanishes when r_1 is allowed to approach zero. Hence, from Equations 5.17 to 5.19 it follows that

$$\int_{\gamma_1} f(p)\,dp = -j2\pi b_1 \tag{5.20}$$

However, the coefficient b_1 is, by definition, equal to the residue of the pole at $p = p_1$. Similarly, the integral of $f(p)$ round the circle γ_2 is equal to $-j2\pi$ times the residue of the pole at $p = p_2$ and so on for

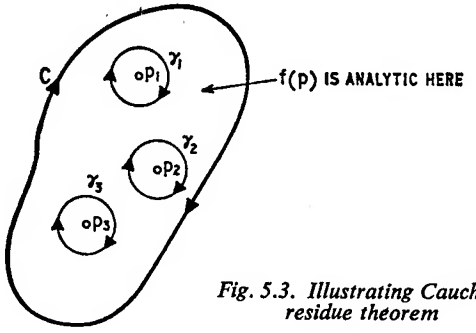

Fig. 5.3. Illustrating Cauchy's residue theorem

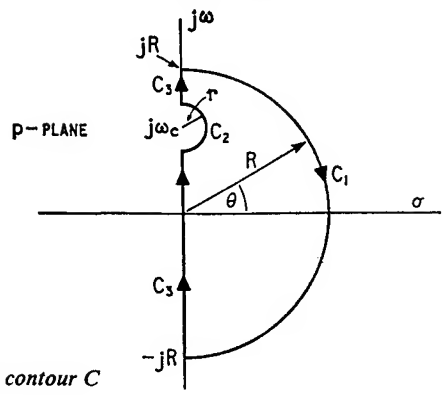

Fig. 5.4. The contour C

the remaining poles. Thus, Equation 5.15 leads to *Cauchy's residue theorem* which states that

$$\int_C f(p)\,dp = -j2\pi \sum (\text{residues of poles of } f(p) \text{ inside contour } C) \tag{5.21}$$

5.1.3 RELATIONS BETWEEN REAL AND IMAGINARY PARTS

Consider a rational function $f(p)$ that is analytic everywhere in the right half of the p-plane and on its $j\omega$-axis. Also, suppose that $f(p)$ has a finite value equal to $f(\infty)$ when p is allowed to become infinitely large. Then, applying Cauchy's theorem to the related function $f(p)/(p - j\omega_c)$ leads to the result

$$\int_C \frac{f(p)}{p - j\omega_c}\,dp = 0 \tag{5.22}$$

where the closed contour C is as shown in Fig. 5.4. It consists of three parts: the large semicircle C_1 of radius R, the small semicircular indentation C_2 (of radius r) round the point $p = j\omega_c$, and the $j\omega$-axis C_3. The indentation C_2 has been introduced to avoid the pole of the function $f(p)/(p - j\omega_c)$ at the point $p = j\omega_c$ and so ensure that this function is analytic at all points on and within the contour C, thereby justifying the result of Equation 5.22.

Along the semicircle C_1 we have $p = Re^{j\theta}$ and $dp = jRe^{j\theta}$. Therefore

$$\int_{C_1} \frac{f(p)}{p - j\omega_c}\,dp = \int_{\pi/2}^{-\pi/2} \frac{f(Re^{j\theta})}{Re^{j\theta} - j\omega_c} jRe^{j\theta}\,d\theta \tag{5.23}$$

Now let R become infinitely large: then

$$\int_{C_1} \frac{f(p)}{p - j\omega_c}\,dp = jf(\infty)\int_{\pi/2}^{-\pi/2} d\theta$$
$$= -j\pi f(\infty) \qquad (5.24)$$

When $p = j\omega$, we have

$$f(j\omega) = x(\omega) + jy(\omega) \qquad (5.25)$$

where the real part $x(\omega)$ is an even function of ω, and the imaginary part $y(\omega)$ is an odd function of ω. Hence, $y(\omega)$ can have either a zero or a pole at infinity, and so if $f(\infty)$ is to be finite, then $y(\omega)$ must be zero at infinity. Thus, $f(\infty) = x(\infty)$ and Equation 5.24 becomes

$$\int_{C_1} \frac{f(p)}{p - j\omega_c}\,dp = -j\pi x(\infty) \qquad (5.26)$$

Next, along the small semicircle C_2 we have $p = j\omega_c + re^{j\theta}$ and $dp = jre^{j\theta}\,d\theta$. Then, the integral round C_2 is

$$\int_{C_2} \frac{f(p)}{p - j\omega_c}\,dp = \int_{-\pi/2}^{\pi/2} \frac{f(j\omega_c + re^{j\theta})}{re^{j\theta}}\,jre^{j\theta}\,d\theta \qquad (5.27)$$

Now let r approach zero; thus

$$\int_{C_2} \frac{f(p)}{p - j\omega_c}\,dp = jf(j\omega_c)\int_{-\pi/2}^{\pi/2} d\theta$$
$$= j\pi f(j\omega_c) \qquad (5.28)$$

where $f(j\omega_c)$ is the value of $f(p)$ at the point $p = j\omega_c$.

Along the $j\omega$-axis we have $p = j\omega$ and $dp = jd\omega$. Therefore, the integral along the portion C_3 of the $j\omega$-axis is given by

$$\int_{C_3} \frac{f(p)}{p - j\omega_c}\,dp = \int_{-R}^{\omega_c - r} \frac{f(j\omega)}{\omega - \omega_c}\,d\omega + \int_{\omega_c + r}^{R} \frac{f(j\omega)}{\omega - \omega_c}\,d\omega \qquad (5.29)$$

In the limit when $r = 0$ and $R = \infty$, Equation 5.29 reduces to

$$\int_{C_3} \frac{f(p)}{p - j\omega_c}\,dp = \int_{-\infty}^{\infty} \frac{f(j\omega)}{\omega - \omega_c}\,d\omega \qquad (5.30)$$

The integral along the contour C is equal to the sum of the three integrals of Equations 5.26, 5.28 and 5.30. Hence, adding these three contributions and using Equation 5.22, we get

$$\int_{-\infty}^{\infty} \frac{f(j\omega)}{\omega - \omega_c}\,d\omega = j\pi[x(\infty) - f(j\omega_c)] \qquad (5.31)$$

If next we combine Equations 5.25 and 5.31 and then separate the real and imaginary parts, we obtain the following two important results

$$x(\omega_c) = x(\infty) - \frac{1}{\pi}\int_{-\infty}^{\infty} \frac{y(\omega)}{\omega - \omega_c}\,d\omega \qquad (5.32)$$

$$y(\omega_c) = \frac{1}{\pi}\int_{-\infty}^{\infty} \frac{x(\omega)}{\omega - \omega_c}\,d\omega \qquad (5.33)$$

Equation 5.33 states that if the real part of a complex function $f(j\omega)$ is specified over all frequencies, then its imaginary part is uniquely determined provided that the function $f(p)$ has no poles in the right half and on the $j\omega$-axis of the p-plane. Similarly, from Equation 5.32 we see that if the imaginary part of $f(j\omega)$ is specified over all frequencies, then its real part is completely determined except for the additive constant $x(\infty)$.

The integrals of Equations 5.32 and 5.33 are improper in that, in each case, the integrand has a singularity at the point $\omega = \omega_c$ along the path of integration. They must be evaluated according to Fig. 5.4; thus, in the case of Equation 5.32 we have

$$\int_{-\infty}^{\infty} \frac{y(\omega)}{\omega - \omega_c}\,d\omega = \underset{\substack{r\to 0\\ R\to\infty}}{\text{Limit}} \left[\int_{-R}^{\omega_c - r} \frac{y(\omega)}{\omega - \omega_c}\,d\omega + \int_{\omega_c + r}^{R} \frac{y(\omega)}{\omega - \omega_c}\,d\omega\right] \qquad (5.34)$$

In a similar way the integral of Equation 5.33 can be evaluated. The apparent difficulty presented by the impropriety of the integrands can in fact be removed by making use of the fact that†

$$\int_{-\infty}^{\infty} \frac{d\omega}{\omega - \omega_c} = 0 \qquad (5.35)$$

---

† $$\int_{-\infty}^{\infty} \frac{d\omega}{\omega - \omega_c} = \underset{\substack{r\to 0\\ R\to\infty}}{\text{Limit}} \left[\int_{-R}^{\omega_c - r} \frac{d\omega}{\omega - \omega_c} + \int_{\omega_c + r}^{R} \frac{d\omega}{\omega - \omega_c}\right]$$
$$= \underset{\substack{r\to 0\\ R\to\infty}}{\text{Limit}} [\log_e(-r) - \log_e(-R - \omega_c) + \log_e(R - \omega_c) - \log_e r]$$
$$= \underset{\substack{r\to 0\\ R\to\infty}}{\text{Limit}} \log_e\left(\frac{-r}{-R - \omega_c}\cdot\frac{R - \omega_c}{r}\right) = \log_e 1 = 0$$

Then, we can add any convenient constant to $y(\omega)$ or $x(\omega)$ in the integrands without changing the values of the integrals. Adding the constant $-y(\omega_c)$ to the numerator of the integrand in Equation 5.32 and the constant $-x(\omega_c)$ to the numerator of the integrand in Equation 5.33 we get

$$x(\omega_c) = x(\infty) - \frac{1}{\pi}\int_{-\infty}^{\infty} \frac{y(\omega) - y(\omega_c)}{\omega - \omega_c}\,\mathrm{d}\omega \tag{5.36}$$

$$y(\omega_c) = \frac{1}{\pi}\int_{-\infty}^{\infty} \frac{x(\omega) - x(\omega_c)}{\omega - \omega_c}\,\mathrm{d}\omega \tag{5.37}$$

where, in each case, we now see that the numerator and denominator of the integrand vanish at $\omega = \omega_c$. Accordingly the integrands are both perfectly proper in Equations 5.36 and 5.37.

5.1.4 THE ENCIRCLEMENT THEOREM

Consider a function $f(p)$ having a zero of order m_1 at the point $p = z_1$. In the neighbourhood of this zero we can express $f(p)$ as

$$f(p) = (p - z_1)^{m_1} g(p) \tag{5.38}$$

where $g(p)$ is non-zero and analytic at $p = z_1$. Differentiating both sides of Equation 5.38 with respect to p we obtain

$$f'(p) = m_1(p - z_1)^{m_1 - 1} g(p) + (p - z_1)^{m_1} g'(p) \tag{5.39}$$

where $f'(p)$ and $g'(p)$ are the derivatives of $f(p)$ and $g(p)$ with respect to p. Dividing Equation 5.39 by 5.38 we get

$$\frac{f'(p)}{f(p)} = \frac{m_1}{p - z_1} + \frac{g'(p)}{g(p)} \tag{5.40}$$

The second term on the right hand side is analytic at $p = z_1$. Therefore, the function $f'(p)/f(p)$ has a simple pole at $p = z_1$, with a residue equal to m_1.

Suppose next that $f(p)$ has a pole of order n_1 at $p = p_1$. Then, in the neighbourhood of this pole, $f(p)$ can be expressed by

$$f(p) = \frac{h(p)}{(p - p_1)^{n_1}} \tag{5.41}$$

where $h(p)$ is non-zero and analytic at $p = p_1$. If again we differentiate both sides of Equation 5.41 with respect to p we get

$$f'(p) = \frac{-n_1 h(p)}{(p - p_1)^{n_1 + 1}} + \frac{h'(p)}{(p - p_1)^{n_1}} \tag{5.42}$$

Dividing Equation 5.42 by 5.41, we have

$$\frac{f'(p)}{f(p)} = \frac{-n_1}{p - p_1} + \frac{h'(p)}{h(p)} \tag{5.43}$$

In this case we see that the function $f'(p)/f(p)$ has a simple pole at $p = p_1$ with a residue equal to $-n_1$.

Thus, if in the general case the function $f(p)$ has zeros of orders $m_1, m_2, \ldots m_r$ at the points $z_1, z_2, \ldots z_r$ respectively, and poles of orders $n_1, n_2, \ldots n_q$ at the points $p_1, p_2 \ldots p_q$ respectively, all located inside a closed contour C in the p-plane, then the related function $f'(p)/f(p)$ will have simple poles at the points $z_1, z_2, \ldots z_r$ and $p_1, p_2 \ldots p_q$ with residues equal to $m_1, m_2, \ldots m_r$ and $-n_1, -n_2 \ldots -n_q$ respectively. Integrating $f'(p)/f(p)$ round the contour C and applying Cauchy's residue theorem (i.e. Equation 5.21) we find that

$$\begin{aligned}\int_C \frac{f'(p)}{f(p)}\,\mathrm{d}p &= -\mathrm{j}2\pi[(m_1 + m_2 + \ldots + m_r) - (n_1 + n_2 + \ldots + n_q)] \\ &= -\mathrm{j}2\pi\left(\sum_{i=1}^{r} m_i - \sum_{k=1}^{q} n_k\right) \\ &= -\mathrm{j}2\pi(M - N)\end{aligned} \tag{5.44}$$

where $M = \sum_{i=1}^{r} m_i$ and $N = \sum_{k=1}^{q} n_k$. Thus, M and N denote total number of zeros and poles of $f(p)$ inside the contour C, respectively, with each zero and pole counted according to its order of multiplicity. The integration is assumed to be in the clockwise direction. Next, we note that

$$\frac{\mathrm{d}}{\mathrm{d}p}[\log_e f(p)] = \frac{f'(p)}{f(p)} \tag{5.45}$$

Therefore, from Equations 5.44 and 5.45 we get

$$\int_C \mathrm{d}[\log_e f(p)] = -\mathrm{j}2\pi(M - N) \tag{5.46}$$

Expressing $f(p)$ in terms of its magnitude and phase angle, we have

$$\log_e f(p) = \log_e |f(p)| + \mathrm{j}\angle f(p) \tag{5.47}$$

Suppose that the variable p starts at an arbitrary point s_1 on the contour C and returns to the point s_1' after traversing C once, as shown in Fig. 5.5 Then

$$\int_C d[\log_e f(p)] = \log_e f(s_1') - \log_e f(s_1)$$
$$= \log_e |f(s_1')| + j\angle f(s_1') - \log_e |f(s_1)| - j\angle f(s_1) \quad (5.48)$$

If the point s_1' is infinitely close to s_1, we have

$$\log_e|f(s_1')| = \log_e|f(s_1)|$$

and Equation 5.48 reduces to

$$\int_C d[\log_e f(p)] = j[\angle f(s_1') - \angle f(s_1)] \quad (5.49)$$

Hence, combining Equations 5.46 and 5.49 we get the result

$$\begin{bmatrix}\text{Change in the phase angle of } f(p) \text{ in} \\ \text{traversing contour } C \text{ in the } p\text{-plane}\end{bmatrix} = -2\pi(M - N) \quad (5.50)$$

Let us next represent the function $f(p)$ on a complex plane of its own. Then, as the variable p moves round the contour C in the p-plane, as in Fig. 5.6 (a), we find that $f(p)$ describes a closed curve in the $f(p)$-plane, as in Fig. 5.6 (b). Now a change in the phase angle of $f(p)$ equal to -2π radians corresponds to one encirclement of the origin of the $f(p)$-plane by the plot of $f(p)$ in the clockwise direction. Therefore, from Equation 5.50 we deduce that if a function $f(p)$ has a total number of M zeros and N poles inside a closed contour C in the p-plane, then as a result of the variable p moving round the contour C once in the clockwise direction, the plot of $f(p)$ will encircle the origin of the $f(p)$-plane in the clockwise direction (which is in the same sense as that of contour C) a number of times equal to $M - N$. This is known as the *encirclement theorem* which is the basis of Nyquist's stability criterion.

5.2 Nyquist's criterion

The closed-loop gain $K'(p)$ of a single-loop feedback circuit is given by Equation 4.10 which is reproduced here in the form

$$K'(p) = t_{sl}(p) + \frac{K(p)}{F(p)} \quad (5.51)$$

where $F(p) = 1 + T(p)$ is the return difference expressed as a function of p, and $T(p)$ is the open-loop gain function. The feedback circuit is stable if it can be established that it has no closed-loop poles in the right half of the p-plane, that is $F(p)$ has no zeros in the right half of the p-plane. This problem can be studied

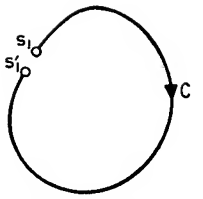

Fig. 5.5. Contour C

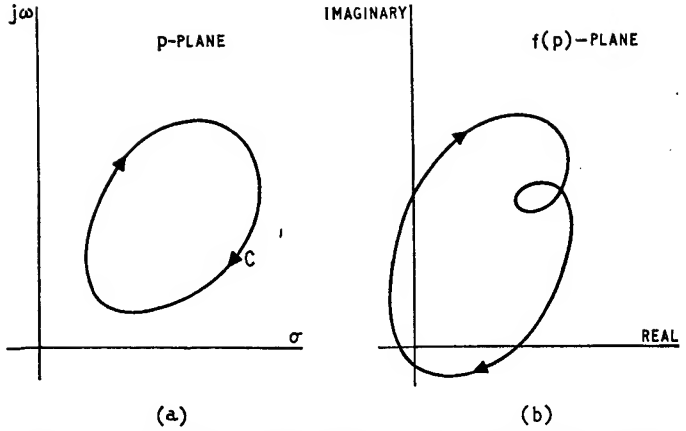

Fig. 5.6. (a) Contour C in p-plane, (b) Locus of f(p) in f(p)-plane

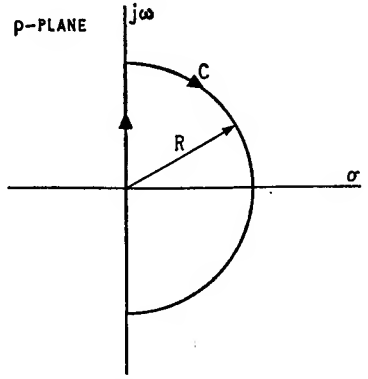

Fig. 5.7. Contour used in the derivation of Nyquist's criterion (note that $R \to \infty$)

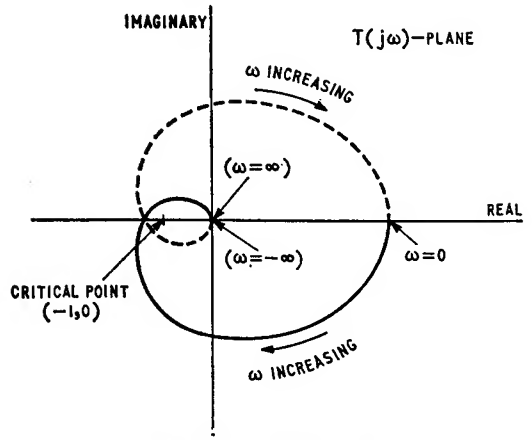

Fig. 5.8. Nyquist locus

by applying the encirclement theorem to the return difference $F(p)$. For this purpose the contour C is chosen to be an infinitely large semicircle in the right half of the p-plane built on the jω-axis, as shown in Fig. 5.7. Then, this contour will enclose all the possible zeros of $F(p)$ that may be located in the right half of the p-plane.

Now the poles of $F(p)$ are the same as the poles of $T(p)$ and the zeros of $F(p)$ are the same as the closed-loop poles. Further, we normally find that the amplifier is stable when the feedback loop is opened, which means that all the poles of the open-loop gain function $T(p)$ are confined to the left half of the p-plane. Therefore, in a single-loop feedback circuit neither the open-loop gain function $T(p)$ nor the return difference $F(p)$ can have poles in the right half of the p-plane. Thus, when applying the encirclement theorem to $F(p)$, we have $N = 0$. As p traverses the contour C of Fig. 5.7 the plot of $F(p)$ will encircle the origin of the $F(p)$-plane M times, where M is equal to the total number of zeros of $F(p)$ located in the right half of the p-plane. At infinite frequency the open-loop gain function $T(p)$ is reduced to zero with the result that $F(p)$ approaches unity as p approaches infinity. Hence, the plot is essentially of the function $F(j\omega)$. We thus deduce that if, as a result of varying ω between the limits $-\infty$ to $+\infty$, the plot of $F(j\omega)$ encircles the origin of the $F(j\omega)$-plane M times, then the return difference $F(p)$ has M of its zeros located in the right half of the p-plane. If the feedback circuit is to be stable, that is, $M = 0$, then the plot of $F(j\omega)$ must not enclose the origin of the $F(j\omega)$-plane.

In practice it is found more convenient to work with the open-loop gain function $T(j\omega)$ rather than $F(j\omega)$ because $T(j\omega)$ is directly measurable. The difference between a plot of $F(j\omega)$ and that of

$T(j\omega)$ is simply a shift in the imaginary axis. Since $F(j\omega) = 1 + T(j\omega)$ it follows that the origin of the $F(j\omega)$-plane corresponds to the point $(-1,0)$ in the $T(j\omega)$-plane. Therefore, the feedback circuit is stable if the plot of $T(j\omega)$ does not enclose the *critical point* $(-1,0)$ of the $T(j\omega)$-plane as ω is varied from $-\infty$ to $+\infty$. This is known as *Nyquist's criterion for stability.*

The required plotting of $T(j\omega)$ can be simplified by observing that the magnitude of $T(j\omega)$ is an even function of ω, and its phase angle is an odd function of ω, that is

$$|T(j\omega)| = |T(-j\omega)| \tag{5.52a}$$

$$\angle T(j\omega) = -\angle T(-j\omega) \tag{5.52b}$$

Therefore, it is necessary only to plot $T(j\omega)$ for positive frequencies from $\omega = 0$ to $\omega = \infty$. The plot for negative frequencies from $-\infty$ to 0 can be inserted as the mirror image of this part with respect to the real axis of the $T(j\omega)$-plane, as illustrated in Fig. 5.8. The plot for negative frequencies is needed only when it is required to determine the number of zeros of $F(p)$ located in the right half of the p-plane. If, however, the problem is simply to determine whether or not the feedback circuit is stable, then the plot for positive frequencies can be sufficient. Thus, if the critical point $(-1, 0)$ is not enclosed by the plot of $T(j\omega)$ for positive frequencies as in Fig. 5.9 (a), the feedback circuit is stable. On the other hand, the plot of Fig. 5.9 (b), where the critical point $(-1,0)$ is enclosed by the plot of $T(j\omega)$, corresponds to an unstable feedback circuit. The plots of Fig. 5.9 are usually referred to as *Nyquist loci.*

When the Nyquist locus passes through the critical point $(-1,0)$,

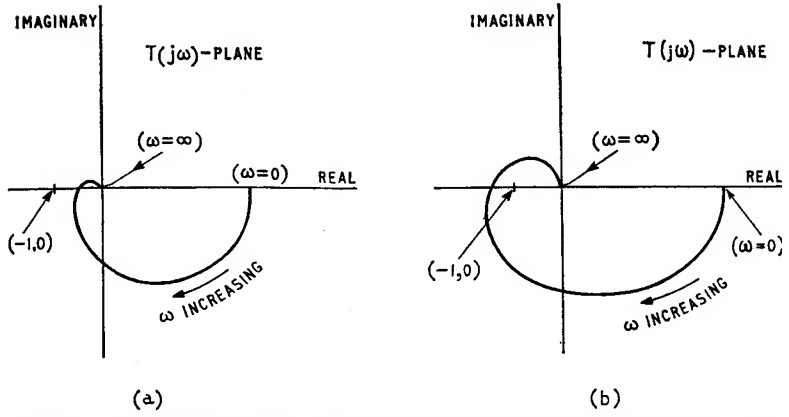

Fig. 5.9. (a) Nyquist locus for stable circuit, (b) Nyquist locus for unstable circuit

the feedback circuit is on the threshold of instability. This corresponds to the characteristic equation of the feedback circuit having a pair of conjugate roots on the jω-axis of the p-plane.

5.2.1 STABILITY MARGINS

From the Nyquist diagram of Fig. 5.10, which corresponds to a stable feedback circuit, we see that when the phase angle of the open-loop gain function equals $-180°$, its magnitude equals $1/T_m$. The quantity $20 \log_{10} T_m$ is equal to the *gain margin* expressed in decibels. The angular frequency ω_p at which $T(j\omega_p) = T_m^{-1} \angle -180°$ is termed the *phase crossover frequency*.

In Fig. 5.10 we also see that when the magnitude of the open-loop gain equals unity, its phase angle equals $-180° + \phi_m$. The phase angle ϕ_m is termed the *phase margin*; it is equal to the additional phase lag (at unity magnitude) required to just cause instability. The angular frequency ω_g at which $T(j\omega_g) = 1 \angle -180° + \phi_m°$ is termed the *gain crossover frequency*. In an absolutely stable feedback circuit ω_g is necessarily smaller than the phase crossover frequency ω_p.

The gain and phase margins are the generally accepted measures of the degree of stability of a feedback amplifier. They are intended to guard against the variations occurring in valve or transistor parameters as a result of supply voltage changes, temperature variations and other causes. In practice it is found that gain margins of 6 to 12 dB and phase margins of 20° to 40° are quite adequate.

5.2.2 APPLICATION OF NYQUIST'S CRITERION TO MULTIPLE-LOOP FEEDBACK AMPLIFIERS

Nyquist's criterion, developed above for a single-loop amplifier, can be also applied to any loop of a multiple-loop feedback amplifier, provided that the amplifier remains stable when the particular loop is broken. If, however, it is found that the amplifier becomes unstable when one of its loops is broken then to apply Nyquist's criterion it is necessary to find a mesh of the amplifier which, if broken, will simultaneously break all the feedback loops.

As an example consider the two-loop feedback amplifier of Fig. 5.11 (a) where the $\beta_1(j\omega)$-feedback network constitutes a *minor loop* applying local feedback to the $K_1(j\omega)$-amplifier, and the $\beta_2(j\omega)$-feedback network constitutes a *major loop* applying overall feedback to both $K_1(j\omega)$ and $K_2(j\omega)$ amplifier stages. The closed-loop gain $K'(j\omega)$ of such an amplifier is

$$K'(j\omega) = \frac{K_1(j\omega)K_2(j\omega)}{1 + \beta_1(j\omega)K_1(j\omega) + \beta_2(j\omega)K_1(j\omega)K_2(j\omega)} \qquad (5.53)$$

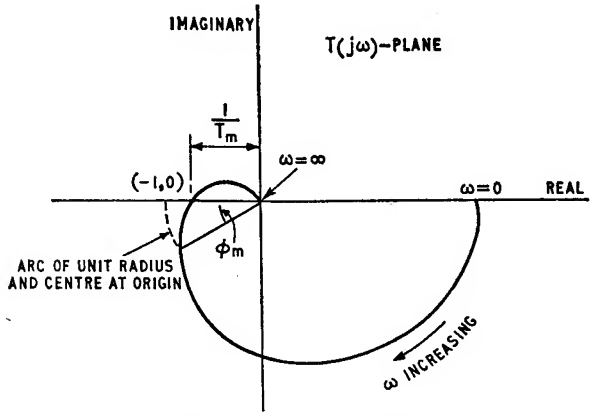

Fig. 5.10 Stability margins

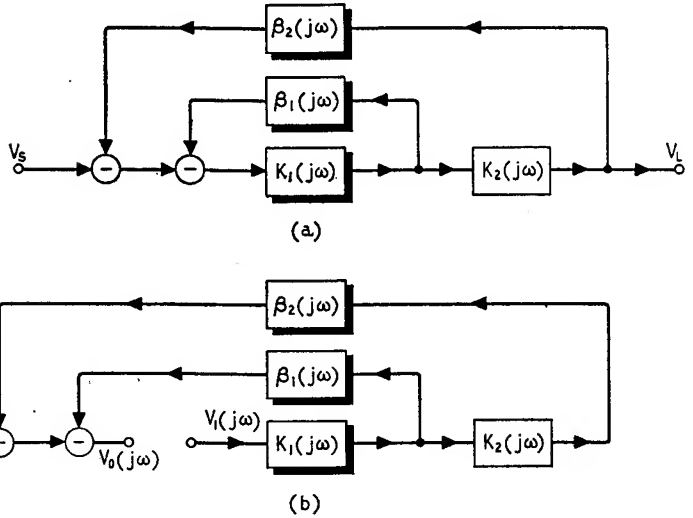

Fig. 5.11. (a) Block diagram of multiple-loop feedback circuit, (b) Block diagram showing the simultaneous opening of both feedback loops

Hence the stability performance of the amplifier is determined by the frequency response of $\beta_1(j\omega)K_1(j\omega) + \beta_2(j\omega)K_1(j\omega)K_2(j\omega)$ which can be obtained by breaking both loops at the input of $K_1(j\omega)$-stage, as in Fig. 5.11 (b) and evaluating the frequency dependence of the voltage ratio $V_0(j\omega)/V_1(j\omega)$. The complete amplifier is stable if the Nyquist locus of $-V_0(j\omega)/V_1(j\omega)$ does not encircle the critical point $(-1,0)$.

5.2.3 EXAMPLES

Single-stage feedback amplifier

In the real frequency domain the open-loop gain function of a single-stage feedback amplifier, with a purely resistive feedback network, is

$$T(j\omega) = \frac{T(0)}{1 + \frac{j\omega}{\omega_0}} \tag{5.54}$$

where $T(0)$ is the low frequency open-loop gain, and ω_0 is the stage cut off frequency. For positive frequencies the Nyquist locus of Equation 5.54 is a semicircle as shown in Fig. 5.12. For all positive values of $T(0)$ the locus remains in the fourth quadrant of the $T(j\omega)$-plane, and so a single-stage amplifier with negative feedback is inherently stable.

Two-stage feedback amplifier

The open-loop gain function of a two-stage amplifier with a purely resistive feedback network, providing overall negative feedback, is

$$T(j\omega) = \frac{T_0}{\left(1 + \frac{j\omega}{\omega_1}\right)\left(1 + \frac{j\omega}{\omega_2}\right)} \tag{5.55}$$

where ω_1 and ω_2 are the individual stage cut off frequencies. As in the previous case, $T(j\omega) = T(0)$ at zero frequency.

Each pole factor contributes a phase angle of $-90°$ at infinite frequency. Hence, with two pole factors as in Equation 5.55, the

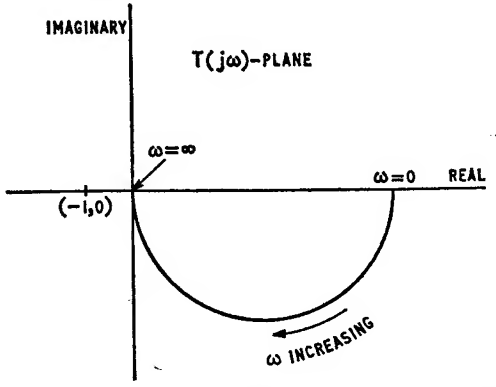

Fig. 5.12. Nyquist locus for single-stage feedback amplifier

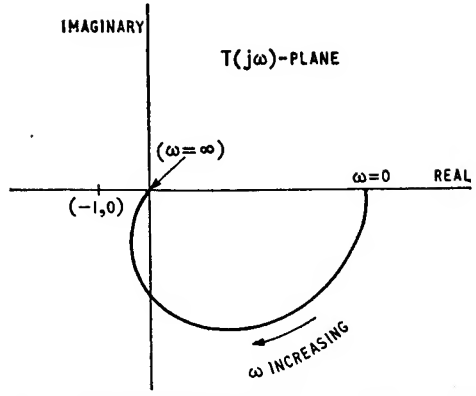

Fig. 5.13. Nyquist diagram for two-stage feedback amplifier

phase angle equals $-180°$ at infinite frequency. For positive frequencies the Nyquist locus of Equation 5.55 is thus shown as in Fig. 5.13. The Nyquist locus will not enclose the critical point $(-1,0)$ no matter how large the value of $T(0)$ is. Therefore, for all positive values of $T(0)$ the two-stage feedback amplifier having the open-loop gain function of Equation 5.55 is always stable.

Three-stage feedback amplifier

Consider next a three-stage feedback amplifier having a purely resistive feedback network. We shall assume that its open-loop gain function is given by

$$T(j\omega) = \frac{T(0)}{(1 + j10\omega)(1 + j\omega)(1 + j0{\cdot}5\omega)} \tag{5.56}$$

The denominator polynomial can be also expressed as

$$1 + j11{\cdot}5\omega - 15{\cdot}5\omega^2 - j5\omega^3$$

Hence the phase angle of $T(j\omega)$ is

$$\angle T(j\omega) = -\tan^{-1}\left(\frac{11{\cdot}5\omega - 5\omega^3}{1 - 15{\cdot}5\omega^2}\right)$$

This angle reaches the value of $-180°$ when

$$11{\cdot}5\omega - 5\omega^3 = 0$$

that is, when $\omega = 1.52$. Therefore the phase crossover frequency

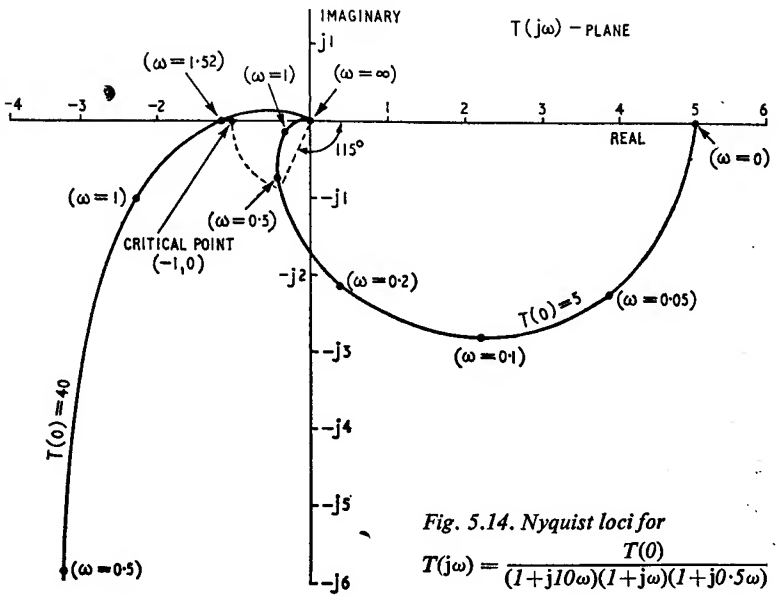

Fig. 5.14. Nyquist loci for $T(j\omega) = \dfrac{T(0)}{(1+j10\omega)(1+j\omega)(1+j0{\cdot}5\omega)}$

ω_p equals 1·52 rad/sec. At this frequency $T(j\omega)$ has the following magnitude

$$|T(j\omega_p)| = \frac{T(0)}{\left[1+\left(\frac{1{\cdot}52}{0{\cdot}1}\right)^2\right]^{1/2}[1+(1{\cdot}52)^2]^{1/2}\left[1+\left(\frac{1{\cdot}52}{2}\right)^2\right]^{1/2}}$$

$$= \frac{T(0)}{34{\cdot}7}$$

which shows that the amplifier is stable provided $T(0)$ is less than 34·7.

Next we note that, with three pole factors, the phase angle of $T(j\omega)$ is equal to $-270°$ at $\omega = \infty$; accordingly the Nyquist locus goes through three quadrants as ω is increased from zero to infinity. The diagram of Fig. 5.14 shows the Nyquist loci for two different values of $T(0)$. When $T(0) = 5$ we see that the critical point $(-1,0)$ is not encircled by the Nyquist locus. The corresponding gain margin is

$$20\log_{10}\frac{34{\cdot}7}{5} = 16{\cdot}8 \text{ dB}$$

From Fig. 5.14 we also see that the phase margin is 65°. On the

other hand, when $T(0) = 40$ we find that the resulting Nyquist locus does encircle the critical point $(-1,0)$, and so the feedback circuit becomes unstable. In Fig. 5.14 only the high frequency portion of the Nyquist locus for $T(0) = 40$ is shown plotted.

Let us next evaluate the effect of adding a zero factor to the open-loop gain function; thus

$$T(j\omega) = T(0)\frac{1+j2\omega}{(1+j10\omega)(1+j\omega)(1+j0{\cdot}5\omega)}$$

The high frequency portion of the Nyquist locus of this open-loop gain function is shown plotted in Fig. 5.15 when $T(0) = 40$. In this diagram we have also included the corresponding high frequency portion of the Nyquist locus for the open-loop gain function without

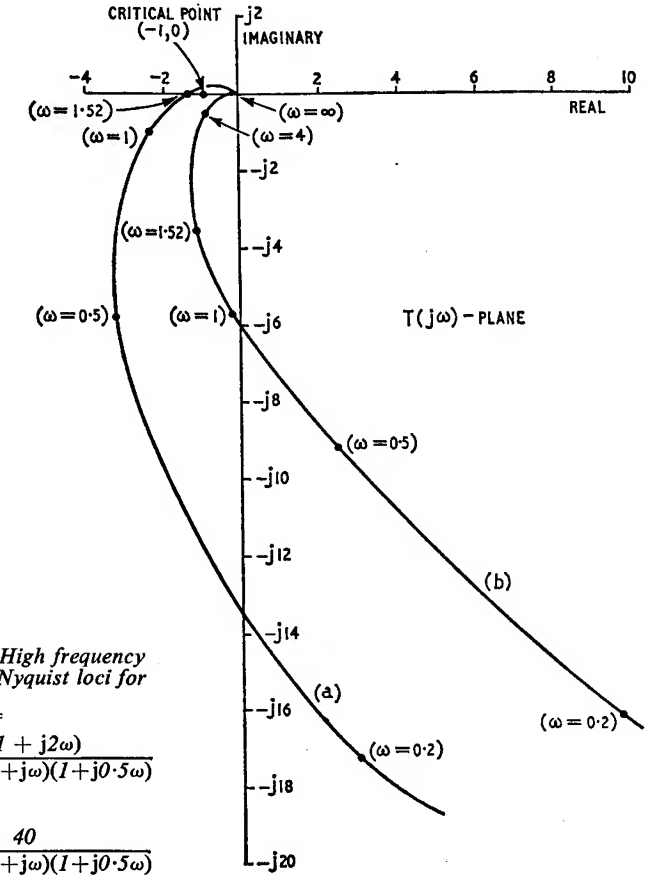

Fig. 5.15. High frequency portions of Nyquist loci for

(*a*) $T(j\omega) = \dfrac{40(1+j2\omega)}{(1+j10\omega)(1+j\omega)(1+j0{\cdot}5\omega)}$

(*b*) $T(j\omega) = \dfrac{40}{(1+j10\omega)(1+j\omega)(1+j0{\cdot}5\omega)}$

the zero factor $(1 + j2\omega)$. On examining these two loci we clearly see the stabilising influence of the added zero factor. At high frequencies, the zero factor has the combined effect of increasing the magnitude of the open-loop gain, and reducing the phase angle by introducing a phase advance into the open-loop frequency response.

Conditional stability

For our final example we shall consider the open-loop gain function

$$T(j\omega) = T(0)\frac{1 + 0{\cdot}1j\omega - 0{\cdot}1\omega^2}{(1 + j\omega)(1 + j\omega - \omega^2)} \qquad (5.57)$$

The denominator polynomial is equal to

$$1 + j2\omega - 2\omega^2 - j\omega^3$$

and so the phase angle of $T(j\omega)$ is

$$\angle T(j\omega) = \tan^{-1}\left(\frac{0{\cdot}1\omega}{1 - 0{\cdot}1\omega^2}\right) - \tan^{-1}\left(\frac{2\omega - \omega^3}{1 - 2\omega^2}\right)$$

When this angle reaches the value of $-180°$ we have

$$\frac{0{\cdot}1\omega}{1 - 0{\cdot}1\omega^2} - \frac{2\omega - \omega^3}{1 - 2\omega^2} = 0$$

which simplifies as follows

$$\omega^4 - 10\omega^2 + 19 = 0$$

This is a quadratic equation in ω^2 and has the two positive roots

$$\omega = 1{\cdot}6 \text{ and } \omega = 2{\cdot}73$$

Therefore, the open-loop gain function of Equation 5.57 has two crossover frequencies at $\omega_{p_1} = 1{\cdot}6$ rad/sec and $\omega_{p_2} = 2{\cdot}73$ rad/sec. At $\omega = \omega_{p_1} = 1{\cdot}6$ we see from Equation 5·57 that $T(j\omega)$ has a magnitude equal to

$$|T(j\omega_{p_1})| = T(0)\frac{[(1 - 0{\cdot}1 \times 1{\cdot}6^2)^2 + (0{\cdot}1 \times 1{\cdot}6)^2]^{1/2}}{(1 + 1{\cdot}6^2)^{1/2}[(1 - 1{\cdot}6^2)^2 + 1{\cdot}6^2]^{1/2}}$$
$$= \frac{T(0)}{5{\cdot}5}$$

At $\omega = \omega_{p_2} = 2{\cdot}73$ we find that $T(j\omega)$ has the magnitude

$$|T(j\omega_{p_2})| = T(0)\frac{[(1 - 0{\cdot}1 \times 2{\cdot}73^2)^2 + (0{\cdot}1 \times 2{\cdot}73)^2]^{1/2}}{(1 + 2{\cdot}73^2)^{1/2}[(1 - 2{\cdot}73^2)^2 + 2{\cdot}73^2]^{1/2}}$$
$$= \frac{T(0)}{54{\cdot}5}$$

We therefore deduce that if $T(0)$ is less than 5·5, the Nyquist locus is as shown in Fig. 5.16 (a) and the amplifier is stable. If $T(0)$ is greater than 5·5 but less than 54·5, the Nyquist locus encloses the

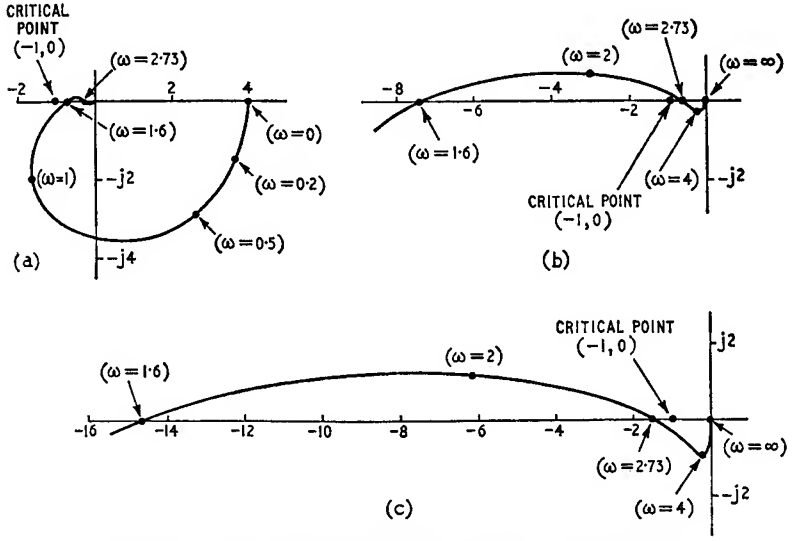

Fig. 5.16. Illustrating conditional stability associated with

$$T(j\omega) = T(0)\frac{1 + 0{\cdot}1j\omega - 0{\cdot}1\omega^2}{(1 + j\omega)(1 + j\omega - \omega^2)}$$

(a) $T(0) = 4$, (b) $T(0) = 40$, (c) $T(0) = 80$

critical point $(-1,0)$ as in Fig. 5.16 (b), and the amplifier becomes unstable. If $T(0)$ is greater than 54·5, the Nyquist diagram assumes the form illustrated in Fig. 5.16 (c), which shows the amplifier to be stable. Hence a feedback amplifier having the open-loop gain function of Equation 5.57 is conditionally stable, and for stability we must have $T(0) < 5{\cdot}5$ or else $T(0) > 54{\cdot}5$.

The results of the above four examples concerning the stability performance of feedback amplifiers, and obtained from Nyquist locus consideration are, as to be expected, in perfect agreement

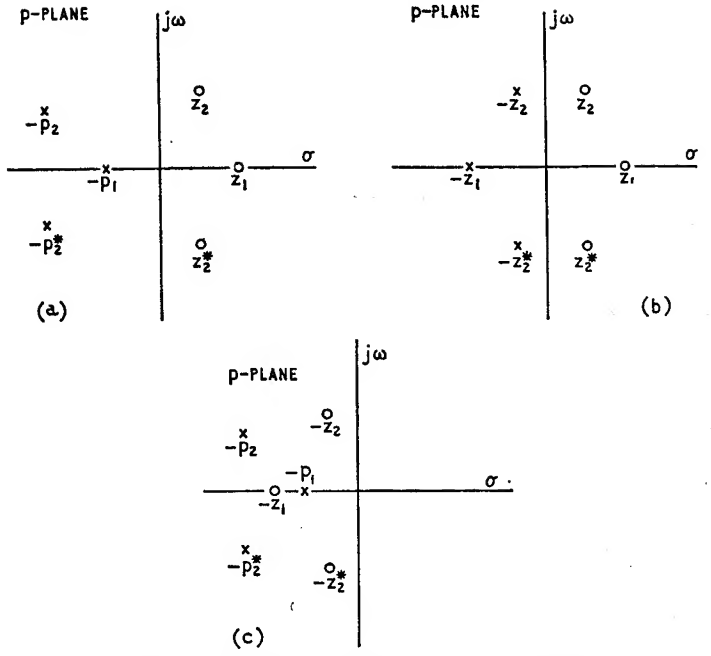

Fig. 5.17. Pole-zero patterns: (a) Non-minimum phase function, (b) All-pass function, (c) Minimum phase function

with those which we deduced earlier when the same examples were investigated in Chapter 4 in terms of the root locus diagram.

5.3 Gain-phase analysis

5.3.1 MINIMUM PHASE TRANSFER FUNCTIONS

In Section 4.1 (p. 168) we showed that if a transfer function is to correspond to a stable circuit, then all its poles must be restricted to the left half of the p-plane. We shall now discuss the effect of the location of zeros in the right half of the p-plane. Consider a transfer function $G_1(p)$ having the pole-zero pattern of Fig. 5.17 (a) where the poles at $-p_1$, $-p_2$ and $-p_2^*$ are all located in the left half of the p-plane, and the zeros at z_1, z_2 and z_3^* are all located in the right half. Then

$$G_1(p) = \frac{(p - z_1)(p - z_2)(p - z_2^*)}{(p + p_1)(p + p_2)(p + p_2^*)} \tag{5.58}$$

This transfer function can be also expressed as follows

$$G_1(p) = G_0(p) \,.\, G(p) \tag{5.59}$$

where

$$G_0(p) = \frac{(p - z_1)(p - z_2)(p - z_2^*)}{(p + z_1)(p + z_2)(p + z_2^*)} \tag{5.60}$$

$$G(p) = \frac{(p + z_1)(p + z_2)(p + z_2^*)}{(p + p_1)(p + p_2)(p + p_2^*)} \tag{5.61}$$

The transfer functions $G_0(p)$ and $G(p)$ correspond to stable circuits and have the pole-zero patterns of Figs. 5.17 (b) and 5.17 (c) respectively. The sum of these two patterns is the same as the pole-zero pattern of Fig. 5.17 (a) when it is remembered that a pole and a zero located at the same point in the p-plane cancel each other.

A transfer function whose zeros are the negatives of its poles is called an *all-pass* function. For stability, the poles must be located in the left half plane; hence, the zeros of an all-pass function are all located in the right half plane. From the pole-zero pattern of Fig. 5.17 (b) we see that $G_0(p)$ is an all-pass function. The factor $(p - z_1)/(p + z_1)$ is termed a *first order all-pass function* and the factor $(p - z_2)\,(p - z_2^*)/(p + z_2)\,(p + z_2^*)$ is called a *second order all-pass function*; in each case the order refers to the number of poles. If, in Equation 5.60, we put $p = j\omega$, we find that $|G_0(j\omega)| = 1$. Therefore, an all-pass function has the property that, along the $j\omega$-axis, its magnitude is equal to unity for all values of ω. However, its phase angle is frequency dependent. Thus, the phase angle of the first order all-pass function $(j\omega - z_1)/(j\omega + z_1)$, for example, is equal to $-2\tan^{-1}(\omega/z_1)$, which continuously decreases from 180° at zero frequency to zero degree at infinite frequency.

Next, a transfer function that has all its poles and zeros located in the left half plane is called a *minimum phase function*. From the pole-zero pattern of Fig. 5.17 (c) we see that $G(p)$ is a minimum phase function. Such a transfer function has the important property that, as we shall see later, its magnitude and phase angle characteristics are uniquely related to each other. Further, for a specified magnitude characteristic, it has the minimum phase lag possible. It is to be noted that a minimum phase function is permitted to have simple poles, and zeros of any order of multiplicity along the $j\omega$-axis.

A minimum phase transfer function is permitted to have only simple poles along the $j\omega$-axis of the p-plane because of stability considerations. As an illustration, consider the transfer function

$$G(p) = \frac{\omega_0^2}{(p^2 + \omega_0^2)^2}$$

which has double poles at $p = \pm j\omega_0$ along the $j\omega$-axis. Assuming that the excitation is a unit impulse, we find that the response

transform $\phi_0(p)$ is also equal to $\omega_0^2/(p^2 + \omega_0^2)^2$. From pair no. 15 of the Laplace transform pairs Table 2.1, we see that the response function $\phi_0(t)$ is

$$\phi_0(t) = \frac{1}{2\omega_0}(\sin \omega_0 t - \omega_0 t \cos \omega_0 t)$$

The amplitude of the resulting oscillations becomes infinitely large at $t = \infty$. Therefore, a transfer function which has double, or higher order, poles along the jω-axis is unstable. In other words, any poles of a stable transfer function which are located along the jω-axis of the p-plane must be simple.

The product of an all-pass function and a minimum phase function is termed a *non-minimum phase function*, which is, therefore, characterised in having zeros in the right half plane. Thus, from the pole-zero pattern of Fig. 5.17 (a) we see that $G_1(p)$ is an example of a non-minimum phase function. Since $|G_0(j\omega)| = 1$ it follows that the non-minimum phase function $G_1(j\omega)$ and the minimum phase function $G(j\omega)$ have exactly the same magnitudes, but they differ in phase by an amount equal to the phase angle of the all-pass function $G_0(j\omega)$. Therefore, the magnitude and phase angle characteristics of a non-minimum phase function cannot be uniquely related to each other because the phase angle characteristic can be changed as desired by the addition of an all-pass function without affecting the magnitude characteristic at all.

5.3.2 PHASE AREA THEOREM

Let $\Gamma(j\omega)$ denote the natural logarithm of a steady state transfer function $G(j\omega)$. Then, in terms of the magnitude and phase angle of $G(j\omega)$, we can express $\Gamma(j\omega)$ as follows

$$\begin{aligned}\Gamma(j\omega) &= \log_e G(j\omega) \\ &= A(\omega) + jB(\omega) \qquad (5.62)\end{aligned}$$

where

$$\begin{aligned}A(\omega) &= \text{logarithmic gain in nepers} \\ &= \log_e |G(j\omega)| \qquad (5.63) \\ B(\omega) &= \text{phase angle in radians} \\ &= \angle G(j\omega) \qquad (5.64)\end{aligned}$$

Suppose that $G(p)$ is a minimum phase function; then, it cannot vanish or become infinite in the right-half plane because it has no poles or zeros in this region. Therefore, the logarithm of $G(p)$, that is, $\Gamma(p)$ is analytic in the right half plane. Since it is permissible for $G(p)$ to have simple poles, and zeros of any order along the $j\omega$-axis, it follows that $\Gamma(p)$ can have *logarithmic singularities* along this axis.

Let us integrate the function

$$\frac{\Gamma(p)}{p - j\omega_c} = \frac{\log_e G(p)}{p - j\omega_c}$$

round the contour C shown in Fig. 5.18. This contour has been indented to the right, not only round the point $p = j\omega_c$ but also round any of the logarithmic singularities of $\Gamma(p)$ that may be found along the jω-axis. Then, by Cauchy's theorem it follows that the integral round the contour C will be equal to zero. In the limit, when the radii of the various small semicircles are allowed to approach zero, we find that the logarithmic singularities will contribute nothing at all to the contour integral.† Therefore, we can use Equations 5.32 and 5.33 or Equations 5.36 and 5.37 to relate the gain and angle functions $A(\omega)$ and $B(\omega)$.

Let it be assumed that $A(\omega)$ has finite values equal to $A(0)$ and $A(\infty)$ at zero and infinite frequencies, respectively. This condition restricts the transfer function $G(p)$ to have an equal number of poles and zeros. Then, noting that $\Gamma(j\omega)$, $A(\omega)$ and $B(\omega)$ correspond to the functions $f(j\omega)$, $x(\omega)$ and $y(\omega)$ considered in Section 5.1, we find from Equation 5.32 that

---

† Suppose that $\Gamma(p)$ has a logarithmic singularity at the point $p = j\omega_0$ as shown in Fig. 5.18. Then we can write

$$G(p) = (p - j\omega_0)g(p)$$

where $g(p)$ is non-zero and analytic at $p = j\omega_0$. Therefore

$$\Gamma(p) = \log_e G(p) = \log_e (p - j\omega_0) + \log_e g(p)$$

Integrating round the semicircular indentation (call it $\mathscr{C}$) of radius r and centre at $p = j\omega_0$, we get

$$\int_{\mathscr{C}} \Gamma(p)\,dp = \int_{\mathscr{C}} \log_e (p - j\omega_0)\,dp + \int_{\mathscr{C}} [\log_e g(p)]\,dp$$

As the radius r is allowed to approach zero, we find that the second integral on the right hand side approaches zero too, and so it is sufficient to consider the first integral only. Along the semi-circle $\mathscr{C}$, we have $p - j\omega_0 = re^{j\theta}$ and $dp = jre^{j\theta}d\theta$. Thus,

$$\begin{aligned}\int_{\mathscr{C}} \log_e (p - j\omega_0)\,dp &= \int_{-\pi/2}^{\pi/2} \log_e (r\,e^{j\theta})\,jr\,d\theta \\ &= jr \log_e r \int_{-\pi/2}^{\pi/2} d\theta - r \int_{-\pi/2}^{\pi/2} \theta\,d\theta\end{aligned}$$

Now

$$\lim_{r \to 0} r \log_e r \to 0$$

Therefore, the contribution of a logarithmic singularity to the contour integral approaches zero as r approaches zero.

$$A(\omega_c) = A(\infty) - \frac{1}{\pi}\int_{-\infty}^{\infty} \frac{B(\omega)}{\omega - \omega_c}\,d\omega \tag{5.65}$$

When $\omega_c = 0$, Equation 5.65 gives

$$A(0) = A(\infty) - \frac{1}{\pi}\int_{-\infty}^{\infty} \frac{B(\omega)}{\omega}\,d\omega \tag{5.66}$$

Since the phase angle $B(\omega)$ is as odd function of ω, it follows that $B(\omega)/\omega$ is an even function of ω. Hence,

$$\int_{-\infty}^{\infty} \frac{B(\omega)}{\omega}\,d\omega = 2\int_{0}^{\infty} \frac{B(\omega)}{\omega}\,d\omega \tag{5.67}$$

In practice, it is found convenient to plot the gain and phase angle characteristics on a logarithmic frequency scale; thus, let us define

$$u = \log_e\left(\frac{\omega}{\omega_c}\right) \tag{5.68}$$

Then, we find that $du = d\omega/\omega$. Also, $u = -\infty$ when $\omega = 0$ and $u = \infty$ when $\omega = \infty$. Therefore, combining Equations 5.66 to 5.68, we get

$$\int_{-\infty}^{\infty} B(\omega)\,du = \frac{\pi}{2}[A(\infty) - A(0)] \tag{5.69}$$

This equation states that the area under the phase angle characteristic, plotted on a logarithmic frequency scale, is equal to $\pi/2$

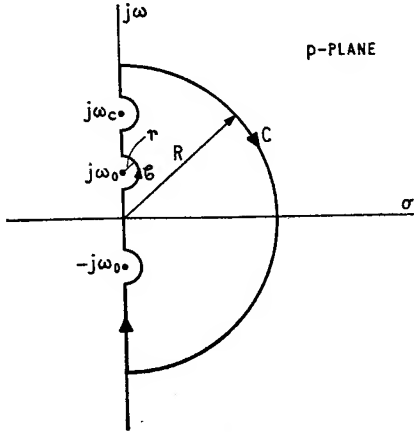

Fig. 5.18. The contour C

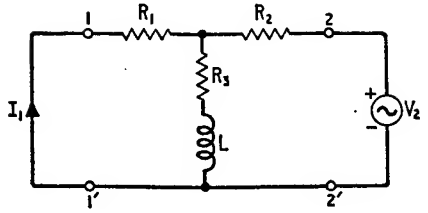

Fig. 5.19. Feedback network with compensating inductor

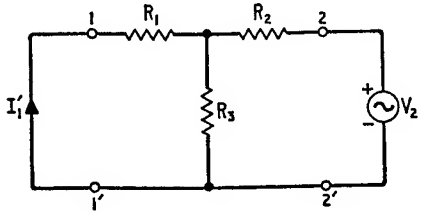

Fig. 5.20. Feedback network with inductor L removed from circuit

times the difference between the infinite frequency and zero frequency values of the gain function $A(\omega)$, and that it is independent of the way in which the gain function varies between these two limits. This is known as the *phase area theorem.*

To illustrate this theorem, consider the T-network of Fig. 5.19 which is the feedback network component of a shunt-shunt type of feedback amplifier. The internal amplifier component is assumed to consist of a cascade of three common emitter stages. The terminal 1 of Fig. 5.19 is connected to the base of the input transistor, and terminal 2 is connected to the collector of the output transistor. We shall assume that the resistors R_1 and R_2 are large compared to the input impedance of the internal amplifier and the load impedance, respectively. This is, in effect, equivalent to short-circuiting the input port of the feedback network and feeding its output port from a voltage source V_2 equal to the load voltage, as in Fig. 5.19. Then, the reverse short-circuit transfer admittance $y_{12}(j\omega)$ becomes a direct measure of the reverse transfer function $\beta(j\omega)$ of the feedback network. From Fig. 5.19, we find that

$$y_{12}(j\omega) = \frac{I_1}{V_2} = \frac{-(R_3 + j\omega L)}{R_1R_2 + (R_1 + R_2)(R_3 + j\omega L)} \tag{5.70}$$

If the inductor L is removed from circuit as in Fig. 5.20, we have

$$y_{12}(0) = \frac{I_1'}{V_2}$$

$$= \frac{-R_3}{R_1R_2 + R_3(R_1 + R_2)} \tag{5.71}$$

Hence, the effect of inserting the inductor L in circuit can be expressed by

$$e^{\Gamma(j\omega)} = \frac{y_{12}(j\omega)}{y_{12}(0)}$$

$$= \frac{m(j\omega + \omega_l)}{j\omega + m\omega_l} \tag{5.72}$$

where

$$\left.\begin{aligned} \omega_l &= \frac{R_3}{L} \\ m &= 1 + \frac{R_1R_2}{R_3(R_1 + R_2)} \end{aligned}\right\} \tag{5.73}$$

Evaluating the gain and phase angle functions, we get

$$A(\omega) = \log_e\left[\frac{1 + (\omega/\omega_l)^2}{1 + (\omega/m\omega_l)^2}\right]^{1/2} \tag{5.74}$$

$$B(\omega) = \tan^{-1}\left(\frac{\omega}{\omega_l}\right) - \tan^{-1}\left(\frac{\omega}{m\omega_l}\right) \tag{5.75}$$

These are shown plotted in Fig. 5.21 for three difference values of L. We see that at all frequencies, the phase angle is positive. Therefore, the effect of adding the inductor L to the feedback network is to introduce a phase advance into the open-loop frequency response.

From Equation 5.74 we find that at zero frequency, $A(0) = 0$ and at infinite frequency

$$A(\infty) = \log_e m \tag{5.76}$$

Therefore, the phase area theorem (that is Equation 5.69) gives

$$\int_{-\infty}^{\infty} B(\omega)\, du = \frac{\pi}{2}\log_e m \tag{5.77}$$

This result can be verified by direct integration of Equation 5.75.

We thus see that the total area under the phase angle characteristic is independent of the inductor L. The effect of varying the inductor L is to shift the frequency at which the phase advance attains its

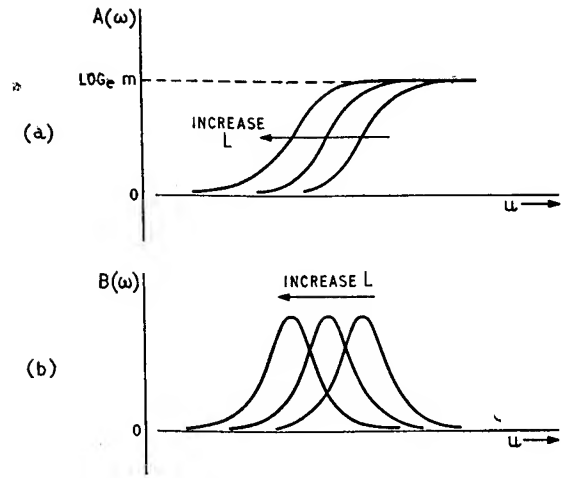

Fig. 5.21. Effects of inserting inductor L: (a) Gain characteristic, (b) Phase characteristic

maximum value. Further, the larger the feedback resistor R_3, the smaller the value of m and the smaller is the area of phase advance available for compensation. However, for given values of R_1 and R_2, the larger the feedback resistor R_3, the greater is the amount of feedback applied to the circuit in the useful frequency band. Therefore, as the applied feedback is increased, the available phase advance is reduced and it becomes more difficult to achieve stability with phase advance compensation in the feedback path.

5.3.3 GAIN-SLOPE THEOREM

The phase area theorem enables the calculation of the phase integral when the behaviour of the associated gain characteristic at zero and infinite frequencies is known. This theorem, however, gives no information whatsoever about the value of the phase angle at any specified frequency. In practice, it is often required to compute the phase angle characteristic from a knowledge of the gain characteristic over all frequencies. For this purpose, we can make use of Equation 5.37 from which we deduce that the angle and gain functions are related as follows

$$B(\omega_c) = \frac{1}{\pi}\int_{-\infty}^{\infty} \frac{A(\omega) - A(\omega_c)}{\omega - \omega_c}\, d\omega$$

$$= \frac{1}{\pi}\int_{-\infty}^{0} \frac{A(\omega) - A(\omega_c)}{\omega - \omega_c}\, d\omega + \frac{1}{\pi}\int_{0}^{\infty} \frac{A(\omega) - A(\omega_c)}{\omega - \omega_c}\, d\omega \tag{5.78}$$

Replacing ω with $-\omega$ in the first integral of the second line of Equation 5.78 and changing the limits of integration accordingly, we obtain

$$\int_{-\infty}^{0} \frac{A(\omega) - A(\omega_c)}{\omega - \omega_c}\,d\omega = \int_{\infty}^{0} \frac{A(-\omega) - A(\omega_c)}{-\omega - \omega_c}(-d\omega)$$

$$= -\int_{0}^{\infty} \frac{A(\omega) - A(\omega_c)}{\omega + \omega_c}\,d\omega \qquad (5.79)$$

where we have used the relationship $A(\omega) = A(-\omega)$, which states that the gain function is an even function of frequency. Substituting the result of Equation 5.79 into Equation 5.78 we get

$$B(\omega_c) = -\frac{1}{\pi}\int_{0}^{\infty} \frac{A(\omega) - A(\omega_c)}{\omega + \omega_c}\,d\omega + \frac{1}{\pi}\int_{0}^{\infty} \frac{A(\omega) - A(\omega_c)}{\omega - \omega_c}\,d\omega$$

$$= \frac{2\omega_c}{\pi}\int_{0}^{\infty} \frac{A(\omega) - A(\omega_c)}{\omega^2 - \omega_c^2}\,d\omega \qquad (5.80)$$

If we change to a logarithmic frequency scale by the use of Equation 5.68 we find that Equation 5.80 modifies to

$$B(\omega_c) = \frac{1}{\pi}\int_{-\infty}^{\infty} \frac{A(\omega) - A(\omega_c)}{\sinh u}\,du \qquad (5.81)$$

Integrating the right hand side of this equation by parts leads to the following result†

$$B(\omega_c) = \frac{1}{\pi}\int_{-\infty}^{\infty} \frac{dA(\omega)}{du} \log_e\left(\coth\left|\frac{u}{2}\right|\right) du \qquad (5.82)$$

† On integrating by parts, we find from Equation 5.81 that

$$B(\omega_c) = -\frac{1}{\pi}\left[(A(\omega) - A(\omega_c))\log_e\left(\coth\frac{u}{2}\right)\right]_{-\infty}^{\infty} + \frac{1}{\pi}\int_{-\infty}^{\infty} \frac{dA(\omega)}{du}\log_e\left(\coth\frac{u}{2}\right)du$$

Now $\coth u/2 = (e^u + 1)/(e^u - 1)$; hence, when $u = \infty$, $\coth u/2 = 1$ and $\log_e(\coth u/2) = 0$. Further, when $u = -\infty$, $\coth u/2 = -1 = e^{j\pi}$ and so $\log_e(\coth u/2) = j\pi$. Also, $A(\omega) = A(0)$ when $u = -\infty$ because this corresponds to $\omega = 0$. Therefore, the integrated part of the above equation reduces to $j[A(0) - A(\omega_c)]$.

Next, for negative values of u, we note that $\coth u/2$ is negative and its logarithm is complex; thus

$$\log_e\left(\coth\frac{u}{2}\right) = \log_e\left(\coth\left|\frac{u}{2}\right|\right) + j\pi$$

where $u < 0$

Therefore

$$\frac{1}{\pi}\int_{-\infty}^{\infty} \frac{dA(\omega)}{du}\log_e\left(\coth\frac{u}{2}\right)du = \frac{1}{\pi}\int_{-\infty}^{\infty} \frac{dA(\omega)}{du}\log_e\left(\coth\left|\frac{u}{2}\right|\right)du + j\int_{-\infty}^{0} \frac{dA(\omega)}{du}\,du$$

$$= \frac{1}{\pi}\int_{-\infty}^{\infty} \frac{dA(\omega)}{du}\log_e\left(\coth\left|\frac{u}{2}\right|\right)du + j\left[A(\omega)\right]_{u=-\infty}^{u=0}$$

$$= \frac{1}{\pi}\int_{-\infty}^{\infty} \frac{dA(\omega)}{du}\log_e\left(\coth\left|\frac{u}{2}\right|\right)du + j\,[A(\omega_c) - A(0)]$$

where it is noted that $\omega = \omega_c$ at $u = 0$, and $\omega = 0$ at $u = -\infty$.

Finally, combining the above results, we get Equation 5.82.

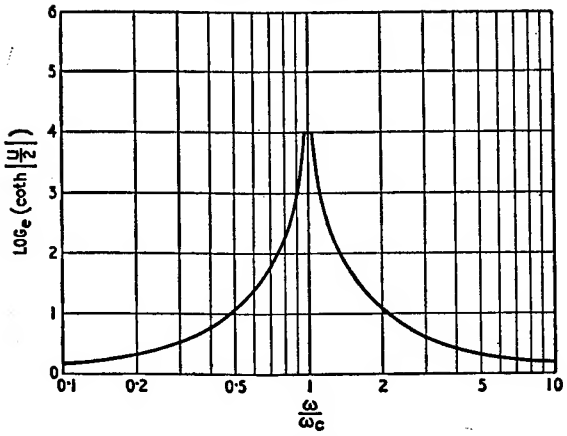

Fig. 5.22. Weighting factor

This equation states that the phase angle at any particular frequency depends on the slope of the gain characteristic (plotted on a logarithmic frequency scale) at all frequencies. The relative importance of the gain-slope at different frequencies is determined by the *weighting factor*

$$\log_e\left(\coth\left|\frac{u}{2}\right|\right) = \log_e\left|\frac{\omega + \omega_c}{\omega - \omega_c}\right| \qquad (5.83)$$

This is shown plotted in Fig. 5.22 where we see that it becomes logarithmically infinite at $\omega = \omega_c$. At frequencies high compared with ω_c the weighting factor approximates to $2\omega_c/\omega$, and at frequencies low compared with ω_c it approximates to $2\omega/\omega_c$. Therefore, the slope of the gain characteristic at a frequency lying close

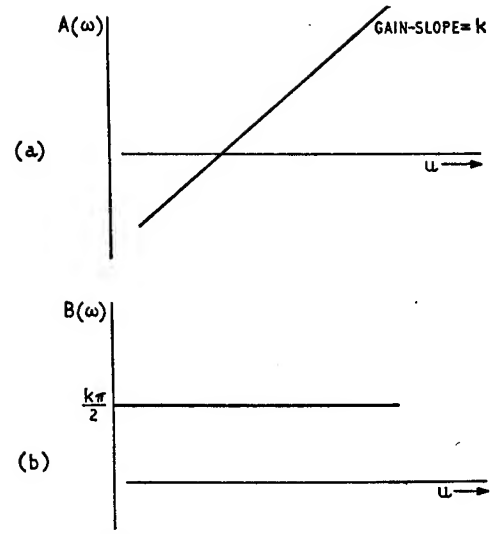

Fig. 5.23. Constant gain-slope: (a) Gain characteristic, (b) Phase characteristic

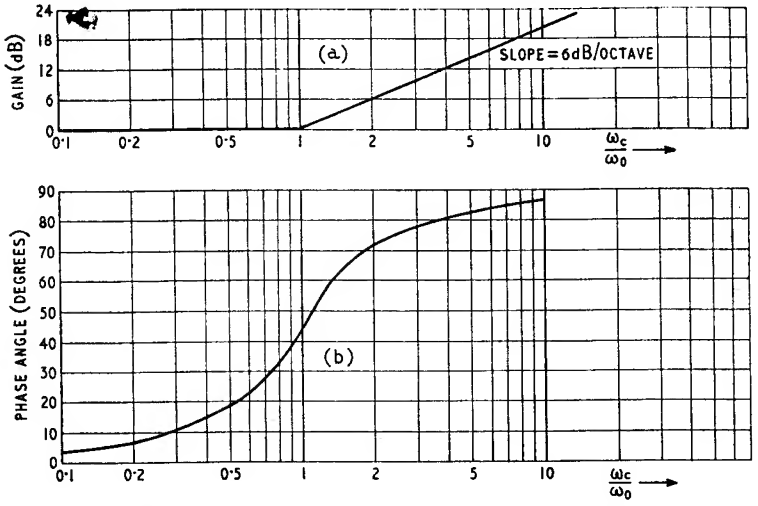

Fig. 5.24. Semi-infinite constant slope: (a) Gain characteristic, (b) Phase angle characteristic

to ω_c, where the phase angle is being determined, has a much larger effect than the gain-slope at a more remote frequency. We thus find that the phase angle at ω_c is effectively determined by the slope of the gain characteristic in the frequency range extending from $\omega_c/10$ to $10\omega_c$. It is to be noted that the gain slope theorem defined by Equation 5.82 applies to all minimum phase transfer functions whether or not they have poles and zeros at infinite frequency. On the other hand, in the case of the phase area theorem, poles and zeros at infinity are excluded.

5.3.4 EXAMPLES

Constant gain-slope

This is the simplest possible gain characteristic and is shown plotted on a logarithmic frequency scale in Fig. 5.23 (a). The gain-slope is equal to k at all frequencies. Therefore, $dA(\omega)/du = k$, and so Equation 5.82 becomes

$$B(\omega_c) = \frac{k}{\pi}\int_{-\infty}^{\infty} \log_e\left(\coth\left|\frac{u}{2}\right|\right) du \qquad (5.84)$$

The definite integral is known to be equal to $\pi^2/2$ so that

$$B(\omega_c) = \frac{k\pi}{2} \qquad (5.85)$$

Therefore, the phase angle is constant and independent of frequency as indicated in Fig. 5.23 (b). It is equal to 90° for a *unit slope*, that is, $k = 1$. A unit slope is equivalent to a change in $A(\omega)$ by one neper per unit change of u. A unit change of u, in turn, corresponds to a change in frequency by the factor $e = 2.718$ and is therefore equal to $1/\log_e 2$ octaves. Since, one neper equals 8.69 dB, it follows that a unit slope is the same as 6 dB per octave.

Semi-infinite slope

For the second example, we shall consider the problem of evaluating the exact phase angle characteristic associated with the *semi-infinite constant slope* characteristic of Fig. 5.24 (a). The gain is zero up to $\omega_c = \omega_0$, beyond which it has a constant unit slope (i.e. 6 dB per octave). Let

$$u_c = \log_e\left(\frac{\omega_0}{\omega_c}\right)$$

then the gain is zero in the range below u_c, and Equation 5.82 gives the phase angle at any frequency ω_c to be

$$B(\omega_c) = \int_{u_c}^{\infty} \log_e \left(\coth \left| \frac{u}{2} \right| \right) du \qquad (5.86)$$

This definite integral has been computed and tabulated by Thomas[1] for different values of ω_c. The results of the integration are shown plotted in Fig. 5.24 (b).

If ω_c is low compared to the corner frequency ω_0, we can show from Equation 5.86 that

$$B(\omega_c) \simeq \frac{2\omega_c}{\pi\omega_0} \qquad (\omega_c \ll \omega_0) \qquad (5.87)$$

which states that, at low frequencies, the phase angle of the semi-infinite constant slope characteristic of Fig. 5.24 (a) varies practically in a linear manner with frequency. In the general case of a semi-infinite characteristic of slope equal to k dB per octave we have

$$B(\omega_c) \simeq \frac{2k\omega_c}{\pi\omega_0} \qquad (\omega_c \ll \omega_0) \qquad (5.88)$$

5.4 Ideal loop gain characteristic

5.4.1 CONSTANT PHASE CUT OFF

Up till now, we have considered evaluating the minimum phase angle characteristic associated with a gain characteristic specified

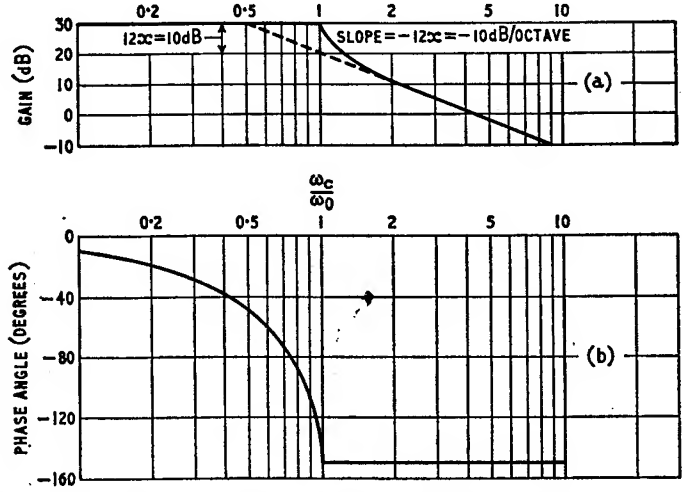

Fig. 5.25. Constant phase cut off characteristic

throughout the complete frequency range from zero to infinity. It is also possible to specify the gain function in one frequency range and the phase angle function for all other frequencies outside this range. Let us thus assume that the gain is specified to be constant at a level equal to A_0 nepers up to a frequency of ω_0, and from ω_0 upwards the phase angle is specified to be constant at a level equal to $-x\pi$ radians. Then, the problem is that of evaluating the gain for all frequencies greater than ω_0 and the phase angle for frequencies less than ω_0. This problem has been solved by Bode[2] and the result is that when $\omega_c < \omega_0$, we have

$$\left.\begin{aligned} A(\omega_c) &= A_0 \\ B(\omega_c) &= -2x \sin^{-1}\left(\frac{\omega_c}{\omega_0}\right) \end{aligned}\right\} \qquad (5.89)$$

and when $\omega_c > \omega_0$,

$$\left.\begin{aligned} A(\omega_c) &= A_0 - 2x \log_e \left[\left(\frac{\omega_c}{\omega_0}\right) + \left[\left(\frac{\omega_c}{\omega_0}\right)^2 - 1 \right]^{1/2} \right] \\ B(\omega_c) &= -x\pi \end{aligned}\right\} \qquad (5.90)$$

Fig. 5.25 shows $A(\omega_c)$ and $B(\omega_c)$ plotted for the case of $A_0 = 3{\cdot}46$ nepers = 30 dB and $x = 5/6$. We shall refer to this characteristic as the *constant phase cut off characteristic.*

When the frequency ω_c becomes large compared with ω_0 we find from Equation 5.90 that the gain approximates to

$$A(\omega_c) \simeq A_0 - 2x \log_e \left(\frac{2\omega_c}{\omega_0}\right) \qquad (\omega_c \gg \omega_0) \qquad (5.91)$$

Therefore, at high frequencies, the gain decreases asymptotically at the rate of $-12x$ dB/octave. If this asymptote is extended to the left, it intersects the flat portion of the gain characteristic at $\omega_0/2$, as can be deduced by setting $A(\omega_c) = A_0$ in Equation 5.91. We thus see that the gain characteristic of Fig. 5.25 bears a resemblance to the semi-infinite constant slope characteristic except that the flat portion extends one octave higher in frequency.

Further, the high frequency asymptote cuts a vertical line drawn through the frequency ω_0 at a point located below the horizontal line A_0 by an amount equal to $2x \log_e 2$ nepers, that is, $12x$ dB. This can be confirmed by putting $\omega_c = \omega_0$ in Equation 5.91.

5.4.2 BODE'S IDEAL LOOP GAIN CHARACTERISTIC

In the practical design of feedback amplifiers, the requirements are usually for a specified constant open-loop gain throughout the useful

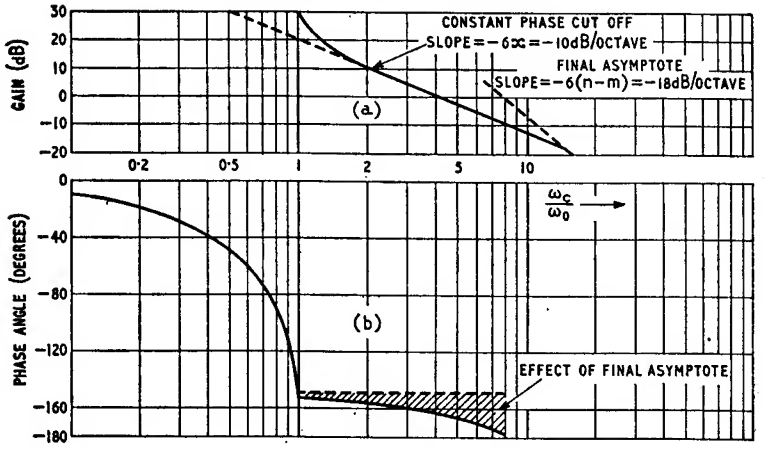

Fig. 5.26. Illustrating effect of final asymptote on gain and phase characteristics

frequency band and for specified gain and phase margins. These design requirements can be satisfied simultaneously if it were possible to realise a constant phase cut off type of characteristic for the open-loop frequency response, that is, if $A(\omega) = \log_e |T(j\omega)|$ and $B(\omega) = \angle T(j\omega)$ have the characteristics shown in Fig. 5.25. Then, the constant phase base can be set at an angle of $-x\pi$ radians thereby providing a constant phase margin of $(1-x)\pi$ radians, where $x < 1$. Also, the flat portion of the gain characteristic, extending up to ω_0, provides a constant open-loop gain throughout the useful frequency band.

In practice, however, the open-loop frequency response can be shaped to follow the constant phase cut off characteristic only up to a certain frequency for the following reason. If the open-loop gain function $T(p)$ has m zeros and n poles, then it follows that as the frequency approaches infinity, we have

$$\underset{\omega\to\infty}{\text{Limit}} T(j\omega) = H\frac{(j\omega)^m}{(j\omega)^n} = H\cdot(j\omega)^{-(n-m)} \qquad (5.92)$$

where H is a scale factor. On a logarithmic frequency scale, Equation 5.92 represents a straight line, referred to as the *final asymptote*, with a slope equal to $-6(n-m)$ dB per octave. Since, the logarithmic gain of a common cathode or common emitter stage falls off ultimately at the rate of -6 dB per octave it is clearly impossible for $(n-m)$ to be less than the number of valves or transistors that make up the internal amplifier component of the feedback circuit. Further, in negative feedback amplifiers where there is likelihood of instability occurring we find that the slope of the

final asymptote is greater in absolute value than that of the constant phase cut off characteristic, that is, $6(n-m) > 12x$. Therefore, the constant phase cut off can be realised only up to the frequency where it intersects the final asymptote, as shown illustrated in Fig. 5.26 (a) for the practical case of $n-m=3$ and $x=5/6$.

The effect of the final asymptote can be taken into account by adding, to the constant phase cut off characteristic, a semi-infinite constant slope characteristic of a slope equal to $-6(n-m-2x)$ dB per octave and a corner frequency equal to the intersection frequency. This added semi-infinite characteristic modifies the total phase angle to the form shown in Fig. 5.26 (b), where we see that the much desired constant phase feature has been completely destroyed. However, we can counteract this effect, at least within a limited frequency range, by introducing a minor transition region in the form of a horizontal step between the constant phase cut off slope and the final asymptote as shown in Fig. 5.27 (a). The horizontal step is located below the zero dB line by an amount equal to the specified gain margin. The design then becomes complete once the frequency ω_b is determined.

The characteristic of Fig. 5.27 (a) can be resolved into the sum of a constant phase cut off characteristic extending to infinity and two semi-infinite constant slope characteristics, one of which starts at the frequency ω_b and has a positive slope of $12x$ dB per octave, and the other starts at ω_d and has a negative slope equal to that of the final asymptote, that is $-6(n-m)$ dB per octave. From Equation 5.88 we deduce that, at low frequencies, the phase angle of the first semi-infinite asymptote is equal to $4x\omega_c/\pi\omega_b$ radians,

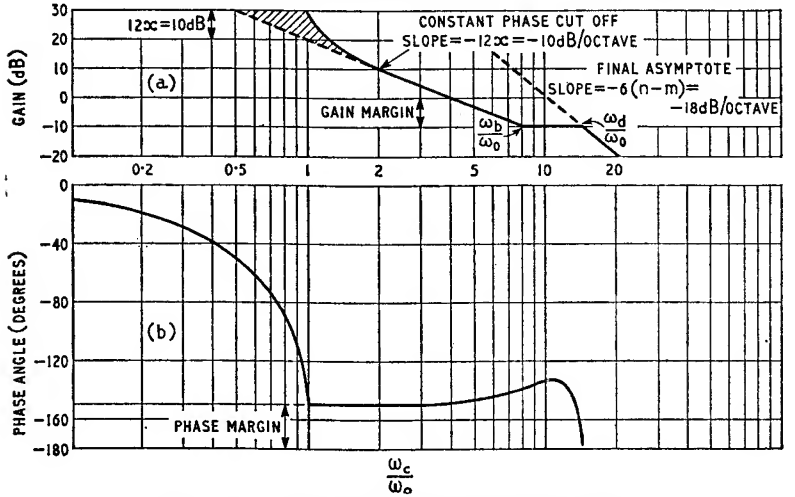

Fig. 5.27. Bode's ideal loop gain characteristic

and the phase angle of the second one is equal to $-2(n-m)\omega_c/\pi\omega_a$ radians. These two phase angles can be made to cancel each other provided that we choose

$$\omega_b = \frac{2x\omega_a}{n-m} \tag{5.93}$$

Then, at low frequencies, the total phase angle associated with the gain characteristic of Fig. 5.27 (a) becomes practically the same as that obtained from a constant phase cut off characteristic. For the case of $x = 5/6$ and $n - m = 3$, the complete phase angle characteristic is as shown in Fig. 5.27 (b). The gain characteristic of Fig. 5.27 (a) is known as *Bode's ideal loop gain characteristic.*

In the examples considered in the next chapter, we shall illustrate how the above characteristic can be used in the practical design of feedback amplifiers.

5.5 An approximate evaluation of the principal oscillatory mode of the closed-loop transient response from the open-loop frequency response

In a great majority of feedback amplifiers the closed-loop transient response is dominated by the principal oscillatory mode which is due to a pair of closed-loop poles nearest the jω-axis of the p-plane (see Section 4.7). The closer these two poles move to the jω axis the smaller will be the resulting stability margins of the open-loop

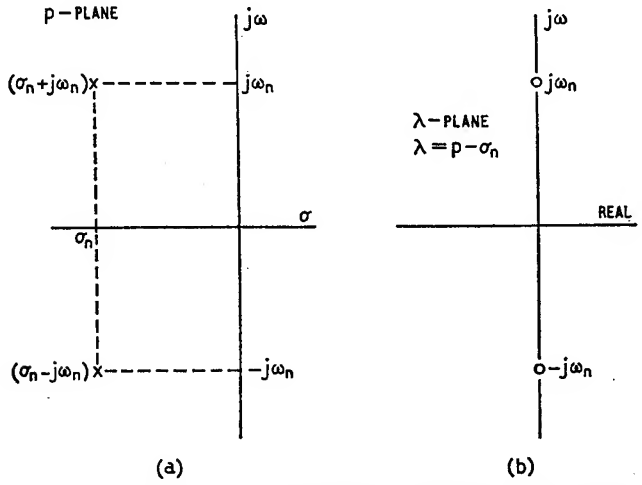

Fig. 5.28. (a) A pair of dominant closed-loop poles in the p-plane, (b) The two roots of $1 + T_1(\lambda) = 0$ located on the imaginary axis of the λ-plane

frequency response. This relationship between the principal oscillatory mode of the closed-loop transient response and the stability margins of the open-loop frequency response can be put on to a quantitative basis by examining the Nyquist locus around the critical point ($-$ 1,0).

Consider Fig. 5.28 (a) showing a pair of dominant closed-loop poles at $p = \sigma_n \pm j\omega_n$, with the remaining poles located far out to the left in the p-plane. The closed-loop poles are the same as the roots of $F(p) = 1 + T(p) = 0$ where $T(p)$ is the open-loop gain function of the feedback amplifier. Further, let the open-loop

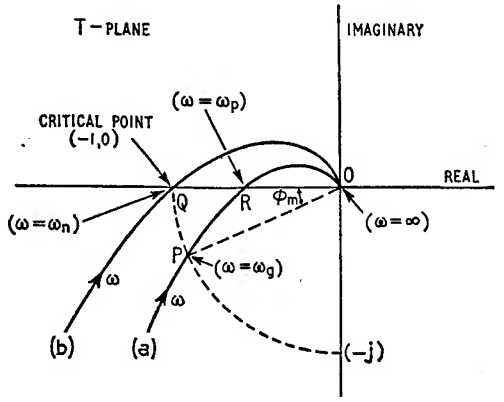

Fig. 5.29. Curve (a) is the Nyquist plot of $T(j\omega)$, Curve (b) is the Nyquist plot of $T(\sigma_n + j\omega)$

frequency response of the amplifier be represented by the Nyquist locus (a), Fig. 5.29, which is obtained by putting $p = j\omega$ and then plotting $T(j\omega)$, with ω varying from zero up to infinity. If, next, we put $p = \sigma_n + \lambda$, where λ is a new complex variable, we obtain $T_1(\lambda) = T(\sigma_n + \lambda)$. Then we find that $1 + T_1(\lambda) = 0$ has a pair of roots at $\lambda = \pm j\omega_n$ along the imaginary axis of the λ-plane, as in Fig. 5.28 (b). Accordingly, if λ is put equal to jω, and a Nyquist locus of $T_1(j\omega) = T(\sigma_n + j\omega)$ is plotted, we see that this locus just passes through the critical point ($-$ 1,0), as shown by curve (b) in Fig. 5.29. The frequency at which this occurs is equal to the oscillation frequency ω_n of the principal oscillatory mode. In other words it is required to determine the values of σ_n and ω_n which satisfy the equation $1 + T(\sigma_n + j\omega_n) = 0$.

Expressing the open-loop gain function in its logarithmic form, we have

$$\begin{aligned} \log_e T(p) &= \log_e T(\sigma + j\omega) \\ &= A(\sigma,\omega) + jB(\sigma, \omega) \end{aligned} \tag{5.94}$$

where $A(\sigma,\omega)$ is the open-loop gain in nepers and $B(\sigma,\omega)$ is the open-loop phase in radians, both being functions of σ as well as ω. Suppose that σ and ω are allowed to change by the small amounts $\delta\sigma$ and $\delta\omega$, respectively. Then to a first order of approximation, we find from the total differential theorem that the corresponding changes δA and δB in the values of $A(\sigma,\omega)$ and $B(\sigma,\omega)$, respectively, are given by

$$\left.\begin{aligned}\delta A &= \frac{\partial A}{\partial \sigma}\,\delta\sigma + \frac{\partial A}{\partial \omega}\,\delta\omega \\ \delta B &= \frac{\partial B}{\partial \sigma}\,\delta\sigma + \frac{\partial B}{\partial \omega}\,\delta\omega\end{aligned}\right\} \tag{5.95}$$

The logarithmic function $\log_e T(p)$ is, however, analytic in the region surrounding the critical point $(-1,0)$ in the T-plane; therefore, the functions $A(\sigma,\omega)$ and $B(\sigma,\omega)$ must satisfy the Cauchy-Riemann Equations 5.3 where the functions $x(\sigma,\omega)$ and $y(\sigma,\omega)$ correspond to $A(\sigma,\omega)$ and $B(\sigma,\omega)$, respectively. Therefore

$$\left.\begin{aligned}\frac{\partial A}{\partial \omega} &= -\frac{\partial B}{\partial \sigma} \\ \frac{\partial A}{\partial \sigma} &= \frac{\partial B}{\partial \omega}\end{aligned}\right\} \tag{5.96}$$

Eliminating $\partial A/\partial\sigma$ and $\partial B/\partial\sigma$ between these relations and Equations 5.95, we get

$$\left.\begin{aligned}\delta A &= \frac{\partial B}{\partial \omega}\,\delta\sigma + \frac{\partial A}{\partial \omega}\,\delta\omega \\ \delta B &= -\frac{\partial A}{\partial \omega}\,\delta\sigma + \frac{\partial B}{\partial \omega}\,\delta\omega\end{aligned}\right\} \tag{5.97}$$

Let us apply these generalised results to the case of Fig. 5.29 when we shift from the point P (where $\sigma = 0$, $\omega = \omega_g$) to the point Q (where $\sigma = \sigma_n$, $\omega = \omega_n$). We thus have $\delta\sigma = \sigma_n$ and $\delta\omega = \omega_n - \omega_g$, where ω_g is the gain crossover frequency. In Fig. 5.29 we see that the points P and Q are both unit distance from the origin; hence, the function $T(p)$ does not change in magnitude, that is, $\delta A = 0$. We also see that the phase angle of $T(p)$ changes by the amount $\delta B = -\pi - (-\pi + \phi_m) = -\phi_m$, where ϕ_m is the phase margin in radians. Substituting these changes into Equations 5.97, we get

$$\left.\begin{aligned}0 &= \frac{\partial B}{\partial \omega}\sigma_n + \frac{\partial A}{\partial \omega}(\omega_n - \omega_g) \\ -\phi_m &= -\frac{\partial A}{\partial \omega}\sigma_n + \frac{\partial B}{\partial \omega}(\omega_n - \omega_g)\end{aligned}\right\} \tag{5.98}$$

The derivatives $\partial A/\partial\omega$ and $\partial B/\partial\omega$ are equal to the rates of change of the open-loop gain and phase with frequency, respectively, both being measured at the gain crossover frequency ω_g. Putting $S_A = \partial A/\partial\omega$ and $S_B = \partial B/\partial\omega$, and then solving Equations 5.98 for σ_n and ω_n, we get

$$\sigma_n = \frac{S_A\,\phi_m}{S_A^2 + S_B^2} \tag{5.99}$$

$$\omega_n = \omega_g - \frac{S_B\,\phi_m}{S_A^2 + S_B^2} \tag{5.100}$$

In a stable feedback amplifier all the closed-loop poles are located in the left half of the p-plane; therefore, the parameter σ_n must necessarily have a negative value. This, in turn, requires the product term $S_A\,\phi_m$ to be always negative. Further, in Equation 5.99 we see that the absolute value of σ_n decreases with decreasing ϕ_m. In other words, the smaller the phase margin, the nearer will the dominant closed-loop poles move to the jω-axis and the greater will be the overshoot exhibited by the resulting closed-loop transient response.

It must be emphasised that, when using Equations 5.99 and 5.100, greater accuracy is obtained for highly oscillatory feedback amplifiers for which the Nyquist locust passes close to the critical point $(-1,0)$. This, of course, is to be expected because Equations 5.95, which are the results of first order approximation, are then reasonably well justified. For damping ratios less than 0·5, the accuracy can be of the order of 30 per cent, or better.

If at the unity-gain point P the Nyquist locus is nearly tangential to the radius OP, a case which arises when, for example, the open-loop frequency response of the feedback amplifier has been shaped to follow Bode's ideal loop gain characteristic, then the phase slope S_B is small (or zero) compared to the gain slop S_A. For such a feedback amplifier we find from Equations 5.99 and 5.100 that

$$\sigma_n \simeq \frac{\phi_m}{S_A} \tag{5.101}$$

and that the frequency of oscillation ω_n of the principal oscillatory mode is very nearly equal to the gain crossover frequency ω_g.

It is also possible to relate the open- and closed-loop responses of a feedback amplifier by considering the $-180°$ phase point R on the Nyquist locus†. Then as we move from the point R to point Q, the loop gain changes by an amount δA equal to the gain margin in nepers. The phase change δB is zero because both points Q and R lie on the imaginary axis of the T-plane. Using these results in

† See J. C. West and J. Potts[3]

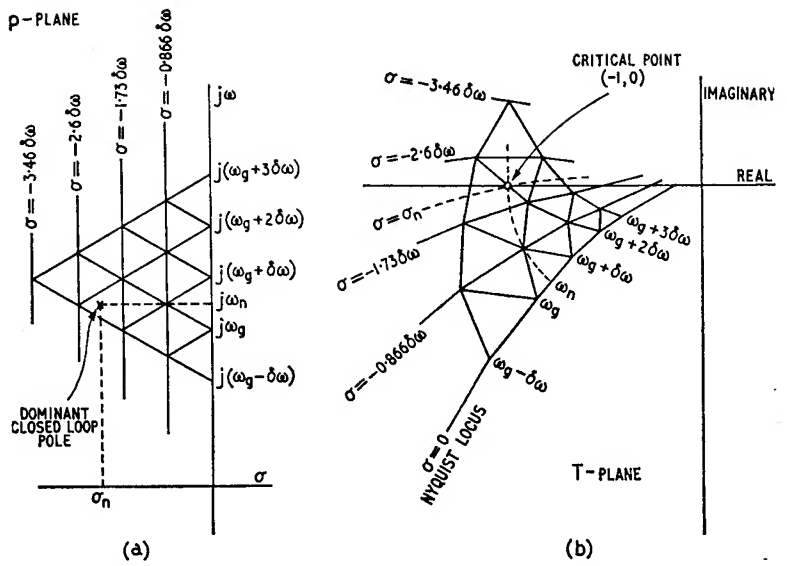

Fig. 5.30. Graphical construction for evaluating the principal oscillatory mode of closed-loop transient response: (a) p-plane, (b) T-plane

Equations 5.97, we can then solve for the parameters σ_n and ω_n of the principal oscillatory mode in terms of the gain margin, phase crossover frequency ω_p, and gain and phase slopes measured at $\omega = \omega_p$. However, in general, the results of this evaluation are less accurate than those of Equations 5.99 and 5.100 based on the phase margin concept.

5.5.1 A GRAPHICAL METHOD FOR EVALUATING THE PRINCIPAL OSCILLATORY MODE

The parameters of the principal oscillatory mode can be also evaluated by applying a graphical technique due to J. C. West,[4,5] which uses the frequency scale on the Nyquist locus to construct an orthogonal diagram such that the T-plane becomes a conformal transformation of the p-plane. In a conformal transformation any small geometrical figure in the p-plane is transformed into a similar figure in the T-plane with the angles of intersection and the approximate geometrical shapes being preserved as we go from one plane to the other. Accordingly, we find that a set of small equilateral triangles based on the $j\omega$-axis of the p-plane, as in Fig. 5.30 (a), is transformed, in the T-plane, into a corresponding set of curvilinear triangles based on the Nyquist locus. If, however, the elementary

triangles in the p-plane are chosen small enough, then the corresponding curvilinear triangles in the T-plane can be approximated with straight sided triangles, as in Fig. 5.30 (b).

To determine the principal oscillatory mode, we first select on the Nyquist locus a number of points which represent equal increments $\delta\omega$ of frequency starting from (or close to) the gain crossover frequency ω_g. The successive points are joined together by straight lines, and on each line as base an equilateral triangle is constructed. Then the apices of successive triangles are connected with a new set of straight lines, and the process is continued till the graphical construction crosses the real axis of the T-plane.

The curves drawn through the apices of successive rows of triangles represent loci for which σ changes at increments of $-\delta\omega \cdot \sin 60° = -0{\cdot}866\delta\omega$. The number of such increments lying between the Nyquist locus and the critical point $(-1,0)$ is equal to the real co-ordinate σ_n of the dominant closed-loop poles. To determine the imaginary co-ordinate ω_n of these poles, we construct a line to pass through the critical point $(-1,0)$ and at right angles to the constant σ loci; the frequency at which this line intersects the Nyquist locus equals ω_n. Provided the frequency increment $\delta\omega$ is chosen sufficiently small then, at the expense of a greater constructional effort, it is possible to achieve fairly accurate results with this graphical method.

PROBLEMS

1. By applying Nyquist's criterion, determine whether the feedback circuits represented by the following open-loop gain functions are stable or not:

   (a) $$T(j\omega) = \frac{20}{(1 + j5\omega)(1 + j\omega)(1 + j\omega/5)}$$

   (b) $$T(j\omega) = \frac{100}{(1 + j10\omega)(1 - \omega^2 + j\omega)}$$

2. For the open-loop gain function of Problem 2, Chapter 4, calculate by means of Nyquist's criterion the range of values of $T(0)$ for which the amplifier is unstable.
3. A three-stage amplifier has the open-loop gain function

   $$T(j\omega) = \frac{20/3}{(1 + j\omega/\omega_0)^3}$$

   where $\omega_0 = 10^6$ rad/sec is the angular cut off frequency of each of the individual stages. Sketch the Nyquist locus and show that the amplifier is stable.

What is the value of $T(0)$ necessary for sustained oscillations, and what is the corresponding frequency of oscillation?

4. A compensating network is added to the three-stage amplifier of Problem 3 modifying its open-loop gain function to

$$T(j\omega) = \frac{T(0)}{\left(1 + \frac{j\omega}{\omega_0}\right)^2 \left(1 + \frac{j\omega}{10\omega_0}\right)}$$

If $T(0) = 20$, determine the gain margin in dB and the phase cross over frequency.

5. A single-loop feedback amplifier involves three stages having angular cut off frequencies of 10^6, 2×10^6 and 4×10^6 rad/sec. The low frequency open-loop gain has a value of 40 dB.

Construct Bode's ideal loop gain characteristic so as to realise a phase margin of 45° and a gain margin of 12 dB. Hence determine the loss characteristic of the interstage compensating network required for addition to the internal amplifier component.

Plot the Nyquist locus for the compensated amplifier, and then using West's graphical technique determine approximate values for the co-ordinates of the principal oscillatory mode of the resulting closed-loop transient response.

6. Negative feedback is applied to a synchronously tuned three-stage amplifier resulting in the following open-loop gain function:

$$T(j\omega) = \frac{c}{\left(1 + \frac{j\omega}{\omega_r} + \frac{\omega_r}{j\omega}\right)^3}$$

where c is a constant equal to the value of the open-loop gain at the resonance frequency ω_r. Sketch the Nyquist locus for this amplifier and determine (a) the phase crossover frequencies, (b) the critical value of c for which the amplifier is on the verge of instability.

7. The feedback loop of a linear circuit consists of an amplifier and a lossless transmission line of fixed delay τ. The open-loop gain function of the circuit is

$$T(j\omega) = T(0) \frac{e^{-j\omega\tau}}{1 + j\omega/\omega_0}$$

Discuss the effect of the delay factor $e^{-j\omega\tau}$ on the Nyquist locus, and show that the circuit oscillates at an angular frequency ω given by

$$\omega = -\omega_0 \tan(\omega\tau)$$

provided at this frequency

$$T(0) = \frac{1}{\cos \omega\tau}$$

Hence demonstrate that an infinity of values for ω is possible.

8. In a certain application it is required to establish that a negative feedback amplifier is not only stable but also that its dominant closed-loop poles have a real part more negative than a specified real number $-\sigma_0$. Show that such a requirement can be investigated by applying Nyquist's criterion to the modified function $T(jx)$ which is obtained from the open-loop gain function $T(j\omega)$ by substituting $j\omega = jx - \sigma_0$. Hence, establish whether or not the dominant closed-loop poles of a negative feedback circuit with

$$T(j\omega) = \frac{3}{1 + 3(j\omega) + 2(j\omega)^2 + (j\omega)^3}$$

have a real part more negative than $-0{\cdot}5$.

REFERENCES

1. THOMAS, D. E., 'Tables of phase associated with a semi-infinite unit slope of attenuation', *Bell Syst. Tech. J.*, **26**, 870 (1947).
2. BODE, H. W., *Network Analysis and Feedback Amplifier Design*, Van Nostrand, New York (1945).
3. WEST, J. C., and POTTS, J., 'A Simple Connection Between Closed-Loop Transient Response and Open-Loop Frequency Response', *Proc. I.E.E.*, Part II, **100**, 201 (1953).
4. WEST, J. C., *Servomechanisms*, English Universities Press (1953).
5. TAYLOR, P. L., *Servomechanisms*, Longmans (1960).
6. BLECHER, F. H., 'Transistor Multiple-Loop Feedback Amplifiers', *Proc. National Electronics Conference*, **13**, 19 (1957).
7. BOTHWELL, F. E. 'Nyquist Diagram and The Routh-Hurwitz Stability Criterion', *Proc. I.R.E.*, **38**, 1345 (1950).
8. CAMPBELL, W. W., 'Stability From Nyquist Diagram', *Ministry of Supply Servo Library*, G.74 (1945).
9. CHESTNUT, H., and MAYER, R. W., *Servomechanisms and Regulating System Design*, Vol. 1, Wiley, New York (1959). Second Edition.
10. DOUCE, J. L., *An Introduction To The Mathematics of Servomechanisms*, English Universities Press (1963).
11. DUERDOTH, W. T. 'Some Considerations in the Design of Negative Feedback Amplifiers', *Proc. I.E.E.*, Part III, **97**, p. 138 (1950).
12. LYNCH, W. A., 'The Stability Problem in Feedback Amplifiers', *Proc. I.R.E.*, **39**, 999 (1951).
13. NYQUIST, H., 'Regeneration Theory', *Bell System Tech. J.*, **11**, 126 (1932).
14. THOMASON, J. G., *Linear Feedback Analysis*, Pergamon Press (1955).
15. VAZSONYI, A., 'A Generalisation of Nyquist's Stability Criterion', *J. Appl. Phys.*, **20**, 863 (1949).

CHAPTER 6

Design of Compensating Networks

In Chapter 3 we saw that a large value of open-loop gain is required in order to appreciably reduce harmonic distortion, sensitivity of gain to parameter variations, etc., and so improve the circuit performance of a negative feedback amplifier. On the other hand, in Chapters 4 and 5 we saw that it is possible for a feedback amplifier having a large open-loop gain to become unstable. The designer of a feedback amplifier is therefore faced with the difficult problem of having to realise a large open-loop open gain inside the useful frequency band and yet having to guard against instability with satisfactory margins. In order to achieve these two conflicting objectives it is necessary to suitably shape the open-loop frequency response, outside the useful band, by adding compensating circuit elements to the feedback network or the internal amplifier component

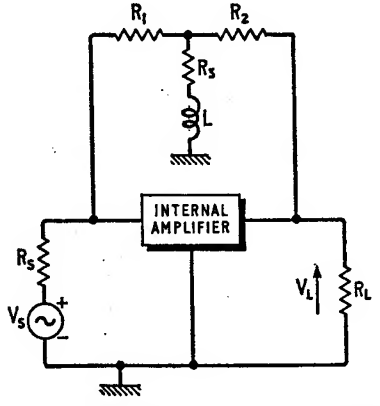

Fig. 6.1. Shunt-shunt feedback amplifier with phase advancing feedback network

or both. In this chapter we shall consider these two methods of stabilisation.

6.1 Compensation in the feedback path

The stability performance of a feedback amplifier can be improved by introducing a phase advance into the open-loop frequency response so as to partially counteract the phase lag associated with the frequency response of the internal amplifier at high frequencies. As an example consider the shunt-shunt feedback amplifier of Fig. 6.1. In Section 5.3 we showed that the effect of adding the inductor L to the feedback network is to multiply the uncompensated open-loop gain function by the following transfer function

$$G(j\omega) = \frac{m(j\omega + \omega_l)}{j\omega + m\omega_l} \tag{6.1}$$

where

$$\omega_l = \frac{R_s}{L} \tag{6.2}$$

$$m = 1 + \frac{R_1 R_2}{R_s(R_1 + R_2)} \tag{6.3}$$

With $j\omega = p$ we obtain the pole-zero pattern of Fig. 6.2 for the transfer function $G(p)$ which has a real zero at $p = -\omega_l$ and a real

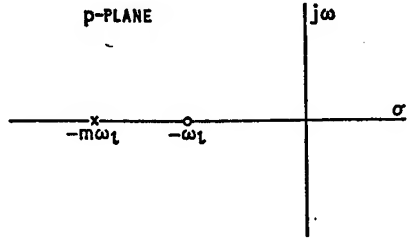

Fig. 6.2. Pole-zero pattern for feedback network of Fig. 6.1

pole at $p = -m\omega_l$. The parameter m is necessarily greater than unity; hence the pole is located to the left of the zero.

From Equation 6.1 we deduce that the gain $A'(\omega)$ in dB and the phase angle $B(\omega)$ in radians are given by, respectively

$$A'(\omega) = 20 \log_{10} |G(j\omega)|$$

$$= 10 \log_{10} \left[\frac{1 + (\omega/\omega_l)^2}{1 + (\omega/m\omega_l)^2} \right] \tag{6.4}$$

$$B(\omega) = \angle G(j\omega)$$

$$= \tan^{-1}\left[\frac{\omega\omega_l(m-1)}{\omega^2 + m\omega_l^2}\right] \tag{6.5}$$

The gain characteristic can be approximated by three line segments, as in Fig. 6.3 (a). The phase angle, shown plotted in Fig. 6.3 (b),

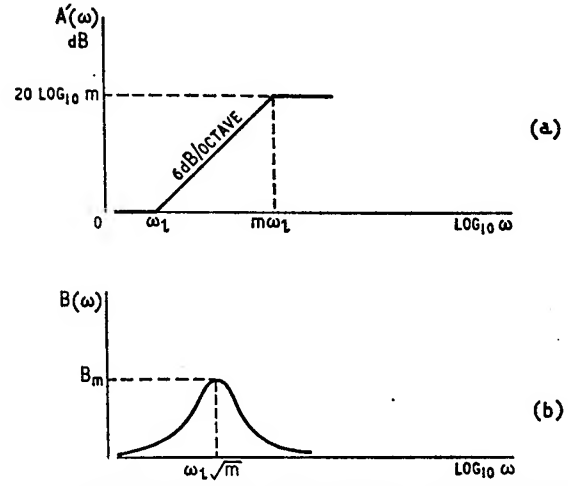

Fig. 6.3. (a) Approximate gain characteristic, (b) Phase characteristic

reaches a maximum value B_m at an angular frequency ω_m equal to the geometric mean of the two corner frequencies ω_l and $m\omega_l$ that is,

$$\omega_m = \omega_l\sqrt{m} \tag{6.6}$$

At $\omega = \omega_m$, we have from Equation 6.5

$$B_m = \tan^{-1}\left(\frac{m-1}{2\sqrt{m}}\right) \tag{6.7}$$

which can also be expressed in the following equivalent form

$$B_m = \sin^{-1}\left(\frac{m-1}{m+1}\right) \tag{6.8}$$

The corresponding value A_m of the gain function is obtained from Equation 6.4 to be

$$A_m = 10\log_{10}\left(\frac{1+m}{1+1/m}\right) \text{ dB} \tag{6.9}$$

The gain function $A'(\omega)$ attains its maximum value of $20\log_{10} m$ at infinite frequency. Therefore, the maximum values of both $A'(\omega)$ and $B(\omega)$ are independent of the compensating inductor L.

It is important to note that as the open-loop gain is increased in magnitude, the feedback resistor R_3 becomes smaller for fixed values of R_1 and R_2, the parameter m decreases tending to approach unity, and accordingly the maximum phase advance B_m decreases.

The compensating inductor L is chosen such that the angular frequency ω_m of maximum phase advance coincides with the gain crossover frequency ω_g at which the uncompensated open-loop gain drops to zero dB. Then from Equations 6.2 and 6.6 we find

$$L = \frac{R_3\sqrt{m}}{\omega_g} \tag{6.10}$$

In a practical design problem the elements R_1, R_2 and R_3 of the feedback network are first evaluated, in the manner described in Section 3.8.5, so as to realise a specified value for the open-loop gain in the useful frequency band of the amplifier. Next, the gain and phase characteristics of the uncompensated open-loop response are plotted, and the gain crossover frequency ω_g is located. Then, Equations 6.3 and 6.10 are used to evaluate the compensating inductor L, and the stability performance of the compensated

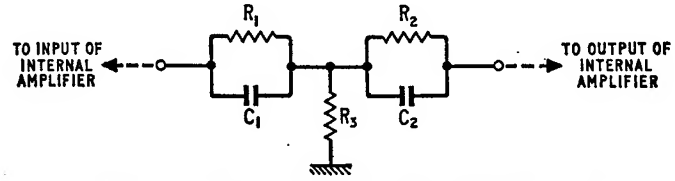

Fig. 6.4. Another phase advancing feedback network

system is assessed by examining the open-loop response that results from adding the gain and phase characteristics, as calculated from Equations 6.4 and 6.5, to the uncompensated open-loop gain and phase response, respectively.

Another way of introducing phase advance into the open-loop response of a feedback amplifier is by adding two capacitors in parallel with the feedback resistors R_1 and R_2, as in Fig. 6.4. In this case it is convenient to choose C_1 and C_2 such that

$$C_1R_1 = C_2R_2 = \frac{1}{\omega_c} \tag{6.11}$$

Then analysis of the feedback network of Fig. 6.4 shows that its reverse short-circuit transfer admittance $y_{12}(p)$ has a double zero at

$p = -1/\omega_c$ and a simple pole at $p = -m\omega_c$ where the parameter m is as defined in Equation 6.3. At high frequencies the feedback network of Fig. 6.4 can produce quite an appreciable loading effect. In the case of a transistor amplifier the loading effect at the output port is greater than that at the input port, and it can be taken into account by adding a pole at $p = -1/C_2R_L$ to the compensated open-loop gain function; R_L is the load resistance. Therefore, as a result of adding the capacitors C_1 and C_2 to the feedback network of

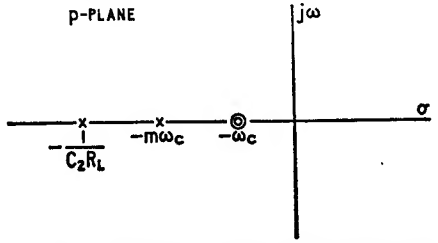

Fig. 6.5. Pole-zero pattern of Equation 6.12

Fig. 6.4, the uncompensated open-loop gain function becomes multiplied by a transfer function having the pole-zero pattern of Fig. 6.5 and given by

$$G(p) = \frac{(1 + p/\omega_c)^2}{(1 + p/m\omega_c)(1 + pC_2R_L)} \tag{6.12}$$

6.2 Compensation in the forward path

Another widely used method of shaping the open-loop frequency response of a feedback amplifier is to modify its internal amplifier component. This can be achieved by applying local feedback to the particular stage which has the largest cut off frequency, thereby increasing the threshold open-loop gain, as discussed in Section 4.4

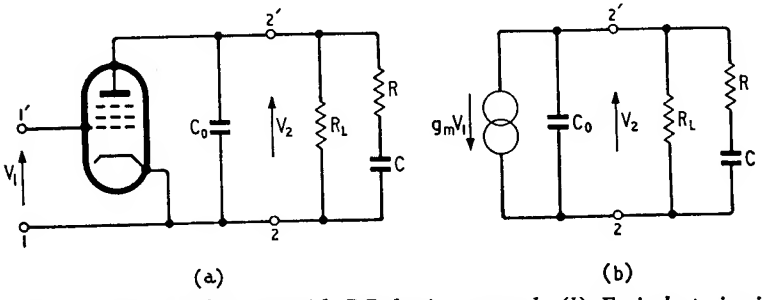

Fig. 6.6. (a) Pentode stage with RC-shaping network, (b) Equivalent circuit

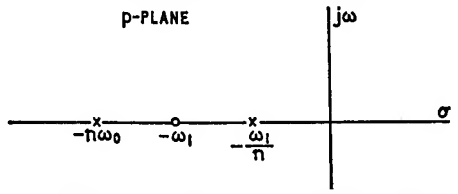

Fig. 6.7. Pole-zero pattern of pentode stage of Fig. 6.6 (a)

(p. 174). Alternatively, the open-loop response can be shaped by means of interstage networks. We shall illustrate the design of such networks by considering two examples, one involving valves and the other involving transistors.

6.2.1 THE RC-INTERSTAGE NETWORK

Consider the pentode stage of Fig. 6.6 (a) where R_L is the load resistance, C_0 is the total shunt capacitance, and the elements R, C have been added for the purpose of stabilisation. The voltage gain function of this stage can be calculated from the equivalent circuit of Fig. 6.6 (b); thus

$$V_2 = \frac{-g_mV_1}{(1/R_L) + pC_0 + pC/(1 + pCR)} \tag{6.13}$$

Let

ω_0 = uncompensated stage cut off frequency

$$= \frac{1}{C_0R_L} \tag{6.14}$$

$$\omega_1 = \frac{1}{CR} \tag{6.15}$$

Then in terms of ω_0 and ω_1 we can re-write Equation 6.13 as follows

$$\frac{V_2}{V_1} = \frac{-g_mR_L\omega_0(p + \omega_1)}{p^2 + p(\omega_0 + \omega_1 + \omega_0\omega_1CR_L) + \omega_0\omega_1} \tag{6.16}$$

Expressing the denominator polynomial as the product of two real pole factors, we get

$$\frac{V_2}{V_1} = \frac{-g_mR_L\omega_0(p + \omega_1)}{(p + n\omega_0)(p + \omega_1/n)} \tag{6.17}$$

where

$$\omega_0 + \omega_1 + \omega_0\omega_1CR_L = n\omega_0 + \frac{\omega_1}{n} \tag{6.18}$$

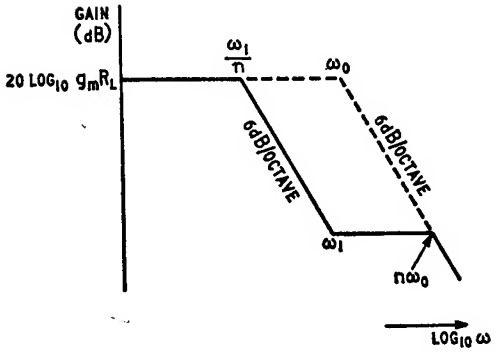

Fig. 6.8. Approximate gain characteristic of pentode stage of Fig. 6.6 (a)

Therefore, the pole-zero pattern of the pentode stage of Fig. 6.6 (a) is as shown in Fig. 6.7. In the absence of the compensating elements R and C, the voltage gain function of the stage has a pole at $p = -\omega_0$. We thus see that the effect of adding the elements R and C has been to move the pole originally associated with the stage. Further if we put $p = j\omega$ in Equation 6.17 we find that the gain characteristic of the stage of Fig. 6.6 (a) can be approximated by four straight line segments as in Fig. 6.8. The dashed portion of this diagram represents the approximation to the gain characteristic of the stage without the elements R and C.

We shall regard the quantities ω_1 and n as design parameters, in terms of which we find from Equation 6.18 that the compensating element C is given by

$$C = \frac{n-1}{R_L}\left(\frac{1}{\omega_1} - \frac{1}{n\omega_0}\right) \tag{6.19}$$

Then Equation 6.15 gives the element R to be

$$R = \frac{1}{\omega_1 C} \tag{6.20}$$

Example

To illustrate the procedure for evaluating the parameters ω_1 and n let it be supposed that the internal amplifier consists of a cascade of three identical pentodes with two RC-interstage shaping networks, as shown in Fig. 6.9. The last stage has a voltage gain function equal to $-g_m R_L \omega_0/(p + \omega_0)$, whereas that of each of the first two stages is given by Equation 6.17. Hence we deduce that the overall voltage gain $K(p)$ of the internal amplifier is equal to

$$K(p) = \frac{(-g_m R_L \omega_0)^3 (p+\omega_1)^2}{(p+\omega_0)(p+n\omega_0)^2 (p+\omega_1/n)^2} \tag{6.21}$$

If we choose ω_1 equal to the uncompensated stage cut off frequency ω_0, a pole-zero cancellation takes place and Equation 6.21 simplifies to

$$K(p) = \frac{(-g_m R_L \omega_0)^3 (p+\omega_0)}{(p+n\omega_0)^2 (p+\omega_0/n)^2} \tag{6.22}$$

Further, if we assume that the feedback network is purely resistive and that it presents negligible loading to the internal amplifier, then

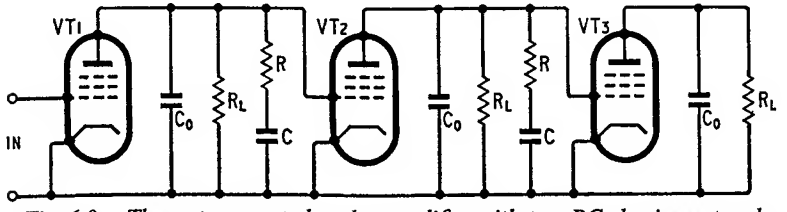

Fig. 6.9. Three-stage pentode valve amplifier with two RC-shaping networks

we find that the reverse transfer function $\beta(p)$ of the feedback network is purely real and equal to β, and the resulting open-loop gain function $T(p) = \beta(p)K(p)$ is given by

$$T(p) = \frac{\omega_0^3 T(0)(p+\omega_0)}{(p+n\omega_0)^2 (p+\omega_0/n)^2} \tag{6.23}$$

where $T(0) = -\beta g_m^3 R_L^3$ is the low frequency valve of the open-loop gain. The open-loop pole-zero pattern corresponding to Equation 6.23 is shown in Fig. 6.10, where we see that $T(p)$ has a simple zero at $p = -\omega_0$ and a double pole at each of $p = -n\omega_0$ and $p = -\omega_0/n$.

Suppose next the design requirements are for low frequency open-loop gain (in dB) $= 20 \log_{10} T(0) = 30$ dB (that is $T(0) = 31{\cdot}6$)

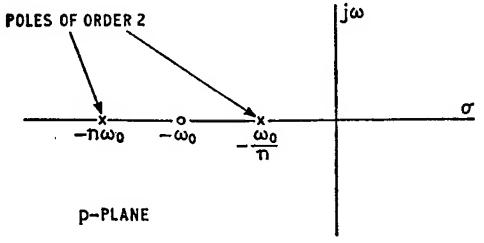

Fig. 6.10. Pole-zero pattern of Equation 6.23

Phase Margin $\geqslant 30°$

Gain Margin $\geqslant 10$ dB

Then noting that the uncompensated open-loop gain function is equal to $T(0)\,(1 + j\omega/\omega_0)^{-3}$ and following the procedure described in Section 5.4.2 we can construct Bode's ideal loop gain characteristic shown in Fig. 6.11. After a few trials it is found that this characteristic can be approximated reasonably closely by four straight line segments corresponding to the open-loop gain function of Equation 6.23 with $p = j\omega$ and the parameter $n = 5$.

Assuming that

$R_L = 10\ \text{k}\Omega$

$C_0 = 4\ \text{pF}$

we find from Equation 6.14 that

$$\omega_0 = \frac{1}{4 \times 10^{-12} \times 10^4} = 25 \times 10^6\ \text{rad/sec}$$

Remembering that ω_1 was chosen equal to ω_0, and using the value $n = 5$ deduced from Fig. 6.11 we find from Equations 6.19 and 6.20 that the elements C and R of the compensating interstage networks of Fig. 6.8 have the following values

$$C = \frac{5-1}{10^4}\left(\frac{1}{25 \times 10^6} - \frac{1}{5 \times 25 \times 10^6}\right)$$
$$= 12{\cdot}8 \times 10^{-12}\ \text{F} = 12{\cdot}8\ \text{pF}$$
$$R = \frac{1}{25 \times 10^6 \times 12{\cdot}8 \times 10^{-12}}$$
$$= 3{\cdot}12 \times 10^3\Omega = 3{\cdot}12\ \text{k}\Omega$$

Compensated open-loop frequency response

Let us next evaluate the gain and phase margins actually realised by the compensated amplifier with $T(0) = 31{\cdot}6$. Putting $p = j\omega$ and $n = 5$ in Equation 6.23 we get

$$T(j\omega) = \frac{31{\cdot}6\omega_0^3\,(j\omega + \omega_0)}{(j\omega + 5\omega_0)^2\,(j\omega + \omega_0/5)^2}$$
$$= \frac{31{\cdot}6(1 + j\omega/\omega_0)}{(1 + j\omega/5\omega_0)^2\,(1 + j5\omega/\omega_0)^2} \qquad (6.24)$$

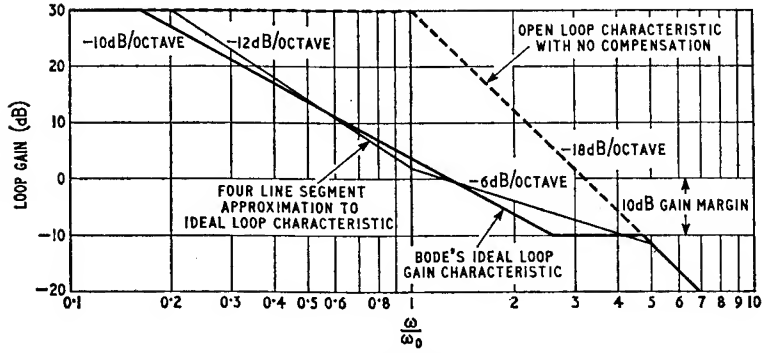

Fig. 6.11. Construction of Bode's ideal loop gain characteristic

The gain and phase characteristics for each of the zero and pole factors of this expression are shown plotted in Fig. 6.12, these characteristics have been obtained as follows. The factor $(1 + j\omega/\omega_0)$ has a corner frequency ω_0 and leads to the gain and phase curves labelled *a* which are of the same form as those of Fig. 2.28, but inverted; this is because $(1 + j\omega/\omega_0)$ is a zero factor whereas the characteristics of Fig. 2.28 apply to a pole factor. Next, the pole factor $(1 + j\omega/5\omega_0)^2$ is of order 2 and has a corner frequency of $5\omega_0$; therefore, to obtain its contribution we shift the actual gain and phase characteristics of Fig. 2.28 along the frequency scale such that the 3 dB point occurs at the corner frequency $5\omega_0$, then multiply each characteristic by 2 which is the order of the factor $(1 + j\omega/5\omega_0)^2$. We thus obtain curves *b* of Fig. 6.12. Similarly, the second order pole factor $(1 + j5\omega/\omega_0)^2$ has a corner frequency at $\omega_0/5$ and leads to curves *c*. Finally the scale factor $T(0) = 31{\cdot}6$ contributes a constant gain of $20 \log_{10} 31{\cdot}6 = 30$ dB and a constant phase angle of 0°. Adding these contributions to curves *a*, *b* and *c* of Fig. 6.12 we obtain the total gain and phase characteristics of Fig. 6.13 for the open-loop gain function of Equation 6.24. Therefore, the gain and phase margins of the compensated amplifier are 15 dB and 39° respectively; these margins are both greater than the required values of 10 dB and 30°, thereby satisfying the design specifications.

Closed-loop response

To complete the design problem we shall determine the closed-loop response by constructing the root locus diagram. Putting $n = 5$ in Equation 6.23, we have

$$T(p) = \frac{\omega_0^3 T(0)\,(p + \omega_0)}{(p + 5\omega_0)^2\,(p + 0{\cdot}2\omega_0)^2} \qquad (6.25)$$

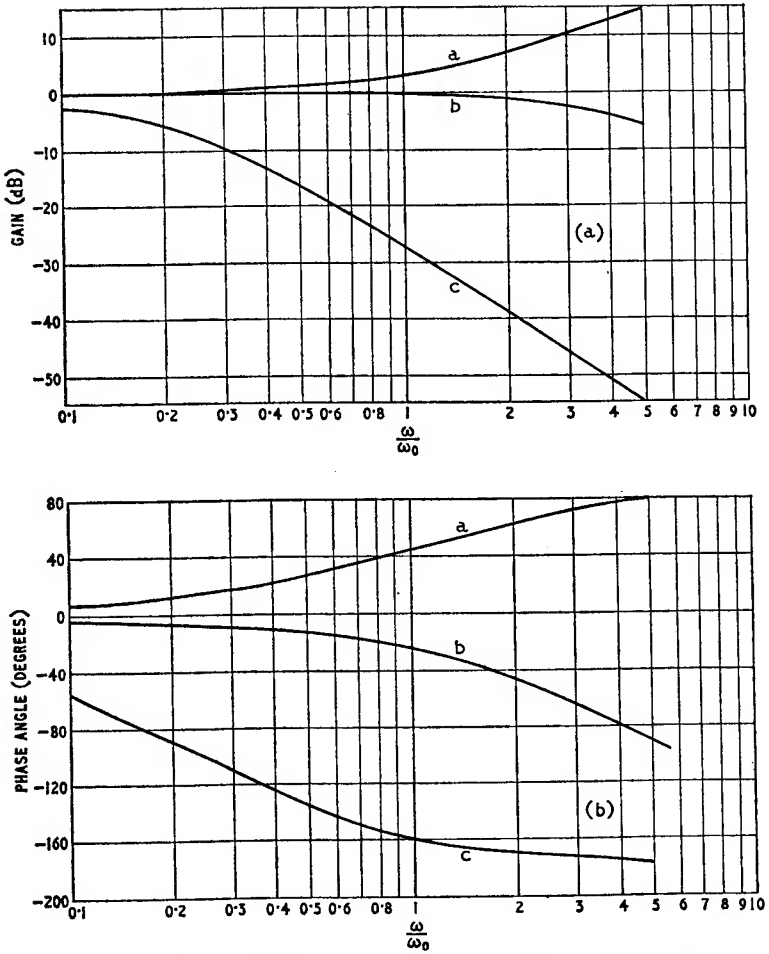

Fig. 6.12. (a) Gain-frequency characteristics, (b) Phase angle-frequency characteristic

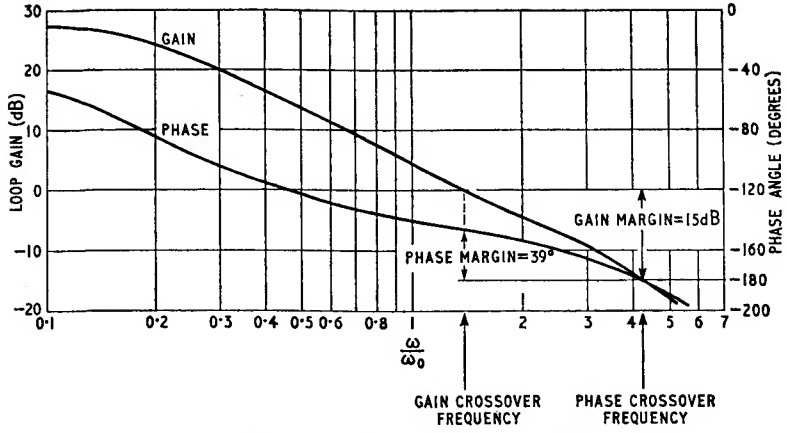

Fig. 6.13. Open-loop response of compensated amplifier

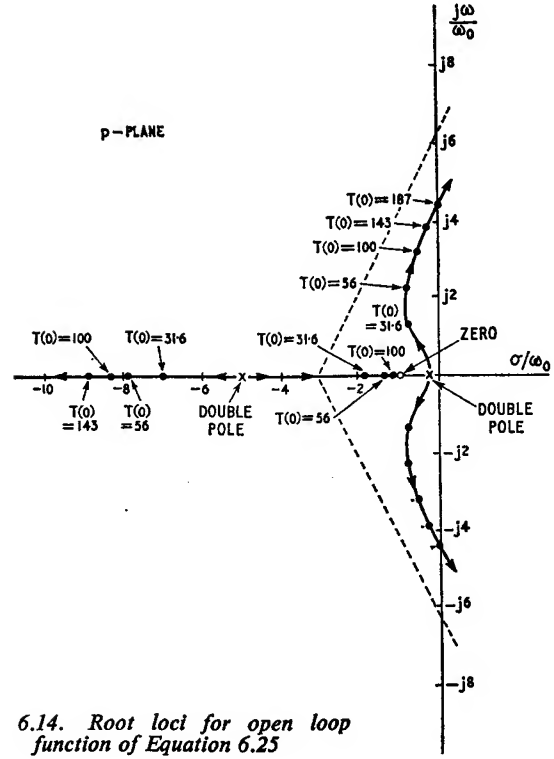

Fig. 6.14. Root loci for open loop function of Equation 6.25

This open-loop gain function has one zero and four poles; hence the root locus diagram has three asymptotes making angles of $-60°$, $-180°$ and $+60°$ with the σ-axis of the p-plane. From Equation 4.60 we find that the asymptotes intersect at the point $p = \sigma_0$ where

$$\sigma_0 = \frac{-2 \times 5\omega_0 - 2 \times 0{\cdot}2\omega_0 + \omega_0}{4 - 1}$$

$$= -3{\cdot}13\omega_0$$

There are four root loci, equal to the number of the open-loop poles; one root locus terminates on the open-loop zero at $p = -\omega_0$, and the remaining three terminate at infinity. With the aid of rule No. 5 (p. 179), we can then construct the root locus diagram, as in Fig. 6.14. Here we see that when $T(0)$ assumes the design value of 31.6, the closed-loop poles are at

$$p = -1{\cdot}86\omega_0$$
$$p = -7{\cdot}02\omega_0$$
$$p = -0{\cdot}76\omega_0 \pm \mathrm{j}\,1{\cdot}39\omega_0$$

Assuming that the direct transmittance from the source to the load is negligible, we find that with a purely resistive feedback network we can express the closed-loop gain function $K'(p)$ as follows

$$K'(p) = \frac{1}{\beta} \cdot \frac{T(p)}{1 + T(p)} \tag{6.26}$$

Then the closed-loop zeros are the same as the open-loop zeros, and the closed-loop poles are the same as the zeros of $1 + T(p)$. Since the open-loop gain function $T(p)$ of Equation 6.25 has a zero at $p = -\omega_0$, it follows that for $T(0) = 31{\cdot}6$ the complete pole-zero pattern for the closed-loop gain function $K'(p)$ is as shown in Fig. 6.15. The value of $K'(p)$ at $p = 0$ is closely equal to $1/\beta$ because $T(0) \gg 1$; we therefore have

$$K'(p) = \frac{1}{\beta} \cdot \frac{1{\cdot}86 \times 7{\cdot}02(0{\cdot}76^2 + 1{\cdot}39^2)\omega_0^3(p + \omega_0)}{(p + 1{\cdot}86\omega_0)\,(p + 7{\cdot}02\omega_0)\,[(p + 0{\cdot}76\omega_0)^2 + (1{\cdot}39\omega_0)^2]}$$

$$= \frac{1}{\beta} \cdot \frac{32{\cdot}6\omega_0^3(p + \omega_0)}{(p + 1{\cdot}86\omega_0)\,(p + 7{\cdot}02\omega_0)\,[(p + 0{\cdot}76\omega_0)^2 + (1{\cdot}39\omega_0)^2]} \tag{6.27}$$

The pole at $= -7{\cdot}02\omega_0$ lies so far out to the left in the p-plane that it contributes negligibly to the closed-loop transient response. Accordingly if the input signal is a unit-step function, we find that the transform $V_L(p)$ of the output signal $v_L(t)$ is effectively given by

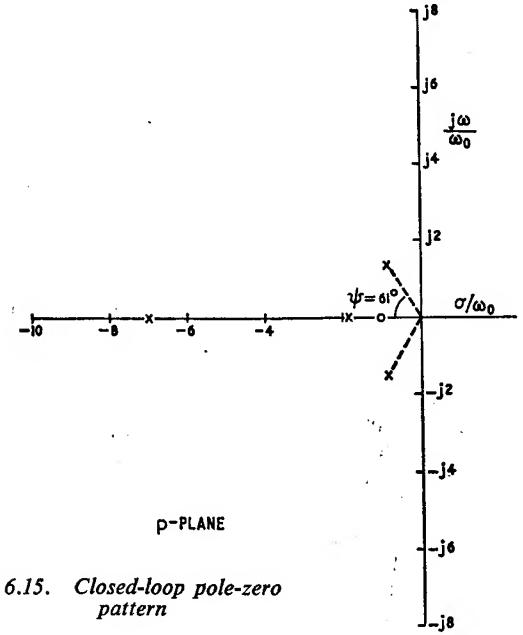

Fig. 6.15. Closed-loop pole-zero pattern

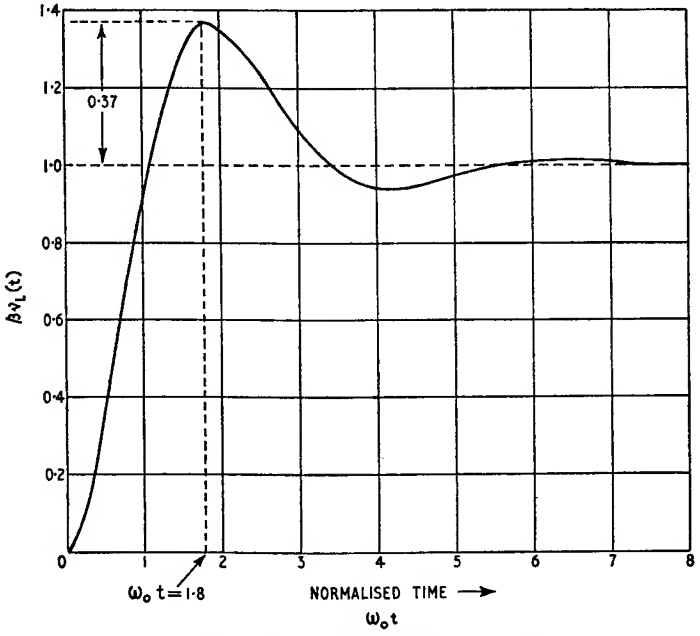

Fig. 6.16. Closed-loop transient response

$$V_L(p) \simeq \frac{1}{\beta} \cdot \frac{4{\cdot}68\omega_0^2(p + \omega_0)}{p(p + 1{\cdot}86\omega_0)\,[(p + 0{\cdot}76\omega_0)^2 + (1{\cdot}39\omega_0)^2]}$$

Expanding into partial fractions, we get

$$V_L(p) \simeq \frac{1}{\beta}\left[\frac{1}{p} + \frac{0{\cdot}685}{p + 1{\cdot}86\omega_0} - 1{\cdot}685\frac{p + 0{\cdot}76\omega_0}{(p + 0{\cdot}76\omega_0)^2 + (1{\cdot}39\omega_0)^2}\right]$$

Hence, we deduce that the output signal $v_L(t)$ is

$$v_L(t) \simeq \frac{1}{\beta}\left[1 + 0{\cdot}685\,e^{-1{\cdot}86\omega_0 t} - 1{\cdot}685\,e^{-0{\cdot}76\omega_0 t}\cos(1{\cdot}39\omega_0 t)\right] \quad (6.28)$$

This is shown plotted in Fig. 6.16 where we see that $v_L(t)$ reaches its first maximum value of $1{\cdot}37/\beta$ at $t = 1{\cdot}8/\omega_0$. Since the ultimate value of $v_L(t)$ is approximately $1/\beta$, it follows that the closed-loop transient response exhibits a fractional overshoot equal to 37%.

The closed-loop frequency response can be determined from Equation 6.27 by putting $p = j\omega$ and then summing the contributions of of the various pole and zero factors; the result is shown in Fig. 6.17.

In this diagram we see that the 'closed-loop cut off frequency', at which the closed loop gain drops by 3 dB below its zero frequency value $K'(0)$, is equal to $2{\cdot}55\ \omega_0$.

The closed loop cut off frequency can be also determined from the loop gain frequency characteristic more directly by noting that it is approximately equal to the frequency at which the open loop gain, in decibels, drops to†

$$-20\log_{10}[\cos\phi_m + \sqrt{(1 + \cos^2\phi_m)}]$$

where ϕ_m is the phase margin. This relation assumes that the amplifier employs a purely resistive feedback network, and that its

† From Equation 6.26 we have

$$K'(j\omega) = \frac{1}{\beta}\frac{1}{1 + T^{-1}(j\omega)}$$

If $T(0) \gg 1$, the zero frequency valve $K'(0)$ of the closed-loop gain is effectively equal to $1/\beta$. Therefore, at the closed-loop cut off frequency $|K'(j\omega)| \simeq 1/(\beta\sqrt{2})$, that is

$$|1 + T^{-1}(j\omega)| = \sqrt{2}$$

In the neighbourhood of the frequency at which this relation is satisfied the open-loop phase angle is practically constant and equal to $-180° + \phi_m$, where ϕ_m is the phase margin. This assumes that the open-loop frequency response follows Bode's ideal loop gain characteristic with a gain margin of at least 10 dB.

Let T_x denote the magnitude of $T(j\omega)$ at the closed-loop cut off frequency; then at this frequency we have

$$T^{-1}(j\omega) = \frac{1}{T_x}e^{j(180° - \phi_m)} = \frac{-1}{T_x}(\cos\phi_m - j\sin\phi_m)$$

Therefore,

$$\left|\left(1 - \frac{\cos\phi_m}{T_x}\right) + \frac{j\sin\phi_m}{T_x}\right| = \sqrt{2}$$

Evaluating the magnitude of the expression on the left hand side leads to

$$\frac{1}{T_x^2} - \frac{2\cos\phi_m}{T_x} - 1 = 0$$

Since T_x must have a positive value, only the following solution of this quadratic equation is acceptable

$$\frac{1}{T_x} = \cos\phi_m + \sqrt{(1 + \cos^2\phi_m)}$$

We thus see that the closed-loop cut off frequency is approximately equal to the frequency at which the open-loop gain drops to

$$20\log_{10}T_x = -20\log_{10}[\cos\phi_m + \sqrt{(1 + \cos^2\phi_m)}]\ \text{dB}$$

open loop frequency response has been shaped to follow Bode's ideal loop gain characteristic. It is also assumed that $T(0) \gg 1$ and the gain margin is at least 10 dB. These conditions are satisfied by the characteristic of Fig. 6.13 for which $\phi_m = 39°$ and $\cos\phi_m = 0{\cdot}776$. Therefore, in the example being considered

$$-20\log_{10}[\cos\phi_m + \sqrt{(1 + \cos^2\phi_m)}] = -20\log_{10}(0{\cdot}776 + \sqrt{1{\cdot}6}) = -6{\cdot}2\ \text{dB}$$

In Fig. 6.13 we see that the open loop gain drops to $-6{\cdot}2$ dB at $\omega = 2{\cdot}35\ \omega_0$. Hence, the approximate value of the closed loop cut off frequency is $2{\cdot}35\ \omega_0$, a result which agrees fairly well with that of $2{\cdot}55\ \omega_0$ obtained from the closed-loop frequency response of Fig. 6.17.

Evaluation of the principal oscillatory mode from the open-loop frequency response

Lastly, it is instructive to use the open-loop frequency response of Fig. 6.13 to determine the co-ordinates σ_n and ω_n of the dominant closed-loop poles, and compare the results with those deduced from the root locus diagram. In Fig. 6.13 we see that the rate of change of the open-loop phase angle with frequency is negligibly small around the gain crossover frequency ω_g which is equal to $1{\cdot}41\ \omega_0$. Therefore, it follows that

$$\omega_n \simeq \omega_g = 1{\cdot}41\ \omega_0$$

where ω_n is the angular frequency of oscillation of the principal oscillatory mode of the closed-loop transient response (see

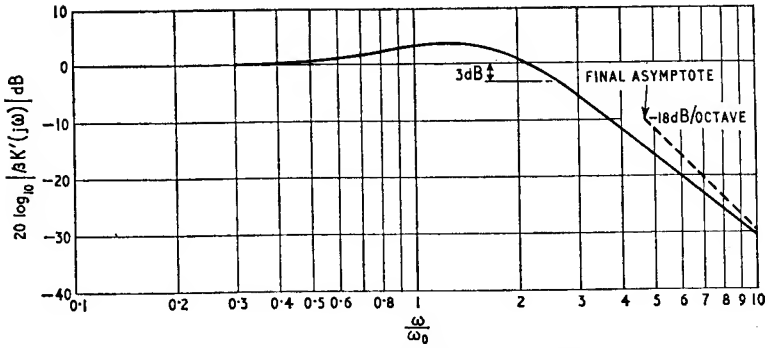

Fig. 6.17. Closed-loop frequency response

Section 5.5, page 241). Next, from Fig. 6.13 we deduce that at $\omega = \omega_g$ the open-loop response has a gain slope

$$S_A = -\frac{1{\cdot}01}{\omega_0} \text{ nepers-sec./rad.}$$

Since the phase margin $\phi_m = 39° = 0{\cdot}68$ radians, it follows from Equation 5.101 that the real co-ordinate σ_n of the dominant closed-loop poles is given by

$$\sigma_n \simeq \frac{\phi_m}{S_A}$$

$$= \frac{0{\cdot}68}{-1{\cdot}01/\omega_0} \simeq -0{\cdot}673\,\omega_0$$

From the open-loop frequency response of Fig. 6.13 we thus find that the dominant closed-loop poles are located at

$$p = \sigma_n \pm j\omega_n \simeq -0{\cdot}673\,\omega_0 \pm j\,1{\cdot}41\,\omega_0$$

This result compares moderately well with the actual positions of

$$p = -0{\cdot}76\,\omega_0 \pm j\,1{\cdot}39\,\omega_0$$

as deduced from the root locus diagram (see the closed-loop pole-zero pattern of Fig. 6.15).

6.2.2 THE RCL-INTERSTAGE NETWORK

Another interstage network widely used in shaping the open-loop response of a feedback amplifier is the so-called *trap circuit* which consists of the series combination of a resistor, a capacitor and an

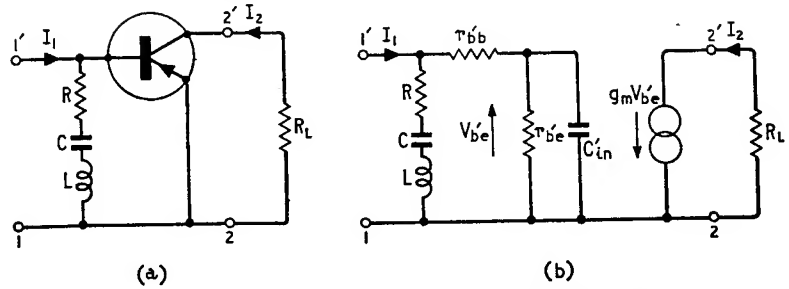

Fig. 6.18. (a) Common emitter stage with an RCL-shaping network, (b) Equivalent circuit

inductor. Fig. 6.18 (a) shows such a network connected across the input port of a common emitter stage. The effect of inserting this network can be calculated from Fig. 6.18 (b) where the transistor has been replaced by its simplified hybrid-π equivalent circuit; thus

$$I_2 = g_m V_{b'e}$$

$$= g_m \frac{Z(p) I_1}{Z(p) + Z_{in}(p)} \cdot \frac{r_{b'e}}{1 + pC_{in}' r_{b'e}} \tag{6.29}$$

where

$Z(p)$ = impedance of the interstage network

$$= R + pL + \frac{1}{pC} \tag{6.30}$$

$Z_{in}(p)$ = input impedance of the common emitter stage

$$= r_{bb'} + \frac{r_{b'e}}{1 + pC_{in}' r_{b'e}} \tag{6.31}$$

$$C_{in}' = C_{b'e} + C_{b'c} g_m R_L \tag{6.32}$$

Assuming that

ω_a = uncompensated stage cut off frequency

$$= \frac{1}{C_{in}' r_{b'e}} \tag{6.33}$$

r_i = low frequency value of $Z_{in}(p)$

$$= r_{bb'} + r_{b'e} \tag{6.34}$$

and considering the special case of the elements R, C and L satisfying the condition

$$LC = \frac{R^2C^2}{4} = \frac{1}{\omega_3^2} \tag{6.35}$$

then the current gain of the stage of Fig. 6.18 (a) is given by

$$\frac{I_2}{I_1} = \frac{g_m r_{b'e}\left(1 + \frac{p}{\omega_3}\right)^2}{1 + p\left(\frac{2}{\omega_3} + \frac{1}{\omega_a} + Cr_t\right) + p^2\left(\frac{1}{\omega_3^2} + \frac{2}{\omega_3\omega_a} + \frac{Cr_{bb'}}{\omega_a}\right) + \frac{p}{\omega_a\omega_3^2}} \tag{6.36}$$

Next, expressing the denominator polynomial in factorised form, we have

$$\frac{I_2}{I_1} = \frac{g_m r_{b'e}\left(1 + \frac{p}{\omega_3}\right)^2}{\left(1 + \frac{p}{\omega_2}\right)\left(1 + 2\delta\frac{p}{\omega_4} + \frac{p^2}{\omega_4^2}\right)} \tag{6.37}$$

where

$$\frac{1}{\omega_2} + \frac{2\delta}{\omega_4} = \frac{2}{\omega_3} + \frac{1}{\omega_a} + Cr_t \tag{6.38}$$

$$\frac{1}{\omega_4^2} + \frac{2\delta}{\omega_2\omega_4} = \frac{1}{\omega_3^2} + \frac{2}{\omega_3\omega_a} + \frac{Cr_{bb'}}{\omega_a} \tag{6.39}$$

$$\omega_2\omega_4^2 = \omega_a\omega_3^2 \tag{6.40}$$

To simplify the design equations we shall assume that ω_2 is small compared to ω_4, that is,

$$\frac{1}{\omega_2} \gg \frac{1}{\omega_4}$$

The validity of this assumption will be demonstrated later. Equations 6.38 and 6.39 then simplify as follows, respectively

$$\frac{1}{\omega_2} \simeq \frac{2}{\omega_3} + \frac{1}{\omega_a} + Cr_t \tag{6.41}$$

$$\frac{2\delta}{\omega_2\omega_4} \simeq \frac{1}{\omega_3^2} + \frac{2}{\omega_3\omega_a} + \frac{Cr_{bb'}}{\omega_a} \tag{6.42}$$

If the cut off frequencies ω_2 and ω_3 are regarded as design parameters, and Equation 6.41 is solved for the compensating element C, we get

$$C \simeq \frac{1}{r_t}\left(\frac{1}{\omega_2} - \frac{1}{\omega_a} - \frac{2}{\omega_3}\right) \tag{6.43}$$

Having evaluated C, we can then determine the remaining elements L and R of the interstage network from Equations 6.35, thus

$$L = \frac{1}{\omega_3^2 C} \tag{6.44}$$

$$R = \frac{2}{\omega_3 C} \tag{6.45}$$

Next, Equations 6.40 and 6.42 can be used to evaluate the parameters ω_4 and δ and so we get

$$\omega_4 = \omega_3\sqrt{\left(\frac{\omega_a}{\omega_2}\right)} \tag{6.46}$$

$$\delta = \frac{\sqrt{(\omega_a\omega_2)}}{2}\left(\frac{2}{\omega_a} + \frac{1}{\omega_3} + \frac{\omega_3 Cr_{bb'}}{\omega_a}\right) \tag{6.47}$$

If it turns out that the parameter δ is greater than unity, then the quadratic term in the denominator of Equation 6.37 can be factorised further into the product of two linear factors. The resulting pole-zero pattern of the current gain function I_2/I_1 of the stage will be of the form shown in Fig. 6.19 (a), and the gain-frequency characteristic can be approximated by five straight line segments as in Fig. 6.19 (b). If, on the other hand, the parameter δ is less than unity, then the current gain function I_2/I_1 will have a pair of complex conjugate poles as shown in the pole-zero pattern of Fig. 6.20 (a); the corresponding gain-frequency characteristic is approximated by

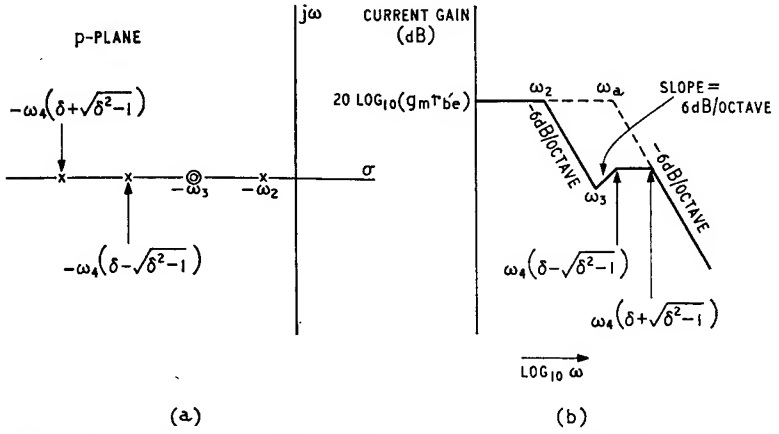

Fig. 6.19. (a) Pole-zero pattern with $\delta > 1$, (b) Corresponding approximation to gain-frequency characteristic

four line segments as in Fig. 6.20 (b). The dashed portions of Figs. 6.19 (b) and 6.20 (b) represent approximations to the gain characteristic of the stage in the absence of the compensating elements R, C and L.

Example

Suitable values for the design parameters ω_2 and ω_3 can be obtained from knowledge of the uncompensated open-loop response of the feedback amplifier and approximation to Bode's ideal loop gain

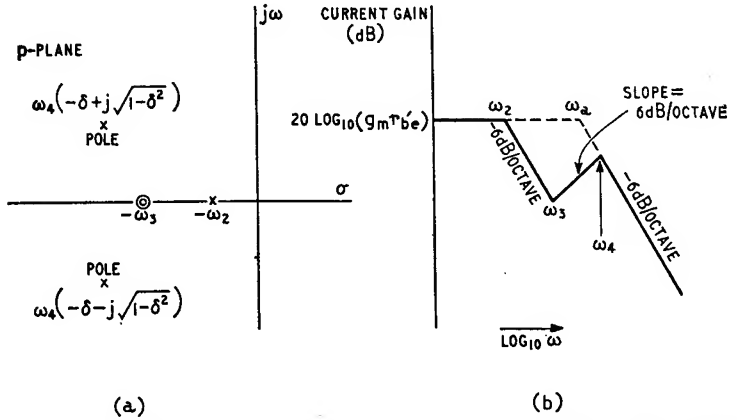

Fig. 6.20. (a) Pole-zero pattern with $\delta < 1$, (b) Corresponding approximation to gain-frequency characteristic

characteristic. As an illustration let us consider a transistor feedback amplifier involving a cascade of three common emitter stages with a purely resistive feedback network and an *RCL*-interstage shaping network connected across the input port of the output stage. Then the current gain functions of the first two stages will each have a pole at $p = -\omega_a$ while the current gain function of the output stage will be as given by Equation 6.37. We therefore deduce that the open-loop gain function of the feedback amplifier is equal to

$$T(p) = \frac{T(0)\left(1+\frac{p}{\omega_3}\right)^2}{\left(1+\frac{p}{\omega_a}\right)^2\left(1+\frac{p}{\omega_2}\right)\left(1+2\delta\frac{p}{\omega_4}+\frac{p^2}{\omega_4^2}\right)} \qquad (6.48)$$

where $T(0)$ is the low frequency value of $T(p)$. Let us next suppose that the amplifier is to satisfy the following specifications:

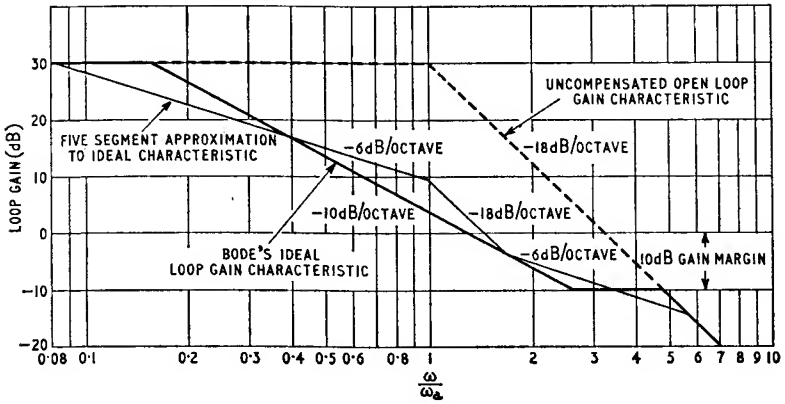

Fig. 6.21. Construction of Bode's ideal loop gain characteristic

Low frequency open-loop gain = 20 $\log_{10} T(0)$ = 30 dB (that is $T(0) = 31{\cdot}6$).

phase margin $\geqslant 30°$
gain margin $\geqslant$ 10 dB

and that the transistor has the following hybrid-π parameters

$$r_{bb'} = 40\ \Omega$$
$$r_{b'e} = 1{,}140\ \Omega$$
$$g_m = 40\ \text{mA/V}$$
$$C_{b'e} = 700\ \text{pF}$$
$$C_{b'c} = 10\ \text{pF}$$

The load resistance $R_L = 1\ \text{k}\Omega$

To determine the elements of the interstage shaping network, we first note that the uncompensated open-loop gain function of the amplifier has a triple pole at $p = -\omega_a$. Hence the uncompensated and Bode's ideal loop gain characteristics will be as shown in Fig. 6.21. After a few trials we find that this ideal characteristic can be approximated by the open-loop gain function of Equation 6.48 having

$$\omega_2 = 0{\cdot}0834\ \omega_a$$
$$\omega_3 = 1{\cdot}67\ \omega_a$$
$$\omega_4 = 5{\cdot}78\ \omega_a$$

Here we see that the inequality $\omega_4 \gg \omega_2$, which we assumed earlier, is perfectly justified.

Next, Equations 6.32 to 6.34 give

$$C_{in}' = 700 + 10 \times 40 \times 10^{-3} \times 10^{3}$$
$$= 1{,}100 \text{ pF}$$
$$\omega_a = \frac{10^{12}}{1{,}100 \times 1{,}140} = 0{\cdot}8 \times 10^{6} \text{ rad/sec}$$
$$r_i = 40 + 1{,}140 = 1{,}180\ \Omega$$

Then from Equations 6.43 to 6.45 we find

$$C = \frac{10^{-6}}{1{,}180 \times 0{\cdot}8}\left(\frac{1}{0{\cdot}0834} - 1 - \frac{2}{1{\cdot}67}\right)$$
$$= 10{,}400 \times 10^{-12} \text{ F} = 10{,}400 \text{ pF}$$
$$L = \frac{1}{(1{\cdot}67 \times 0{\cdot}8)^2 \times 10{,}400}$$
$$= 54 \times 10^{-6} \text{ H} = 54\ \mu\text{H}$$
$$R = \frac{2}{1{\cdot}67 \times 0{\cdot}8 \times 10{,}400 \times 10^{-6}}$$
$$= 144\ \Omega$$

Equation 6.47 gives the parameter δ to be

$$\delta = \frac{\sqrt{(0{\cdot}0834)}}{2}\left(2 + \frac{1}{1{\cdot}67} + 1{\cdot}67 \times 0{\cdot}8 \times 10{,}400 \times 10^{-6} \times 40\right)$$
$$= 0{\cdot}455$$

Hence with δ less than unity, it follows that the open-loop gain function will have a pair of complex conjugate poles at

$$p = -\delta\omega_4 \pm j\omega_4\sqrt{(1 - \delta^2)}$$
$$= -0{\cdot}455 \times 5{\cdot}78\ \omega_a \pm j5{\cdot}78\ \omega_a\sqrt{(1 - 0{\cdot}455^2)}$$
$$= -2{\cdot}64\ \omega_a \pm j5{\cdot}15\ \omega_a$$

Compensated open-loop response

To evaluate the gain and phase margins actually realised by the compensated amplifier with $T(0) = 31{\cdot}6$, we replace p with $j\omega$ in Equation 6.48, thus

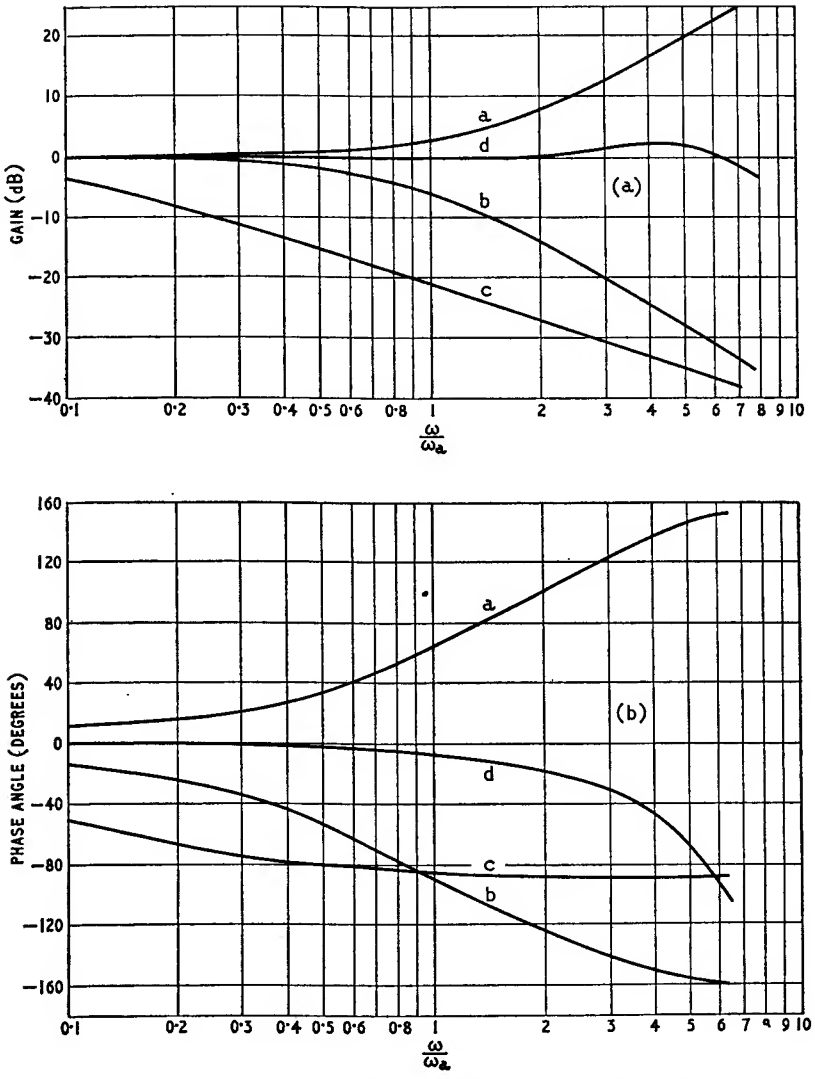

Fig. 6.22. (a) Gain-frequency characteristics, (b) Phase angle-frequency characteristics

$$T(j\omega) = \frac{31{\cdot}6\left(1 + \frac{j\omega}{\omega_3}\right)^2}{\left(1 + \frac{j\omega}{\omega_a}\right)^2 \left(1 + \frac{j\omega}{\omega_2}\right)\left(1 + j2\delta\frac{\omega}{\omega_4} - \frac{\omega^2}{\omega_4{}^2}\right)} \qquad (6.49)$$

The zero factor $(1 + j\omega/\omega_3)^2$ is of order 2 and has a corner frequency at $\omega = \omega_3 = 1{\cdot}67\ \omega_a$; it leads to the gain and phase curves *a* of Fig. 6.22. The second order pole factor $(1 + j\omega/\omega_a)^2$ has a cut off frequency at $\omega = \omega_a$ and, therefore, contributes the curves *b* of Fig. 6.22. The simple pole factor $(1 + j\omega/\omega_2)$ has a corner frequency at $\omega = \omega_2 = 0{\cdot}0834\ \omega_a$ and contributes the gain and phase curves *c*. The quadratic pole factor, for which $\delta = 0{\cdot}455$ and $\omega_4 = 5{\cdot}78\ \omega_a$,

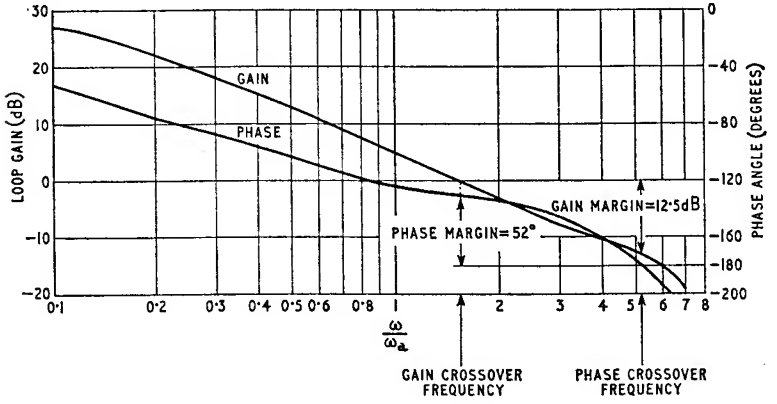

Fig. 6.23. Compensated open-loop response

leads to the gain and phase curves *d*. Adding the gain and phase curves *a*, *b*, *c* and *d* of Fig. 6.22 to the constant gain of 30 dB and constant phase angle of 0°, respectively, contributed by the scale factor $T(0) = 31{\cdot}6$ we obtain the total gain and phase characteristics of Fig. 6.23 for the open-loop gain function of Equation 6.49. We thus find that the gain and phase margins of the compensated amplifier are equal to 12·5 dB and 52°, both of which satisfy the design requirements.

Root locus diagram of compensated amplifier

Let us next construct the root locus diagram for the purpose of evaluating the resulting closed-loop response. Substituting in Equation 6.48 the values obtained for ω_2, ω_3, ω_4 and δ, we see that the open-loop gain function has a double zero at $p = -\omega_3 = -1{\cdot}67\ \omega_a$

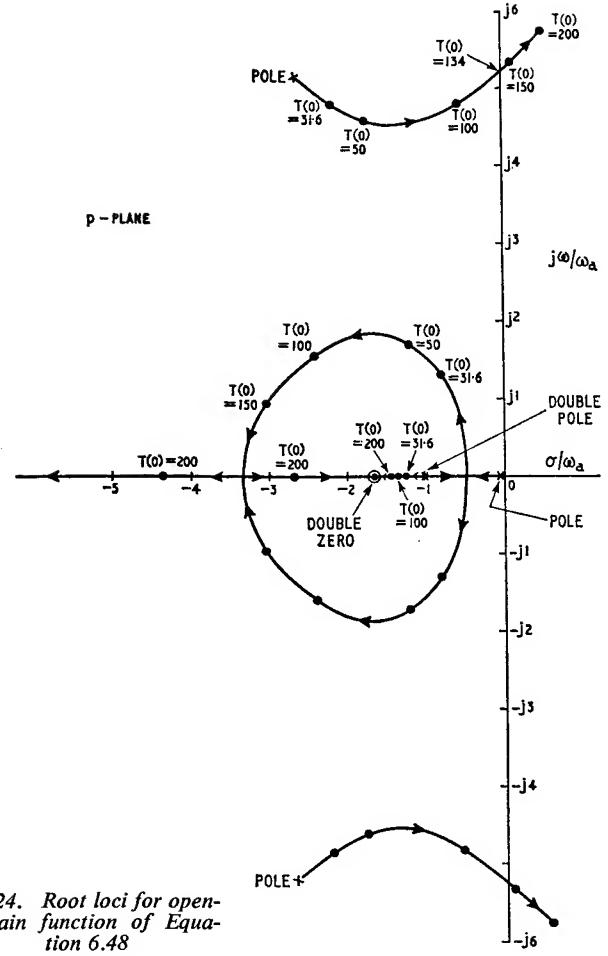

Fig. 6.24. Root loci for open-loop gain function of Equation 6.48

a simple pole at $p = -\omega_2 = -0{\cdot}0834\ \omega_a$, a double pole at $p = -\omega_a$ and a pair of complex conjugate poles at $p = -2{\cdot}64\ \omega_a \pm j5{\cdot}15\ \omega_a$. Then as $T(0)$ is increased in magnitude, starting from the value of zero, we obtain the root locus diagram of Fig. 6.23. At the design value of $T(0) = 31{\cdot}6$ we find that the compensated amplifier has the following five closed-loop poles.

$$p = -1{\cdot}31\ \omega_a$$
$$p = -0{\cdot}84\ \omega_a \pm j\ 1{\cdot}33\ \omega_a$$
$$p = -2{\cdot}17\ \omega_a \pm j\ 4{\cdot}81\ \omega_a$$

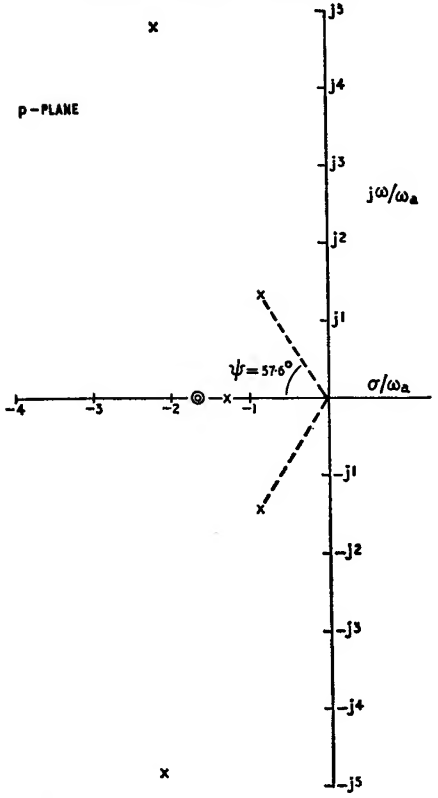

Fig. 6.25. Closed loop pole-zero pattern

Further with the feedback network assumed purely resistive, we deduce from Equations 6.26 and 6.48 that the closed-loop gain function $K'(p)$ has a double zero at $p = -\omega_3 = -1{\cdot}67\ \omega_a$. Therefore, the complete pole-zero pattern of $K'(p)$ is, for $T(0) = 31{\cdot}6$, as shown in Fig. 6.25. In a manner similar to the example of Section 6.2.1, the pole-zero pattern of Fig. 6.25 can be used for determining the closed-loop transient and frequency response of the amplifier. These evaluations, together with the evaluation of the co-ordinates of the dominant closed-loop poles from the open-loop frequency response of Fig. 6.23 are left as exercises for the reader.

REFERENCES

1. ALMOND, J., and BOOTHROYD, A. R., 'Broadband Transistor Feedback Amplifiers', *Proc. I.E.E.*, **103B**, 93 (1956).

2. BLECHER, F. H. 'Design Principles for Single-Loop Transistor Feedback Amplifiers', *I.R.E. Trans.*, **CT-4**, 145 (1957).
3. BODE, H. W., *Network Analysis and Feedback Amplifier Design*, Van Nostrand, New York (1945).
4. COTE, A. J., and OAKES, J. B., *Linear-Vacuum Tube and Transistor Circuits*, McGraw-Hill (1961).
5. GHAUSI, M. S., and PEDERSON, D. O., 'A New Design Approach for Feedback Amplifiers', *I.R.E. Trans.* **CT-8**, 274 (1961).
6. HAKIM, S. S., 'Synthesis of Correcting Network for a Feedback Amplifier', *Proc. I.E.E.*, **111**, 27 (1964).
7. HAKIM, S. S., 'Feedback Amplifier Stabilisation', *Industrial Electronics* **1**, 273 (1963).
8. MULLIGAN, J. H., 'Transient Response and the Stabilisation of Feedback Amplifiers', *Trans. A.I.E.E.*, Part II, **78**, 495 (1960).
9. BRIERLEY, H. G., and HAKIM, S. S., 'Transistor Feedback Amplifier Design', *Proc. I.E.E.*, **112**, 1825 (1965)

CHAPTER 7

The Impedance Concept

In the previous three chapters we have studied the stability performance of a feedback circuit in terms of its closed-loop transient response and open-loop frequency response. In this chapter we shall study the stability problem by considering the behaviour of the impedance or admittance measured looking into either the input or output port of the circuit under closed-loop conditions. Such an approach is particularly useful when it is required to determine the terminating conditions under which the circuit is likely to become unstable, if at all. This study is, however, by no means restricted to feedback circuits; it can be applied, for example, to a linear circuit containing a negative resistance element.

We shall first examine the significance of the location of the poles and zeros of driving-point impedance and admittance functions in the p-plane. Then, we shall apply Nyquist's criterion to determine the relationship between stability and the behaviour of these functions in the real frequency domain. In this way, we shall make use of some of the ideas and concepts developed in Chapters 4 and 5. Finally, we shall illustrate the driving-point impedance aspect of the stability problem by considering a number of different examples.

7.1 Open-circuit and short-circuit stability

Consider Fig. 7.1 where a current source $i_n(t)$ is connected across the port n,n' of a linear circuit consisting of passive elements and controlled sources only. Then, if $v_n(t)$ is the voltage developed across this port, we have

$$V_n(p) = Z_n(p)I_n(p) \tag{7.1}$$

where $Z_n(p)$ is the driving-point impedance function at the port n,n' and $V_n(p)$ and $I_n(p)$ are the Laplace transforms of $v_n(t)$ and $i_n(t)$, respectively. Thus, $V_n(p)$ is the response transform and $I_n(p)$ is the excitation transform.

In general, the impedance function $Z_n(p)$ can be expressed as follows

$$Z_n(p) = H\cdot\frac{(p-z_1)(p-z_2)\ldots(p-z_q)}{(p-p_1)(p-p_2)\ldots(p-p_r)} \tag{7.2}$$

where H is a scale factor, and $z_1, z_2, \ldots z_q$ are the zeros of $Z_n(p)$ and $p_1, p_2 \ldots p_r$ are its poles. For a driving-point impedance function, any of the following three cases is possible

$$\left.\begin{array}{l} q = r-1 \\ \text{or} \\ q = r \\ \text{or} \\ q = r+1 \end{array}\right\} \tag{7.3}$$

Combining Equations 7.1 and 7.2 gives

$$V_n(p) = H\cdot\frac{(p-z_1)(p-z_2)\ldots(p-z_q)}{(p-p_1)(p-p_2)\ldots(p-p_r)}I_n(p) \tag{7.4}$$

If the driving function $i_n(t)$ is a unit impulse, its Laplace transform $I_n(p)$ is equal to unity, and Equation 7.4 simplifies to

$$V_n(p) = H\cdot\frac{(p-z_1)(p-z_2)\ldots(p-z_q)}{(p-p_1)(p-p_2)\ldots(p-p_r)} \tag{7.5}$$

Suppose that $q = r-1$. Then, we can expand the rational function of Equation 7.5 into partial fractions as follows

$$V_n(p) = \frac{A_1}{p-p_1} + \frac{A_2}{p-p_2} + \ldots\frac{A_r}{p-p_r} \tag{7.6}$$

where $A_1, A_2, \ldots A_r$ are the residues of the poles at $p_1, p_2, \ldots, p_r$. Using pair No. 5 of the Laplace transform pairs Table 2.1, we find from Equation 7.6 that the response function $v_n(t)$ is given by

$$v_n(t) = A_1 e^{p_1 t} + A_2 e^{p_2 t} + \ldots + A_r e^{p_r t} \tag{7.7}$$

Therefore, $p_1, p_2, \ldots p_r$ are the *natural transient frequencies* of the circuit arrangement of Fig. 7.1. Now an ideal current source has

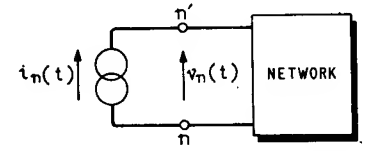

Fig. 7.1. One-port network with terminating current source

infinite shunt impedance, and so as far as the natural transient frequencies of the circuit of Fig. 7.1 are concerned, the current source $i_n(t)$ presents an open-circuit to the port n,n'. We thus see that the poles of the driving-point impedance function $Z_n(p)$ are the *open-circuit natural frequencies* of the system.

If the poles $p_1, p_2, \ldots p_r$ of $Z_n(p)$ are all located in the left half of the p-plane, then the resulting response function $v_n(t)$ of Fig. 7.1 will

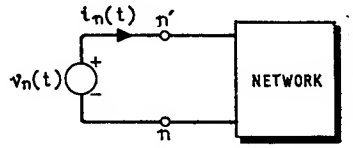

Fig. 7.2. One-port network with terminating voltage source

ultimately decay to zero, and the system is said to be *open-circuit stable*. If, however, any of the poles of $Z_n(p)$ are located in the right half of the p-plane, then the response function $v_n(t)$ will increase with time and the system is said to be *open-circuit unstable*.

Consider next the circuit arrangement of Fig. 7.2 where the driving function is a voltage source $v_n(t)$ connected across the port n,n'. If $i_n(t)$ is the resulting current response function, we find that

$$I_n(p) = Y_n(p)V_n(p) \tag{7.8}$$

where $Y_n(p)$ is the *driving-point admittance function* at the port n,n'. Now $Y_n(p)$ is equal to the reciprocal of $Z_n(p)$; hence

$$Y_n(p) = \frac{1}{H}\cdot\frac{(p-p_1)(p-p_2)\ldots(p-p_r)}{(p-z_1)(p-z_2)\ldots(p-z_q)} \tag{7.9}$$

Thus, the poles of $Y_n(p)$ are the same as the zeros of $Z_n(p)$ and vice versa. Assuming that the applied voltage $v_n(t)$ is a unit impulse, it follows that its Laplace transform $V_n(p)$ is unity.

Then, from Equations 7.8 and 7.9 we obtain

$$I_n(p) = \frac{1}{H}\cdot\frac{(p-p_1)(p-p_2)\ldots(p-p_r)}{(p-z_1)(p-z_2)\ldots(p-z_q)} \tag{7.10}$$

If, as before, we have $q = r - 1$ (that is, $r = q + 1$), the rational function of Equation 7.10 can be expanded into partial fractions as follows

$$I_n(p) = B_\infty p + B_0 + \frac{B_1}{p-z_1} + \frac{B_2}{p-z_2} + \ldots + \frac{B_q}{p-z_q} \tag{7.11}$$

From this, we find that the response function $i_n(t)$ is

$$i_n(t) = B_\infty u_{+1}(t) + B_0 u_0(t) + B_1 e^{z_1 t} + \ldots + B_q e^{z_q t} \tag{7.12}$$

where $u_0(t)$ is a unit impulse and $u_{+1}(t)$ is the first derivative of a unit impulse. At infinite time, both the unit impulse and its derivatives are reduced to zero. Therefore, the stability or instability of the circuit arrangement of Fig. 7.2 is completely determined by the location of its natural transient frequencies $z_1, z_2, \ldots z_q$ in the p-plane. Since an ideal voltage source has zero series impedance, it follows that as far as the natural transient frequencies of Fig. 7.2 are concerned, the voltage source $v_n(t)$ presents a short-circuit to the port n,n'. Hence, the poles of the admittance function $Y_n(p)$, that is, the zeros of the impedance function $Z_n(p)$ are the *short-circuit natural frequencies* of the system.

If all the zeros of $Z_n(p)$ are located in the left half of the p-plane, the resulting current response function $i_n(t)$ of Fig. 7.2 will ultimately reduce to zero and the system is said to be *short-circuit stable*. If, on the other hand, any of the zeros of $Z_n(p)$ is in the right half of the p-plane, then the response function $i_n(t)$ increases with time, and the system is said to be *short-circuit unstable*.

A system which is open-circuit as well as short-circuit stable, and which remains stable when any external impedance is connected across the port n,n' is said to be *absolutely stable* with respect to the port n, n'. But if a system becomes unstable under certain terminating conditions, it is said to be *potentially unstable*. An example of potential instability is a system that is open-circuit stable, but short-circuit unstable.

7.1.1 OPEN-CIRCUIT AND SHORT-CIRCUIT STABILITY CONSIDERATIONS OF SINGLE-LOOP FEEDBACK AMPLIFIERS

Consider the series-series feedback circuit of Fig. 7.3. Normally, the internal amplifier component is stable on its own under all possible terminating conditions. The feedback network component is usually passive with the result that it is always stable too. There-

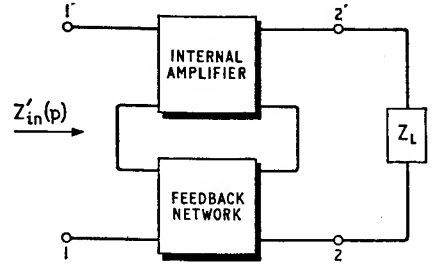

Fig. 7.3. Series-series feedback circuit

fore, if the input port 1,1′ of the complete feedback amplifier is open-circuited, then the flow of signal round the feedback loop is interrupted so that the feedback circuit of Fig. 7.3 is inherently open-circuit stable at its input port. For the same reason, the condition of open-circuit stability applies at the output port 2,2′.

Next, in the case of the shunt-shunt feedback circuit of Fig. 7.4, we see that if either the input port 1,1′ or output port 2,2′ is short-circuited, the open-loop gain of the resulting circuit is reduced to

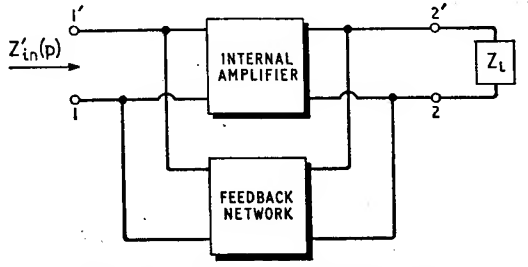

Fig. 7.4. Shunt-shunt feedback circuit

zero. Hence the feedback amplifier of Fig. 7.4 is short-circuit stable at both of its input and output ports.

The above results can be generalised as follows. A single-loop feedback amplifier is open-circuit stable at its input port if the internal amplifier and feedback network are connected in series at this port; it is short-circuit stable if they are connected in parallell Similar remarks apply to the behaviour at the output port.

7.2 Nyquist's Criterion applied to driving-point impedance and admittance functions

Suppose that a particular feedback amplifier is known to be open-circuit stable at its input port. Then, the input impedance function $Z_{in}'(p)$ with feedback will have no poles in the right half of the p-plane. In the sinusoidal steady state condition, we have p replaced with $j\omega$ resulting in the impedance function $Z_{in}'(j\omega)$. If we vary ω between the limits $-\infty$ to $+\infty$ and so plot a Nyquist diagram for $Z_{in}'(j\omega)$, it follows from Nyquist's Criterion that the number of times the plot encircles the origin of the $Z_{in}'(j\omega)$-plane in the clockwise direction is equal to the number of zeros of $Z_{in}'(p)$ in the right half of the p-plane. Therefore, the feedback amplifier will also be short-circuit stable at its input port if the Nyquist plot of $Z_{in}'(j\omega)$ does not encircle the origin; otherwise, it is short-circuit unstable.

When in Section 5.2 we applied the encirclement theorem to the return difference $F(p)$, we used the contour C of Fig. 7.5 which consists

of the $j\omega$-axis and a large semicircle in the right half of the p-plane. Because $F(p)$ approached unity at infinite frequency, we dismissed the semicircular part of the contour C when its radius R was allowed to become infinitely large. The same simplification applies when considering $Z_{in}'(p)$ provided that it approaches a constant value at infinite frequency. This occurs when $Z_{in}'(p)$ has an equal number of poles and zeros, that is, $q = r$ in Equation 7.2. In this case, $Z_{in}'(p)$ becomes purely resistive at infinite frequency, as shown in the Nyquist diagram of Fig. 7.6 (a).

However, in Section 7.1 it was pointed out that it is possible to have $q = r - 1$ or $q = r + 1$. In the former case, we find that at high frequencies $Z_{in}'(p)$ approaches the purely capacitive form $1/(pC_\infty)$. Therefore, the Nyquist diagram must be modified to include a very small semicircle round the origin of the $Z_{in}'(j\omega)$-plane,

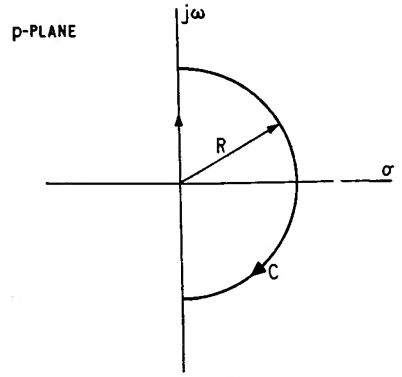

Fig. 7.5. Contour C

as illustrated in Fig. 7.6 (b), so as to represent the values assumed by the function $Z_{in}'(p)$ along the very large semicircular part of the contour C of Fig. 7.5.

When $q = r + 1$ we find that $Z_{in}'(p)$ approaches the purely inductive form pL_∞ at high frequencies. In this case, the Nyquist diagram must include a very large semicircle, as shown in Fig. 7.6 (c), to represent the values of $Z_{in}'(p)$ along the very large semicircular part of the contour C.

Each of the three Nyquist diagrams of Fig. 7.6 encircles the origin twice, hence, in each case $Z_{in}'(p)$ has two zeros in the right half of the p-plane and so corresponds to a feedback amplifier that is short-circuit unstable at its input port.

The complete Nyquist plot of $Z_{in}'(j\omega)$ is required only when it is necessary to know the number of zeros of $Z_{in}'(p)$ located in the right half of the p-plane. If the problem is to determine whether or not the amplifier is short-circuit stable, then the Nyquist plot of

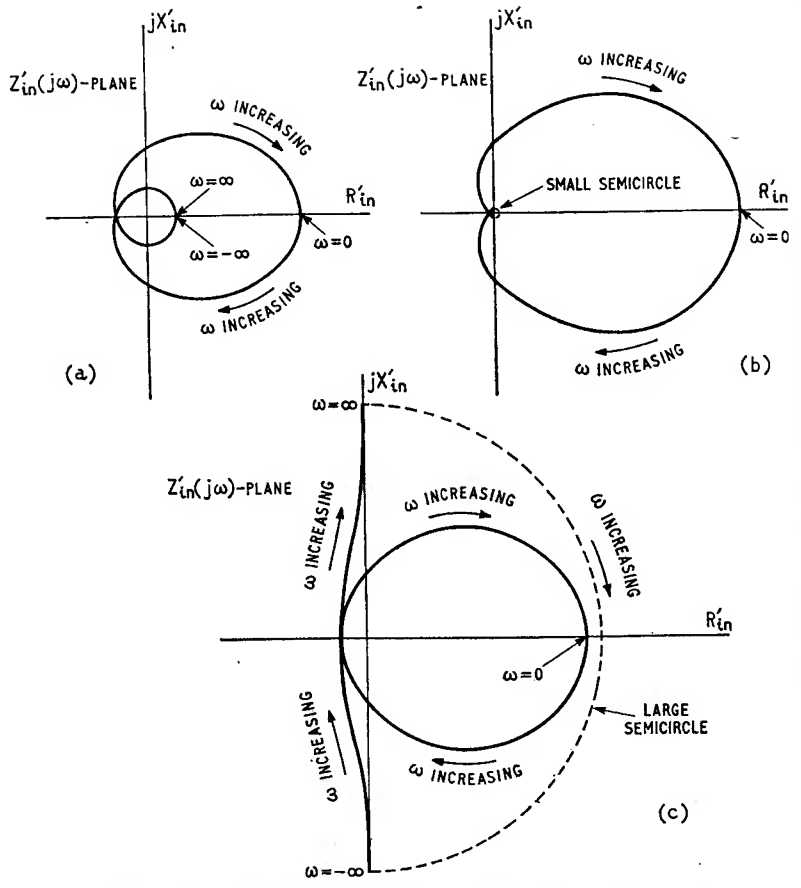

Fig. 7.6. Nyquist diagramis for $Z_{in}'(j\omega)$: (a) $q = r$, (b) $q = r - 1$, (c) $q = r + 1$ (Note that $Z_{in}'(j\omega) = R_{in}' + jX_{in}'$)

$Z_{in}'(j\omega)$ for the frequency range $\omega = 0$ to $\omega = \infty$ is quite adequate. Thus, if the origin of the $Z_{in}'(j\omega)$-plane is not enclosed by the plot of $Z_{in}'(j\omega)$ when going from zero to infinite frequency as in Fig. 7.7 (a), the amplifier is short-circuit stable. On the other hand, it is short-circuit unstable if the Nyquist diagram encloses the origin of the $Z_{in}'(j\omega)$-plane as in Fig. 7.7 (b). In this latter diagram, we see that in the frequency range $\omega_2 > \omega > \omega_1$ the input impedance $Z_{in}'(j\omega)$ has a negative resistive component. Suppose that an external impedance $Z_S = R_S + jX_S$ is connected across the input port of the feedback amplifier having the plot of 7.7 (b). Then, the

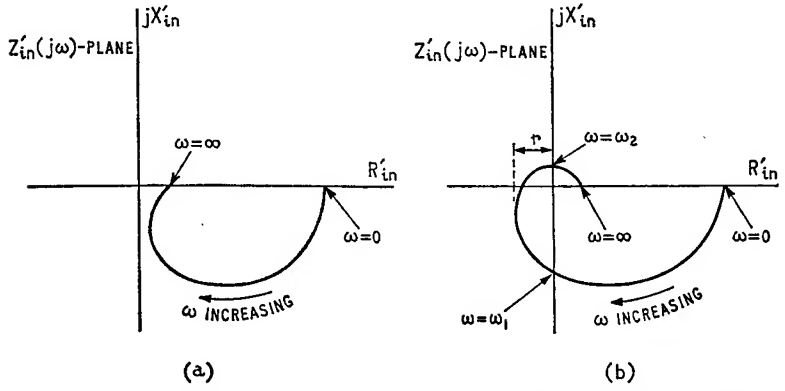

Fig. 7.7. (a) Nyquist diagram for short-circuit stable system, (b) Nyquist diagram for short-circuit unstable system

total impedance of the input mesh is equal to $Z_{in}' + Z_S$. The resistive component of this total impedance is positive at all frequencies from zero to infinity, thereby resulting in a stable amplifier independently of X_S, provided we have $R_S > r$, where $-r$ is the most negative value of R_{in}' as shown defined in Fig. 7.7 (b). But if $R_S < r$, the amplifier remains potentially unstable.

Let us next consider the case of a feedback amplifier which is short-circuit stable at its input port. Then, the input admittance $Y_{in}'(p)$ with feedback has no poles in the right half of the p-plane. If we draw a Nyquist plot of $Y_{in}'(j\omega)$ for ω varying from $-\infty$ to $+\infty$, the number of times the plot encircles the origin of the $Y_{in}'(j\omega)$-plane will be equal to the number of zeros of $Y_{in}'(p)$ in the right half plane. The amplifier will be also open-circuit stable at the input port provided that the Nyquist diagram of $Y_{in}'(j\omega)$ does not encircle the origin; otherwise, it is open-circuit unstable. Here again we must give special consideration to the two cases of $q = r - 1$ and $q = r + 1$. In the first case, $Y_{in}'(p)$ approaches pC_∞ at infinite frequency and so the Nyquist diagram of $Y_{in}'(j\omega)$ must include a very

large semicircle in a similar way to Fig. 7.6 (c). On the other hand when $q = r + 1$ we find that $Y_{in}'(p)$ approaches $1/(pL_\infty)$ at infinite frequency; hence, the Nyquist diagram of $Y_{in}'(j\omega)$ must be modified to include a very small semicircle round the origin of the $Y_{in}'(j\omega)$-plane in a manner similar to Fig. 7.6 (b).

Unless it is necessary to know how many of the zeros of $Y_{in}'(p)$ are located in the right half of the p-plane, we do not require the complete Nyquist diagram of $Y_{in}'(j\omega)$. Thus, the amplifier is open-circuit stable if the origin of the $Y_{in}'(j\omega)$-plane is not enclosed by the plot of $Y_{in}'(j\omega)$ obtained by varying ω from zero to infinity, as in Fig. 7.8 (a). It is open-circuit unstable if the plot of $Y_{in}'(j\omega)$ encloses the origin of the $Y_{in}'(j\omega)$-plane as in Fig. 7.8 (b),

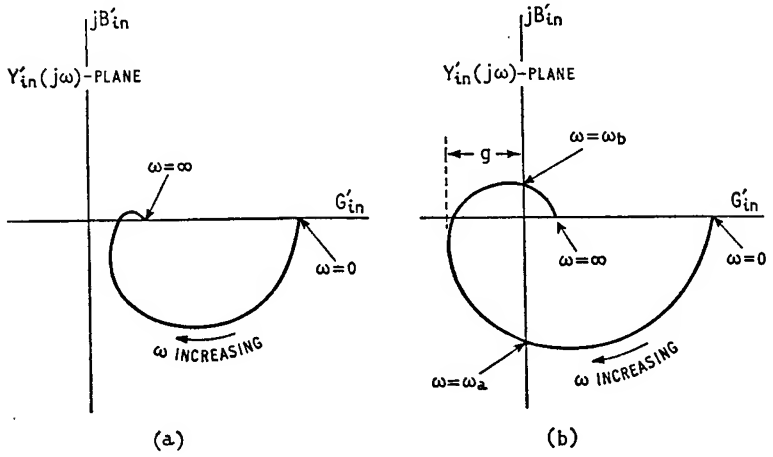

Fig. 7.8. (a) Nyquist diagram for open-circuit stable system, (b) Nyquist diagram for open-circuit unstable system (Note than $Y_{in}'(j\omega) = G_{in}' + jB_{in}'$)

where we see that $Y_{in}'(j\omega)$ has a negative conductive component in the frequency range $\omega_b > \omega > \omega_a$. Suppose that an external admittance $Y_S = G_S + jB_S$ is connected across the input port of the amplifier having the plot of Fig. 7.8 (b) resulting in a total admittance of $Y_{in}' + Y_S$ at the input node. If $G_S > g$ where g is indicated in Fig. 7.8 (b), then the conductive component of the total admittance is positive at all frequencies and the amplifier is stable independently of B_S. If, $G_S < g$ the amplifier remains potentially unstable.

We can summarise the above results as follows. If a single-loop feedback amplifier is open-circuit stable at its input port, then the stability performance under other terminating conditions across this port can be studied by considering the Nyquist diagram for $Z_{in}'(j\omega)$. If, on the other hand, the amplifier is short-circuit stable at the input

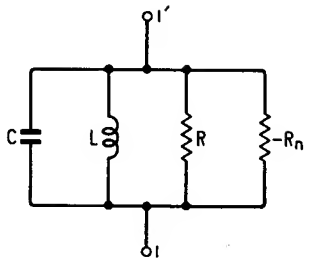

Fig. 7.9. Negative resistance oscillator

port, the effect of other terminating conditions, at this port, on the stability performance can be studied by considering the Nyquist diagram for $Y_{in}'(j\omega)$. Again, similar remarks apply to the behaviour of the feedback amplifier at its output port.

7.3 Examples

7.3.1 NEGATIVE RESISTANCE OSCILLATOR

For this example consider Fig. 7.9 showing the equivalent circuit of a parallel tuned *negative resistance oscillator*. The shunt resistance R represents the combined effect of the load resistance and the losses associated with the tuning inductor. The element $-R_n$ represents

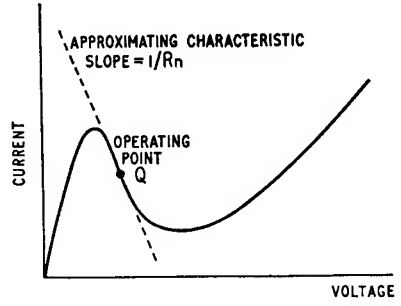

Fig. 7.10. Characteristic curve of a tunnel diode

the incremental resistance of a negative resistance device, e.g. a tunnel diode having the static characteristic curve of Fig. 7.10 and operated at the point Q.

The admittance $Y_1(p)$ measured between the terminals 1,1' is given by

$$Y_1(p) = pC + (G - G_n) + \frac{1}{pL}$$

$$= \frac{C}{p}\left[p^2 + \frac{p}{C}(G - G_n) + \frac{1}{LC}\right] \qquad (7.13)$$

where $G = 1/R$ and $G_n = 1/R_n$. The admittance $Y_1(p)$ has a pole at $p = 0$, and two zeros at

$$p = \frac{-G + G_n}{2C} \pm \sqrt{\left[\left(\frac{G - G_n}{2C}\right)^2 - \frac{1}{LC}\right]} \qquad (7.14)$$

As the conductance G is varied between the limiting values of infinity and zero, we find that the two zeros of $Y_1(p)$ move inside the

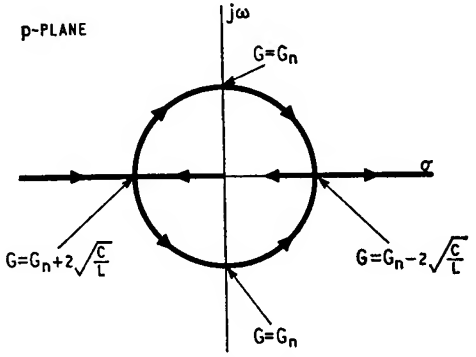

Fig. 7.11. Migration of the zeros of $Y_1(p)$ inside the p-plane with varying G

p-plane in the manner shown in Fig. 7.11. For values of G lying in the range

$$\infty > G > G_n + 2\sqrt{[C/L]}$$

the two zeros of $Y_1(p)$ are located on the negative σ-axis of the p-plane. When $G = G_n + 2\sqrt{[C/L]}$, the two zeros are coincident and located at

$$p = \frac{-G + G_n}{2C} = -\frac{1}{\sqrt{[LC]}}$$

When $G < G_n + 2\sqrt{[C/L]}$, the two zeros separate from the negative σ-axis and move along the arcs of a circle of centre at the origin and of radius $1/\sqrt{[LC]}$.

When $G = G_n$ the two zeros lie on the jω-axis at $p = \pm j/\sqrt{[LC]}$. A further reduction in the value of G permits the negative conductance element to predominate, and causes the two zeros to move into the right half of the p-plane. The two zeros meet again when

$G = G_n - 2\sqrt{[C/L]}$; hereafter they separate along the positive σ-axis. In Fig. 7.11 we are assuming that $G_n > 2\sqrt{[C/L]}$.

We therefore deduce that the two zeros of $Y_1(p)$ are located in the left half of the p-plane, and the circuit is stable, when $G > G_n$, that is $R < R_n$. On the other hand when $G < G_n$, that is $R > R_n$ the two zeros are located in the right half of the p-plane, and the circuit is unstable and its output voltage signal is exponentially increasing in amplitude. In practice the amplitude of oscillations becomes limited by the nonlinearities associated with the negative resistance device.

7.3.2 INSTABILITY IN ACTIVE TWO-PORT NETWORKS

For the second example consider Fig. 7.12 which shows an active two-port network terminated at its output port with a load of admittance Y_L and driven, at its input port, from a current source I_S

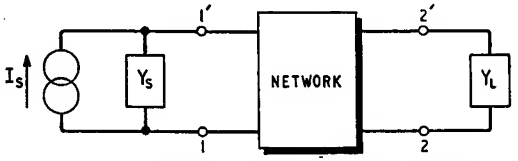

Fig. 7.12. Double-terminated two-port network

of shunt admittance Y_S. The input admittance $Y_{in}(j\omega)$ of such a stage is given in terms of the y-parameters as follows (see Table 2.4)

$$Y_{in}(j\omega) = y_{11} - \frac{y_{12}y_{21}}{y_{22} + Y_L} \qquad (7.15)$$

where all the y-parameters and Y_L are functions of jω. The finite value of y_{12} is responsible for the internal feedback existing in the two-port network. Suppose that

$$\left.\begin{aligned} y_{11} &= G_{11} + jB_{11} \\ y_{12}y_{21} &= M + jN \\ y_{22} &= G_{22} + jB_{22} \\ Y_L &= G_L + jB_L \\ Y_S &= G_S + jB_S \end{aligned}\right\} \qquad (7.16)$$

Then, we can re-write Equation 7.15 in the following form

$$Y_{in}(j\omega) = G_{11} + jB_{11} - \frac{M + jN}{(G_{22} + G_L) + j(B_{22} + B_L)}$$

$$Y_{in}(j\omega) = G_{11} + jB_{11} - \frac{(M + jN)[(G_{22} + G_L) - j(B_{22} + B_L)]}{(G_{22} + G_L)^2 + (B_{22} + B_L)^2} \tag{7.17}$$

Let G_{in} be the conductive part of $Y_{in}(j\omega)$ and B_{in} be its susceptive part. Then from Equation 7.17 we get

$$G_{in} = G_{11} - \frac{M(G_{22} + G_L) + N(B_{22} + B_L)}{(G_{22} + G_L)^2 + (B_{22} + B_L)^2} \tag{7.18}$$

$$B_{in} = B_{11} - \frac{N(G_{22} + G_L) - M(B_{22} + B_L)}{(G_{22} + G_L)^2 + (B_{22} + B_L)^2} \tag{7.19}$$

To find the maximum and minimum values of G_{in}, we set $(dG_{in}/dB_L) = 0$, which, together with Equation 7.18, leads to the following condition

$$\left(\frac{B_{22} + B_L}{G_{22} + G_L}\right)^2 + \frac{2M}{N}\left(\frac{B_{22} + B_L}{G_{22} + G_L}\right) - 1 = 0 \tag{7.20}$$

This is a quadratic equation in the term $(B_{22} + B_L)/(G_{22} + G_L)$ and has the following two roots

$$\frac{B_{22} + B_L}{G_{22} + G_L} = -\frac{M}{N} \pm \sqrt{\left[\frac{M^2}{N^2} + 1\right]} \tag{7.21}$$

One of these two roots is positive while the other is negative. The positive root gives the minimum value of G_{in}, and the negative one gives the maximum value. From the stability point of view, the former solution is of more direct interest because then there is a likelihood of G_{in} having negative value. Using this solution for $(B_{22} + B_L)/(G_{22} + G_L)$ in Equations 7.18 and 7.19, we see that the minimum value of G_{in} and corresponding value of B_{min} are given by

$$G_{min} = G_{11} - \frac{M + \sqrt{[M^2 + N^2]}}{2(G_{22} + G_L)} \tag{7.22}$$

$$B_{min} = B_{11} - \frac{N}{2(G_{22} + G_L)} \tag{7.23}$$

When $G_L = 0$, the conductance G_{min} assumes the value G_0 given by

$$G_0 = G_{11} - \frac{M + \sqrt{[M^2 + N^2]}}{2G_{22}} \tag{7.24}$$

Therefore, the frequencies for which G_0 is negative are the frequencies of potential instability. For the terminated two-port network of

Fig. 7.12 to be absolutely stable, we find that it is necessary to have $G_0 > 0$, that is

$$G_{11} > \frac{M + \sqrt{[M^2 + N^2]}}{2G_{22}}$$

or

$$2G_{11}G_{22} - M > \sqrt{[M^2 + N^2]} \tag{7.25}$$

Using the definitions of Equation 7.16, we see that the condition of Equation 7.25 means the following

$$2\mathscr{R}(y_{11}) \cdot \mathscr{R}(y_{22}) - \mathscr{R}(y_{12}y_{21}) > |y_{12}y_{21}| \tag{7.26}$$

The boundary between potential instability and absolute stability is therefore defined by

$$2\mathscr{R}(y_{11}) \cdot \mathscr{R}(y_{22}) - \mathscr{R}(y_{12}y_{21}) = |y_{12}y_{21}| \tag{7.27}$$

where $\mathscr{R}$ signifies the real part of the expression which follows it.

We thus see that it is possible for an active two-port network, such as a transistor, having tuned source and load impedances to become unstable under certain conditions, without applying any form of external feedback. For a given transistor, say, and a specified value of G_L, we can determine the value of G_S required to ensure stability as follows. The terminated two-port network is stable provided that $G_{in} + G_S$ is positive at all frequencies. Then, from Equation 7.22 we deduce that in order to ensure stability, we must have

$$G_{11} + G_S - \frac{M + \sqrt{[M^2 + N^2]}}{2(G_{22} + G_L)} > 0 \tag{7.28}$$

This inequality can be rearranged to give $S > 1$, where

$$S = \frac{2(G_{11} + G_S)(G_{22} + G_L)}{M + \sqrt{[M^2 + N^2]}} \tag{7.29}$$

The term S is referred to as the *stability factor*. The terminated two-port network is stable if $S > 1$, otherwise it is unstable. It is of interest to note that the stability factor S depends only on the conductive components of Y_S and Y_L and it is independent of their susceptive components. For the special case of $G_S = G_L = 0$, the stability factor assumes the value S_0 which, from Equation 7.29, follows to be

$$S_0 = \frac{2G_{11}G_{22}}{M + \sqrt{[M^2 + N^2]}} \tag{7.30}$$

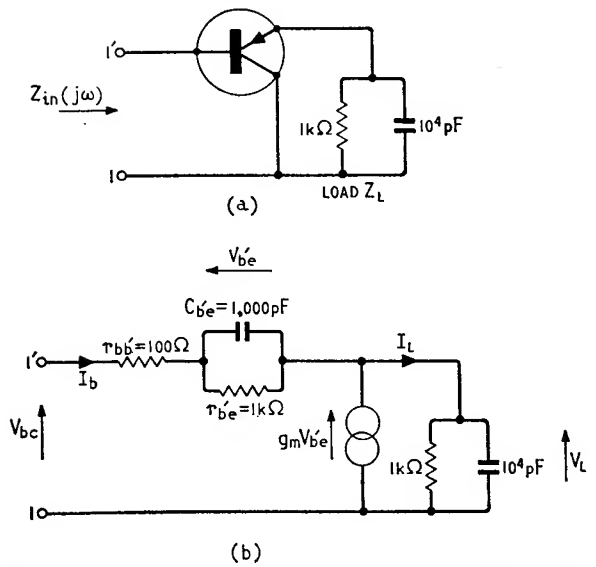

Fig. 7.13. (a) Common collector stage with capacitive load, (b) Equivalent circuit

The condition $S_0 = 1$ corresponds to the boundary between potential instability and absolute stability.

7.3.3 COMMON COLLECTOR STAGE WITH CAPACITIVE LOAD

A transistor having the following hybrid-π parameters: $r_{bb'} = 100\ \Omega$, $r_{b'e} = 1$ kΩ, $C_{b'e} = 1000$ pF, $g_m = 40$ mA/V is operated as a common collector stage as in Fig. 7.13 (a). The load consists of a 1 kΩ resistor connected in parallel with a 10^4 pF capacitor, and the effect of $C_{b'c}$ can be assumed negligible. It is required to investigate the stability of such a stage.

Replacing the transistor with its simplified hybrid-π equivalent circuit, we obtain Fig. 7.13 (b). Assuming that I_b is the input base current, we find that

$$V_{b'e} = \frac{I_b}{(1/r_{b'e}) + j\omega C_{b'e}}$$

$$= \frac{I_b}{10^{-3} + j\omega \times 10^{-3}} = \frac{10^3 I_b}{1 + j\omega}$$

$$I_L = I_b + g_m V_{b'e}$$

$$I_L = I_b + \frac{40 \times 10^{-3} \times 10^3 I_b}{1 + j\omega} = \frac{41 + j\omega}{1 + j\omega} I_b$$

where ω is normalised with respect to 10^6 rad/sec. Therefore, the input voltage V_{bc} is

$$V_{bc} = r_{bb'} I_b + V_{b'e} + Z_L I_L$$

$$= 100 I_b + \frac{10^3 I_b}{1 + j\omega} + \frac{10^3}{1 + j\omega \times 10^3 \times 10^{-2}} \cdot \frac{41 + j\omega}{1 + j\omega} I_b$$

$$= \left[0{\cdot}1 + \frac{1}{1 + j\omega} + \frac{41 + j\omega}{(1 + j10\omega)(1 + j\omega)}\right] 10^3 I_b$$

$$= \frac{(42{\cdot}1 - \omega^2) + j12{\cdot}1\omega}{(1 - 10\omega^2) + j11\omega} \times 10^3 I_b$$

The ratio V_{bc}/I_b gives the input impedance Z_{in}; thus

$$Z_{in} = \frac{(42{\cdot}1 - \omega^2) + j12{\cdot}1\omega}{(1 - 10\omega^2) + j11\omega}\ \text{k}\Omega$$

Rationalising, that is, multiplying the numerator and denominator by the complex conjugate of the denominator, we get

$$Z_{in} = \frac{[(42{\cdot}1 - \omega^2) + j12{\cdot}1\omega][(1 - 10\omega^2) - j11\omega]}{[(1 - 10\omega^2) + j11\omega][(1 - 10\omega^2) - j11\omega]}$$

$$= R_{in} + jX_{in}$$

where

$$R_{in} = \frac{(42{\cdot}1 - \omega^2)(1 - 10\omega^2) + 133\omega^2}{(1 - 10\omega^2)^2 + 121\omega^2}$$

$$= \frac{10\omega^4 - 289\omega^2 + 42{\cdot}1}{100\omega^4 + 101\omega^2 + 1}\ \text{k}\Omega \qquad (7.31)$$

$$X_{in} = \omega \frac{12{\cdot}1(1 - 10\omega^2) - 11(42{\cdot}1 - \omega^2)}{(1 - 10\omega^2)^2 + 121\omega^2}$$

$$= -\omega \frac{110\omega^2 + 451}{100\omega^4 + 101\omega^2 + 1}\ \text{k}\Omega \qquad (7.32)$$

The resistive component becomes negative when

$$10\omega^4 - 289\omega^2 + 42{\cdot}1 < 0$$

Factorising the quadratic in ω^2 on the left hand side gives

$$(\omega^2 - 0{\cdot}147)(\omega^2 - 28{\cdot}6) < 0$$

We therefore see that $R_{in} < 0$ when $28{\cdot}6 > \omega^2 > 0{\cdot}147$, that is, $5{\cdot}35 > \omega > 0{\cdot}384$. From Equation 7.32 we find that when $\omega = 0{\cdot}384$, $X_{in} = -10$ kΩ and when $\omega = 5{\cdot}35$, $X_{in} = -0{\cdot}23$ kΩ.

To find the most negative value of R_{in}, we set $(dR_{in}/d\omega^2) = 0$. Then, differentiating the right hand side of Equation 7.31 with respect to ω^2, putting the result equal to zero and simplifying, we get

$$30\omega^4 - 8{\cdot}4\omega^2 - 4{\cdot}54 = 0$$

This is a quadratic equation in ω^2; its two roots are $\omega^2 = -0{\cdot}275$ and $\omega^2 = 0{\cdot}555$. Only the latter solution leads to a real value for the frequency ω. We, therefore, find from Equation 7.31 that at $\omega = \sqrt{(0{\cdot}555)} = 0{\cdot}745$, $R_{in} = -1{\cdot}31$ kΩ. The corresponding value of X_{in} is obtained from Equation 7.32 to be −4.34 kΩ.

Next, from Equation 7.31 we see that $R_{in} = 42{\cdot}1$ kΩ at $\omega = 0$ and $R_{in} = 0{\cdot}1$ kΩ at $\omega = \infty$. At both of these limiting frequencies, $X_{in} = 0$.

Using all the above results, we obtain the Nyquist diagram of Fig. 7.14 for $Z_{in}(j\omega)$. In this diagram we observe that although the common collector stage with a capacitive load is open-circuit as well as short-circuit stable, it is however potentially unstable in the frequency range $5{\cdot}35 > \omega > 0{\cdot}384$. Thus, if the stage of Fig. 7.13 (a) is driven from a voltage source having an inductive series impedance $Z_S = R_S + j\omega L_S$, then it will become unstable if $R_S < 1{\cdot}31$ kΩ and L_S resonates with the input capacitance C_{in} at a frequency in the range $5{\cdot}35 > \omega > 0{\cdot}384$. On the other hand, if $R_S > 1{\cdot}31$ kΩ then the stage is stable for all values of L_S.

7.3.4 NEGATIVE IMPEDANCE CONVERTER

Consider the circuit of Fig. 7.15 involving an impedance Z_L and a current-controlled current source αI_1, where α is a dimensionless control parameter. From Fig. 7.15 we see that the current I_L through the impedance Z_L is equal to $(1 + \alpha)I_1$. Also, the voltage drop across Z_L is the same as the input voltage V_1. Therefore we have

$$V_1 = (1 + \alpha)I_1 Z_L \tag{7.33}$$

The ratio V_1/I_1 equals the input impedance Z_{in} at the port 1,1′; thus

$$Z_{in} = (1 + \alpha)Z_L \tag{7.34}$$

A particular case of interest occurs when $\alpha = -2$. Then, we have $Z_{in} = -Z_L$. Thus, a positive impedance (i.e. an impedance with a

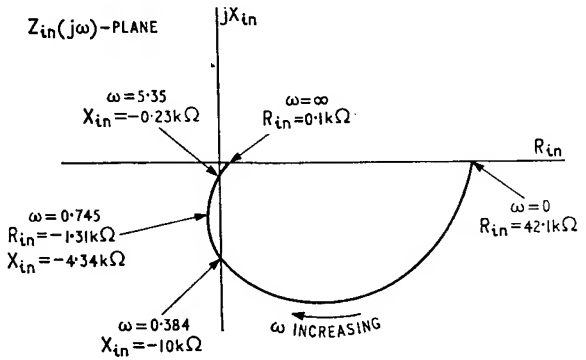

Fig. 7.14. Nyquist diagram for $Z_{in}(j\omega)$ of common collector stage of Fig. 7.13 (not to scale)

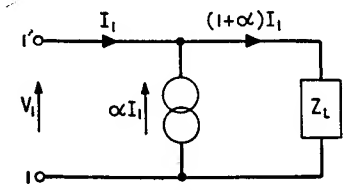

Fig. 7.15. Ideal negative impedance converter

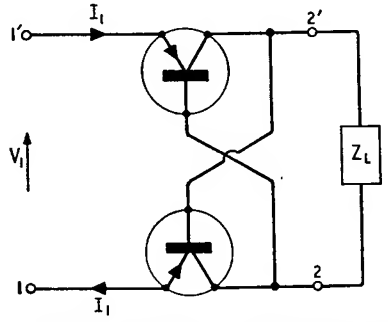

Fig. 7.16. Negative impedance converter using two transistors

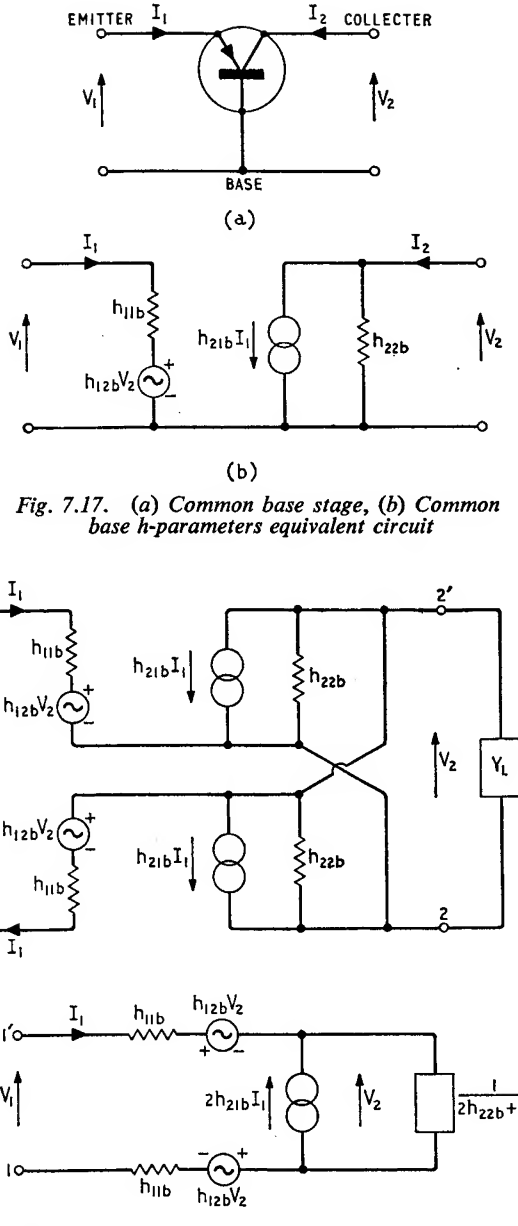

Fig. 7.17. (a) Common base stage, (b) Common base h-parameters equivalent circuit

Fig. 7.18. (a) Equivalent circuit of negative impedance converter of Fig. 7.16, (b) Simplified equivalent circuit

positive resistive component) has been converted into a negative impedance (i.e. an impedance with negative resistive component), and so the controlled current source arrangement of Fig. 7.15 is referred to as a *negative impedance converter*. Owing to the presence of the negative resistive component, it follows that a negative impedance converter is by nature potentially unstable.

The idealised controlled source of Fig. 7.15 can be fairly closely realised in practice by the double-transistor circuit of Fig. 7.16. To demonstrate this, let us replace each transistor by the common base *h*-parameters equivalent circuit of Fig. 7.17. Then, the circuit of Fig. 7.16 becomes equivalent to that of Fig. 7.18 (a), which can be simplified into the form of Fig. 7.18 (b). In this latter diagram, we see that if the idealised circuit of Fig. 7.15 is to be realised with $\alpha = -2$, the common base *h*-parameters h_{11b}, h_{12b}, h_{21b} and h_{22b} must satisfy the following ideal set of conditions

$$\left.\begin{aligned} h_{11b} &= 0\,\Omega \\ h_{12b} &= 0 \\ h_{21b} &= -1 \\ h_{22b} &= 0\,\mho \end{aligned}\right\} \qquad (7.35)$$

These conditions are reasonably closely met by a practical transistor, for which the following values are a typical set of common base *h*-parameters

$$h_{11b} = 20\,\Omega \qquad h_{21b} = -0{\cdot}99$$
$$h_{12b} = 10^{-4} \qquad h_{22b} = 10^{-6}\,\mho$$

Let us next examine the stability performance of the converter of Fig. 7.16. When the output port is short-circuited (i.e. $V_2 = 0$), the controlled source $2h_{21b}I_1$, which is responsible for the generation of the negative impedance, is by-passed with the result that the input impedance measured looking into the port 1,1′ becomes equal to $2h_{11b}$. In such a situation there is no likelihood of instability arising irrespective of the nature of the terminating source impedance so long as it remains passive.

If, on the other hand, the input port 1,1′ is open-circuited, then $I_1 = 0$ and the controlled source $2h_{21b}I_1$ becomes inactivated. An output admittance of $2h_{22b}$ is now presented to the load. Again there is no likelihood of any instability irrespective of the passive load impedance. We therefore conclude that the negative impedance converter of Fig. 7.16 is open-circuit stable at its input port 1,1′ and short-circuit stable at its output port. It is, however, short-circuit unstable at the port 1,1′, and open-circuit unstable at port 2,2′.

PROBLEMS

1. Fig. 7.19 shows the equivalent circuit of a negative resistance oscillator. It consists of a parallel tuned circuit connected across a negative resistance element $-R$. By evaluating the impedance measured between terminals 1,1′ determine the minimum necessary condition for sustained oscillations, and the frequency of oscillation.
2. Sketch the root locus diagram for the two poles of the

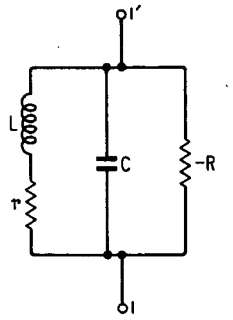

Fig. 7.19

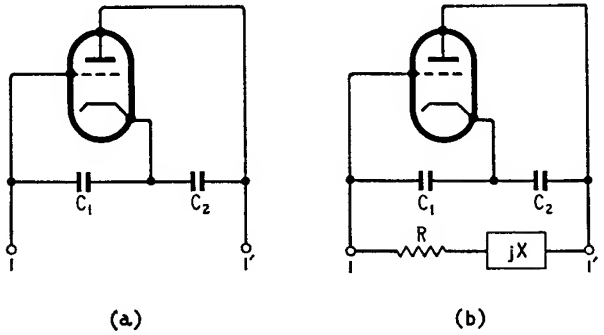

(a) (b)

Fig. 7.20

impedance measured between terminals 1,1′ of Fig. 7.19, as R is varied from zero to infinity.

3. Determine the impedance Z_1 measured between terminals 1,1′ of Fig. 7.20 (a), and show that the condition $\mu C_2 > C_1$ is necessary if the impedance Z_1 is to have a negative resistive component.

   If $C_1 = 0{\cdot}02\ \mu$F, $C_2 = 0{\cdot}001\ \mu$F and the valve parameters are $r_a = 10$ kΩ and $\mu = 24$, and an impedance $R + jX$ is connected across terminals 1,1′, as in Fig. 7.20 (b), calculate:

(*a*) The nature and magnitude of the reactance X so as to cause oscillation at a frequency of 15·9 kc/s, and
(*b*) the maximum permissible value of the resistance R for which the circuit will oscillate.

4. An active one-port network has the following driving-point impedance:

$$Z(p) = \frac{3p^3 + p^2 + 2p + 4}{p^3 + 3p^2 + 3p + 1}$$

Is this network short-circuit stable?
Is it open-circuit stable?

REFERENCES

1. BODE, H. W., *Network Analysis and Feedback Amplifier Design*, Van Nostrand, New York (1945).
2. DE PIAN, L., *Linear Active Network Theory*, Prentice-Hall, Englewood Cliffs (1962).
3. LINVILL, J. G., 'Transistor Negative Impedance Convertors', *Proc. I.R.E.*, **41**, 725 (1953).
4. MAYO, C. G., and HEAD, J. W., 'The Impedance Concept: Its Relation to Stability and Feedback', *Wireless Engineer*, **33**, 96 (1956).
5. PAGE, D. F. and BOOTHROYD, A. R., 'Instability in Two-Port Active Networks', *I.R.E. Trans.*, **CT–5**, 133 (1958).

CHAPTER 8

Wideband Amplifiers

A *wideband amplifier* is an amplifier the useful frequency range of which extends up to relatively high frequencies, of the order of several megacycles and higher. The design considerations of such an amplifier largely depend on the particular application for which it is intended. If the objective is to amplify pulses, then the amplifier is designed to have a step function response that rises to its ultimate value in the least possible time and exhibits the least possible amount of overshoot. If, on the other hand, the frequency response of the amplifier is of particular concern, then it is normally designed to provide a gain-frequency characteristic that is flat over the widest possible frequency band.

Negative feedback is often used in the design of wideband amplifiers because of the improvement which it can result in the frequency as well as transient response of the amplifier. However, before going on to the study of specific feedback circuits, we shall find it useful to develop first a number of general concepts.

8.1 General considerations

Consider a single-stage amplifier having a transfer function $K(p)$ given by

$$K(p) = \frac{K_0}{1 + p/\omega_0} \tag{8.1}$$

where K_0 is the low frequency value of $K(p)$, and ω_0 is the stage's angular cut off frequency. Suppose a unit-step function is applied to the input port of this stage. Then we obtain the following expression for the response transform $V_2(p)$, that is, the Laplace transform of the output signal $v_2(t)$

$$V_2(p) = \frac{K_0}{p(1 + p/\omega_0)} \tag{8.2}$$

Therefore $v_2(t)$ is given by (see Section 2.2.6)

$$v_2(t) = K_0(1 - e^{-t\omega_0}) \tag{8.3}$$

which is shown plotted in Fig. 8.1. The *rise time* τ_r, indicated in this diagram, is defined as the time taken for the output signal $v_2(t)$ to rise from 10 per cent to 90 per cent of its ultimate value.

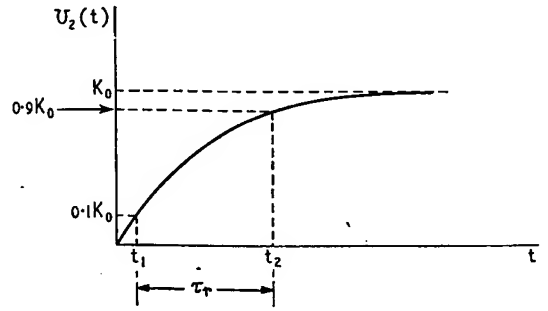

Fig. 8.1. Step function response of single-amplifier stage

In Fig. 8.1 we see that $v_2(t) = 0{\cdot}1\ K_0$ at time $t = t_1$; hence substituting these values in Equation 8.3, we get

$$0{\cdot}1 = 1 - e^{-t_1\omega_0}$$

Solving for t_1, we have

$$t_1 = \frac{1}{\omega_0}\log_e\left(\frac{1}{0{\cdot}9}\right)$$

$$= \frac{0{\cdot}1}{\omega_0} \tag{8.4}$$

Similarly, $v_2(t) = 0{\cdot}9\ K_0$ at $t = t_2$, and Equation 8.3 gives

$$t_2 = \frac{1}{\omega_0}\log_e 10$$

$$= \frac{2{\cdot}3}{\omega_0} \tag{8.5}$$

Hence, the rise time τ_r is equal to

$$\tau_r = t_2 - t_1$$

$$= \frac{2{\cdot}2}{\omega_0} \tag{8.6}$$

The above definition for rise time is the generally accepted one when carrying out practical measurements on the step function response of amplifiers. We have seen that in a single-stage amplifier having one pole only, as in Equation 8.1, the definition leads to quite a simple relationship between the rise time τ_r and the stage cut off frequency ω_0. But if the transfer function of the amplifier is more complex, as it is very often the case, then calculation of the 10 to 90 per cent rise time can be quite a difficult task. To overcome this

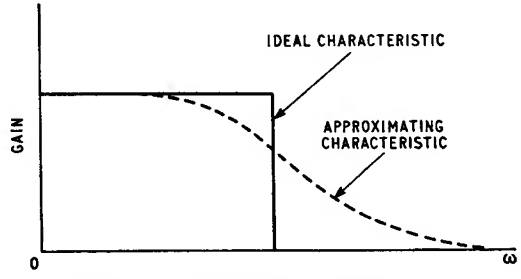

Fig. 8.2. Gain-frequency characteristic

difficulty W. C. Elmore[1] has introduced an alternative definition for the rise time which can be calculated directly from the transfer function, thereby avoiding the need for evaluating the inverse Laplace transform. Thus, if the transfer function of an amplifier is given by

$$K(p) = K_0 \frac{1 + c_1 p + c_2 p^2 + \ldots + c_m p^m}{1 + d_1 p + d_2 p^2 + \ldots d_n p^n} \tag{8.7}$$

where c_1 to c_m and d_1 to d_n are all real coefficients, then according to Elmore the rise time is given by

$$\tau_r = \sqrt{[2\pi(d_1^2 - c_1^2 + 2c_2 - 2d_2)]} \tag{8.8}$$

It is, however, important to note that this relationship applies only to a system which does not exhibit any overshoot and whose response rises *monotonically* to its ultimate value. Thus, if for example, all the poles and zeros of the transfer function $K(p)$ of Equation 8.7 are located on the negative σ-axis of the p-plane, then the resulting step function response will be monotonic and Equation 8.8 can be applied to evaluate the rise time τ_r.

In the case of the simple transfer function of Equation 8.1 we see that the coefficient $d_1 = 1/\omega_0$ and all the remaining coefficients c_1 to c_m and d_2 to d_n are zero; hence Equation 8.8 gives Elmore's rise time τ_r to be

$$\tau_r = \frac{\sqrt{2\pi}}{\omega_0} = \frac{2{\cdot}5}{\omega_0} \tag{8.9}$$

This agrees moderately well with the result of Equation 8.6.

8.1.1 CONDITIONS FOR MAXIMAL FLATNESS

If in Equation 8.7 we put $p = j\omega$ and evaluate the squared magnitude of $K(j\omega)$, we obtain a result of the following generalised form

$$\left|\frac{K(j\omega)}{K_0}\right|^2 = \frac{1 + a_2\omega^2 + a_4\omega^4 + \ldots + a_{2m}\omega^{2m}}{1 + b_2\omega^2 + b_4\omega^4 + \ldots + b_{2n}\omega^{2n}} \tag{8.10}$$

where the coefficients a_2 to a_{2m} are related to the coefficients c_1 to c_m of Equation 8.7, and the coefficients b_2 to b_{2n} are related to the coefficients d_1 to d_n. Using the normal process of long division the rational function of Equation 8.10 can be expanded as follows

$$\left|\frac{K(j\omega)}{K_0}\right|^2 = 1 + (a_2 - b_2)\omega^2 + [(a_4 - b_4) - b_2(a_2 - b_2)]\omega^4 + \ldots \tag{8.11}$$

which shows that the coefficients of the resulting expansion are related to the differences of the corresponding coefficients of like powers in the numerator and denominator polynomials of Equation 8.10.

Let us suppose next that it is required to approximate the ideal low-pass frequency characteristic of Fig. 8.2 by means of the magnitude function of Equation 8.10, the approximation being in a *maximally flat* manner about the point $\omega = 0$. From Equation 8.10 we deduce directly that m must be less than n. Further from Equation 8.11 the required approximation can be achieved provided that the various coefficients satisfy the following conditions

$$\left.\begin{aligned} a_2 &= b_2 \\ a_4 &= b_4 \\ &\ldots\ldots \\ a_{2m} &= b_{2m} \end{aligned}\right\} \tag{8.12}$$

Then Equation 8.10 modifies to

$$\left|\frac{K(j\omega)}{K_0}\right|^2 = \frac{1 + a_2\omega^2 + a_4\omega^4 + \ldots a_{2m}\omega^{2m}}{1 + a_2\omega^2 + a_4\omega^4 + \ldots a_{2m}\omega^{2m} + b_{2n}\omega^{2n}} \tag{8.13}$$

Such a characteristic is referred to as a *maximally flat magnitude function* in that the first $2n - 1$ derivatives with respect to ω are zero at $\omega = 0$.

8.2 Common emitter stage with local series feedback

The circuit of Fig. 8.3 shows local series feedback applied to a single-common emitter stage by means of the resistor R_e connected in series with the emitter terminal. The stage is driven from a sinusoidal voltage source V_S of internal resistance R_S. To evaluate the effect of the resistor R_e on the frequency response of the stage, the

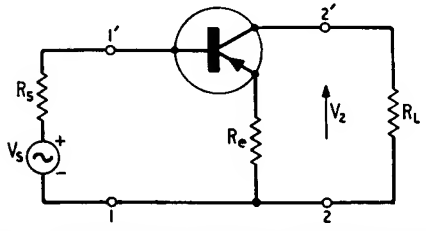

Fig. 8.3. Common emitter stage with local series feedback

transistor is replaced by its simplified hybrid-π equivalent circuit, as in Fig. 8.4 (a). The controlled current source $g_m V_{b'e}$ in this circuit is next replaced by an equivalent pair of controlled sources to obtain the equivalent circuit of Fig. 8.4 (b). Here we see that the voltage $V_{b'}$ at the node b' with respect to the common terminal is equal to

$$V_{b'} = V_{b'e} + R_e(g_m + y_{b'e})V_{b'e} \tag{8.14}$$

where $y_{b'e}$ is the admittance of the resistance $r_{b'e}$ and capacitance $C_{b'e}$ in parallel, that is,

$$y_{b'e} = \frac{1}{r_{b'e}} + j\omega C_{b'e} \tag{8.15}$$

Equation 8.14 gives the voltage drop $V_{b'e}$ in terms of $V_{b'}$ to be

$$V_{b'e} = \frac{V_{b'}}{1 + R_e(g_m + y_{b'e})} \tag{8.16}$$

Since the current $I_{b'}$ shown defined in Fig. 8.4 (b) is equal to $y_{b'e}V_{b'e}$ it follows that the equivalent circuit of Fig. 8.4 (b) can be reduced to the simpler form shown in Fig. 8.4 (c). This can be further simplified by adding an admittance of

$$j\omega C_{b'c} \cdot \frac{g_m R_L}{1 + R_e(g_m + y_{b'e})}$$

between the node b' and the common terminal so as to account for the Miller effect of the feedback capacitance $C_{b'c}$. We thus obtain

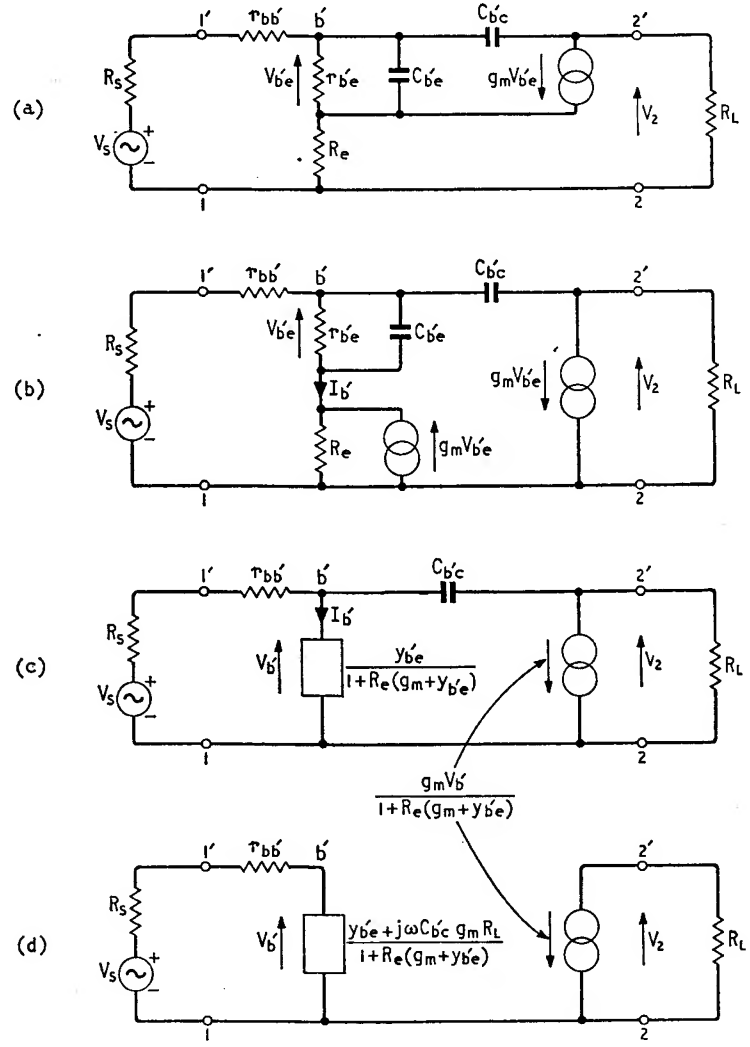

Fig. 8.4. Equivalent circuit for the transistor stage of Fig. 8.3, and its various simplifications

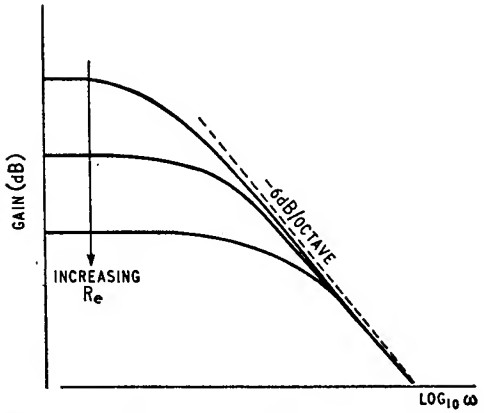

Fig. 8.5. Illustrating effect of local feedback on gain-frequency response

the simplified equivalent circuit of Fig. 8.4 (d) for the transistor stage of Fig. 8.3. From the equivalent circuit of Fig. 8.4 (d) we deduce directly that the output voltage V_2 is equal to

$$V_2 = \frac{-g_m R_L V_S}{1 + R_e(g_m + y_{b'e}) + (R_S + r_{bb'})(y_{b'e} + j\omega C_{b'c} g_m R_L)} \quad (8.17)$$

Using Equation 8.15 for $y_{b'e}$ and then evaluating the external voltage gain V_2/V_S of the stage, we obtain

$$K'(j\omega) = \frac{V_2}{V_S}$$

$$= \frac{K_0'}{1 + j\omega/\omega_v} \quad (8.18)$$

where K_0' = low frequency value of $K'(j\omega)$

$$= \frac{-g_m r_{b'e} R_L}{R_S + r_{bb'} + r_{b'e} + R_e(1 + g_m r_{b'e})} \quad (8.19)$$

ω_v = angular cut off frequency of the stage

$$= \frac{R_S + r_{b'b} + r_{b'e} + R_e(1 + g_m r_{b'e})}{r_{b'e}[R_e C_{b'e} + (R_S + r_{bb'})(C_{b'e} + C_{b'c} g_m R_L)]} \quad (8.20)$$

Equations 8.19 and 8.20 give the *voltage gain-bandwidth product* denoted by *VGBP*, to be

$$VGBP = |K_0'|\omega_v$$

$$VGBP = \frac{g_m R_L}{R_e C_{b'e} + (R_S + r_{bb'})(C_{b'e} + C_{b'c} g_m R_L)} \quad (8.21)$$

This product is maximum when $R_S = 0$. We therefore deduce that the series feedback stage of Fig. 8.3 is best driven from a voltage source of low internal impedance. Another good reason for using a voltage source of low internal impedance is that, for a given transistor, load resistance and feedback resistance R_e, the return difference with reference to the mutual conductance g_m attains its maximum value when the source resistance R_S is zero†.

In Fig. 8.5 the gain-frequency characteristic of the stage is shown plotted for different values of the feedback resistor R_e. We see that

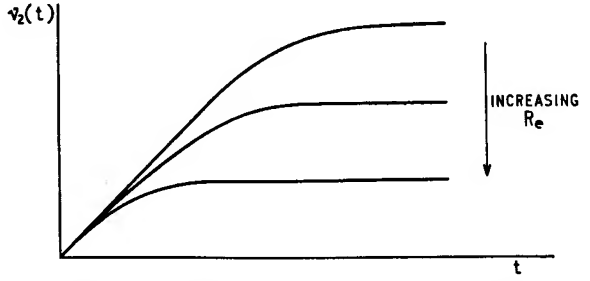

Fig. 8.6. Illustrating effect of local feedback on transient response

the stage cut off frequency is increased with increasing R_e; this is however, achieved at the expense of reduced low frequency gain. Provided that the feedback resistor R_e is small compared with $(R_S + r_{bb'})(1 + C_{b'c} g_m R_L/C_{b'e})$, then to a first order of approximation the gain-bandwidth is independent of R_e, and at high frequencies the curves for all values of R_e become asymptotic to the dashed line which has a slope of −6 dB per octave.

Next to evaluate the transient response of the stage, suppose that it is driven from a voltage source providing a unit-step function; then the transfer function of the stage is

$$K'(p) = \frac{K_0'}{1 + p/\omega_v} \quad (8.22)$$

and from Equation 8.3 the resulting response $v_2(t)$ is given by

† Assuming that the effects of the elements $r_{b'c}$ and r_{ce} are negligible, we find that in the stage of Fig. 8.3 the return difference with reference to g_m is given by

$$F \simeq 1 + \frac{g_m r_{b'e} R_e}{R_S + R_e + r_{bb'} + r_{b'e}}$$

from which we clearly see that F has its maximum value when $R_S = 0$.

$$v_2(t) = K_0'(1 - e^{-t\omega_v}) \tag{8.23}$$

The 10 to 90 per cent rise time of the stage is equal to $2{\cdot}2/\omega_v$; it is reduced with increasing R_e as illustrated in Fig. 8.6.

8.2.1 HIGH FREQUENCY COMPENSATION

For a given value of feedback resistor R_e the response of the stage of Fig. 8.3 can be further improved by connecting a capacitor C_e in parallel with the resistor R_e, as in Fig. 8.7. In this case the low

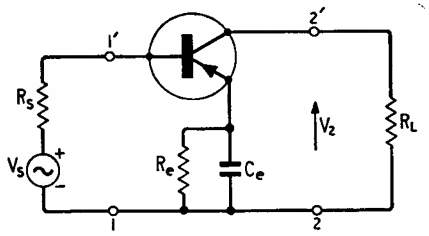

Fig. 8.7. Series feedback stage with high frequency compensation

frequency gain of the stage remains at the value K_0' given by Equation 8.19.

As a result of adding the capacitor C_e we see that the total feedback impedance Z_e connected in series with the emitter terminal is equal to

$$Z_e = \frac{R_e}{1 + j\omega C_e R_e} \tag{8.24}$$

If therefore we replace R_e with Z_e in Equation 8.17 and then use the relationship of Equation 8.15, we find that the external voltage gain $K_c'(j\omega)$ of the capacitively compensated stage of Fig. 8.7 can be expressed as follows

$$K_c'(j\omega) = \frac{V_2}{V_S} = \frac{K_0'(1 + j\omega C_e R_e)}{1 + j\omega\left(\frac{1}{\omega_v} + \lambda C_e R_e\right) - \omega^2\left(\frac{C_e R_e}{\mathscr{K}\omega_v}\right)} \tag{8.25}$$

where ω_v is as defined in Equation 8.20 and the parameters λ and $\mathscr{K}$ are given by

$$\lambda = \frac{R_S + r_{bb'} + r_{b'e}}{R_S + r_{bb'} + r_{b'e} + R_e(1 + g_m r_{b'e})} \tag{8.26}$$

$$\mathscr{K} = 1 + \frac{R_e C_{b'e}}{(R_S + r_{bb'})(C_{b'e} + C_{b'c} g_m R_L)} \tag{8.27}$$

Evaluating the magnitude of the external voltage gain and then squaring, we get

$$\left|\frac{K_c'(j\omega)}{K_0'}\right|^2 = \frac{1 + \omega^2 C_e^2 R_e^2}{1 + \omega^2\left[\left(\frac{1}{\omega_v} + \lambda C_e R_e\right)^2 - \frac{2C_e R_e}{\mathscr{K}\omega_v}\right] + \omega^4\left(\frac{C_e R_e}{\mathscr{K}\omega_v}\right)^2} \tag{8.28}$$

Fig. 8.8 shows the effect of varying the compensating capacitor C_e on the gain-frequency characteristic of the stage of Fig. 8.7. The value of C_e which makes this characteristic maximally flat can be determined from the necessary condition

$$C_e^2 R_e^2 = \left(\frac{1}{\omega_v} + \lambda C_e R_e\right)^2 - \frac{2C_e R_e}{\mathscr{K}\omega_v} \tag{8.29}$$

which is a quadratic equation in C_e. However, only the following solution leads to a positive value for C_e

$$C_e = \frac{1}{\omega_a R_e} \tag{8.30}$$

where

$$\omega_a = \frac{\omega_v \mathscr{K}(1 - \lambda^2)}{\lambda\mathscr{K} - 1 + \sqrt{[\mathscr{K}^2 - 2\lambda\mathscr{K} + 1]}} \tag{8.31}$$

To demonstrate the improvement in the frequency response resulting from addition of the capacitor C_e, we shall evaluate the

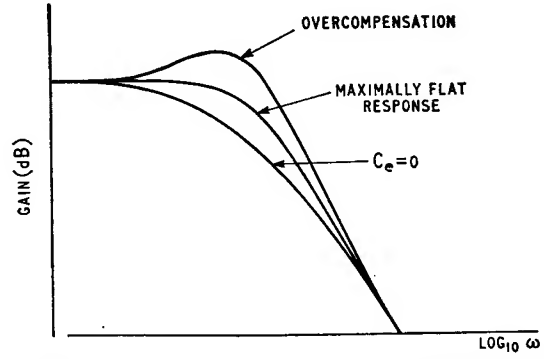

Fig. 8.8. Effect of compensating capacitor on gain-frequency response

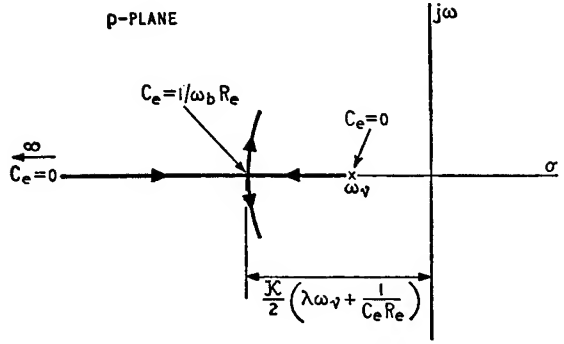

Fig. 8.9. Locus of poles of compensated stage as C_e is increased from zero

angular cut off frequency of the stage with C_e having the value given by Equations 8.30 and 8.31. Substituting this value in Equation 8.28 we find that the maximally flat magnitude characteristic of the stage is given by

$$\left|\frac{K_c'(j\omega)}{K_0'}\right|^2 = \frac{1+\left(\frac{\omega}{\omega_a}\right)^2}{1+\left(\frac{\omega}{\omega_a}\right)^2+\frac{\omega_a^2}{\mathcal{K}^2\omega_v^2}\left(\frac{\omega}{\omega_a}\right)^4} \tag{8.32}$$

Let ω_c denote the angular cut off frequency of the stage for the maximally flat case. Then, by definition, at $\omega = \omega_c$ we have

$$|K_c'(j\omega)| = \frac{|K_0'|}{\sqrt{2}}$$

and so Equation 8.32 leads to

$$\frac{\omega_a^2}{\mathcal{K}^2\omega_v^2}\left(\frac{\omega_c}{\omega_a}\right)^4 - \left(\frac{\omega_c}{\omega_a}\right)^2 - 1 = 0 \tag{8.33}$$

This is a quadratic equation in $(\omega_c/\omega_a)^2$, but has only one positive real root. We thus get the solution

$$\omega_c = \mathcal{K}\omega_v\left(\frac{1}{2}+\sqrt{\left[\frac{1}{4}+\frac{\omega_a^2}{\mathcal{K}^2\omega_v^2}\right]}\right)^{1/2} \tag{8.34}$$

If, as is often the case, the feedback resistor R_e satisfies both of the following two inequalities

$$R_e \gg \frac{R_S + r_{bb'} + r_{b'e}}{1+g_m r_{b'e}} \tag{8.35}$$

$$R_e \ll \frac{1}{C_{b'e}}(R_S + r_{bb'})\,(C_{b'e} + g_m R_L C_{b'c}) \tag{8.36}$$

then we find from Equations 8.26 and 8.27 that $\lambda \ll 1$ and $\mathcal{K} \simeq 1$. Accordingly Equation 8.31 approximates to

$$\omega_a \simeq \frac{\omega_v}{-1+\sqrt{2}}$$
$$= 2{\cdot}42\omega_v \tag{8.37}$$

and therefore the expression for ω_c, as given by Equation 8.34 reduces to

$$\omega_c \simeq 1{\cdot}73\omega_v \tag{8.38}$$

This states that the angular cut off frequency of the capacitively compensated stage of Fig. 8.7 with a maximally flat gain characteristic is approximately 1·73 times the uncompensated stage's angular cut off frequency.

Let us next investigate the transient response of the stage of Fig. 8.7. Putting $j\omega = p$ in Equation 8.25, we have

$$K_c'(p) = \frac{K_0'(1+pC_eR_e)}{1+p\left(\frac{1}{\omega_v}+\lambda C_eR_e\right)+\frac{p^2C_eR_e}{\mathcal{K}\omega_v}} \tag{8.39}$$

Hence $K_c'(p)$ has a zero at $p = -1/C_eR_e$ and two poles at

$$p_1, p_2 = \frac{\mathcal{K}\omega_v}{2C_eR_e}\left[-\left(\frac{1}{\omega_v}+\lambda C_eR_e\right) \pm \sqrt{\left\{\left(\frac{1}{\omega_v}+\lambda C_eR_e\right)^2 - \frac{4C_eR_e}{\mathcal{K}\omega_v}\right\}}\right] \tag{8.40}$$

The locus of these two poles as C_e varies is shown in Fig. 8.9. If the resulting response to a step function is to be critically damped and so exhibit no overshoot, then the two poles must be real and coincident. To meet this requirement the compensating capacitor C_e must in turn satisfy the following condition

$$\left(\frac{1}{\omega_v}+\lambda C_eR_e\right)^2 - \frac{4C_eR_e}{\mathcal{K}\omega_v} = 0 \tag{8.41}$$

which is a quadratic equation in C_e; however only the following positive real root is acceptable

$$C_e = \frac{1}{\omega_b R_e} \tag{8.42}$$

where $$\omega_b = \frac{\omega_v \lambda^2 \mathscr{K}}{2 - \lambda\mathscr{K} - 2\sqrt{[1 - \lambda\mathscr{K}]}} \tag{8.43}$$

If the capacitor C_e has a value greater than that given by the above two equations, the poles p_1 and p_2 become complex conjugate, thereby giving rise to an oscillatory response.

With the condition for critical damping satisfied, the transfer function of Equation 8.39 modifies to

$$K_c'(p) = \frac{K_0'\left(1 + \frac{p}{\omega_b}\right)}{1 + \frac{2p}{\sqrt{[\mathscr{K}\omega_b\omega_v]}} + \frac{p^2}{\mathscr{K}\omega_b\omega_v}} = \frac{K_0'\left(1 + \frac{p}{\omega_b}\right)}{\left(1 + \frac{p}{\sqrt{[\mathscr{K}\omega_b\omega_v]}}\right)^2} \tag{8.44}$$

Further, if the excitation is a unit-step function, its Laplace transform is equal to $1/p$ and the Laplace transform $V_2(p)$ of the resulting output signal is given by

$$V_2(p) = \frac{K_c'(p)}{p} = \frac{K_0'\left(1 + \frac{p}{\omega_b}\right)}{p\left(1 + \frac{p}{\sqrt{[\mathscr{K}\omega_b\omega_v]}}\right)^2} \tag{8.45}$$

Expanding this rational function into partial fractions and then using the Laplace transform pairs table, it can be shown that the output signal $v_2(t)$ developed across the load is equal to

$$v_2(t) = K_0'\left[1 - e^{-t\sqrt{[\mathscr{K}\omega_b\omega_v]}}\left\{1 + t(\sqrt{[\mathscr{K}\omega_b\omega_v]} - \mathscr{K}\omega_v)\right\}\right] \tag{8.46}$$

Evaluation of the 10 to 90 per cent rise time from this response is by no means an easy task. Therefore, in an effort to obtain an estimate of the improvement resulting from addition of the capacitor C_e, we shall evaluate Elmore's rise time; this is perfectly justified in the case of the transfer function of Equation 8.44. Thus comparing the function given in the first line of Equation 8.44 with that of Equation 8.7, and evaluating Elmore's rise time from Equation 8.8 we obtain τ_r' = rise time of the stage compensated for critical damping.

$$\tau_r' = \sqrt{\left[2\pi\left(\frac{4}{\mathscr{K}\omega_b\omega_v} - \frac{1}{\omega_b^2} - \frac{2}{\mathscr{K}\omega_b\omega_v}\right)\right]} = \frac{1}{\omega_v}\sqrt{\left[2\pi\left(\frac{2\omega_v}{\mathscr{K}\omega_b} - \frac{\omega_v^2}{\omega_b^2}\right)\right]} \tag{8.47}$$

The transfer function of the stage in the absence of the capacitor C_e is given by Equation 8.22. We therefore deduce that Elmore's rise time τ_r for the uncompensated stage is equal to $\sqrt{[2\pi]}/\omega_v$. Thus as a measure of the improvement in transient response we can define the *rise time improvement factor* η for the capacitively compensated stage of Fig. 8.7 as follows

$$\eta = \frac{\tau_r}{\tau_r'} = \frac{1}{\sqrt{\left[\frac{2\omega_v}{\mathscr{K}\omega_b} - \frac{\omega_v^2}{\omega_b^2}\right]}} \tag{8.48}$$

Assuming that the feedback resistor R_e satisfies the inequalities of Equations 8.35 and 8.36, we have $\lambda \ll 1$ and $\mathscr{K} \simeq 1$. Accordingly Equation 8.43 approximates to

$$\omega_b \simeq 4\omega_v \tag{8.49}$$

and Equation 8.48 gives

$$\eta \simeq \frac{4}{\sqrt{7}} = 1{\cdot}51 \tag{8.50}$$

This shows that the rise time of the capacitively compensated stage of Fig. 8.8 adjusted for critical damping is approximately $\frac{2}{3}$ times that of the uncompensated stage.

8.3 Common emitter stage with local shunt feedback

In Fig. 8.10 local shunt feedback is applied to a single-common emitter stage by means of a resistor R_c connected between the base and collector terminals. In this case it is convenient to represent the driving source as a current source I_S shunted by the resistance R_S. To determine the response of the stage we can apply the feedback theory developed in Chapter 3 or the nodal method of analysis to the circuit of Fig. 8.11 where the transistor has been replaced by its simplified hybrid-π equivalent circuit. Then we find that the external current gain I_2/I_S of the stage is given by

$$\frac{I_2}{I_S} = \frac{K_0'}{1 + j\omega/\omega_t} \tag{8.51}$$

where K_0' = low frequency value of external current gain

$$= \frac{g_m r_{b'e} R_S R_c}{(R_S + r_{bb'} + r_{b'e})(R_c + R_L) + g_m r_{b'e} R_S R_L} \tag{8.52}$$

ω_t = angular cut-off frequency of the stage

$$= \frac{(R_S + r_{bb'} + r_{b'e})(R_c + R_L) + g_m r_{b'e} R_S R_L}{r_{b'e}(r_{bb'} + R_S)[C_{b'e}(R_c + R_L) + C_{b'c} g_m R_c R_L]} \tag{8.53}$$

These results are subject to the following conditions which are normally justified

$$\left.\begin{aligned} R_c &\gg r_{bb'} \\ C_{b'e} &\gg C_{b'c} \\ g_m &\gg \omega C_{b'c} \\ \frac{1}{R_c} + \frac{1}{R_L} &\gg \omega C_{b'c} \\ g_m R_c &\gg 1 + \frac{r_{bb'}}{r_{b'e}} \\ g_m R_c &\gg \omega C_{b'e} r_{bb'} \end{aligned}\right\} \tag{8.54}$$

From Equations 8.52 and 8.53 the *current gain-bandwidth product*, denoted by *CGBP*, for the stage of Fig. 8.10 is equal to

$$CGBP = \frac{g_m R_S R_c}{(r_{bb'} + R_S)[C_{b'e}(R_c + R_L) + C_{b'c} g_m R_c R_L]} \tag{8.55}$$

which has its maximum value when $R_S = \infty$. Hence the shunt feedback stage of Fig. 8.10 is best driven from an ideal current source having an infinitely large shunt resistance. Futhermore, it is of interest to note that, for a given transistor, load resistance and feedback resistance R_c, the return difference with reference to g_m has its maximum value when the source resistance R_S is infinite†.

The frequency and transient response of the stage can be further improved by connecting an inductor in series with the feedback resistance as in Fig. 8.12. The resulting improvement can be determined in a similar manner to the compensated stage of Fig. 8.7.

† Assuming that the elements $r_{b'c}$ and r_{ce} have negligible effects, we find that in the stage of Fig. 8.10 the return difference with reference to g_m is given by

$$F \simeq 1 + \frac{g_m r_{b'e} R_L}{(R_c + R_L)[1 + (r_{bb'} + r_{b'e})/R_S]}$$

which clearly shows that F has its maximum value when $R_S = \infty$.

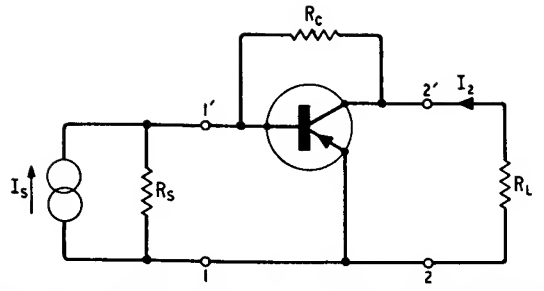

Fig. 8.10. Common emitter stage with local shunt feedback

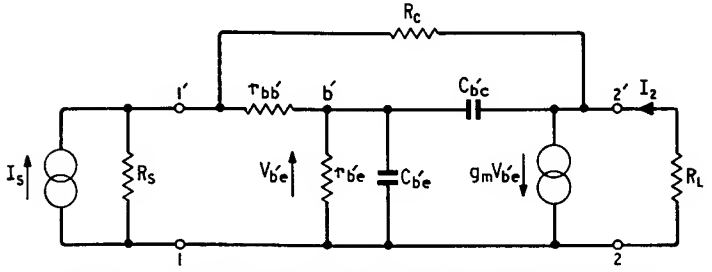

Fig. 8.11. Equivalent circuit of the feedback stage of Fig. 8.10

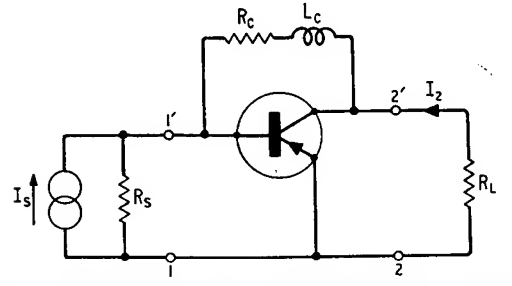

Fig. 8.12. Shunt feedback stage with high frequency compensation

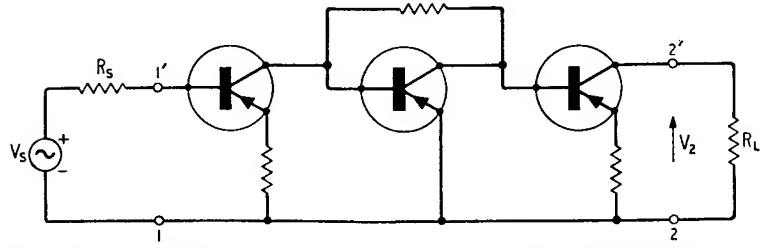

Fig. 8.13. A cascade of three common emitter stages with alternate local series and shunt feedback

8.4 Cascades of transistor feedback stages

In a series feedback stage we have seen that the maximum value of voltage gain-bandwidth product is obtained when the stage is driven from an ideal voltage source, whereas in a shunt feedback stage the maximum value of current gain-bandwidth product is achieved by driving it with an ideal current source. Now remembering that a series feedback stage has a relatively high output impedance and a shunt feedback stage has a relatively low output impedance, it follows that when cascading a number of transistor feedback stages it is best to employ series and shunt feedback stages arranged such that they alternate in the manner shown in Fig. 8.13. The interaction between stages in such a combination is negligibly small in the useful frequency band because there exists a gross impedance mismatch between the adjacent stages. Therefore each stage can be designed independently starting from the load end.†

8.5 A valve feedback pair

The diagram of Fig. 8.14 shows a widely used *feedback pair* involving two pentode valves operated as common cathode stages. The resistor R connected between the two anodes applies local shunt feedback to the second stage only. Replacing each valve with its

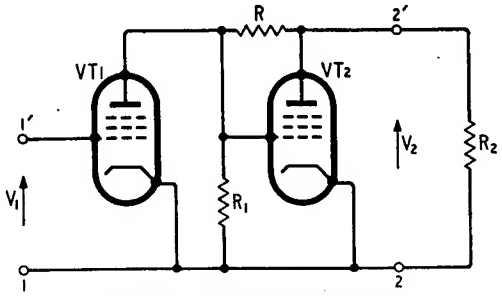

Fig. 8.14. Valve feedback pair

equivalent circuit we obtain Fig. 8.15 where C_2 is the output capacitance of the second stage, and C_1 is the sum of the output capacitance of the first stage and the input capacitance of the second stage. g_{m1} and g_{m2} are the mutual conductances of the two valves. Subject to the condition that the feedback resistance R is large compared to both anode load resistances R_1 and R_2, we can show that the overall voltage gain function $K'(p) = V_2/V_1$ of the circuit of Fig. 8.15 is

† For a more detailed treatment see E. M. Cherry and M. E. Hooper.[2]

$$K'(p) = \frac{K_0}{F_0 + p\left(\frac{1}{\omega_1} + \frac{1}{\omega_2}\right) + \frac{p^2}{\omega_1\omega_2}} \tag{8.56}$$

where

$$K_0 = g_{m1}R_1 g_{m2}R_2 \tag{8.57}$$

ω_1 = angular cut off frequency of the first stage

$$= \frac{1}{C_1R_1} \tag{8.58}$$

ω_2 = angular cut off frequency of the second stage

$$= \frac{1}{C_2R_2} \tag{8.59}$$

F_0 = low frequency value of the return difference with reference to g_{m2}

$$= 1 + \frac{g_{m2}R_1R_2}{R} \tag{8.60}$$

Equation 8.56 can be also expressed as follows

$$K'(p) = \frac{K_0'}{1 + 2\zeta\frac{p}{\omega_0} + \frac{p^2}{\omega_0^2}} \tag{8.61}$$

where $K_0' = K_0/F_0$ is the low frequency value of the overall gain, ζ is the damping ratio and ω_0 is the undamped frequency of oscillation, as defined in Section 2.2.7. Therefore

$$2\zeta\omega_0 = \omega_1 + \omega_2 \tag{8.62}$$

$$\omega_0^2 = \omega_1\omega_2'F_0 \tag{8.63}$$

and the return difference F_0 required to realise a specified damping ratio is given by

$$F_0 = \frac{(\omega_1 + \omega_2)^2}{4\omega_1\omega_2\zeta^2} \tag{8.64}$$

The transient response to a step function is critically damped provided ζ equals unity (see Section 2.2.7). Then, Equation 8.64 gives the corresponding value of F_0' of the return difference to be

$$F_0' = \frac{(\omega_1 + \omega_2)^2}{4\omega_1\omega_2} \tag{8.65}$$

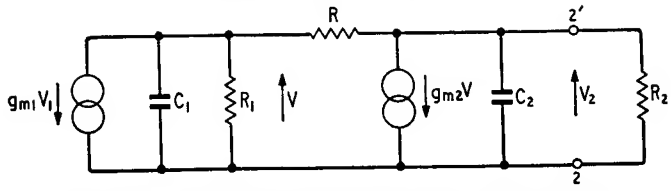

Fig. 8.15. Equivalent circuit of the valve feedback pair

When F_0 has this value, the gain function $K'(p)$ will have a double pole at $p = -\frac{1}{2}(\omega_1 + \omega_2)$, as shown in Fig. 8.16 (a).

If, however, the objective is to realise a maximally flat gain-frequency characteristic, then to determine the required value of ζ we put $p = j\omega$ in Equation 8.56 obtaining

$$K'(j\omega) = \frac{K_0'}{\left(1 - \frac{\omega^2}{\omega_0^2}\right) + j2\zeta\frac{\omega}{\omega_0}} \tag{8.66}$$

Evaluating the magnitude and squaring, we have

$$\left|\frac{K'(j\omega)}{K_0'}\right|^2 = \frac{1}{1 + 2(2\zeta^2 - 1)\frac{\omega^2}{\omega_0^2} + \frac{\omega^4}{\omega_0^4}} \tag{8.67}$$

Hence for a maximally flat frequency response we must have

$$2\zeta^2 - 1 = 0$$

that is, $\zeta = 1/\sqrt{2}$. Equation 8.64 then gives the corresponding value F_0'' of the return difference with reference to g_{m2} to be

$$F_0'' = \frac{(\omega_1 + \omega_2)^2}{2\omega_1\omega_2} \tag{8.68}$$

in which case Equation 8.67 simplifies to

$$\left|\frac{K'(j\omega)}{K_0'}\right|^2 = \frac{1}{1 + \frac{\omega^4}{\omega_0^4}} \tag{8.69}$$

This expression shows that, when the conditions for maximal flatness are satisfied, the angular cut off frequency ω_0' at which the gain $20 \log_{10} |K'(j\omega)|$ drops by 3 dB below its low frequency value $20 \log_{10} K_0'$ is equal to ω_0. From Equations 8.63 and 8.68 we therefore see that ω_0' is related to the individual stage cut off frequencies ω_1 and ω_2 by

$$\omega_0' = \frac{1}{\sqrt{2}}(\omega_1 + \omega_2) \tag{8.70}$$

Further when $\zeta = 1/\sqrt{2}$ we find from Equation 8.61 that the resulting two poles of $K'(p)$ are complex conjugate located at

$$p = \frac{\omega_1 + \omega_2}{2}(-1 \pm j)$$

as indicated in Fig. 8.16 (b).

Comparing the values F_0' and F_0'' given by Equations 8.65 and 8.68 we see that, for any values of ω_1 and ω_2, the condition for a critically damped transient response permits a low frequency return difference F_0 that is only one half that required for a maximally flat frequency response.

PROBLEMS

1. (a) A common emitter stage is driven from a voltage source of internal resistance 600 Ω. The load resistance is 500 Ω, and the transistor has the following hybrid-π parameters

$$r_{bb'} = 100\ \Omega$$
$$r_{b'e} = 1{,}000\ \Omega$$
$$C_{b'e} = 200\ \text{pF}$$
$$C_{b'c} = 5\ \text{pF}$$
$$g_m = 40\ \text{mA/V}$$

Calculate the low frequency value of the external voltage gain,

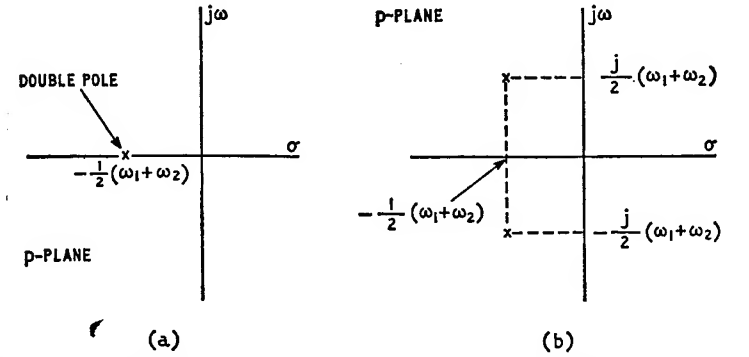

Fig. 8.16. Pole-zero patterns: (a) Critically damped transient response, (b) Maximally flat frequency response

the cut off frequency and the 10 to 90 per cent rise time of the stage.

(b) If the cut off frequency is to be extended to 2 Mc/s by applying local series feedback to the stage, determine the required value of the feedback resistor. What are the resulting values of the gain with feedback, and the return difference with reference to g_m?

2. The feedback pair circuit of Fig. 8.17 uses two identical pentodes valves, each with an output shunt capacitance of

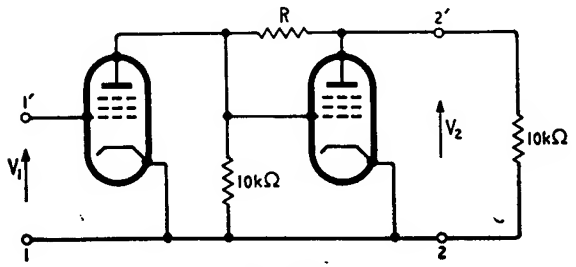

Fig. 8.17

5 pF and a mutual conductance g_m of 4 mA/V. Determine the value of the feedback resistor R required for a maximally flat gain-frequency response. For this particular value of R calculate

(a) The 3 dB cut off frequency of the gain-response, and

(b) the percentage overshoot of the transient response to an input step function.

3. A two-stage amplifier, with its output terminals on open-circuit, has a voltage amplification given by $250/(1 - x^2 + j2x)$ and

$$x = \left(\frac{f}{20} - \frac{1}{20f}\right)$$

where f is the frequency in kc/s. The output resistance is 48 Ω, and a load resistance of 12 Ω is connected across the output terminals. A high resistance potential divider is connected in parallel with the load, and a fraction $1/N$ of the output voltage is fed back to give negative feedback at 1 kc/s.

(a) Determine the value of N required to give an overall voltage amplification of 12.5 at 1 kc/s.

(b) Derive an expression which shows how the overall voltage amplification varies with frequency when N is 50/9 and determine the magnitude of the amplification at 60 kc/s. Sketch curves showing the frequency response (i) without feedback

and (ii) when N is 50/9. Comment on the relative shapes of the curves.

(London University, B.Sc., Eng., Part III, Electronics, 1961)

4. A negative feedback amplifier with a purely resistive feedback network has the following open-loop gain function:

$$T(p) = T(0)\frac{1 + 0{\cdot}5p}{(1 + p)^2}$$

Determine the required value of $T(0)$ if the closed-loop gain function of the amplifier is to have a maximally flat frequency response. What are the positions of the closed-loop poles and zeros of the resulting amplifier?

5. A three-stage negative feedback amplifier is to have a low-frequency open-loop gain $T(0) = 99$. The closed-loop poles of the amplifier are required to be located at $p = -1$ and $p = (-1 \pm j\sqrt{3})/2$ so as to result in a maximally flat frequency response for the closed-loop gain function. Determine the necessary positions of the open-loop poles, and sketch the resulting root-locus diagram. What is the gain margin of the amplifier?

REFERENCES

1. ELMORE, W. C., 'The transient response of damped linear networks with particular regard to wideband amplifiers, *J. Appl. Phys.*, **19**, 55 (1948).
2. CHERRY, E. M. and HOOPER, M. E., 'The Design of Wideband Transistor Feedback Amplifiers', *Proc. I.E.E.*, **110**, 375 (1963).
3. BRUNN, G., 'Common Emitter Transistor Video Amplifier Design', *Proc. I.R.E.*, **44**, 1561 (1956).
4. FLOOD, J. E., 'Negative Feedback Amplifiers', *Wireless Engineer*, **27**, 201 (1950).
5. LYNCH, W. A., 'The Role Played by Derivative Adjustment in Broadband Amplifier Design', *Proceedings of Symposium on Modern Network Synthesis*, Polytechnic Institute of Brooklyn, New York, 192 (1952).
6. REDDI, V. G. K., 'Transistor Pulse Amplifiers', *Semiconductor Prod.*, 23 (1961).
7. REEVES, R. J. D., 'Feedback Amplifier Design', *Proc. I.E.E.*, Part IV, **99**, 383 (1952).
8. STEWART, J. L., *Circuit Theory and Design*, Wiley, New York (1956).
9. VALLEY, G. E. and WALLMAN, H., *Vacuum Tube Amplifiers*, McGraw-Hill, New York (1948).

CHAPTER 9

Operational Amplifiers

An *operational amplifier* consists basically of a high gain direct-coupled amplifier to which negative feedback is applied, and provides signal amplification in the frequency range from zero to a few hundred cycles per second. It is capable of performing the mathematical operations of differentiation and integration with respect to time, summation and multiplication by a negative constant and various combinations of these operations; hence, the name of operational amplifier.

9.1 The basic operational amplifier circuit

Consider the feedback circuit of Fig. 9.1 where the internal amplifier component provides a phase shift of 180° between its input and output voltage signals. This 180° phase shift is necessary if the applied feedback is to be negative. The input voltage $v_1(t)$ is any time function subject to the condition that it is zero for $t < 0$ and that it is Laplace transformable. $v_1(t)$ is applied to the internal amplifier through a passive two-terminal network of impedance

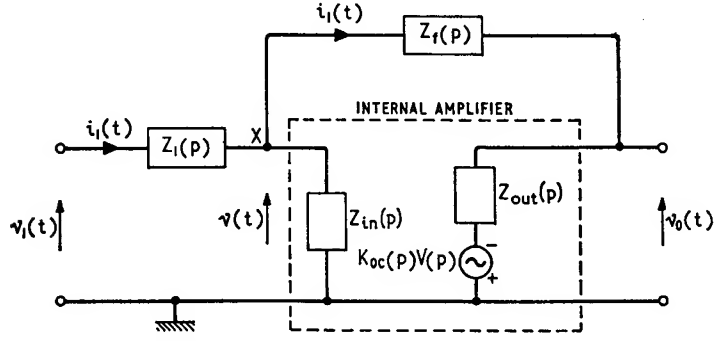

Fig. 9.1. Basic operational amplifier circuit

$Z_1(p)$. The output signal $v_2(t)$ is fed back to the input through another passive two-terminal network of impedance $Z_f(p)$.

Let it be assumed that the internal amplifier is unilateral providing signal transmission in the forward direction only, and that it has an input impedance $Z_{in}(p)$, an output impedance $Z_{out}(p)$ and an open-circuit voltage gain $K_{oc}(p)$. Then on neglecting the direct transmittance from the source to the load, we obtain the following expression for the closed-loop gain $K'(p)$ of the shunt–shunt feedback circuit of Fig. 9.1

$$K'(p) = \frac{V_0(p)}{V_1(p)}$$

$$= \frac{-Z_f(p)Z_{in}(p)K_{oc}(p)}{[Z_1(p) + Z_{in}(p)][Z_f(p) + Z_{out}(p)] + Z_1(p)Z_{in}(p)[1 + K_{oc}(p)]} \tag{9.1}$$

where $V_1(p)$ and $V_0(p)$ are the Laplace transforms of the input and output voltages $v_1(t)$ and $v_0(t)$, respectively. The minus sign in Equation 9.1 is due to the 180° phase shift associated with the internal amplifier at low frequencies.

When the input impedance $Z_{in}(p)$ is very high compared to $Z_1(p)$ and the output impedance $Z_{out}(p)$ is very small compared to the feedback impedance $Z_f(p)$, we find that Equation 9.1 reduces to

$$K'(p) \simeq \frac{-Z_f(p)K_{oc}(p)}{Z_f(p) + Z_1(p)[1 + K_{oc}(p)]} \tag{9.2}$$

If also the voltage gain of the internal amplifier is high such that, in the frequency domain, the following inequality is satisfied

$$|K_{oc}(j\omega)| \gg \left|\frac{Z_f(j\omega)}{Z_1(j\omega)}\right|$$

then Equation 9.2 simplifies further to the form

$$K'(p) = \frac{V_0(p)}{V_1(p)} \simeq -\frac{Z_f(p)}{Z_1(p)} \tag{9.3}$$

We therefore see that provided the gain of the internal amplifier on its own is very large, the closed-loop gain becomes effectively a function only of the linear passive circuit elements which constitute the input and feedback networks of Fig. 9.1.

Let $i_1(t)$ be the input current shown defined in Fig. 9.1. Then, with the input impedance of the internal amplifier assumed high, it follows that $i_1(t)$ flows on through the feedback network. Hence, if $I_1(p)$ is the Laplace transform of $i_1(t)$ and $V(p)$ is the transform of

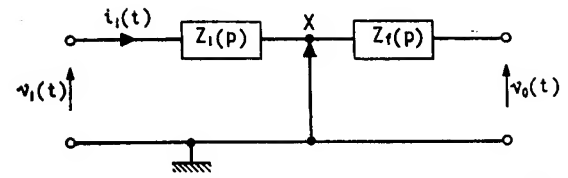

Fig. 9.2. Virtual earth in the basic operational amplifier

the voltage $v(t)$ developed at the input point X of the internal amplifier, then

$$\left.\begin{aligned} V_1(p) &= I_1(p)Z_1(p) + V(p) \\ V_0(p) &= -I_1(p)Z_f(p) + V(p) \end{aligned}\right\} \tag{9.4}$$

which, together with Equation 9.3, gives $V(p) \simeq 0$. In other words, the internal amplifier input point X is maintained virtually at earth potential. For this reason, the point X is known as a *virtual earth*. This is depicted in Fig. 9.2 where the arrow joining point X signifies the virtual earth. Notice that the input current $i_1(t)$ continues past the virtual earth.

9.2 Mathematical operations

Equation 9.3 can be re-written as follows

$$V_0(p) \simeq K'(p)V_1(p) = -\frac{Z_f(p)}{Z_1(p)}V_1(p) \tag{9.5}$$

Since $V_1(p)$ and $V_0(p)$ are the Laplace transforms of the time functions $v_1(t)$ and $v_0(t)$, it follows that $v_0(t)$ is the output signal which results when the particular operational amplifier configuration

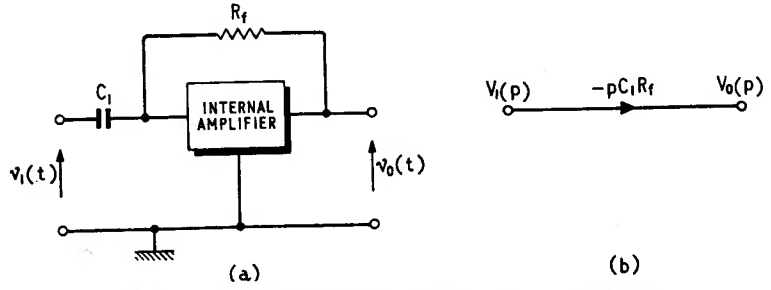

Fig. 9.3. (a) Differentiating amplifier circuit, (b) Signal flow graph representation

operates on the input signal $v_1(t)$ in the time domain. $v_0(t)$ can be determined by taking the inverse Laplace transform of $V_0(p)$ which, in turn, results when the closed-loop gain function $K'(p)$ operates on the excitation transform $V_1(p)$ in the complex frequency domain.

Using Equation 9.5, we shall next demonstrate the basic mathematical operations of differentiation, integration, scale changing (i.e. multiplication by a constant) and summation.

9.2.1 DIFFERENTIATION

In Fig. 9.3 (a), the input network consists of a capacitor C_1 and the feedback network consists of a resistor R_f. Hence, $Z_1(p) = 1/pC_1$ and $Z_f(p) = R_f$, and so Equation 9.5 gives

$$V_0(p) = -pC_1R_fV_1(p) \tag{9.6}$$

This corresponds to the signal flow graph of Fig. 9.3 (b).

Assuming that the initial value of $v_1(t)$ is zero, we have that $pV_1(p)$ is equal to the Laplace transform of $dv_1(t)/dt$ (see Section 2.2). Therefore, taking the inverse Laplace transforms of both sides of Equation 9.6, we get

$$v_0(t) = -C_1R_f\frac{dv_1(t)}{dt} \tag{9.7}$$

This means that the circuit arrangement of Fig. 9.3 (a) performs on the input signal $v_1(t)$ the operations of differentiation with respect to time and multiplication by a gain constant equal to $-C_1R_f$.

It is of interest to evaluate the frequency response of the *differentiating amplifier* of Fig. 9.3 (a). Putting $p = j\omega$ we see from Equation 9.6 that

$$\begin{aligned} K'(j\omega) &= \frac{V_0(j\omega)}{V_1(j\omega)} \\ &= -j\omega C_1R_f \end{aligned} \tag{9.8}$$

which gives the logarithmic gain in dB to be

$$20\log_{10}|K'(j\omega)| = 20\log_{10}(C_1R_f) + 20\log_{10}\omega \tag{9.9}$$

This corresponds to the gain-frequency characteristic of Fig. 9.4 (a), where we see that the gain increases at the rate of 6 dB per octave. At $\omega = 1/(C_1R_f)$, the gain is equal to zero dB. The phase angle of $K'(j\omega)$ is deduced from Equation 9.8 to be constant and equal to $-90°$ at all frequencies, as illustrated in Fig. 9.4 (b). In this diagram it is assumed that the internal amplifier component of Fig. 9.3 (a) is perfect in that it has infinite voltage gain and infinite bandwidth.

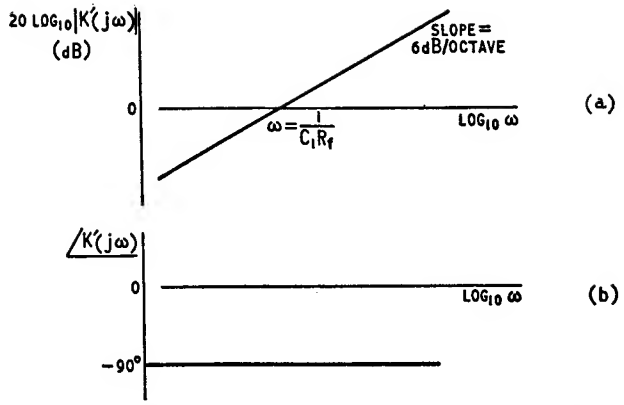

Fig. 9.4. Steady-state response of differentiating circuit, (a) gain characteristic, (b) phase angle characteristic

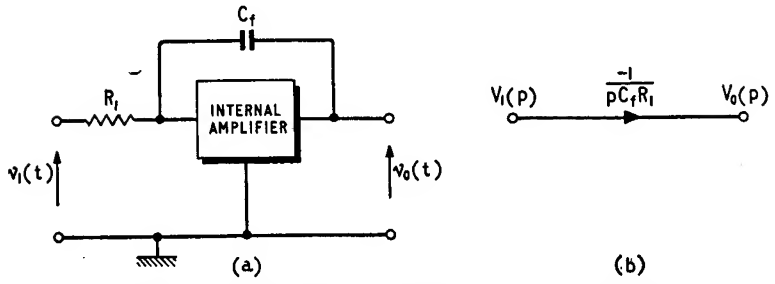

Fig. 9.5. (a) Integrating amplifier circuit, (b) Signal flow graph representation

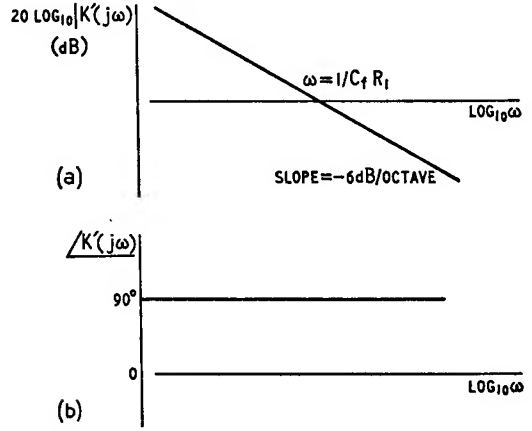

Fig. 9.6. Steady-state response of integrating amplifier: (a) gain characteristic, (b) phase angle characteristic

9.2.2 INTEGRATION

Consider next Fig. 9.5 (a) where the input network consists of a resistor R_1 and the feedback network consists of a capacitor C_f. Then, $Z_1(p) = R_1$ and $Z_f(p) = 1/pC_f$, and Equation 9.5 gives

$$V_0(p) = -\frac{1}{pC_fR_1}V_1(p) \tag{9.10}$$

The overall behaviour of the circuit of Fig. 9.5 (a) can thus be represented by the simple signal flow graph of Fig. 9.5 (b).

In section 2.2 we saw that $V_1(p)/p$ is the Laplace transform of $\int v_1(t)\,dt$ providing the initial conditions are zero. Therefore, taking the inverse Laplace transforms of both sides of Equation 9.10, we obtain

$$v_0(t) = -\frac{1}{C_fR_1}\int v_1(t)\,dt \tag{9.11}$$

This equation shows that the circuit of Fig. 9.5 (a) performs on the input signal the operations of integration with respect to time and multiplication by the gain constant of $-1/C_fR_1$.

Suppose that the input signal $v_1(t)$ is a unit-step function, that is, $v_1(t) = u_{-1}(t) = 1$ for $t > 0$. Equation 9.11 gives the corresponding output signal to be

$$v_0(t) = -\frac{1}{C_fR_1}\int dt$$

$$= -\frac{t}{C_fR_1} \tag{9.12}$$

Hence, the output signal is a linear function of time, that is, a ramp function of a slope equal to the gain constant $-1/C_fR_1$. Equation 9.12 shows that, for a prescribed accuracy of operation the larger the time constant C_fR_1 the longer is the permissible integration time t.

To determine the frequency response of the integrating circuit of Fig. 9.5 (a), we put $p = j\omega$ in Equation 9.10; then

$$K'(j\omega) = \frac{-1}{j\omega C_fR_1} \tag{9.13}$$

Evaluating the logarithmic gain in dB, we get

$$20\log_{10}|K'(j\omega)| = -20\log_{10}(C_fR_1) - 20\log_{10}\omega \tag{9.14}$$

Therefore, the gain of an *integrating amplifier* decreases at the rate of 6 dB per octave and becomes equal to zero dB at $\omega = 1/C_fR_1$ as shown in Fig. 9.6 (a). Further, from Equation 9.13 we see that the

phase angle of K' (jω) is constant and equal to $+ 90°$ as in Fig. 9.6 (b). Here again we are assuming that the internal amplifier component is perfect.

9.2.3 SCALE CHANGING

In Fig. 9.7 (a), the input and feedback networks are both resistive; thus, $Z_1(p) = R_1$ and $Z_f(p) = R_f$. From Equation 9.5, we obtain

$$V_0(p) = -\frac{R_f}{R_1} V_1(p) \tag{9.15}$$

which leads to the signal flow of graph Fig. 9.7 (b).

Taking the inverse Laplace transforms of both sides of Equation 9.15, we find that

$$v_0(t) = -\frac{R_f}{R_1} v_1(t) \tag{9.16}$$

The output signal $v_0(t)$ of Fig. 9.7 (a) is thus equal to the input signal $v_1(t)$ multiplied by the gain constant $-R_f/R_1$. A special case occurs when $R_f = R_1$, then $v_0(t) = -v_1(t)$, that is, the output signal is the negative of the input signal.

9.2.4 SUMMATION

Let the input signals $v_1(t)$ and $v_2(t)$ be applied to the internal amplifier via the resistors R_1 and R_2, respectively, as in Fig. 9.8 (a). The resistor R_f constitutes the feedback network. Since the input point of the internal amplifier is virtually at earth potential, it follows from Fig. 9.8 (a) that the input currents $i_1(t)$ and $i_2(t)$ are given by

$$\left.\begin{aligned} i_1(t) &= \frac{v_1(t)}{R_1} \\ i_2(t) &= \frac{v_2(t)}{R_2} \end{aligned}\right\} \tag{9.17}$$

Therefore, the output voltage $v_0(t)$ is

$$\begin{aligned} v_0(t) &= -R_f[i_1(t) + i_2(t)] \\ &= -\frac{R_f}{R_1} v_1(t) - \frac{R_f}{R_2} v_2(t) \end{aligned} \tag{9.18}$$

The transform of this equation can be represented by the signal

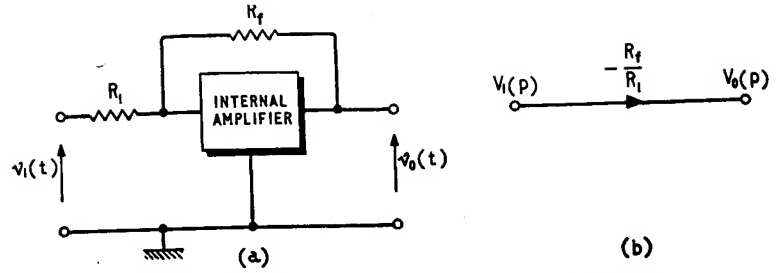

Fig. 9.7. (a) Scale changing amplifier, (b) Signal flow graph representation

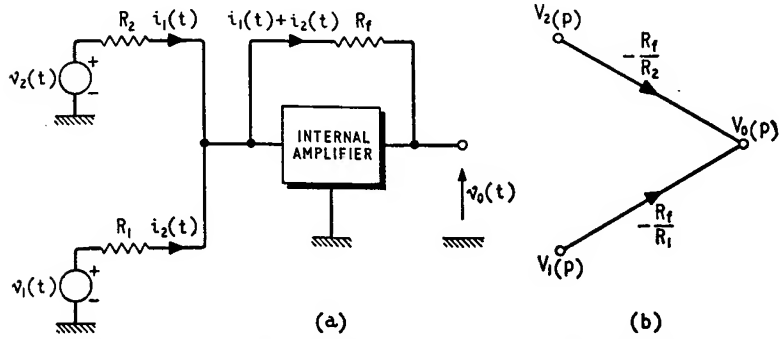

Fig. 9.8. (a) Summing amplifier with two input channels, (b) Flow graph representation

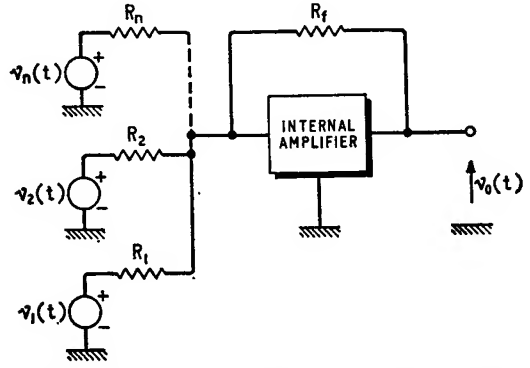

Fig. 9.9. Summing amplifier with n input channels

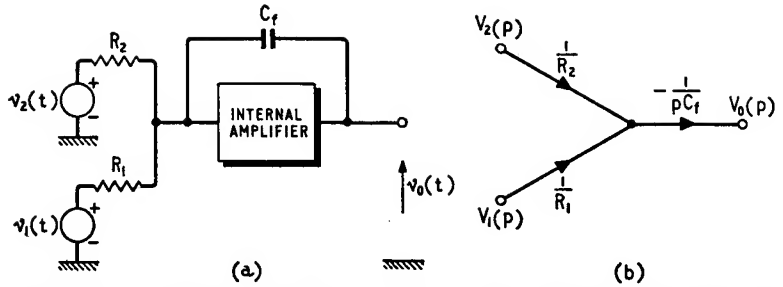

Fig. 9.10. (a) Summing integrator with two input channels, (b) Signal flow graph representation

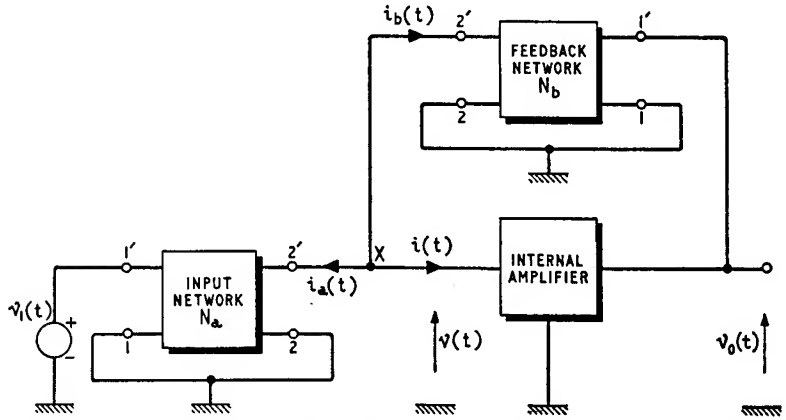

Fig. 9.11. Operational amplifier with two-port input and feedback network

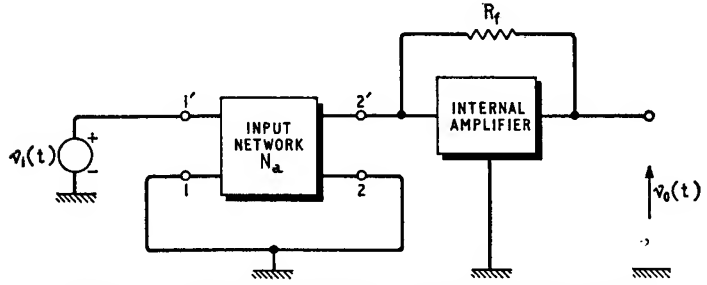

Fig. 9.12. Operational amplifier with two-port input network

flow graph of Fig. 9.8 (b). We thus see that the circuit of Fig. 9.8 (a) performs on the input signals $v_1(t)$ and $v_2(t)$ the operation of summation after multiplication with the gain constants of $-R_f/R_1$ and $-R_f/R_2$, respectively. In the general case of Fig. 9.9 having n input channels, the output voltage is given by

$$v_0(t) = -\frac{R_f}{R_1}v_1(t) - \frac{R_f}{R_2}v_2(t) - \ldots - \frac{R_f}{R_n}v_n(t) \qquad (9.19)$$

For the special case of $R_f = R_1 = R_2 = \ldots = R_n$ we have

$$v_0(t) = -v_1(t) - v_2(t) - \ldots - v_n(t)$$

$$= -\sum_{k=1}^{n} v_k(t) \qquad (9.20)$$

This corresponds to the operation of summation with 180° phase shift.

An extension of the *summing amplifier* of Fig. 9.8 (a) leads to the *summing integrator* shown in Fig. 9.10 (a) where the transform $V_0(p)$ of the output voltage is given by

$$V_0(p) = -\frac{1}{pC_fR_1}V_1(p) - \frac{1}{pC_fR_2}V_2(p) \qquad (9.21)$$

This equation corresponds to the signal flow graph of Fig. 9.10 (b) where we see that each input signal is multiplied by its own gain constant, with the sum appearing at the output. When $R_1 = R_2$ the output voltage $v_0(t)$ becomes proportional to the integral of the sum of the input voltages $v_1(t)$ and $v_2(t)$.

9.3 Operational amplifiers with two-port input and feedback networks

Consider the operational amplifier of Fig. 9.11 where the input and feedback networks are both two-port networks each having one input and one output terminal earthed. If the voltage gain of the internal amplifier is high, then the applied negative feedback will cause the internal amplifier input point X to be virtually at earth potential. Therefore, the output ports 2,2′ of both the input and feedback networks are effectively short-circuited such that if $y_{21a}(p)$ is the forward short-circuit transfer admittance of the input network N_a and $y_{12b}(p)$ is the reverse short-circuit transfer admittance of the feedback network N_b, we have

$$y_{21a}(p) = \left[\frac{I_a(p)}{V_1(p)}\right]_{V(p)=0} \qquad (9.22)$$

$$y_{12b}(p) = \left[\frac{I_b(p)}{V_0(p)}\right]_{V(p)=0} \tag{9.23}$$

where $I_a(p)$, $I_b(p)$, $V_1(p)$, $V(p)$ and $V_0(p)$ are the Laplace transforms of $i_a(t)$, $i_b(t)$, $v_1(t)$, $v(t)$ and $v_0(t)$, respectively. The condition $V(p) = 0$ is closely satisfied in practice because as explained earlier, $v(t) \simeq 0$ in the circuit arrangement of Fig. 9.11.

Assuming that the input impedance of the internal amplifier is very high, we have $i(t) \simeq 0$ and accordingly

$$i_a(t) \simeq -i_b(t) \tag{9.24}$$

Taking the Laplace transforms of both sides of this equation gives

$$I_a(p) \simeq -I_b(p) \tag{9.25}$$

Therefore, using Equations 9.22, 9.23 and 9.25 to evaluate the closed-loop gain $K'(p)$, we get

$$K'(p) = \frac{V_0(p)}{V_1(p)} \simeq -\frac{y_{21a}(p)}{y_{12b}(p)} \tag{9.26}$$

This relationship is a generalisation of Equation 9.3.

The following two cases can be of interest:

(a) The input network is a two-port network and the feedback network consists of a resistor R_f as in Fig. 9.12. Here we see that $y_{12b}(p) = -1/R_f$ and Equation 9.26 becomes

$$\frac{V_0(p)}{V_1(p)} \simeq R_f y_{21a}(p) \tag{9.27}$$

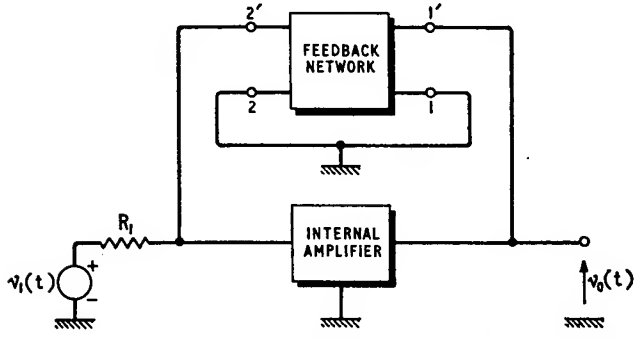

Fig. 9.13. Operational amplifier with two-port feedback network

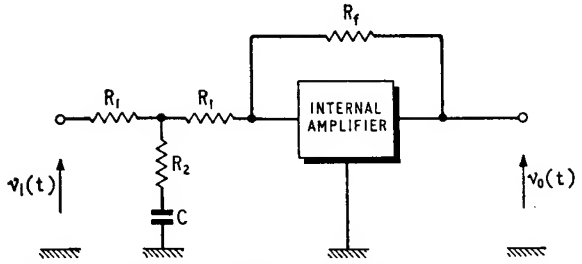

Fig. 9.14. Operational amplifier with an RC two-port input network

This means that the poles and zeros of the closed-loop gain function of Fig. 9.12 are the same as the poles and zeros of $y_{21a}(p)$, respectively.

(b) The input network consists of a resistor R_1 and the feedback network is a two-port network, as in Fig. 9.13. Then, $y_{21a}(p) = -1/R_1$ and Equation 9.26 gives

$$\frac{V_0(p)}{V_1(p)} \simeq \frac{1}{R_1 y_{12b}(p)} \tag{9.28}$$

Here, the poles and zeros of the closed-loop gain function are the same as the zeros and poles of $y_{12b}(p)$, respectively.

9.3.1 EXAMPLE

As an illustration, consider the operational amplifier of Fig. 9.14. Analysis of the input two-port network shows that

$$y_{21a}(p) = -\frac{1}{2R_1}\frac{1 + pCR_2}{1 + pC(R_2 + R_1/2)} \tag{9.29}$$

Combining Equations 9.27 and 9.29, we get

$$\frac{V_0(p)}{V_1(p)} \simeq -\frac{R_f}{2R_1}\frac{1 + pCR_2}{1 + pC(R_2 + R_1/2)} \tag{9.30}$$

We therefore see that by using a single operational amplifier in Figs. 9.11 to 9.13, it is possible to perform relatively complicated operations.

9.4 Some practical considerations

In practice, we find that an operational amplifier can perform satisfactorily only when the input signal level is limited to within a

specified range of values. Outside this range the amplifier can become overloaded with the result that there no longer exists a true correspondence between the applied input signal and the resulting output signal Thus, in the case of a differentiating amplifier overloading can occur due to two major causes. First, the output of such an operational amplifier is proportional to the rate of change of the input signal, which if it is too fast, can produce an output signal that is large enough to overload the amplifier. Second, the closed-loop gain of a differentiating amplifier increases with increasing frequency (see Fig. 9.4 (a)). Therefore, any high frequency noise component contaminating the input signal may become amplified sufficiently to overload the amplifier. For these reasons differentiating amplifiers are avoided in practice wherever possible.

In the case of an integrating amplifier subjected to an input step function, the resulting output signal will be a ramp function. If the output signal is allowed to persist for a long period of time, then it can eventually cause the amplifier to become overloaded. Therefore, when using an integrating amplifier it is necessary to limit the integration time so as not to overload the amplifier.

9.5 Transfer function simulation

One of the most important applications of operational amplifiers is in the *simulation* of transfer functions. In this respect, it is found convenient to develop first a signal flow graph representing the given transfer function. Then, the flow graph is modified, if necessary, in such a way that it can be transformed directly into an equivalent system, termed the *simulator*, involving a number of operational amplifiers. However, in the formulation of an acceptable signal flow graph we must remember that: (1) the signal flow graph should not involve any branch with a transmittance proportional to $-p$ so as to avoid performing the operation of differentiation for

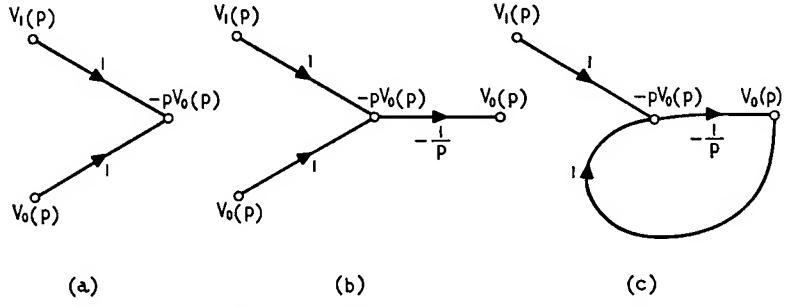

Fig. 9.15. Signal flow graphs for Equation 9.33

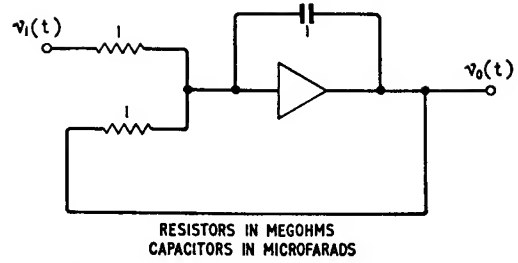

Fig. 9.16. Simulator for simple pole factor

reasons explained above. (2) Any operation performed by an operational amplifier is always accompanied by a minus sign; hence, any branch of the flow graph with a minus sign necessitates the use of a corresponding operational amplifier in the final simulator.

9.5.1 SIMPLE POLE FACTOR

For our first illustration, we shall simulate a transfer function having one simple pole at -1; thus let

$$\frac{V_0(p)}{V_1(p)} = \frac{-1}{p+1} \tag{9.31}$$

where $V_0(p)$ and $V_1(p)$ are the Laplace transforms of the input signal $v_1(t)$ and output signal $v_0(t)$, respectively. Assuming that the initial conditions are zero, the transfer function of Equation 9.31 corresponds to the first order differential equation

$$\frac{dv_0(t)}{dt} + v_0(t) = -v_1(t) \tag{9.32}$$

To avoid the use of a differentiating amplifier, we shall re-write Equation 9.31 with only $pV_0(p)$, that is, the transform of the first derivative of $v_0(t)$ on the left hand side. This leads to

$$-pV_0(p) = V_1(p) + V_0(p) \tag{9.33}$$

which can be represented by the partial signal flow graph of Fig. 9.15 (a). Next, we add the branch representing the auxiliary relationship $V_0(p) = (-1/p)[-pV_0(p)]$ as in Fig. 9.15 (b). Here we see that the common nodes $V_0(p)$ can be coalesced; when this is done, the signal flow graph modifies to the form shown in Fig. 9.15 (c). The latter signal flow graph can be transformed directly into the simulator of Fig. 9.16 where, for convenience, we have

used —▷— to symbolise the internal amplifier component of the operational amplifier. In the simulator of Fig. 9.16 it should be noted that the resistors are in terms of megohms and the capacitors are in terms of microfarads. Time t is in seconds.

9.5.2 SECOND ORDER POLE FACTOR

Consider next the simulation of a transfer function having two poles and no finite zeros; thus

$$\frac{V_0(p)}{V_1(p)} = \frac{-1}{p^2 + 2\zeta p + 1} \tag{9.34}$$

This corresponds to the following second order differential equation

$$\frac{d^2v_0(t)}{dt^2} + 2\zeta\frac{dv_0(t)}{dt} + v_0(t) = -v_1(t) \tag{9.35}$$

where the initial conditions are assumed to be zero.

Again to avoid the use of differentiating amplifiers, we shall

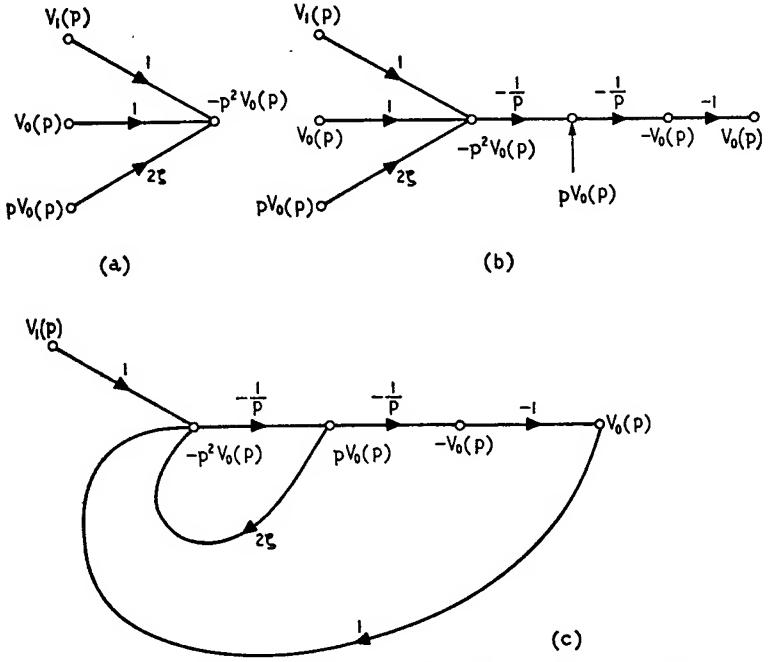

Fig. 9.17. Signal flow graph representations of Equation 9.36

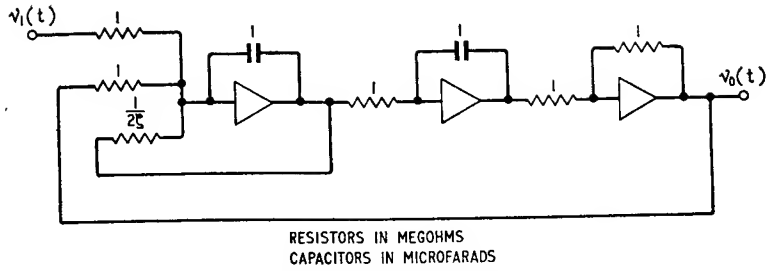

Fig. 9.18. Simulation of second order pole factor

re-write Equation 9.34 with only $p^2V_0(p)$, that is, the transform of the second derivative of $v_0(t)$ on the left hand side. We thus get

$$-p^2V_0(p) = V_1(p) + V_0(p) + 2\zeta pV_0(p) \tag{9.36}$$

This leads to the partial signal flow graph of Fig. 9.17 (a). To this diagram, we next add branches representing the auxiliary relationships

$$pV_0(p) = -\frac{1}{p}[-p^2V_0(p)] \tag{9.37}$$

and

$$V_0(p) = \left(-\frac{1}{p}\right)(-1)[pV_0(p)] \tag{9.38}$$

The result is shown in Fig. 9.17 (b). If the common nodes at $pV_0(p)$ and $V_0(p)$ are coalesced, then we shall obtain the modified signal flow graph of Fig. 9.17 (c) which can be realised directly by the simulator of Fig. 9.18.

In both the simulators of Figs. 9.16 and 9.18 we have assumed that the initial conditions are zero. If, however, this is not the case, then we can introduce the specified initial conditions simply by placing an appropriate charge on the feedback capacitor of the integrator in the particular simulator set up.

9.5.3 TRANSPORT DELAY

A system is said to exhibit a true *transport delay* when it satisfies the following equation

$$v_0(t) = v_1(t - \tau) \tag{9.39}$$

where τ is the delay. Equation 9.39 states that to obtain the output signal $v_0(t)$, we replace t by $t - \tau$ wherever it appears in the

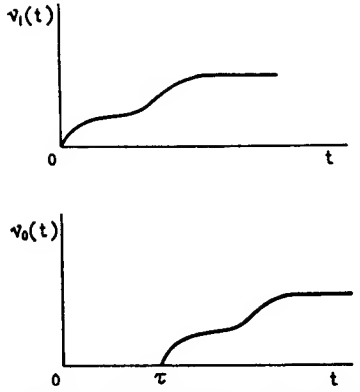

Fig. 9.19. Illustrating true transport delay

expression for the input signal $v_1(t)$. Hence, if the input signal is zero for $t < 0$, it follows that the output signal remains identically zero for $t < \tau$, as in Fig. 9.19.

Taking the Laplace transforms of both sides of Equation 9.39 and making use of the shifting theorem (see Section 2.2), then

$$\frac{V_0(p)}{V_1(p)} = e^{-\tau p} \tag{9.40}$$

It is instructive to examine the frequency response of this transfer function. Replacing p with $j\omega$ gives

$$\frac{V_0(j\omega)}{V_1(j\omega)} = e^{-j\omega\tau} \tag{9.41}$$

Evaluating the magnitude and phase angle, we obtain

$$\left.\begin{aligned} \left|\frac{V_0(j\omega)}{V_1(j\omega)}\right| &= 1 \\ \angle\frac{V_0(j\omega)}{V_1(j\omega)} &= -\omega\tau \end{aligned}\right\} \tag{9.42}$$

We therefore see that the frequency response of a linear system exhibiting a true transport delay shows no attenuation and a linear phase angle characteristic. Such a frequency response can be satisfied only by a lossless transmission line.

The transcendental function of Equation 9.40 can be approximated by a second order Pade type of rational function as follows[1]

$$\frac{V_0(p)}{V_1(p)} \simeq \frac{\tau^2p^2 - 6\tau p + 12}{\tau^2p^2 + 6\tau p + 12} \tag{9.43}$$

which is recognised to be an all-pass transfer function having two zeros at $p = (3 \pm j\sqrt{3})/\tau$ and two poles at $p = (-3 \pm j\sqrt{3})/\tau$. Putting $p = j\omega$, we get

$$\frac{V_0(j\omega)}{V_1(j\omega)} \simeq \frac{\omega^2\tau^2 + j6\omega\tau - 12}{\omega^2\tau^2 - j6\omega\tau - 12} \tag{9.44}$$

The magnitude of this transfer function is equal to unity as required. The phase angle equals $2\tan^{-1}[6\omega\tau/(\omega^2\tau^2 - 12)]$ which is shown plotted in Fig. 9.20. The maximum value of $\omega\tau$ for a one-degree error in phase is equal to 1.7 radians.

To simulate the approximating function of Equation 9.43, we first re-write it in the following form

$$\begin{aligned} &\tau^2p^2V_0(p) + 6\tau pV_0(p) + 12V_0(p) \\ &\qquad = \tau^2p^2V_1(p) - 6\tau pV_1(p) + 12V_1(p) \end{aligned} \tag{9.45}$$

Dividing both sides of this equation by τ^2p^2 and re-arranging

$$\begin{aligned} V_0(p) &= V_1(p) - \frac{6}{p\tau}[V_1(p) + V_0(p)] + \frac{12}{p^2\tau^2}[V_1(p) - V_0(p)] \\ &= V_1(p) - \frac{6}{p\tau}\left[V_1(p) + V_0(p) - \frac{2}{p\tau}[V_1(p) - V_0(p)]\right] \end{aligned} \tag{9.46}$$

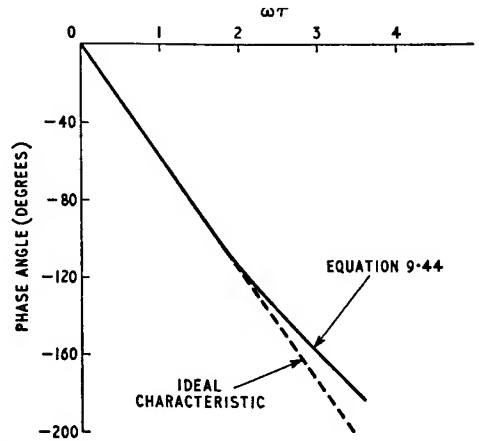

Fig. 9.20. Approximation to ideal transport delay characteristic

This equation can be represented by the signal flow graph of Fig. 9.21 (a). If the common nodes at $V_1(p)$, $V_0(p)$ and $-V_0(p)$ are coalesced, we obtain the modified signal flow graph of Fig. 9.21 (b) which we can simulate by the set up of Fig. 9.22. Here again the resistors are in megohms and the capacitors are in microfarads.

9.5.4 TIME SCALING

When simulating a transfer function, or solving a differential equation, by means of operational amplifiers it is usually found that, for convenience, a certain time scaling is necessary. The 'time scale' is simply the proportionality ratio between the 'simulator time' and the 'real time' which takes the actual event, being simulated, to occur. Thus a time scale of a means that a seconds of simulator time correspond to one second of real time. In certain applications we may have to slow down the event by choosing $a > 1$, while in other cases we may find it necessary to speed up the event by choosing $a < 1$.

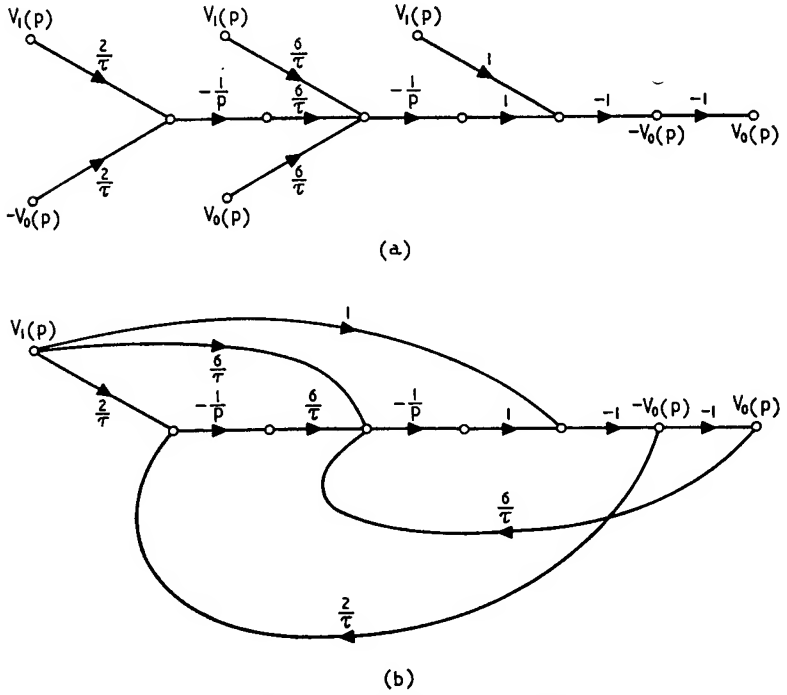

Fig. 9.21. Flow graph representations of Equation 9.46

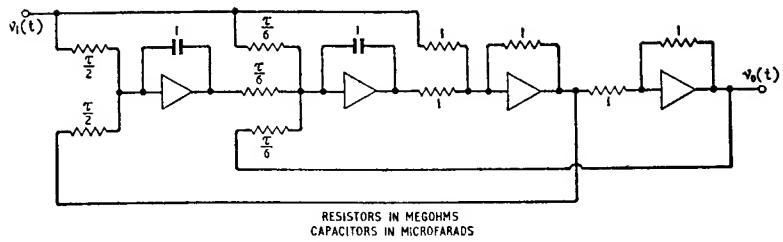

Fig. 9.22. Simulator for Equation 9.43

Let t denote real time and t' denote simulator time; then we have

$$t' = at$$

Remembering that differentiation (i.e. $\mathrm{d}/\mathrm{d}t$) in real time is equivalent to multiplication by the complex frequency variable p, we find that

$$p = ap'$$

where $p' \equiv \mathrm{d}/\mathrm{d}t'$ denotes differentiation in simulator time.

Now in each of the transfer functions of Equations 9.10, 9.21 and 9.30 we see that, whenever an operational amplifier involves a capacitor, the variable p is always multiplied by the product of a resistance and a capacitance. Therefore, if C and R refer to capacitance and resistance values in real time, C' and R' refer to the corresponding capacitance and resistance values in simulator time, and if we demand that $pCR = p'C'R'$ and $p = ap'$, then it follows that the time constant CR in real time must equal $C'R'/a$ in simulator time. This means that when the simulator set up uses the integrator of Fig. 9.5, we can realise a specified time scale a by multiplying the capacitor C_f or resistor R_1 by the factor a.

Similarly, when the simulator involves a more complex operational amplifier as that of Fig. 9.14, we see from Equation 9.30 that in order to introduce a time scale a we can either multiply the capacitor C by the factor a or else multiply each of the resistors R_1 and R_2 by a. If, however, we decide to change the input resistors R_1 and R_2, then from Equation 9.30 we see that the feedback resistor R_f must be also changed in exactly the same ratio so as to ensure that the d.c. gain of the operational amplifier of Fig. 9.14, which is equal to $-R_f/2R_1$, remains unchanged as a result of the time scaling.

9.6 Error analysis

The operational amplifier is, in practice, associated with unavoidable errors arising from a number of different sources. The combined

effect of these error sources is to cause the performance of a practical operational amplifier to deviate from the idealised performance considered up till now. The errors are principally due to the following factors:

(1) The operational amplifier is required to respond to input d.c. levels as well as changes in these levels; accordingly it is necessary to directly couple the various stages which make up the internal amplifier component. A major problem encountered in the design of d.c. amplifiers is that of *drift* caused by changes in the d.c. operating conditions of the amplifier, the changes arising from variations in the supply voltage, ambient temperature, etc. Drift affects the performance of a d.c. amplifier because it is incapable of distinguishing between a drift voltage and a change in the input d.c. signal.

To evaluate the effects of drift, consider Fig. 9.23 where the voltage source $V_d(p)$, connected in series with the input of the internal amplifier, represents the *equivalent drift voltage*. It is equal to the change in output voltage solely due to drift voltages divided by the overall voltage gain of the internal amplifier. Assuming that this amplifier has a high input impedance, a low output impedance and a high voltage gain, we find that the output voltage $V_0(p)$ produced by the combined effects of the externally applied input voltage $V_1(p)$ and the equivalent drift voltage $V_d(p)$ is given by

$$V_0(p) = -\frac{Z_f(p)}{Z_1(p)}V_1(p) + \left[1 + \frac{Z_f(p)}{Z_1(p)}\right]V_d(p) \qquad (9.47)$$

From this equation we see that for a satisfactory performance it is essential to minimise the contribution of the equivalent drift voltage $V_d(p)$. Various techniques have been developed for achieving this, in practice; a particular method that is widely used is the *chopper stabilised d.c. amplifier* developed by E. A. Goldberg[2].

From Equation 9.47 we see also that in order to keep low the output voltage due to drift, it is desirable to have the impedance $Z_1(p)$ high compared to the feedback impedance $Z_f(p)$.

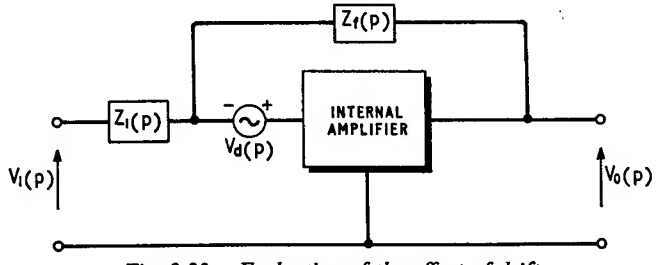

Fig. 9.23. Evaluation of the effect of drift

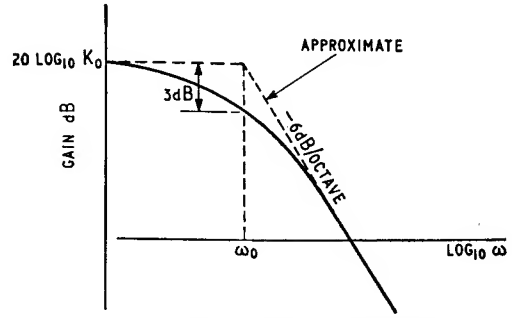

Fig. 9.24. Gain-frequency characteristic

(2) The second major source of error in operational amplifiers is the finite value of the open-circuit voltage gain $K_{oc}(p)$ the magnitude and phase angle of which vary with frequency. To evaluate this effect let us replace the gain $K_{oc}(p)$ in Equation 9.2 by the approximate expression

$$K_{oc}(p) \simeq \frac{K_0}{1 + p/\omega_0} \qquad (9.48)$$

which corresponds to a d.c. amplifier having the gain-frequency characteristic of Fig. 9.24. At high frequencies most operational amplifiers cut off more rapidly than the — 6 dB per octave rate shown in Fig. 9.24. But as far as error analysis is concerned, the approximation of Equation 9.48 is quite adequate. The complete frequency response of the amplifier need only be considered when investigating the stability performance of the operational amplifier.

Using Equations 9.2 and 9.48 we get

$$K'(p) = \frac{V_0(p)}{V_1(p)} = \frac{-Z_f(p)}{Z_1(p) + \frac{1}{K_0}\left(1 + \frac{p}{\omega_0}\right)[Z_1(p) + Z_f(p)]} \qquad (9.49)$$

As an illustration consider the case of a scale changer for which we have $Z_1(p) = R_1$ and $Z_f(p) = R_f$. Then noting that normally $K_0 \gg 1$, we find that for a scale changer Equation 9.49 gives

$$\frac{V_0(p)}{V_1(p)} \simeq -\frac{R_f}{R_1}\frac{1}{1 + \frac{p}{\omega_0 K_0}\left(1 + \frac{R_f}{R_1}\right)} \qquad (9.50)$$

which shows that the effective cut-off frequency of a scale changer is equal to $\omega_0 K_0 R_1/(R_1 + R_f)$. To make this cut off frequency assume a high value, the resistance R_1 should be large compared with R_f, ω_0 should be high and K_0 should be large.

9.7 Some considerations of the stability problem

An operational amplifier, like any other high gain amplifier to which negative feedback is applied, can become unstable and therefore break into oscillation unless special precautions are taken

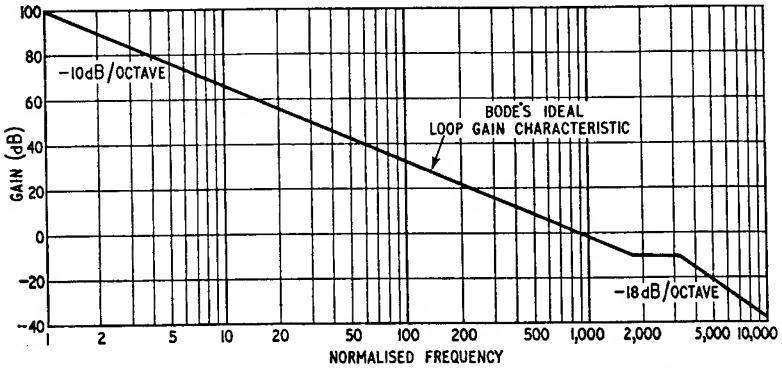

Fig. 9.25. Loop gain characteristic of operational amplifier

in shaping its open-loop response up to frequencies well beyond the useful frequency range of the amplifier. Assuming the input impedance of the internal amplifier component to be high and its output impedance to be low, we find that the open-loop gain of the basic operational amplifier circuit of Fig. 9.1 is

$$T(p) = \frac{Z_1(p) \cdot K_{oc}(p)}{Z_1(p) + Z_f(p)} \tag{9.51}$$

Consider first the case of a scale changer having $Z_1(p) = R_1$ and $Z_f(p) = R_f$; for these conditions Equation 9.51 gives

$$T(p) = \frac{R_1 K_{oc}(p)}{R_1 + R_f} \tag{9.52}$$

Here we see that the frequency dependence of the open-loop response is determined principally by the gain-frequency characteristic of the internal amplifier. Further, the open-loop gain has its maximum low frequency value when the feedback resistor R_f is small compared to the input resistor R_1; then we have $T(p) \simeq K_{oc}(p)$.

As an illustration suppose that the low frequency value K_0 of the gain $K_{oc}(p)$ is equal to 10^5, which corresponds to a voltage gain of 100 dB. Also let it be required to realise a phase margin of 30° and a gain margin of 10 dB. Then for the special case of R_f small compared to R_1, we deduce from Bode's ideal loop gain considerations that the gain-frequency characteristic of the internal amplifier should be shaped to follow the form shown in Fig. 9.25. It is assumed that the internal amplifier has a final asymptote of −18 dB per octave slope. We can approximate to the ideal characteristic of Fig. 9.25 by the addition of suitable interstage shaping networks to the internal amplifier, as discussed in Section 6.2.

If the useful frequency range of the amplifier is required to extend up to 100 c/s (say), then from Fig. 9.25 we see that it is necessary to control the shaping of the amplifier frequency response up to 325 kc/s, at least, so as to realise the required high value of low frequency open-loop gain and the stability margins. This clearly shows why high gain operational amplifiers can perform satisfactorily up to only a few hundred cycles per second.

Consider next the case of an integrator having $Z_1(p) = 1/R_1$ and $Z_f(p) = 1/pC_f$. Then Equation 9.51 gives

$$T(p) = \frac{K_{oc}(p)}{1 + 1/pC_fR_1} \tag{9.53}$$

At frequencies high compared to $1/C_fR_1$ we have $T(p) \simeq K_{oc}(p)$ The inclusion of the feedback capacitor C_f causes the open-loop response to fall off at the rate of − 6 dB per octave at very low frequencies. However, such a rate of fall off is not large enough to produce instability at very low frequencies irrespective of the value of $K_{oc}(p)$ at zero frequency. We therefore see that the stability performance of the integrator is also determined by the gain-frequency characteristic of the internal amplifier.

PROBLEMS

1. Show that the circuit of Fig. 9.26 can be so designed that the potential of point X does not deviate appreciably from that of earth. Derive the necessary conditions.

   Show how the circuit may be modified to obtain an output voltage approximating closely to the integral with respect to time of the input voltage.

   What are the desirable features of an amplifier for use in an analogue computer? Why are integrating circuits preferred to differentiating circuits in such a computer?

   (London University, B.Sc. Eng., Part III, Electronics, 1963).
2. Determine the transfer function $V_2(p)/V_1(p)$ for each of the simulators shown in Fig. 9.27.

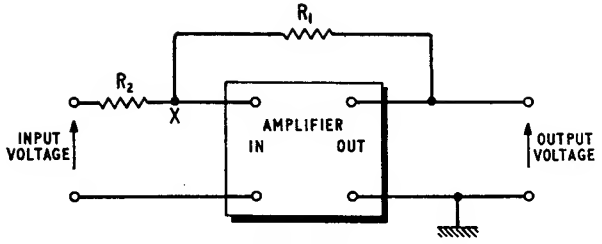

Fig. 9.26

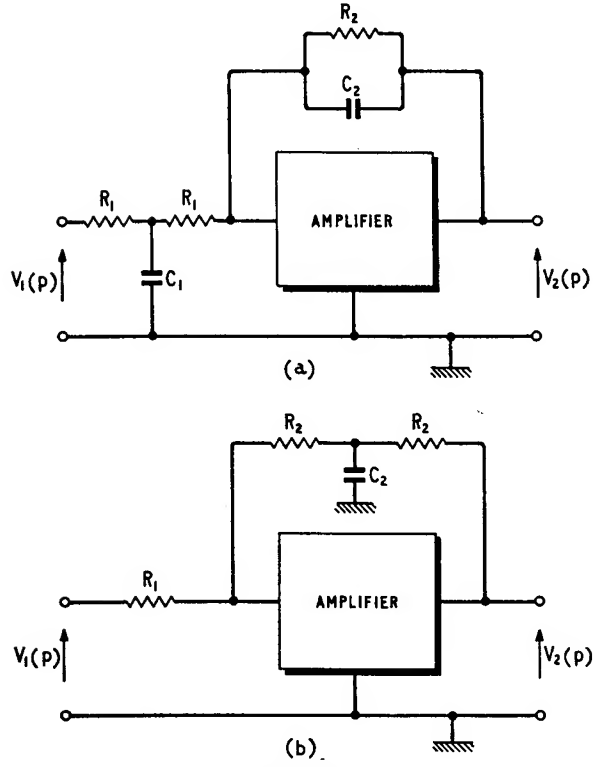

Fig. 9.27

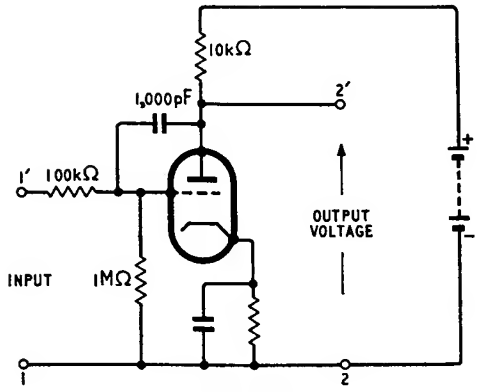

Fig. 9.28

3. A unit-step function is applied to the input port of the *Blumlein integrator* of Fig. 9.28. The triode has the parameters $g_m = 3\text{mA/V}$ and $r_a = 10\ \text{k}\Omega$. Determine the output voltage as a function of time, assuming that the cathode by-pass capacitor is large enough to have negligible effect.
4. Simulate the following transfer functions, giving values of resistors and capacitors in each computer set up:

$$\text{(a)}\ \frac{V_2(p)}{V_1(p)} = \frac{5(p+10)}{p+5}$$

$$\text{(b)}\ \frac{V_2(p)}{V_1(p)} = \frac{(p+2)}{(p+1)(p+3)}$$

5. A feedback amplifier with a purely resistive feedback network has the open-loop gain function

$$T(p) = \frac{9}{(1+p)^2}$$

The closed-loop gain is equal to 10 at zero frequency. Determine the closed-loop gain function of the feedback amplifier, and simulate it with a computer set up complete with component values.

6. Show that for the operational amplifier circuit of Fig. 9.29

$$\frac{V_0(p)}{V_1(p)} = \frac{-R_2/R_1}{a_2p^2 + a_1p + 1}$$

where

$$a_1 = \frac{C_2}{R_1}(R_2R_3 + R_3R_1 + R_1R_2)$$

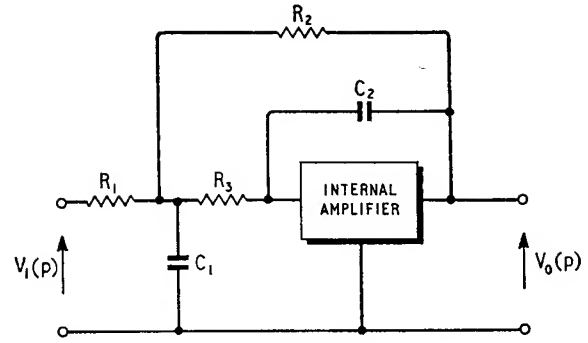

Fig. 9.29

$$a_2 = R_2R_3C_1C_2$$

Hence using Fig. 9.29 simulate a second order system having the following transfer function

$$\frac{V_0(p)}{V_1(p)} = \frac{-1}{p^2 + 2\zeta p + 1}$$

assuming that $R_1 = R_2$, $C_1 = 1\mu F$ and $C_2 = (\zeta^2/2)$.

REFERENCES

1. TRUXAL, J. G., *Automatic Feedback Control System Synthesis*, McGraw-Hill, New York (1955).
2. GOLDBERG, E. A., 'Stabilisation of d.c. amplifiers', *R.C.A. Review*, **2**, 296 (1950).
3. CHESTNUT, H., and MAYER, R. W., *Servomechanisms and Regulating System Design*, Vol. 1, Wiley, New York (1959), Second Edition.
4. KONISBERG, R. L., 'Operational Amplifiers', *Advan. Electron. Electron Phys.* **11**, 225 (1959).
5. KORN, G. A., and KORN, T. M., *Electronic Analog Computers*, McGraw-Hill, New York (1956), Second Edition.
6. WASS, C. A. A., *Introduction to Electronic Analogue Computers*, Pergamon Press (1955).
7. WILLIAMS, F. C., and MOODY, N. F., 'Ranging Circuits, Linear Time Base Generators and Associated Circuits', *J.I.E.E.*, Part IIIA, **93**, 1181 (1946).

CHAPTER 10

Feedback Oscillators

In the design of a negative feedback amplifier one of the principal objectives is to ensure that the amplifier will remain stable under all possible operating conditions. On the other hand, when a feedback circuit is required to function as an oscillator, positive feedback is applied and the elements of the feedback network component are purposely chosen to produce instability. Consequently, as soon as the d.c. power supply is switched on, the amplitude of the resulting oscillations will progressively increase until it becomes limited by the inherent non-linearities of the active elements constituting the amplifier component of the oscillator.

There are various types of feedback oscillators differing from each other in the type of feedback network and details of the amplifier used. Thus some feedback networks have reverse voltage transfer functions with 180° phase shift at or near the frequency of oscillation, and must therefore be used in conjunction with an amplifier whose voltage gain also has a 180° phase shift so as to produce the required positive feedback. In such cases it is normally found that a single common cathode or common emitter amplifier is quite satisfactory. It is also possible to construct an oscillator by means of an amplifier and a feedback network both of which have zero phase shifts at or near the frequency of oscillation.

However, before going on to the study of specific oscillator circuits, let us first develop general formulae for determining the frequency of oscillation and condition for oscillation.

10.1 Generalised oscillator circuit

A feedback oscillator consists basically of an amplifier and a feedback network coupled together in the manner shown in Fig. 10.1. Assuming that the feedback loop is broken, we find that the voltage V_1 and current I_1 at the port 1,1′ are related to the voltage V_2 and current I_2 at the port 2,2′ by

$$\begin{bmatrix} V_1 \\ I_1 \end{bmatrix} = \begin{bmatrix} a_{11} & a_{12} \\ a_{21} & a_{22} \end{bmatrix} \begin{bmatrix} V_2 \\ -I_2 \end{bmatrix} \tag{10.1}$$

where a_{11}, a_{12}, a_{21} and a_{22} are elements of the overall a-matrix of the amplifier and feedback network connected in tandem. In Fig. 10.1 we see that the whole of the signal developed at the port 2,2′ is fed back to the port 1,1′; therefore

$$\begin{bmatrix} V_2 \\ -I_2 \end{bmatrix} = \begin{bmatrix} V_1 \\ I_1 \end{bmatrix} \tag{10.2}$$

Eliminating the column matrix $\begin{bmatrix} V_2 \\ -I_2 \end{bmatrix}$ between Equations 10.1 and 10.2, we get

$$\begin{bmatrix} V_1 \\ I_1 \end{bmatrix} = \begin{bmatrix} a_{11} & a_{12} \\ a_{21} & a_{22} \end{bmatrix} \begin{bmatrix} V_1 \\ I_1 \end{bmatrix}$$

which, in turn, leads to

$$\begin{bmatrix} a_{11} - 1 & a_{12} \\ a_{21} & a_{22} - 1 \end{bmatrix} \begin{bmatrix} V_1 \\ I_1 \end{bmatrix} = 0 \tag{10.3}$$

Equation 10.3 has a non-trivial solution $\begin{bmatrix} V_1 \\ I_1 \end{bmatrix}$ if and only if the determinant of the square matrix $\begin{bmatrix} a_{11} - 1 & a_{12} \\ a_{21} & a_{22} - 1 \end{bmatrix}$ is zero, that is

$$\begin{vmatrix} a_{11} - 1 & a_{12} \\ a_{21} & a_{22} - 1 \end{vmatrix} = 0 \tag{10.4}$$

Expanding this determinant, we have

$$\Delta_a + 1 - a_{11} - a_{22} = 0 \tag{10.5}$$

where

$$\Delta_a = a_{11}a_{22} - a_{12}a_{21} \tag{10.6}$$

Equation 10.5 is the characteristic equation of the oscillator circuit; it determines the frequency of oscillation and the necessary condition for oscillation.

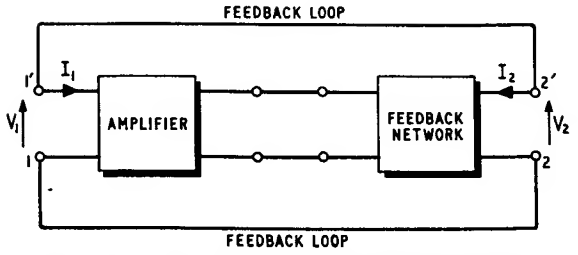

Fig. 10.1. Block diagram of generalised oscillator

Now in Section 2.5.3 we showed that the overall a-matrix of any two-port networks connected in cascade is equal to the product of the a-matrices of the individual networks. Therefore, if a_{11}', a_{12}', a_{21}' and a_{22}' denote the elements of the a-matrix of the oscillator's amplifier component, and a_{11}'', a_{12}'', a_{21}'' and a_{22}'' denote the elements of the a-matrix of the feedback network, we find that the overall a-matrix of these two networks connected in cascade is given by

$$\begin{bmatrix} a_{11} & a_{12} \\ a_{21} & a_{22} \end{bmatrix} = \begin{bmatrix} a_{11}' & a_{12}' \\ a_{21}' & a_{22}' \end{bmatrix} \begin{bmatrix} a_{11}'' & a_{12}'' \\ a_{21}'' & a_{22}'' \end{bmatrix} \tag{10.7}$$

Expanding the matrix product, we have

$$\begin{bmatrix} a_{11} & a_{12} \\ a_{21} & a_{22} \end{bmatrix} = \begin{bmatrix} (a_{11}'a_{11}'' + a_{12}'a_{21}'') & (a_{11}'a_{12}'' + a_{12}'a_{22}'') \\ (a_{21}'a_{11}'' + a_{22}'a_{21}'') & (a_{21}'a_{12}'' + a_{22}'a_{22}'') \end{bmatrix} \tag{10.8}$$

The determinant Δa of this overall a-matrix can be shown to have the value

$$\Delta a = \Delta a' \Delta a'' \tag{10.9}$$

where

$$\left.\begin{aligned} \Delta a' &= a_{11}'a_{22}' - a_{12}'a_{21}' \\ \Delta a'' &= a_{11}''a_{22}'' - a_{12}''a_{21}'' \end{aligned}\right\} \tag{10.10}$$

A special case of practical importance occurs when the amplifier component of the oscillator circuit is unilateral or exhibits negligible internal feedback. Then the determinant $\Delta a'$ of its a-matrix becomes equal to zero, and the characteristic Equation 10.5 correspondingly reduces to

$$1 - a_{11} - a_{22} = 0 \tag{10.11}$$

which, together with Equation 10.8 gives

$$1 - (a_{11}'a_{11}'' + a_{12}'a_{21}'') - (a_{21}'a_{12}'' + a_{22}'a_{22}'') = 0 \quad (10.12)$$

If further the feedback network is lossless, that is, it consists of inductors and capacitors only, we find that a_{11}'' and a_{22}'' are both real whereas a_{12}'' and a_{21}'' are both imaginary. Therefore, provided that the operating frequency is sufficiently low for the a-matrix parameters of the internal amplifier to assume real values, and separating the real and imaginary terms in Equation 10.12, we get

$$1 - a_{11}'a_{11}'' - a_{22}'a_{22}'' = 0 \quad (10.13\,(a))$$

$$a_{12}'a_{21}'' + a_{21}'a_{12}'' = 0 \quad (10.13\,(b))$$

Equation 10.13 (a) defines the minimum necessary condition for oscillation, and Equation 10.13 (b) determines the frequency of oscillation.

10.2 LC-Oscillators

10.2.1 HARTLEY OSCILLATOR

Fig.10.2 (a) shows the valve version of the well known *Hartley Oscillator* circuit. In Fig. 10.2 (b) it has been rearranged so as to correspond to the generalised oscillator of Fig. 10.1. The two inductors L_1 and L_2 of the feedback network are magnetically coupled and have a mutual inductance of $-M$. Such a pair of coupled inductors can be represented by the π circuit of Fig. 10.3 (see Section 2.1).

Therefore, the complete feedback network consisting of the coupled inductors and capacitor C is equivalent to the π section of Fig. 10.4 having the following elements

$$\left.\begin{aligned} Y_1 &= \frac{L_2 + M}{j\omega(L_1L_2 - M^2)} \\ Z_2 &= \frac{-j\omega(L_1L_2 - M^2)}{M + \omega^2 C(L_1L_2 - M^2)} \\ Y_3 &= \frac{L_1 + M}{j\omega(L_1L_2 - M^2)} \end{aligned}\right\} \quad (10.14)$$

The a-matrix of the π section of Fig. 10.4, and therefore the feedback network, is given by

$$\begin{bmatrix} a_{11}'' & a_{12}'' \\ a_{21}'' & a_{22}'' \end{bmatrix} = \begin{bmatrix} 1 & 0 \\ Y_1 & 1 \end{bmatrix} \begin{bmatrix} 1 & Z_2 \\ 0 & 1 \end{bmatrix} \begin{bmatrix} 1 & 0 \\ Y_3 & 1 \end{bmatrix}$$

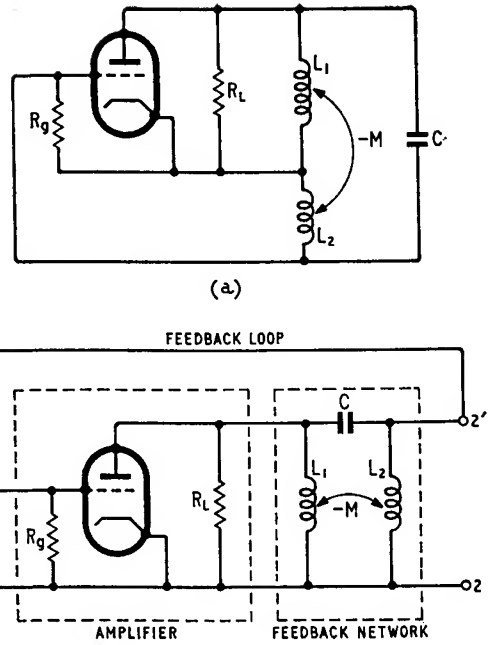

Fig. 10.2. (a) Hartley oscillator, (b) Hartley oscillator re-drawn to correspond to Fig. 10.1

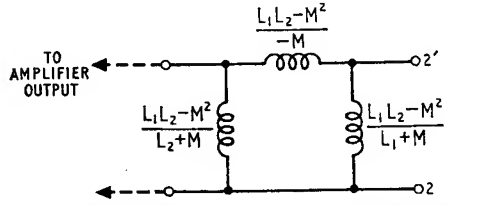

Fig. 10.3. Equivalent circuit of two coupled inductors

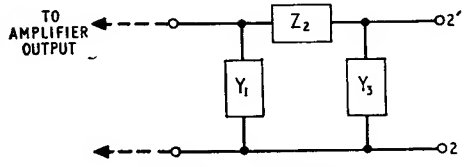

Fig. 10.4. π-Section

$$\begin{bmatrix} a_{11}'' & a_{12}'' \\ a_{21}'' & a_{22}'' \end{bmatrix} = \begin{bmatrix} 1 + Z_2Y_3 & Z_2 \\ Y_1 + Y_3(1 + Y_1Z_2) & 1 + Y_1Z_2 \end{bmatrix} \quad (10.15)$$

Combining Equations 10.14 and 10.15, we get

$$\begin{bmatrix} a_{11}'' & a_{12}'' \\ a_{21}'' & a_{22}'' \end{bmatrix} = \frac{-1}{M + \omega^2 C(L_1L_2 - M^2)} \cdot \begin{bmatrix} L_1 - \omega^2 C(L_1L_2 - M^2) & j\omega(L_1L_2 - M^2) \\ \dfrac{1 - \omega^2 C(L_1 + L_2 + 2M)}{j\omega} & L_2 - \omega^2 C(L_1L_2 - M^2) \end{bmatrix} \quad (10.16)$$

Next, consider the common cathode amplifier component of the Hartley Oscillator of Fig. 10.2 (b); it has the equivalent circuit

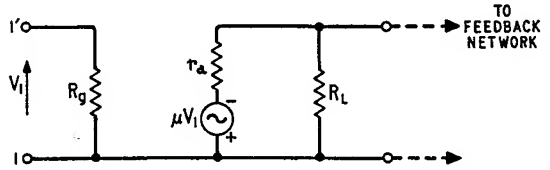

Fig. 10.5. Equivalent circuit of terminated common cathode stage

shown in Fig. 10.5 from which we directly deduce the following a-matrix by applying the definitions of Equations 2.123.

$$\begin{bmatrix} a_{11}' & a_{12}' \\ a_{21}' & a_{22}' \end{bmatrix} = \frac{-1}{\mu} \begin{bmatrix} \dfrac{R_L + r_a}{R_L} & r_a \\ \dfrac{R_L + r_a}{R_LR_g} & \dfrac{r_a}{R_g} \end{bmatrix} \quad (10.17)$$

where R_g is the grid resistor, R_L is the anode load resistor, and μ and r_a are the amplification factor and anode slope resistance of the triode valve. Hence, using Equations 10.13 (b), 10.16 and 10.17 we find that the angular frequency of oscillation ω is given by

$$\frac{1}{\omega^2} = C(L_1 + L_2 + 2M) + \frac{1}{R_g}\left(\frac{1}{R_L} + \frac{1}{r_a}\right)(L_1L_2 - M^2) \quad (10.18)$$

where the first term on the right hand side is due to the resonant

frequency of the tuned circuit, while the second term is due to the damping of the tuned circuit produced by the shunt conductances $1/R_g$ and $(R_L + r_a)/R_Lr_a$. To ensure that the frequency of oscillation is independent of the valve parameter r_a and the terminating resistors R_g and R_L, it is necessary to have

$$C(L_1 + L_2 + 2M) \gg \frac{1}{R_g}\left(\frac{1}{R_L} + \frac{1}{r_a}\right)(L_1L_2 - M^2) \quad (10.19)$$

This inequality can be satisfied if the ratio C/L_2 is large, and if the two inductors of the feedback network are tightly coupled magnetically in which case the mutual inductance M closely approaches $\sqrt{[L_1L_2]}$. Assuming that the inequality is satisfied, Equation 10.18 gives the frequency of oscillation to be

$$f = \frac{\omega}{2\pi} = \frac{1}{2\pi}\sqrt{\left[\frac{1}{C(L_1 + L_2 + 2M)}\right]} \quad (10.20)$$

The minimum necessary condition for sustained oscillations is obtained from Equations 10.13 (a), 10.16 and 10.17 to be

$$1 = \frac{R_L + r_a}{\mu R_L} \cdot \frac{L_1 - \omega^2 C(L_1L_2 - M^2)}{M + \omega^2 C(L_1L_2 - M^2)} + \frac{r_a}{\mu R_g} \cdot \frac{L_2 - \omega^2 C(L_1L_2 - M^2)}{M + \omega^2 C(L_1L_2 - M^2)} \quad (10.21)$$

where ω is as defined by Equation 10.18. Normally the grid resistor R_g is quite large compared to the anode load resistor, R_L; therefore Equation 10.21 reduces to

$$1 \simeq \frac{R_L + r_a}{\mu R_L} \cdot \frac{L_1 - \omega^2 C(L_1L_2 - M^2)}{M + \omega^2 C(L_1L_2 - M^2)} \quad (10.22)$$

Assuming that the inequality of Equation 10.19 is satisfied, we can eliminate ω between Equations 10.20 and 10.22, and simplify the result to obtain

$$\frac{\mu R_L}{R_L + r_a} = \frac{L_1 + M}{L_2 + M} \quad (10.23)$$

This equation states that, for sustained oscillations the magnitude of the voltage gain of the common cathode stage of Fig. 10.2 (b) with a load resistance R_L must be at least equal to the ratio $(L_1 + M)/(L_2 + M)$. If the voltage gain of the stage is greater than this value, then the amplitudes of oscillations will progressively

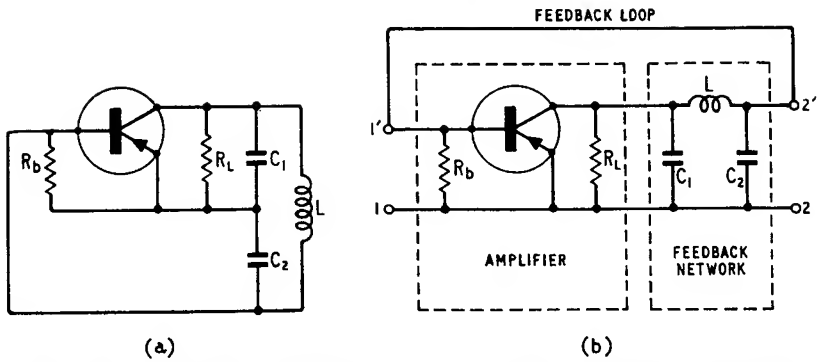

Fig. 10.6. (a) Colpitts oscillator, (b) Colpitts oscillator re-drawn to correspond to Fig. 10.1

increase until the stage becomes overloaded, as a result of which the average value of r_a reaches the steady state value.

10.2.2 COLPITTS OSCILLATOR

In Fig. 10.6 (a) we have the transistor version of the *Colpitts Oscillator*. It is re-drawn in Fig. 10.6 (b) to correspond to the generalised oscillator of Fig. 10.1. The resistor R_b accounts for the shunting effect of biasing resistors connected to the base terminal, and R_L is the collector load resistance. The frequency selective feedback network composed of capacitors C_1, C_2 and inductor L is seen to be also in the form of the π-section of Fig. 10.4 where

$$\left.\begin{aligned} Y_1 &= j\omega C_1 \\ Z_2 &= j\omega L \\ Y_3 &= j\omega C_2 \end{aligned}\right\} \qquad (10.24)$$

Hence, from Equations 10.15 and 10.24 we find that the feedback network of Fig. 10.6 has the following a-matrix

$$\begin{bmatrix} a_{11}'' & a_{12}'' \\ a_{21}'' & a_{22}'' \end{bmatrix} = \begin{bmatrix} 1-\omega^2 LC_2 & j\omega L \\ j\omega C_1 + j\omega C_2(1-\omega^2 LC_1) & 1-\omega^2 LC_1 \end{bmatrix} \qquad (10.25)$$

In Fig. 10.6 (b) the transistor is shown operated in its common emitter mode, and so it can be represented by the equivalent circuit of Fig. 10.7, where the parameter h_{12e} responsible for internal feedback has been ignored. This is quite justified provided

$$(h_{11e} + R_b)\left(h_{22e} + \frac{1}{R_L}\right) \gg h_{12e}h_{21e} \qquad (10.26)$$

where h_{11e}, h_{12e}, h_{21e} and h_{22e} are the common emitter h-parameters. By using the definitions of Equations 2.123 for the a-matrix parameters, we deduce from Fig. 10.7 that

$$\begin{bmatrix} a_{11}' & a_{12}' \\ a_{21}' & a_{22}' \end{bmatrix} = \frac{-1}{h_{21e}} \begin{bmatrix} h_{11e}\left(h_{22e} + \frac{1}{R_L}\right) & h_{11e} \\ \left(1 + \frac{h_{11e}}{R_b}\right)\left(h_{22e} + \frac{1}{R_L}\right) & 1 + \frac{h_{11e}}{R_b} \end{bmatrix} \qquad (10.27)$$

Therefore, using Equations 10.13 (b), 10.25 and 10.27 we find that the frequency of oscillation can be determined from

$$\omega^2 = \frac{1}{L}\left(\frac{1}{C_1} + \frac{1}{C_2}\right) + \frac{1}{C_1 C_2}\left(\frac{1}{h_{11e}} + \frac{1}{R_b}\right)\left(h_{22e} + \frac{1}{R_L}\right) \qquad (10.28)$$

The first term on the right hand side of this equation is due to resonance of the tuned circuit comprising C_1, C_2 and L all connected in series. The second term is due to the damping of this tuned

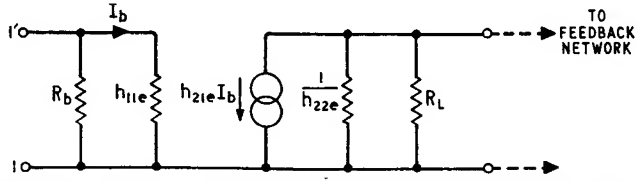

Fig. 10.7. Equivalent circuit of terminated common emitter stage

circuit produced by the shunt conductances $(h_{11e} + R_b)/h_{11e}R_b$ and $(h_{22e} + 1/R_L)$. If, however, the elements of the feedback network satisfy the inequality

$$\frac{1}{L}(C_1 + C_2) \gg \left(\frac{1}{h_{11e}} + \frac{1}{R_b}\right)\left(h_{22e} + \frac{1}{R_L}\right) \qquad (10.29)$$

then the resulting frequency of oscillation becomes practically independent of transistor parameters as well as the terminating resistors R_b and R_L; thus

$$f = \frac{\omega}{2\pi}$$

$$f \simeq \frac{1}{2\pi}\sqrt{\left[\frac{1}{L}\left(\frac{1}{C_1}+\frac{1}{C_2}\right)\right]} \tag{10.30}$$

The minimum necessary condition for sustained oscillations follows from Equations 10.13 (a), 10.25 and 10.27 to be

$$1+\frac{h_{11e}}{h_{21e}}\left(h_{22e}+\frac{1}{R_L}\right)(1-\omega^2LC_2)+\frac{1}{h_{21e}}\left(1+\frac{h_{11e}}{R_b}\right)(1-\omega^2LC_1)=0 \tag{10.31}$$

Eliminating ω^2 between Equations 10.30 and 10.31 and simplifying, we find that for sustained oscillations the forward current amplification factor h_{21e} of the transistor must at least have the following value

$$h_{21e}=\frac{C_1}{C_2}\left(1+\frac{h_{11e}}{R_b}\right)+\frac{C_2h_{11e}}{C_1}\left(h_{22e}+\frac{1}{R_L}\right) \tag{10.32}$$

10.2.3 LOSSLESS T SECTION FOR FEEDBACK NETWORK

The feedback networks considered up till now have been basically in the forms of π sections. Alternatively, the feedback network can be in the form of a lossless T section, as shown in the transistor oscillator of Fig. 10.8. For the feedback network of this circuit we deduce the following a-matrix

$$\begin{bmatrix} a_{11}'' & a_{12}'' \\ a_{21}'' & a_{22}'' \end{bmatrix} = \begin{bmatrix} 1 & \frac{1}{j\omega C_1} \\ 0 & 1 \end{bmatrix}\begin{bmatrix} 1 & 0 \\ \frac{1}{j\omega L} & 1 \end{bmatrix}\begin{bmatrix} 1 & \frac{1}{j\omega C_2} \\ 0 & 1 \end{bmatrix}$$

$$= \begin{bmatrix} 1-\frac{1}{\omega^2LC_1} & \frac{1}{j\omega C_1}+\frac{1}{j\omega C_2}\left(1-\frac{1}{\omega^2LC_1}\right) \\ \frac{1}{j\omega L} & 1-\frac{1}{\omega^2LC_2} \end{bmatrix} \tag{10.33}$$

The a-matrix of the terminated common emitter stage is still given by Equation 10.27. Therefore, using Equations 10.13 (b), 10.27 and 10.33 we find that the oscillation frequency is given by

$$\frac{1}{\omega^2}=L(C_1+C_2)+\frac{C_1C_2h_{11e}R_bR_L}{(h_{11e}+R_b)(1+h_{22e}R_L)} \tag{10.34}$$

where again the second term is due to the loading effects of the

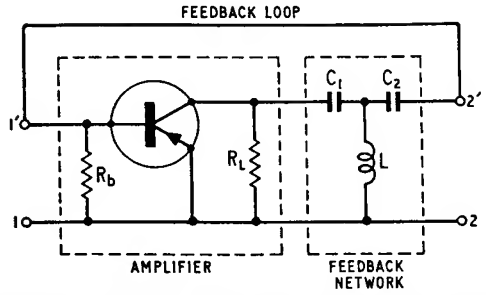

Fig. 10.8. Transistor oscillator with lossless T-section for feedback network

transistor and terminating resistors R_b and R_L upon the frequency selective network. This loading can be minimised if

$$L\left(\frac{1}{C_1}+\frac{1}{C_2}\right) \gg \frac{h_{11e}R_bR_L}{(h_{11e}+R_b)(1+h_{22e}R_L)} \tag{10.35}$$

Then the frequency of oscillation becomes determined effectively by the feedback network,

$$f=\frac{\omega}{2\pi}$$

$$=\frac{1}{2\pi}\sqrt{\left[\frac{1}{L(C_1+C_2)}\right]} \tag{10.36}$$

The minimum necessary condition for sustained oscillations is deduced from Equations 10.13 (a), 10.27 and 10.33 to be

$$1+\frac{h_{11e}}{h_{21e}}\left(h_{22e}+\frac{1}{R_L}\right)\left(1-\frac{1}{\omega^2LC_1}\right)+\frac{1}{h_{21e}}\left(1+\frac{h_{11e}}{R_b}\right)\left(1-\frac{1}{\omega^2LC_2}\right)=0 \tag{10.37}$$

which, together with Equation 10.36, simplifies as follows

$$h_{21e}=\frac{C_2h_{11e}}{C_1}\left(h_{22e}+\frac{1}{R_L}\right)+\frac{C_1}{C_2}\left(1+\frac{h_{11e}}{R_b}\right) \tag{10.38}$$

It is of interest to note that the above oscillator circuits can also be analysed by other alternative methods. For example, in the Hartley oscillator of Fig. 10.2 (a) and the Colpitts oscillator of Fig. 10.6 (a) the amplifier and feedback network components can be

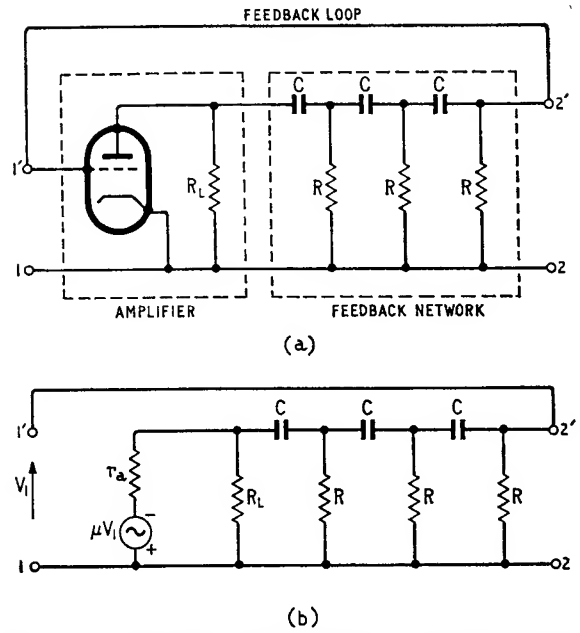

Fig. 10.9. (a) RC-phase shift oscillator, (b) Equivalent circuit

considered as connected in parallel at both their input as well as output ports. Then in terms of the *y*-parameters we can set up the characteristic equation from which the frequency of oscillation and condition for oscillation are determined. On the other hand, in the oscillator circuit of Fig. 10.8 the two components can be considered as connected in series at their input and output ports, and so the characteristic equation is conveniently formulated in terms of the *z*-parameters.

10.3 RC-oscillators

10.3.1 RC-PHASE SHIFT OSCILLATOR

It is also possible to construct an oscillator circuit with the feedback network consisting of resistors and capacitors only. The *RC phase shift oscillator* of Fig. 10.9 (a) is an example of such a class of oscillator circuit. It consists of a common cathode stage and a ladder network having three *RC*-sections.

In Fig. 10.9 (b) the triode valve has been replaced with its equivalent circuit involving a controlled voltage source. We therefore deduce the following *a*-matrix for the amplifier component

$$\begin{bmatrix} a_{11}' & a_{12}' \\ a_{21}' & a_{22}' \end{bmatrix} = \frac{-1}{\mu} \begin{bmatrix} \frac{R_L + r_a}{R_L} & r_a \\ 0 & 0 \end{bmatrix} \tag{10.39}$$

Here we see that a_{21}' and a_{22}' are both zero, in which case the characteristic equation 10.12 reduces to

$$1 - (a_{11}'a_{11}'' + a_{12}'a_{21}'') = 0 \tag{10.40}$$

The product term $a_{12}'a_{21}''$ is representative of the loading effect of the *RC*-feedback network upon the common cathode amplifier. This loading effect can be justifiably ignored if the following inequality is satisfied.

$$R \gg \frac{r_a R_L}{r_a + R_L} \tag{10.41}$$

Then Equation 10.40 reduces further to the following simple but approximate form

$$a_{11}'' \simeq \frac{1}{a_{11}'} \tag{10.42}$$

This equation states that for sustained oscillations the reciprocal of the open-circuit voltage gain of the feedback network, in the forward direction of signal transmission, must equal the voltage gain of the common cathode stage, both networks being considered individually.

The feedback network consists basically of a cascade of three *RC*-sections, each one of which has the following *a*-matrix

$$\begin{bmatrix} 1 + \frac{1}{j\omega CR} & \frac{1}{j\omega C} \\ \frac{1}{R} & 1 \end{bmatrix}$$

The *a*-matrix of the complete feedback network is equal to the product of the *a*-matrices of the three *RC*-sections; therefore,

$$\begin{bmatrix} a_{11}'' & a_{12}'' \\ a_{21}'' & a_{22}'' \end{bmatrix} = \begin{bmatrix} 1 + \frac{1}{j\omega CR} & \frac{1}{j\omega C} \\ \frac{1}{R} & 1 \end{bmatrix}^3 \tag{10.43}$$

from which it follows that the element a_{11}'' is given by

$$a_{11}'' = \left(1 + \frac{1}{j\omega CR}\right)\left[\left(1 + \frac{1}{j\omega CR}\right)^2 + \frac{1}{j\omega CR}\right] + \frac{1}{j\omega CR}\left(2 + \frac{1}{j\omega CR}\right)$$

$$= \left(1 - \frac{5}{\omega^2 C^2 R^2}\right) + \frac{j}{\omega CR}\left(\frac{1}{\omega^2 C^2 R^2} - 6\right) \qquad (10.44)$$

Here we see that a_{11}'' has a purely real value when

$$\frac{1}{\omega^2 C^2 R^2} - 6 = 0$$

that is

$$\omega = \frac{1}{CR\sqrt{6}} \qquad (10.45)$$

When the angular frequency has this value, we find from Equation 10.44 that the corresponding value of a_{11}'' is -29. Hence, Equation 10.42 gives the minimum necessary condition for sustained oscillations to be $(1/a_{11}') = -29$, that is (see Equation 10.39)

$$\frac{\mu R_L}{R_L + r_a} = 29 \qquad (10.46)$$

The feedback circuit of Fig. 10.9 (a) will thus oscillate at the angular frequency of $1/RC\sqrt{6}$ provided the magnitude of the voltage gain of the common cathode stage with a load resistance R_L has a minimum value of 29.

10.3.2 WIEN-BRIDGE OSCILLATOR

The *RC*-oscillator circuit of Fig. 10.10 (a) employs a *Wien-bridge* for its feedback network component. The frequency selective branches, comprising the parallel and series combinations of the elements R and C, apply the positive feedback necessary for regeneration and so determine the frequency of oscillation. On the other hand, the purely resistive branches, comprising the elements R_1 and R_2, apply negative feedback to the circuit. At the frequency of oscillation the positive feedback predominates, whereas at harmonic frequencies the negative feedback predominates and, therefore, reduces the harmonic distortion in the output signal.

In the following analysis we shall assume that the load resistance R_{L_2} of the stage $VT2$ operated as common grid is small compared to the resistive elements of the bridge, and that the *cathode-coupled pair* comprising $VT1$ and $VT2$ has an overall voltage gain K_0. Then we obtain the equivalent circuit of Fig. 10.10 (b) from which we can

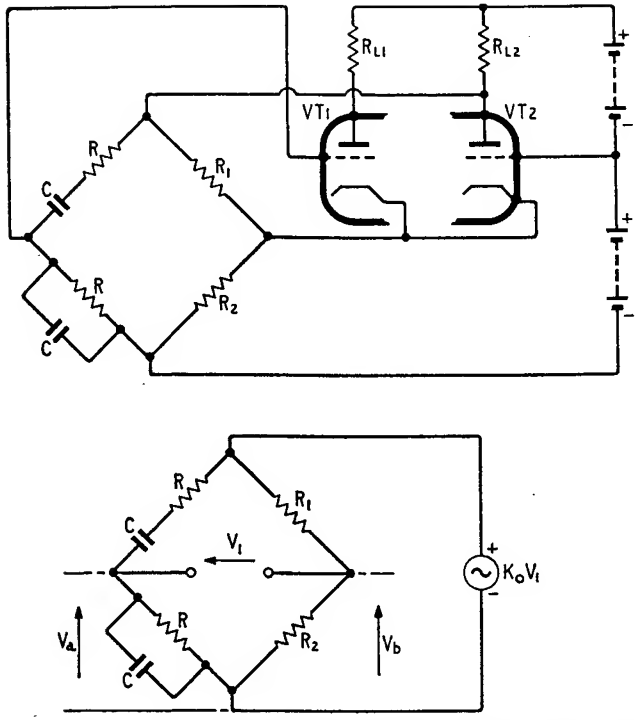

Fig. 10.10. (a) Wien-bridge oscillator, (b) Equivalent circuit

determine the return difference $F(j\omega)$ with reference to the control parameter K_0 by using the following relation (see Section 3.6)

$$F(j\omega) = 1 - K_0 t_{ba}(j\omega) \qquad (10.47)$$

where the transmittance $t_{ba}(j\omega)$ is equal to the value of the voltage $V_1 = V_a - V_b$ which results when the controlled source $K_0 V_1$ is replaced by an independent voltage source of 1 volt. Then with $K_0 V_1 = 1$ volt we find from Fig. 10.10 (b) that

$$V_a = \frac{\dfrac{R}{1 + j\omega CR}}{R + \dfrac{1}{j\omega C} + \dfrac{R}{1 + j\omega CR}}$$

$$= \frac{j\omega CR}{1 - \omega^2 C^2 R^2 + j3\omega CR} \qquad (10.48)$$

and
$$V_b = \frac{R_2}{R_1 + R_2}$$
$$= \frac{1}{a+1} \qquad (10.49)$$
where
$$a = R_1/R_2$$

Remembering that $t_{ba}(j\omega) = V_a - V_b$ when $K_0V_1 = 1$ volt, we deduce from Equations 10.47 to 10.49 that the return difference with reference to K_0 is given by

$$F(j\omega) = 1 + K_0 \frac{1 - \frac{\omega^2}{\omega_0^2} + \frac{j\omega}{\omega_0}(2-a)}{(1+a)\left(1 - \frac{\omega^2}{\omega_0^2} + j3\frac{\omega}{\omega_0}\right)} \qquad (10.50)$$

where $\omega_0 = 1/CR$. Now from Nyquist's criterion we know that for sustained oscillations we must have $F(j\omega) = 0$. From Equation 10.50 we see that this condition is satisfied at $\omega = \omega_0$ provided that the voltage gain K_0 of the internal amplifier has a minimum value given by

$$K_0 = \frac{3(a+1)}{a-2} \qquad (10.51)$$

Then, with this minimum necessary condition satisfied, we find that the circuit of Fig. 10.10 oscillates at a frequency equal to $1/(2\pi CR)$.

It is of interest that the Wien-bridge of Fig. 10.10 is perfectly balanced at $\omega = 1/CR$ and when $a = (R_1/R_2) = 2$. Equation 10.51 thus shows that the closer the bridge is to its balanced condition the greater is the value of the voltage gain K_0 necessary for sustained oscillations.

10.4 Frequency stability

In practice it is found that the oscillation frequency invariably drifts from the desired value, the drift having been caused by any of the following factors:

1. Aging of the active as well as passive network elements of the oscillator circuit.
2. Variations in valve or transistor parameters due to a shift in the quiescent operating point produced by changes in the d.c. supply voltage and/or ambient temperature.
3. Changes in external loading conditions and parasitic capacitances.

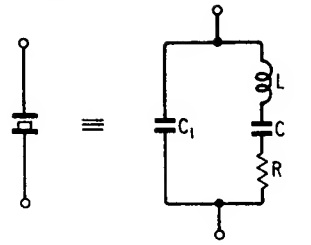

Fig. 10.11. Equivalent circuit of piezoelectric crystal

The effect of parameter variations can be reduced by applying negative feedback to the internal amplifier component of the oscillator circuit. It can be reduced also by the proper choice of the element values of the frequency selective feedback network. In the case of the Colpitts oscillator, for example, this can be achieved by choosing the ratio $(C_1 + C_2)/L$ of the feedback network to be sufficiently large, as shown in Section 10.2.2. In addition, a large value for this ratio tends to filter out the harmonics resulting in further improvement in the overall oscillator performance.

In the case of the Hartley oscillator we can reduce the dependence of the oscillation frequency on valve or transistor parameters by ensuring that the two inductors of the feedback network component have a coefficient of coupling close to unity.

The frequency stability can be improved also by using a *piezoelectric crystal*, as the frequency controlling element. A vibrating piezoelectric crystal has the equivalent circuit shown in Fig. 10.11. The capacitance C_1 represents the electrostatic capacitance between the crystal electrodes when it is not vibrating. The series LCR-branch represents the electrical equivalent of the vibrational characteristics of the crystal. The elements of the equivalent circuit normally have such values that the series and parallel resonant frequencies are very close together (see Problem 7).

Practically any oscillator circuit, having an inductor in its feedback network, can be converted to a crystal controlled oscillator by replacing the inductor with a crystal. Thus in the crystal oscillator of Fig. 10.12 we have used a crystal in place of the inductive component of a Colpitts oscillator. The resulting oscillation frequency

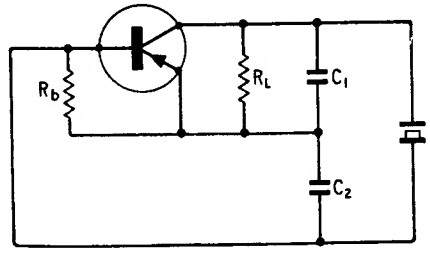

Fig. 10.12. Crystal controlled oscillator

is only slightly greater than the series resonant frequency of the crystal. Another method of improving the frequency stability of an oscillator is to use a feedback network in the form of a bridge; an example of such a method is the Wien-bridge oscillator considered in Section 10.3.2. The closer the bridge is to its balanced condition the better is the frequency stability.

10.4.1 FREQUENCY STABILISATION FACTOR

Suppose that initially the angular oscillation frequency of an oscillator is equal to ω_0. Then from Nyquist's criterion we deduce that the phase angle $B(\omega)$ of the open-loop gain function $T(j\omega)$ of the oscillator circuit is 180° at $\omega = \omega_0$. If, next, the various factors cause the phase angle $B(\omega)$ to change by a small amount δB at $\omega = \omega_0$, then the necessary condition for oscillation will no longer be satisfied at $\omega = \omega_0$. Accordingly, the frequency of oscillation shifts to a new value at which the phase angle of the open-loop gain function is restored to 180°. The resulting frequency shift is given as follows

$$\delta\omega = \left[\frac{\partial\omega}{\partial B(\omega)}\right]_{\omega=\omega_0} \delta B \tag{10.52}$$

and so the modified frequency of oscillation is

$$\omega_0 + \delta\omega = \omega_0\left(1 + \frac{\delta B}{S_f}\right) \tag{10.53}$$

where

$$S_f = \omega_0\left[\frac{\partial B(\omega)}{\partial\omega}\right]_{\omega=\omega_0} \tag{10.54}$$

S_f is defined as the *frequency stabilisation factor*. We see that, for a given value of δB, the larger the value of S_f the smaller is the frequency drift.

As an illustration we shall evaluate the frequency stabilisation factor for the Wien-bridge oscillator. From Equation 10.50 we deduce that for this oscillator the open-loop gain function is given by

$$T(j\omega) = K_0 \frac{1 - \frac{\omega^2}{\omega_0^2} + j\frac{\omega}{\omega_0}(2 - a)}{(a+1)\left(1 - \frac{\omega^2}{\omega_0^2} + j\frac{3\omega}{\omega_0}\right)} \tag{10.55}$$

where $\omega_0 = 1/CR$ is the normal frequency of oscillation. Therefore

$$B(\omega) = \angle T(j\omega)$$

$$B(\omega) = \tan^{-1}\left[\frac{\frac{\omega}{\omega_0}(2 - a)}{1 - \frac{\omega^2}{\omega_0^2}}\right] - \tan^{-1}\left[\frac{\frac{3\omega}{\omega_0}}{1 - \frac{\omega^2}{\omega_0^2}}\right] \tag{10.56}$$

Differentiating with respect to ω, and then putting $\omega = \omega_0$ we get

$$\left[\frac{\partial B(\omega)}{\partial\omega}\right]_{\omega=\omega_0} = -\frac{2(a+1)}{3\omega_0(a-2)} \tag{10.57}$$

Hence Equation 10.54 gives the frequency stabilisation factor of the Wien-bridge oscillator to be

$$S_f = -\frac{2(a+1)}{3(a-2)} \tag{10.58}$$

where the minus sign indicates that the phase angle decreases with increasing frequency. Equation 10.58 shows that the magnitude of the S_f increases as the parameter a approaches the value of 2. In other words, the closer the Wien-bridge is to its perfectly balanced condition, the better is the resulting frequency stability. But, as pointed out earlier, the voltage gain of the internal amplifier required for sustained oscillations becomes greater as the bridge approaches its balanced condition. Therefore, in practice a compromise is necessary between the desired value for the frequency stabilisation factor S_f and the possible value for the voltage gain of the amplifier.

10.4.2 REACTIVE STABILISATION OF LC-OSCILLATORS

The frequency stability of an *LC*-oscillator can be greatly improved by adding to the frequency selective feedback network an extra branch which is purely reactive. If the feedback network is in the form of a π section (see Fig. 10.13 (a)), then frequency stabilisation can be achieved by adding the purely reactive series branch of impedance Z_0, as in Fig. 10.13 (b). If, on the other hand, the feedback network is in the form of a T-section (see Fig. 10.14 (a)), then for frequency stabilisation we can add a purely reactive shunt arm, as in Fig. 10.14 (b), or a purely reactive bridge arm, as in Fig. 10.14 (c).

To illustrate this method of stabilisation, consider Fig. 10.15 showing the valve version of the Colpitts oscillator. The inductance L_0 has been added for the purpose of frequency stabilisation. Therefore, the a-matrix of the feedback network modifies to

$$\begin{bmatrix} a_{11}'' & a_{12}'' \\ a_{21}'' & a_{22}'' \end{bmatrix} = \begin{bmatrix} 1 & j\omega L_0 \\ 0 & 1 \end{bmatrix} \begin{bmatrix} 1 & 0 \\ j\omega C_1 & 1 \end{bmatrix} \begin{bmatrix} 1 & j\omega L \\ 0 & 1 \end{bmatrix} \begin{bmatrix} 1 & 0 \\ j\omega C_2 & 1 \end{bmatrix}$$

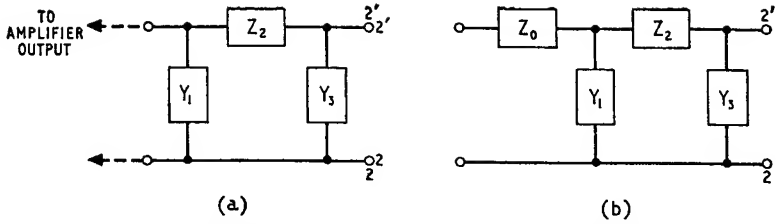

Fig. 10.13. (a) π-section for feedback network, (b) Feedback network with frequency stabilising element Z_0

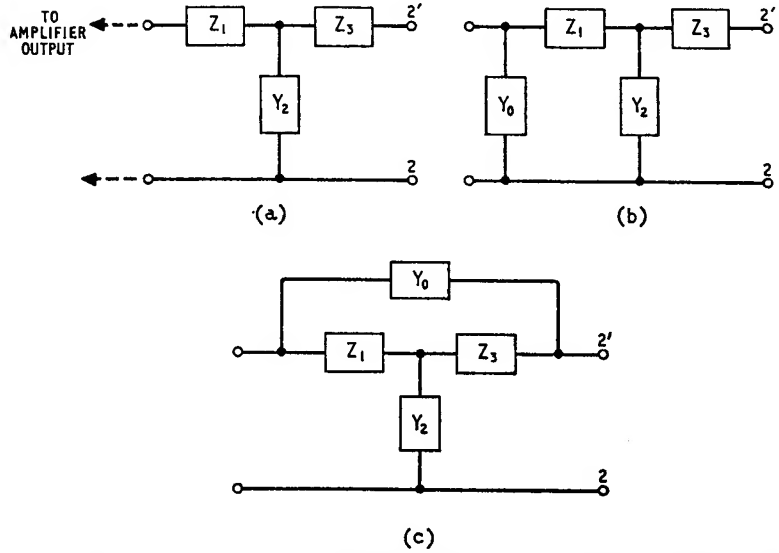

Fig. 10.14. (a) T-section for feedback network, (b) Feedback network with frequency stabilising shunt element Y_0, (c) Feedback network with frequency stabilising bridge arm Y_0

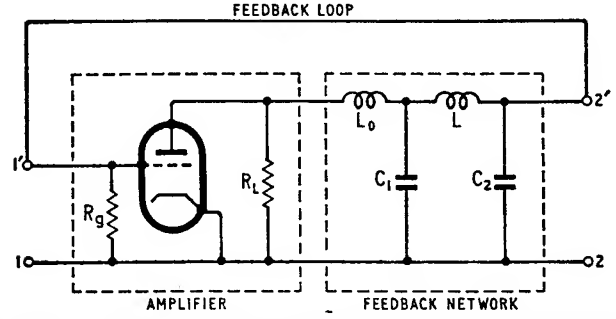

Fig. 10.15. Colpitts oscillator with frequency stabilisation element L_0

$$\begin{bmatrix} a_{11}'' & a_{12}'' \\ a_{21}'' & a_{22}'' \end{bmatrix} = \begin{bmatrix} 1-\omega^2 L_0 C_1 & j\omega L_0 \\ j\omega C_1 & 1 \end{bmatrix} \begin{bmatrix} 1-\omega^2 LC_2 & j\omega L \\ j\omega C_2 & 1 \end{bmatrix}$$

After expanding this matrix product, we obtain

$$\left.\begin{aligned} a_{11}'' &= (1-\omega^2 L_0 C_1)(1-\omega^2 LC_2) - \omega^2 L_0 C_2 \\ a_{12}'' &= j\omega L(1-\omega^2 L_0 C_1) + j\omega L_0 \\ a_{21}'' &= j\omega C_1(1-\omega^2 LC_2) + j\omega C_2 \\ a_{22}'' &= 1-\omega^2 LC_1 \end{aligned}\right\} \quad (10.59)$$

The frequency of oscillation is determined by Equation 10.13 (b) which is reproduced here for convenience

$$a_{12}'a_{21}'' + a_{21}'a_{12}'' = 0$$

For perfect frequency stabilisation, the frequency of oscillation must be independent of the matrix parameters a_{12}' and a_{21}', contributed by the amplifier. This can be achieved if and only if the parameters a_{12}'' and a_{21}'' of the feedback network component are both simultaneously zero at the desired frequency of oscillation, that is,

$$a_{12}'' = 0 \quad (10.60\text{ (a)})$$

$$a_{21}'' = 0 \quad (10.60\text{ (b)})$$

These two relationships together determine the frequency of oscillation and the necessary condition for frequency stabilisation.

Equations 10.60 can be both satisfied by means of the feedback network of Fig. 10.15; thus when they are used in conjunction with Equation 10.59, we find that they lead to

$$L(1-\omega^2 L_0 C_1) + L_0 = 0 \quad (10.61\text{ (a)})$$

$$C_1(1-\omega^2 LC_2) + C_2 = 0 \quad (10.61\text{ (b)})$$

where we have excluded the trivial solution $\omega = 0$. The frequency of oscillation can be determined from Equation 10.61 (b); hence

$$\omega = \sqrt{\left[\frac{1}{L}\left(\frac{1}{C_1} + \frac{1}{C_2}\right)\right]} \quad (10.62)$$

Next, eliminating ω^2 between Equations 10.61 (a) and 10.62, we get

$$L_0 C_1 = LC_2 \quad (10.63)$$

We therefore see that the frequency of oscillation is independent of the inductance L_0, which acts solely as a frequency stabilising circuit element.

The a-matrix parameters of the amplifier component are given by Equations 10.17. Hence, if the values of a_{11}'' and a_{22}'', given by these equations, are substituted in Equation 10.13 (a), we obtain

$$1 + \frac{R_L + r_a}{\mu R_L}[(1 - \omega^2 L_0 C_1)(1 - \omega^2 L C_2) - \omega^2 L_0 C_2] + \frac{r_a}{\mu R_g}(1 - \omega^2 L C_1) = 0 \tag{10.64}$$

Eliminating ω^2 between Equation 10.62 and 10.64 and then using Equation 10.63, we find that the minimum necessary condition for sustained oscillations is

$$\mu = \frac{C_2}{C_1}\left(1 + \frac{r_a}{R_L}\right) + \frac{C_1}{C_2}\cdot\frac{r_a}{R_g} \tag{10.65}$$

The expression on the right hand side of this equation has its minimum value when

$$\left(\frac{C_2}{C_1}\right)^2 = \frac{r_a R_L}{R_g(r_a + R_L)}$$

in which case the magnitude $\mu R_L/(R_L + r_a)$ of the voltage gain of the common cathode amplifier must equal the required value of $2C_2/C_1$.

PROBLEMS

1. Three impedances are connected together in a single closed circuit and the anode, cathode and grid of a valve (A, K and G) are tapped on at the points of junction. Prove that such a circuit is capable of sustained sinusoidal oscillation, provided that

$$r_a(Z_{GK} + Z_{AK} + Z_{AG}) = -Z_{AK}(Z_{GK} + \mu Z_{GK} + Z_{AG})$$

If the three impedances, Z_{GK}, Z_{AK} and Z_{AG}, are pure reactances, jX_{GK}, jX_{AK}, jX_{AG}, prove that, for sustained oscillation, the circuit elements in the grid-cathode, and anode-cathode circuits must be either both capacitive or both inductive.

Give the circuits of any three oscillators which are based on the above reasoning.

A certain tuned-anode/tuned-grid oscillator uses two identical coil-capacitor circuits. The resonance frequency of each is 4 Mc/s, and in each, the tuning capacitance is four times the grid-anode capacitance. What will be the frequency of oscillation? (Neglect the effect of coil resistance on oscillation frequency).
(Institute of Electrical Engineers, Part III, Electronic Engineering, June, 1960).

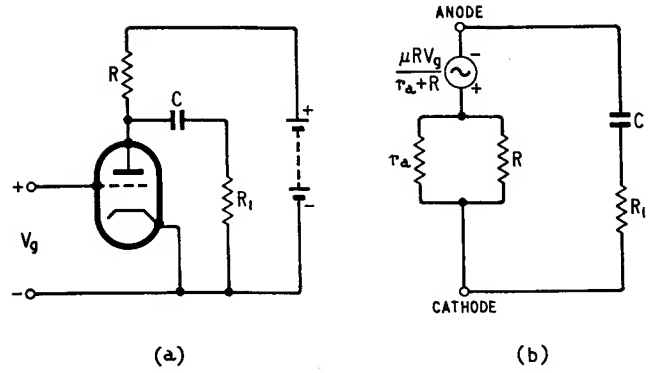

Fig. 10.16

2. Show that the circuit shown in Fig. 10.16 (b) is an equivalent circuit for that in Fig. 10.16 (a).

An oscillator is formed from a 3-stage RC-coupled amplifier by feeding back the whole output voltage to the input terminals of the first valve. The three valves are identical and the three anode load resistances have the same value, R. The three coupling capacitors are C_1, C_2 and C_3, and the three coupling resistors are R_1, R_2 and R_3. Prove that the frequency of oscillation is given by

$$\frac{1}{2\pi\sqrt{[r_1 r_2 C_1 C_2 + r_2 r_3 C_2 C_3 + r_3 r_1 C_3 C_1]}}$$

where r_1 denotes the resistance of R_1 in series with the parallel combination of R and the valve incremental impedance r_a, and similarly for r_2 and r_3.
(Institute of Electrical Engineers, Part III, Electronic Engineering, June, 1961).

3. The amplifier component of the oscillator circuit of Fig. 10.17 has a large input impedance, a small output impedance, and a voltage gain K_0. Determine the open-loop gain $T(p)$ of the circuit; hence find the frequency of oscillation and the value of K_0 necessary for sustained oscillations.
4. In the RC-phase shift oscillator circuit of Fig. 10.18 the triode valve has an anode slope resistance of 7 kΩ. Neglecting the

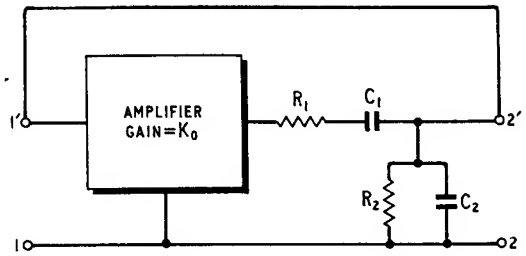

Fig. 10.17

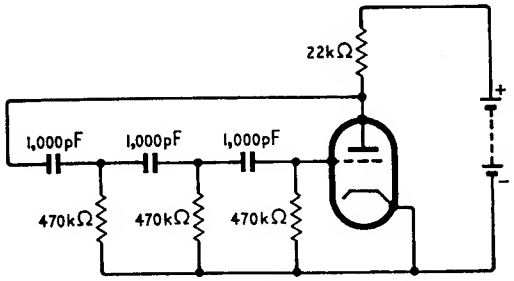

Fig. 10.18

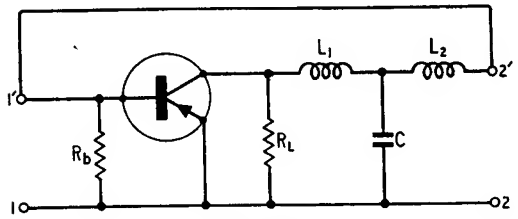

Fig. 10.19

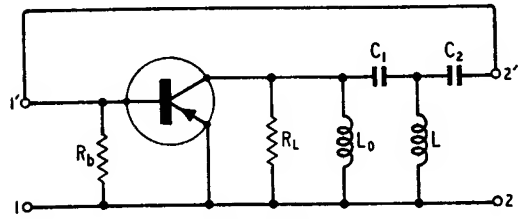

Fig. 10.20

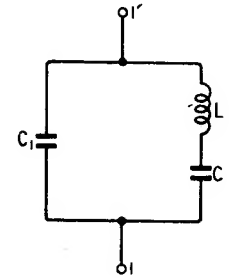

Fig. 10.21

loading effect of the feedback network, determine the minimum value of the amplification factor μ necessary for sustained oscillations. What is the frequency of oscillation?

5. Fig. 10.19 shows a transistor oscillator with a feedback network in the form of a T-section. Assuming that there exists no magnetic coupling between the inductors L_1 and L_2, and neglecting the effect of the h_{12e} parameter, determine the frequency of oscillation, and the condition to be satisfied if this frequency is to be almost independent of transistor parameters. What is the minimum necessary condition for sustained oscillations?
6. In the transistor oscillator of Fig. 10.20 the inductance L_0 has been added for the purpose of frequency stabilisation. Determine the value of L_0 required for perfect stabilisation. What are the frequency of oscillation and minimum necessary condition for oscillation? Neglect the effect of the h_{12e} parameter.
7. Fig. 10.21 shows the equivalent circuit for a piezoelectric crystal. Determine the reactance measured between terminals 1,1'; hence sketch the reactance-frequency characteristic.

   Using the typical values $L = 0{\cdot}57$ H, $C = 0{\cdot}16$ pF, and $C_1 = 40$ pF, show that the series and parallel resonance frequencies are very close together.

REFERENCES

1. COTE, A. J., and OAKES, J. B., *Linear Vacuum Tube and Transistor Circuits*, McGraw-Hill, New York (1961).
2. EDSON, W. A., *Vacuum Tube Oscillators*, Wiley, New York (1953).
3. JEFFERSON, H., 'Stabilisation of Feedback Oscillators', *Wireless Engineer*, **22**, 384 (1945).
4. NICHOLS, K. G., 'The Use of Transfer Matrices in the Analysis of Conditions of Oscillation', *J. Brit. I.R.E.*, **23**, 41 (1963).
5. REICH, H. J., *Functional Circuits and Oscillators*, Van Nostrand, New York (1961).
6. STRAUSS, L., *Wave Generation and Shaping*, McGraw-Hill, New York (1960).
7. GLADWIN, A. S., 'Constant Frequency Oscillators', *Wireless Engineer*, **33**, 13 (1956)

APPENDIX

Further Applications of Routh's Criterion

In Section 4.3 we showed that by applying Routh's criterion to a feedback circuit's characteristic equation

$$f(p) = \alpha_0 p^n + \alpha_1 p^{n-1} + \alpha_2 p^{n-2} + \ldots + \alpha_{n-1} p + \alpha_n = 0 \quad \text{(A.1)}$$

where all the coefficients α_0 to α_n are real, it is possible to detect the existence, or non-existence, of roots in the right half of the p-plane. If all the roots are found to be located inside the left half of the

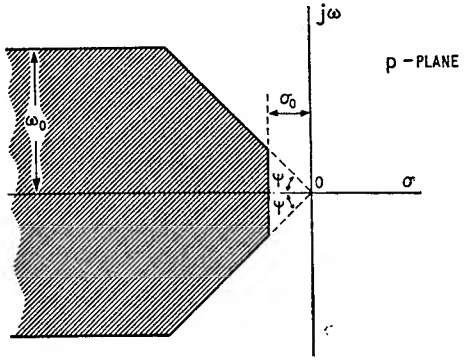

Fig. A.1

p-plane, and therefore the feedback circuit is stable, the next problem is to examine the nature of the resulting closed-loop transient response by establishing whether or not all the roots of the characteristic equation are located inside the shaded region of Fig. A.1 (see Section 4.7). In this appendix we shall demonstrate that it is possible to explore the entire left half of the p-plane by first making

certain transformations and then applying Routh's criterion to the transformed characteristic equation.

We shall consider four extensions which are of particular importance:

To establish whether or not every root of the characteristic equation has a real part more negative than a specified real number $-\sigma_0$.

This test is useful when it is required to ascertain that every one of the terms constituting the closed-loop transient response has a multiplying exponential factor $e^{-\sigma t}$ with $\sigma \geqslant \sigma_0$, thereby ensuring that the time required for the transient response to decay will not exceed a

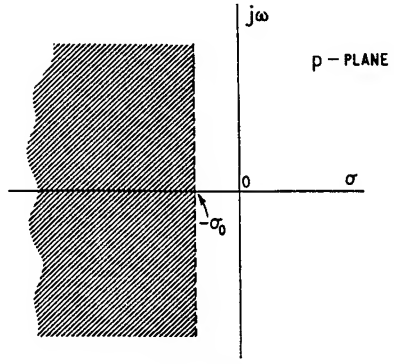

Fig. A.2

specified value determined by σ_0. To satisfy this requirement it is necessary for all the closed-loop poles, i.e. the roots of the characteristic equation to be located inside the shaded region of Fig. A.2.

Let us put

$$p = s - \sigma_0 \quad \text{(A.2)}$$

in which case Equation A.1 is transformed as follows

$$g(s) = [f(p)]_{p=s-\sigma_0}$$
$$= \alpha_0(s-\sigma_0)^n + \alpha_1(s-\sigma_0)^{n-1} + \alpha_2(s-\sigma_0)^{n-2} + \ldots + \alpha_{n-1}(s-\sigma_0) + \alpha_n \quad \text{(A.3)}$$

The effect of using s as the independent variable instead of p is to displace all the roots of the characteristic equation $f(p) = 0$ horizontally and to the right by a distance equal to σ_0. Hence if $f(p)$ happens to have a zero between the jω-axis of the p-plane and the

shaded region of Fig. A.2, then the polynomial $g(s)$, as defined by Equation A.3 will have a corresponding zero in the right half of the s-plane, and this is shown up when Routh's criterion is applied to $g(s)$. If, on the other hand, after applying Routh's criterion we find that all the zeros of $g(s)$ are confined to the left half of the s-plane then directly we deduce that all the zeros of $f(p)$ are confined to the shaded region of Fig. A.2.

Example 1

Suppose that it is required to know whether or not the polynomial

$$f(p) = p^3 + 2p^2 + 3p + 4$$

has any zero with a negative real part less than 0·5 in absolute value (i.e. $\sigma_0 = 0{\cdot}5$)

Putting $p = s - 0{\cdot}5$ we get

$$\begin{aligned} g(s) &= (s - 0{\cdot}5)^3 + 2(s - 0{\cdot}5)^2 + 3(s - 0{\cdot}5) + 4 \\ &= s^3 + 0{\cdot}5s^2 + 1{\cdot}75s + 2{\cdot}87 \end{aligned}$$

Application of Routh's criterion to this polynomial reveals that it has two zeros in the right half of the s-plane. Also on applying Routh's criterion to $f(p)$ we find that it has no zeros in the right half of the p-plane. It therefore follows that $f(p)$ has two zeros between the jω-axis of the p-plane and the shaded region of Fig. A.2 with $\sigma_0 = 0{\cdot}5$.

To establish whether or not every pair of complex conjugate roots, if any, of the characteristic equation has an imaginary part whose absolute value is less than a certain positive real number ω_0.

This test is useful in detecting whether or not a given feedback circuit satisfies the requirement that the frequency of oscillation of each oscillatory term, if any, contained in the closed-loop transient response and due to the presence of complex conjugate roots is less than a specified value ω_0. Such a requirement is satisfied if it can be established that all the characteristic roots are located inside the shaded region of Fig. A.3.

For this purpose let us put

$$p = \mathrm{j}(z + \omega_0) \tag{A.4}$$

The effect of this transformation is first to rotate the zeros of the polynomial $f(p)$ through 90° in the clockwise direction, and then displace them all horizontally and to the left by a distance equal to ω_0. Thus Equation A.1 modifies to

$$G_1(z) = \alpha_0 \mathrm{j}^n (z + \omega_0)^n + \alpha_1 \mathrm{j}^{n-1}(z + \omega_0)^{n-1} \ldots + \alpha_{n-1}\mathrm{j}(z + \omega_0) + \alpha_n \tag{A.5}$$

Remembering that $\mathrm{j}^2 = -1$, we find that the polynomial in the new variable z can be expressed as follows

$$G_1(z) = M_1(z) + \mathrm{j}N_1(z) \tag{A.6}$$

where $M_1(z)$ and $N_1(z)$ are polynomials in z, both having real coefficients.

We cannot apply Routh's criterion, in its normal form, to the polynomial $G_1(z)$ because of the presence of some imaginary

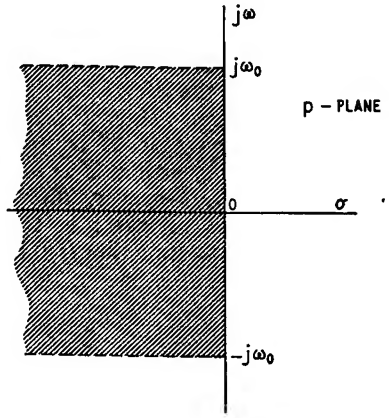

Fig. A.3

coefficients†. To overcome this difficulty let us construct a second polynomial $G_2(z)$ obtained from $f(p)$ by using the transformation

$$p = -\mathrm{j}(z + \omega_0) \tag{A.7}$$

The effect of this transformation is to rotate the zeros of the polynomial $f(p)$ through 90° in the anticlockwise direction, and then displace them horizontally and to the left by a distance ω_0. The result of the transformation is that

$$G_2(z) = M_1(z) - \mathrm{j}N_1(z) \tag{A.8}$$

where $M_1(z)$ and $N_1(z)$ are as defined earlier. Here again we

† An extension of Routh's criterion for polynomials with complex coefficients is given by E. Frank.[1]

cannot apply Routh's criterion owing to the presence of some imaginary coefficients.

A polynomial in z having real coefficients and containing the rotated zeros of both $G_1(z)$ and $G_2(z)$ is obtained by multiplying these two polynomials; we thus get

$$\begin{aligned} G(z) &= G_1(z) \cdot G_2(z) \\ &= M_1^2(z) + N_1^2(z) \end{aligned} \tag{A.9}$$

Owing to the rotation of the original zeros of $f(p)$ in opposite directions, we find that the zeros of $G(z)$ occur in complex conjugate pairs and, accordingly, the coefficients of $G(z)$ are all real. Also the order of the polynomial $G(z)$ is twice that of $f(p)$, that is, if the highest power of p in the polynomial $f(p)$ is n then the highest power of z in $G(z)$ is $2n$.

Suppose the original polynomial $f(p)$ has a pair of complex conjugate roots which lie inside the left half of the p-plane but outside the shaded region of Fig. A.3. Then the modified polynomial $G(z)$ will have a corresponding pair of complex conjugate zeros in the right half of the z-plane, and this is detected by applying Routh's criterion to $G(z)$. If, however, after applying Routh's criterion we find that $G(z)$ has no zeros in the right half of the z-plane, then we immediately conclude that $f(p)$ has no zeros outside the shaded region of Fig. A.3.

Example 2

Let it be required to find whether or not the polynomial

$$f(p) = p^3 + 2p^2 + 2p + 1$$

has a pair of complex conjugate roots with an imaginary part greater than 1 in absolute value (i.e. $\omega_0 = 1$). Putting $p = \mathrm{j}(z + 1)$ we get

$$\begin{aligned} G_1(z) &= \mathrm{j}^3(z+1)^3 + 2\mathrm{j}^2(z+1)^2 + 2\mathrm{j}(z+1) + 1 \\ &= M_1(z) + \mathrm{j}N_1(z) \end{aligned}$$

where

$$\begin{aligned} M_1(z) &= -(2z^2 + 4z + 1) \\ N_1(z) &= -(z^3 + 3z^2 + z - 1) \end{aligned}$$

Therefore, we have from Equation A.9 that

$$\begin{aligned} G(z) &= (2z^2 + 4z + 1)^2 + (z^3 + 3z^2 + z - 1)^2 \\ &= z^6 + 6z^5 + 15z^4 + 20z^3 + 15z^2 + 6z + 2 \end{aligned}$$

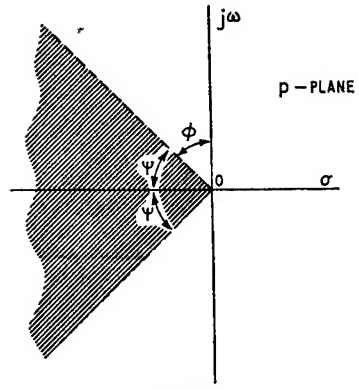

Fig. A.4

On applying Routh's criterion to this polynomial we find that $G(z)$ contains no zeros inside the right half of the z-plane, and so therefore we deduce that all the zeros of $f(p)$ are located inside the shaded region of Fig. A.3 with $\omega_0 = 1$.

To establish whether or not the characteristic equation has a pair of complex conjugate roots with a damping ratio less than a specified value ζ.

This test is useful when it is required to establish that the fractional overshoot of the closed-loop response to a step function input does not exceed a permissible value determined by ζ (see Section 2.2). To satisfy such a requirement it is necessary to demand that all the roots of the characteristic equation are located inside the shaded sector of Fig. A.4 with $\psi = \cos^{-1}\zeta$.

Let the roots of the characteristic equation $f(p) = 0$ be rotated through an angle $\phi = \pi/2 - \psi$ in a clockwise direction. This is achieved by making the following change of variable

$$p = w\,\mathrm{e}^{\mathrm{j}\phi} \tag{A.10}$$

Eliminating p between Equations A.1 and A.10 gives

$$Q_1(w) = \alpha_0\,\mathrm{e}^{\mathrm{j}n\phi}w^n + \alpha_1\,\mathrm{e}^{\mathrm{j}(n-1)\phi}w^{n-1} + \ldots + \alpha_{n-1}\,\mathrm{e}^{\mathrm{j}\phi}w + \alpha_n \tag{A.11}$$

Next, if the roots of the characteristic equation are rotated through an angle ϕ in an anticlockwise direction by making the change of variable

$$p = w\,e^{-j\phi} \tag{A.12}$$

we get

$$Q_2(w) = \alpha_0\,e^{-jn\phi}w^n + \alpha_1\,e^{-j(n-1)\phi}w^{n-1} + \ldots \alpha_{n-1}\,e^{-j\phi}w + \alpha_n \tag{A.13}$$

The polynomials $Q_1(w)$ and $Q_2(w)$ are both characterised in having complex coefficients and cannot, therefore, be tested by means of Routh's criterion in the usual way. If, however, these two polynomials are multiplied together, we obtain a polynomial $Q(w)$ which has real coefficients and which has all the zeros of $Q_1(w)$ and $Q_2(w)$; thus

$$Q(w) = Q_1(w).Q_2(w) \tag{A.14}$$

The polynomial $Q(w)$ will have all its zeros confined to the left half of the w-plane provided that the original polynomial $f(p)$ contains no zeros outside the shaded sector of Fig. A.4. On the other hand, if $f(p)$ has any pair of complex conjugate zeros outside this shaded sector, then the modified polynomial $Q(w)$ will possess a corresponding pair of zeros inside the right half of the w-plane. This is readily established by applying Routh's criterion to $Q(w)$.

Example 3

It is required to examine the polynomial

$$f(p) = p^3 + 2p^2 + 2p + 1$$

for the existence of a pair of complex conjugate zeros with $\zeta \leqslant 0{\cdot}707$. This corresponds to $\psi = \pi/4$ and $\phi = \pi/4$. Therefore putting $p = w\,e^{j\pi/4}$ gives

$$Q_1(w) = e^{j3\pi/4}w^3 + 2\,e^{j\pi/2}w^2 + 2\,e^{j\pi/4}w + 1 \tag{A.15}$$

But

$$e^{jm\phi} = \cos m\phi + j \sin m\phi$$

Therefore we can express $Q_1(w)$ as follows

$$Q_1(w) = \left(\cos\frac{3\pi}{4}.w^3 + 2\cos\frac{\pi}{2}.w^2 + 2\cos\frac{\pi}{4}.w + 1\right) + j\left(\sin\frac{3\pi}{4}w^3 + 2\sin\frac{\pi}{2}w^2 + 2\sin\frac{\pi}{4}w\right)$$

$$= (-0{\cdot}707w^3 + 1{\cdot}414w + 1) + j(0{\cdot}707w^3 + 2w^2 + 1{\cdot}414w)$$

Next, putting $p = w\,e^{-j\pi/4}$ leads to

$$Q_2(w) = (-0{\cdot}707w^3 + 1{\cdot}414w + 1) - j(0{\cdot}707w^3 + 2w^2 + 1{\cdot}414w)$$

We thus get

$$Q(w) = Q_1(w).Q_2(w)$$
$$= (-0{\cdot}707w^3 + 1{\cdot}414w + 1)^2 + (0{\cdot}707w^3 + 2w^2 + 1{\cdot}414w)^2$$
$$= w^6 + 2{\cdot}828w^5 + 4w^4 + 4{\cdot}242w^3 + 4w^2 + 2{\cdot}828w + 1$$

Application of Routh's criterion to the polynomial $Q(w)$ reveals that it has a pair of complex conjugate zeros in the right half of the w-plane. It therefore follows that the original polynomial $f(p)$ contains a pair of complex conjugate zeros with a damping ratio of ζ less than 0.707.

To establish whether or not all the roots of the characteristic equation are located along the negative σ-axis of the p-plane

This test is useful when it is required to ascertain that the closed loop transient response to a step function does not exhibit any overshoot†. Such a requirement demands that all the closed-loop poles, i.e. the roots of the characteristic equation are located along the negative σ-axis of the p-plane.

Consider a characteristic equation expressed in its generalised form as in Equation A.1. Differentiating with respect to p gives

$$'(p) = \frac{d}{dp}f(p)$$
$$= \alpha_0 np^{n-1} + \alpha_1(n-1)p^{n-2} + \alpha_2(n-2)p^{n-3} + \ldots + \alpha_{n-1} \tag{A.16}$$

If next we introduce a new variable λ related to p by

$$p = \lambda^2 \tag{A.17}$$

then in terms of λ we can express Equations A.1 and A.16 as follows, respectively,

$$P_1(\lambda) = [f(p)]_{p=\lambda^2} \tag{A.18}$$
$$= \alpha_0\lambda^{2n} + \alpha_1\lambda^{2n-2} + \ldots \alpha_{n-1}\lambda^2 + \alpha_n$$
$$P_2(\lambda) = [f'(p)]_{p=\lambda^2}$$
$$= \alpha_0 n\lambda^{2n-2} + \alpha_1(n-1)\lambda^{2n-4} + \ldots + \alpha_{n-1} \tag{A.19}$$

† It is also found useful in the study of transfer functions realised by networks composed of resistors and capacitors only; see A. T. Fuller.[2]

Let us next construct another polynomial $P(\lambda)$ related to $P_1(\lambda)$ and $P_2(\lambda)$ as follows

$$P(\lambda) = P_1(\lambda) + \lambda P_2(\lambda) \tag{A.20}$$

that is,

$$P(\lambda) = \alpha_0\lambda^{2n} + \alpha_0 n\lambda^{2n-1} + \alpha_1\lambda^{2n-2} + \alpha_1(n-1)\lambda^{2n-3} + \ldots \ldots + \alpha_{n-1}\lambda + \alpha_n \tag{A.21}$$

Now if the original polynomial $f(p)$ is to have all its zeros located on the negative σ-axis of the p-plane, then it is necessary and sufficient for the polynomial $P(\lambda)$ to have all its zeros confined to the left half of the λ-plane. Hence by applying Routh's criterion to $P(\lambda)$ we can establish whether or not all the zeros of $f(p)$ are located along the negative σ-axis of the p-plane.

As an illustration consider the simple case of a polynomial $f(p)$ having only two zeros on the negative σ-axis of the p-plane, that is

$$\begin{aligned} f(p) &= (p + \sigma_1)(p + \sigma_2) \\ &= p^2 + (\sigma_1 + \sigma_2)p + \sigma_1\sigma_2 \end{aligned} \tag{A.22}$$

whether σ_1 and σ_2 are both positive real numbers. Differentiating $f(p)$ with respect to p gives

$$f'(p) = 2p + (\sigma_1 + \sigma_2) \tag{A.23}$$

Therefore,

$$P_1(\lambda) = \lambda^4 + (\sigma_1 + \sigma_2)\lambda^2 + \sigma_1\sigma_2 \tag{A.24}$$

$$P_2(\lambda) = 2\lambda^2 + (\sigma_1 + \sigma_2) \tag{A.25}$$

$$\begin{aligned} P(\lambda) &= P_1(\lambda) + \lambda P_2(\lambda) \\ &= \lambda^4 + 2\lambda^3 + (\sigma_1 + \sigma_2)\lambda^2 + (\sigma_1 + \sigma_2)\lambda + \sigma_1\sigma_2 \end{aligned} \tag{A.26}$$

Applying Routh's criterion to $P(\lambda)$ leads to the following table

1	$(\sigma_1 + \sigma_2)$	$\sigma_1\sigma_2$
2	$(\sigma_1 + \sigma_2)$	0
$\frac{1}{2}(\sigma_1 + \sigma_2)$	$\sigma_1\sigma_2$	0
$\dfrac{(\sigma_1 - \sigma_2)^2}{(\sigma_1 + \sigma_2)}$	0	0
$\sigma_1\sigma_2$	0	0

Since σ_1 and σ_2 are both positive real numbers, by assumption, it follows that all elements of the first column of this table are positive, and therefore all zeros of $P(\lambda)$ are located in the left half of the λ-plane. We can generalise this result by stating that if on applying Routh's criterion to the polynomial $P(\lambda)$ of Equation A.21 we find that all the zeros of $P(\lambda)$ are located inside the left half of the λ-plane, then all the zeros of the original polynomial $f(p)$ are necessarily located along the negative σ-axis of the p-plane.

REFERENCES

1. FRANK, E., 'On the Zeros of Polynomials with Complex Coefficients', *Bull. Am. Math. Soc.*, **52**, 144 (1946).
2. FULLER, A. T., 'Stability Criterion for Linear Systems and Realisability Criterion for RC Networks', *Proc. Cambridge Phil. Soc.*, **53**, 878 (1957).
3. USHER, T., 'A New Application of the Hurwitz-Routh Stability Criteria', *Trans. A.I.E.E.*, Part I, **78**, 530 (1957).
4. WALL, H. S., *Analytic Theory of Continued Fractions*, Van Nostrand, New York (1948).

Chapter 2

1. $v_{oc} = 0{\cdot}667\, v_S$ $\qquad Z_{out} = 3{\cdot}33\ \text{k}\Omega$

2. $i_{sc} = -4{\cdot}93\, i_S$ $\qquad Z_{out} = 1{\cdot}68\ \text{k}\Omega$

3. (a) $v(t) = \dfrac{E}{5}(1 - \mathrm{e}^{-1{\cdot}25t/CR})$

   (b) $\left[\dfrac{\mathrm{d}}{\mathrm{d}t} i(t)\right]_{t=0} = \dfrac{E}{16CR^2}$

4. $v_R(t) = \dfrac{1}{2C}\mathrm{e}^{-t/CR}$

   $v_s(t) = -\dfrac{1}{2C}(1 - \mathrm{e}^{-t/CR})$

5. $i_L(t) = 1 - \dfrac{\mathrm{e}^{-Rt/2L}}{\omega_0\sqrt{[LC]}}\cos(\omega_0 t - \theta)$

   where

   $\omega_0 = \sqrt{\left[\dfrac{1}{LC} - \dfrac{R^2}{4L^2}\right]} \qquad \theta = \sin^{-1}\left(\dfrac{R}{2}\sqrt{\left[\dfrac{C}{L}\right]}\right)$

6. $i(t) = \dfrac{-ER}{R^2 + \omega^2 L^2}\mathrm{e}^{-tR/L} + \dfrac{E}{\sqrt{[R^2 + \omega^2 L^2]}}\cos(\omega t + \theta$

   where

   $\theta = -\tan^{-1}\left(\dfrac{\omega L}{R}\right)$ and $R = R_0 + R_1$

7. $v_1(t) = CR(1 - \mathrm{e}^{-t/CR})$

$$v_2(t) = -g_m CR^2\left(1 - e^{-t/CR} - \frac{t}{CR}e^{-t/CR}\right)$$

9. $T(p) = \dfrac{31{\cdot}6\omega_0^3(p+\omega_0)}{(p+0{\cdot}1\omega_0)^2(p+10\omega_0)^2}$

10. Angular cut-off frequency $= 2{\cdot}91\ \omega_0$
    At $\omega = 2{\cdot}91\ \omega_0$, phase angle $= -67°$

13. $Z_{in} = 30\ \Omega$
    $Z_{out} = 490\ k\Omega$
    $K_V = 325$
    $K_I = -0{\cdot}975$

14. $Z_{in} = 1370\ \Omega$
    $K_V = 12{\cdot}2 \times 10^3$

15. $K_V = -19{\cdot}3$

16. $K_V = 7{\cdot}75$

18. $K_{p\,max} = 1000$

Chapter 3

2. 3%

3. 24·6

4. $F = 1 + h_{21e}\dfrac{R_S R_L + R_e(R_S + R_L + R_f)}{(h_{11e} + R_e)(R_S + R_L + R_f) + R_S(R_L + R_f)}$

   $Z_{in}' = \dfrac{(R_L + R_f)[h_{11e} + R_e(1 + h_{21e})]}{h_{11e} + R_f + (R_e + R_L)(1 + h_{21e})}$

7. 0·236

8. $K' = 9{\cdot}65$
   $Z_{in}' = 30{\cdot}5\ k\Omega$

9. $K' = 85$
   $Z_{out}' = 678\ \Omega$

10. (a) $F_h = 0{\cdot}98$

(b) $F_y = 1{\cdot}021$
(c) $F_z = 1{\cdot}09$
(d) $F_g = 0{\cdot}907$

Chapter 4

1. (a) Stable
   (b) Unstable
   (c) Unstable
   (d) Stable

2. $2 < T(0) < 20$

3. Asymptotes intersect at $p = -2{\cdot}07$
   Point of departure from σ-axis at $p = -0{\cdot}58$
   Point of intersection with jω-axis at $p = \pm$ j 2·49
   Threshold open-loop gain = 37·5
   For critical damping, $T(0) = 0{\cdot}7$

4. Angle of departure = 25°
   Point of intersection with jω-axis at $p = \pm$ j 1·05
   Threshold open-loop gain = 11·1
   For $T(0) = 10$, percentage overshoot = 92·5%

5. Closed loop poles at $p = -1{\cdot}46$
   $p = -0{\cdot}02 \pm$ j 0·665
   20 per cent increase in $T(0)$ causes closed loop poles to move to
   $p = -1{\cdot}51$,
   $p = 0{\cdot}005 \pm$ j0·718

6. $47{\cdot}5 \times 10^6$ rad/sec, or $10^6/47{\cdot}5$ rad/sec

7. T(0) = 5
   The remaining closed-loop pole is at $p = -2{\cdot}71$
   Overshoot = 73·6%

Chapter 5

1. (a) Stable
   (b) Unstable
2. $2 < T(0) < 20$
3. Critical value of $T(0) = 8$
   Frequency of oscillation $= \sqrt{3}\omega_0$
4. Gain margin = 1·66 dB
   Phase crossover frequency $= 4{\cdot}58\ \omega_0$
6. Critical value of c is 8.
   Phase crossover frequencies are at $2{\cdot}19\ \omega_r$ and $0{\cdot}455\ \omega_r$

Chapter 7

1. $L = rRC$

$$f = \frac{1}{2\pi}\sqrt{\left[\frac{1}{LC}\left(1 - \frac{r}{R}\right)\right]}$$

3. $$Z_1 = \frac{(1+\mu) + j\omega(C_1 + C_2)r_a}{j\omega C_1(1 + j\omega C_2 r_a)}$$

   (a) $X = 11{\cdot}5$ kΩ; the reactance X is therefore inductive
   (b) $R = 1$ kΩ
4. The network is open-circuit stable but short-circuit unstable.

Chapter 8

1. (a) $K_0 = -11{\cdot}8$
   $f_0 = 1{\cdot}29$ Mc/s
   $\tau_r = 0{\cdot}27\ \mu$sec
   (b) $R_e = 24{\cdot}4\ \Omega$
   $K_0' = -7{\cdot}4$
   $F = 1{\cdot}57$
2. $R = 400$ kΩ
   (a) 4·5 Mc/s

   (b) 4·3%
3. (a) $N = \frac{50}{3}$
   (b) $K' = 8{\cdot}2$
   Without feedback the 3-dB cut-off frequencies are at 75 c/s and 13 kc/s. With feedback the 3-dB cut-off frequencies are at 10 c/s and 91 kc/s.
4. $T(0) = 3{\cdot}5$
   Closed-loop zero at $p = -2$
   Closed-loop poles at $p = -1{\cdot}86 \pm j$
5. Required open-loop poles are at $p = -1/200$ and $p = -1 \pm j$.
   Gain margin = 12·1 dB.

Chapter 9

2. (a) $$K'(p) = -\frac{R_2}{2R_1}\frac{1}{(1 + \frac{1}{2}pC_1R_1)(1 + pC_2R_2)}$$
   (b) $$K'(p) = -\frac{2R_2}{R_1}(1 + \tfrac{1}{2}pC_2R_2)$$
3. $-13{\cdot}6\ (1 - e^{-0{\cdot}69t})$ where t is in millisec
5. $$K'(p) = \frac{100}{p^2 + 2p + 10}$$
6. $$R_1 = R_2 = \frac{2}{\zeta}$$
   $$R_3 = \frac{1}{\zeta}$$

Chapter 10

1. 3·26 Mc/s
3. $$T(p) = \frac{-j\omega C_1R_2K_0}{1 + j\omega(C_1R_1 + C_2R_2 + C_1R_2) - \omega^2C_1R_1C_2R_2}$$
   $$\omega = \sqrt{\left[\frac{1}{C_1R_1C_2R_2}\right]}$$

$$K_0 = 1 + \frac{R_1}{R_2} + \frac{C_2}{C_1}$$

4. $\mu = 38{\cdot}2$

   $f = 138$ c/s

5. If $\dfrac{L_1 + L_2}{C} \gg \dfrac{h_{11e}R_bR_L}{(R_b + h_{11e})(1 + h_{22e}R_L)}$

   then $\omega \simeq \sqrt{\left[\dfrac{1}{C}\left(\dfrac{1}{L_1} + \dfrac{1}{L_2}\right)\right]}$

   $$h_{21e} = \frac{L_1}{L_2}h_{11e}\left(h_{22e} + \frac{1}{R_L}\right) + \frac{L_2}{L_1}\left(1 + \frac{h_{11e}}{R_b}\right)$$

6. $L_0 = \dfrac{LC_2}{C_1}$

   $$\omega = \sqrt{\left[\frac{1}{L(C_1 + C_2)}\right]}$$

   $$h_{21e} = \frac{C_1}{C_2}\left(1 + \frac{h_{11e}}{R_b}\right) + \frac{C_2}{C_1}h_{11e}\left(h_{22e} + \frac{1}{R_L}\right)$$

7. $X(\omega) = -\dfrac{1 - \omega^2LC}{\omega(C + C_1 - \omega^2LCC_1)}$

   Series resonance frequency $= f_1 = \dfrac{1}{2\pi}\sqrt{\left[\dfrac{1}{LC}\right]} = 0{\cdot}527$ Mc/s

   Parallel resonance frequency $= f_2 = \dfrac{1}{2\pi}\sqrt{\left[\dfrac{1}{L}\left(\dfrac{1}{C} + \dfrac{1}{C_1}\right)\right]}$

   $$\frac{f_2 - f_1}{f_1} \simeq \frac{C}{2C_1} = 0{\cdot}002$$

Index